THE DEVELOPMENT OF COASTAL BLUFFS IN A PERMAFROST ENVIRONMENT, KIVITOO PENINSULA, BAFFIN ISLAND, CANADA

by Mitchell Algus

A thesis submitted to the faculty of Graduate Studies and Research in partial fulfillment of the requirements for the degree of Doctor of Philosophy

Department of Geography
McGill University
Montreal, Quebec

© March, 1986

ABSTRACT

Bluffs developed in Quaternary sediments are found in a permafrost environment along the coast of the Kivitoo Peninsula, Baffin Island. Four bluff types are identified, their distribution being primarily a function of local stratigraphy and intensity of marine undercutting.

Bluffs possessing an undissected planform and straight slopes mantled by coarse sediments develop where thick coarse-grained stratigraphic units cap the bluffs. Since this debris-mantle is highly permeable, active layer saturation and flattening below the soil's angle of repose is not favored and, consequently, bluff dissection is inhibited.

Bluffs displaying faceted scarp slopes and dissected by steep, shallow hollows form in interbedded, predominantly sandy lithologies. Hollows develop as laterally prefential failure along the bluff face leads to localized slope reduction.

Bluffs with broad arcuate embayments ('debris-bowls') possessing steep side walls and gentler tongue slopes occur where thick fine-grained units are present, the tongue slopes developing at the level of these sediments. Debris-bowls are an extreme case of hollow development in which the axial slope has flattened and broadened in response to soil failure and transport processes capable of operating on low-gradient slopes. Under more moderate erosion rates adjacent tongue slopes may join to form a continuous surface. The prominent bench along the northwest end of the bluffs has formed in this manner.

A stability analysis considering excess pore pressures generated by thaw-consolidation is applied to low-angle single-event landslides along the mid-bluff bench. Although stability is predicted most of the time -- as is consistent with the apparent infrequency of landslide events and low in situ pore pressures -- failure could occur during the exceptional year when icy soil at the base of the active layer is subject to prolonged or rapid thaw. Periods of intensive instability may therefore coincide with climatic warming, soil movements becoming less frequent as the icy zone is restablished at the base of the thickened active layer.

Undercutting of soft muddy sediments resulting in undrained failure and retrogressive spalling of the newly created scarp, is, in association with debris evacuation by flowage, a significant mechanism of low-gradient active layer stripping.

Short-lived, areally confined liquefaction of sandy soils in which grain contacts have been eliminated by frost action, lowering the soil's friction angle and resulting in failure initiation upon thaw, can account for the widespread, shallow gelifluction-type movements occurring on gentle slopes.

RESUME

Dans une région de pergélisol sur la côte de la Péninsule Kivitoo (Terre de Baffin), on retrouve des escarpements formés dans des sédiments quaternaires. Quatre principaux types d'escarpement sont identifiés; leur distribution dépend surtout de la stratigraphie locale et de l'intensité du sapement marin.

Des escarpements dont le plan est non-disséqué et possedant des pentes rectilignes recouvertes de sédiments à gros grains se sont dévelopés là où d'épaisses unités à gros grains coiffent les escarpements. En raison de la grande perméabilité de ce manteau de débris, la saturation du mollisol et l'aplanissement en deçà de l'angle d'équilibre du sol ne sont pas favorisés et ceci, par conséquent, empêche la dissection des escarpements.

Des escarpements présentant des pentes facettées et disséqués par des creux peu profonds, à pentes abruptes, se forment au sein de lithologies sablonneuses interstratifées. Les creux se développent par rupture préférentielle latérale le long du front de l'escarpement, menant à une réduction locale de la pente.

Là où d'épaisses unités à grain fin sont présentes, on retrouve des escarpements avec de vastes creux arqués (cuvettes de débris). Ces creux présentent des murs latéraux à forte pente et des talus en forme de langue, à pente plus faible. Ces talus se développent au niveau des sédiments fins. Les cuvettes de débris représentent un cas extrême de développement de cuvette au cours duquel la pente axiale a été aplanie et élargie en réponse à des processus de rupture du sol et de transport capables d'opérer sur des pentes faibles. Lorsque les taux d'érosion sont plus modérés, des langues adjacentes peuvent se rejoindre pour former une surface continue. Le replat prononcé des escarpements de la section nord-ouest a été crée de cette façon.

Les surpressions interstitielles causées par la consolidation lors de la fonte ont fait l'objet d'une analyse de stabilité appliquée aux glissements de terrain uniques à faible pente se produisant le long du replat au milieu des escarpements. Quoique la stabilité de la pente est prédite dans la plupart des cas -- tel que confirmé par le nombre apparemment peu élevé de glissements de terrain et par les faibles pressions interstitielles in situ -- des ruptures pourraient se produire au cours d'années exceptionnelles où le sol glacé à la base du mollisol subirait un dégel rapide ou prolongé. Par conséquent, des périodes d'instabilité intense peuvent coincider avec un réchauffement du climat, les mouvements de sol devenant moins fréquents alors que la zone glacée est rétablie a la base du mollisol maintenant plus épais.

Le sapement de sédiments boueux mous causant une rupture non draînée et un effritement rétrogressif de l'escarpement nouvellement créé représente, associé à l'évacuation des débris par écoulement, un mécanisme significatif de décapage des mollisols à pente faible.

On peut expliquer les mouvements répandus et peu profonds de type 'gélifluxion' notés sur des pentes douces par une liquéfaction des sols sablonneux. Au cours de cette liquéfaction, de courte durée et limitée dans l'espace, les contacts entre grains ont été éliminés par l'action du gel, ce qui réduit l'angle de frottement du sol et initie la rupture au dégel.

ACKNOWLEDGEMENTS

Prof. M.A. Carson acted as thesis advisor. His interest in, and insight into, this research were invaluable, as was his patience and encouragement duing the preparation of the text. Prof. Carson also, gamely and under adverse conditions, joined the party in the field in July, 1983. I sincerely thank him for his tutorship and understanding throughout.

Prof. J.B. Bird supervised the initial stages of this research and laid the groundwork for the present study through his visit to the Kivitoo area in 1976. Prof. Bird's knowledge of northern geography provided the ground from which this research grew. His help in securing financial support and guidance in the last stages of manuscript preparation are also greatly appreciated.

Jeffrey Berman and Todd Moses proved intelligent and selfless field assistants during 1977 and 1983 respectively. Their companionship and enthusiasm under difficult and isolated circumstances contributed in no small part to the present research.

The initial field season was made considerably easier through the experience and company of Alan Nelson and Terry Brown (then of the University of Colorado) with whom we shared our camp at Kivitoo in 1977. Alan Nelson also gave generously of his knowledge of the Kivitoo bluffs. Without his stratigraphic work this reseach would have been disadvantaged.

I would also like to thank Prof. J.T. Andrews and the Institute for Arctic and Alpine Research of the University of Colorado for logistical support. Parks Canada extended to us permission to conduct our study within the confines of Auyuittuq National Park, and kept track of us through their Broughton Island office.

Funding for this reseach came from the Arctic Institute of North America and the Center for Northern Studies of McGill University in 1977. Financial support for the 1983 field season was received through an Energy, Mines and Resouces grant to Prof. J.B. Bird; J.A. Heginbottom of the Terrain Sciences division was instrumental in helping to secure this aid. A Max Bell Fellowship from McGill University helped support data analysis and laboratory work during 1983 - 1984.

This project has benefited greatly from discussions with colleagues at both McGill University and the University of Colorado. Profs. William Howland and Hardy Granberg, Paul MacLean, Alan Colvill, Scott Morris and Peter Palmer, among others, had their say. Prof. Rick Wright facilitated drafting of data using the geography department's computer facilities. Prof. Prapote Boonsinsuk allowed me the use of the (McGill) Geotechnical Research Centre's consolidation device. The CRREL corer was lent by the Civil Engineering Department of the University of Montreal. Betsy Howland contributed the drafting of Figures I.1 and IV.4, while Charlotte Granberg assisted in typing of the manuscript. Marie-Andrhe Dubreuil did the translation of the abstract.

Finally, I would like to thank all those who put up with the various and difficult personal traumas surrounding this

thesis. Many friends, including Charlotte Mayes, Jane Algus and the Berman family, have felt the impact of this work in their lives and displayed faith and understanding. My grandparents likewise contributed heartening advice and perspective. My parents though lived this project vicariously, providing ineffable support. This thesis is their's as well.

List Of Contents

Chapter I: Introduction.....1
A. Field area.....4
B. Quaternary and sea level history.....8
C. Previous work on coastal bluffs in high latitude regions.....14
D. Objectives.....16
E. Organization.....18

Chapter II: Physical Geography of the Kivitoo Peninsula.....19
A. The terrain of the Kivitoo Peninsula
1. Permafrost.....19
2. Nivation and snowpack distribution.....21
B. Climate.....23
C. The coastal environment and coastal retreat.....26
1. Pack ice, landfast ice and the ice foot.....27
2. Coastal energy regime: Tides, wave action and storm surges.....28
3. Coastal retreat.....30
4. Long term variations in erosion intensity.....31
D. Stratigraphy and character of the Kivitoo bluff sediments.....32

Chapter III: Field Methods and Theoretical Background.....37
A. Methods of field investigation and data collection...38
B. Bluff dissection.....40
C. Slope stability analysis.....42
D. Introduction to the morphological divisions of the Kivitoo Bluffs; Chapters IV, V, VII, and VIII.....46

Chapter IV: The Planar Debris-Mantled Bluffs.....48
A. Stratigraphy.....48
B. Terrace morphology.....49
C. The bluff slope.....54

Chapter V: The Steep Dissected Bluffs.....63
A. Stratigraphy.....63
B. Form and development of scarp slopes.....65
1. Active layer thickness and frost table depth..66
2. Analysis of the profiles.....66
a. Talus segments.....67
b. Undercut segments with a sandy colluvial regolith.....69
c. Slope segments in in situ sediment.....71
d. High-angle slope elements.....72
3. Observation of process on scarp slopes.....77
C. Form and Development of Bluff-Face Hollows.....81
1. Literature review.....84
2. Morphology and hydrologic conditions of the terrace along the steep dissected bluffs.....87
3. Bluff-face hollows: Morphology and process....94
a. Initiation and genesis of form.....96
b. Observation of process.....98
c. 'Nivation': The role of snow in

hollow development.....101
d. Sideslope undercutting and axial incision.....102
4. Taluvial lag slopes: Extreme conversion.....104
5. The spacing of bluff-face hollows.....107
D. Summary.....110

Chapter VI: Soil Movements on Low-Angle Slopes: Observations and Theory
Introduction.....112
A. Low-angle, single-event landslides.....116
1. Observations of low-angle Landslides on the Kivitoo bench slopes: Case studies and ground ice conditions.....117
a. Description of slides.....118
b. Active layer soils of the Kivitoo bench slopes
i. Soil profiles, moisture content and ground ice.....122
ii. Freezing-induced structure of the Kivitoo soils.....131
iii. Piezometric observations along Kivitoo bench.....137
c.Observations of soil movement during the 1977 and 1983 field seasons.....139
2. Mechanisms of low-angled movement of thawing soils: Literature Review.....146
a. Confined aquifer mechanisms.....147
b. Liquefaction of sandy soils.....151
c. In situ formation of debris flow by ped slaking during thaw.....154
d. Thaw-consolidation mechanism for single-event slides: Theory.....158
3. Thaw-consolidation mechanism: application to Kivitoo.....167
a. Solution of the thermal problem
i. Derivation of the thermal constant (α) for Kivitoo.....167
ii. Analytical definition of the thermal constant and back-calculation of average seasonal thawing temperatures.....169
iii. Year-to-year variation in thaw rate and active layer depth.....173
b. Determination of the coefficient of consolidation (Cv) for the fine-grained soils along the Kivitoo bench....180
c. Calculation of the thaw consolidation ratio (R) for the Kivitoo bench slopes...183
d. The Special Case of Active Layers With continuous icy Layers at depth.....185
e. Application of thaw consolidation theory to Kivitoo bench slides: Discussion.....193
f. Conclusion.....199
4. Post-failure behavior of landslides along

the Kivitoo bench.....200
B. Retrogressive Active Layer Failure.....207
1. Description of retrogressive active layer failures along the Kivitoo Bluffs.....209
2. Mechanics of failure initiation.....212
3. Movement of the debris lobe.....214
C. Gelifluction.....217
D. Endnote.....226

Chapter VII: Morphology and Development of the Bluffs with Debris-Bowls
A. Introduction.....227
B. Stratigraphy.....228
C. Terrace conditions along the bluffs with debris-bowls.....229
D. Debris-bowl morphology
1. General characteristics.....231
2. Debris-bowl profiles and their relationship to bluff stratigraphy.....237
E. Debris-bowl development.....239
1. Initiation of the bowl form.....240
2. Soil movement along the tongue slope.....243
a. Stability of the debris-bowl tongue slopes.....244
b. The tongue as a transport slope for failure initiated on the debris-bowl walls.....247
c. Soil movement by seepage and slope wash...248
3. Retreat of the debris-bowl back slope.....249
4. The foot slope.....251
5. Inter-bowl ribs, debris-bowl side slopes and coast-parallel slopes.....252
F. Taluvial debris slopes.....254
G. Endnote.....256

Chapter VIII: The Benched Bluffs
A. Introduction.....257
B. The origin of the mid-bluff bench.....259
1. Bench development.....261
2. Other instances of bench formation.....264
3. The location of low-angle landslides.....266
C. Rates of toe erosion and the development of vegetated colluvial slopes.....268
D. The bench back slope.....270
E. Endnote.....271

Chapter IX: Discussion and Suggestions For Future Research.....273

References.....286

Appendices.....301
A. Addenda to text, tilting box and consolidation data
B. Bluff profiles and bluff-top survey lines
C. Photographic panorama of the Kivitoo Bluffs and Stratigraphy of the Kivitoo Bluffs

List of Tables

Tables are gathered together at the end of each chapter.

Table II.1 Glossary of permafrost terminology
II.2 Summary of weather records for Broughton Island and Cape Hooper (1961-1970)
II.3 Facies classification for sediments of the Kivitoo Peninsula

Table V.1 Bulk unit weight and moisture content of steep facets in sand

Table VI.1 Morphology of low-angle, single-event landslides at Kivitoo
VI.2 Summary of soil properties
VI.3 Thermal solutions for Kivitoo
VI.4 Length of thaw season, eqivalent step temperature, depth of thaw and value of the thermal constant for the years 1960-1983
VI.5 Consolidation test results
VI.6 Field hydraulic conductivity
VI.7 Physical properties of some gelifluction soils from Kivitoo

List of Figures

To facilitate use, figures are located at the end of each chapter, following the Tables.

Figure I.1 Place map of the Kivitoo Peninsula, Baffin Island
I.2 Map of field area
I.3 Air photo of field area, July 5, 1958
I.4 Oblique view of the field area looking towards the southeast
I.5 Mid-Foxe ice margins (ca 60 - 80,000 BP)
I.6 Relative sea level at Kivitoo, Mid-Foxe to present

Figure II.1 Neve-type coastline west of Kangeeak Point
II.2 24-hour storm rainfall events at Cape Hooper
II.3 Daily Mean Temperature at Broughton Island (June - August, 1977, 1983)
II.4 View southeast alond coast in the vicinity of the stream at K900
II.5 Generalized bathymetry off the coast of the Kivitoo Peninsula

Figure III.1 Analysis of the stabiltiy of an infinite slope
III.2 Distribution of bluff types within the Kivitoo study area

Figure IV.1 Planar debris-mantled bluffs southeast of Camp I
IV.2 Oblique view of tall debris-mantled bluff
IV.3 Terrace surface along Survey Line III
IV.4 Schematic representation of the morphology of the raised terrace surface
IV.5 Selected transects across the raised terrace surface
IV.6 Sediment fans along bluff southeast of Camp I
IV.7 Gully retrogressing onto sand wedge fissure
IV.8 Surface pitting formed by pipe collapse behand incipient gully
IV.9 Planar debris-mantled bluff face along Survey Line III
IV.10 Representative profiles of the debris-mantled bluffs
IV.11 Grain-size curves for samples from the debris-mantled bluffs
IV.12 Cross section of the active layer along a debris-mantled bluff slope
IV.13 Schematic cross section showing effect of mantle on phreatic zone development
IV.14 Landslide at base of a debris-mantled bluff slope
IV.15 Bluffs southeast of Camp I demonstrating the stabilizing effect of the coarse mantle

Figure V.1 Stratigraphy along the steep dissected bluffs
V.2 Profiles of representative scarp slopes along the steep dissected bluffs
V.3 Bar graph of scarp slope segment angles
V.4 Schematic model of an undercut scarp slope
V.5 Photographs of scarp slope at K268; 1976, 1977, 1983
V.6 'Ice-cored' talus apron
V.7 Grain-size curve from steep slope in bedded bedded sand
V.8 Exfoliation and spalling of lightly cemented sand along high angled scarp slope
V.9 Accumulation of talus at base of sandy scarp by granular disintegration in late August
V.10 Debris-hopper at K127
V.11 Bluff-face ravines at K291
V.12 Schematic representation of bluff-face hollows along the steep dissected bluffs
V.13 Surface drainage on terrace behind a debris-hopper
V.14 Distribution of bluff morphology along the steep dissected bluffs
V.15 Survey Line II
V.16 Subsidence of terrece surface behind a bluff-face hollow
V.17 'Organic mat' -type terrace surface northwest K240
V.18 'Stabilized' channel behind bluff-face hollow near K305
V.19 Long profiles of small 'hanging' gullies along the steep dissected bluffs
V.20 Undercutting of permafrost along a gully side
V.21 Collapse of the modern beach due to pseudo-pipe formation
V.22 Bar graph of mean inclinations of bluff-face hollows
V.23 Schematic profile of a bluff-face hollow
V.24 Slope failure along hollow axis
V.25 Slope failure in bluff-face hollow at K635
V.26 Schematic cross section showing effect of a thin clayey unit on along-slope seepage
V.27 Excavation above a snow patch at the top of a debris-hopper along Survey Line II
V.28 Schematic presentation of the effects of a snow patch in a bluff-face hollow
V.29 Bluff-face ravine showing pseudo-pipe development

Figure VI.1 Description of Slide 1
VI.2 Description of Slide 2
VI.3 Description of Slide 3
VI.4 Description of Slide 5
VI.5 Trench across mid-bluff bench at K1063
VI.6 Moisture content data from CRREL core sites along the mid-bluff bench

VI.7 Schematic representation of reticulate cryogenic structure in a fine-grained soil
VI.8 Excavation of frozen silty clay
VI.9 Exposure of thawed silty clay
VI.10 Grain-size of some reticulate-structured soils
VI.11 Piezometric data from sites along the mid-bluff bench
VI.12 Description of a recent landslide at K890 (Slide 8)
VI.13 Thawed, fine-grained soils from the mid-bluff bench
VI.14 Graphic solution to the two-layer thawing problem for a representitive active layer
VI.15 Frozen fine-garained consolidation test sample
VI.16 Typical consolidation test results for remolded and frozen/thawed silty clay
VI.17 Stage-loaded consolidation tests on remolded and frozen/thawed silty clay loam
VI.18 Graphic solution for determination of excess pore pressures at a soil/ice interface
VI.19 Diagramatic presentation of the possible post-failure behavior of a soil in shear
VI.20 Description of retrogressive active layer failure at K896
VI.21 Description of retrogressive active layer failure alongside stream at K900
VI.22 Arrested retrogressive failure at edge of debris-bowl tongue slope at K660
VI.23 Soil ripples at bottom of bench back slope
VI.24 Solifluction slope study site at K1145
VI.25 Schematic of ice growth at inter-grain contacts in sand

Figure VII.1 View along bluffs with debris-bowls south of K682
VII.2 Stratigraphy along the bluffs with debris-bowls
VII.3 Dry channel on terrace surface at K667
VII.4 Schematic profile and plan of a well-developed debris-bowl
VII.5 Description of the debris-bowl at K660
VII.6 Seepage steps retrogressing over debris-bowl tongue slope
VII.7 Minor retrogressive instability at the edge of a debris-bowl tongue slope
VII.8 Profiles through debris-bowls
VII.9 Large 'perched' debris-bowl at K860
VII.10 Schematic model of debris-bowl development
VII.11 Schematic diagram of seepage through a slope compried of a gentle segment below a steeper segment
VII.12 Bar graph of slope segment angles along debris-bowl tongue slopes

VII.13 Failure of rib end at K668
VII.14 Apron of wet and fluid debris at base of bluff southeast of Profile B-1 (K625)
VII.15 Pocket penetrometer log at base of bluff shown in Figure VII.14
VII.16 Taluvial lag slopes at K754 - K765

Figure VIII.1 View west along the mid-bluff bench from K1020
VIII.2 View east along the mid-bluff bench from K1245
VIII.3 Bench and back slope west of K1105
VIII.4 Bar graph of slope segment angles along the mid-bluff bench
VIII.5 Bluff profiles and stratigraphy for two locations along the benched bluffs
VIII.6 Excavation at the downslope edge of the mid-bluff bench at K955
VIII.7 Excavation at the downslope edge of the mid-bluff bench near K1250
VIII.8 Profile and stratigraphy of the bluffs at K1250 showing two bench slope segments
VIII.9 Schematic plan and photograph of the mid-bluff bench and its extension along the side of the stream at K1145
VIII.10 Profile and stratigraphy of the mid-bluff bench at K1128
VIII.11 Schematic representation of the wide section of the mid-bluff bench at K1215 - K1235
VIII.12 View of the mid-bluff bench looking east from K1250
VIII.13 Quasi-stable colluvial slope below mid-bluff bench
VIII.14 Bar graph of stable and quasi-stable colluvial slope segment angles
VIII.15 Bar graph of lower bluff slope segment angles along the benched bluffs
VIII.16 Bar graph of slope segment angles from the bench back slope

Figure IX.1 Schematic model for the morphological development of the Kivitoo bluffs

Symbols Used In The Text

α	thermal constant (Neumann Solution)
γ	total bulk unit weight of soil
γ'	submerged (buoyant) bulk unit weight of soil
γ_i	unit weight of ice
γ_w	unit weight of water
N	stability factor (see Equation VI.16)
σ	total normal stress
σ'	effective normal stress (prime denotes effective stress conditions)
$\sigma'r$	residual stress in a soil after thaw (see Capter VI)
ϕ'	angle of internal friction
ϕ'_p	peak angle of internal friction
ϕ'_r	residual angle of internal friction
ϕ'_{cv}	value of $\phi'p$ for a soil specimen which displays no volume change at failure
ϕ_i	angle of initial yield (following Carson 1977a)
ϕ_{rep}	angle of repose or rest after avalance-type failure (see Carson 1977a)
c'	cohesion intercept in Mohr-Coulomb usage
Cv	coefficient of consolidation
D	vertical depth of potential failure surface (see X)
Ku	thermal conductivity of an unfrozen soil
kw	hydraulic conductivity (Darcy's permeability coefficient)
L	latent heat content of a unit volume of frozen soil
Mv	coefficient of volume change
Po	applied normal load
R	thaw consolidation ratio (see Chapter VI)
S	shear strength

Su	undrained shear strength
T	shear stress acting to promote sliding
Tf	temperature at a thawed soil/ice interface
Ts	thawing step temperature
u	total pore pressure
u'	pore pressure corresponding to saturated, slope parallel flow
u_e	excess pore pressure
X	vertical thickness of soil above a thaw plane

CHAPTER I:
INTRODUCTION

Wave-eroded bluffs developed in Quaternary glacial and marine sediments form the outer coast of Kivitoo Peninsula, Baffin Island, N.W.T., Figure I.1. The bluffs display, along their length, considerable morphological variation. Not only does the gross morphology vary along the 15 km of coast which constitutes the study area (Figure I.2) -- slope height ranges from less than 4 m to over 30 m -- but a wide variety of slope types and bluff features are encountered. These range from low, undissected debris-mantled bluffs, to steeper, highly dissected scarp slopes to gentler, vegetated colluvial slopes.

Recent studies have employed a geotechnical approach in the study of natural slopes (e.g. Carson, 1971; Brunsden and Jones, 1972; Tam, 1975). Many of these investigations, done by engineers, have been concerned with coastal slopes and river banks (Lohnes and Handy, 1968; Hutchinson, 1967, 1973; Barton, 1973). These studies have included detailed geomorphological mapping and a geographical approach, considering not only problems of slope stability but those of slope developement as expressed both temporally and spatially.

Unfortunately, geotechnically oriented slope studies have, for the most part, been limited to humid-temperate and semi-arid environments. Researchers interested in slope processes and development in cold regions have attempted to incorporate a geotechnical perspective (e.g. Williams, 1959;

Harris, 1977). However, these efforts have been limited by the lack of a suitable body of geotechnical literature concerned with permafrost soils, as well as inadequate presentation and application of geotechnical principles in the geomorphological literature.

With increasing activity in the north, a body of work addressing slope problems in permafrost has been developing. The research of Chandler (1972), McRoberts and Morgenstern (1974), and Mackay (1977a) is particularly notable as initial attempts, still largely unincorporated into the mainstream of geomorphological research, at establishing a physical context through which to approach periglacial slope studies.

This thesis considers the development of the Kivitoo bluffs as a problem in coastal slope development, with the additional and extremely important factor of permafrost and ground ice. Much work in high latitudes has tended to emphasize (or at least call attention to in order to deemphasize) the uniqueness of these realms. Hence their geomorphology has often been seen firstly in a regional context and only secondarily in the context of 'normal' geomorphology (e.g. slope studies, coastal sedimentation, etc.). The broader approach taken here allows for a greater variety of research to be drawn from and a wider application of conclusions to be made, while still respecting the very real differences which do exist between the morphogenetic environments of high latitude and temperate regions.

During the summer of 1976, Professor J.B. Bird (McGill University) visited the field area with the intent of making 'periglacial studies along the coast of the Kivitoo foreland' (Bird, 1977). (Nelson (1978) uses the spelling 'Qivitu' based on local syllabic translations.) Bird noted that the 'most environmentally fragile areas of the peninsula are the contemporary (coastal) cliffs' and suggested that they are undergoing rapid retreat. These observations led, in turn, to the present research, begun the following summer. During the initial field season the party remained at Kivitoo from June 28 until August 28, 1977. The second field season, in 1983, lasted from June 25 until August 18.

The Kivitoo bluffs present a unique opportunity for the study of coastal slope developement in an arctic environment. Foremost among the reasons for this is the exceptional detailed stratigraphy of the bluffs prepared by Nelson (1978; see Appendix C) which serves, along with a photographic panorama of the study area (Appendix C), as the descriptive framework for this study. The relatively small size of the bluffs, their ease of access to a single base camp, and (in 1977) the support of the University of Colorado's facilities on Broughton Island, 60 km to the south, all tended to minimize the difficulties usually associated with research in remote areas.

But perhaps the single most intriguing aspect is the bluffs themselves: the wide range of lithology, surficial conditions and erosional environments encountered over so short a stretch of coastline. This variety facilitated the use of comparative

techniques and ergodic principles (the substitution of a spatial series for a temporal one). It also allowed a more 'geographical' approach to be taken. That is, the study of a spatially distributed set of slope types and slope features, rather than concentration on any one particular kind of bluff morphology.

A. Field Area

The Kivitoo Peninsula is the southern-most in a series of coastal lowlands extending into Baffin Bay and Davis Strait, along the east coast of Baffin Island. These lowlands, which Ives and Andrews (1963) have referred to as the 'continental forelands', include the Clyde foreland, Cape Aston and Cape Henry Kater, and represent the only subdued topography along a predominantly steep, rocky coast. As such they are of great interest to development concerns as locations for shore facilities. The Kivitoo Peninsula is included within the boundaries of Auyuittuq National Park.

Bounded to the east and west by Quajon and Narpaing Fiords respectively, the Kivitoo Peninsula is fronted by a gently sloping coastal plain blanketed by glacial and marine sediments. Deposited during the Quaternary as waxing and waning of glacier ice and associated isostatic-eustatic changes resulted in several glacial and marine transgressive-regressive episodes, the sediments outcrop in the coastal bluffs. Occupying the center of the peninsula, above the marine limit at 85 m, is a low upland mantled by blocky debris and

interpreted by Nelson (1980) as a glacio-fluvial outwash plain. Several small felsenmeer-covered bedrock hills rise above the general level of the foreland surface. The highest of these is Quaviq (360 m) along Quajon Fiord between Kangeeak Point and Kangitukuluk. Natinaq (150 m) and Nattiurusiq are the only two bedrock hills which occur fully within the marine limit along the outer coast.

The Kivitoo foreland is separated from the low hills and plateau surfaces (below 1,000 m elevation) which occupy the mid-fiord positions by a series of minor glacial troughs occupied by Narpait Lake and Itillikuluk along Narpaing Fiord and Kangitukuluk, which enters onto Quajon Fiord (see Figure I.1). South and west of this, the terrain rises spectacularly to the 1,500 to 2,000 m summits and deeply entrenched inner fiords of the Penny Highlands. The most prominent geological feature of the region is the Penny Ice Cap, covering an area of 6000 km^2, 30 km inland from the coast. Further to the west, elevations decrease as plateau surfaces step down to the gentle lowlands surrounding Foxe Basin which forms Baffin Island's western coast.

The imposing eastern edge of the Penny Highlands (and the entire upland region from Bylot Island south to Labrador) has been interpreted as the result of uplift and antithetic tilting associated with the opening of the Baffin Bay - Labrador Sea basin during the Tertiary (King, 1972; McMillan, 1973; Pelletier et al., 1974). The origin of the low coastal forelands is more difficult to explain. They may have been formed as down-faulted blocks during the opening of Baffin Bay.

Alternatively, they may be interpreted as strandflat (e.g. Reuch, 1844; Nanssen, 1922) cut into bedrock by a combination of marine planation (John and Sugden, 1971) and glacial erosion (Holtendahl, 1959).

The bedrock along the east coast of Baffin Island forms the eastern edge of the Churchill Province of the Canadian Shield. In the Cumberland Peninsula region, the crystalline bedrock may be either massive or layered; predominantly granite, fine to medium grained granitic gneiss (often interbedded with biotite-garnet gneiss) and quartz para-gneiss (Jackson and Taylor, 1972; Pheasant and Andrews, 1973; Sugden and Watts, 1977). Only two bedrock exposures could be found in the field area below the marine limit along the outer coast; a small tor about 5 m high at ca 35 m above sea level (asl) and a tiny outcrop along the coastal bluffs within the mouth of Narpaing Fiord (visible at K1232). Both of these exposures were intensely frost-shattered but only slightly weathered (equal to, or younger than Weathering Class III, as defined by Andrews and Miller 1976). The possibility exists that these are in fact large glacial erratics, but the lack of glacial abrasion and the close agreement of their jointing to regional patterns (Nelson pers. comm. 1977) argues against such an interpretation. The configuration and depth of the bedrock surface below the sediment cover is not known. The outcrops mentioned above, few small protruding hills and low height of the bluffs suggest that the bedrock surface is gently undulating and that the sediment blanket is probably not much thicker than 50-100 m.

The continental shelf off the Kivitoo Peninsula is about 40 km wide, as measured to the slope break at a depth of 200 m. Major troughs with basinal enclosure originating in the fiords traverse the shelf. The continental slope is gentle for glaciated coasts (3-5°; Loken and Hodgeson, 1971) and no fault lines or pronounced irregularities are evident.

Aerial photographic coverage of the northeastern coast of the Cumberland Peninsula is limited to small scale (1:60,000-1:40,000) vertical and oblique tri-metrogon black and white panchromatic imagery. The best coverage available is on Canadian Geological Survey photos A-16087-129/130, 143/44 (at 1:60,000, July 5, 1958), showing a partially snow-covered peninsula (Figure I.3), and A-16985-68/69 (1:60,000, 1960). Tri-metragon imagery, T326R-152/153 (1:40,000, July 22, 1949; Figure I.4) provides an oblique view towards the southeast of the northern portion of the peninsula.

Available topographic map coverage is even less useful, being of a very small scale (1:250,000). As the 68°N parallel cuts the Kivitoo Peninsula in two, both the Okoa Bay, District of Franklin map sheet (contour interval 500 feet) and the Home Bay, District of Franklin map sheet (contour interval 200 feet) are necessary for complete coverage of the research area. Since the bluffs are at no point greater than 100 feet high, and most of the topography of the peninsula is below 500 feet, these maps are of limited use.

B. Quaternary and Sea-Level History

The east coast of Baffin Island in general, and the northeastern Cumberland Peninsula specifically, has been an area of intensive interest to students of the Quaternary. Andrews et al. (1975) proposed that the Quajon-Narpaing Fiord area be studied as a type locality for a glacial response model of the northern margin of the Laurentide Ice Sheet. This could then be used as a reference for comparison with chronologies from the southern margin. It has become increasingly evident that the fluctuations of the northern and southern margin are not in phase (Pheasant and Andrews, 1973) and that glaciation is time transgressive, with ice appearing first in the north and then moving south as zones of maximum nourishment are 'pushed ahead' of the advancing margin, thereby leaving the northern regions snow-starved. Recently this picture has become considerably more complicated with the suggestion that the Laurentide Ice Sheet was not the monolithic ice body that has been assumed (Andrews and Barry 1978). Instead, several independent ice centers and/or contiguous ice sheets probably existed at any one time. Also, inter-stadial events may have been longer and more 'temperate' than previously suspected and there is good evidence from pollen and faunal assemblages in the Clyde (Baffin Island) cliffs (Miller et al. 1977; Fehling-Hansen, 1976) that periods of glacier build-up occurred during conditions that were, in fact, warmer than during the present non-glacial interval.

The significance of the Baffin Island region during

periods of glaciation has been recognized by Andrews et al. (1972). Often cited are its climatic sensitivity (Bradley and Miller, 1972; Andrews and Barry, 1972) and proximity to full glacial conditions. The nearness of the contemporary snowline to large upland plateaus has led to the concept of 'instantaneous glacierization', originally suggested for the Labrador-Ungava region by Ives et al. (1975), although this concept has been questioned by Barry et al. (1975) on the grounds that it would be physically impossible to build a sufficiently large ice sheet in the required time. Several smaller ice bodies would help to mitigate this objection. The special location of the Baffin coast with respect to critical and sensitive oceanic-atmospheric circulation systems has been discussed in an interesting paper by Johnson and McClure (1976).

In order to avoid unfounded correlations between the latest period of glacial activity in the eastern Canadian Arctic and the events to the south, Andrews (1968) proposed the term 'Foxe glaciation' to refer specifically to the most recent glaciation of Baffin Island. This replaces the use of 'Wisconsinan' which is retained for the southern margins. The usage has since been adopted by others (Miller et al., 1977; Dyke, 1979; and Nelson, 1980). The Foxe glaciation has been divided into early, middle and late stades (defined locally) and terminates with the recession of glaciers in the fiords ca. 8,000 yrs. B.P. The chronologies developed by Dyke (1977) and Nelson (1980) have used stadial names originally applied to the stratigraphic sequence exposed in the Clyde bluffs by Miller et

al. (1977).

The initial glacio-climatic and sea level chronologies for the Quajon-Narpaing Fiord area were developed by Pheasant (1971), Pheasant and Andrews (1973) and Andrews et al. (1975). These were based on the recognition of surficial weathering zones (usually occurring one above the other along the fiords) and stratigraphic evidence. The highest weathering zone, Weathering Zone I, may never have been glaciated, although this is disputed by Sugden and Watts (1977). Weathering Zone II pre-dates the last glaciation and is recognized by the presence of a weathered till. Weathering Zone III includes those areas affected by the Foxe glaciation and is characterized by the slight weathering of bedrock and glacial deposits. All of the Kivitoo Peninsula, with the possible exception of the summits of the higher hills, lies within the margins of Weathering Zone III (Nelson, 1980).

Three major glacial episodes within the Foxe glaciation, each of succeedingly lesser ice extent, have been recognized in the Kivitoo area. According to Pheasant and Andrews (1973), the oldest stade, dated at 115,000 yrs B.P., is the Alikdjuak stade, named after the moraine features deposited during this advance along Narpaing Fiord. Relative sea level at this time was coincident with the marine limit at 85 m and is marked by deltaic deposits at the front of the Alikdjuak moraine and by numerous smaller deltas and beach ridges on the central interior of the foreland (Figure I.5). Following the Quajon interstade, ice readvanced to mid-fiord positions and the limit of this advance, dated at greater than 40,000 yrs B.P., is

marked by the moraines bracketing Napait Lake and Pamiuja. Associated relative sea levels along the outer coast are 72 m and 40 m. Nelson (1978, 1980) has argued that the Alikdjuak Moraine is mid-Foxe in age and was formed 60,000 to 80,000 yrs B.P. at a tide-water ice margin. This would make the Alikdjuak stade correlative with the Ayr Lake till at Clyde (Miller et al., 1977) and thus older than previously thought. Consequently, the Napait and Keketurnak moraines represent mid-Foxe recessional stands and the 85, 72 and 40 m sea levels are all mid-Foxe in age. The mid-Foxe advance (Ayr Lake Stade) was followed by the retreat of the fiord glaciers (the inter-stade), Figure I.5.

During the late Foxe readvance (Baffinland Stade; prior to 10,000 yrs B.P.) glaciers probably did not extend much past the heads of the fiords and relative sea level at this time (24,000 to 10,000 yrs B.P.) may have been below present. During the late Foxe, the climate on Baffin Island was probably cool and dry, due to permanent sea-ice cover and the blockage of storm tracks by ice to the south which would result in decreased snowfall and consequently glacier thinning. In response to this thinning, restrained isostatic rebound coupled with low eustatic sea - levels may have combined to produce a local relative sea level as much as 30 m below present sea level (Nelson 1980). This is a possible reason for the lack of radiocarbon dates between 24,000 and 10,000 yrs B.P. If low relative sea levels were indeed the case, this would mean that near-shore permafrost may be thick and that streams along the foreland have experienced large infill sedimentation in their

lower reaches as they regraded to a higher relative sea level. Nelson (1978) suggests that the large beach ridges on the foreland surface marking a 25 m sea level date from ca. 25,000 yrs B.P. and were formed during transgression from the low sea level stand in response to a glacier advance at this time. However, no dates associated with this strandline are available. A more recent pre-Holocene advance, following several minor sea level and glacial fluctuations, climaxed ca 8,000 yrs B.P., during which time the raised beaches on the foreland surface at 15 m and below were formed. The inferred sea level curve for Kivitoo, derived from various sources, is given in Figure I.6.

Miller (1973) has constructed a climatic history for the Kivitoo-Home Bay area during Holocene and recent times. After the late Foxe readvance, climatic warming climaxed during the Hypsithermal (6,000-5,000 yrs B.P.). This was followed by the onset of a cooling trend, the neo-glaciation which has been marked by several periods of ice activity, mostly confined to the cirques, the most recent of which is the Little Ice Age (17th-19th centuries). Along the Kivitoo bluffs, this period is marked by the deposition of aeolian sand deposits interbedded with organic layers.

Pheasant and Andrews (1973) suggest that at present, relative sea levels along the east coast of the Cumberland Peninsula are rising. They attribute this recent submergence (begun 1,200 yrs B.P.) to the lowering of the eastern coast of Baffin Island on the distal side of an isostatic forebulge as this moves inward towards the zone of maximum isostatic

depression. As evidence they cite, in addition to the confirmed submergence in the Maritime provinces, the submergence and destruction of Inuit sites by wave action, the blocking of streams by shingle ridges and the covering of vegetation mats by beach depostis. An additional argument is the presence of a 6 m asl wave-cut notch which occurs at several locations in the area which is thought (Pheasant and Andrews 1973) to mark the sea level at isostatic equilibrium.

The evidence for submergence is compelling and is important in a discussion of bluff retreat. However, much of the evidence may be interpreted in a different manner. 'Normal' erosion processes may account for much of the observed coastal retreat, the construction of shingle ridges and the blocking of streams may have more to do with changes in the operation of subareal processes and the action of ice on the beach. The wave-cut notch must also be carefully interpreted for, as Nielson (1979) has shown, this feature may be related more to the quarrying action of the ice foot several meters above sea level than to wave action. Accelerated frost action, due to the effects of sea spray, could also result in increased weathering of the rock some distance above the waterline. In addition, beach ridges 1-3 m asl within the mouth of Narpaing Fiord are being stabilized by lichen and plant cover and overridden by gelifluctin lobes suggesting that this section of the coast is not being submerged.

C. Previous Work on Coastal Bluffs in High Latitude Regions

Over the last decade and a half increased activity along high latitude coasts has led to a renewal of interest in their geomorphology. John and Sudgen (1975) point out that this area of coastal research has largely been neglected in the past, further noting that much of the work which has been done is concerned with raised, rather than contemporary, marine features. This emphasis is understandable in the light of the significance of strandlines as paleoclimatic indicators and guideposts towards glacial chronologies, subjects which have been of primary interest to geomorphologists in high latitude regions. Geomorphological study of coastlines in the eastern Arctic has been more limited than work in the west owing to the more extensive economic development in the latter region over the past 25 years.

Researchers have consistently pointed to the importance of sea and shore fast ice in the morphogenesis of arctic coasts. Ice performs a protective role, reducing both the intensity of wave related processes and the period of the year during which these processes are effective. Arctic coasts are generally considered to be low energy environments (Davies, 1964, 1972; Dolan et al., 1973), even though they may lie within regions subject to intensive storm activity. (The energy regime on the Kivitoo coast is discussed in Chapter II.)

The literature concerned with the development of coastal bluffs in permafrost regions is limited. Much of the work which has been done deals with bedrock erosion forms such as

strandflat and other wave cut features in rock. Studies of coastal bluffs eroded into unconsolidated sediments focus almost exclusively on those which occur along coasts comprised entirely of ice-rich fine-grained tundra materials. Moreover, this work has been broadly descriptive, emphasizing processes of thermal erosion and degradation and rates of bluff retreat. With the exception of Kerfoot (1969), detailed studies of process and form have been lacking. The literature on river bank erosion is, perhaps, more process oriented and is drawn upon here to supplement coastal studies.

Permafrost coasts may undergo dramatic or dramatic appearing retreat when massive ground ice or ice-rich sediments are exposed to the combined action of marine and subareal processes. Observations by Leffingwell (1919) along the coast of the Beaufort Sea suggested rates of retreat as high as 30 m/yr. Lewellen (1970) reported retreat exceeding 10 m/yr east of Point Barrow and Zenkovich (1967) quotes remarkable retrogression on the order of 50-100 m/yr in Northern Siberia. Clearly these are exceptional, and retreat rates on the order of 0-5 m/yr are probably more typical.

The emphasis on ice-rich coastal slopes probably gives an incorrect impression of the rate of retreat of unconsolidated bluffs in permafrost regions in general. Harper (1978) calculated a mean retreat of 0.31 m/yr (1949-1976) for the unconsolidated clays, silts and sands of the Gubik Formation just west of Barrow, Alaska. (Much of the previously published work concerns bluffs developed in this formation.) Mackay (1963), assessing the rates of retreat of coastal bluffs near

Tuktoyaktuk, N.W.T., found that slopes comprised of sand and gravel were retreating at a considerably slower rate than those in finer-grained deposits. In fact, erosion rates along temperate coastlines may be comparable or greater than those along most permafrost coasts. Newbury et al. (1978) found that initial coastal erosion rates following the creation of a reservoir in a permafrost region were less than the rates along shorelines of reservoirs in non-permafrost regions (comparing volume of material eroded). In some cases, permafrost may actually slow down shoreline erosion since the frozen ground must first be thawed in order to free sediment for removal. Once the active layer is stripped, the rate of erosion during a storm surge will depend upon the rate of thaw of the bluff materials. This may be slow if air and sea-water temperature is at or below 0° C. Hartwell (1972) notes that late lying snow may also be a factor in slowing bluff retreat by preventing thermal degradation and protecting the bluff from the attack of waves.

Other previous work on bluff process and morphology is discussed in the course of the text.

D. Objectives

This thesis is, necessarily, a reconnaisance study. The small literature on related slope problems in permafrost combined with the general physiographic and Quaternary stratigraphic bent of previous workers in the field area, provided no clear idea of the range of bluff morphology to be

encountered. In light of this, the initial objective of this research was to present a comprehensive description of the coastal bluffs along the Kivitoo Peninsula and to identify the main processes active in their development. Reconnaisance during the initial field season entailed extensive photographic documentation, including a panorama of the entire study area, slope profiling and local surveys. These provided a descriptive record of a permafrost coastline unique in its detail and range.

From the beginning the emphasis of this research was on the morphology and mechanisms of bluff slope development, viewed in a geotechnical context, rather than the rates at which these processes operate or the rate at which the bluffs are retreating. This approach avoids, to some degree, the problems inherent in process studies where detailed observation over a period of time is required. The necessarily limited period of research presents substantial, though unavoidable, problems in that some of the processes under investigation occur infrequently making direct observation impossible. Still, the second field season, coming five years after the initial field season, provided a worthwhile perspective on the rates of process operation and the relative frequency of geomorphic events.

Once specific areas of interest were identified, a more detailed investigation of relevant processes could be undertaken during the second field season. The data presented here should provide a base for further, more prolonged study of the temporal aspects of bluff slope development in cold regions

in general and at Kivitoo in particular.

E. Organization

After the introduction, in Chapter II, a brief description of the geomorphology of the Kivitoo Peninsula is given in order to 'set the scene' as well as provide some observations on a remote region. This is followed by a description of the three major independent environmental variables in bluff development: climate, erosional environment, and bluff stratigraphy. Chapter III presents some methodological and theoretical considerations. After addressing the problems inherent in slope profile measurement and the extension of the two-dimensional profile into a three dimensional context, a short presentation of basic slope stability analysis is given. The core of the study lies in Chapters IV to VIII, which discuss the form and development of the four major morphological divisions of the Kivitoo bluffs. Chapter VI presents a detailed description and analysis of mass-movement processes on the low-gradient slopes found along the northwestern portion of the Kivitoo coastline.

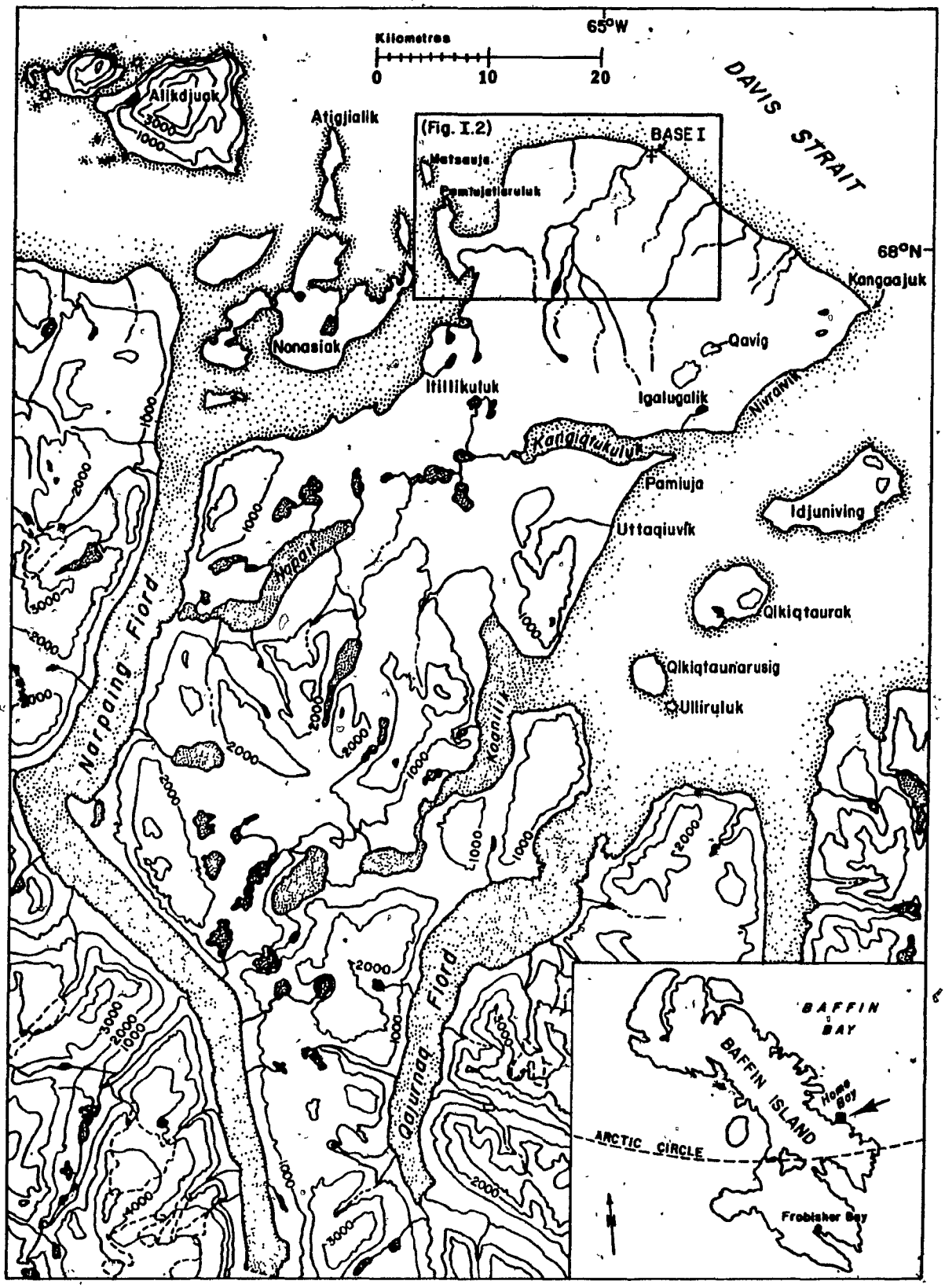


Figure I.1 Place map of the Kivitoo Peninsula, Baffin Island, N.W.T. Inuck place names courtesy Anana and Anilnilk Panniluk, Broughton Island (in Nelson 1980).

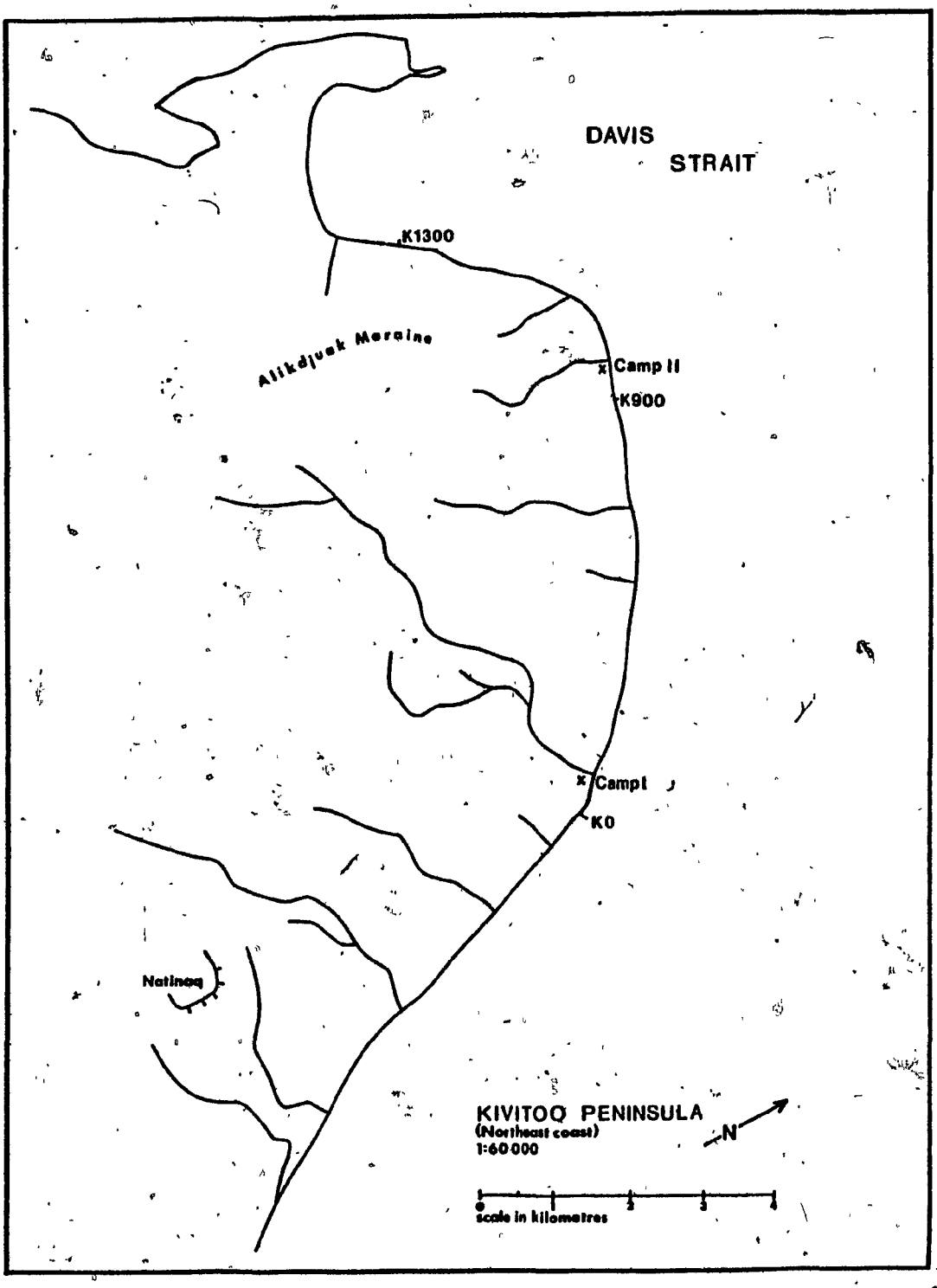


Figure I.2 Field area, Kivitoo Peninsula, Baffin Island, N.W.T. Numbers correspond to numeration of panoramic photographs, Appendix E.



Figure I.3 Partially snow-covered Kivitoo Peninsula, July 5, 1958. Raised marine terrace surface along outer coast is largely free of snow. Camps I and II are marked.



Figure I.4 Oblique tri-metragon imagery of the Kivitoo Peninsula (July 22, 1949). View, looking to the southeast, is of the northwest section of the study area. Pamiujatiaruluk (Figure I.1) is in the immediate foreground.

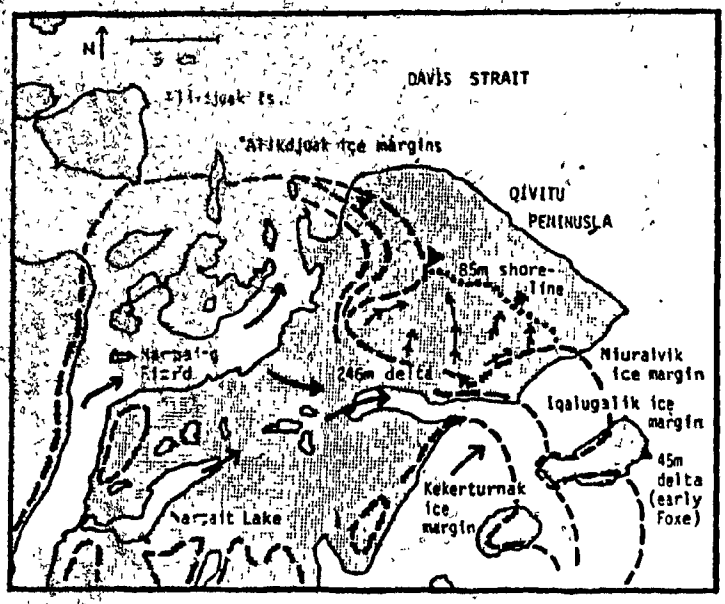


Figure I.5 Mid-Foxe ice margins (ca 60,000 - 80,000 BP). Triangles represent raised deltas deposited during this time. Alikdjuak moraines and proglacial marine delta deposited on the Kivitoo Foreland along the east interior margin of the Narpaing Fiord lobe. Outwash deposited on the central portion of the Foreland between the glacier margin and sea level at 85 m. (Illustration from Nelson 1980.)

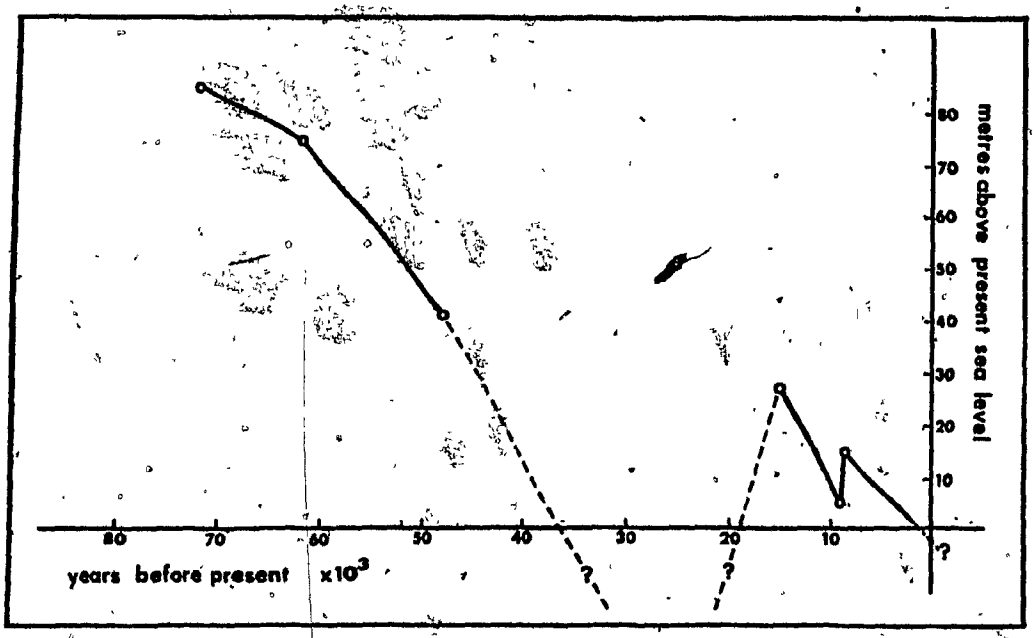


Figure I.6 Relative sea level along the outer coast of the Kivitoo Peninsula from mid-foxe time to the present. (Compiled from data in Pheasant and Andrews 1973; Andrews, Isherwood and Szabo 1975; Nelson 1978.)

CHAPTER II:

PHYSICAL GEOGRAPHY OF THE QIVITU PENINSULA

A. The terrain of the Kivitoo Peninsula

1. Permafrost

Baffin Island lies entirely within the zone of continuous permafrost (Mackay, 1972a; R.J.E. Brown, 1972). The thickness of frozen ground is uncertain but probably ranges from less than 300 m in southern Baffin Island to around 600 m in the high Arctic (Brown, 1972).

Problems arise in the literature since words such as high-ice, ice-rich and thaw-unstable, are used loosely. The terminology used here for description of permafrost, ground ice and frozen soils is defined in Table II.1.

Active layer depths were determined using a metal probe pushed to refusal (Mackay, 1977b) or by excavation. These methods are not thermal so that the frost table is defined as the depth at which ground ice or ice-bonded materials are encountered. For particularly coarse, well-drained active layers and other ice-poor soils, this method may result in an over-estimation of the active layer thickness or an inability to locate the frost table. However, few locations along the Kivitoo bluff slope itself presented this problem.

Active layer thickness on the foreland surface ranges from 30-150 cm depending upon such factors as soil texture, ice

content, surface drainage conditions and insulation by organic materials. Average thickness is 70-90 cm in the moist silty sands or loams most commonly encountered. On steeper, shaded slopes, such as the bluffs, the active layer may be relatively thin, 40-70 cm.

Massive ground ice or ice wedges were not found anywhere along the Kivitoo bluffs. Ice wedges may develop in the wetter interior, but available aerial photography is of too poor a resolution to use to confirm this.

Sand wedge fissures, developed in coarse-grained materials on the terrace surface (particularly in raised beach deposits), are common. These fissures develop low ramparts (5-50 cm high) along a central trough which often forms a surface drainage line. The sand wedge itself is usually slightly finer-grained than the surrounding soils, and is notably more oxidized. Sand wedges may be considered an indicator of arid climatic conditions or well drained permeable materials (e.g. Embleton and King, 1975).

Permafrost occurs beneath the contemporary beach. The thickness of the active layer on the beach is 50-70 cm. Frozen ground may exist off-shore as a relic of bluff retreat (e.g. Mackay, 1972b) and the lower relative sea level during the late Foxe stade which would have exposed extensive areas of the inner shelf to subaerial freezing.

The magnitude of long term variations in the mean active layer thickness is not known. Fluctuations on the order of ten or more centimetres are likely to have occurred in Holocene times.

Where it occurs along the Kivitoo foreland, patterned ground is not well developed. Poorly defined stone nets, comprised of frost-shattered debris, are encountered in wet depressions behind beach ridges where meltwater accumulates and fines are concentrated by slope wash. Mudboils (or non-sorted circles, Washburn, 1973) with centers of brown fine-grained soils are common in wetter areas where the active layer is comprised of materials which are sufficiently fine-grained. The soils in the vicinity of K 900 proved to be very susceptible to such cryostatic convection processes. Interestingly, the mudboils found on the valley side of streams crossing the bluffs in the northwest bring fossil mollusks (from in situ marine units) to the surface.

2. Nivation and Snowpack Distribution

The regional or climatic snowline along the Cumberland Peninsula lies between the glaciation limit and the local cirque glacier equilibrium line (Andrews and Miller 1972). Along the Kivitoo Peninsula, this would place the regional snowline between 900 and 1,000 m. In maritime climates, the topographic snowline is generally 400-500 m below the climatic snowline (Manley 1959). Therefore the highest portions of Kivitoo should lie just below the topographic snowline. In reality, certain areas of the forelands retain perennial snow right down to sea level.

Along the coast, wind keeps the top of the bluffs nearly free of snow. In the interior, thin (< 1 m), areally

extensive, snowpack accumulates. This usually melts by the end of July so that no snow remains on the foreland surface except in a few topographically favorable locations, such as along the slopes of the Alikdjak moraine. Another favored location is in the lee of raised beach ridges where it forms an important local source of the meltwater intercepted at the bluff line. Within the study area, snow is the latest lying along valley sides and in gullies where, during winter, the thicknesses of the snow-drift may be accordant with terrace surface. Drift may be as thick as 10 m in the more deeply incised gullies. Along the larger valleys the snowpack tends to drift in against south and east facing slopes. This preferential distribution probably accounts for the distinctive asymmetry of the larger valleys with their steeper north-facing slopes. Most of the late-lying snow in these locations melts out by the end of August.

The distribution of snowpack is variable along the coast. Along the low bluffs south of Camp I (the 1977 base camp), snow covered the base of the bluff until late August in 1977, and only in a few places did it melt out entirely by the time the field party departed on August 28. Early on, these drifts completely buried low bluffs, forming a snow ramp from the ice foot to the terrace surface. Southeast of Kangeeak Point, deep snowpack completely covered the 15-20 m high bluffs in late August, Figure II.1. The beach at this location, however, was clear of snow and the ice foot by the end of July. At the present time, it is unlikely that these snowpacks ever completely melt out during the summer. This particular section

of the Kivitoo coastline may be termed a névé coast (Zenkovich 1967). Isolated patches of snow persist into late summer in favorable locations along the bluffs north of Camp I, e.g. in the bluff face hollows between K100 and K140.

The areal photograph in Figure I.3 shows the snowpack distribution on July 5, 1958. The outer coast is largely snow free. Gullies are drifted in and prominent beach ridges are outlined by the snowpack. (This is particularly noticable southeast of Camp I.) The rough surface of the colluvial rubble and felsenmeer above the marine limit is seen to have the greatest snow retention.

A qualitative assessment of 1977 and 1983 snow conditions compared with the same time in 1958 (July 5), would suggest that there was more snow in both these years, especially more complete coverage along the outer coast. The sea ice at the mouths of major streams had not yet broken up and snowbanks along these streams were more extensive. These observations are consistent with a climatic deterioration during the past 20 years (Bradley and Miller, 1972), although it is difficult to make meaningful comparisons based on casual observations of three years' snow conditions.

B. Climate

The climate of Baffin Island is fully arctic and although the island is nearly 1,500 km long, remarkably uniform, being characterized by cool, short summers and long, cold winters. Although relative humidity is usually high (greater than 80%,

McGill University, 1963), the low moisture capacity of the cold air makes this region quite arid.

Along the east coast of the Cumberland Peninsula, summers are cool and moist, even though absolute amounts of precipitation are low, generally less than 15 cm water equivalent. The coast is often fog-bound and low altitude temperature inversions, a result of cold water temperatures coupled with a low angle of solar incidence, are common. A regional temperature inversion persists along the coast, at least through July, at the 1,000 to 950 mb level, or approximately 650-1,000 m asl (Bradley 1972).

In summer, the ocean has an important moderating effect on the coastal climate such that, in conjunction with the fog, cloud cover and the 24 hour daylight, diurnal temperature fluctuations are small, usually less than 5°C. The coastal climate is considerably different from that in the fiords and inland mountains. In these locations, without the maritime influence, seasonal and diurnal temperature variations are more pronounced and, although average relative humidity is lower, precipitaiton is relatively high (due to orographic effects). During the particularly cloudless summer of 1977, storms were often noted over the highlands, while the outer coast was clear. On Baffin Island topographic variations in climate tend to be more pronounced than regional variations.

There are no continuous long-term weather observations for Kivitoo Peninsula. The two nearest permanent weather stations, each with about 25 years of record, are at 580 m elevation on Broughton Island, 70 km southeast along the coast and 400 m

elevation at Cape Hooper, 90 km north of Home Bay. Temperature and precipitation data are summarized in Table II.2, compiled by Miller and Bradley (1976) for the years 1961-1970. Application of these weather observations to the study area must be done with caution since the stations may be above the local temperature inversion and local lapse rates tend to be high and variable (0.5-3.0°C/100 m, with an average of 0.75°C, (Andrews and Miller 1972). Mean annual temperatures are -11°C and -11.5°C at Broughton Island and Cape Hooper respectively, with average diurnal temperature changes of 5-6°C at both stations. Average summer (June-July-August) temperatureat Broughton Island for the period 1961 - 1970 was 1.6°C and, at Cape Hooper 2.5°C (average daily maximum temperatures are 5.3°C and 5.0°C respectively; Table II.2. Daily fluctuations of temperature are least from August to October due to the presence of open water along the coast, the influence of which more than offsets the diurnal change which would be expected from variations in solar radiation.

Mean precipitation at Broughton Island is 24.4 cm water equivalent in winter and 6.6 cm in summer. Snow may fall at any time of year, but in summer the bulk of the precipitation falls as rain. Rain can be expected from June through September although rain storms have occurred in May and October. Church et al. (1979) note that rainfall amounts in the Home Bay area are high for the eastern Canadian Arctic in general. Summer rainfall tends to occur as prolonged period of light rain or drizzle. Maximum 24-hour precipitation is of interest because of its potential effects on soil moisture and

soil thawing and, therefore, slope stability. Maximum rainfalls of 2.5-3.5 cm/24-hr have been recorded at both Broughton Island and Cape Hooper. Church et al. (1979) have compiled a distribution and frequency diagram of 24-hour rainfall events at Cape Hooper, Figure II.2. However, during the 1977 field season, the driest on record, no 24-hour falls in excess of 0.2 cm were observed.

Temperature data for the 1977 and 1983 field seasons (June, July, and August) are reproduced in Figure II.3. Initial thawing began in mid-June, although mean daily temperatures above 0°C were common prior to this. In 1977 freeze-back began around August 25-26, when the daily mean temperature dropped below 0°C. July and August, 1977 were also unusually dry: Cape Hooper received only 29% and 33% of normal precipitation in July and August respectively. Maximum daily precipitation was 7.1 mm at Broughton Island on July 16, 1977.

C. The Coastal Environment and Coastal Retreat

The general impression of the Kivitoo coast is that of a low energy shoreline whose morphological characteristics are in large part determined by the infrequent storm event. This is typical of Arctic coasts where the presence of pack and landfast ice throughout most of the year, severely limits the effectiveness of wave action.

1. Pack ice, landfast ice and the ice foot

The Kivitoo coast is ice bound for an average of nine months of the year. Break-up generally begins in early to mid-July with the opening of shore leads and accumulation of surface melt on top of the sea ice. The Ice Atlas of Canada (Swithinbank 1960) indicates that, on average, the first significant open water along the northeastern coast of the Cumberland Peninsula occurs during early mid-August and that scattered ice distribution (10-50% coverage) is attained by late August. Open water may appear early off prominent points of land, such as the Kivitoo Peninsula and Cape Broughton, as portions of the landfast ice break off and join the moving pack. Mitigating attrition of the landfast ice is the deeply embayed coastline and many islands, the latter constituting anchor points for the ice. Open water or scattered pack may persist for two to three months. During freeze-up, sea ice coverage of 50-80% is usually formed by mid to late October with complete coverage by mid to late November (Oceanographic Atlas of the Polar Seas, 1958).

During the summer of 1977 break-up began in mid-July. Following break-up, coverage was dependent upon wind conditions and ranged from broken to scattered ice to open water, often over very short periods of time (<24 hr). At no time during the 1977 field season was the pack out of sight and only on two occasions was coverage within 10 km of the shore less than 20%. Travel along the coast between Kivitoo and Broughton Island was still difficult at the end of August. In the cooler summer of

1983, the ice began to break-up during the second week in July. However ice remained packed in along the shore, at least through mid-August. The few periods of off-shore winds only opened up small shore leads. The persistence of ice off Kivitoo appears to be consistent with the experience of other workers in the region over the past ten years.

Early in the summer an ice foot is present along the entire Kivitoo coast. This is narrow (<5m) and thin (<1m) owing to the steepness of the beach and the limited tidal range. Following the formation of shore leads, a small notch quickly develops along the outer edge of the ice foot leading to collapse and ultimately removal of all but the highest ice. Where drift snow or ice push has significantly increased its thickness, the ice foot may persist for several weeks following break up.

Ice push ridges, Figure II.4, are a common feature along the Kivitoo coast. These are best developed to either side of stream mouths, since it is here that the greatest amount of smaller cobbles and pebbles are available for excavation.

2. Coastal energy regime: Tides, wave action and storm surges

Observed tidal range along the Kivitoo coast was on the order of 1.0-1.5 m and was diurnal. McGill University (1963) reports tidal fluctuations of 1.2 m in Home Bay, increasing both to the north and south. Since the slope of the beach ranges from 12° to less than 5° (depending upon sediment size) the horizontal extent of tidal action is limited to 5-17 m,

with a mode of 5-7 m.

Few observations of wave action or storm surges along the east coast of Baffin Island are available. According to the Oceanographic Atlas of the Polar Seas (1958), swell greater than 1.5 m in height occurs in Baffin Bay off the northeast coast of the Cumberland Peninsula during less than 10% of the period of open water.

The nearest wind records are from Clyde River to the north and Cape Dyer to the south. These data show that, at both locations, northwesterly winds prevail and are also the strongest: yearly mean velocity of 17.3 km/hr compared with an all-direction mean velocity of 10.6 km/hr (compiled by P. Drake from Monthly Record 1955-1972). Maximum recorded wind velocity at Clyde River for the open water period from September to November, is 19.8 km/hr.

Figure II.5 presents the generalized bathymetry off the Kivitoo Peninsula. The direction of greatest fetch is to the northeast and east with no obstruction across the width of Baffin Bay and Davis Strait.

During 1977 field season, no waves greater than about 0.3 m in height were observed and nowhere did the sea ever reach the base of the bluffs. In 1983, persistent near-shore ice effectively eliminated all wave action during the field season. Yet, undercutting of bluff slopes, rapid removal of finer sediment to below the low tide line, slumped-over storm ridges and large pieces of driftwood well above the high tide line attest to the occurrence of effective storm events. At one location a tree trunk about 10 m long was deposited in a stream

mouth 25 m from (ca 3 m above) the high tide line.

3. Coastal Retreat

Although determination of the rate of bluff retreat was not a feasible objective of this research, several general observations can be made. Resurvey, in 1977, of bluff top survey lines set out by J.B. Bird in 1976 show no unequivocal retreat of the top of the bluff over the period of one year. Remeasurement of the Survey Lines in 1983, likewise, indicated little retreat of the bluff top, except at the head of the larger hollows which carried substantial surface run-off. One hollow along Survey Line IV had retreated by more than 10 m. However, the mode of retreat here was not undercutting or flattening of the bluff slope, but rather the predominantly fluvial processes of gully (drainage net) extension. Reexamination of photographs of the bluff face from 1976 to 1983 (such as Figures V.5a - 5c), likewise indicate few dramatic changes besides minor basal trimming and removal of loose sediments. The importance of wave action in bluff retreat is nonetheless obvious. Nearly all of the coast parallel slopes along the outer coast are undercut; the regrading mechanisms, however, appear to operate rather slowly, with what is apparently a prolonged lag time between basal undercutting and knick-line response. Thus retreat of the top of the bluff following an undercutting event may take several years or longer. That the bluffs are, in fact, retreating is demonstrated by such evidence as the intersection, by the bluff

edge, of old stone circles (two locations) and the oblique transection of valley sides. The average rate of coastal retreat is certainly less than 1 m/yr. Retreat rates are probably greatest along the low bluffs south of base camp due, simply, to their lower height and therefore the smaller amount of sediment it is necessary to remove for a similar rate of bluff retreat. In any case, the rapid rates of coastal retreat observed along fine-grained tundra coasts do not occur at Kivitoo.

4. Long term variations in erosion intensity

Since sea ice plays a major role in regulating the efficacy of wave action, long term variations may be expected to affect the intensity of marine erosion. King (1969) and John and Sugden (1971) have cited changes in pack ice density to account for periods of beach formation and wave cutting indicated in the raised marine morphological record. Based on these assumptions, McGhee (1972) has suggested greater amounts of open water along the Baffin coast between 1100 and 800 BP. Periods of warmer weather and presumably more prolonged open water also occurred ca 4000 BP (Dekin, 1972; Barry et al., 1977; McGhee and Tuck, 1976) and from 4600-3600 BP (Nichols, 1967). Following the Little Ice Age, the early portion of this century was marked by a warming trend. However, by 1914 observations in Home Bay and off Kivitoo indicated that closed pack still lay off the coast as late as September 12. It is important to remember that since pack ice reforms each year,

response to short-term climatic changes is immediate (Barry et al., 1977). Also, the relationship between temperature and pack ice persistence may be complex, as warming can result in increased snowfall and therefore thicker and longer lasting ice cover.

D. Stratigraphy and Character of the Kivitoo Bluff Sediments.

The stratigraphic framework of the Kivitoo Bluffs used here is based on the work of Nelson (1978, 1981). An earlier reconnaisance of the bluff stratigraphy has been published by Anderson, Isherwood and Szabo (1975) and brief reference to the coastal lithology is given by Pheasant and Andrews (1973).

Fifty-four stratigraphic sections, of which forty-one fall within the present study area, were described by Nelson (1978) emphasizing sediment texture, color, type of stratification and fossil occurrence. Nelson's entire stratigraphy is reproduced in Appendix C and section locations are marked on the photographic panorama. Textural classification is based largely on field determinations with selected samples analyzed in the laboratory. Qualitative evaluations of plasticity were noted by Nelson (pers. comm., 1977) for many units. One surprising outcome of Nelson's laboratory analysis is the unexpectedly high clay-sized particle content of many of the units, which may be in excess of 25%. While this is not unusual for glacial sediments, which would be expected to contain large amounts of rock flour, it was not predicted by field determinations using standard criteria of plasticity and

stickiness. Due to the abundance of rock flour, as opposed to clay minerals, many of the finer-grained units have lower liquid limits and plasticity indices than their textural parameters would seem to indicate (see Table VI.2). Also consistent with such sediments are the high residual internal friction angles, $\phi' > 32°$, determined in laboratory shear tests (Smalley, 1971).

Lateral correlation between individual stratigraphic sections is difficult due to cut and fill, local mass wasting, erosional unconformities, and rapid facies changes. Fossils collected for amino acid analysis proved to be a valuable tool in the tracing of stratigraphic units, as was the biostratigraphic work done by Fehling-Hanson (unpublished).

Nelson groups the lithology of the Kivitoo bluffs into six major lithofacies, 'A' through 'E', and one biofacies, 'W'. He points out that many facies are gradational and that the boundaries between them are therefore somewhat subjective. Table II.3 reproduces Nelson's classification along with representative textural and sedimentary parameters. Brief mention of representative ice contents for each facies is made below. These refer to the ice content of the active layer and may not be representative of the ice content of the permafrost. In some instances, where stripping of surficial sediments has occurred, the soil at the frost table may be previously unthawed permafrost. In most locations, however, the sediments at the frost table may have been exposed to thawing previously, and their ice content is not necessarily that of the underlying permafrost. For the purposes of this study, in which the

genetic interpretation of each facies is not of the first concern, the term 'facies' is often replaced by 'unit' when referring to specific occurrences in the bluffs.

Facies A is comprised of gravelly and coarse sand units and may include cobble and boulder beds. Texturally, this facies ranges from predominantly cobbles and boulders to medium to coarse sand grading into the interbedded sand and gravel of facies B1. Nelson interprets these as high energy marine and beach deposits, although some may have been formed by reworking of older beach and glacio-marine sediments. Frozen in situ sediments have relatively low ice contents, generally less than 10% (field estimation) and are only weakly cemented. In some locations however, the sediments may be ice cemented with larger water contents. As these units generally contain no significant fine particles, ice lens formation is uncommon.

Facies B sediments are mostly well-sorted sands containing little coarser material, although this may be present as gravel and pebble lenses. Many units display planar bedding. Nelson suggests that facies B sediments were laid down in a nearshore environment but that some may be proximal glacio-marine or glacio- fluvial in origin. Ice content of facies B units is variable, ranging from less than 15% to over 30% in the finer sands. Ice lenses are usually absent, most of the ice existing as pore ice. However, the fine and very fine sands may show substantial ice lens formation. When frozen these sediments are well cemented.

Nelson defines facies C as being comprised of alternating beds of predominantly sandy sediment with up to 35% silt and a

small fraction of pebbles and cobbles. These beds may range from thin laminations to layers over 50 cm thick. The poorly-sorted nature of these units, their relatively low clay-size fraction and extensive lateral variation and irregular bedding, suggest a proximal glacio-marine genesis. Gradational contacts between facies C and adjacent facies are typical. Nelson also notes that mottling is often found near the top and bottom of these units.

Ice content of facies C sediment is variable. As would be expected, those units with a significant silt fraction have well developed horizontal ice lenses (to several cm thick), and water content in excess of 40% are not uncommon. A rough estimate of average ice content would be 30-40%.

Facies D units are typically fine-grained and massive. Texturally, facies D ranges from sandy silt, clayey silt and loamy sediment to silty clay and clay. Nelson's criteria stipulates non-stratified units with greater than 35% silt and clay. An average textural composition would be % sand/silt/clay = 20/40/30, although some samples had clay-sized particle contents as high as 68% (Nelson 1981). The fine-grained and massive nature of these sediments indicates a distal glacio-marine or deep marine origin.

The ice content of these sediments is also highly variable. In general, frozen water content is slightly less than that of Facies C units. Ice is often present in the form of thin ice partings arranged in a three-dimensional cellular network rather than the horizontal lenses of facies C units. The cryogenic structure of these sediments has important

implications for slope stability and is examined in detail in Chapter VI.

Nelson includes within facies E, diamictons with greater than 25% pebbles, cobbles and boulders. Matrix texture ranges from poorly sorted sand to silty clay. These deposits, despite their till-like appearance, are classified as inner distal glacio-marine deposits, although some units may have been created by the illuviation of fines into coarser textured sediments or by cryoturbation. Units are typically thin, <1 m. Facies E sediments appear densely packed (and till-like), a function of their wide range of grain sizes, although no in situ bulk density values are available. Ice content is again variable, but where ice lenses occur, may be as high as 60%.

Facies W is gradational with facies B and D, but is distinguished by the abundance of mollusk shells and unabraded fragments. These units are generally well sorted fine sand and silty sand and are recognized by a distinctive green-grey colour. Facies O are organic units, mostly peat interbedded with sand and silt and were probably deposited in an inter-tidal or supra-tidal environment behind beach ridges.

TABLE II.1

GLOSSARY OF PERMAFROST TERMINOLOGY

Active layer
: The thickness of surficial soil which each year thaws and refreezes.

Ice-rich or high ice content soils
: Soils which have frozen water contents in excess of those expected for the soil in a normally consolidated, saturated state. Synonymous with 'excess ice' (French, 1975).

Ice-poor or low ice content soils
: Soils with frozen water contents below those of the saturated, normally consolidated soil.

Ice partings or veins
: Any planer or lenticular clear ice inclusion, whether oriented horizontally or vertically.

Granular ice
: Coarse, usually rounded and weakly bonded ice crystals.

Pore ice
: Ice which fills the soil voids without significant segregation or bulking of the soil.

Reticulate, cellular or ataxic ice
: Clear ice arranged in a three dimensional structure of more or less normally oriented partins.

Ice-bonded
: Soil held strongly together in the frozen state but lacking ice lenses or other forms of segregated ice. Also referred to as ice-cemented.

Thaw-unstable soils
: Soils which, upon thawing, undergo significant loss of strength leading to mobilization under the influence of gravity (Linell and Kaplar, 1966).

TABLE II.2

SUMMARY OF WEATHER RECORDS FOR BROUGHTON ISLAND and CAPE HOOPER FOR THE YEARS 1961 to 1970 (from Miller and Bradley 1976)

Cape Hooper (400 m)

	Jan.	Feb.	Mar.	Apr.	May	June	July	Aug.	Sept.	Oct.	Nov.	Dec.	Annual
Average daily maximum temperature (°C)	−22	−23	−21	−14	−5	2	8	5	0	−6	−13	−19	−9
Average daily minimum temperature (°C)	−28	−28	−27	−20	−10	−3	2	1	−3	−9	−18	−24	−14
Extreme maximum temperature (°C) (14 year record)	−2	−1	−2	1	11	18	19	17	13	5	2	3	19
Extreme minimum temperature (°C) (14 year record)	−41	−39	−41	−34	−28	−9	−7	−6	−12	−25	−26	−41	−41
Number of days with frost	31	28	29	30	31	27	13	19	27	31	30	31	327
Greatest precipitation in 24 hours (centimetres)	2.3	2.2	1.6	2.3	1.9	3.3	2.0	2.6	1.9	2.5	2.4	2.3	3.3
Number of days with measurable precipitation	4	6	3	5	8	6	5	8	10	10	9	6	80

Broughton Island (580 m)

	Jan.	Feb.	Mar.	Apr.	May	June	July	Aug.	Sept.	Oct.	Nov.	Dec.	Annual
Average daily maximum temperature (°C)	−21	−22	−20	−14	−4	2	8	6	0	−6	−12	−19	−8
Average daily minimum temperature (°C)	−27	−28	−27	−20	−10	−3	2	1	−4	−10	−18	−24	−14
Extreme maximum temperature (°C) (12 year record)	0	2	−2	6	7	15	18	18	14	7	3	5	18
Extreme minimum temperature (°C) (13 year record)	−42	−40	−39	−33	−28	−12	−6	−6	−12	−21	−31	−37	−42
Number of days with frost	31	28	31	30	31	27	12	16	27	31	30	31	325
Greatest precipitation in 24 hours (centimetres)	3.2	1.4	0.7	2.3	2.0	3.6	1.0	2.6	3.3	3.8	3.3	2.2	3.8
Number of days with measurable precipitation	4	5	3	4	10	7	4	5	10	11	8	5	76

TABLE II.3

FACIES CLASSIFICATION
for sediments of the Kivitoo Peninsula
(From Nelson 1978)

Subfacies	Texture, stratification and other features*
Facies A (gravel)	>30% pkb (pebbles, cobbles & boulders), <5% silt & clay, well to semi-stratified
A1	>90% kb
A2	15-50% kb
A3	<15% kb
Facies B (sand)	<5% clay, well to semi-stratified
B1	sand and gravel, interbedded
B2	sand with gravel lenses
B3	f-v cos, 10-25% p
B4	m-v cos, <10% p, parallel and wavy bedded
B5	f-ms, <2% p, parallel bedded
B6	f-ms, <2% p, wavy bedded
B7	vf-fs, <2% p, parallel bedded
B8	vf-fs, <2% p, wavy bedded
B9	vf-ms, <2% p, convoluted, flow structures
B10	vf-ms, <2% p, deformed and/or faulted beds
B11	vf-ms, <2% p, planar cross-stratified
B12	vf-ms, <2% p, trough cross-stratified
B13	vf-cos, <25% p, non-stratified
Facies C (alternating sands and silts)	<25% pkb, well-semi-stratified
C1	parallel to wavy laminated (beds <1cm thick)
C2	parallel to wavy interbedded (beds >1cm)
C3	flaser bedding (beds <3cm)
C4	uneven bed thickness(>3cm), mostly continuous bedding
C5	irregular bed thickness, discontinuous bedding
C6	>25% pkb, irregular bed thickness, discontinuous bedding
C7	vf-cos, uneven bed thickness, discontinuous beds
Facies D (massive, sandy, silts and clays)	>30% silt & clay, <25% pkb
D1	<10% pkb
D2	10-25% pkb
D3	strong angular blocky structure
D1-F	vesicular structure - upper part of fragipan soil horizon?
Facies E (diamicton)	>25% pkb, >15% silt and clay, non-stratified
E1	<50% sand
E2	>50% sand
Facies W (greenish-gray silts and sands)	<2% pkb, 2.5Y or 5Y hues, unabraded macrofossils common
W1	<5% clay, <35% silt, well stratified
W2	>5% clay, >30% silt, non-stratified
Facies O (organic-rich sediments)	%organics > 0.5%, value <3

*Characteristics of main facies apply to all subfacies unless otherwise indicated



Figure II.1 Névé-type coast west of Kangaajuk (Kangeeak Point) in late July, 1977. Snowpack is probably perennial. View is southwest towards the head of Quajurnaq Fiord.



Figure II.4 View southeast along coast in the vicinity of the stream at K900. Well developed ice-push ridges are clearly evident. Note also the well-sorted nature of the cobbles which form them. Broken pack conditions prevail near the shore (mid-July, 1977).

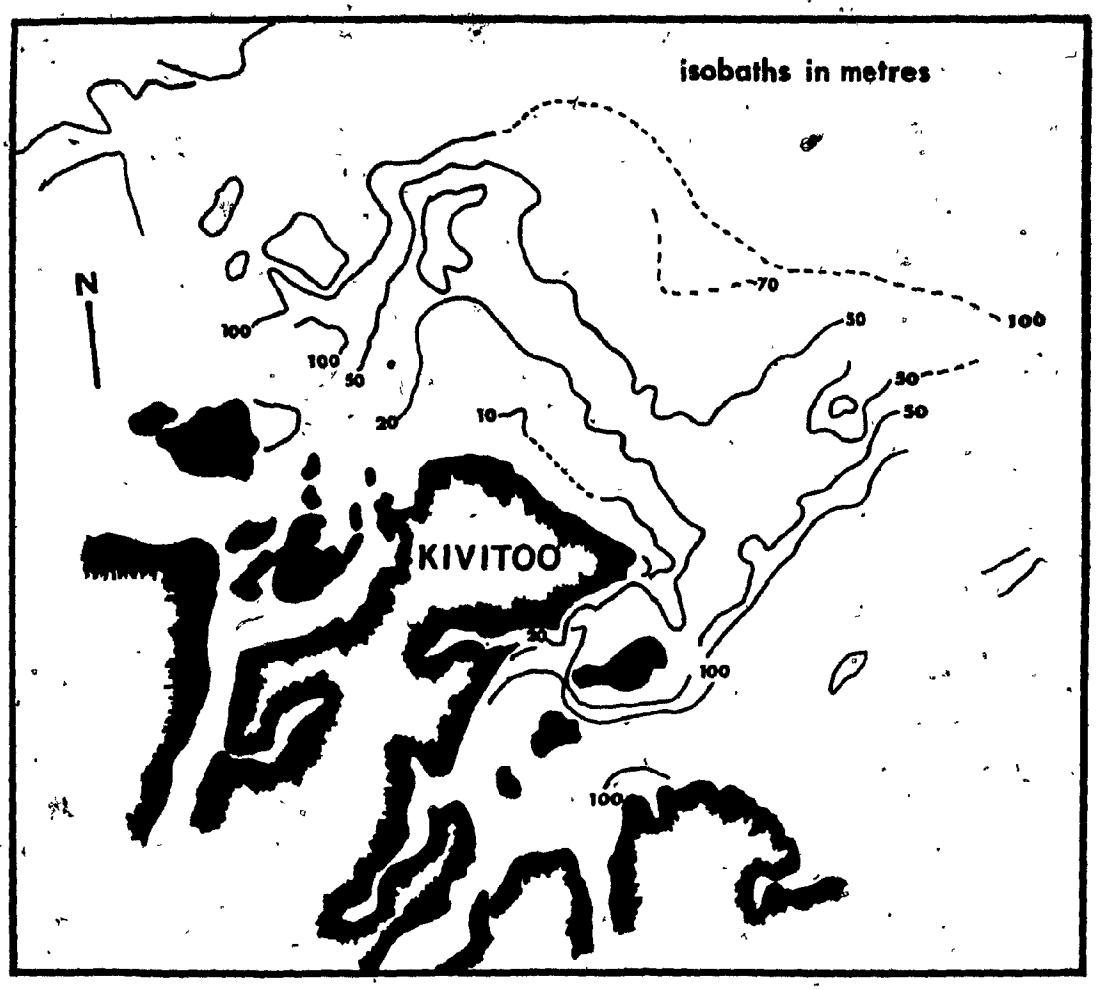


Figure II.5 Generalized bathymetry off the coast of the Kivitoo Peninsula. Note the small deltaic 'bulge' in the 10 m isobath seaward of the mouth of the major stream on which Camp I was situated.

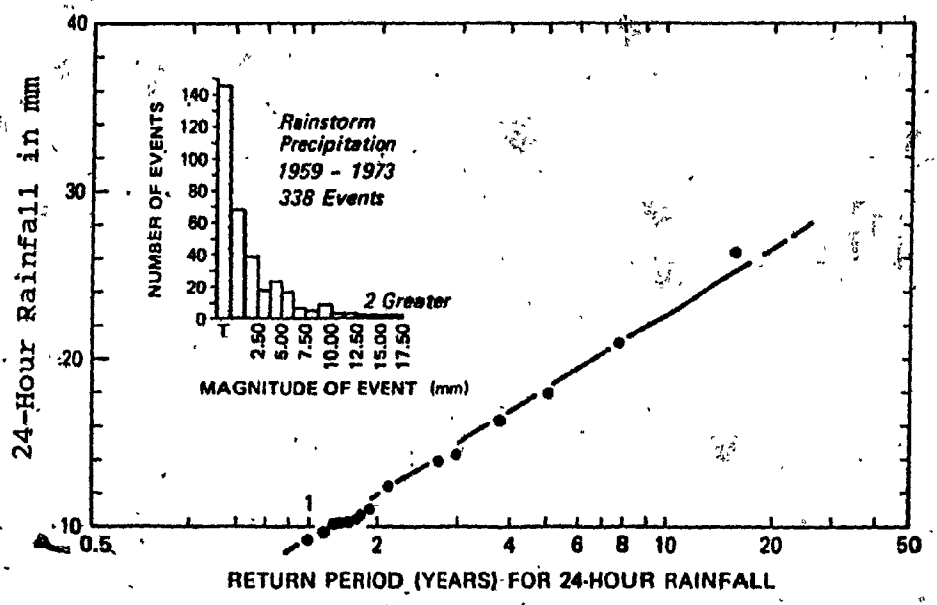
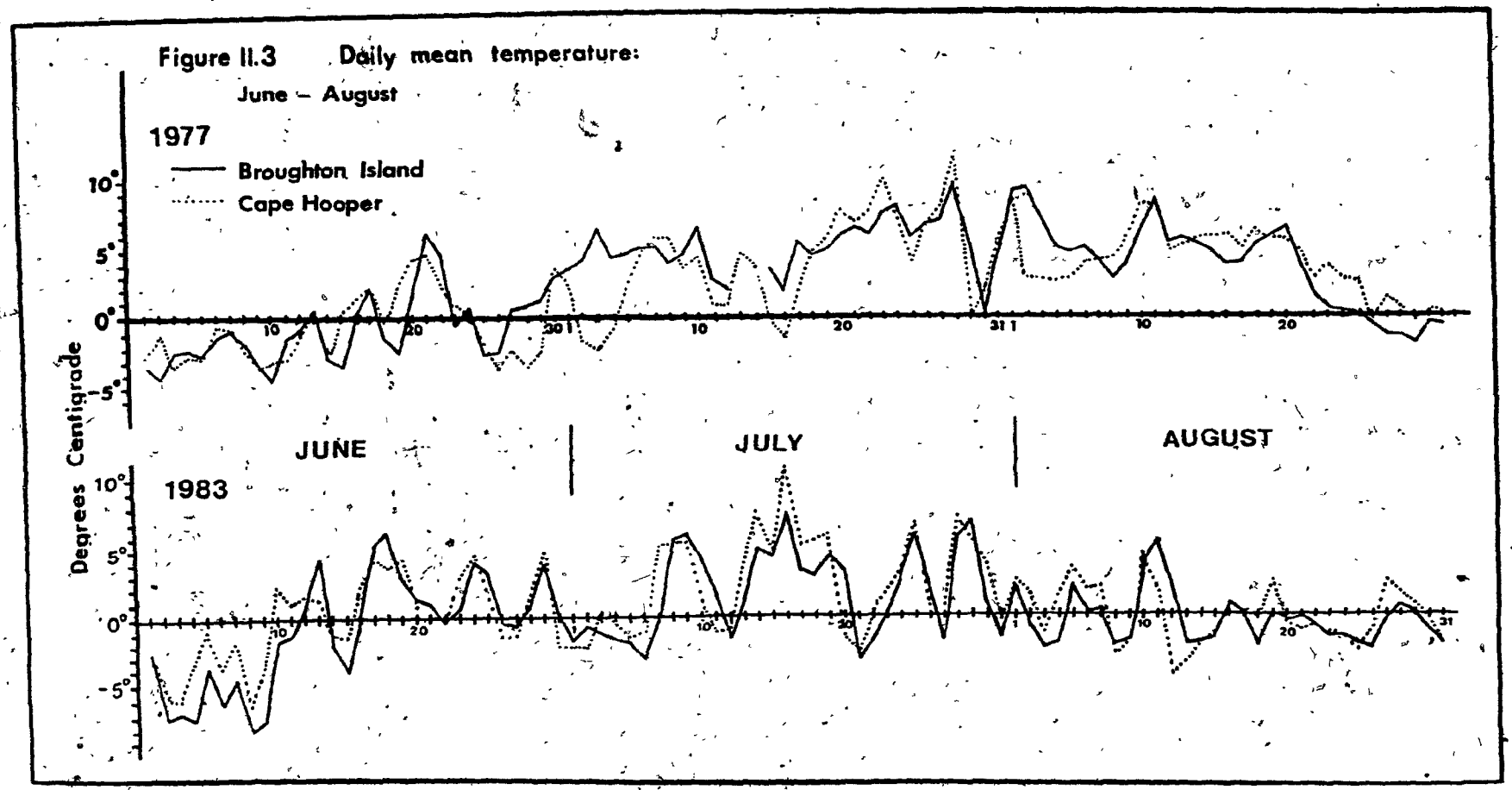


Figure II.2 Intensity, distribution and recurrence interval of 24-hour storm rainfall events at Cape Hooper (80 km north of Kivitoo) for the period 1959-1973. (From Church et al, 1979.)


Figure II.3 Daily mean temperature:
June – August
1977
Broughton Island
Cape Hooper
10°
5°
0°
-5°
JUNE
JULY
AUGUST
1983
Degrees Centigrade
10
20
30
1
10
20
31
1
10
20
10
20
1
10
20
31

CHAPTER III:

FIELD METHODS AND THEORETICAL BACKGROUND

The principal unit of investigation used in this study is the slope profile and its extension, the coastal zone transect, which includes the bluff slope, the topography inland from the edge of the bluff, the beach and nearshore profile (although the latter was unobtainable).

The term 'bluff' is preferred over 'cliff' as used by Nelson (1980) and others as cliff implies a steep slope along which in situ sediment or bedrock is exposed, and along which debris does not accumulate. The surface inland from the top of the top of the bluff is refered to as the 'terrace' since it is in fact a raised marine terrace surface (Nelson, 1978; Pheasant and Andrews, 1973), mantled by beach sediments deposited during transgressive - regressive episodes. The crest of the bluff, at the point where the bluff face meets the the terrace, is also referred to as the knick-line. Particularly steep portions of the bluff face, along which in situ sediments are exposed, are sometimes referred to as scarp slopes or facets.

Several terms are also applied to a discussion of the plan form of the bluffs. A 'planar' section of the bluff face is one which is straight in plan, with contours running parallel to the beach. The term 'coast-parallel' is also used to refer to such a slope. 'Contour curvature' is used to denote deviations from the planar or coast-parallel trend of the bluff face. For example, concave contour curvature indicates a

hollow or embayment along the bluff face, whereas convex contour curvature refers to a nose or spur.

A. Methods of Field Investigation and Data Collection

Field investigation involved bluff profiling, local surveys of the terrace edge, and more detailed mapping of selected individual bluff sections and slope features.

The photographic panorama in Appendix C is the main reference for this study. This has been marked off in centimetres, beginning just southeast of Camp I and stretching northwest to the end of the bluffs (within the mouth of Narpaing Fiord; see also Fig. I.2). The scale refers only to distances as measured along the photographs themselves and is not consistently scaled with respect to actual distances since the distance of the photo base to the shoreline varies. All references to the panorama in the text are prefixed by 'K'; for example, Camp I is located at K62. The separate photographs are fitted together so that the bluff base is continuous. Parallax affects the more distant topography so that, along bluff sections where the top of the bluff is set back from the beach, there may be considerable duplication of background features between adjacent photographs. To compensate for this, a line has been drawn connecting a point at the top of the bluff with the same point in the following picture. Along the steep bluffs the duplication of distant features is not as apparent. For further aid in location of areas of interest named reference points include Base Camp I at K62 and Camp II

at K980.

Bluff profiles were made from the high tide line which was functionally identified as the line of oxidation present on the beach, the limit of foam and flotsam occurrence, or the point at which interstitial fines significantly increased within the coarser beach matrix. The profiles continue to a point on the terrace just inland of the knick-line (usually 10-30 m). This latter distance was increased if it appeared that the terrace surface was very irregular or unusually steep. The inland extent of the profiles was rarely more than 50 m.

Profiles were made using a 50 m tape, a stadia rod marked off at eye level, and an Abney level. Since the same Abney level was used for all measurements and was subject to rigorous abuse, it was regularly checked by backsighting techniques. For short or very steep slopes, where Abney level measurements were difficult to make, a Brunton compass placed on a metre long board was employed.

Slope profiling in the field is necessarily a subjective activity and has been the subject of some debate in the literature. Much of this argument centers around whether a standard segment length should be used (e.g. Young, 1971) or if a slope is best represented by a series of segments of variable lengths defined by the recognition of breaks and changes of slope. Slopes which were notably concave and convex were, in the present work, dealt with by increasing the number of slope measurements (for example, Brunsden and Jones, 1972) or recording the inclination of a chord joining the upslope and

downslope ends of the convexity or concavity, and adding supplemental notation of the unit's curvature using symbols such as Savigear's (1965).

In this study the slope segment length was variable depending upon the complexity of the slope profile. A segment was functionally defined as the angle and distance between recognizable breaks or changes of slope. Where long straight segments occurred a standard length, usually of 5, 10 or 20 m, was used. Slopes appearing to be broadly convex or concave were similarly surveyed using a standard length. Where the rounded section was short a single measurement was taken and the type of curvature noted.

B. Bluff Dissection

Carson and Kirkby (1972) recognized that contour curvature will effect slope processes and development, mainly through the convergence or divergence of water and sediment flow lines. Where the effects of contour curvature are important along-slope or downslope variations in process type and rates may produce slope features or form-elements characterized by a particular grouping of slope processes and forms. (The term 'form-element' is Strahler's (1950a,b).) The drainage basin, which is for all intents and purposes the primary unit of non-coastal landscapes (Derbyshire et al., 1979) may be considered as the large scale expression of such a form-element (Hack and Goodlet, 1960). Similar form-elements at a smaller scale are the erosion cells recognized by Tam (1975). Carson

(1976) has discussed the development of form-elements:

> If ... movements (of debris) show preferential development in certain parts (laterally) of the hillside slope, the retreating slope surface will display a distinctly three-dimensional character, e.g. rockwall chutes and talus cones in high altitude areas (Rapp, 1960; Luckman, 1971) and combes cut into coastal clay cliffs (Brunsden and Jones, 1972). Indeed it should be emphasized that slope development is not entirely a matter of slope profile development but also a reflection of the rate of abolition of side slopes by the growth of hollows and noses.

Slope dissection is a useful concept in a discussion of the Kivitoo bluffs. Dissection can be considered as an extension of the concept of contour curvature and can be used to refer to contour curvature on a somewhat smaller scale where the initial linearity or planar form of the bluff plan is being disrupted by the laterally different rates of operation of process. Bluffs which display little contour curvature and have an unbroken coast parallel (planar) knick-line and bluff face -- except where crossed by established steams or gullies -- are referred to as 'undissected'. Where localized contour curvature is pronounced breaking the linearity of the knick-line and bluff face, the bluff may be said to be 'dissected'. The preceeding terms refer only to dissection by non-fluvial, mass wasting, processes. Fluvial dissection is (as is pointed out in Chapter V) considered to be a separate, though not necessarily unrelated, process. As shown below, mass-wasting and small scale fluvial processes may be mutually interdependent in the development of some of the Kivitoo bluff features. However, while fluvial dissection may be locally

important (for example, where streams exit onto the beach), it is not considered to be a primary shaper of the morphology of the Kivitoo bluffs.

C. Slope Stability Analysis

The stability of natural slopes with respect to shallow translational failure has been sucessfully considered using an infinite slope stability analysis (Skempton and DeLory, 1957; Carson and Petley, 1970). As this analysis is referred to extensively in Chapters IV to VIII, its formulation below serves as a useful prologue to the following text.

The condition of limiting stability will occur along a potential failure plane, such as A - A' in Figure III.1, when

$$S = T \qquad \text{(III.1)}$$

where S is the shear strength resisting sliding and T is the shear stress acting to promote sliding.

The shear stress along A - A' is defined as

$$T = \gamma D \cos i \sin i \qquad \text{(III.2)}$$

where γ is the total bulk unit weight of the soil, D is the depth of the potential failure surface and i is the slope angle.

The shear strength along A - A' is given by Mohr-Coulomb criteria as

$$S' = c' + \sigma' \tan\phi' \qquad \text{(III.3)}$$

where c' is the cohesion intercept and $\tan\phi'$ is the relevant angle of internal friction, both with respect to effective stresses (Skempton and Bishop, 1950), and σ' is the effective normal stress or that part of the normal stress effective in mobilizing friction. For the long term stability of a slope the relevant ϕ' may be taken as ϕ'_r, the residual friction angle (Skempton and DeLorey 1957; Hutchinson 1967).

Studies have shown that the presence of water under pressure in the soil voids will reduce the force (via buoyancy) that can be mobilized against displacement. Therefore it is appropriate to define shear strength in terms of the effective normal stress, σ', rather than the total normal stress, σ. The effective normal stress is defined by

$$\sigma' = \sigma - u \qquad \text{(III.4)}$$

where σ is the total normal stress on the failure surface and u is the pore fluid pressure. The total normal stress is given by

$$\sigma = \gamma D \cos^2 i \qquad \text{(III.5)}$$

Substituting Eq. III.5 in Eq. III.3 (and assuming a cohesionless soil; c = 0)

$$S' = [\ (\gamma D \cos^2 i) - u\ ] \tan\phi' \qquad \text{(III.6)}$$

The pore pressure (in the normal case where the pore fluid is water and flow is parallel to the slope) is given by

$$u = \gamma_w dl \cos^2 i \qquad \text{(III.7)}$$

where γ_w is the unit weight of water and dl is the height of the water table above the potential failure surface.

Substituting Eq. III.7 in Eq. III.6

$$S' = (\gamma D - \gamma_w dl) \cos^2 i \tan \phi' \qquad \text{(III.8)}$$

Now, applying a balance of forces as in Eq. III,1, but substituting Eq. III.2 and Eq. III.8

$$\tan i = \frac{\gamma D - \gamma_w dl}{\gamma D} \tan \phi' \qquad \text{(III.9)}$$

If the ratio of the thickness of the phreatic zone (dl) to the depth of the potential failure plane (D) is defined as 'm', where

$$m = \frac{dl}{dl+d2} = \frac{dl}{D} \qquad \text{(III.10)}$$

Then, substituting Eq. III.10 into Eq. III.9 gives

$$\tan i = 1 - \frac{m \cdot \gamma_w}{\gamma} \tan\phi' \qquad \text{(III.11)}$$

For the limiting case where the entire thickness of the soil above the failure plane is dry (m = 0), the pore pressure at the failure plane is zero (u = 0) and

$$\tan i = \tan\phi' \qquad \text{(III.12)}$$

If the water table is at the surface (i.e. m = 1) and flow is parallel to the slope then, in many cases, where γ is approximately $2\gamma_w$,

$$\tan i = 1/2 \tan\phi' \qquad \text{(III.13)}$$

Equations III.12 and III.13 have been shown to identify many slope stability thresholds in nature (Carson 1971). These limiting slope gradients have been called the frictional (Eq. III.12) and semi-frictional (Eq. III.13) threshold slopes.

It must be stressed that this analysis assumes a soil mass which is thin relative to the areal extent of the failure, minimal side and end friction or passive restraint downslope, and a planar shear surface. Evidence has shown these assumptions to be reasonable when considering many different thin, cohesionless regoliths (e.g. Carson, 1975; Chandler, 1972, 1973; Hutchinson, 1969). As some of the landslides encountered along the Kivitoo bluff slopes are small, the effects of side friction or passive restraint downslope must be considered as likely (e.g. Chandler, 1972).

D. Introduction To The Morphological Divisions Of the Kivitoo Bluffs: Chapers IV, V, VII and VIII.

The division of the Kivitoo bluffs into morphological units is based upon the recognition of geographically discrete groupings of specific slope types and bluff features. After several weeks in the field it became evident that the bluff morphology could be usefully represented by four distinctive morphological types. These formed a regular geographic sequence along the coast, with only one morphological division significantly expressed at two locations within the study area. The morphology of the bluffs south of Camp II is rather complex, but may be viewed as being transitional in nature, complicated (morphologically) by the fact that here the coast is cutting back onto an old valley side which obliquely intersects the bluff.

It must be emphasized that, while the four recognized morphological divisions are distinctive, there is, in reality, a continuum of form which exists between these divisions. Thus their exact delimitation is, to a degree, artificial and necessarily idealized. Features which define one morphological division may grade into other features which, when fully expressed, define a different morphological division. It is believed, however, that the best developed features within any one morphological division define distinctive morphological entities, which can be explained by real differences in bluff stratigraphy, erosional environment and local hydrological conditions.

The four major morphological divisions are defined and discussed in the following chapters are: (1) The planar debris-mantled bluffs, Chapter IV; (2) The steep dissected bluffs, Chapter V; (3) The bluffs with debris-bowls, Chapter VII and (4) The benched bluffs, Chapter VIII. The distribution of these bluff types within the study area is shown in Figure III.2. A fifth type of bluff morphology, the neve coast, where the bluff is perennially covered by drift snow may be recognized (and has already been mentioned; Figure II.1). Owing to the limited occurrence of this bluff type, the difficulty involved its study, and the remoteness of these bluffs from the base camp they were not the subject of detailed study.

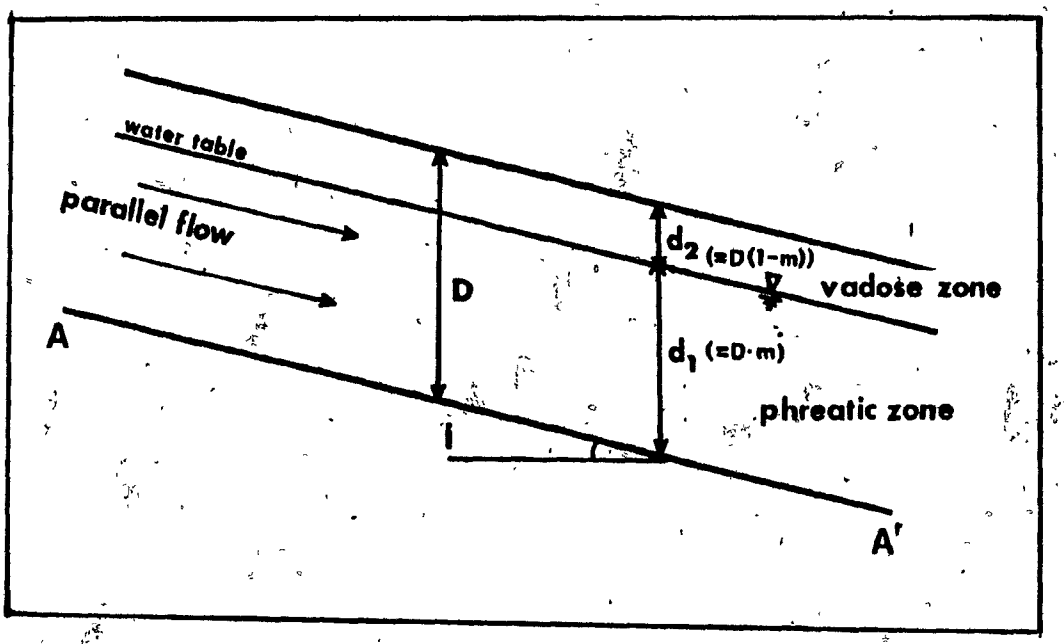


Figure III.1 Analysis of the stability of an infinite slope failure. A-A' represents the potential failure plane. D is the depth from the surface to A-A' and d1 is the thickness of the phreatic zone. Numerical analysis and further explanation of diagram in text.

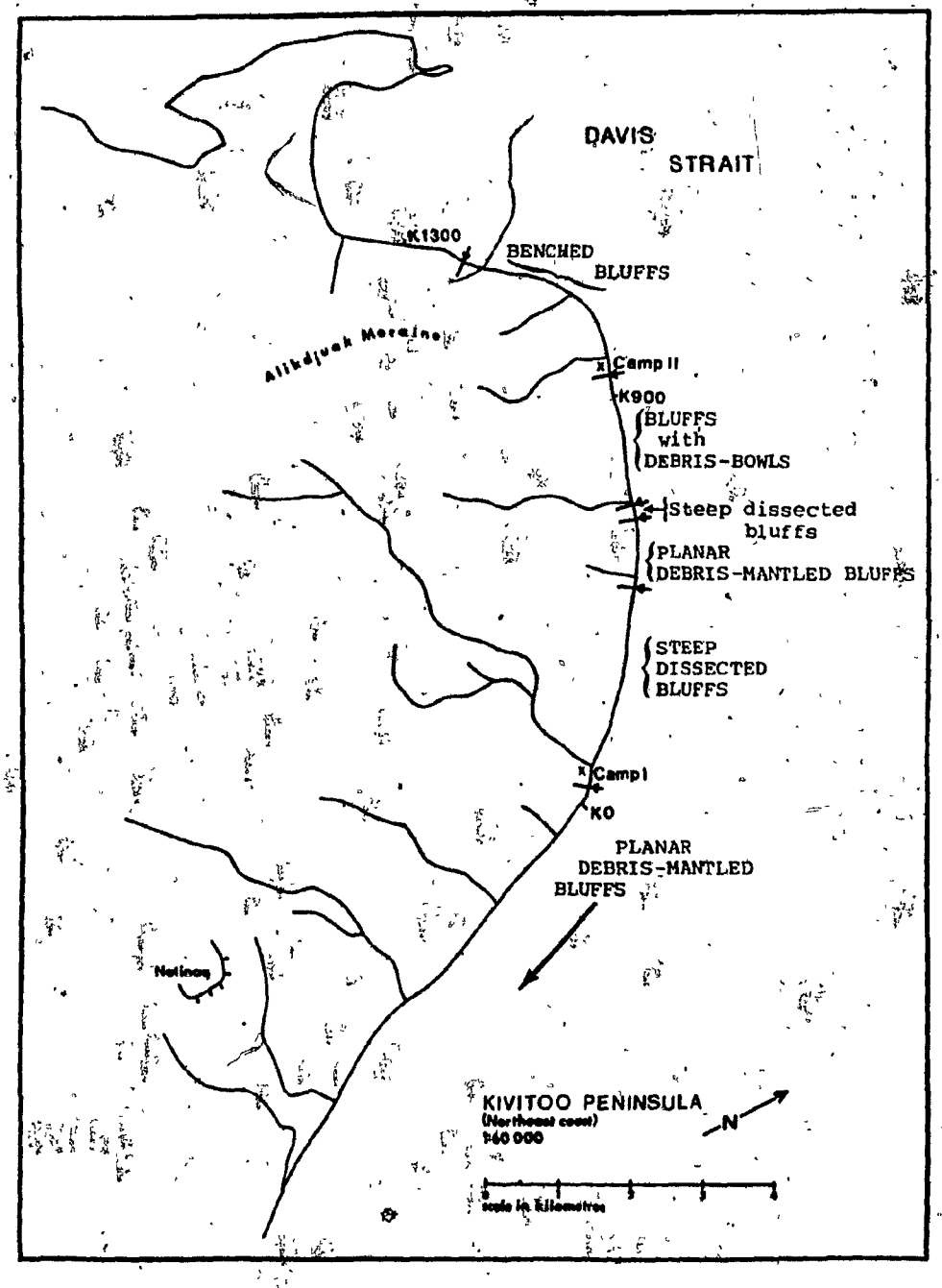


Figure III.2 Distribution of bluff types within the Kivitoo study area.

CHAPTER IV:

THE PLANAR DEBRIS-MANTLED BLUFFS

Straight slopes, mantled by a veneer of coarse debris and topped by an undissected linear knick-line (except where crossed by gullies) form the predominant bluff morphology southeast of K32 extending south to Kageeak Point at the mouth of Quajon Fiord; Figures IV.1 and IV.2. Similar bluffs are found between K415 and K650, being best developed from K550 to K600. These bluff sections are characterized by low bluffs (less than 15 m, and generally below 10 m tall) which contain, in the upper part of the stratigraphic section, a relatively thick coarse-grained sedimentary unit. The planar debris-mantled bluffs differ from the bluffs to the northwest of Camp I in their lack of free-face segments and other pronounced profile irregularities and in their regular planar, coast-parallel plan which is a result of the lack of contour curvature and dissection along the bluff knick-line.

A. Stratigraphy

The typical stratigraphic section along the debris-mantled bluffs consists of an upper thick, coarse-grained unit comprised of sandy gravel to gravelly sands (facies A), underlain by fine to medium sands (facies B) and silty sands (facies C). Fine-grained units (facies D) are, for the most part, absent from the stratigraphy along the debris-mantled bluffs. The sediments which make up the coarse-grained units

are derived from beach or other 'high-energy' marine deposits. The coarse-grained cap unit is typically 2-4 m thick, but may be as thick as 6 m (Sec. 48-49). These coarse-grained cap units therefore occupy from 15% to 65% of the bluff height, with a mean value of 30%.

Where present, the underlying frozen silty sands (facies C) typically have high ice contents and may be a source of groundwater flow through, and seepage along, the bluff slope. Excess water contents of 10-30% were obtained for three frozen samples following a procedure outlined by French (1975). Ice content of these sediments, by weight, ranges from less than 30% to over 60%.

Stratigraphic sections found along portions of the debris-mantled bluffs include sections 50-53 to 39-19 southeast of Camp I and sections 25-42 to 19-8 between K415 and K650; Appendix C.

B. Terrace Morphology

The terrace surface above the debris-mantled bluffs is formed from the raised beach deposits (sand and gravel units) which cap the stratigraphic section along them. These paleo-shorelines are distinctive in their coarse-grained and well-drained xeric surfaces, lack of vascular vegetation and extremely subdued micro-relief. The raised beach deposits, occurring along bluffs less than 15 m in height, are also the most recent sediments which form the terrace surface along the Kivitoo Bluffs. Raised beach ridges 0.5 to 3 m in height are

often found 50 to 150 m inland from the bluff edge. These ridges may occur singly or in small series. Sparsely distributed large boulders mark the seaward edge of the beach ridges, presumably moved to this location by the action of the sea ice. Seaward of the beach ridges a smooth, gently sloping (less than 2°) boulder-free raised foreshore, Figure IV.3, is found. A shallow depression, which may collect meltwater, is usually present in front of and running parallel to the beach ridges, probably representing a former, poorly defined, longshore trough. Figure IV.4 is a schematic representation of a typical portion of the terrace surface along the debris-mantled bluffs. Representative profiles across the bluff and terrace surface at points 1 km southeast of Camp I (along Survey Line VII) and at K565 (along Survey Line VIII) are reproduced in Figure IV.5.

Due to the coarseness of the raised beach deposits, the terrace surface is highly permeable. (While no in situ infiltration or hydraulic conductivity tests could be made, observation showed that water poured onto the terrace surface would infiltrate the surface without a noticable lag. (The hydraulic conductivity of similar materials is on the order of $10 - 10^{-3}$ cm/sec; e.g. Lambe and Whitman, 1969.) Rapid drainage of water from the ground behind the bluffs is enhanced by the rapid and deep penetration of the frost table during initial thaw. Active layer depths of over 1.5 m were observed in early July. Desiccation and drainage of the surface deposits prior to freeze-back in autumn could leave a soil which is freely draining even while frozen.

Sand 'seeps' (deposits of fine sand eroded from within the terrace active layer) are commonly found seaward of raised beach ridges. This internal erosion of finer sediments is effected by groundwater, the source of which is the snowmelt which often accumulates behind the raised beach ridges. The drop in elevation between the front and back of the beach ridges provides the requisite differential head, resulting in flow out of the slope at the seaward edge of the ridge. Silt/fine sand 'seeps', comprised of finer and better-sorted materials than the local active layer, have been noted by Chandler (1972) along similar raised beach deposits in Vestspitzbergen.

Movement of fine soil particles through the active layer by groundwater (suffusion) is probably common in raised beach deposits in permafrost regions. Taylor (1980) noted an increase in sand content from 10% to 22% going from the surface to the frost table on contemporary gravel beaches on Somerset Island. He attributes this to the illuviation of finer-grained particles suggesting that sand may be 'further transported downslope by subsurface rills'. (Winnowing by wind may also be responsible for the creation of a surficial lag deposit.) The deep active layer in these freely draining gentle raised foreshore slopes would seem to be conducive to such processes.

Soil pits excavated on the terrace at K10, 20 m from the edge of the bluff, showed the active layer to be comprised of oxidized gravel to coarse sand. A typical soil profile will grade downward from oxidized coarse sand with approximately 10% gravel to a coarse stony gravel with an admixture of pebbles

and cobbles at a shallow depth (30-50 cm). This downward coarsening of material may represent a former wave-cut platform, veneered by a lag deposit overlain by finer foreshore deposits. In many locations groundwater was encountered within the active layer, often flowing into the pits making further excavation difficult.

A conspicuous feature found along the bluffs just southeast of Survey Line I was deposits of oxidized coarse sand, up to 50 cm thick, overlying snow-drifts at the base of the bluffs, Figure IV.6. Similar 'sediment fans' were also noted along low coastal bluffs south of Quajon Fiord.

While two of these deposits were clearly associated with fresh-appearing short, shallow (less than 50 cm deep), flat bottomed, dendritic channels on the terrace surface, a third deposit (marked C in figure IV.6) was not associated with any such surface feature. Internal erosion (piping) of the active layer is a possible genesis for this deposit. Supporting this genetic interpretation, strong water flow was observed emerging from the bluff face at the intersection of the snow and bluff slope at C (Figure IV.6). At the time of observation, the flow carried no sediment. Emergent flow was also noticed just upslope of the snow/bluff contact along Survey Line III. The deposits do not contain any large pebbles or cobbles, though these larger clasts are found on the terrace and bluff slope. There did not appear to be any significant difference in the texture of the sediments in the three deposits, although no sediment samples were taken for laboratory analysis. Sand fans, due to subsurface erosion, may be common along permafrost

bluffs developed in coarse-grained sediments, although no reports of similar features could be found in the literature.

Sand wedges (such as those visible in Figure IV.3, many of which are bordered by low (less than 50 cm high) ramparts, are common features of the terrace surface. These often function as drainage lines bringing water to the bluff edge. Gullies which intersect the bluff can be seen retrogressing onto these fissures as in Figure IV.7. Along the debris-mantled bluffs gully development may begin as a series of small collapse pits (such as those shown in Figure VI.8) strung-out along subsurface drainage lines coalesce, creating a subareal gully along the path of the former pipe (e.g. Tuckfield, 1964; Mosley, 1972).

The raised beach deposits described above were deposited at the end of the most recent marine transgressive-regressive cycle (approximately 7,000 BP) the upper limit of which is placed at 15 +/- 2 m (Nelson, 1980). The terrace morphology developed on these surfaces is therefore found on bluffs whose crests are below the 15 m elevation. Some of the lower bluffs are not topped by the freely draining, raised forebeach deposits due either to retreat of the local bluff line inland of the facies (as in Figure VI.15, below), or masking of the deposits by aeolian deposition or in-washing of fines (discussed in Chapter V). Elsewhere at Kivitoo, the bluff crest lies above 15 m and the bluff-line is cutting back onto different terrace surface types.

C. The Bluff Slope

A typical view along the debris-mantled bluffs south of Camp I is shown in Figure IV.9. Representative bluff profiles, reproduced in Figure IV.10, show that these are straight (or rectilinear) slopes. In the photographs the planar, undissected plan of the bluffs is clearly seen. The knick-line is sharply defined and thin gravel and pebble lines (lag surfaces atop old beach deposits) are being exposed in situ near the top of the bluff. The smooth, uniform nature of the coarse-grained debris-mantle which forms the slope surface is also evident in the photographs. Rounded, rill-like micro-relief, produced by small 'runs' of granular materials down the bluff face, is commonly encountered. Contour curvature along the bluff face is insignificant so that sediment and ground water flow lines tend to remain straight and evenly spaced from the knick-line to the slope base. Large-scale instability appears to be limited along these bluffs, the primary mechanism of slope regrading in response to undercutting being small avalanches of dry, granular debris. Where larger landslides do occur, the scars are rapidly infilled with coarse debris derived from above and the small hollow created by the slide is effectively obscured.

The texture of the debris-mantle, which is derived from dry avalanching of the cap unit, ranges from gravelly coarse sand to medium - coarse sand with up to 20% pebbles. (Figure IV.11 reproduces representative grain size curves.) As noted above, in the case of the surface deposits, the hydraulic

conductivity of such materials is typically very high (10 to 10^{-3} cm/sec; Lambe and Whitman, 1969). The thickness of the colluvial veneer ranges from 0 cm at the top of the bluff to less than 40 cm in the vicinity of the slope mid-point (as in Figure IV.12) and tends to thin towards the slope base due to the removal of the active layer by wave action and/or regrading of the underlying colluvium (discussed below). Figure IV.12 is a photograph of an excavation of the bluff regolith just northwest of profile A-1. The excavation is approximately 7 m asl at the level of a thin clayey unit (facies W, Section 39-19). The texture of the active layer grades downward from the coarse-grained debris mantle to medium to fine sand and loamy soil just above the frost table, which lies at a depth of 65 cm.

Twenty slope profiles along Survey Line III were made by sighting from the knick-line to the base, a procedure considered adequate in view of the low height of the bluffs (in this case below 4 m) and the lack of conspicuous changes in slope angle along the profiles. The mean slope angle was 33° with a very narrow range of 32° to 34° and a standard deviation of 0.75°. These gradients are consistent with reported inclinations of undercut slopes, developed in similar loose granular materials, which have since been abandoned and allowed to regrade (Sharpe 1966; Rahn 1969).

To determine the particular mechanical properties of the debris-mantle, and the relationship between these properties and the natural slopes, a sample of coarse sand (grain size data in Figure IV.11) was taken from the upper 10 cm of the

bluff slope along Survey Line III. Tilting box experiments were performed following a procedure outlined by Carson (1977a). The sediment was placed in a box 15 cm wide and 40 cm long with one side constructed of Plexiglas. The ratio of box width to the diameter of the largest particle was greater than 30, thereby minimizing the effects of side friction. The sediment was shaped into a smooth slope at one end of the box and the slope surface marked on the Plexiglas by a straight line. The box was then tilted until avalanching occurred creating a new slope. The angle of this newly created slope, as well as the present angle of the previously marked slope (i.e. the angle of the original slope at the inclination at which it failed), was recorded. Following Allen (1969) and Carrigy (1970), the latter measurement is the angle of initial yield, ϕ_i, for the particular soil, while the inclination of the new slope is equal to the angle of rest, ϕ_{rest}. In discussing the semantics surrounding the usage of the term 'angle of repose', Carson (1977a) concluded that ϕ_{rest} -- 'the angle of rest after avalanching has occurred in a ... tilting box' -- is, for large avalanches and when measured at a suitable distance from the effects of sidewall friction, equal to ϕ_{rep}, the angle of repose (as measured by cone accumulation). (For conventianal purposes, since ϕ_{rep} is widely used it will be retained in the discussion to follow.) Angles of initial failure, ϕ_i, would be expected to vary depending upon the degree of particle interlocking, and therefore the conditions under which the initial slope was shaped and tamped.

The results of the tests, presented in Appendix A, show

that angles of initial failure (ϕ_i) range from 45° for well-tamped material to 38° for more loosely-formed slopes. The ϕ_i values define the steepest slope which the material, in a specific state of packing, can maintain. The angle of repose (ϕ_{rep}) was 34° with a small standard deveiation of 0.8°. Test results are in reasonable agreement with the inclinations of the natural slopes and it is concluded that the debris-mantled bluffs do indeed stand at the angle of repose of the colluvial mantle and are therefore formed via dry avalanching of the debris-mantle which has, in turn, been derived from the cap unit. Thus, these slopes are, in effect, talus slopes, with the regolith being derived not from a free face, but an upper cap unit which itself stands at the angle of repose of its constituent materials. The slightly higher repose angle obtained in the laboratory -- 34° versus the natural angle of 33° -- is not considered significant and may be a consequence of scale (small size of the test slope as compared with the natural slope) or the relatively good sorting of the sample.

Because the thickness of the colluvial debris-mantle is zero at the knick-line, the conformity of the upper portions of the bluff profile to the rectilinearity of the entire slope means that the top-most sediments almost instantaneously assume their repose angle rather than remaining at a higher friction angle. This would also account for the rapid infilling of slide scars and 'smoothing out' of an undercut base.

The general resistance of the debris-mantled bluffs to slope flattening and dissection at the knick-line arises from the infrequency of positive pore water pressure occurrence

(relative to the rate of undercutting) within the highly permeable, freely draining debris-mantle and cap deposits. Positive pore pressures, if they occur, would result in a decrease of the effective stresses within the regolith. Since the slopes are already standing at the angle of repose ($i=\phi_{rep}$), any further reduction in regolith strength should result in slope failure and ultimately regrading to a lower equilibrium angle. Such lower slope gradients are infrequently encountered. (It should be noted here that ϕ_{rep} is the relevant friction angle to use in Equation III.12. The angle of repose is often slightly less than ϕ'_r, the residual angle of internal friction. Since ϕ_{rep} may be slightly less than ϕ'_r, the value of m in Equation III.11 (i.e. the thickness of the phreatic zone relative to the thickness of the potential slide mass) may have some small value before slope failure will occur.)

In sum, the effect of the coarse sediment mantle is to provide a freely draining surcharge which reduces (to insignificace) the thickness of the phreatic zone above any potential failure plane. Restated in terms of the infinite slope stability analysis (Eq. III.11), the ratio (m) of the height of the water table above the potential failure plane to the total regolith thickness is seldom greater than zero. The stable slope angle, i, therefore approaches ϕ_{rep}. This analysis, outlined in Figure VI.13, assumes that the potential failure plane lies in the vicinity of the frost table and that the thickness of the phreatic zone (dl) is kept small in relation to the total regolith thickness by the the effective surcharge drainage provided by the debris-mantle.

In addition to their large hydraulic conductivity, the low ice content and deep thaw penetration within the terrace deposits and debris-mantle, further reduces the probability of thick phreatic zone development (relative to the total active layer thickness) providing an additional check against positive pore pressure build up.

The use of a gravel fill blanket for the stabilization of thawing slopes has been suggested by Lane (1948: 283). He noted that "Nature's remedy" for the stabilization of "frost-sloughing" slopes was to create "a more pervious surface layer as from soil creep carrying down a pervious soil from a cap deposit." Lane felt "that the value of a pervious cover comes from its weight consolidating the melting soil below back to its normal density and shear strength and from its drainage ability, removing excess water expelled by such consolidation." Pufahl and Morganstern (1979) have provided a more analytical discussion of the value of a freely-draining gravel surcharge in the stabilization of thawing slopes. Their analysis assumes pore pressure conditions that result from a combination of steady state seepage, thaw-consolidation (see Chapter VI) due to self weight loading of the thawing soil, and the additional pore water pressure generated as a result of the added weight of the surcharge load itself. The surcharge load was found to increase the effective normal stress on a potential failure surface by an amount that offset any increase in total pore pressure which is a direct result of the transfer of some portion of the added weight of the fill to the interstitial melt-water. While the thaw-consolidation process may be

effective in generating positive pore pressures along certain portions of the debris-mantled bluffs, the debris mantle appears able, in most cases, to mitigate the effects of any small phreatic zone which may arise in this manner.

In contrast to the general stability of the debris-mantled bluffs, larger slope failures, such as that shown in Figure IV.14, do occur, particularly along the taller debris-mantled bluffs where numerous non-plastic finer-grained (silty sand to fine sand) units are present. Such slopes occur just south of Camp I and between K415 and K650. These taller slopes may represent a limiting case, where the cap unit is just sufficiently thick to provide a surcharge which inhibits most, but not all, potential failure. The ice content of the finer-grained units is typically 40-60%. The water content of the slide debris is in the range 10-15% and post-failure movement takes the form of limited flowage. This difference in water content and the lack of a clay sized fraction suggests that movement is associated with liquefaction/saturated grain flow (see Chapter VI.G), rather than true debris flow. This is borne out not only by the limited displacement of the debris but by its apparent resistance to remobilization following undercutting at the toe and the film of water flowing over the surface of the fresh debris. Thes water film is thought to be supplied, in part, by the expulsion of pore-water associated with grain settlement. The high ice content of the local sediments suggests that the instability noted here can occur independently of water supply from the terrace, though the ultimate source of the ground ice (whether seepage from the

terrace or thawing of permafrost) is not known. High ice contents (up to 40%) in some frozen coarse-grained materials (clearly not frost susceptible) suggest that refreezing of seepage within existing pore spaces may be an important meltwater source.

If the processes which lead to slope flattening operate preferentially along the bluff face and the initial failure retrogresses upslope to intersect the knick-line, then dissection of the slope crest would result. The resistance of the debris-mantled bluffs to slope dissection initiated by preferential failure along the slope is inhibited by rapid back-filling of any slide scars, such as those just discussed, by the coarse debris-mantle. This in-filling may render portions of the bluff with old slide scars relatively stable due to the increased thickness of coarse fill.

The effectiveness of the debris-mantle and beach cap in stabalizing and preventing dissection of the bluff slopes is seen dramatically in Figure IV.15. At this location (K35) the bluff edge cuts obliquely across a beach ridge. In front of the ridge (to the left in the photograph), the terrace surface is developed on a thick, coarse-grained, and permeable, forebeach deposit. Behind the beach ridge the surface has greater micro-topographic irregularity, a finer textured soil and a better developed vegetation cover. Thus, along the bluffs to the right in the photograph, there is no thick, coarse-grained source unit from which to derive a debris-mantle. The stratigraphy along both bluff sections (which includes numerous thin, ice-rich, fine-grained units) is

similar except for this lack of a thick beach cap unit along the bluffs to the right.

The bluff slope below the coarse sand and gravel capped sections is relatively straight with a sharp, well defined knick-line and stands at the angle of repose of the debris-mantle. The only conspicuous signs of instability are small, localized sediment flows at the slope base. The slope on the right, however, shows marked instability. Sections of the bluff slope have gradients as low as 26°. There is also considerable rill development and the knick-line is not sharply defined but displays some profile convexity (due to slope wash and creep processes) and dissection. Small sediment flows are ubiquitous along the bluff slope, building a small debris 'apron' behind the ice-push ridges on the beach at the slope base.

(The rilled, lower-angled section discussed above is, along with a similar stretch of the bluff northwest of Camp I, a unique but apparently minor, bluff type which occurs nowhere else. This bluff type grades into the dissected bluff morphology discussed in the following chapter. These particular bluff sections therefore appear to be transitional in nature, the peculiar morphology being a result of the presence of fine-grained units, high surface run-off, and low over-all bluff height as well as the absence of the coarse-grained cap unit.)

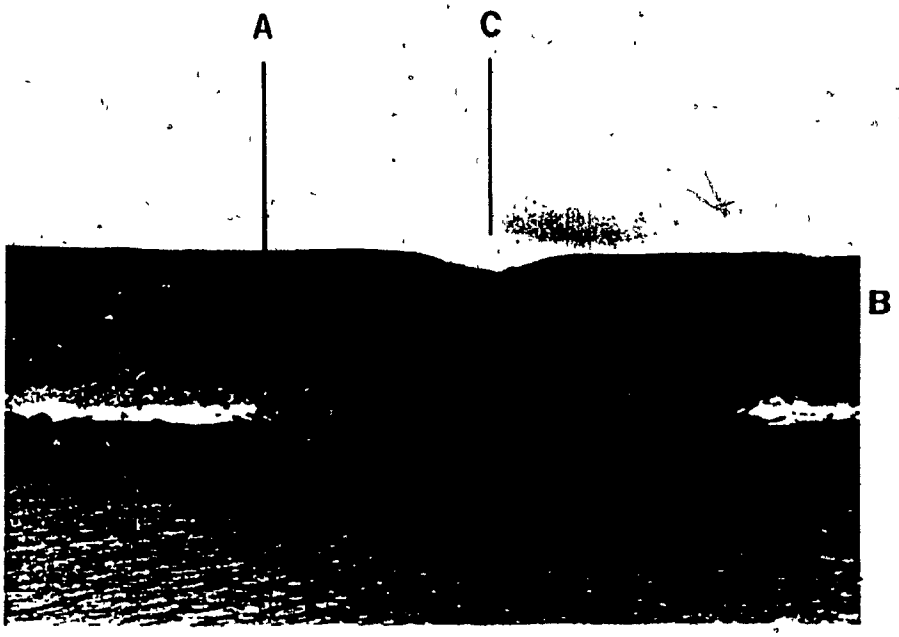


Figure IV.1 Planar debris-mantled bluffs just southeast of Camp I (ca K30) showing the undissected linear knick-line, coarse-grained colluvial mantle, cobble and pebble lines (A) and minor instability associated with the development of a perched phreatic zone at the level of a thin clay unit (B). Incipient gully crosses the bluff line at C.

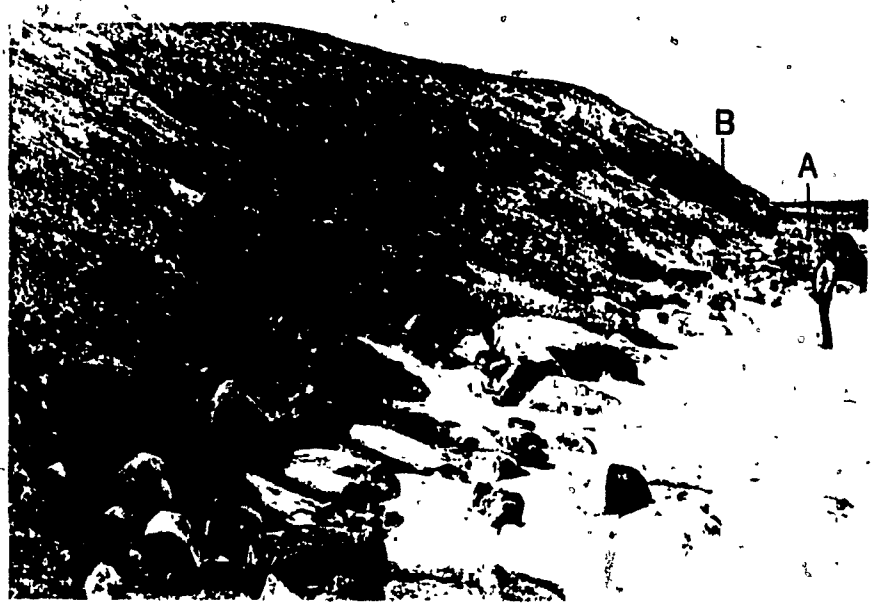


Figure IV.2 View northwest along a tall section of the debris-mantled bluffs. The large rock in the background (A) is located at K5 on the bluff panorama (Appendix C). Small debris flows occur at the slope base due to basal trimming and the presence of ice-rich finer-grained sediments at this level. Overall, however, the bluff slope is straight and covered by a variable thickness of coarse sediment derived from the cap unit. The mid-bluff break in slope, visible in the background (B), occurs in response to a local thickening of an ice-rich fine-grained unit and local slope steepening by basal trimming. This break may, over time, be 'smoothed out' by avalancing of debris from above.



Figure IV.2 View northwest along a tall section of the debris-mantled bluffs. The large rock in the background (A) is located at K5 on the bluff panorama (Appendix C). Small debris flows occur at the slope base due to basal trimming and the presence of ice-rich finer-grained sediments at this level. Overall, however, the bluff slope is straight and covered by a variable thickness of coarse sediment derived from the cap unit. The mid-bluff break in slope, visible in the background (B), occurs in response to a local thickening of an ice-rich fine-grained unit and local slope steepening by basal trimming. This break may, over time, be 'smoothed out' by avalancing of debris from above.



Figure IV.3 Raised marine terrace surface along Survey Line III (Appendix C). This section of the terrace is shown schematically in Figure IV.4. Raised beach ridge is marked by line of ice-pushed boulders (A). Seaward of the beach ridge is a wet depression (B) which is a source for melt water feeding a small gully system (C). Surface slope near the knick-line is 0°-2° seaward (see profiles in Figure IV.5). Sand wedge fissures are marked with an 'x'.

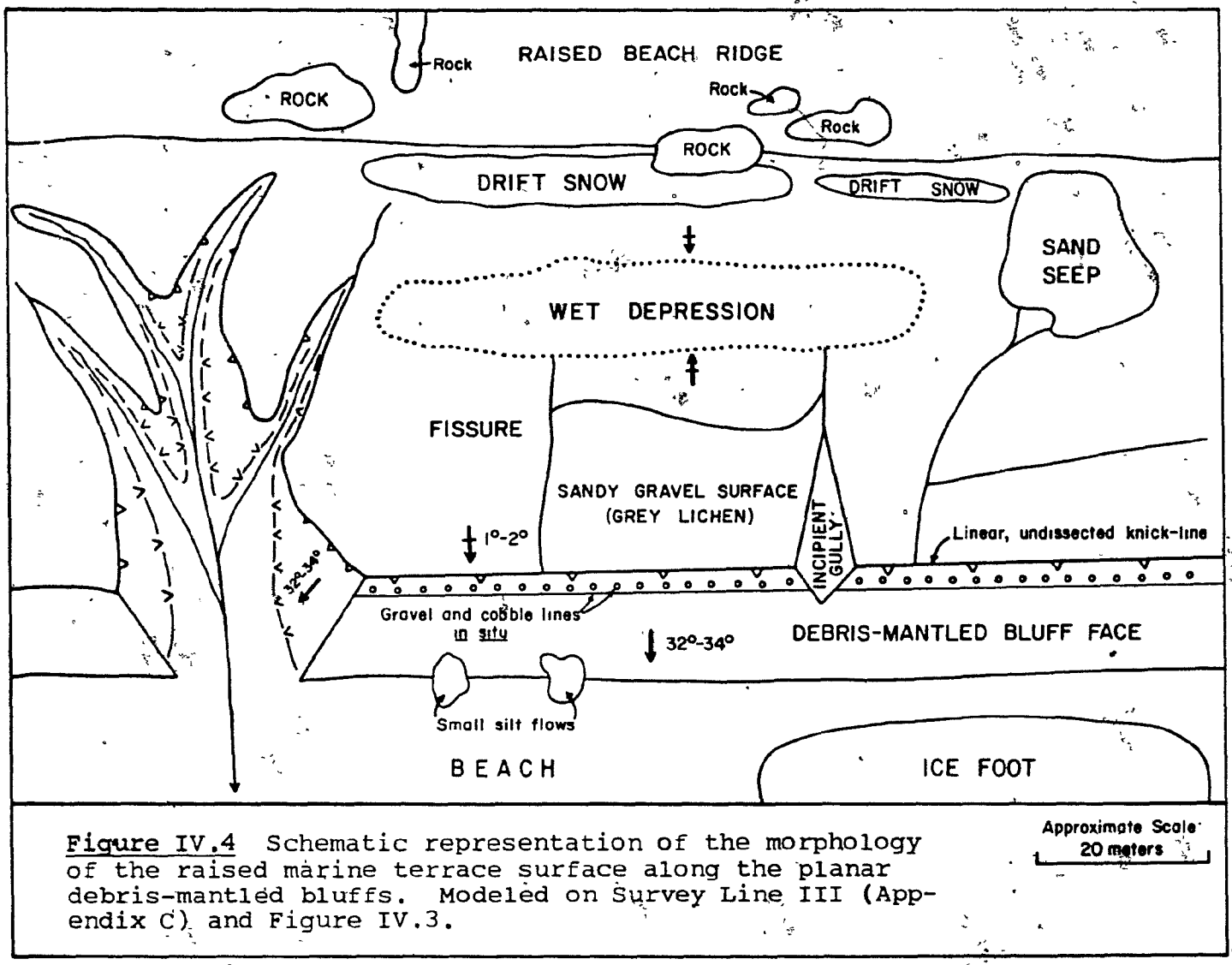


Figure IV.4 Schematic representation of the morphology of the raised marine terrace surface along the planar debris-mantled bluffs. Modeled on Survey Line III (Appendix C) and Figure IV.3.

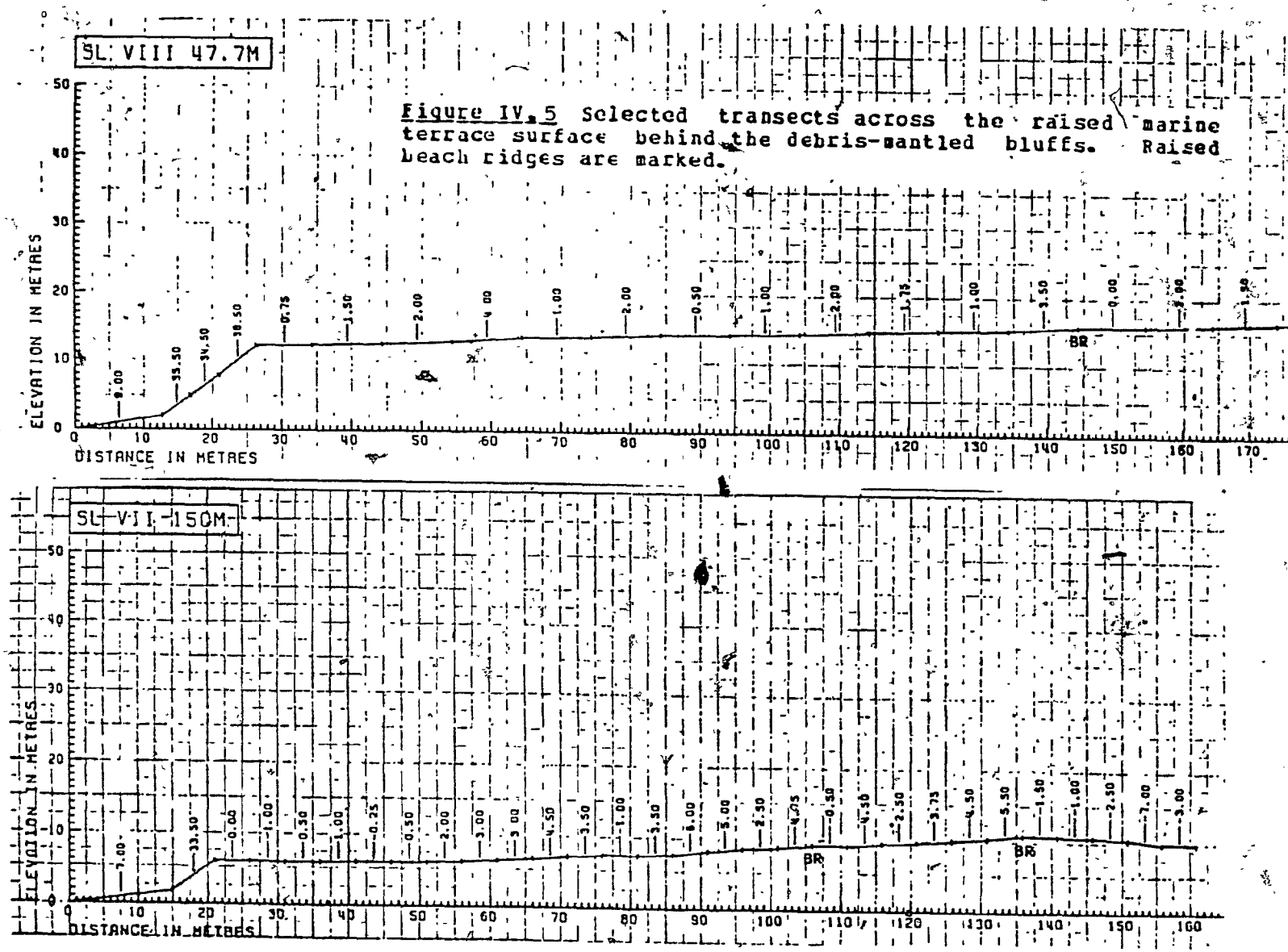


Figure IV.5 Selected transects across the raised marine terrace surface behind the debris-mantled bluffs. Raised beach ridges are marked.

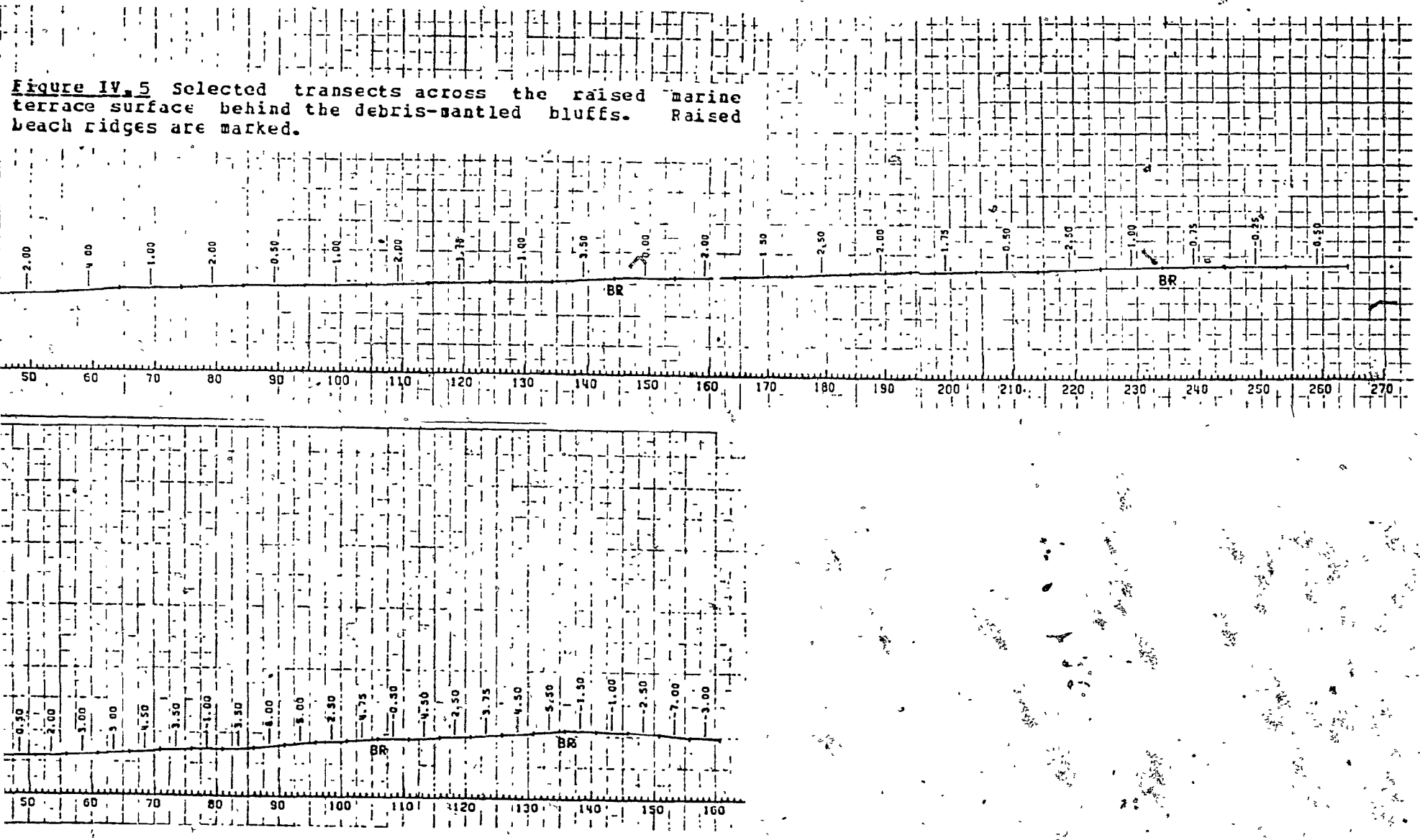


Figure IV.5 Selected transects across the raised marine terrace surface behind the debris-mantled bluffs. Raised beach ridges are marked.

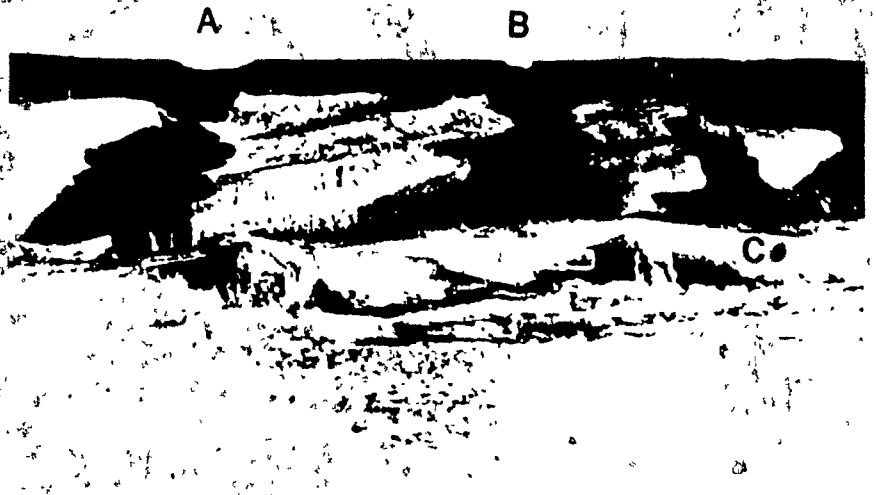


Figure IV.6 Sediment fans along bluff southeast of Camp I. A and B are associated with small subaerial gullies on the terrace surface. Fan C does not have an obvious subaerial source, but is associated with a strong flow of melt water arising along the bluff slope, suggesting deposition by emergent subsurface flow.

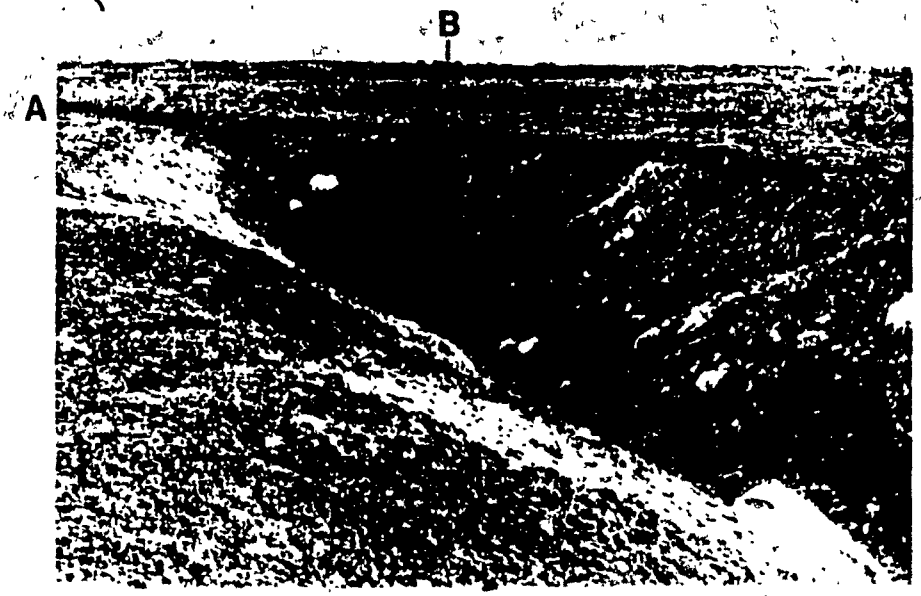


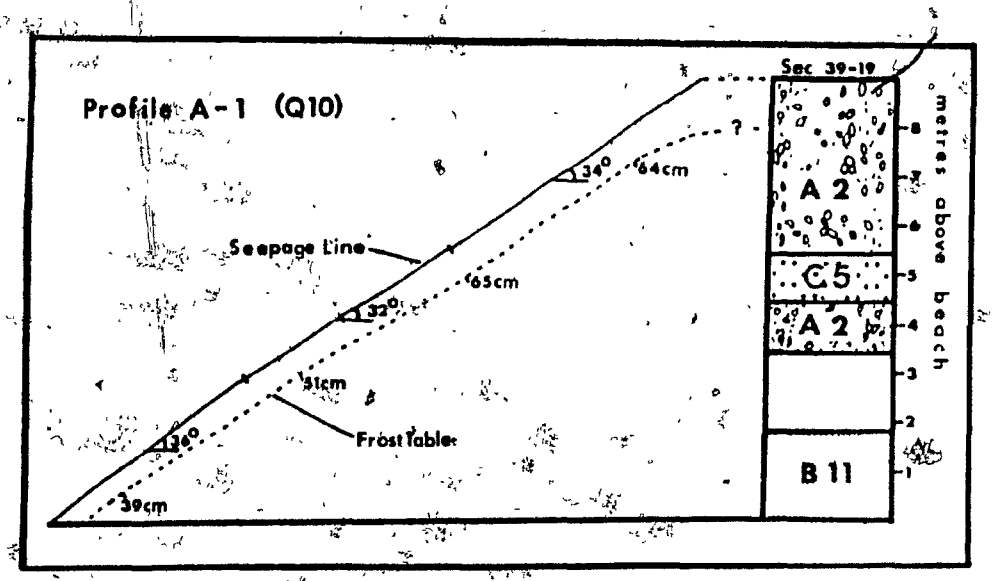
Figure IV.7 Gully retrogressing onto sand wedge fissure (A) at K557 (Survey Line VII, Appendix C). View is inland from bluff edge. Raised beach ridges in background are marked by large ice-pushed boulders (B).



Figure IV.8 Surface pitting formed by pipe collapse behind an incipient gully at the bluff edge. Such discontinuous surface depressions represent an early stage of gully development. Location is southeast of Camp I (not on panorama).



Figure IV.9 Planar debris-mantled bluff face along Survey Line III showing distinct knick-line break, linear, undissected slope and pebble and cobble lines near crest. The bluff is approximately 4 m high, the slope angle is 33°. (Sandy mounds are small sediment fans in front of a small gully: These are just veneers of sediment over snow.)



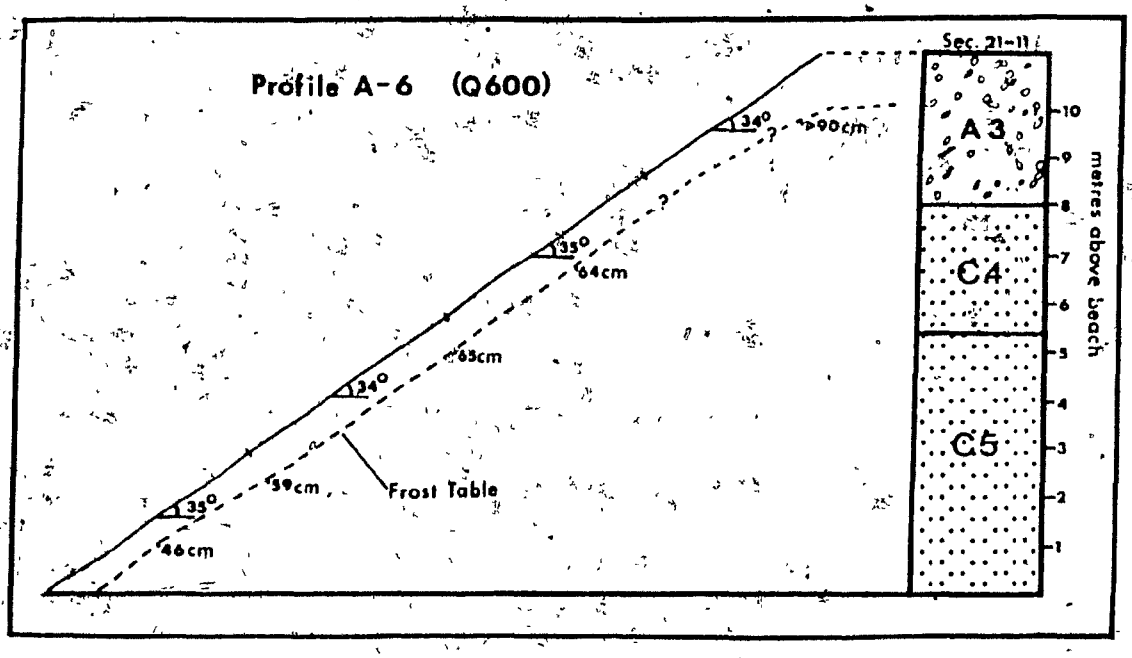
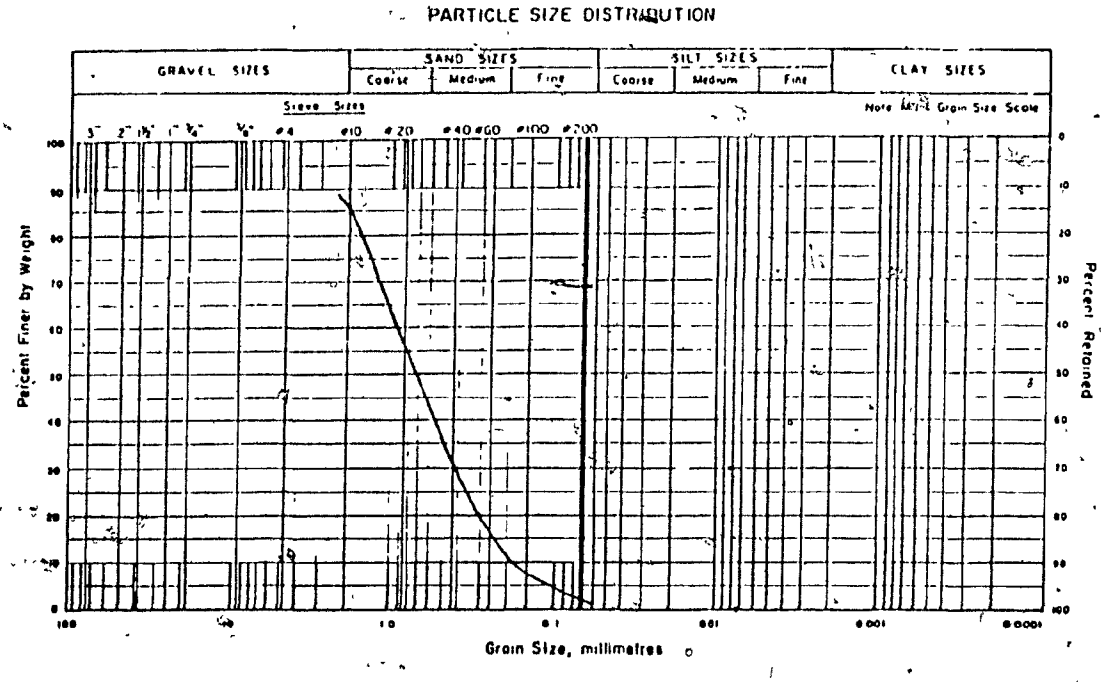
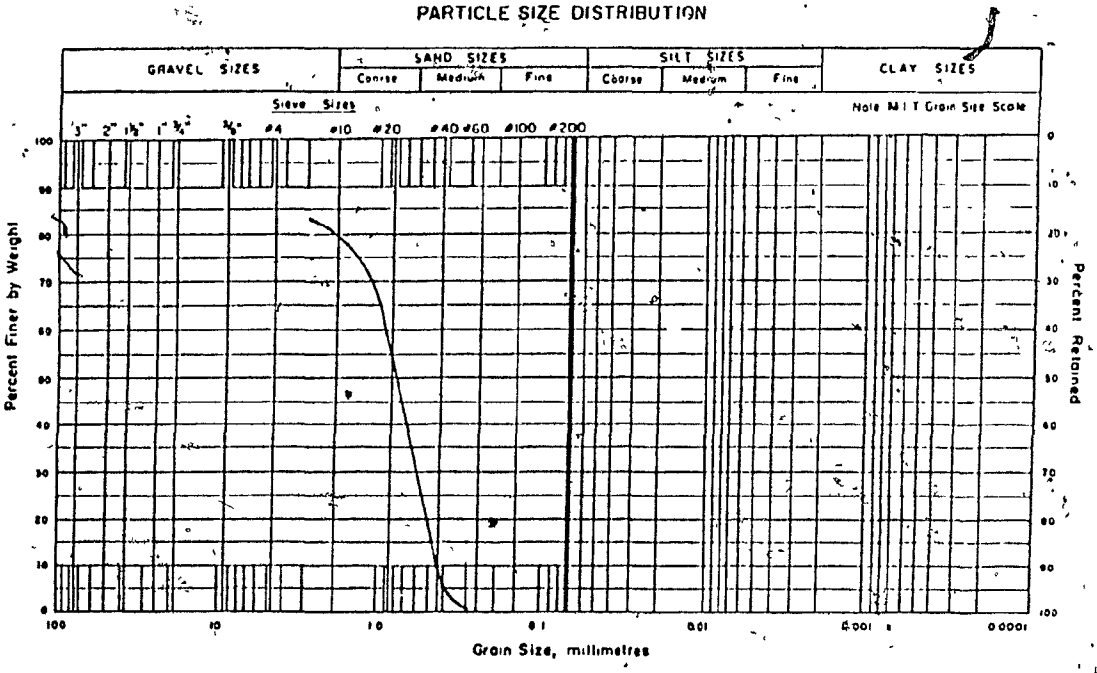


Figure IV.10 Representative profiles of the debris-mantled bluffs including local stratigraphy and frost table depth as of early August (1977). (Stratigraphic symbols explained in Table II.3.)



Sample from debris-mantled bluff slope; 50 cm depth.



Tilting box sample. From surface of bluff slope along Survey Line III.

Figure IV.11 Grain-size curves for samples from the debris-mantled bluffs.

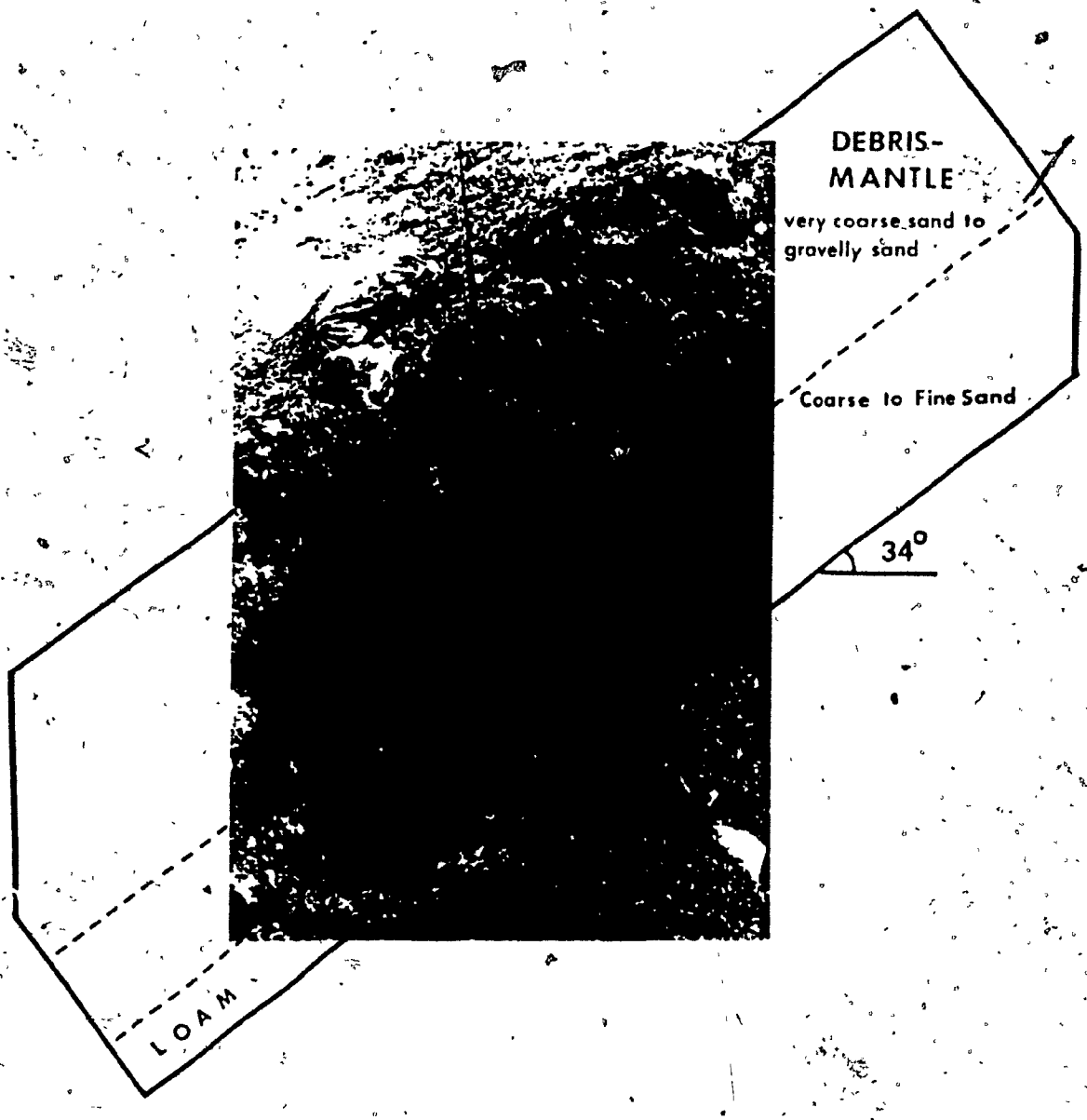


Figure IV.12 Cross section of the active layer along a debris-mantled bluff slope near Profile A-1, Figure IV.10. The excavation is at the elevation of a thin clayey unit (facies D) which is seen in situ at the base of the active layer (A). The white inclusions at the bottom of the excavation are ice veins.

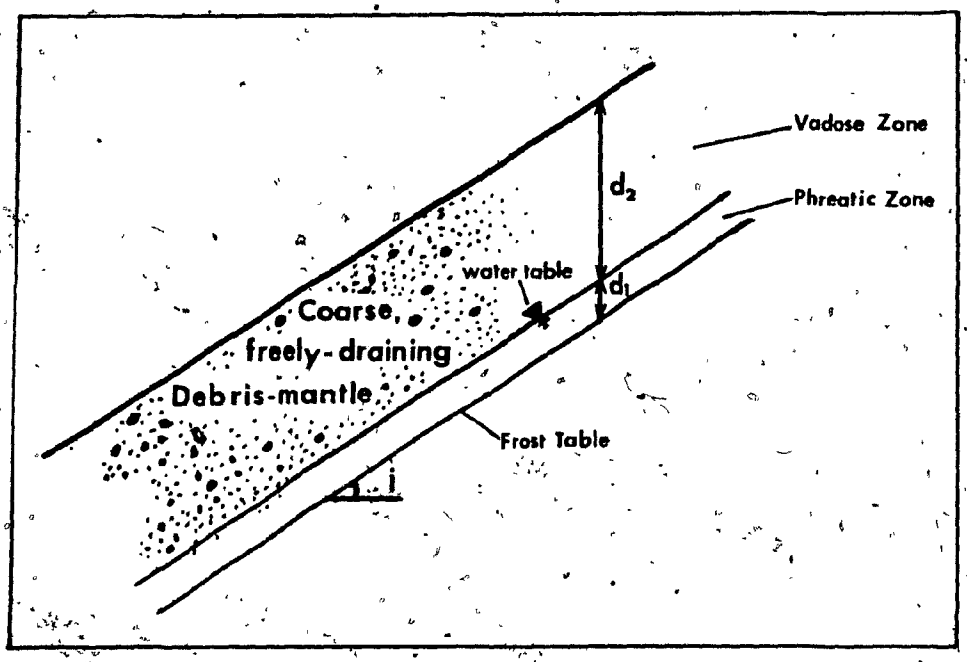


Figure IV.13 Cross section of active layer showing, schematically, the effect of a coarse-grained mantle on ground water through-flow and phreatic zone development. The thick, freely draining surcharge keeps the thickness of the phreatic zone (d1) small in relation to the total active layer thickness. Thus, the effective normal stress at the frost table is never much less than the total normal stress and slope failure due to pore pressure generation is unlikely.



Figure IV.14 Landslide along the lower portion of a debris-mantled bluffs south of Camp 1. The stratigraphy of the lower bluff contains silty sand and thin clayey units. The landslide was most likely the result of the development of a thin phreatic layer above the frost table. Such landslides however are infrequent and do not affect significant changes in the plan form of the bluff, as their scars are quicky back-filled with debris from above.

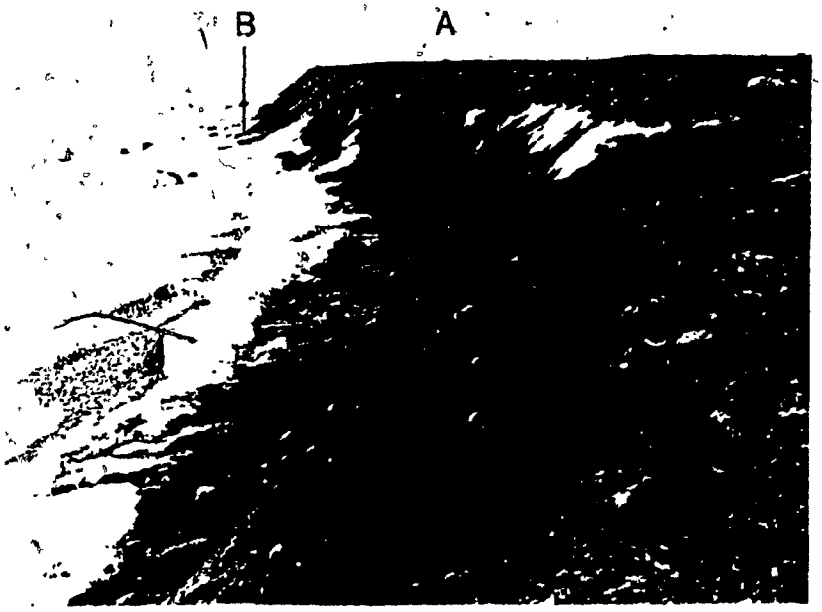


Figure IV.15 Bluffs southeast of Camp I showing the stabilizing effect of the coarse-grained debris-mantle. To the left of 'A' the bluff is covered by coarse sand and gravel derived from the beach facies (facies A2) which forms the cap unit. This cap unit is absent from the stratigraphic section to the right of 'A'. The bluffs here therefore lack a source unit for the debris-mantle. Rilling and slope instability is ubiquitous along the unmantled bluffs. This has led to the accumulation of a mud flow apron at the bluff base. Small basal sediment flows are the only signs of instability along the debris-mantled bluff in the background (B).

CHAPTER V:

THE STEEP DISSECTED BLUFFS

Steep bluffs dissected by funnel-shaped hollows (debris-hoppers) and short steep ravines compose the bluff morphology between K45, just southeast of Camp I and the major stream at K405. Bluffs similar in appearance also occur at K630-645 and K905-975, although this latter section is transitional in nature. Bluff height is generally greater than that of the debris-mantled bluffs, increasing from 10-12 m in the vicinity of Camp I to over 16 m at K275 and 20 m at K905. In comparison to the bluffs to the south of Camp I, fluvial dissection by gullies and streams is frequent. The streams also exhibit a wider range of profile gradings and channel lengths than along the debris-mantled bluffs.

A. Stratigraphy

The stratigraphy of the steep dissected bluffs, which is shown in Figure V.1, is also quite different from that of the bluffs described in the previous chapter and it is this difference that is in large part responsible for the differences in bluff morphology. The lithology is predominantly very fine to medium sand and silty sand with interbedded with stoney diamicts, poorly sorted gravelly sands, boulder lines and the occasional massive fine-grained unit. Where present, the latter units are usually thin, but in some

locations may be a metre or more in thickness. Locally, the thicker fine-grained units may have some morphological expression giving rise to complex, transitional bluff forms.

The most continuous and conspicuous units found along the steep dissected bluffs are comprised of well-sorted cross-stratified fine to medium sand (facies B). Locally these units account for up to 80% of the bluff section (e.g. Sec. 30-12). Long, continuous and prominent free-faces, such as those between K275 and K405, are often formed on these sand units. Interbedded sand and silty sand units (facies C) occupy the lower portions of the bluffs northwest of K300 and compose most of Section 19-8. Thin fine-grained units (facies D) are present in the upper part of the bluff between K49 (Section 38-14) and K220 (Section 31-5) and can be traced laterally on the panorama as darker-toned lines. The darker tone indicates moist or wet sediments, often marking zones of saturation or seepage. A particularly thick fine-grained unit (for this portion of the bluffs) occurs in the vicinity of K220-240 (Sec. 32-31) at 7.4-10 m asl.

Where gravelly and coarse sand units (facies A) are present near the top of the stratigraphic section (most notably K275-347), they are usually overlain by other finer-grained sediments. While it is facies A2 which forms the cap unit along the debris-mantled bluffs, the 'A' facies here is predominantly A3 indicating the presence of a greater proportion of fine grain sizes. (An exception to this is the facies A2 unit in Section 19-8, but this unit is thin relative to the height of the bluff.)

The lines of cobbles and boulders (facies A1) which are commonly found along the steep dissected bluffs are most likely lag deposits marking erosional discontinuities at unit contacts. Thick, dense and pooorly-sorted units with a high admixture of larger clasts are also found, forming cemented strata (facies V13, Sec. 30-12). The absence of carbonates in laboratory samples (Nelson, 1978, p.75) suggests that the source of cementation is the silt/clay fraction (6-10% silt, 2% clay) or iron oxides (mottling is often evident in these units).

B. Form and Development of Scarp Slopes

The planar scarp slopes along the steep dissected bluffs differ from the debris-mantled bluffs, not only in their lack of a continuous coarse colluvial blanket but in the steepess and irregularity of their profiles. Overall bluff slope inclinations (beach to knick-line) of 38° to 44° are typical. In situ sediment is often exposed in short free-face segments, some of which approach the vertical. Along any single profile, high-angled facets may be interspersed with less steep colluvium-covered segments.

Detailed slope profiles indicating regolith character and frost table depth are reproduced in Figure V.2 and Appendix B. (Frost table measurements were made in mid-August when the active layer was near its maximum thickness.) Where available, local stratigraphy is indicated on the profile.

1. Active layer thickness and frost table depth

In 1977 and 1983 the maximum seasonal frost table lay roughly parallel to the bluff slope, ranging in depth from 40 cm to 75 cm and increasing abruptly to over 90 cm at the knick-line. Along any single profile the active layer thickness may vary by as much as 30 cm depending upon such factors as sediment texture, ice content, soil moisture and slope angle. At no location along the bluffs was the frost table exposed. There seems to be a tendency for steeper sections of the profile (which are usually developed in relatively dense in situ sediment) to have a slightly thinner active layer than the (less dense and often drier) colluvium on gentler slope segments. In relation to thaw, it should be noted that even the north-facing slopes at Kivitoo receive direct insolation from late afternoon to early morning during June and July (the period of initial thaw) when the sun is still high over the horizon in the north.

2. Analysis of the profiles

A coastal scarp slope subject to alternating periods of basal erosion, debris removal and quiescence, would be expected to display longshore variations in bluff profile reflecting the local patterns of undercutting, failure, regrading, debris accumulation and removal. In addition to differences in the erosional environment, differences in the mechanical strength, weathering behavior and hydraulic conductivity of the

individual units which make up the stratigraphic section, as well as their rapidly changing sequence, gives rise to a second level of profile variation.

The range of slope segment angles encountered along the scarp slopes is shown by the bar graph in Figure V.3, which has been constructed from the bluff profiles and spot measurements. Sampling of slope segments was representative, not systematic, and as these bluffs are low and segments short, a minimum segment length of 1.5 m was used. This sampling procedure is considered adequate since it is the range of slope inclinations present, rather than their frequency, which is of primary interest here. As such, most of the slope segments fall between 34° and 47° with some segments up to 78° and occasional short facets as steep as 90° (not included on bar graph).

In light of the many possible individual bluff profiles it is useful to consider a comprehensive theoretical profile, Figure V.4, of an idealized undercut scarp slope along the Kivitoo bluffs. This profile is loosely modeled after the slope shown in Figure V.5.

a. Talus Segments

With the accumulation of granular debris derived from the slope above, a talus apron standing at the angle of repose of the debris, is formed at the base of the bluff: Segment A, Figure V.4. For a variety of fairly well-sorted, rounded to subangular sandy debris this angle will be 33-35° (as discussed in the previous chapter).

A well developed talus apron (of greater than 1 m in height) was not a ubiquitous feature along the base of the scarp slopes when the party arrived in the field in 1977. Where present, much of the talus accumulation which had taken place (as well as depositon of debris from the bluff hollows) did so over snow drifted in against the base of the bluff. Snow or ice was found to underlie most basal talus segments. Protected by the overlaying material, this frozen core persisted in many locations throughout the summer. Where significant melting had occurred, the effect was to lower the angle of the talus through subsidence.

Although evidence of basal trimming, such as that shown in Figure V.6, was widespread in both 1977 and 1983, the talus segments were taller and more laterally continuous in 1983. (See also Figure V.5c.) Snow or ice underlaying the basal talus was also less frequently encountered. These observations suggest that in 1977 the bluffs had recently been extensively undercut, and that it takes a period of time (at least a year) for a substantial basal accumulation slope to be reformed. (Process along scarp slopes is discussed in section V.B,3, below.)

Where units comprised of coarse beach sediments (facies A2) are found, short, debris-mantled slope segments, similar to the longer slopes found along the debris-mantled bluffs, develop at the top of the steep dissected bluffs; Segment F, Fig. V.4. However, along these bluffs such units are not thick enough relative to bluff height to provide a geomorphologically effective surcharge cover over the entire slope.

b. Undercut Segments With a Sandy Colluvial Regolith

Above the talus apron in Figure V.4 is a slope segment -- Segment B -- mantled by a 30-60 cm thick veneer of sandy colluvium, derived both from the slope above and from the underlying in situ sediment. These slopes account for most of the segments of 36° to 39° on the bargraph. Colluvial segments are particularly common along the lower half of the bluff between K220 and K430. Aside from the steeper gradients, the regolith of these colluvial segments differs from that of the debris-mantled bluffs in several ways: (1) it is finer textured, usually moderately well-sorted medium sand in a loose state of packing (dry bulk unit weights of 14.5-15.5 kN/m^3 are typical); (2) a thin, weak surficial crust (as seen in Figure V.6) is often present; and (3) laterally extensive mass instability with limited displacement (indicated by cracking of the surficial crust) is common. (These cracks are apparent half-way up the bluff face on the panorama between K275 and K405.) The ubiquitous, but minor, instability along these slopes indicates that they are inclined at an an angle near that of limiting equilibrium. The 36-39° inclinations of these slope segments correspond to reported residual angles of internal friction (ϕ'_r) and angles of initial failure (ϕ_i) for loose, relatively well-sorted sandy colluvium comprised of subangular to subrounded grains, as well as to reported modes of undercut slope segments developed in similar loose materials (e.g. Chandler 1973). Thus, these are truly colluvial slopes, rather than strictly debris accumulation slopes. The primary

control on slope angle is not the dry avalanching found along the debris-mantled bluffs and talus segments, but rather instability initiated by slope undercutting or pore pressure build-up. Thus slope gradient corresponds to the angle of initial failure (ϕ_i) rather than to the slightly lower angle of repose (ϕ_{rep}, as discussed in the precious chapter). For loosely-packed colluvium, the angle of initial yield is roughly correlative with the constant volume shearing angle, ϕ'_{cv} (Chandler, 1973).

The limited displacement indicated by cracks on the slope surface suggests that some form of colluvial 'creep' (failure with limited displacement) of laterally extensive sections of the active layer is occurring. As the slope material is inclined at its frictional threshold angle, any (transient) occurrence of positive pore-water pressures (due to ground-ice thaw, downslope seepage or precipitation) could potentially result in downslope movement. However, positive pore pressures, when they occur, appear to be small and/or transient in nature so that significant and prologed strength reduction resulting in major transitional movements and stripping of the active layer was not observed. The lateral extension of cracks along the slope surface implies that failure is in response to a laterally extensive cause, such as the slope steepening due to marine undercutting or removal of basal debris, rather than to fluctuations in the local groundwater conditions.

Slope flattening to gradients less steep than the frictional threshold value is limited in the sandy colluvium by the inferred high rates of undercutting, low precipitation and

the fact that run-off and seepage is funnelled to either side of the slopes into the bluff-face hollows. Also, negative pore pressures arising from the unsaturated state of the soil, coupled with surface crust formation, make the colluvium resistant to dry avalanching and permit steeper undercut basal slopes to be temporarily retained.

c. Slope segments in in situ sediment

Inspection of the slope profiles and the panorama indicates that along large portions of the bluffs in situ sediment (with bedding planes etched out by wind deflation) is exposed: Segment D, Figure V.4. The bar graph, Figure V.3 shows that most of these elements are inclined at 45-50°, though some (discussed next) are much steeper. The two thickest and most prominent units supporting such steep slopes are stratified fine to medium sands which outcrop along the entire length of the steep dissected bluffs, most notably between K240 and K975.

From the absence of carbonates and iron staining it is assumed that these faces lack any source of cohesion when thawed, and are standing at angles close to the peak angle of internal friction (ϕ'_p) of the in situ sand. For sand in a normally dense state of packing, ϕ'_p values are widely reported to be about 45° (e.g. Kirkpatrick, 1965). The two segment sequence represented by Segments D and B in Figure V.4 is comparable to that reported on many other undercut slopes of granular, non-cohesive materials where the water table is well

below the slope surface; as in the slopes described by Strahler (1950a,b) in weathered granite in southern California, and Chandler (1973), along marine eroded talus terraces on Vestspitzbergen. Most previous studies (e.g. Carson, 1969; Chandler, 1973), have interpreted the steeper slope in terms of ϕ'_p for the densely packed soil and the gentler slope in terms of ϕ'_{res} (or perhaps ϕ_{rep}) for the same soil when loosened by weathering processes or when forming a basal accumulation slope via discrete rockfall and dry avalanching. Unfortunately, no undisturbed samples could be retrieved due to the difficulty of transporting such specimens from the field. Some evidence that the profiles at Kivitoo are determined in this way is provided by the maximum angle of stability (the angle of initial yield, ϕ_i) obtained for coarse-sand in tilting-box tests: ϕ_i = 38-45° while ϕ_{rep} = 32-34°. Other segments along which in situ poorly-sorted sediment is exposed may be easily accounted for by the high internal friction angles typical of such material.

d. High-angled slope elements

Slope elements standing at greater angles (55-80°) are not so easily explained. According to Mohr-Coulomb strength criteria, a soil must have either a very large coefficient of internal friction or cohesion if it is to be strong enough to maintain such steep slopes. Angles of internal friction in excess of 45° are unusual, particularly for granular soils which are not poorly-sorted. In some instances the stability of steep sand slopes may be attributed to cohesion provided by

cementation (either by carbonates or iron oxides) while in others, small amounts of fine (cohesive) sediment may provide the requisite cohesion. Yet, the major free face-forming units -- e.g. Segment E: Figure V.4 and Figure V.5 -- are found, not in poorly-sorted sediments, but in well-sorted medium sand, lacking fine sediment and without any carbonate cement (Nelson, 1978) or evidence of iron-staining. Another possible explaination for the strength of the Kivitoo sands, is the large effective stress which can be generated in a soil if pore-water tensions (capillary forces) exist in the unsaturated soil providing an apparent cohesion. In terms of Mohr-Coulomb strength criteria capillary tension translates to negative pore pressure. Since the sand forming the major free-face segments does not appear to be cemented, the stability of such slopes would require either unusually high angles of internal friction or capillary tensions.

Considering the possibility that the Kivitoo sands have unusually high friction angles, it is interesting that Dusseault and Morgenstern (1978a,b; 1979) have documented very steep slope segments (50-80°; with slopes of 50° being as tall as 70 m) in the Athabaska Oil Sands. Dusseault and Morgenstern explained such high, steep slopes as the result of exceptionally high peak friction angles (ϕ'_p = 47-64° in direct shear tests at low effective stress levels).

The Athabaska sands are very dense and comprised of highly interlocked, but not cemented, grains. (The Mohr-Coulomb strength envelope was highly curved tending to zero at low effective normal stress, indicating the lack of cohesion.) The

'locked' structure of these sands was attributed to diagenic 'suturing' of individual grains under high overburden pressures (such as those which are thought to occur under an ice sheet) and over long periods of time. Dusseault and Morgenstern argue that when subject to such conditions, sands of highly quartose mineralogy will develop 'sutures' or silica over-growths between grains creating a 'dense and interpenetrative structure' similar in effect to a jigsaw puzzle with individual interlocked pieces formed of aggregates of bonded and fitted sand grains. Although no grain size curves are given, such a sand would be expected to have a wide range of 'particle sizes'. Whether or not the sands of the Kivitoo bluffs could also belong in the category of 'locked sands' is an intriguing question.

The Athabaska Oil Sands have dry bulk unit weights of 20.7-22.8 kN/m^3, and porosities as low as 18.4%. By contrast, a naturally-packed, well-sorted, dense sand would be expected to have a dry bulk unit weight of 14-17 kN/m^3 and a porosity in the range of 25-35% (e.g. Dusseault and Morgenstern, 1978b; Pettibone and Keally, 1971). The Kivitoo sands were found (by in situ density sampling) to have dry bulk densities of 15.0-15.9 kN/m^3 and a porosity of 39-42% (assuming Gs = 2.65); Table V.1. These values are well within the expected range for such sediments in a normal state of packing. (For example, sand strata in the Champlain Sea sediments examined by Dredge and Thom (1976) had an in situ bulk density of 15.6 KN/m^3, corresponding to a porosity of 40% (assuming Gs = 2.65).) The relatively high porosity of the Kivitoo sand, in comparison to

that expected for a 'dense-normal' state of packing, suggests that these sands have angles of internal friction which are not much greater than the residual friction values.

In addition to the differences in porosity, the Kivitoo sands show little physical resemblance to the Athabaska locked sands. No evidence of sutured grain contacts was found by microscopic examination; the grain size curve, Figure V.7, shows very good sorting; the sand is predominantly feldspar not quartz; and the Kivitoo sediment is considerably younger (<250,000 years; Nelson, 1978).

The possibility that stability is being maintained by capillary tensions seems a logical one for several reasons. First, the water content of 7-18% indicates that the sand is not saturated. For a bulk unit weight of 15-16 kN/m^3, 100% saturation corresponds to a water content of 24-28%. Second, subsurface seepage from the terrace above does not appear to move uniformly down the bluff slopes, but is localized along certain flow axes that give rise to the 'hollows' (discussed below), leaving the bluff face with no ready external source of water for soil saturation. And third, in the humid atmosphere of the Baffin Island coast it is only late in the summer that effective drying of the slope surface occurs, eliminating capillary films and thereby leading to granular disintegration. This desiccation appears to be due, at least in part, to refreezing of the active layer (see next section). As the active layer is thin (approximately 50-70 cm), only small capillary tensions would be required to provide the apparent cohesion necessary to support the steep slope facets along the

Kivitoo Bluffs. Although large capillary tensions can develop only in clay soils, the small capillary tensions required at Kivitoo are possible in sandy soils (e.g. Lane and Washburn, 1946).

Examination of a steep sandy slope facet south of Camp II suggests that there is some cohesive component to slope strength (in this case from either cementation or capillary tensions). These slopes are tall (>7 m) and up to 70° steep. At K934 the failure of a large slab of sand approximately 40 cm thick, has occurred on a 60-70° slope. Examination of the failure scar revealed a system of sub-parallel fissures -- shown in Figure V.8 -- dipping at an angle slightly steeper than the slope. Normally, cohesionless sediment does not develop tension cracks.

The origin of these high angle fissures at K934 is not known. Frequently such features are attributed to pressure release and 'exfoliation' parallel to the slope (Dusseault and Morgenstern 1979; Terzaghi, 1962), but this still does not provide an explanation for the initial slope angle to which the fissures are sub-parallel. From soil mechanics theory (e.g. Wu 1966), rapid undercutting of a cliff may produce an active state of stress immediately behind the cliff with 'failure planes' inclined at an angle of $(45 + \phi'/2)$. For ϕ'_p in the range 30-40°, the fissures should be 60-65°. DePloey (1977), in fact, noted a mean fissure inclination in slopes of lightly cemented Tertiary sandstones of 70° and attributed these to failure planes developed in response to the in situ active

state of stress. Thus, if the capillary tension (or true cohesion) in the sand unit is large enough to maintain slopes tall enough for active stress fractures to develop, these slopes may, in turn, stand at angles determined by these fracture patterns. Along the Kivitoo coast the sand unit south of Camp II is, apparently, the only unit thick enough for such tall slopes to develop.

3. Observation of process on scarp slopes

Over the course of the 1977 and 1983 field seasons, little sediment movement was noted along the scarp slopes. Small sediment flows of well-sorted, fine to medium sands occurred locally but did not move large amounts of material and are not thought to be a principle mechanism of sediment movement along the scarp slopes. These sediment flows were generated by failure associated with the local rise in pore (seepage) pressure at the base of steep slopes in well-sorted sands. As high pore pressure conditions are rapidly dissipated in permeable sandy materials, the sediment flows often 'freeze' in place on the slope after only limited displacement, and individual failures seldom show marked retrogression. These small sediment flows may be a result of either true liquefaction, saturated grain-flow, or some combination of the two. An in-depth discussion of post-failure movements in sandy materials is undertaken in Chapter VI.

Although long portions of the bluff base were undercut, extensive talus aprons did not accumulate along the base of

scarp slopes during most of the 1977 field season. However, during the last week of August (1977) there was a sudden onset of rapid granular disintegration along steep, sandy scarp slopes and, consequently, the development of a basal talus. Sediment movement took the form of dry avalanching and grain flow. The 'hissing' sound of sand cascading down the bluff face was clearly audible. Talus slopes, some as tall as 2 m, formed over the short period of 2-3 days. Figure V.9 shows such a recently formed talus.

The onset of this activity coincided with the first prolonged drop in air temperature below 0°C, during the 1977 field season (August 24-25, 1977). During this entire period the temperature at Kivitoo remained below 0°C. Prior to this, while nightime temperature would drop as low as -5°C, daytime temperature would always rise above 0°C. Temperature data from Broughton Island, Figure II.3, confirmed these observations. Precipitation in the days preceeding this period was negligable. The period of rapid granular disintegration therefore occurred while the active layer was beginning to refreeze, not, as would be expected, when the sediment was thawing or thawed.

Considering that the process of sediment failure was granular disintegration rather than more extensive forms of mass wasting and the sandy nature of the sediment released, it is likely that the reason for this activity was the elimination of the caplillary tensions holding the sand grains on the slope. Freezing at the surface of the in situ sand could cause such desiccation. Mechanical disturbance and loosening of

dense or lightly cemented sands by expansion of freezing water at partical contacts (Beskow, 1935 cited in Williams, 1967; p.98) may also loosen sand particles.

If sand grains are being held on a steep slope by capillary tension (as discussed above), dessication of the inter-grain menisci would be eliminate any apparent cohesion releasing the sand grain. Significant drying of the surficial soil apparently did not occur at Kivitoo prior to this time, even though the summer of 1977 was particularly dry, sunny and warm. It is possible that as the freezing plane advances into the active layer it effectively cuts off the supply of capillary moisture being supplied at the thaw interface allowing the inter-grain menisci to be eliminated. Sublimation of any inter-grain ice in the frozen surface layers may also occur promoting grain release.

A simple test performed in the laboratory supports this hypothesis: A sample of well-sorted medium sand from the bluff was saturated and allowed to dry until sufficient capillary tensions were developed to allow small (2 cm^3) cubes of soil to be cut. One cube was placed in a freezer at -10°C and the other allowed to air dry. After freezing over-night, desiccation (indicated by a lightening of color) had occurred on the surface of the small cube and a small amount of sand grains had fallen around the cube. No such drying or grain release was noted for the control specimen.

Based on the 1977 observations it likely that talus accumulation occurs each fall during freeze-back as long as scarp slope facets are present along the bluff face. The

absence of extensive basal talus upon arrival in late June (1977) and the presence of 'ice cores' in what talus did exist, suggests that much of the talus which had accumulated did so prior to the thawing of the surficial sediments i.e. while the active layer was frozen. Kerfoot (1969) has also observed that steep slopes in sandy marine bluffs along the coast of Garry Island, N.W.T., failed late in the summer resulting in active layer stripping. However, the mechanism of failure was not addressed in his study.

Infrequent, intense rainfall events are a possible cause of active layer stripping along the Kivitoo scarp slopes, effecting a type of parallel retreat. Yet, in light of the low precipitation at Kivitoo, the steepness of the slopes and the fact that run-off from the terrace is directed away from the scarp slopes into the hollows, it is unlikely that such stripping is a frequent event.

Evidence of the relative inactivity of scarp slopes with respect to instability which is not a direct result of slope steepening as a result of basal trimming is given in Figures V.5a, 5b and 5c. These photographs of a section of the steep dissected bluffs show only minor changes in the slope morphology during the period 1976 - 1983. Comparison of Figures VI.5b (1977) and VI.5c (1983) indicate only minor (0.5-1.0 m) basal retreat. This recession of the slope base may be largely accounted for by the removal of the basal talus, and once this reforms the apparent retreat may be mostly mitigated. Active layer sloughing along the steep scarp slope ($i>38°$) in response to undercutting is also evident ('E' in

Figure VI.5c). Analysis of the many photographs taken during 1977 with the condition of the bluff face in 1983, indicates that there is a tendency for the steeper scarp slope facets to regrade in the absence of severe episodes of basal undercutting. This regrading occurs as dense or slightly cohesive sediments become loosened and assume a lower gradient slope coincident with the angle of internal friction of this loose debris.

C. Form and Development of Bluff-Face Hollows

The dissection of the bluff face represented by the development of steep incised hollows such as those shown in Figures V.10 and V.11, can be considered as a form of preferential slope flattening and knick-line retreat, linked to both terrace and bluff slope conditions which interact to effect lateral variation in slope stability and rates of debris supply and removal. The process of bluff dissection is enhanced by the overall steepness of the bluff face, since even minor variations in the strength of the bluff materials could potentially lead to localized slope failure, slope reduction and hence the development of contour curvature. Once initiated, incipient contour concavity may further localize erosion through the induced convergence of sediment and groundwater flow lines (Carson and Kirkby, 1972; Kirkby, 1978), promoting the continued growth of the initial hollow.

Hollows may continue to develop almost exclusively by mass wasting processes as debris shed by failure along the steep

side slopes of an upper funnel-shaped 'debris-hopper' (Figure V.10) is evacuated to the beach along an axial slope below the hopper. Debris transport may be via the break-up of landslide waste and its transformation into a mobile debris flow or, alternatively, debris shed by mass-movements may be removed from the hollow predominantly by fluvial transport and seepage erosion as the convergence of groundwater at the base of the hollow side slopes results in the formation of rills or poorly defined 'channels' along an axial slope at the base of the debris-hopper.

As the geomorphic importance of ground and surface water supplied at the terrace surface increases, fluvial processes may come to predominate over mass-wasting as the predominant mode of debris transport, and at the extreme, debris-hopper development may grade into the processes of gully development and drainage net extension (Carson 1976). Yet, for reasons outlined below, extension of the axial slope onto the terrace and reduction of this slope to gradients less than semi-frictional threshold values (see Chaper III, Eq. III.12) does not frequently occur. Along the Kivitoo coast, bluff face hollows rarely develop into true gullies.

Discussion of the bluff face hollows is hampered by the problems inherent in establishing a nomenclature to refer to and describe features which, in fact, represent a continuum of form. Figure V.12 is a schematic representation of the range of hollow morphology found along the steep dissected bluffs. For convenience all features exhibiting concave-in-plan contour curvature are refered to as bluff face hollows. Debris-hoppers

are defined as the loci of the convergent movement of debris from the upper portions of the bluff to the beach. Hoppers are characterized by a broadly arcuate plan and steep side slopes which are convergent upon a point; Figure VI.12 A. Below this, debris is carried to the base of the bluff along a basal transport slope. This slope may become incised, as it flattens to a lesser gradient than the adjacent steep planar bluff face. This regraded slope may extend upwards to the knick-line, forming what is in effect an axial slope lending a bilateral symmetry to the nitially broadly arcuate hopper. Such steep incised hollows in which the axial slope is more or less two-dimensional, has extended to the knick-line, has steep side slope rising above it and, often, carries significant run-off are referred to as bluff face ravines; Figure V.12 D. These features are 'V'-shaped in cross section. In plan, the side slopes tend to have straight contours (as opposed to the broad concavity of a well developed debris-hopper). Debris, rather than being convergent upon a point as in the debris-hopper, is now convergent upon a line, the axial slope, along which it is moved to the beach. Typically, this transport is accomplished by both fluvial and debris flow processes. Bluff-face ravines are distinct from 'hanging gullies' (Figure V.12 B) which have better developed channels and extend back onto the terrace surface at a low angle. Rigorous application of these distinctions is not possible because of the variety of intermediate forms, but they serve to emphasize important differences. There exists, in reality, a continuum of form between debris-hoppers, bluff-face ravines and small fluvial

gullies, depending upon the relationship between fluvial and mass wasting processes.

1. Literature review

The term 'debris-hopper' is derived from Strahler (1950b) who used it to describe the morphology of ravine heads developed in the meta-sedimentary bedrock of California's Verdugo Hills. Strahler's 'form-elements' seem to be morphologically and genetically analogous to the hollows along the Kivitoo coast, especially in the importance of differential weathering and mass wasting processes. Strahler explains (1950b; 803)

> Hopper walls tend to be nearly straight in profile and make the form of an inverted part-cone. Most of the hopper walls are very steep, greater than 45 degrees in angle. Evidences of rolling and sliding of weathered bedrock are conspicuous. Bedrock exposures comprise from one third to three fourths of the hopper walls. Locally a layer of resistant rock may produce a vertical cliff, but for the most part rock surfaces conform closely to the straight hopper walls. Some hoppers intersect the broadly rounded divide with a sharp clearly defined break in slope, indicating the rapid expansion of the steep hopper slopes by rapid mass movements.

Strahler may have found inspiration for his description in Gilbert's (1880) classic discussion of the (shale) badland topography surrounding the Henry Mountains (Utah):

> The converging surface (of the stream heads) becomes hopper-shaped or funnel-shaped; as the the point of convergence is lowered by corrosion, the walls of the funnel are eaten back equally in all directions . . . . (p. 115).

While both Strahler and Gilbert worked in weak bedrock terrain, the similarity of the Kivitoo features to those described by these authors suggests that such form-elements are important in the development of steep slopes in many different landscapes and can develop under diverse lithological conditions. While debris-hoppers are certainly common along over-steepened bluffs formed of unconsolidated sediments, they have received very limited attention. One of the reasons for this oversight may be a confusion over process; since debris-hoppers may be easily dismissed as 'gullies' their true nature and role in bluff denudation has gone largely unrecognized.

Quigley et al. (1977) have referred to a pattern of 'scallops' and 'ribs' along steep bluffs on the north shore of Lake Erie. The features develop as small mud-slides (caused by the swelling and slaking of the dry, fissured, clayey sediment which comprises sections of the bluffs) becomes mobilized as 'thin flow-slides within each scallop'. The scallops have mean inclinations of 37° with intervening ribs standing at 50-70°. Bryan and Price (1980) have described similar bluff scallops, but on a much larger scale, in the interbedded till, sand and clay deposits found along the north shore of Lake Ontario. They identified two types of scalloped bluffs: (1) Bluffs with 'protected scallops', which have a deeply embayed, arcuate knick-line, and (2) bluffs with 'unprotected scallops', along which large individual features do not develop owing to the more uniform distribution of instability across the bluff face due, according to Bryan and Price, to the absence of a

resistant cap unit. Yet, how the lack of a resistant cap unit results in a more nearly planar bluff face is not clearly stated.

In a permafrost environment, Miles (1977) identified 'cirque-like nivation hollows' along riverbanks formed in unconsolidated sands, silts and clays. These features developed on high, steep banks, in low to medium ice content sediments. Miles noted that snow provided the source of additional moisture which he considered necessary for hollow development. The riverbanks with hollows were thought to differ from planar 'angle of repose banks' (similar to the debris-mantled bluffs discussed in the previous chapter) only in the presence of snow. Yet why hollows should develop on some slopes comprised of low ice-content sediment and not on others remains a problem, as does the mechanism by which the incipient hollow, which serves as the location for snow accumulation, is formed.

Photography of very regularly spaced forms similar in appearance to the Kivitoo features are reproduced by Washburn (1978; Fig.12.2) and Czudek and Demek (1970; Fig.4). Both of these examples appear to be thermokarst features developed along ice wedges as these are intersected by undercut stream banks and exposed to thawing. They are therefore significantly different from the Kivitoo hollows which are the expression of a fundamental mode of the degradation of steep slopes, a degradational mode which occurs along steep slopes in all environments, not just in permafrost terrain. As noted above, no ice wedges were found within the Kivitoo bluffs.

2. Morphology and Hydrology of the Terrace along the Steep Dissected Bluffs

Since the development of bluff face hollows is in most cases closely tied to the morphology and hydrology of the terrace surface, it is useful to consider these by way of introduction.

Two types of terrace topography are found behind the steep dissected bluffs, the principal differentiating factor being the presence of a surficial cover of interbedded organic material and aeolian sand. The division between the two terrace types is made in the vicinity of K240 (Fig. V.14).

The microtopography of the terrace surface southeast of K240 is more irregular and texturally more variable than that found along the debris-mantled bluffs and although the surface is also developed on raised beach deposits, it is considerably wetter. Areas of high soil moisture are readily apparent on the aerial photographs as darker tones, indicating a better developed vegetation or, in the case of the darkest tones, a hydrophilic lichen cover which grows in areas of standing water. Here the active layer soils have a greater amount of fine-grained sediment, mostly fine to medium sand with 10-30% gravel and less than 10% silt/clay. The finer texture of the active layer results in a less permeable and poorly drained surface than along the debris-matled bluffs.

One consequence of the wetter surface and finer-textured soil is the sporadic development of cryogenic features such as mudboils and small gelifluction lobes on these gentle slopes.

Sand wedges are present but not as as well developed as along the coarser-grained terrace surfaces, lacking the distinctive parallel 'ramparts'. Evidence of ice wedges was not found either on the terrace or in bluff exposures. Active layer depth on the terrace reaches a maximum of 60-100 cm in August. In wet lichen or moss covered areas, frozen ground is often encountered at depths of less than 20 cm.

Less permeable soil and thin active layer development leads to considerable surface run-off in early summer. Most of the early season run-off comes from a thin (<1 m) areally extensive snowpack which accumulates inland from the bluff edge, particularly in protected areas behind the raised beach ridges. Wind keeps the terrace surface near the edge of the bluff largely snow free.

Much of the surficial meltwater run-off is unchannelized or limited to poorly defined, vegetated drainage lines formed by the linkage of sand-wedge fissures, surface 'dimples' and shallow depressions (Figure V.13). These 'dimples' may be the result of the collapse of pipes within the active layer. Standing surface water indicates that, in places, saturated surface conditions near the bluff edge may persist into August.

The beach ridges, which are found 50-200 m inland of the bluff edge, are low (less than 1 m high) and more subdued than the strandlines described in the previous chapter. Alteration by gelifluction and cryoturbation processes further obscures many of the smaller raised marine features. As along the debris-mantled bluffs, areas of melt-water accumulation are often associated with raised beach ridges. The locations of

major melt-water accumulation areas, zones of high surface run-off and beach ridge deposits are shown in Figure V.14.

Survey Lines II (K120-137, Fig. V.15) and VI (K630-645, Appendix B), are representative of the surface topography near the bluff edge. The association of drainage lines and surface depressions with bluff morphology is noted. The terrace at the bluff edge slopes seaward at a gradient of 1-4°. The terrace surface slope is steeper (up to 10°) between K150 and K185. At this particular location there is a greater amount of run-off than elsewhere along the steep dissected bluffs. The run-off is also not as concentrated along established drainage lines. The larger quantity of surface run-off, more evenly distributed along the bluff knick-line, aids in the development of the stoney lag deposits which occur on the bluff slope along this section (discussed below).

A distinctive feature of the terrace southeast of K220 and at K630-645 (but best displayed at the northwest end of Survey Line I, Appendix B) is the relatively large number of boulders found on the surface. Many of the boulders are concentrated along amorphous drainage lines oriented roughly normal to the bluff edge. The origin of these 'boulder lines' is problematic. They may be formed as internal erosion of the active layer results in ground subsidence. This is obviously the case in Figure V.16, which shows the terrace just behind a particularly active hollow at K99. Another possible explanation for the association of boulders and drainage lines is as follows. Frost heaving of large stones would result in the creation of a cavity in the active layer where the stone

was previously buried. Collapse of the surrounding soil into this cavity leads to a small amount of subsidence of the ground surface in the vicinity of the boulder. As the terrace topography is very subdued, even this minor irregularity would be sufficient to influence surface drainage. Eventually drainage lines linking these surface depressions become established. Surface wash could also cause additional erosion where it is concentrated as it flows around boulders. Where 'boulder lines' occur they mark drainage paths and are therefore associated with bluff hollows.

The terrace surface northwest of K240 is quite different from that described above, being characterized by a 50-100 cm thick cover of interbedded plant detritus and very fine to medium aeolian sand. This 'organic mat', a representative section of which is shown in Figure V.17, has very subdued micro-topography and a more or less uniformly vegetated surface (grass and sedge) with few boulders or other stones. A large, well-defined beach ridge complex backs most of this section of the terrace. Occurring at an elevation of 24 m asl, it is clearly visible on the aerial photographs 150-250 m inland from the coast (see also Figures V.14). The seaward slope of the terrace here is 1-5°, averaging about 2-3°. The steeper slope gradients which occur locally along the dissected bluffs to the southeast are not encountered. Survey Lines VI (Q247-270) and V (Q319-323), (Appendix B), cover representative sections of the organic-mat terrace type.

The organic mat itself is best developed along a narrow zone, less than 100 m wide inland from the bluff edge. Its

distribution appears to be a direct function of the local sediment composition of the bluffs. As the stratigraphy between K240 and K405 is dominated by very fine to medium sands, deflation of these sands from the bluff face by onshore winds, results in their redeposition on the terrace surface near the bluff crest. Aeolian sedimentation is effective in masking surface irregularities such as small beach ridges, fissures and depressions. Although no systematic measurements were made, the thickness of the interbedded sand and organic deposits should decrease inland from the the bluff reflecting the pattern of wind deposition.

Active layer thickness is generally less than 50cm due to the insulating qualities of the organic mat. Spot measurements along Survey Line V (Appendix B), show a thinning of the active layer away from the bluff knick-line (from over 50 cm at the knick-line to less than 20 cm, 20 m inland).

Along the organic mat surface, wet depressions and areas of melt-water ponding are always associated with the larger bluff hollows (for example at the northwest end of Survey Line IV). Subsurface channels (pipes) are also found at the back of some hollows, often, but not always, following surface fissures. One pipe located at the back of the large hollow along Survey Line V (Appendix B), was identified by a line of small collapse pits strung along a fissure several metres inland from the knick-line. Some low-angled retrogression of the hollow knick-line had taken place along the pipe due to the collapse of the overlying soil.

Although it has not been widely reported, pipe development

within the active layer is probably common in permafrost regions where suitable soil and hyrologic conditions occur. The frost table forms an impermeable lower surface and frost cracks can aid in the development of concentrated through-flow and consequently internal erosion. The organic mat-type surfaces along the Kivitoo bluffs seem particularly susceptible to piping, as fine cohesionless sand is easily moved, and the included organic material provides matrix strength preventing pipe collapse. P. Drake (pers. comm.) has seen frost cracks, infilled with sand, leading downward into pipes in similar active layer soils on the Clyde foreland (to the north of Kivitoo). Linkage of pipe-collapse pits, forming an incipient subareal gully system, is a sequence of events which has been reported in temperate environments (Tuckfield, 1964; Mosley, 1972).

Peculiar features of the organic mat-topped terrace are vegetated, flat-floored linear depressions such as that shown in Figure V.18. These are short stream channels which now appear to be stabilized either because run-off has been reduced by stream piracy or climatic change, or because of increased rates of sediment infill. The depressions have a remarkably similar orientation, trending southeast at approximately 40° to the bluff edge. This fact suggests that they have been formed along old, raised longshore troughs which have since been masked by aeolian deposition. At present the channels carry only ephemeral flow and have hollows developing at their termini at the top of the bluff.

Many of the smaller streams crossing the dissected bluffs

are being trimmed back at the bluff line more rapidly than they can incise into the terrace surface and hence regrade to the new base level. As shown in Figure V.19, this continuous channel shortening creates multi-segment stream profiles with short, steep section near the bluff edge (e.g. the features at K220 and K226). Many stream channels, heavily overburdened and armored by debris, tend to migrate laterally, against the more easily eroded valley sides widening their valleys and undercutting these sideslopes. Stream channels, where they steepen near the bluff edge, may also develop a type of slip-off slope (as at K145) as the stream cuts sideways and downward leaving the old channel as a lag-covered stream terrace above the present channel level.

Lateral erosion into permafrost, undercutting the stream side slope, comonly resulting in the formation of intra-permafrost channels. When the over-steepened bank sloughs back over the laterally incised thermo-erosional niche and refreezes, the channel is left as a conduit within permafrost along the valley side. Figure V.20 shows this process occurring at the side of the stream valley at K325. At one location, shown in Figure V.21, a portion of the contemporary beach collapsed, apparently due to the intersection of such an old valley-side incision, now an intra-permafrost pipe, by the retreating coastline.

Many other instances of lateral stream incision into permafrost were found along the entire length of the Kivitoo bluffs. These occurred not only in sandy sediments, but in fine-grained and ice-rich sediments as well. Lateral widening

of the channel (or 'valley') may be quite extensive, on the order of metres or tens of metres, and can result in the collapse of large portions of the ground surface along the stream. This process was so common along the Kivitoo bluffs that it suggests the process is of widespread importance along streams crossing unconsolidated materials in many permafrost situations.

Two large dendritic gullies, at K270 and K325 (see air photos and Figure V.14), appear to be active and/or recent features and display unusually well-graded profiles in relation to the other small streams along the steep dissected bluffs. These gullies head in melt-water accumulation zones, just seaward of the large beach ridge mentioned above, and it is possible that their development has been at the expense of adjacent drainage lines, to the point at which they have effectively usurped much of the melt-water available along this section of the bluffs.

3. Bluff-face hollows: Morphology and process

Along the steep dissected bluffs, bluff face hollows range in width from 8-16 m and 10-15 m in depth (measured from the trend of the adjacent scarp slope and therefore a function of the mean angle of the scarp slope). A bar graph of the mean axial gradients of 72 bluff face hollows, Figure V.22, shows a range of 24-39°, with the main grouping at 28-35°. The steeper hollows (>36°) are incipient features where the axial slope has not become incised, the hopper discharging directly onto the

steeper bluff face, as at K247. (The mean angle therefore includes a portion of the steeper bluff face.) Many debris-hoppers have, at their base, debris lobes formed of waste from failure along the hollow axis or side slopes. These lobes are rarely more than several metres in height and can have slope gradients of 10-20° or less, giving the profile of the hollow a somewhat concave appearance.

Although the mean inclinations are not, in all cases, true profiles, they are useful, as many axial slopes are relatively straight from the top of the bluff to the base. Some hollows, however, have significantly gentler basal slope segments due to slope flattening along the lower portion of the hollow or the deposition of alluvium or debris flow material. The side slopes of many debris-hoppers and bluff face ravines approach the steepness of the adjacent bluff face (mean slope angle is greater than 38°) and may display its irregular profile. In this case, the debris hoppers may be viewed as the third-dimension equivalent of the planar scarp slopes, the side slopes being grading to the gentler axial slope and away from the bluff face. Figure V.23 presents a schematic profile of a bluff face hollow in which debris flow is the active agent of sediment removal along the axial slope depositing a debris lobe over the beach. Emergent flow within the hollow has also deposited a small alluvial fan on top of and along the edge of the debris lobe.

a. Initiation and genesis of the hollow form

Debris-hoppers and bluff face ravines are initiated by localized slope failure on the bluff face. Since the Kivitoo scarp slopes often stand at angles which are in excess of the angle of internal friction of the constituent sediment in a 'normal' (loose) state of packing, any reduction in the strength of the slope materials could potentially result in slope failure. In situ strength reduction could be caused by an increase in the void ratio of initially dense sediment (deconsolidation) or the eliminaton of cohesion or inter-grain capillary films (as discussed above). Such 'weathering' processes would be favored at locations on the bluff face where soil water is available. If the initial bluff slope is already at or near its frictional threshold angle ($B = \phi'_r / \phi_{rep}$) any further slope failure and flattening requires saturation of a thickness of the active layer with the consequent increase in pore pressure in the potential slide mass. Thus hollows tend to develop where there is a source of moisture from the terrace or where the local sediment contains an ice content sufficient to result in the development of a thin phreatic zone upon thaw.

Once formed, slope failure and regrading may proceed at a more rapid rate within the incipient hollow than along the planar bluff face. Ultimately, the axial slope will regrade to an angle consistent with the frictional properties of the regolith (ϕ'_r, which, for sandy colluvium, is commonly 32° - 36°; e.g. Chandler, 1973) and the local pore pressure regime relative to the rate of profile shotening by coastal retreat.

If failure and regrading is equally distributed along the

hopper's side slopes, the feature will develop a broadly arcuate form, such as that seen in Figure V.10. However, if slope reduction is limited to a particular portion of the hopper's plan, the broadly expressed hollow develops into a feature which has a narrow, regraded, axial slope, above which rise steeper and often straight-contoured side slopes, such as those evident in Figure V.11. When fully expressed, these features are the bluff-face ravines referred to above. The areally confined axial regrading is a result of either a point source of run-off at the back of the hopper knick-line or rapid extension of the axial slope to the terrace and the consequent localization of surface flow paths. Because of this restriction of the moisture source, the side slopes close to the bluff face are left relatively dry and therefore not subject to frequent slope failure and consequent regrading. Side slope reduction is further limited if the local stratigraphy lacks fine-grained or ice-rich units near the top of the bluff. These units where present, would constitute an additional source for the soil water neccessary for failure and regrading of side slopes independent of the run-off from the terrace.

The fact that few bluff face hollows have axial or side slope gradients significantly lower than expected fricitonal values suggests that the rate of undercutting and retreat of the bluff is rapid with respect to the rate of regrading within the hollow. Yet some features, due to their hydrologically and stratigraphically favorable locations, have regraded to expected semi-frictional threshold values.

b. Observation of process

Once the debris-hopper form has developed, continued development by mass-wasting is activated either by the occurrence of positive pore pressures sufficient to cause failure or by undercutting of side slopes. Upward seepage due to the concentration of through-flow in the lower portions of the hopper where flow lines converge can result in the production of a phreatic zone (i.e. positive pore pressures) above the frost table and in failure. Side slope undercutting can result from downward or lateral incision of the axial slope (often in response to marine trimming). Seepage erosion or spring sapping, in which individual soil grains are removed and transported downslope by emergent seepage, may also be an important mechanism of side slope undercutting and retreat. In this way, a steep-walled debris-hopper at the top of the bluff may retrogress as the base of its side slopes is continually undercut and fluvial processes move the entrained sand along a lower angle axial slope.

A typical basal debris flow which has been mobilized by failure of a 31° axial slope, just below the hopper constriction is shown in Figure V.24. Failure was most likely caused by a rise in the water table at this point due to seepage convergence.

Another example of slope failure in a bluff-hollow, shown in Figure V.25a and 25b (K636, Sec. 19-8), occurred on 7/7-7/8, 1977, following two unusully warm days (daytime temperature greater than 7°C, (see Fig. II.3). The sun at this time was

still sufficiently high in the north so that direct insolation was received by these northwest oriented slopes from late afternoon to early morning. The angle of the post-failure slope was 35-36° (measured from the base of the failure to the upslope limit of disturbance). Slope gradients along adjacent debris-hopper axes were slightly lower, in the range of 30-35°.

In the lower portion of the hopper, the broad slightly concave failure surface exposed frozen in situ silty sand (facies C) with numerous sub-parallel ice lenses and an ice content in excess of 40%. When first observed, this slope was smooth and a uniform sheet of water and sediment was moving down over the frozen surface. Several hours later, when the photograph in Figure V.25a was taken, an anastomosing rill system had formed. These tiny rills were 2-5 cm wide, seated on top of frozen sediments and broken by small inter-rill 'ridges' of thawed sediments up to 6 cm high. Steady pulses of water and fluidized sediment were carried in the rills. A disturbed zone of shallow retrogressive sliding extended up-slope of the failure surface, terminating in a small scarp about 2.5 m from the hollow's knick-line. This scarp was retrogressing onto a short debris-mantled section comprised of sediment from a thin beach cap unit. At the base of the hopper, slide debris formed a stoney rampart which had since been breached by the very wet debris flow material being deposited as a small fan over the beach.

The immediate cause of this failure may have been accelerated thawing of the thick ice-rich silty sand unit in the lower portion of the hollow. This could have resulted in

the creation of a thin phreatic layer above the frost table which would have, on this steep slope, created effective stress conditions low enough for failure to occur.

A photographic record of the hopper was made over the course of the 1977 field season. Within a week after the failure, a single master rill had been established and active layer thickness increased to 30-40 cm. By late August (Figure V.25b), the channel had become partially in-filled and the surficial sediments on the slope to the right had been undercut by flowage of wet debris along the hopper's basal slope.

An additional source of phreatic water may be the seepage line apparent in the upper portion of the hopper (marked in Figure V.25a). The seepage here is associated with a clayey unit (facies Wl, D3) above which lay a thin ice-rich silty sand unit (Wc > 40%). It is this latter unit rather than the underlying fine-grained unit which appears to be a source of seepage. (The terrace surface behind the hollow was quite dry.) The rise of the local water table at this point in the hopper is a consequence of the low hydraulic conductivity of the fine-grained unit relative to that of the sandy colluvium. Melt-water moving downslope from the overlying silty sand is therefore 'forced' to the surface, as shown schematically in Fig. V.26. In this particular case, the role of the clayey unit is not as a source of ice-rich (i.e. thaw-unstable) sediment, but rather as the generator of a 'perched' phreatic zone (perched stratigraphically above the slope base as well as perched above the frost table). The unit is also a source of fine-grained sediment promoting the development of post-failure

debris flowage (discussed in the next chapter). Considering the glacial origin of the sediment, and therefore the presumed low clay mineral content of the clay sized fraction (Smalley, 1971), the residual angle of internal friction is probably not much lower than that of the overlying sandy silt (32-36°). Slope failure is therefore not a function of the lower frictional strength of the clayey colluvium, as is often assumed when clayey soils are involved, but rather the higher pore pressures above it. Excavations revealed that the softest material was several cm above the frost table, while the thawed clay at the frost table was quite stiff (frozen samples when thawed and remoulded by hand were only slightly plastic) supporting the contention that failure was seated above the thawed clay and not within the clay, nor at the frost table. Thin fine-grained units may therefore assume a role in promoting the slope failure which results in hollow development by providing relatively low hydraulic conductivity soil which results in the localized development of phreatic layers.

c. 'Nivation' - The role of snow

The lower slope gradients sometimes encountered near the top of the debris-hopper are, in many locations, due to slope regrading associated with saturation of the active layer and seepage at this level. Locally, snow plays an important role in the creation of such groundwater conditions. Where snow patches are present - which is in fewer than half of the bluff face hollows as of late June - the water table rises to the

slope surface at the upslope edge of the patch as groundwater, supplied at the knick-line, moves downslope through the progressively thinning active layer. This results in saturated or seepage conditions at the upslope edge of the snow patch. If the slope above the snow patch is sufficiently steep (i.e. greater than 1/2 tanϕ') failure will occur at this location. Post-failure movement of the debris often takes the form of sediment flows over the snow patch. An upper zone of disturbance is a common feature of debris-hoppers with snow patches. Figure V.27 shows this situation at the northwest end of Survey Line II. Snow patches may also be an important source of ground water throughflow along hollow axes. The combined effects of a snow patch are shown schematically in Figure V.28. One interesting result of slope failure below a snow patch is the creation of a frozen scarplet immediately beneath the patch as thawing of the underlying sediment is prohibited by the overlying snow (see Figure V.28).

The role of 'nivation' in hopper development should not be overstressed. It is obvious that snow is an important source of soil water in many, but not all, of the bluff-face hollows at Kivitoo. As such it may accelerate hopper growth and development but is not necessary where other sources of moisture are available, nor can snow account for the initiation of hollows.

d. Side slope undercutting and axial incision

As the axial slope flattens or becomes incised, it may

become burdened with a coarse lag deposit or poorly-sorted debris flow materials that armors the axis. Water carried along the axial slope is unable to establish a central channel in such materials and migrates towards the edges of the lag debris. Thus, there is a tendency for the flow to become established at the sides of the axial slope where it can cut down into the more easily erodable in situ sediments. This lateral shift results in undercutting of the axial side slopes (as in Figure V.11) and widening of the hollow. Another armoring mechanism observed in several hollows, is the presence of ice frozen to the sediment along the hollow axis. In shaded locations where there is a sustained flow of water, this ice may last well into August.

If, for some reason, such as the intersection of a particularly resistant unit (boulder lines, cemented diamicts, etc.), the axial flow cannot cut downward, it will erode horizontally, cutting a niche into the frozen sediments at the side of the hollow. (The same process is responsible for the undercutting of the banks of the larger streams, as described above.) Figure V.29a shows the basal slope of a bluff face hollow along Survey Line II, in which the flow has cut laterally into frozen fine sands. This horizontal incision appears to have been initiated just above the contact with a compact diamict (facies B13) unit through which the flow was unable to cut down. The outside edge of the laterally incised niche has collapsed and refrozen, creating a 'pseudo-pipe' through which flow has been maintained. This pipe may remain open following flow subsidence and drainage in the autumn,

remaining as a conduit within the permafrost. As the hollow axis retreats with the bluff line, the conduit may be left above the new axial slope and subsequently be exposed high in the hollow side walls (Figure V.29b). Alternatively, the pipe may backfill with water and refreeze, leaving a clear ice cast of the pipe within the bluff (Figure V.29b).

4. Taluvial lag slopes: Extreme conversion

As rilling and unconcentrated surface flow within the hollow removes finer material from the axial slope a very poorly-sorted active layer soil is developed, the coarser materials being left behind as a lag deposit. An example of such a slope can be seen forming the basal slope of the hollow in Figure V.29a. (In this instance the taluvial slope does not extend to the terrace, but is backed by the steep side walls of the bluff face hollow.) This eluviation of fine sediments creates a slope comprised of mixed coarse debris and finer colluvium, sometimes called taluvium (e.g. Wentworth 1943). Such poorly-sorted materials typically have high residual angles of internal friction, generally in the range of 43-46° (Carson 1971).

The bar graph of bluff face hollow gradients in Figure V.22 contains angles of less than 30° and as low as 24-25°. Inspection of the bluff panorama shows that most of these lower limit slopes (e.g. the hollows at K136, 28°; K166, 28°; K168, 28°; K176, 28°; K181, 25°; K182, 25°; K284, 28°) are mantled by lag deposits with a taluvial texture. The 'channels' of

hanging gullies, at the point where they are being cut back by the bluff line (e.g. at K256) are comprised of similar mixed-grain debris. The gradient of these gully segments ranges from 18° to 29° (as taken from the profiles in Figure V.19 and indicated on the bar graph). The steeper channel segment gradients therefore overlap with the inclinations of the more gently inclined of the hollows.

Both the taluvial slopes in the hollows and the gully segments described above occur in wet locations, i.e. they are situated where there is a large amount of run-off is intercepted at the bluff edge. For example, the hollows between K166 and K182 are backed by a steep section of the terrace (slope > 5°) over which unconcentrated surface wash is abundant (as mentioned above). Naturally, the hanging gullies also receive considerable run-off.

The taluvial lag slopes are therefore located in positions where the water table is most likely to reach the surface with some frequency. In addition to the high run-off, these slopes develop where the local stratigrapy contains a wide range of available grain-sizes, particularly where there is a large proportion of larger clasts. Where large amounts of run-off are intercepted along the predominantly sandy bluffs, more deeply incised hollows develop and taluvial lag slopes are absent.

If the groundwater table commonly rises to the surface along these taluvial slopes with flow parallel to the slope, then the ultimate stable slope angle (as defined by the infinite slope analysis) will approach the semi-frictional

value. Substituting the observed range of slope gradients (24-28°) into Eq. III.11, an angle of internal friction of 42-47° is calculated for the slope materials. This result is in reasonable agreement with the values of friction angles for taluvium noted above. Thus, the lower limit for hollow slope development, as well as the upper limit of the steepness of active hanging gully channel segments, appears to be controlled by the semi-frictional angle of the materials which form these taluvial slopes. Of course, at very high rates of undercutting the taluvial slopes may not be able to regrade entirely to semi-frictional values.

From the preceeding discussion it may be concluded that, in most cases, the ultimate effect of dissection by debris-hoppers and bluff face ravines is to produce an axial slope inclined at the relevant semi-frictional theshold angle. Further retrogression of the hollow onto the terrace surface, leading into gully development, cannot occur unless run off is sufficient to entrain the surficial sediment and move it along slopes of lesser gradient than the semi-frictional angle. Low-gradient retrogression and gully development is, however, unlikely in most situations due to the large size of the lag material and ultimately, the limited amount of run-off which is carried within most of the bluff hollows. However, elaboration of the mechanisms of gully development and extension is beyond the scope of this study.

5. The spacing of bluff face hollows and their relationship to moisture sources

The preceeding discussion makes it clear that soil moisture is instrumental to the processes of hollow formation. This water is derived either from the terrace surface behind the bluff or from the thawing of ice-rich sediments on the bluff face. In the former case, the development of the hollow is dependent upon the hydrological conditions on the terrace surface. If ice-rich sediments are found in the bluff, hollow development can be initiated, and in many cases proceed, independently of the run-off received at the bluff knick-line. Hollow development in this case is independent of the terrace hydrology and therefore is primarily a function of bluff face processes and and hence stratigraphic composition.

South of K240, where fine-grained units and ice-rich sediments are present in the upper portions of the bluffs, debris-hoppers are particularly well developed and closely spaced. There is little or no extension of the knick-line between hollows. Most of the available space at the knick-line has been eliminated by the growth of the hollows. The steep, coast-parallel portions of the bluff face are therefore effectively cut off from the terrace surface. Presently only small 'incipient' hollows can form on these spurs suggesting that some supply of surface run-off is necessary for the continued development of hoppers at this location, if not for their initiation. Some smaller features, such as the incipient hollow at K184, which is located on a portion of the bluff face

adjacent to a gully side and consequently relatively dry, are able to develop, albeit slowly, depending entirely upon bluff face processes. Several hollows in hydrologically unfavorable positions were examined. One particularly active hollow at K353 was investigated in some detail. The stratigraphy here was comprised of thick fine to medium sand units with layers of very fine to silty fine sand occurring in the upper half of the bluff. The cap unit was a gravelly coarse sand approximately 2 m thick. The finer-grained sediments had frozen moisture contents of 35-62%. These sediments were unstable on slopes of 30° or more. Small slides continued downslope movement as sediment flows on these steep slopes. Water content of these flows was 22-26% and one 'standing' sample still had excess water on its surface with a water content of only 13%. Thus, these sediments are capable of liquefaction-type flow as considerable water must be expelled before they obtain their normally consolidated state.

The surface drainage lines on the terrace behind this hollow clearly ran towards bracketing gullies and away from the hollow's knick-line. That the source of moisture is the high-ice sediments is indicated by the dark saturation lines marking these units on the nose slopes and hollow side slopes near the bluff face. In other cases, once the initial hollow develops, snow may be an additional moisture source independent of terrace hydrology.

Although there is an obvious relationship between bluff face hollows and surface drainage lines along the bluffs south of K240, this relationship is, in a sense, unimportant with

respect to hollow location. Here, the spacing of the hollows seems to be more a result of 'competition' between hoppers for a relatively uniform supply of water along the bluff edge. The nature of the drainage net at the bluff edge is probably more dependent upon the initial locations of the incipient hollows than vice versa. In other words, once the hollows develop, their location may alter the hydrology of the terrace surface so that run-off now becomes aligned with the hollows. Close spacing of hollows also occurs along the bluff from K630-645 where the stratigraphy contains similar finer-grained units near the top of the bluff.

Northwest of K240 (Fig. V.14) where the bluffs are topped by the organic mat, and where the stratigraphy is predominantly sand and lacks fine-grained units, the hollows are widely spaced and separated by extensive stretches of undissected knick-line. The large hollows along these bluffs are inevitably associated with specific drainage features on the terrace surface (e.g. the depressions along Survey Line IV, or the melt accumulation areas seen in Figure V.14). The hollows here bear the morphological characteristics of bluff face ravines, and large alluvial sand fans spread out on the beach below many of these features. Particularly long undissected sections of the bluff face are found adjacent to the larger streams and in other topographic situations where the flow of water is away from the bluff edge (e.g. at K272-282 or K411-430). The development of hollows along these sandy, organic mat topped bluffs is entirely dependent upon water from the terrace for their initiation and growth.

6. Summary

Steep dissected bluffs occur along undercut sections of coast line where the stratigraphy is comprised primarily of interbedded sandy sediments and lacks thick fine-grained units. The dissection represented by the bluff-face hollows develops as laterally preferential failure of the active layer leads to local slope flattening of the bluff face. This instability is a result of localized saturation of the active layer, due either to thawing of ice-rich sediments or seepage received from the terrace surface behind the bluff. Once the hollow form has become established, it may further concentrate seepage arising both from the terrace and along the hollow walls, resulting in elaboration of the form. Snow which accumulates in the hollow may be an additional source of phreatic water. The development of hollows also tends to divert water away from those portions of the bluff face between the hollows, inhibiting the regrading of these steep slopes. In very sandy bluffs, where icy sediments are lacking, the spacing of hollows is primarily a function of local sources of run-off from the terrace.

The dissection of undercut slopes represented by the Kivitoo hollows is a fundemental, though little recognized, mode of the development of steep slopes in many different environments. Hollows may be separated into debris-hoppers, in which mass movement is more or less evenly distributed along the side walls of the upper hollow producing an inverted cone-shaped form, and bluff-face ravines, in which fluvial

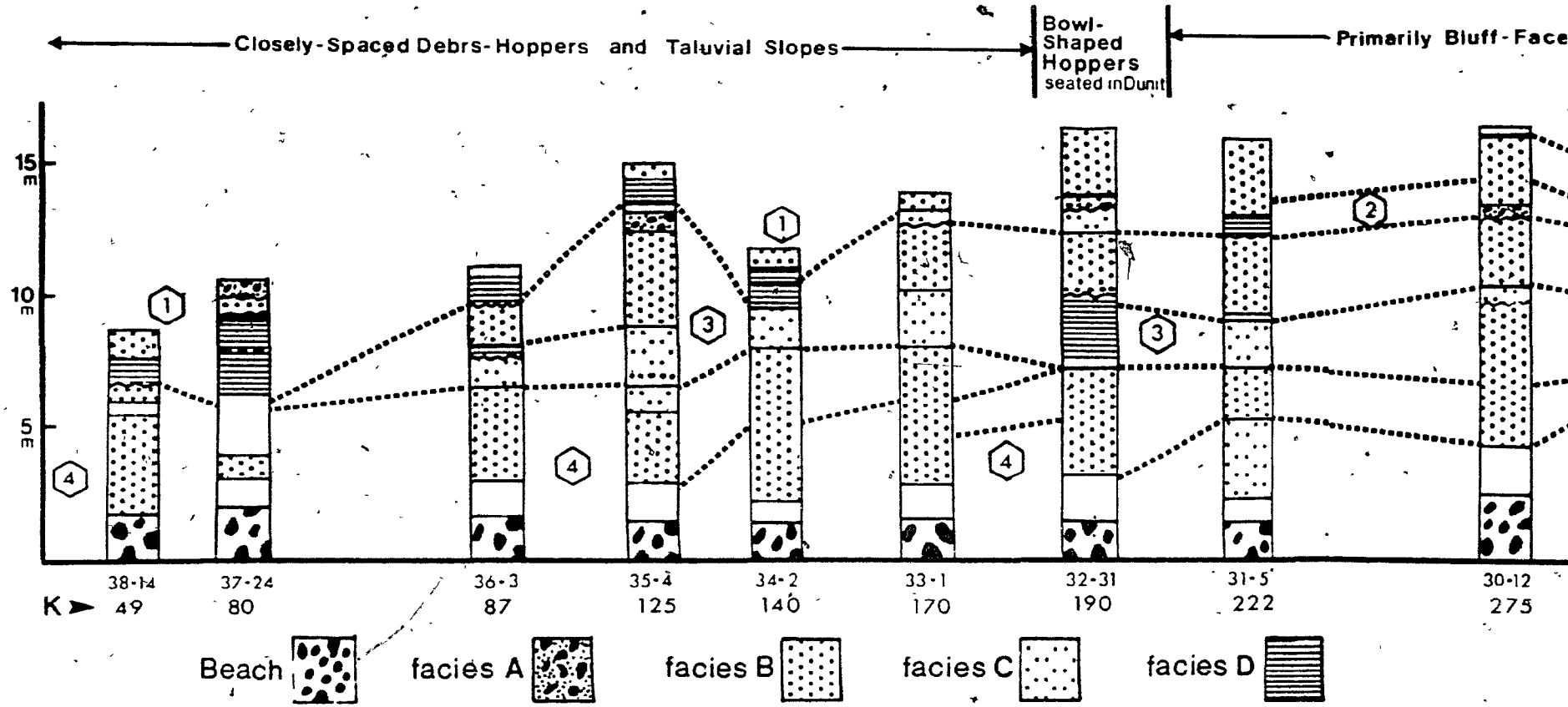
processes and a point source of seepage at the knick-line may be instrumental in creating an incised axial slope and a more elongate planform. The limited run-off intercepted at the bluff edge keeps most bluff-face ravines from developing into true gullies. Hollow axes in wetter areas and stony lithologies may develop into slopes standing at the semi-frictional threshold angle of the poorly-sorted lag (taluvial) deposits which develop along these slopes (via the eluviation of fine materials).

TABLE V.1

BULK UNIT WEIGHT AND MOISTURE CONTENT OF STEEP FACETS IN SAND

Description	No. samples	Moisture content	Bulk unit wt. (dry, kN/m^3)	Porosity
Steep (70-80°) undercut facet along debris-hopper side slope. Same unit maintains 45-65° slope on the face of the bluff. (K143)	4	7%	15.5	40%
Steep undercut facet along bluff face (K116, Profile A-2)	2	18%/13%	15.9/15.7	39%/40%
Well-sorted medium sand (bedded). Slope angle is 45-55°. (K277, A-4) Frozen moisture content is 20%	4	8%	15.0	42%
Sand apron at base of bluff below bedded sand unit. Slope angle is 34-35°.	2	7%/5%	15.3/14.6	41%/44%

Figure V.1 The stratigraphy along the steep dissected bluffs and its relationship to the morphology and development of bluff-face hollows. (Stratigraphy is simplified; see Appendix D for detailed stratigraphy.) From Nelson 1980.



bluffs and its
-face hollows.
d stratigraphy.)

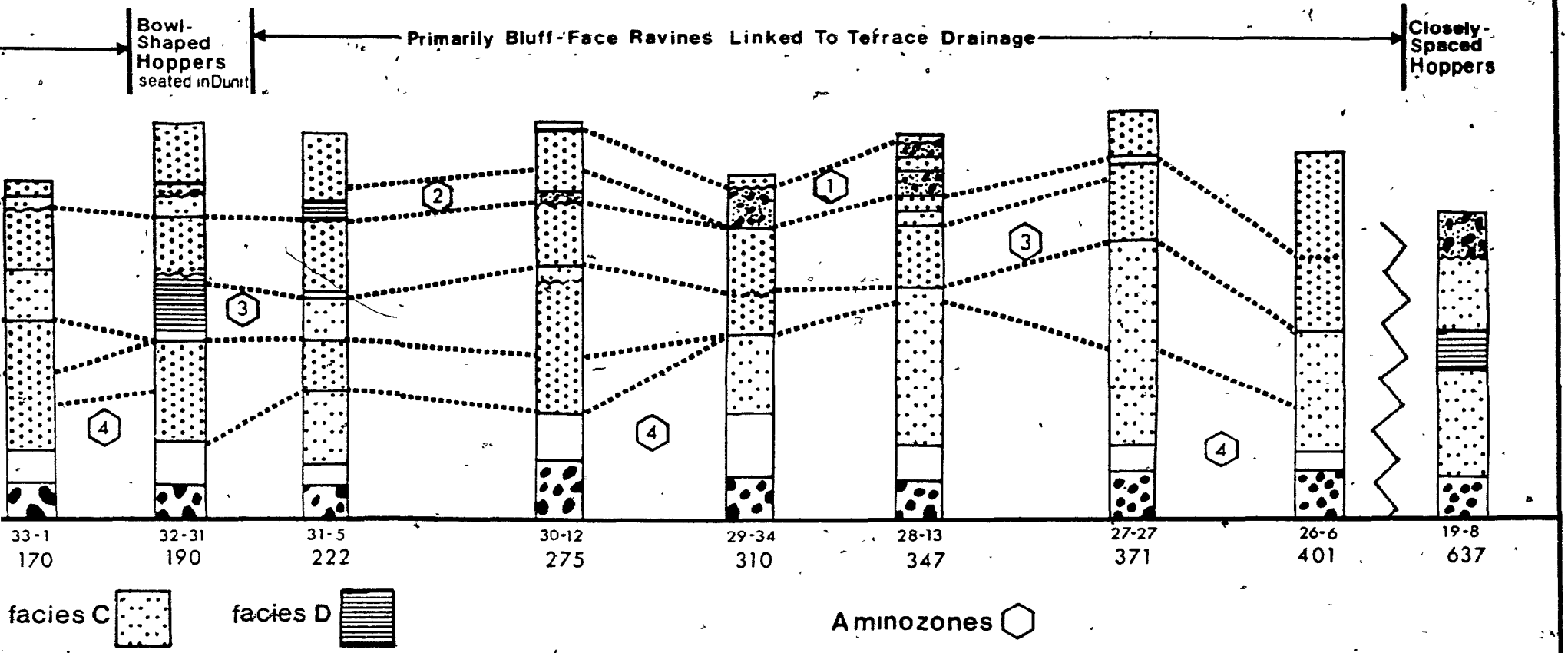
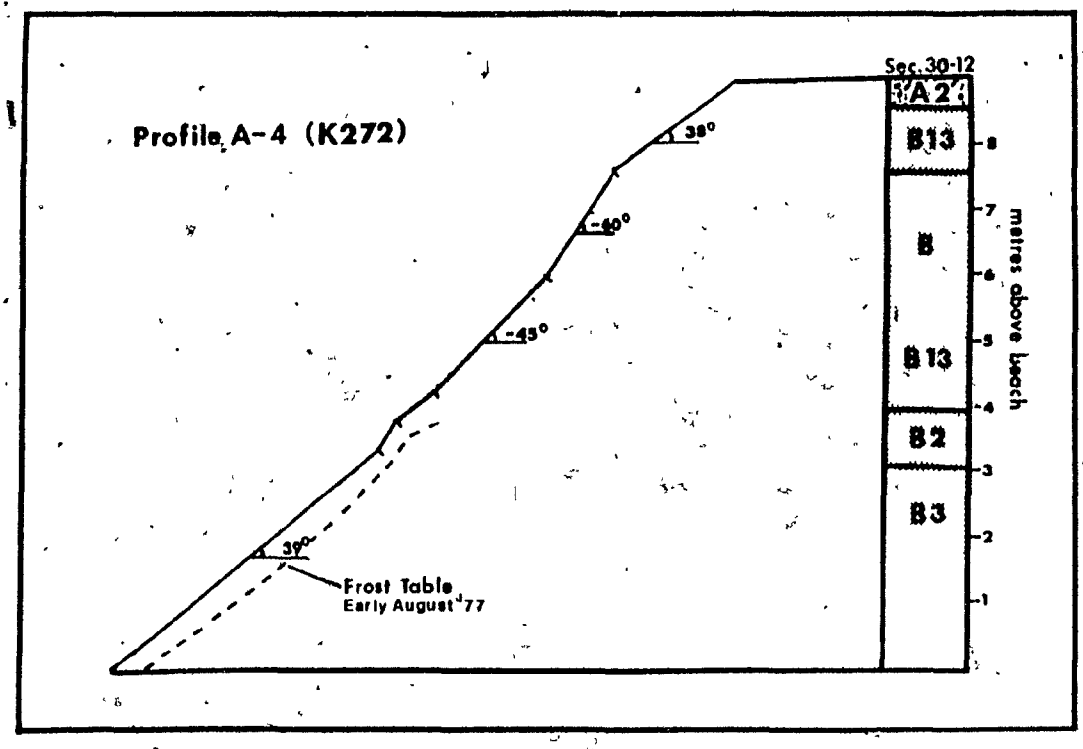
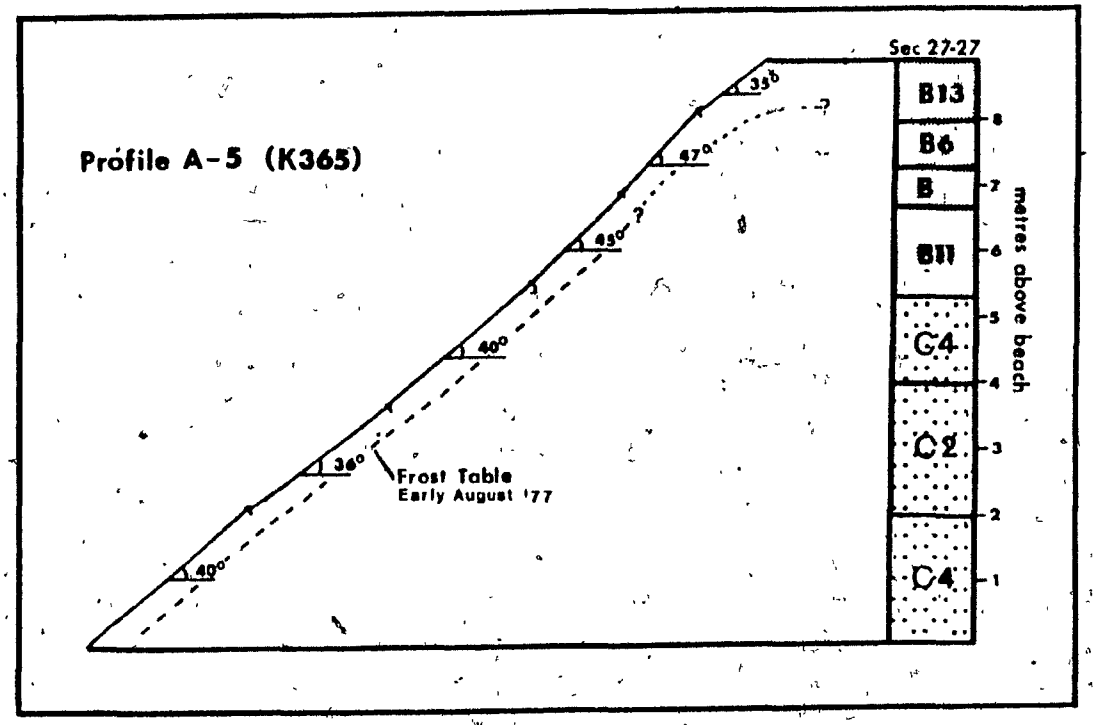


Figure V.2 Profiles of representative scarp slopes along the steep dissected bluffs. Local stratigraphy and frost table depths are shown. Additional profiles in Appendix B.





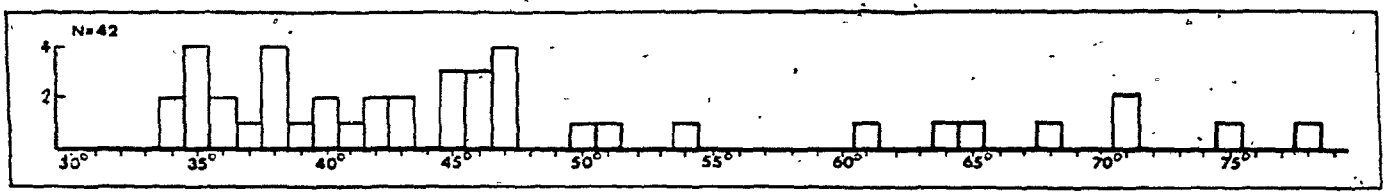


Figure V.3 Bar graph of slope segment angles from scarp slope profiles and spot measurements. Most segments are below 48°.

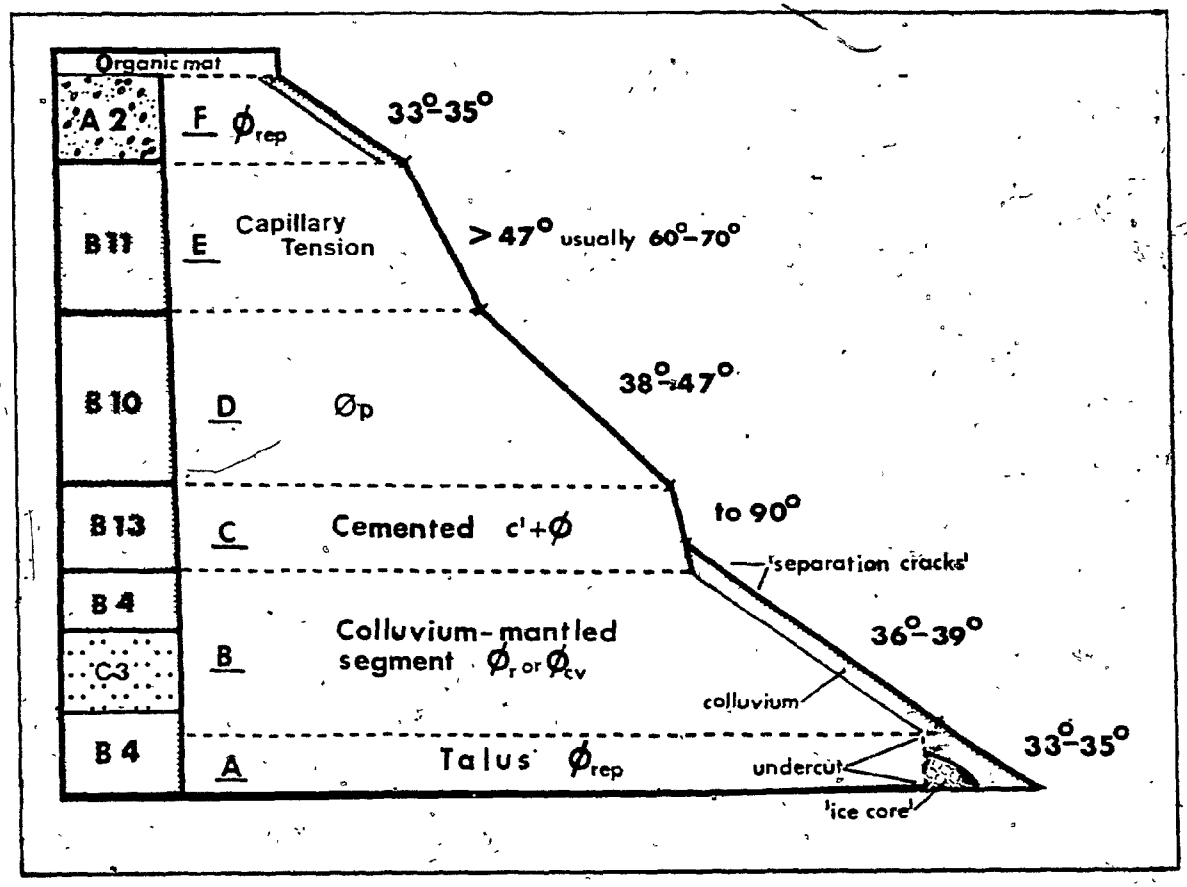


Figure V.4 Schematic model of a theoretical undercut scarp slope developed in interbedded, predominantly sandy sediments. This model is loosely based on the scarp slope shown in Figure V.5. Symbols are explained in the text, stratigraphic notation in Table III.3.



Figure V.5a Scarp slope at K268, July 1977. The following two photographs show this same slope in 1976 and 1983. A - High-angled bedded sands, note etching of bedding planes which are being exposed in situ. B - Cemented diamict, maintains steep slope. C - Basal talus.



Figure V.5b Same scarp slope as in Figure V.5a (above) in August 1976. Slight changes in the basal talus are noticeable, otherwise slope appears to have changed little in one year's time. (Photograph by J.B. Bird.)

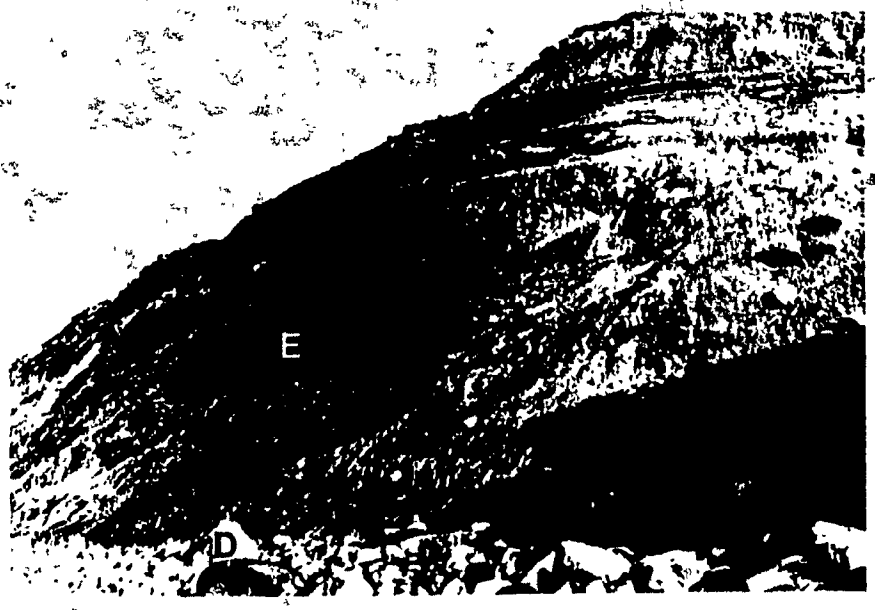


Figure V.5c Scarp slope shown in Figures V.5a and V.5c in mid-July, 1983. Undercutting and minor retreat (ca 0.5-1.0 m) of the slope base is evident. Compare, for example, the position of the rock (D) in relation to the bluff. Much of this retreat, however, may be due to the removal of the basal talus, and once this reforms, the net retreat of the slope base may be less conspicuous. Note also the sloughing of the bedded sands at E, again a response to basal trimming.

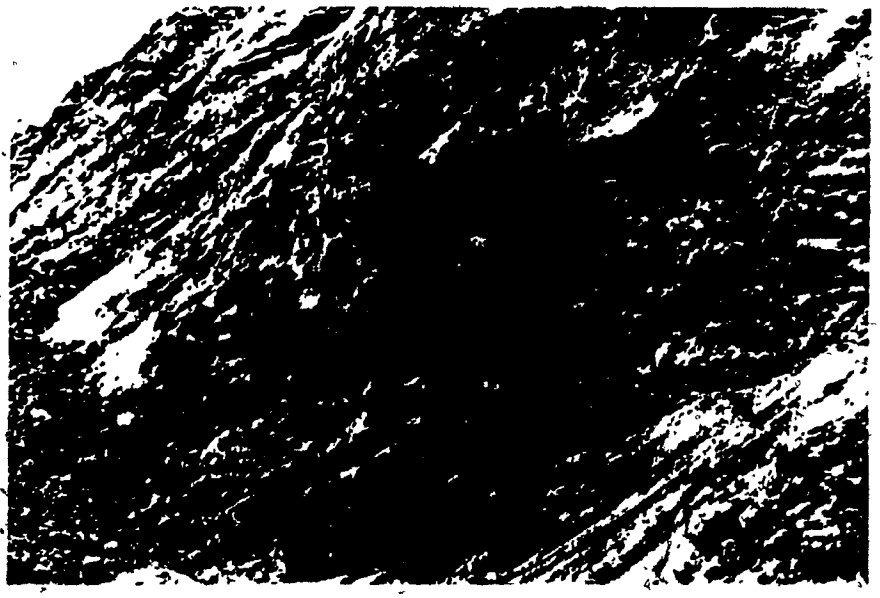


Figure V.6 Trimming of the bluff base by wave action along Survey Line ~~II (K112-132)~~. Steep segment in bedded sands (see below, section V. 2c) is approximately 2 m tall. Little debris from the bluff face has accumulated since the undercutting occurred. Note also the high-angle spalling of the in situ sand unit.

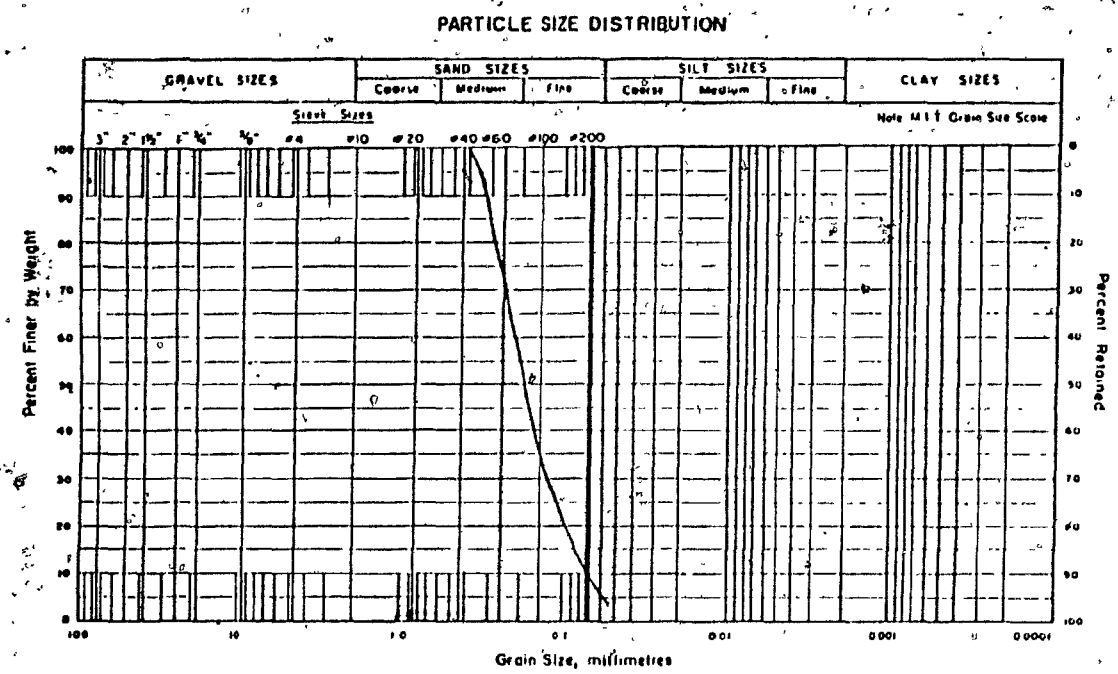


Figure V.7

Grain-size sample from steep slope in bedded sands. Uniformity index (Q60/Q30) is approx. 3, indicating a well-sorted material. The sample is from the bottom of Profile A-2.



Figure V.8 Exfoliation and spalling of lightly cemented, fissured medium to fine sand along high-angled scarp slope at K934. Slope segment is 7 m high. Fissures are subparallel to or slightly steeper than the slope which is inclined at ca 70°.



Figure V.9 Accumulation of talus at base of sandy scarp slope by rapid graular disintegration following several days of below freezing temperatures. Note also undercut basal segment (with bedding planes etched out) which is not being coved by the talus. (August, 27, 1977)

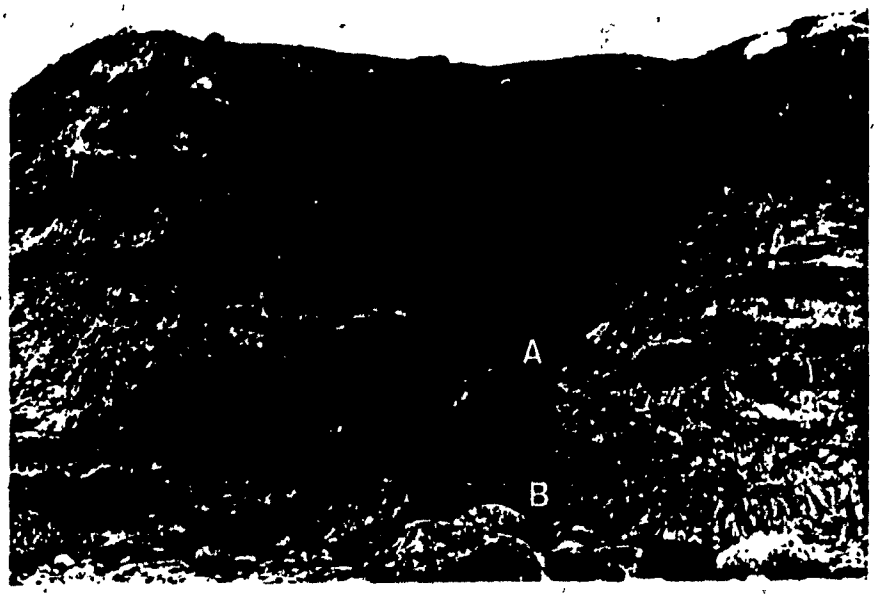


Figure V.10 Debris-hopper at K127. This bluff-face hollow displays a broadly arcuate plan form. The side slopes of the hopper steepen towards the bluff-face. The slopes of the upper debris-hopper are convergent upon the constriction at A. Failure has occurred along the basal slope below A. Poorly-sorted debris flow deposits accumulate at base, B.



Figure V.11 Bluff-face ravines at K291. (6' stadia rod is located below 'X' for scale.) Overall inclination of the incised axial slope is 31 . Side slope contours are predominantly straight-in-plan. Debris movement is convergent upon the length of the axial slope rather than upon a point near the bluff-face, as in the hollow shown in Figure V.10 . The axial slope has also extended to the knick-line. Side slope profiles approach those of the adjacent bluff-face, in response to under-cutting along the axial slope, as at A. Note also debis flow deposits, B, and alluvial sand fans, C.

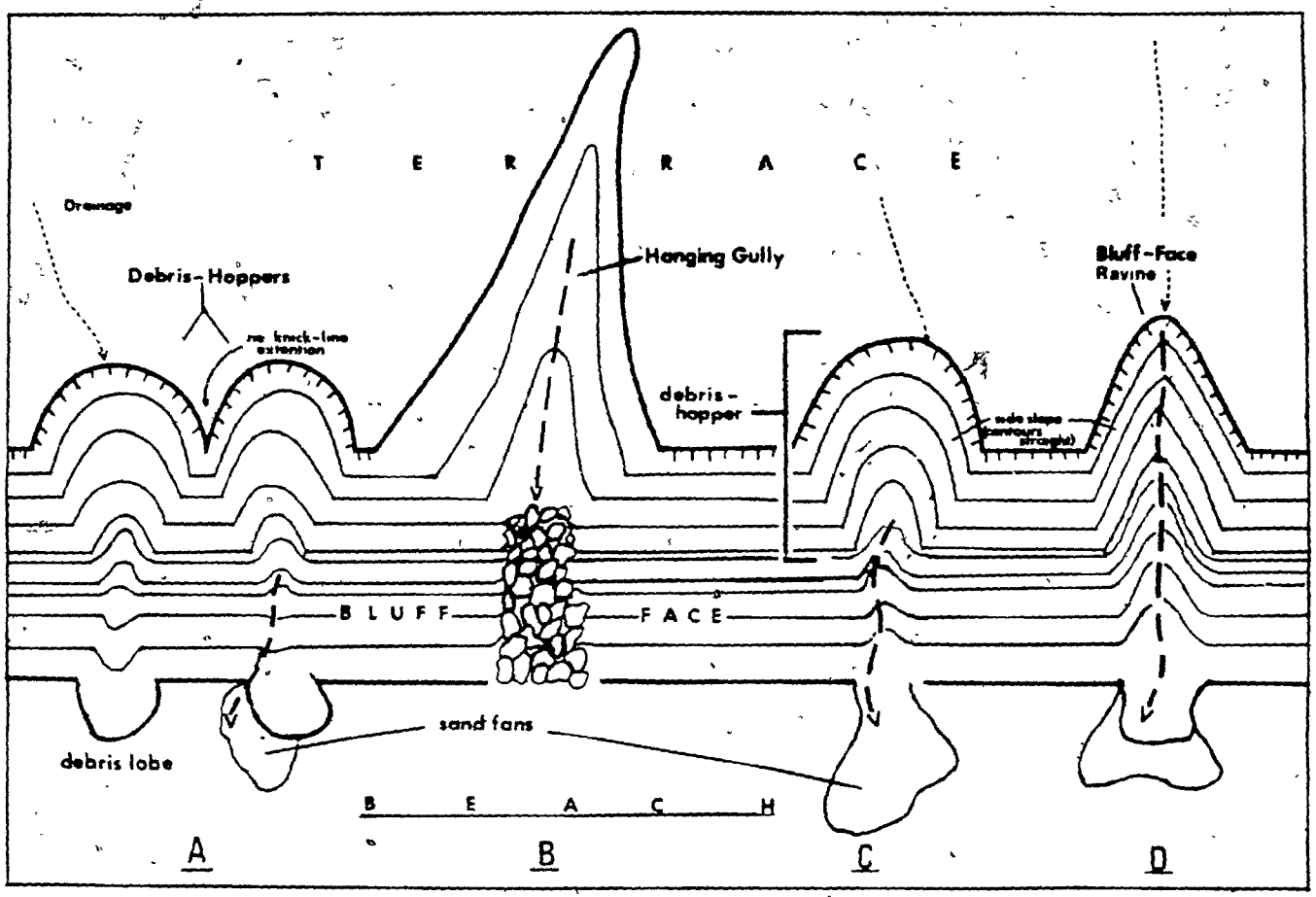


Figure V.12 Schematic representation of bluff-face hollows along the steep dissected bluffs. See text for discussion.



Figure V.13 Surface drainage on terrace behind debris-hopper at the northwest end of Survey Line II (ca K140). Bluff knick-line is marked by probe at A. Linkage of shallow depressions creates an amorphous, discontinuous surface drainage net. (Photograph taken in early July, 1977.)

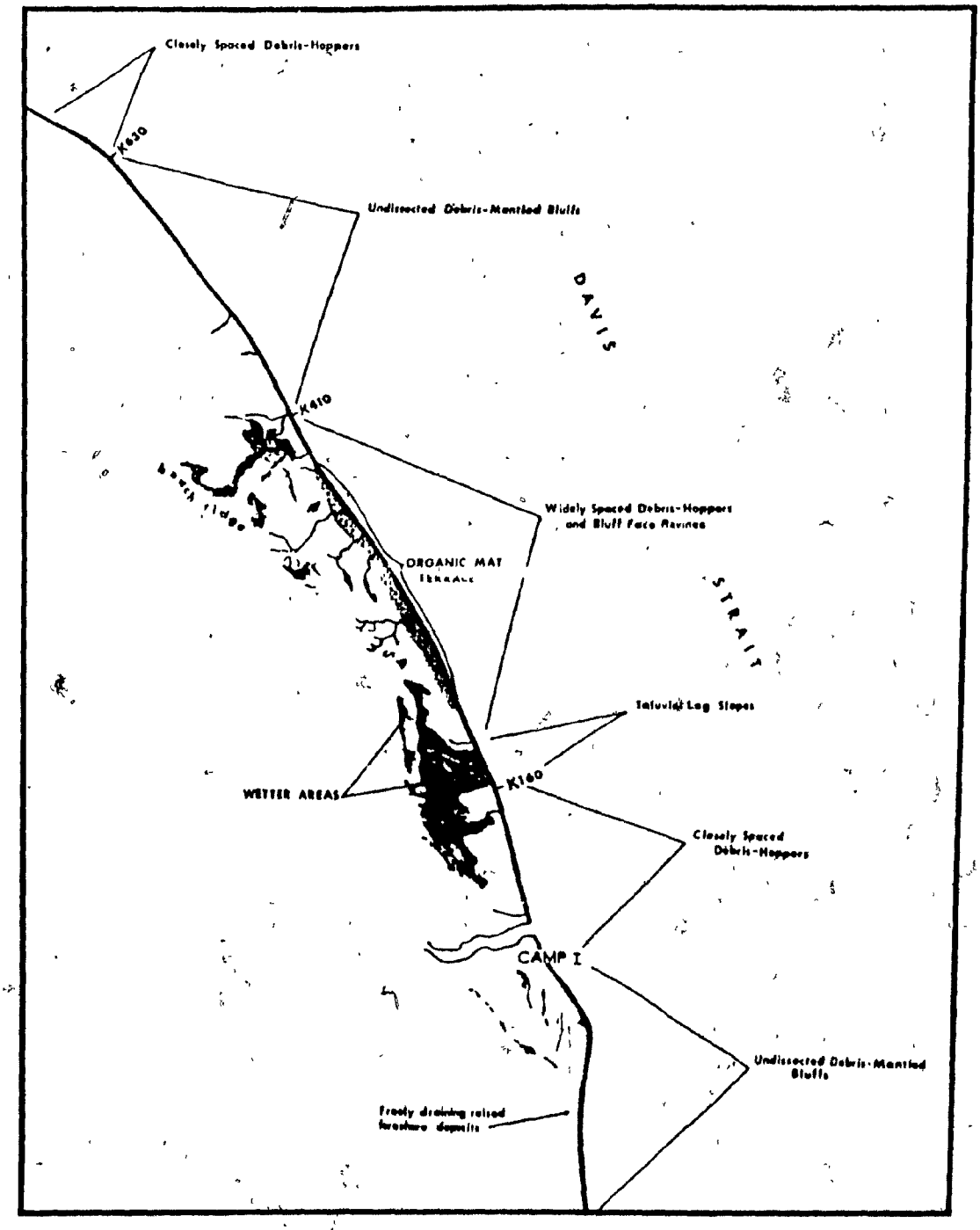
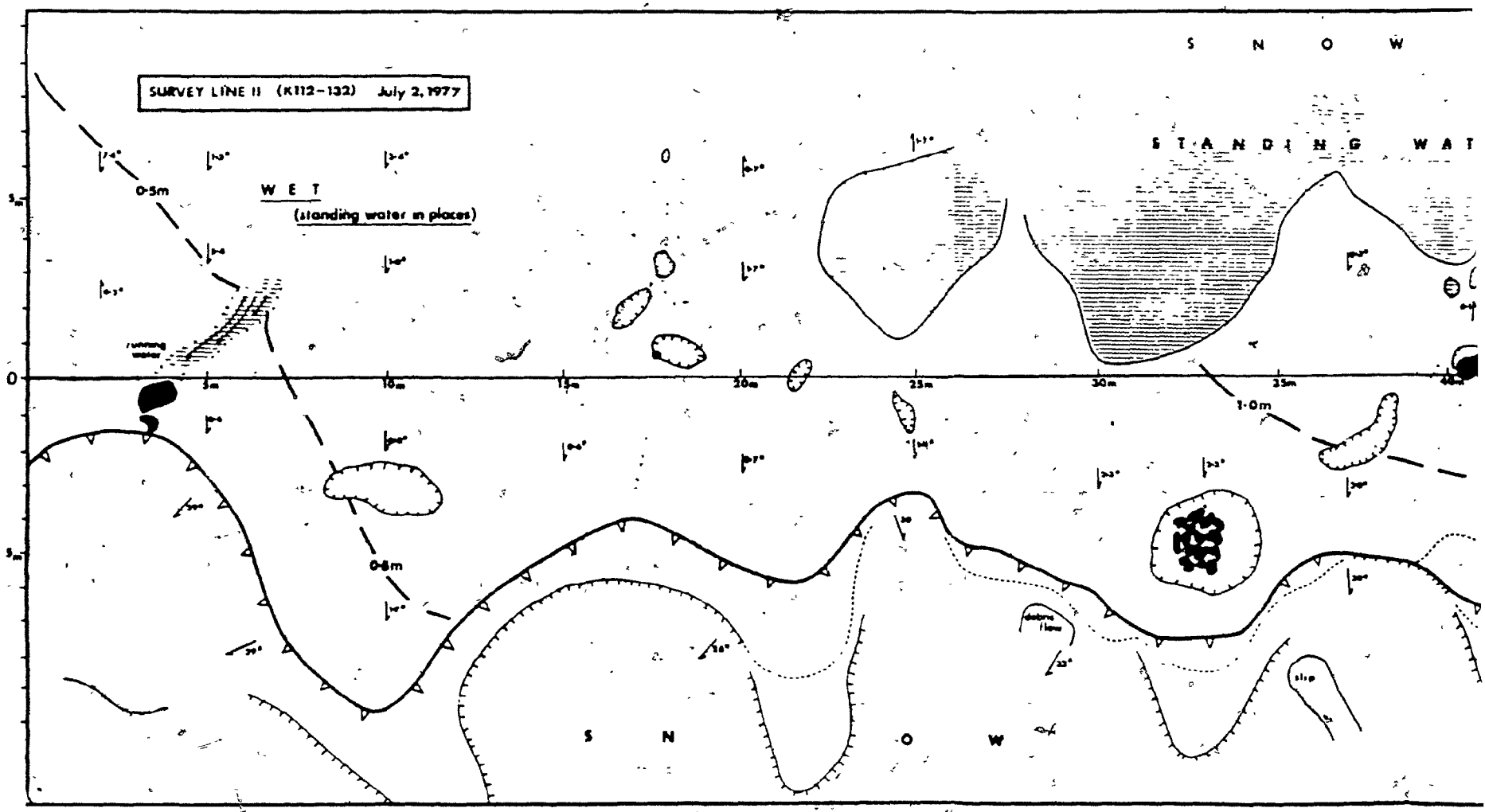


Figure V .14 Distribution of bluff morphology and terrace surface types along the steep dissected bluffs.

Figure V.15 Survey Line II, July 1977. Theodolite survey; contour elevations are relative. The general slope of the terrace surface is towards the lower left of the diagram. The bold line marks the edge of the intact terrace surface, the hatched line marks the major break in slope between the terrace and the bluff face.



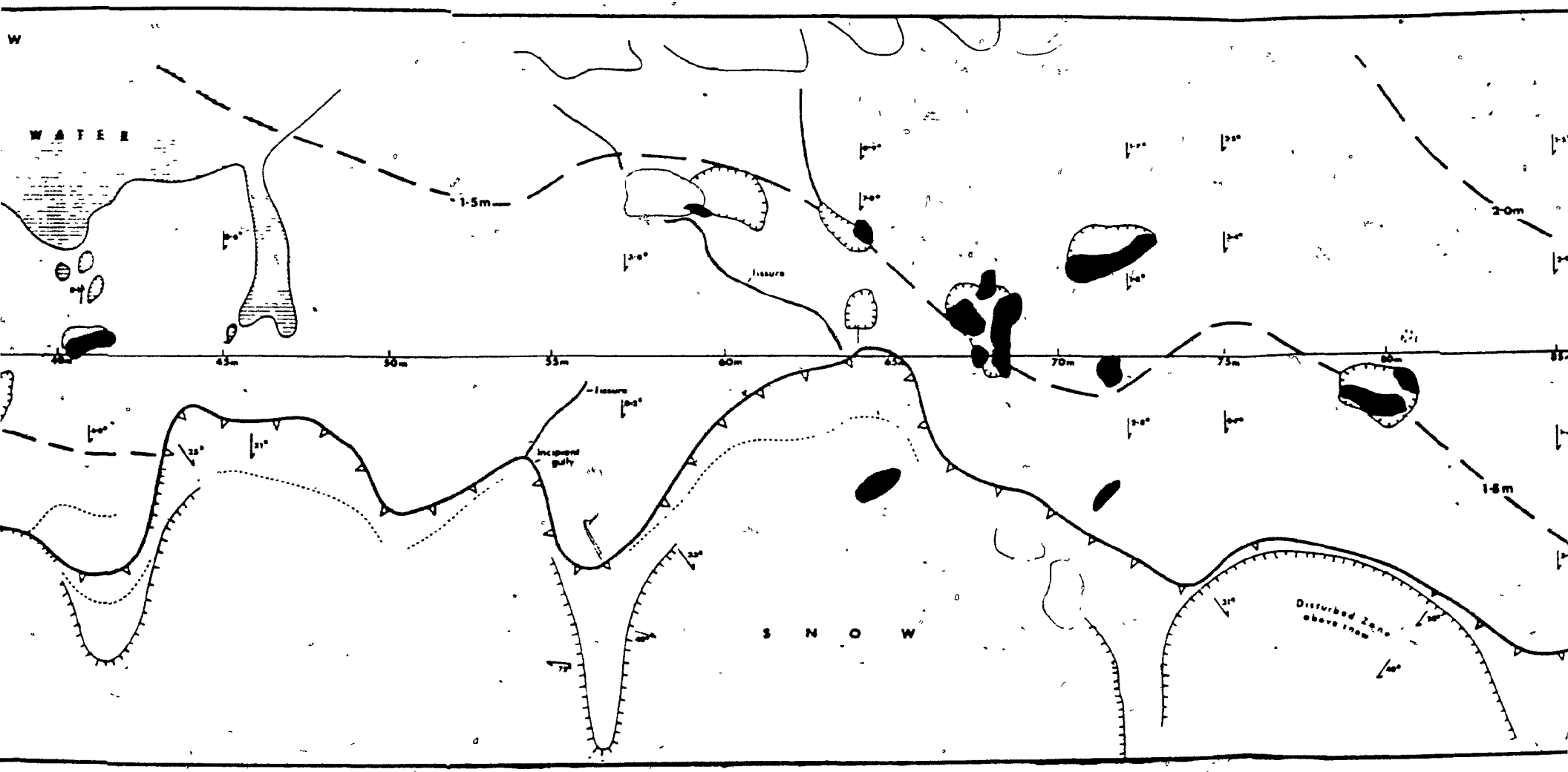

W
WATER
1·5m
2·0m
1·5m
Fissure
Fissure
Incipient gully
SNOW
Disturbed zone above snow
45m
50m
55m
60m
65m
70m
75m



Figure V.16 Subsidence of terrace surface behind bluff-face hollow shown in Figure V.30 (K99). Internal erosion (piping) of the active layer is believed to be the cause of subsidence. Piping was evident at A where the sound of running water beneath the ground surface was clearly audible. (View is inland from bluff edge.)



Figure V.17 'Organic mat' - type terrace surface along the steep dissected bluffs northwest of K240. The low boulder frequency and smooth, uniform ground surface are clearly evident. The upper portions of the bluff-face ravines, well defined knick-line and steep hollow side slopes are also seen. Beach ridges, partly masked by aeolian deposition are seen in the background, A.



Figure V.18 'Stabilized' channel behind bluff-face gully along organic mat terrace surface near K305. Drainage may be along a raised longshore trough which has been masked, in part, by aeolian sedimentation. Note that there is very little low-angled retrogression of the bluff-face ravine onto this swale. The location of the hollow on the bluff is a result of the localization of run-off by the swale.

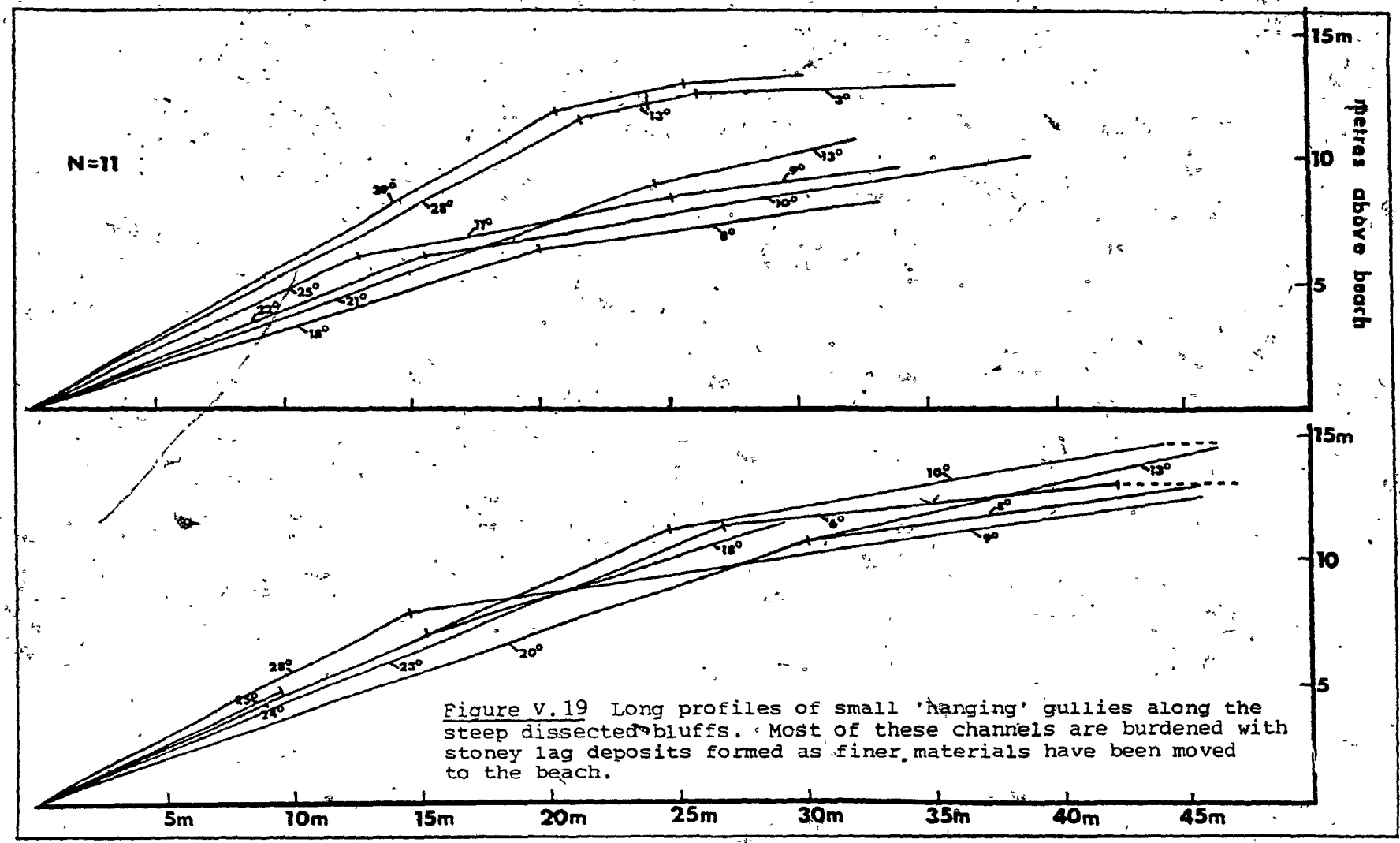


Figure V.19 Long profiles of small 'hanging' gullies along the steep dissected bluffs. Most of these channels are burdened with stoney lag deposits formed as finer materials have been moved to the beach.

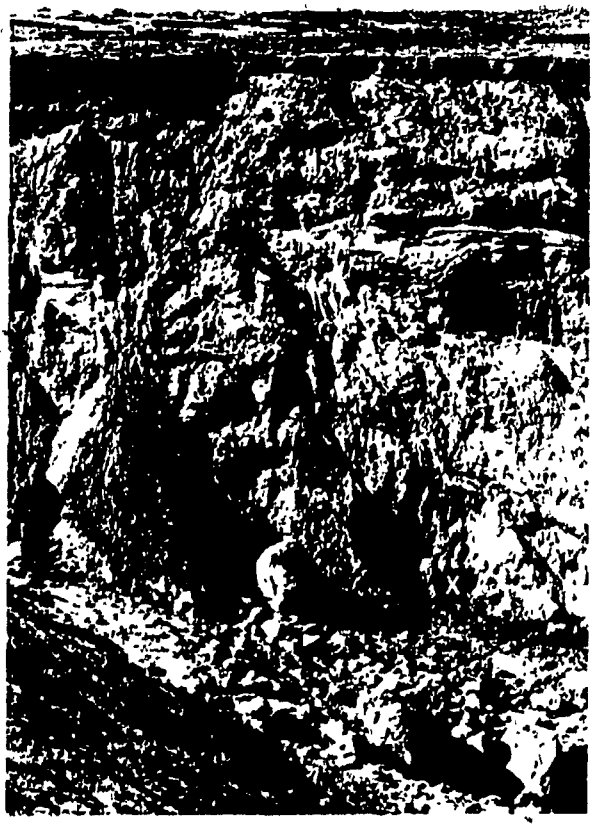


Figure V.20 Undercutting of frozen ground along the side of a gully crossing the dissected bluffs. Avalanching of debris back over the laterally incised niche leaves a conduit isolated within frozen ground, creating a 'pseudo-pipe'. Re-emergence of flow is seen at 'X'. The beach is just out of sight to the lower right of the photograph.



Figure V.21 Collapse of the modern beach as a pseudo-pipe, originally formed along a gully side slope, is intersected by the retreating coastline. Note the thinness of the coarse beach deposits. The frost table along the beach is only 50-70 cm below the surface. Fine sandy sediment is currently being deposited as a micro-delta in the intra-permafrost conduit at 'A'. (Divisions on stadia are one foot (30.5 cm).)

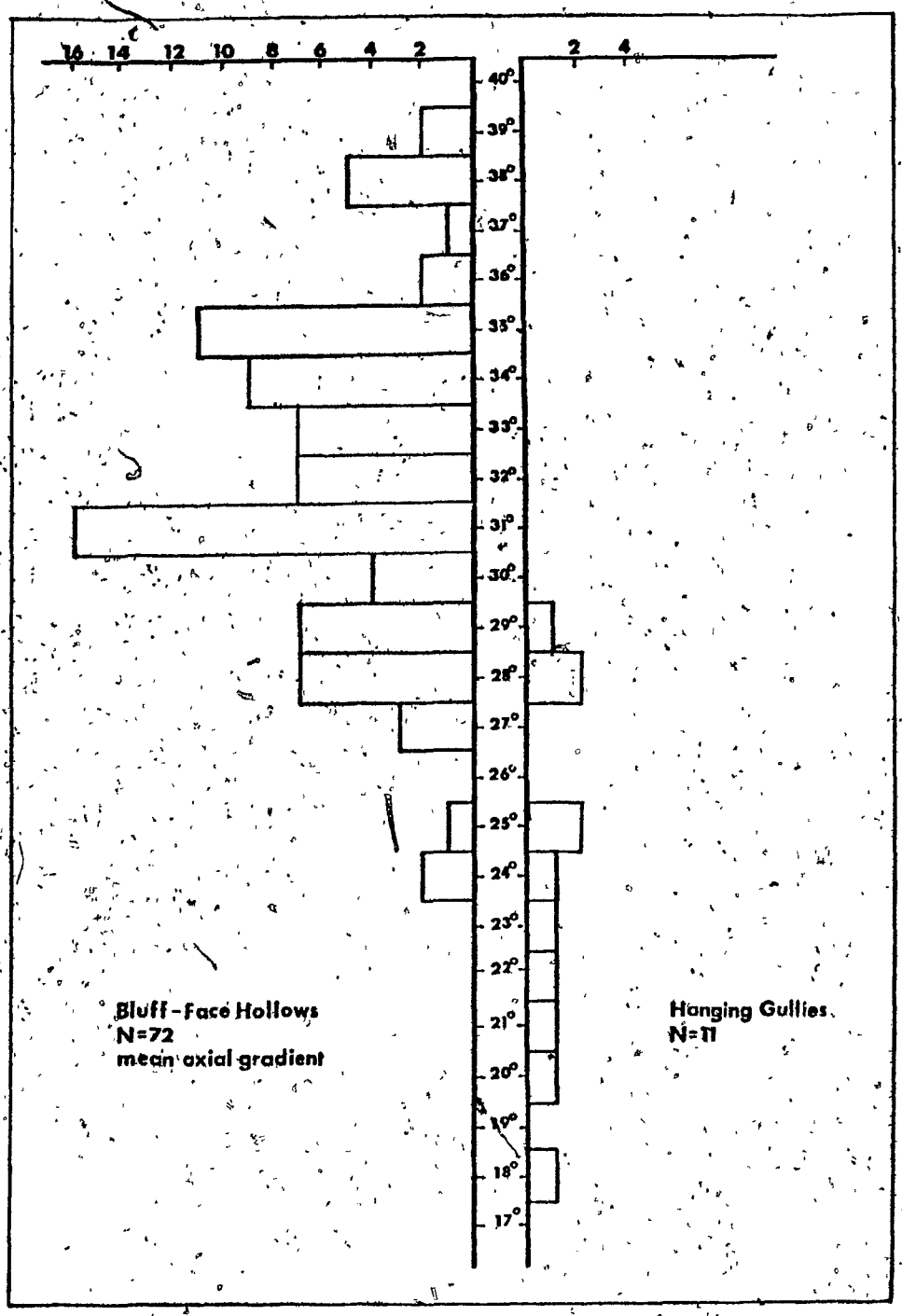


Figure V.22 Bar graph of the mean inclinations (knick-line to beach) of bluff face hollows and steepest segment angles for small hanging gullies along the steep dissected bluffs.

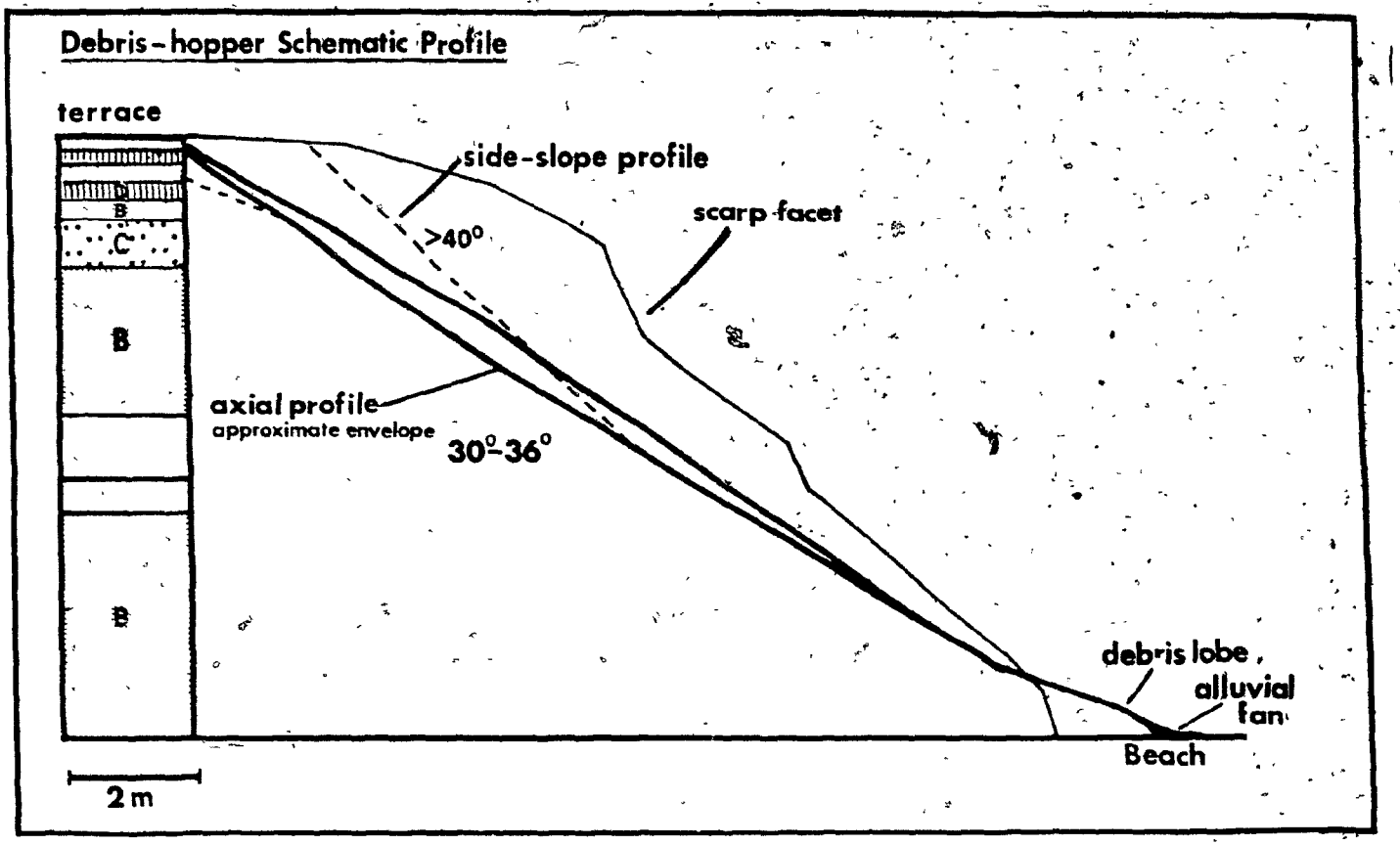


Figure V.23 Schematic profile of a bluff-face h llow. Representative stratigraphy is also given.



Figure V.24 Slope failure along hollow axis, below debris-hopper construction at K230. Slope angle is 32 . Debris has been remolded and transformed into a soil flow. (Perspective view is upslope from beach.)



Figure V.25a Slope failure in a bluff-face hollow at K635. The axial slope is inclined at 35° - 36°. Photograph was taken several hours after failure occurred. Note the small rills forming along the exposed frost table in silty fine sand. Rampart of debris has been breached by flowage of fluid debris from the ablating failure surface. (July 7, 1977)

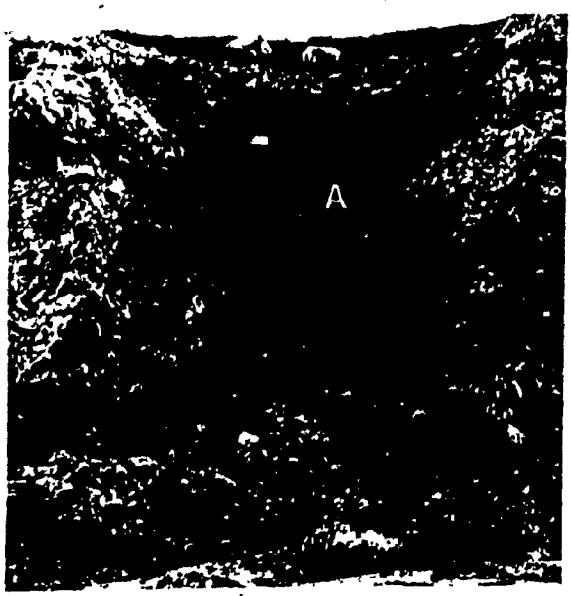


Figure V.25b The same feature seen in Figure V.25a (above) in late August, 1977. A single, incised master rill has been established and the undercut side slopes have regraded somewhat. Note also emergent seepage at base of the upper debris-hopper at 'A'.

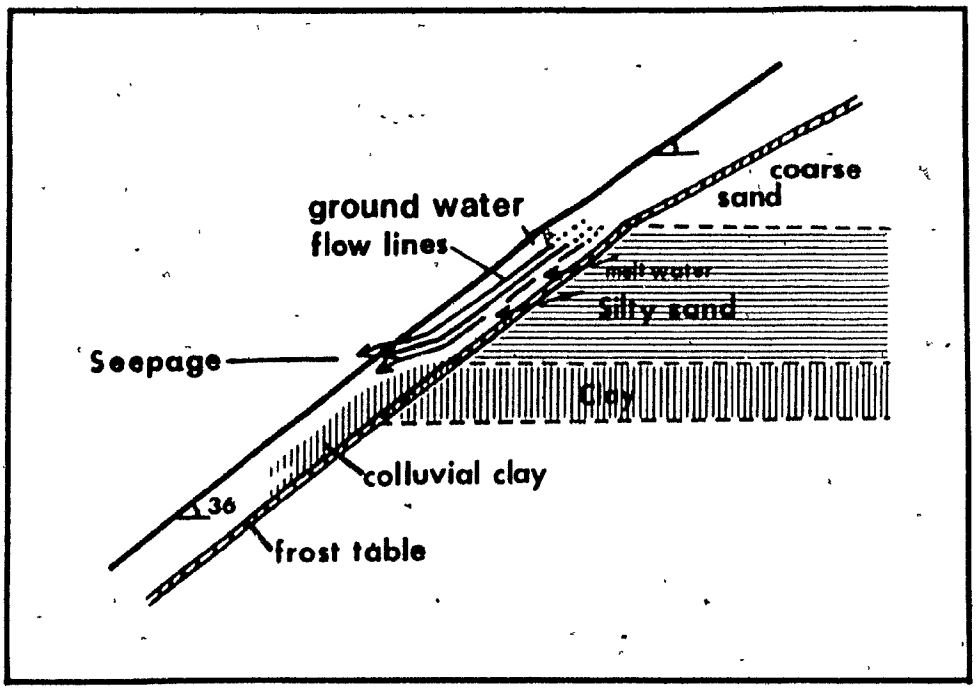


Figure V.26 Schematic slope profile cross section showing the effect of a thin clay unit on ground water through-flow. The low hydraulic conductivity of the clayey soil at the base of the active layer results in the development of a perched water table and seepage at the clay unit's elevation.

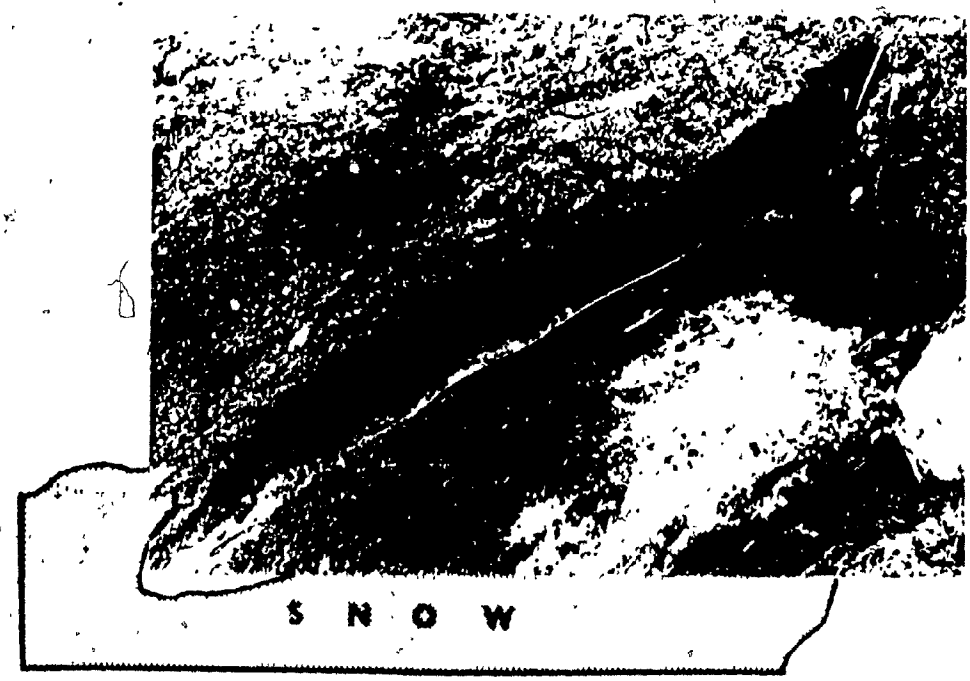


Figure V.27 Excavation above snow patch at the top of a debris-hopper at the northwest end of Survey Line II. Tape lies on the frost table. Retrogressive failure and flowage of sand is associated with seepage and saturation above the snow patch. Slope angle is 32°.

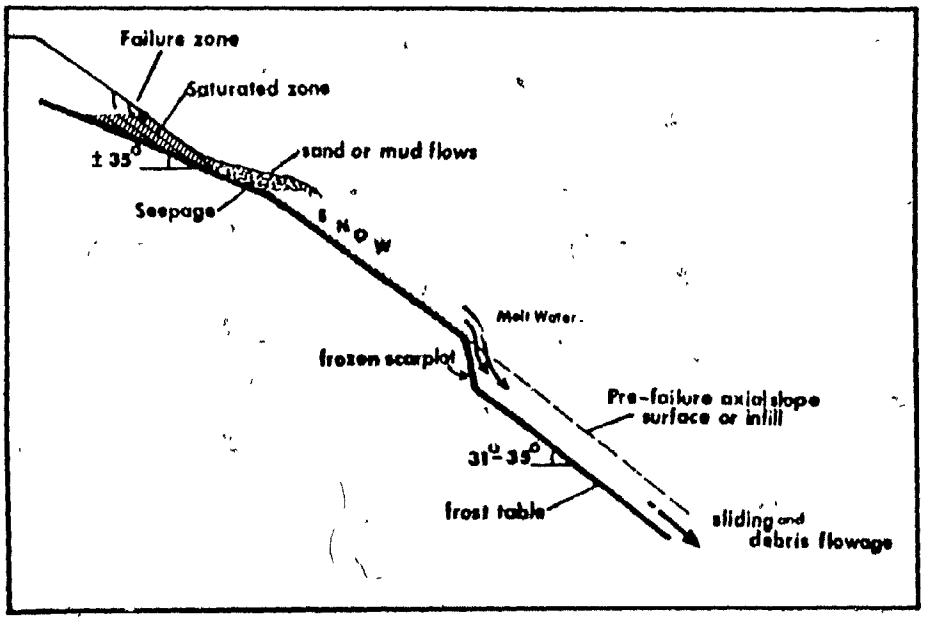


Figure V.28 Schematic presentation of the effects of a snow patch located in a bluff face hollow. Seepage occurs above the snow patch as ground water flows downslope through a progressively thinning active layer. Small scarp below snow patch is maintained by the insulating qualities of the patch.

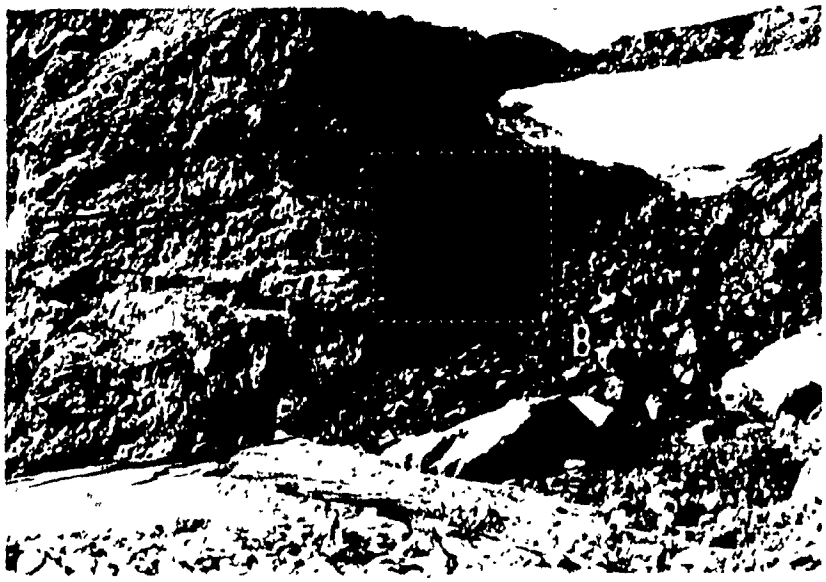


Fig.29b

Figure V.29a Undercut side slope in bluff-face ravine at K99. Basal slope has become armored by a coarse lag deposit (B). Melt water flow has migrated to the sides of the hollow. Box outlines the area shown in Figure V.29b, below.

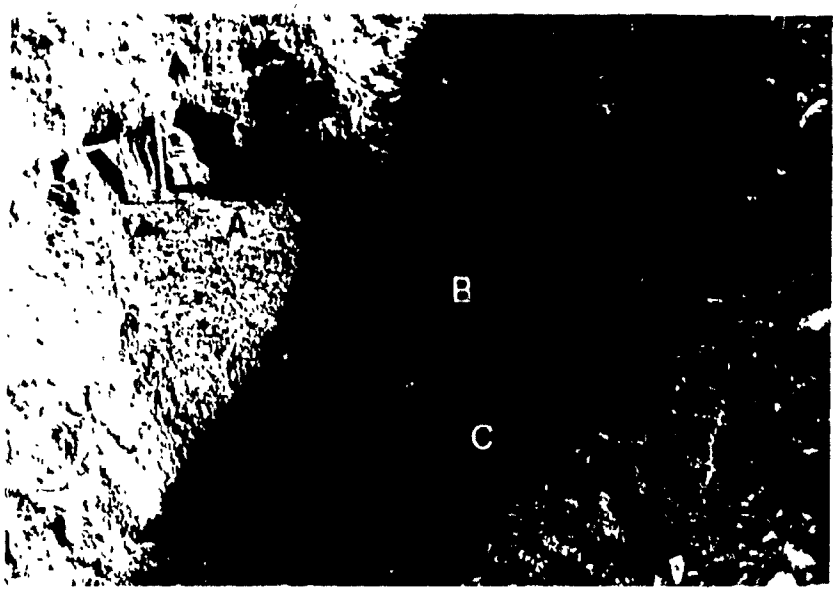


Figure V.29b Pseudo-pipe (A) and casts of clear ice (B) being exposed along the undercut side of the bluff-face ravine seen in Figure V.29a, above. These intra-permafrost conduits form in a manner similar to those along the gully sides in Figure V.20. The lenticular-shaped pseudo-pipe at A has been formed by lateral incision at a unit contact. Above the pipe is a well-sorted fine-medium sand, below it is a pebbly silty sand. Presently flow is emergent at C.

CHAPTER VI:

SOIL MOVEMENTS ON LOW-ANGLE SLOPES: OBSERVATIONS AND THEORY

Introduction.

In the following chapters the remaining morphological sub-divisions of the Kivitoo coast -- the bluffs with debris-bowls and the benched bluffs -- are described. While these two bluff divisions are considered to be morphologically distinct, they have in common the development of gentle slopes (ca 4-16°) along which rapid mass movement occurs. In light of this similarity, and the substantial problems which such low-gradient failure presents to conventional methods of stability analysis, the mechanisms of mass-wasting on low-angle slopes, including relevant observations from both bluff divisions, will be considered below. This is followed, in Chapters VII and VIII, by a discussion of the geomorphological development of these remaining sections of the coastline.

In the preceeding chapters, infinite slope stability analysis has been used to calculate the ultimate angle of limiting stability of many of the different slopes and slope features encountered along the Kivitoo bluffs. In Chapter III it was noted that, as a general assumption, the most critical stability conditions will occur when the water table is at the surface and flow is parallel to the slope. This 'least slope' for failure is given by Eq. III.13 as $\tan i = 1/2 \tan\phi'_r$. For a typical active layer soil with a saturated bulk unit weight of ca 20 kN/m³ and a friction angle of 30-35°, the

semi-frictional threshold slope is 16-19°. Slopes standing at inclinations less steep than semi-frictional angles were not widely encountered along the bluffs south of K650. In the few locations where such slopes are found, they are short and may be attributed to soil wash and creep processes or the continued movement of debris flows generated by failure on steeper, superadjacent slopes. The existence of rapid mass movement on slopes gentler than 16° along the northern part of the coastline thus requires a new explanation.

The term 'low-angle' or 'gentle', as used here, follows Chandler (1972) in denoting 'a slope on which landsliding would not occur, or re-occur, unless the pore-water pressures exceeded those which correspond with the water table being at the ground surface' (and flow parallel to the slope). Williams (1959) was one of the first cold environment geomorphologists to note that mass movement can be initiated on gentle slopes only if the effective stress within the soil is, in some manner, significantly reduced by the presence of 'abnormally' high pore-water pressure within the active layer. However, it is only in recent years that mechanisms capable of inducing such 'artesian' or 'excess' pore-water pressures have been treated analytically.

'Excess' pore pressure can be defined so that the total pore pressure (u) in the soil is equal to the pore pressure corresponding to the 'normal' condition of saturated slope-parallel ground-water flow, (u') (as shown in Figure III.1), plus the excess pore pressure (u_e). Or, formally,

$$u = u' + u_e \qquad \text{(VI.1)}$$

In other words, excess pore pressure at some depth in the soil implies a piezometric surface which is above the elevation of the slope surface. As shown below, such excess pore pressures may occur during thaw of the active layer.

The effect of excess pore pressure on the strength of a soil at a specific depth X can be expressed in terms of effective stress.

$$\sigma' = [Po + (\gamma X - \gamma_w dl)] \cos^2 i - u_e(X) \qquad \text{(VI.2)}$$

where Po is any applied load and $u_e(X)$ is the excess pore pressure at depth X (i.e. $u_e(X) = u(X) - (\gamma_w dl \cos^2 i)$ where u is the total pore pressure and dl is the height of the water table above the potential failure plane). [Note: Depth (vertically) is denoted by X here (rather than D in Chapter III) because D is used by McRoberts and Morgenstern (1974) for thickness (normal to the slope surface).]

In permafrost regions, mass movements have been widely reported on slopes gentler than those predicted by Eq. III.13. Indeed, low-gradient soil movements have been a major topic of periglacial research since Anderson's (1906) pioneering and often quoted observations from Alaska. Extensive documention of low-angle slope failure can be found in the geomorphological literature. Slow solifluction-type movements have attracted by

far the most attention, suited as they are to long-term process studies. Until recently, more rapid single-event failures have received much less detailed study. The work of Chandler (1972) and McRoberts (1973) is notable for its analytical treatment of this specific problem.

(The term 'gelifluction' is used below in preference to solifluction (after Washburn, 1973) to refer to a form of soil movement genetically unique to cold environments, and refers specifically to that component of movement which is in excess of that attributable to frost creep. 'Solifluction' is retained to refer to features, such as solifluction lobes, created by both frost creep and gelifluction, as well as being a general term used to refer to the process which incorporates both of these components of downslope displacement.)

The low-angle soil movements encountered along the northern portion of the Kivitoo bluffs are of three types: (1) single-event translational landslides which may degenerate into debris-flows; (2) bimodal, retrogressive failures in which a steep, retreating backscarp is maintained by the continued downslope movement of debris below this scarp, and (3) slow, year-to-year gelifluction-type movements.

Of these, the single-event translational landslides are thought to be the most significant in bench development and are discussed in the greatest detail below. These landslides also present the best opportunity to investigate the validity of certain failure mechanisms, applicable to low-angle failure,

which have received attention in the literature, but which have not been subject to rigorous verification in the field. Retrogressive failure was not studied in as much detail, partly because its mechanics appear to present fewer problems and partly because it is felt that its role in bench widening is not as significant as that of the 'slab' type failures. Gelifluction-type movements receive more limited treatment in the third section since, while ubiquitous along bench slopes, these movements are not thought to be responsible for the gross morphology of the bench. Also, gelifluction has received extensive treatment elsewhere and an in-depth study would require longer-term observation than was possible in the context of the present research.

Low-gradient failures along the Kivitoo coast are primarily found along the tongue slopes of debris-bowls, on the mid-bluff bench which occurs at the northern end of the bluffs, and along the sides of valleys crossing the bluffs, west of the small stream at K900. It should be stressed that all the slope failures discussed here are mobilized on gentle slopes and do not represent the continued movement of debris shed from failure along steeper slopes. Post-failure debris movement is discussed separately later in this chapter since its mechanics may be different from those responsible for failure initiation, and therefore present quite different problems.

A. Low-angle, single-event landslides

The following discussion of low-angle single event landslides

is organized into four sections. The first section gives detailed descriptions of individual features along the bench slopes at Kivitoo, as well as relevant observations on soil properties, active layer moisture content profiles, piezometric conditions and ground ice. This is followed by a literature review considering alternative mechanisms of low-gradient slope failure in thawing soils. The third section attempts an analysis of the mechanics of the Kivitoo landslides, while the final section presents a qualitative discussion of the post-failure behavior of landslides in active layer soils.

1. Observations of low-angle landslides on the Kivitoo bench slopes ; Case studies and ground ice conditions.

Several translational landslides found on the mid-bluff bench and its extensions along valley sides were examined in detail. For comparison, other 'stable' sites along the bench were also studied. These investigations included geomorphological mapping and excavation of the active layer to examine the soil profile and retrieve samples for determination of moisture content and other physical properties. Particular attention was paid to the physical state of the soil near the thaw plane and the differences in moisture content between the frozen and the thawed soil at this boundary. In order to measure pore pressures in the active layer piezometers were installed at selected sites along the bench.

Sampling of the still frozen active layer and the contemporary permafrost was accomplished using a portable

gasoline-powered drill fitted with a CRREL-type core barrel. Eleven cores, 5 cm in diameter, were obtained, the longest reaching a depth of 160 cm. The presence of stones in the frozen soil, the progressively worsening condition of the cutting shoe on the core barrel, and the extreme difficulty of penetrating cold permafrost at shallow depth prevented deeper coring, as well as limiting the depth of many of the other, shorter cores.

a. Description of landslides

For identification purposes, the landslides examined are numbered 1 to 8 and comprise all of the obvious instability features of this type to be found along the Kivitoo coastline. In addition to the landslides on the bench, the large landslide on the side slope of the valley at K1145 (Slide 7; see Figure VIII.10) and another landslide located at the back of a bench remnant at K890 (Slide 8) were examined.

All of the landslides along the Kivitoo bench extended from the bottom of the bench's back slope (i.e. the upper bluff slope), across the bench, with the initial downslope edge of the landslide located several metres behind the downslope edge of the bench. While most of the landslides involved a short segment of the back slope, the major portion of these failures was seated on the gentler bench slope. None of the soil movements appear to have been initiated principally along the back slope. One landslide (Slide 7) on a 4° slope did not extend to the steeper slope above it.

The landslides along the bench generally range from 7 to 15 m in width (one slide was 30-40 m wide) and in length from 20 to 30 m. Slope angle, as measured along the centre of the slide, is 4° to 9°. Dimensions and inclinations of the eight landslides are given in Table VI.1. Most of the slides overrode the intact surface of the bench downslope (e.g. Figure VI.4) and/or displayed compression ridge development at the toe (e.g. Figure VI.2). While the vegetated surface of the landslide remained intact in some of the failures, in others the slide mass broke-up and continued movement downslope as a debris-flow. In Slides 3, 5 and 7 the soil was completely evacuated, leaving behind a bare scar 60-100 cm deep on the bench surface. Remains of the debris-flows from Slides 3 and 5 can be seen on the lower bluff slope at K1165 and K1228. A particularly well developed debris-flow channel with distinct levees was found downslope of Slide 7, attesting to the fluid nature of the waste and the rapid transformation of the failed active layer into a debris flow. For those slope failures where the active layer remained at least partly intact, distance of travel of the slide mass was 2 to 10 m.

Slides 1 and 2, described in detail in Figures VI.1 and VI.2 respectively, are similar in form, in that the failed active layer did not break up and flow downslope, coming to rest after only limited displacement. The active layer soil profile for both of these landslides is similar to that found in all the other landslides, as well as along stable portions of the bench. The basal portion of the active layer was comprised of fine-grained soil of low plasticity ranging in

texture from sandy loam to silty clay. These basal soils are derived from in situ fine-grained units which occur at the elevation of the bench. (The relationship between the bench and bluff stratigraphy is discussed in Chapter VIII.) The fine-grained soil is usually overlain by a variable thickness of non-plastic sandy colluvium. The relative proportion of basal fine-grained soil to sandy surficial colluvium varies widely, but along intact portions of the bench the colluvium is rarely less than 30 cm thick. An exception to this general soil profile was found in Slide 1 where late season coring of the active layer near the center of the slide mass encountered only sand and slightly silty sand (with a relatively high frozen moisture content of 41-45%) at the frost table. (The significance of this particular soil profile is discussed later.) The fine-grained soil unit , however, was found at shallow depth near the back of the landslide. A trench excavated at the back of Slide 2 (Figure VI.2) shows the typical active layer profile of fine-grained soil overlain by sandy colluvium. Here, the fine-grained soil is clearly derived from the stratigraphic unit which occurs at the bench level. The upper limit of this unit coincides with the base of the bench back slope and the fine-grained basal soil dips back into the permafrost at this level in the trench.

Slide 3, shown in Figure VI.3 occurred on a 4-7° slope. This failure was unusually wide, averaging 35 m. The toe of the landslide, seen in Figure VI.3b, overrode the bench's downslope edge and the bulk of the slide mass was transformed into a debris-flow and evacuated from the scar. Since the

landslide occurred, small channels have been eroded into the bare sediment exposed in the scar and a small, actively downcutting gully, previously situated along the north side of slide 3 now runs across the bench within the scar. En-echelon tension cracks (Hutchinson, 1970; Chandler, 1972) are present in the shear zones along the the sides of the slide. Similar disturbed zones occur along most of the slides.

Excavation at the backscarp of Slide 3 revealed 18 cm of colluvial medium sand overlying 12 cm of silty sand. Below this colluvium, from 30 cm to the frost table at 60 cm, a greyish (unweathered) loamy silt was present. Water content of the frozen soil at the frost table averaged 30-35% while that of the overlying thawed mud was ca 20%. The stable bench alongside Slide 3 had a slightly thicker surficial sandy layer and the ice content near the base of the active layer was slightly higher, in the range of 30-50%.

Slide 5 (K1227), shown in Figure VI.4, was the largest instability feature found, occurring as it did along the widest section of the Kivitoo bench. (See also profile N-14, Appendix C.) Slide 5 is similar to Slide 3; both features being characterized by large bare scars left by debris evacuation and pronounced over-thrusting of the slide toe. Like Slide 3, Slide 5 is situated in proximity to a water source, in this case a sheet of unchannelized run-off flowing over the bench surface, and arising from the hollow just to the north of the landslide. While both of these landslides are situated in wet locations it should be emphasized that not all of the landslides are so located and that other sections of the

Kivitoo bench which do not have 'recent' landslide features are as wet or wetter than these locations. Two cores (nos. 10 and 11) were obtained from the scar and one (no. 9) from the upper half of the 'stable' bench several metres south of the landslide. (The locations of the cores are marked on Figure VI.4a and the moisture content data are given in Figure VI.6.) Again, excavation shows this landslide to be seated in fine-grained sediment. Frozen moisture content at the frost table was 20-30% while that of the overlying soil was less than 20%. The scar itself was 40-90+ cm deep (being shallower along the south side).

b. Active layer soils of the Kivitoo bench slopes

i. Soil profiles, moisture content and ground ice.

Grain-size and moisture content data for the Kivitoo bench have been presented above in the context of the individual landslides. A summary of the physical properties of representative soils is given in Table VI.2 and Appendix A.

A typical soil profile from the Kivitoo bench consists of 30-50 cm of sandy colluvial soil overlying sandy silt to silty clay of low plasticity. (The liquid limit of these fine-grained soils ranges from 22% to 30% with plasticity indices of 5% to 10%, Table VI.2.) Ice content at the frost table in these fine-grained soils ranges from less than 20% to over 55%, but is mostly within the 20-40% range. Water content of the saturated thawed soil immediately above the frost table is almost always less than that of the frozen soil. In some

locations, this difference may reflect real variations in the in situ ice content profile, while in others it is due to post-thaw drainage (consolidation) of the soil above the frost table. (For example, the frozen silty clay from Slide 7 had a void ratio of 0.89 while that of the overlying thawed soil was 0.72.) Drainage may be upward (or laterally) into the thawed soil, or downward into the frozen soil immediately below the frost table. Much of this consolidation, particularly in the ice-rich soils, is a result of the partial closing of gaps left by the melting ice partings rather than a more uniformly distributed consolidation of an initially homogeneous soil. In lower ice content soil, compression following thaw may be insignificant due to the strength of the soil between the ice veins, as well as the lower initial void ratios. The dry bulk density of thawed soils ranges from 13-16 kN/m³. Yet, considering the gaps left by the ice veins and the contribution that these make to the bulk porosity of the soil, bulk density data indicate that the individual soil peds between the gaps must be quite dense. (The post-thaw-consolidation of active layer soils is considered at length in the following sections of this chapter.)

A trench extending from back slope to the seaward edge of the bench was excavated at K1063. A portion of this excavation is seen in Figure VI.5. The overall inclination of the bench at this point was fairly steep (16°) and there were indications of limited instability (tension cracks) at the base of the bench back slope. Small solifluction-type lobes (with risers less than 15 cm high) were present on the bench surface. While

variation in both the relative thickness of the fine-grained and colluvial soil, and in the active layer moisture profile, occurs between sites, the active layer transect exposed in the trench is typical of that found along most of the bench. Frost table depth along the trench was 40-60 cm (22/7/83) and the basal fine-grained layer was 10-20 cm thick. As in the trench at the back of Slide 2 (Figure VI.2), the fine-grained layer dips below the frost table at the top of the trench (i.e. the base of the bench back slope) at an elevation which probably coincides with the top of the stratigraphic unit from which the fine-grained soil is derived. Intrusions of the basal fine-grained soil (such as those seen in Figure VI.5) were found extending into the colluvial sand above the fine-grained contact, although the significance of these is not clearly understood.

Core data from the frozen soil along the Kivitoo bench are reproduced in Figure VI.6. Since the maximum thickness of the active layer on the bench was rarely more than 80-100 cm in 1977 or 1983, the bottom of most of the cores extended into the contemporary permafrost. The moisture content profile of many of the cores shows a marked peak 0 to 30 cm below the frost table. This layer of relatively high ice content may correspond either to the base of the active layer or the top of the contemporay permafrost or both. Beneath this icy layer frozen water content tends to decrease. In core 10 for example, below a peak of 36%, ice content decreased to 15% at a depth of 130 cm. Similar reductions in soil ice content (of 15-50%) are seen in cores 6, 8, 9 and 11. The core data

therefore suggest that the main body of the permafrost itself (or at least that part of the permafrost near the base of the active layer) is not ice rich; only the very top of the permafrost contains large quantities of soil ice.

Interpretation of the core data must be made with care since the thickness of the layer sampled for moisture content will bias the data, particularly if thick, discrete ice layers are present. Yet, in most of the cores ground ice was present in the form of ice veins up to, but usually less than, one cm in thickness. Most often these veins formed a three-dimensional network of horizontal and vertical partings. (Mackay (1981) has also noted that the icy layer is usually comprised of 'ataxic basal ice'.) No massive, continuous clear ice layers were found, though some of the very icy frozen ground contained more ice than soil by volume and this in the form of veins more than one cm thick.

The ice content profiles from the Kivitoo cores resemble those from shallow cores in similar materials reported elsewhere. Stangle et al. (1982); Outcalt (1982); EBA (1979); Mackay (1980, 1981, 1983); Pollard and French (1980); Parmuzina (1978); Tsytovich (1975); and Brown (1969) have all noted the occurrence of icy layers near the base of the seasonal active layer. Such profiles are probably characteristic of active layers developed in fine-grained soils in permafrost in general.

Interpretation of the core data, particularly assessment of the relationship between the icy layer and the depth of maximum seasonal active layer development presents several

difficulties. First, while the presence of icy soils or ice layers at the base of the active layer/top of the permafrost is universally noted, few researchers have made the important distinction between these two levels. Mackay (1981) feels that the icy layers are continuous between the top of the permafrost and the base of the active layer. The Kivitoo data seem to be consistent with this. Thus, the icy layers probably melt out in part in most years but it is only during years of exceptionally thick active layer development that these are subject to deep and prolonged thawing. Another complication made evident by recent research (Mackay and others; cited below) is the demonstration that the ice content profile is not static but may change significantly over the course of the year, both while the active layer is fully frozen and during thaw. Thus, the ice content obtained at a specific depth at any one point in time may not be representative of the ice content at that depth at the time of thaw. As scar depths indicate that the landslides at Kivitoo are seated near the base of the active layer, the core data are felt to adequately represent the ice conditions in the active layer at the time of failure. Although a thorough examination of the dynamics of soil water movement in the active layer is beyond the scope of the present research, a limited treatment of this particular problem is relevant to a discussion of the Kivitoo core data and, ultimately, to the problems of active layer stability.

The icy zone at the base of the active layer forms as the result of two processes. One is the penetration and refreezing

of liquid water in the frozen soil at the top of the permafrost when the active layer approaches its maximum thickness late in the summer. The other process is ice segregation which occurs upon freeze-back in the fall as the active layer begins to refreeze upward from its base.

Recent studies (Mackay, 1981, 1983; Wright, 1981) have shown that, at a thaw front, water can be drawn down into the still frozen soil immediately below the 0° isotherm. This influx of fluid water can occur since frozen soil at near-zero negative temperatures contains unfrozen water and has some hydraulic conductivity. (Also, some frozen soils may be unsaturated and therefore have open void spaces into which melt water can penetrate.) During thaw, pore suctions in the 'warm' frozen soil are such that a downward hydraulic gradient, along which soil water can move, is established (as observed in the field by Guymon, 1976). As liquid water penetrates the frozen ground some of it refreezes increasing the ice content at that level. This refreezing releases latent heat, warming the surrounding frozen soil. Eventually, melting will predominate and the frost table will advance.

Mackay (1983) reviews recent research (much of which is in Russian) showing that ice enrichment below the descending thaw plane may be as much as 20-45% (see his Figure 4). Reinterpreting the data of Michel and Fritz (1981), Mackay (1983) proposes that the zone of ice enrichment at the top of the permafrost may be 10-30 cm thick. This figure appears to correspond well with the thickness of the ice content bulges in the Kivitoo cores. The bulking process can be expected to

occur not only at the base of the seasonal active layer, where it would tend to enrich the top of the permafrost, but may also result in a continuous ice enrichment or frozen moisture bulge preceeding the descending thaw front. The expected magnitude of this ice content bulge is not known, but should vary depending upon the temperature gradient in the vicinity of the 0°C isotherm and soil type, as these factors effect the pressure gradient (maghitude of the suctions), thickness of the 'frozen fringe' (i.e. the still-frozen soil at near-zero temperatures in the thawing zone) and the unfrozen water content and hydraulic conductivity across the thaw line. The development of such a bulge would also depend upon the availability of phreatic water. Dry sites would not be expected to show significant bulking.

The possibility of a mobile ice-bulking phenomenon was of interest since it was thought that the moisture peak below the frost table in some of the core data reflected not the base of the seasonal active layer, but a downwardly mobile ice content bulge. If this were the case, it would mean that the thaw plane would always be descending into frozen ground which has been ice-enriched (though not neccessarily ice-rich), no matter what the pre-thaw ice profiles were like. However, the absence of a second, deeper, moisture peak in most (but not all) of the core data suggests that the active layer at most of the core sites was, in fact, close to its maximum seasonal depth.

These observations of ice enrichment at the base of the active layer also raise the question as to whether there is any limit to the amount of ice bulking which can occur at the base

of the active layer. If the basal soil continued to gain ice this would lead to a continuous heave situation. Wright (pers. comm.) feels that as the ice content of the soil increases, hydraulic conductivity of the frozen soil near the 0°C isotherm would be reduced to the point at which melt water infiltration, and therefore further ice-bulking, would be negligible. The work of Parmuzina (1978; quoted in Mackay, 1983) suggests that moisture can also be extracted from the frozen soil at the top of the permafrost during freeze-back in order to 'feed' ice segregation in the lower active layer as the soil refreezes upward from the top of the permafrost in the fall. This process may further inhibit the development of very thick basal ice layers.

A significant effect of the icy layer near the top of the permafrost would be the formation of a latent heat buffer at depth. This layer would slow the downward progress of an already damped late season thaw plane. Nicholson and Lewis (1976) have noted a year-to-year consistency in seasonal maximum thaw depth which they ascribe to this icy barrier. Similarly, at Kivitoo, year-to-year variations in maximum active layer depth may be substantially reduced by the development of an icy basal layer. Yet, while annual variations in maximum active layer thickness may be somewhat mitigated, the time during which the basal icy layer is exposed to thaw and, ultimately, the amount of water produced by the melting of ground ice (and the rate of this melt water production) may show substantial variations between years. (This point is discussed in a more analytical framework in

section VI,I,c, below.)

Examination of the core data from Kivitoo (Figure VI.6) suggests both the presence of a mobile ice content bulge within the thawing active layer in wet locations and a high ice content zone at the base of the active layer/top of the permafrost in all locations. One core, no. 8, which was in soil that had recently been exposed from beneath a melting snow patch, had two ice enriched layers, one just below the frost table and another at a depth of 90+ cm. The ice content in the middle portion of the core, between 70 and 90 cm, was low (<20%). The depth of the frost table at the time the core was taken (21/7/83) was only 36 cm -- considerably less than the maximum active layer thickness. The upper icy zone in this core may have been formed by the infiltration and refreezing of melt water below the descending thaw front. Ice segregation during the previous fall may also have been a contributing factor. The middle low ice zone is probably a depleted layer from which soil moisture has been drawn to feed ice segregation processes either at the base of the active layer or at its surface during freeze-back. Core 5, which also had a shallow frost table reletive to the maximun active layer depth, suggests a similar (though smaller amount of) ice bulking below the descending thaw front. However, here there is only a slight increase in the frozen water content near the depth of maximun seasonal thaw (90-100 cm). The lack of a pronounced icy layer at depth in this case is most likely a reflection of the site's dry location. Exposure of low ice-content

permafrost within the slide scar within which an active layer has only recently developed may also be a factor which is responsible for low levels of basal enrichment in core 5. As the core data indicate that only the top of the permafrost is ice-rich, following the stripping of the active layer, it would take a period of time before a 'normal' frozen moisture profile is reestablished in the newly created active layer. This may explain why cores 10 and 11, located within the scar of Slide 5, have lower ice contents than core 9, which was located on the stable bench alongside the scar. Indeed, core 9 also had the highest ice content of any of the cores (78%), which may be a reflection of the relatively long period of stability of this portion of the bench, a period during which the top of the permafrost table has become progressively more ice-enriched.

ii. Freezing-induced structure of the Kivitoo soils

In the field, fine-grained soils possess a clearly articulated secondary structure, derived from the formation of ice partings in the frozen soil. This structure may range from predominantly horizontally oriented ice partings (found mostly in the non-plastic silts and silty sands) to a three-dimensional ice texture, with both horizontal and vertical ice partings, which is most commonly encountered in the plastic fine-grained soils. This lattice-like 'cryogenic' texture -- shown schematically in Figure VI.7 and as it occurs in the field in Figure VI.8 -- has been referred to as ataxic, blocky, cellular or reticulate (e.g. Mackay, 1976; Tsytovich,

1975; Roggensack, 1977).

The cryogenic structure of the active layer soils is often maintained in the thawed state, these soils possessing a blocky texture consisting of cubic to platy soil peds like those shown in Figure VI.9. The individual peds in the fine-grained active layer soils on the Kivitoo bluffs are typically less than 1 to 3 cm on a side. (Mackay (1966) has shown blocky structures whose scale is an order of magnitude larger, but this was in permafrost rather than the seasonal active layer.)

The reticulate Kivitoo soils display a wide range of water contents, from less than 20% to over 60%. In a thawed state, after the removal of ice partings, the individual peds are hard (being difficult to crush by hand) and merely moist (water content is generally less than the plastic limit). The peds appear to be overconsolidated and when immersed will slowly readsorb water and disintegrate. In order to determine the relationship between the bulk water content and the water content of the peds in a frozen soil, a sample was collected and as much of the visible ice as possible removed. The water content of the soil blocks was only 18% while that of the total soil was 35%. In another sample, the peds also had a water content of 18% while that of the frozen soil overall was 27%. (The water content determined for the peds is probably high because of the difficulty of removing all the ice partings and the fact that some thawing and readsorption of water inevitably occurs during the process of ice removal.)

Reticulate cryogenic structures have been reported in plastic lacustrine and marine clays in Alaska and Russia

(quoted in Mackay 1974 and Tsytovich, 1975), and in 'thaw exposures' and marine cliffs near Tuktoyaktuk, N.W.T. by Mackay (1974). Yet, the permafrost literature, particularly that produced by geomorphologists, has tended to emphasize horizontal ice lensing. This may have contributed to an unrealistic impression of the structure of active layer soils as they appear in the field, especially that of finer-grained and more plastic soils. It is likely that a cellular structure is the one most characteristic of fine-grained active layer soils. Certainly, this is the case at Kivitoo.

Recent studies (e.g. Roggensack, 1977) have recognized the extreme importance of cryogenic structure to the mechanical behavior of thawing permafrost. Yet the fundamental significance of structuring of active layer soils, and its relevance to geomorphic processes, has not received the attention it requires. As knowledge of the mechanics of permafrost soils increases, and as this knowledge is applied to the field situation, a more accurate picture of the cryogenic structure of active layer soils, and the importance of this structure in terms of active layer processes, should emerge.

Mackay (1974) attributes the development of a reticulate ice vein structure <u>in permafrost</u> (as opposed to the active layer) to the rapid freezing of a plastic soil within a hydrologically closed system -- i.e. no in-flux or out-flow of water. This was thought to account for the relatively low ice contents which he found in reticulate-structured permafrost in contrast to the very high ice contents often found in

horizontally-lensed permafrost. Mackay did not, however, discuss the formation of seasonal ice structures in the active layer.

Nixon and McRoberts (1975) have proposed that the reticulate structure is produced in the still-thawed soil in advance of the freezing plane, and does not require a closed system for its formation. According to Nixon and McRoberts, water is drawn to the 0°C isotherm during refreezing of the active layer, in response to the thermally induced hydraulic gradient. (Soil freezing may be either downward from the surface or upward from the frost table.) This gradient may create large pore suctions in the soil on the warm side of the 0°C isotherm. Shrinkage (consolidation) of the still unfrozen soil occurs in response to these pore tensions, creating a three-dimensional pattern of contraction cracks (see also Penner et al., 1974; Hamilton, 1966). Water expelled from the consolidating soil between the cracks flows into these cracks where it then freezes with the passage of the 0°C isotherm. The formation of small scale contraction cracking is favored by steep hydraulic gradients below the advancing frost front. Steep, shallow hydraulic gradients, form in response to the steep thermal gradients which are induced in rapidly freezing soils (such as those in the active layer). Mackay (1974) proposes that even after the flow of water into the soil behind the 0°C isotherm has nearly stopped (due to the formation of ice in the pores) freezing and ice formation may continue as still-unfrozen water is withdrawn from the surrounding soil to feed ice veins. As ice forms in the veins a secondary thermal

and pore pressure gradient is established and additional water can be withdrawn from the surrounding soil. The induced pore suctions in the soil peds between the growing ice partings in turn increases the effective stress within these peds promoting their consolidation. Added to these consolidation stresses is the increase in effective stress caused by the volume expansion of the water upon freezing, as well as the continued addition of mass to the ice veins. Ultimately, all these factors act to overconsolidate the peds in the freezing soil (as has been demonstrated in an artificially frozen soil by Nixon and Morgenstern, 1973). It is also possible that as the active layer refreezes upward from the top of the permafrost, water may move via gravity into the shrinkage cracks created during the freezing process further enriching the soil at depth.

Mackay notes that permafrost soils with a reticulate structure generally display limited heaving since large amounts of water are not brought up through the soil to feed the growing ice lenses. Nixon and McRoberts (1975) note that this is not because freezing is occurring in a closed system, but rather because of the short, steep hydraulic gradients which do not extend very far into the still-thawed soil. Total heave in a frozen blocky loam may not exceed 9%, i.e. a volume increase which can be accounted for soley by the expansion upon phase change of the soil's pre-existing pore-water. Significant bulking, if it were to occur, would require a more slowly-aggrading permafrost (or freezing active layer). This would allow for a gentler, deeper hydraulic gradient which would allow larger amounts of water to be brought to the

freezing front at any particular depth.

It appears that the most significant factor in the creation of the reticulate cryogenic structure is the presence of a sufficient clay-sized fraction. This would reduce the soil's hydraulic conductivity, which would be conducive to the development of short, steep hydraulic gradients in the freezing soil as well as enhancing the soil's shrinkage capacity, promoting the development of contraction cracks. A larger clay fraction would also increase the unfrozen water content of the soil in the frozen fringe, increasing the amount of unfrozen moisture available behind the 0°C isotherm for the continued growth of ice veins. The grain size data from Kivitoo, plotted in Figure VI.10, along with those of Mackay (1974) and Chandler (1972), show that reticulate ice structures develop in clayey silts and silty clays. This cryogenic structure was also observed at Kivitoo in loamy soils with clay contents less than 15-20%. However, the blocky structure in the low clay content soils is not as well developed as that of the finer-grained soils, and tends towards horizontal ice lenses. In reality, there is a continuum between reticulate structured and horizontally lensed soils and, in fact, both processes can occur simultaneously.

It must be emphasized that ice content is not simply a matter of soil type or the type of ice structure, but is also a function of the availability of soil moisture during freeze-back, as well as of soil moisture redistribution within the frozen soil throughout both the winter and thaw season. In terms of post-thaw consolidation (see next section), even in

reticulate-structured soils which have not become bulked with excess ice, redistribution of the existing pore water in association with the compression of the soil between ice partings, can result in the creation of a soil which is highly compressible upon thaw.

While reticulate-structured soils may contain high ice contents, some of the highest ice content soils found along the Kivitoo bluffs were silty fine sands, such as those which occur at the base of the active layer in Slide 1. These soils tend to display horizontally lensed, rather than reticulate, ice structures. The large hydraulic conductivity of these soils, however, would tend to inhibit the generation of high pore pressures during thaw (for reasons discussed below).

iii. Piezometric observations along the Kivitoo bench

Open standpipe piezometers were installed along the bench slopes in order to monitor the piezometric level in the active layer throughout the 1983 field season. The piezometers were constructed of clear plexiglas tubing with small inside diameters (0.48 and 0.64 cm) in order to minimize the volume change necessary for the piezometer to equilibrate to ambient pore pressures and hence shorten response time. At the base of each tube was a screen made out of a porous styrofoam-like plastic 2.6 cm in diameter and 2.75 cm in length. Each piezometer was fitted with a hard plastic point of the same diameter or smaller than the screen to facilitate insertion.

Standard installation of piezometers into backfilled and

sealed holes was not possible at Kivitoo due to the stoney and/or soft nature of the active layer soils. Piezometers were therefore inserted by gently pushing them down into a previously made hole of a diameter slightly less than that of the screen. In wet, very soft soils the piezometer could be pushed directly into place by hand. After installation the piezometers were filled to a point above the ground surface and allowed to equilibrate to the ambient piezometric conditions.

As the detection of any artesian pore pressures was of particular interest, sites where the water table was at the surface, providing a convenient reference datum, were choice piezometer locations. At some sites piezometers were paired with the tips at the same depth in order to provide a check on the readings. At other sites, where artesian pressures were thought to be most likely due to high ice contents, soft soils or nearby instability, paired piezometers were placed with the tips at different depths so that any upward component in the hydraulic gradient could also be detected. Piezometer locations and soil data from the sites along the bench are reproduced in Figure VI.11.

None of the piezometers installed along the bench registered distinct artesian pressures. Very small artesian pressures were measured at the paired piezometers at Site 2. These were were situated in a midslope position, along a section of the bench where surface flow from melting snowpack was present throughout July. It is thought that the slight artesian pressures measured here were the result of the ponding of water immediately upslope and were therefore not due to

thaw-related processes.

The major hydrologic event to show-up in the piezometric data was a pronounced rise in the local water table during the wet period marked by storms on July 26, 30 and 31. This rise in the piezometric surface is clearly shown in the data for Piezometer Sites 3 and 5 which were located in small hollows (old, revegetated, slide scars) at K1161 and K1175, as well as in data from Piezometer Site 1, which was situated at the back of the bench at K1023.

Only two instances of artesian conditions of significant magnitude were observed in 1983. These high pore pressures were measured within recent or currently active instability features. In one case, this was within a debris flow associated with a retrogressive active layer failure at the base of the bluffs at K896. The other instance of artesian conditions was within a landslide which had recently occurred on a 17° slope at the back of a bench remnant near K890. These pore pressure data are discussed below in the context of the individual slope failures.

c. Observations of soil movement during the 1977 and 1983 field seasons

During the initial field season in 1977, the 'fresh' appearance of the landslide scars and the presence of older degraded scars suggested that single-event low-angle active layer failure was a widespread and frequent process along the Kivitoo bench. However, when the bench was re-examined in 1983

no new slope failures of similar form had occurred in the intervening five years, and the features which were first observed in 1977 still appeared fresh. This spurred speculation as to the true age of the landslides. The revised picture which emerged from the 1983 observations was that the low-gradient slopes of the Kivitoo bench were, in fact, predominantly stable with respect to large single-event landslides. It is now evident that these landslides occur only rarely, in response to exceptional conditions. Stangl et al. (1982; p.145), investigating the stability of low gradient landslides similar to those at Kivitoo, reached the same conclusion: "It appears that the active-layer failures studied [on eastern Melville Island] occurred as isolated events, precipitated by conditions that occur infrequently." This picture is quite different from that given by McRoberts and Morgenstern (1974), Chandler (1972) and others investigating the stability of permafrost slopes. These earlier studies, often pointing to the general impression of instability occasioned by the widespread occurrence of gelifluction-type movements, tend to emphasize the (presumed) marginal stability of thawing active layers. Yet gelifluction-type movements are probably both superficial (being limited to the upper portions of the active layer) and fundamentally different from the more deep-seated low-gradient landslides examined here and in the papers noted above. To date, no far-ranging assessment of the general stability of low-gradient permafrost slopes has been undertaken.

In light of the suspected infrequency of landslide events

the problem, as outlined below, becomes one of explaining the general stability of the Kivitoo slopes, while still being able to account for the production of sufficiently low strength conditions in the thawing active layer so that failure can, occasionally, occur.

During the last week in July, 1983 a landslide (Slide 8) occurred on a 17° slope at K890. The landslide was first noticed on July 25 and its occurrence is most likely related to precipitation on July 21-23. While this landslide did not occur on a gentle slope, the similarity of its location and active layer profile to the landslides found on the bench, may aid in an understanding of these lower-angled landslides.

The landslide was 8-10 m in length and approximately 3 m in width. It was situated in a small, steep-walled hollow at the back of a bench remnant and occupied nearly the entire 'floor' of the hollow. Translational displacement of the slide mass, as indicated by the distance between the slide mass and the back scarp, was approximately 2 m. Distinct bulging had occurred at the landslide toe, which did not override the intact slope surface downslope. Figure VI.12 provides a profile, plan and photographs of Slide 8. Profiles H-12 and H-13 (Appendix B) bracket the feature.

Excavation at the backscarp, sides and center of the slide revealed 30-50 cm of sand and silty sand (with a large number of cobbles and boulders) overlying a silt loam. Soil pit and moisture content data, given in detail in Figure VI.13d, indicate that the water content of the frozen soil at the base

of the active layer at the center of the slide was 49-71%, while that of the thawed soil immediately above this was generally less than 26%, just in excess of the liquid limit (22%). In Pit A, in the center of the slide, the frost table was at 60 cm. Ice content at the frost table was 49%, while the water content of the thawed soil immediately above it was 26%.

The failure zone of the landslide, shown in Figure VI.12c, is assumed to be in the vicinity of the frost table since no clearly defined shear zone could be seen in the pit walls. As disturbance during movement may have caused remolding and the water content of the suspected failure zone was in excess of the liquid limit, it was of particular interest to see if the soil at the base of the landslide had been remolded and thereby transformed into a dense mud slurry. The soil, however, was not fluid. Structurally, it appeared to be a loose aggregation of blocky peds with most of the soil water being contained in the macro-pores between the peds. This structured soil, even though possessing a water content in excess of the liquid limit for the remolded soil, probably retained significant frictional strength. Although determination of the soil's true rheological nature was difficult due to disturbance associated with the excavation of the soil pit -- the fact that a soil pit could be excavated attests to the presence of at least some bearing strength in the active layer -- seepage into the pit appeared to be of clear, not muddy, water. No soil slurry appeared to exist. If remolding had occurred, putting the finer soil particles into suspension and transforming the basal

soil into a debris-flow consistancy, the slurry had settled once movement of the slide mass ceased.

One reason for the observed lack of remolding may be the strength of the individual overconsolidated peds. Roggensack (1977) has shown that thawed blocky soils are dilatant at low effective stress levels (such as those at the base of the active layer, particularly if excess pore-water pressures are present). This observation indicates that (for small strains) the blocky structure of the soil does not break down when sheared under such conditions.

Since this landslide occurred on a 17° slope and was located at the base of a hollow -- a location where the water table would be most likely to reach the surface following a storm event -- the failure can be easily accounted for by the infinite slope analysis (Eq. III.13; $\phi' = 32°$ and applying all the standard assumptions, such as minimal side and end effects). Thus, it does not appear to be neccessary to invoke excess pore-water pressures to account for this particular slope failure.

Three piezometers were placed in the landslide and on the bench beside the toe on July 26. The record from these piezometers, Figure VI.12, shows that large artesian pore pressures were initially recorded. The paired piezometers nos. 5 and 12 clearly show the initial existence of an upward hydraulic gradient. The largest pore pressures were measured at the toe of the slide (piezometer no. 4). Artesian pore pressures had largely subsided at all the piezometer locations by August 5.

The source of the artesian pressures in the landslide is felt to be confined drainage, possibly along a layer of relatively permeable soil just above the frost table; the void ratio of the soil 10-20 cm above the frost table (as indicated by the saturated water content) is lower than that of the thawed soil immediately above the frost table. The piezometric head in this case may have been provided by the ponding of seepage from the hollow side slopes at the back of the landslide scar. A confined aquifer would partly explain why the highest recorded pore pressures were at the toe of the landslide. Upward seepage due to the local reduction in slope may also be responsible for a rise in the piezometric level at this location (for reasons discussed in Chapter VII). The unusual behavior of piezometers 5 and 12, which indicated a transition from upward to downward seepage during the first week in August, would also be consistent with a confined aquifer: Following drainage of water ponded upslope, the zone of high hydraulic conductivity near the frost table may function as a basal drain inducing a downward flow of soil water held within the slide mass. As noted above, the clear water in the soil pit indicated that the measured excess pore pressures are not pore-slurry pressures; that is they are genuine excess pore-WATER pressures rather than pore-FLUID pressures resulting from the suspension of fines in the soil water due to structural collapse of the soil peds. (See section VI.2,c for a further discussion of pore-slurry pressures.)

Examination of this landslide raises two important

questions: (1) Why was the slide mass presently stable despite high pore pressures? Using the piezometer data, an infinite slope stability analysis predicts that any slope steeper than 5° should fail; and (2) Why did the landslide show only limited displacement instead of breaking up and continuing downslope as a debris-flow?

In response to the first question, the slide is relatively small so that side and end effects may be very significant. That is, the infinite slope stability analysis, which requires that the slide mass be thin relative to its length and width, probably does not apply. (The implications of size of the slide mass for the landslides along the bench slopes will be discussed later on.) In addition, the toe with its included boulders and the stable soil immediately downslope from the toe, must provide a substantial passive force against movement. This passive barrier may build up further following failure due to compression bulging of the soil near the landslide's toe or overriding of the ground downslope. Finally, the high pore pressures measured at the centre of the slide may be quite limited in their areal extent, so that the factor of safety calculated <u>over the entire failure surface</u> might be greater than unity, even if side and end effects were not significant. Indeed, given the small size of the landslide some excess pore pressures may have, in fact, been necessary to cause failure. Noting the slide's location on the slope, such excess pressures may have been generated as a result of an upward component to the converging groundwater flow at the base of the steep hollow side slopes, possibly coupled with confined drainage at the

base of the active layer prior to the opening up of the backscarp. Why the landslide did not break up and degenerate into a debris flow is probably explained by a combination of the rapid post-failure build up of passive restraint downslope (due to bulging) which raised the factor of safety, and the possible dilatant shear behavior of the overconsolidated soil peds (which could reduce pore pressure by causing volume expansion in the failure zone). These peds may also have been strong enough not to break down given their initial state of overconsolidation and the low effective stress conditions at the time of failure, as well as limited subsequent strain.

2. Mechanisms of Low-Angled Movement of Thawing Soils: Literature review

A number of researchers have applied standard infinite slope stability analysis to specific instances of slope failures in permafrost soils. Chandler (1972), working in Vestspitbergen, has described failures in silty soils on slopes as low as 9°. His calculations predicted that any slope less steep than 18-20° should be stable. McRoberts and Morgenstern (1974) did a similar analysis for a variety of periglacial soil movements reported in the literature (their Table 2, p. 454), finding that many of these, too, occur on theoretically stable slopes. Others (e.g. Weeks, 1969; Chandler, 1970; Hutchinson, 1974) have analyzed fossil shear surfaces on clay slopes as gentle as 4° in England. (These slopes had been subject to periglacial conditions during the Pleistocene.) Again,

traditional stability analysis with 'normal' ground water conditions could not account for movement.

Several theories which have been presented to account for mass movements on low-angle thawing slopes are reviewed below. All of these theories provide mechanisms by which excess pore pressures may be generated, lowering the effective stress in the soil and thereby reducuing the soil's strength sufficiently for failure to occur on gentle gradients.

a. Confined aquifer mechanisms

One of the few examples of excess pore pressures actually measured in a thawing soil in the field is given by Chandler (1972). He suggested (following Williams, 1954 and Siple, 1952) that excess pore-water pressures could be created by permeability contrasts within the active layer. Assuming that the permafrost table constitutes an impermeable lower boundary, any layers of higher conductivity soil or subsurface channels (pipes) overlain by a less permeable soil could create conditions suitable for the production of a confined aquifer. (Rycroft (1971) has reported this situation in (humid temperate) slopes of weathered shale sandwiched between less permeable material.) Chandler's explanation may, in fact, be correct in relation to his particular study site where seepage erosion was evident and the piezometric record showed consistently high pore pressures -- as if these were determined by a "reservoir" upslope. The slides which he described are also quite shallow (less than 40 cm thick) and the active layer

contained sand lenses and other soils of higher hydraulic conductivity than the surrounding silt.

The 'blanketing' mechanism described by Chandler could not, however, account for fossil solifluction shears on clay slopes in England since these lack (at the present time) recognizable contrasts in permeability in the soil profile. Chandler therefore suggested a mechanism called 'ice-blocked drainage' in which a surficial layer of frozen soil would form the requisite impermeable blanket. This idea of Chandler's has been challenged by McRoberts and Morgenstern (1974) who, however, emphasize the relatively well documented gelifluction-type soil movements rather than single-event translational landslides. These researchers point out that most (gelifluction-type) soil movements occur, not during freeze-back in the fall, but rather during initial thaw in the spring when a frozen surface would not exist. Chandler does suggest that 'surface overnight freezing' may be effective in the early spring. (However, as pointed out below, the larger single-event mass movements at Kivitoo appear to occur later in the thaw season and the contention of McRoberts and Morgenstern that active layer failure occurs predominantly in the spring may not be correct.) Considering the lack of observations of ice-blocked drainage, and the rather special conditions necessary for its implementation, the process must be considered hypothetical at this stage. It should be noted that the location on the slope most susceptible to critical pore pressure conditions generated by confined aquifer mechanisms, and therefore that portion of the slope most likely to fail,

would be in the vicinity of the slope base. There is, however, no evidence to show that preferential failure occurs there, but the problem has not been considered previously. Another problem which arises when invoking confined aquifer mechanisms to account for failure on gentle slopes is that these less steep slopes are potentially more stable than steeper slopes since water must be 'backed-up' further to obtain equivalent excess pressure.

An extreme example of a confined aquifer would be the existence of pipes which have collapsed, so that they no longer have a clear outlet allowing water to 'back-up' the slope. Pierson (1983) has demonstrated the effectiveness of this situation in generating high pore pressures which resulted in slope failure. Despite the occurrence of pipes in the active layer noted in the previous chapters, no pipes were found to be associated with any of the landslides along the bench, nor were any pipes found along other, stable, bench sections. It is also unlikely that a single pipe could account for the more areally extensive landslides.

Savel'yev (1971) summarizes Russian research stating that artesian pressures are indeed 'to be expected' in fine-grained permafrost soils. He contends that thawing (plastic) fine-grained soils will, near to the advancing thaw front, temporarily retain the cryogenic structure imparted by the soil's previous ice network (which in the clayey loams under study was usually cellular or reticulate), significantly increasing the soil's hydraulic conductivity. Saval'yev cites Tsytovich (1955) and Potrashkov and Khrustalev (1961) who found

that the permeability of a fine-grained soil may be increased more than 1,000 times immediately upon thaw. (The topic of the hydraulic conductivity of the active layer will be addressed in more detail later in this chapter.) However, Savel'yev maintains that once thawed, the soil between the former ice partings readsorbs much of the water which had been extracted from it during soil ice formation. The cryogenic structure will thus disintegrate and thereby reduce the soil's permeability. As the thaw plane advances, new layers retaining the cryogenic structure are added while, at the same time, the structure of the overlying soil breaks down. In this way a zone of relatively high permeability -- called the 'contact zone' by Savel'yev -- will be maintained beneath a less permeable surface zone -- the 'thawed layer' -- and in this way create and sustain conditions favorable to confined ground water flow throughout the thaw period. Savel'yev concludes by stating that such artesian conditions -- or 'suspending pressures' as he calls them -- are 'inevitable' on slopes comprised of soils with coefficients of consolidation (for the remolded soil?) of less than 10^{-4} cm^2/sec. Unfortunately Savel'yev provides no detailed field documentation of this process.

Savel'yev's mechanism may be a reasonable one. His observations of soil behavior are consistent with those from the Kivitoo bluffs. At Kivitoo, seepage was also encountered above the frost table in some excavations and the soil in this zone often retained more of the cryogenic structure and had a higher void ratio than the thawed soil above it. (See for

example data from Slide 8, above.)

Savel'yev noted that the ice content of the active layer increases dramatically near the limit of seasonal thaw (from 2-25% near the surface to 10-15% in the middle layers to 30-70% near the maximum depth of the thaw). This may be particularly significant since the higher ice contents may imply naturally higher hydraulic conductivity of the recently thawed soil at the base of the seasonal active layer. Again, Savel'yev's observations are in line with those from Kivitoo. Still, wide application of this mechanism to the Kivitoo situation is appears to be unwarrented as it requires ample supplies of water upslope, conditions which would not likely be met in all of the observed cases. Furthermore, while some of the landslides are associated with wet lines, they do not appear to be more frequently encountered along slopes which have such ready water sources; for example, downslope from snow patches. Another objection to this explaination for all of the landslides is the suspected rarity of these events. If the conditions for this mechanism are as widespread as they appear to be then the landslides would be expected to be of more frequent occurrence.

b. Liquefaction of sandy soils

Liquefaction, caused by the undrained structural collapse of loose soils, is a commonly cited mechanism for failure of low-gradient slopes. Work by Terzaghi and Peck (1948), Cassagrande (1976), Andresen and Bjerrum (1967), Youd (1973), Castro (1975), Seed (1968), and others has shown that the soils

most susceptible to liquefaction are non-cohesive, well-sorted medium to very fine sand with porosities in excess of 45-50%. Soft clays and other sensitive muddy soils may also be subject to liquefaction-type failure under suitable conditions (e.g. Wu and Sangrey, 1978).

The low-angle landslides at Kivitoo occur in slightly plastic silts and clays, soils which are not at the greatest risk of liquefaction-type failure. The retention of the blocky cryogenic structure, by increasing interlocking, further reduces the susceptibility of these soils to liquefaction failure under low total stress conditions. Furthermore, as the major portion of the active layer may be relatively stiff due to low moisture contents and overconsolidation effects, these soils are unlikely to undergo significant structural collapse, even under high stress conditions. (The sandy soils in the upper active layer along the bench may be somewhat more susceptible to liquefaction, but observations show that the landslides along the Kivitoo bench are seated in the underlying muds.) Thus it is only the high void ratio basal soils which would be expected to be sensitive to liquefaction failure.

For liquefaction failure to occur a source of disturbance or an increase in stress in the soil resulting in structural collapse is necessary. A major cause of such structural disturbance, even in marginally susceptible soils, is the loading imposed by seismic shock. Seismic records (Seismological Series, Energy, Mines and Resources, Canada) indicate that the east coast of Baffin Island, and the Home Bay area in particular, are subject to seismic activity. The most

recent significant event was a moderate earthquake of 4.9 intensity (Richter) on December 2, 1970, with its epicenter located in Home Bay (Horner et al., 1975). (The quake rated V on the modified Mercalli scale at Cape Hooper and II-III at Broughton Island. It was the largest earthquake in northern Canada that year.)

While it is beyond the scope of this research to assess the susceptibility of active layer soils to shallow failure under seismic loads, it is evident that any shock which does not coincide with the period of thaw -- and in particular late thaw, when high void ratio soils are exposed at the base of the active layer -- would have no effect. Thus it would have been impossible for the 1970 earthquake to have triggered the Kivitoo slope failures. In addition, the 1970 quake was only of moderate intensity; Seed (1968) suggests that the potential for slope failure exists at a range of 5.5 (Richter) and above.

While it is difficult to envision the rare coincidence of major quake activity with the short period of deep thaw, it is possible that the 'fresh' landslides examined here are all of the same age and could therefore, conceivably, have been caused by the same event. However, the presence of older, degraded landslide scars attests to the continuing occurrence of landslides along the Kivitoo bench and argues forcefully against a single seismic event as a trigger for all of the observed instability features.

c. In situ formation of debris-flow by ped slaking during thaw

Based on observations made during the 1977 field season it was thought that the necessary low effective stress conditions (i.e. high pore-fluid pressures) could be generated and maintained in fine-grained active layer soils if, during thaw, the soil between ice partings slakes into the melt-water, forming, in effect, a muddy pore-fluid. Such a 'pore-slurry', because it has a greater density than clear water, would increase the buoyancy forces within the soil. The 'pore-slurry pressures' thus generated might be sufficient to reduce effective stress conditions to the point at which failure could be initiated, even on gentle slopes. Furthermore, if in situ slaking continued to the point where attrition of fines from individual soil peds reduced the size of these peds so much that they were no longer in contact, becoming suspended in a dense slurry matrix, the reduction in ped-ped contact would lower the soil's coefficient of internal friction (ϕ'), possibly to zero. The only strength the active layer would then have is that due to the rheological properties of the pore-slurry itself.

The pore-slurry model is discussed in this section solely in terms of failure <u>initiation</u> on low-angle slopes; i.e. as being the process by which a thawing active layer can be transformed into a debris-flow <u>in situ</u> without any prior shear strain. This is different from the mechanical generation of a debris flow due to the remolding of the slide mass after the initial failure has taken place. A further analysis of slurry

pressures as a particle support mechanism in post-failure debris-flowage is considered in section VI.A,4, below.

Vallejo (1980), following Bagnold (1954), and citing observations of the texture of mudflow and thaw-related landslide debris reported by McRoberts and Morgenstern (1974) and Chandler (1972), has independently suggested a similar approach to the analysis of the stability of thawing slopes in clayey regoliths.

From the discussion above it is apparent that if this slaking process is common in thawing active layers it would have important implications for slope stability. Recognizing this, a primary objective of the 1983 field season was to assess the validity of this mechanism of landslide initiation.

The pore-slurry model as a valid failure initiation mechanism was seriously questioned, however, by the inability to detect a fluid soil or pore-slurry in any of the numerous excavations at Kivitoo. At no location, either in or adjacent to slide scars, or along 'stable' slopes, was a soil comprised of distinct peds dispersed in a dense slurry matrix observed. (These observations are somewhat qualified by the fact that disturbance of the wetter soils, particularly the siltier non-plastic soils, could result in a fluid condition.) In the few instances where there seemed to be a possibility that a fluid soil did exist, the muddy pore-fluid was thought to be the result of disturbance during excavation rather than in situ ped slaking.

The most thorough examination of the in situ structure of a recently thawed silty clay (% sand/silt/clay = 8/60/32) was

at the back of a large instability feature along the side of the stream at K1145 (see location in Figure VIII.9). The depth to the frost table was less than 20 cm, the soil having been recently exposed from beneath a melting snowpack. When thawed, this soil retained the blocky cryogenic structure and appeared loosely aggregated. The pore-fluid, which could be seen in depressions on the slope surface, was clear water. Mechanical disturbance of the thawed soil would easily create a muddy, fluid condition and the soil had little bearing capacity. In situ water content was 22% near the slope surface, 26% at a depth of 15-20 cm and the frozen water content at the frost table was 27%. Dry bulk unit weights of two undisturbed soil samples were 13.6 kN/m^3 and 14.1 kN/m^3, indicating that the soil was loosely packed with an equivalent bulk porosity of 44-48% (Gs = 2.65). As a result of desaturation of the peds during freezing the soil was not saturated (%S = 75-80%) even though the water table was at the surface. This soil, when lightly remolded at the in situ water content was fluid, its 'flow-limit' being in the range of 18-20%. (The 'flow limit' in this case is lower than the liquid limit of the fully remolded soil due to the poorly-sorted texture imparted by incomplete degradation of soil peds as well as their unsaturated state.)

Piezometers installed at this location failed to register any artesian pore pressures. It is interesting that when disturbed the water column in the piezometers was lowered slightly, suggesting that these loosely aggregated blocky soils, at the very low stress levels near the slope surface,

are dilatant (i.e. interlocked) and may therefore have relatively large coefficients of internal friction due to the cryogenic structuring. (Again, these observations are consistent with the work of Roggensack (1977) mentioned above.)

In order to observe directly what happens when such a soil thaws, frozen reticulate-structured soils from the active layer along the bench were excavated and allowed to thaw in a glass jar. In higher ice content soils, particles released from the slaking peds fell rapidly through the thaw-water, settling out on the peds below. As long as the soil remained 'undisturbed' particle settling appeared to proceed at a rate which was greater than or equal to that at which grains were released by ped slaking. However, minor disturbance would disperse some of the slaked soil in the thaw-water and cause abrasion which would accelerate ped slaking. The density of the pore-fluid created in this way would be a function of the amount of disturbance and the inherent dispersive qualities of the particular soil; silty soils tended to be the most dispersive due, in part, to the more rapid saturation of the peds than in the finer-grained and less permeable clayey soils. The siltier soils were also the soils which, because of their low clay content and larger grains, would settle out of suspension most rapidly.) In lower ice content and clayier soils, a thick layer of softened mud would form around the surface of the peds. However, the peds themselves seldom disintegrated entirely, and a slurry matrix occupying a significant proportion of the 'pore' volume did not develop. The thawed fine-grained soils shown in Figure VI.13 illustrate the

substantial retention of the blocky structure.

These observations of thawing soil, along with those from active layer excavations, suggest that the abrasion/dispersion mechanism associated with in situ conditions is not sufficient in itself to result in the formation of a pore-slurry during thaw at Kivitoo. Considering this, the pore-slurry model must be discounted as a significant failure initiation mechanism at Kivitoo.

d. Thaw-consolidation mechanism for single-event slides: Theory

An alternative mechanism for the development of excess pore pressures in the thawing active layer is the thaw-consolidation process. Originally proposed by Taber (1943) thaw-consolidation has received extensive quantitative development in a series of papers by Nixon, Morgenstern, Smith and others. McRoberts (1973) and McRoberts and Morgenstern (1974) have applied thaw-consolidation theory to the specific problem of the stability of thawing slopes. This research included an attempt at field verification.

McRoberts and Morgenstern (1974) have measured excess pore pressures at the backscarp of active low-angle debris lobes. They attributed the artesian conditions to thaw-consolidation (although the recorded pore-pressures substantially exceed those predicted by their model). However, it is uncertain whether these measurements, recorded at the back of a bimodal flow, are representative of pore pressure conditions beneath the entire debris lobe or, indeed, whether they are in fact the

result of a thaw-consolidation process at all. In McRoberts and Morgenstern's field case, rapid supply of debris by an ablating headscarp may have been effective in generating excess pore pressures at the piezometer location (which was at the back of the mobile debris lobe) due either to undrained loading (Hutchinson and Bhandari, 1971) or an upward pore-pressure gradient established by the reconsolidation of the very wet debris being shed by the backscarp. Alternatively (or in conjunction with the above), the observed excess pore-pressures may have been due to mechanically generated pore-slurry pressures within the moving debris-flow.

The process of thaw-consolidation is discussed below. Following an outline of the theory, the model is applied, in the next section, to the Kivitoo slopes. The work reported here seems to be the first attempt at a rigorous verification of the thaw-consolidation mechanism on natural slopes.

Excess pore-water pressures can be generated in a thawed, previously ice-bulked soil if upon the loss of the structural support of the ice after thaw, the soil tends to reconsolidate to a new lower void ratio. This consolidation occurs since the void ratio of the frozen soil is presumed to be greater than that of the thawed soil under the given ultimate effective stress conditions (i.e. after any excess pore pressures have been dissipated). In a saturated soil such a volume decrease must be accompanied by the expulsion of water (presumably upward). If drainage is prohibited, no volume change can occur, and the pore-water at any point in the soil is forced to

carry the newly-imposed weight of the overlying, thawed soil, increasing the pore pressure by an amount equal to the weight of this (saturated) load.

On the other hand, if drainage can occur at the top of the soil, the pore pressure at this surface is zero, while that at any point inside the sample is, initially, equal to the weight of the imposed overlying load at that point. Thus a gradient in excess pore pressure is established. Water can now flow up and out of the sample along this gradient. Once sufficient water has been expelled for the sample to attain the void ratio corresponding to the ultimate effective stress conditions represented by the overlying (saturated) soil (plus the applied load, if present) all excess pore pressures will have been dissipated. The effective stress at any point in the soil skeleton (i.e. the stress that generates frictional strength) will then be equal to the submerged weight of the overlying soil, $\gamma' X$ (plus that of any applied load).

The rate of dissipation of the excess pore pressures generated during the consolidation process (and therefore the time required for the soil to attain the new void ratio) is a function of the permeability (kw) and compressibility (defined in terms of the coefficient of volume change, Mv) of the soil. Mv defines the magnitude of volume change associated with a given increase in the ultimate effective stress. It therefore defines the amount of water which will be expelled from the soil undergoing consolidation. These factors (kw and Mv) are combined in consolidation theory as the coefficient of

consolidation, Cv, where

$$Cv = \frac{\Delta kw}{\gamma_w \cdot Mv} \qquad \text{(VI.3)}$$

Standard linear consolidation theory assumes that Cv is a constant for a given, normally consolidated soil over a range of consolidation loads. The greater the magnitude of Cv, the more rapidly the excess pore pressures are dissipated and therefore the faster the soil can reconsolidate to the new equilibrium void ratio. The relationship between kw and Mv in Eq.VI.3 indicates that highly permeable soils of low compressibility would have the largest values of Cv and would therefore display the most rapid consolidation. Soils of high compressibility and low permeability would dissipate the excess pore pressure more slowly.

In the example given above the soil is first completely thawed (under undrained conditions) and only then allowed to consolidate under its own weight. The case of a soil undergoing thaw-consolidation in the field is slightly different since new soil of higher void ratio is continuously being added at the descending thaw front while, at the same time, upward drainage is occurring from the consolidating soil at the thaw front. The magnitude of the excess pore pressures at the base of the thawing soil is now dependent <u>also</u> upon the rate at which water is produced at the thaw plane (as well as upon the thawed soil's compressibility and permeability; i.e. Cv). The rate of thaw (generating the excess pore pressures) and the rate of excess pore pressure dissipation (in terms of

Cv) are combined as a single, dimensionless thaw-consolidation ratio (Morgenstern and Nixon, 1971). This ratio (R) defines the rate at which thawed, saturated soil of a given void ratio and compressibility is produced at the thaw plane relative to the rate at which the water from this soil is moved upwards out of the thaw zone allowing consolidation to occur and tending to dissipate the induced excess pore pressures.

Thus R is a measure of the balance between two terms. One is the coefficient of consolidation (Cv; Eq. VI.3). The other term is the thaw rate, defined by the thermal constant, α, given by

$$x = \alpha \sqrt{t} \qquad \text{(VI.4)}$$

where x is the thaw depth, t is time and α is a constant for the given soil and thermal boundary conditions. Equation VI.4 is often referred to as the Neumann Solution (e.g. Jumikis, 1977) and assumes that the rate of thaw for a given soil and thawing temperature is linear with respect to the square root of time. The thaw-consolidation ratio is thus defined by the following relationship

$$R = \frac{\alpha}{2\sqrt{Cv}} \qquad \text{(VI.5)}$$

The effect of R on slope stability may now be considered. For a slope inclined at an angle B and self-weight conditions (i.e. no applied load), the excess pore pressure at depth X (u_e; Eq. VI.1) due to thaw-consolidation is given by McRoberts and Morgenstern (1974: Eq.7) as

$$u_e = \gamma' X \cos^2 i \left[\frac{1}{1 + 1/(2R^2)}\right] \qquad (VI.6)$$

where $\gamma' X$ is the submerged bulk specific weight of the soil ($\gamma' = (\gamma - \gamma_w)$) and ($\gamma' X \cos^2 i$) is the effective normal stress on the lower boundary after complete dissipation of excess pore pressures. The <u>total</u> pore pressure in an (inclined) thawing soil is given by Eq. VI.7 which combines the pore pressure for fully saturated slope parallel groundwater flow conditions [Eq. III.7 and III.10, where m = 1, and dl = D (= X here), i.e. the total thickness of the soil above the thaw front is saturated plus the excess pressure (u_e: Eq.VI.6).

$$u = \gamma_w X \cos^2 i + \left[\frac{\gamma' X \cos^2 i}{1 + 1/(2R^2)}\right] \qquad (VI.7)$$

where, in effect, the term ($\gamma_w + \gamma'/[1 + 1/(2R^2)]$) defines the new $m \cdot \gamma_w$ value (Eq. III.11) under thaw-consolidation conditions.

Combining Eq. VI.7 with the standard infinite slope stability model (Eq. III.11) gives the following solution for the threshold slope angle (i_t) of an infinite slope in a thawing soil.

$$\tan i_t = \frac{\gamma'}{\gamma} \left[1 - \frac{1}{1 + 1/(2R^2)}\right] \tan \phi' \qquad (VI.8)$$

Using Eq. VI.8, and knowing the appropriate values of R, γ' and ϕ', it is now possible to evaluate the potential stability of a thawing slope.

The solution presented above assumes that the initial effective stress in the thawed soil is insignificant. In other words, if the soil is thawed in an undrained situation and subject to self-loading (or an applied load), the increase in the pore pressure within the (saturated) soil will be exactly equal to the buoyant weight of the overlying soil (or the applied load). In this case, the effective stress, as defined by Eq. VI.2, will be zero. If drainage is now permitted, consolidation will occur, no matter how small the load, and continue until all the excess pore pressures are dissipated. For high ice-content soils the assumption that the initial effective stess is zero is probably correct (Nixon and Morgenstern, 1973; Roggensack, 1977).

It has been recognized however (Morgenstern and Nixon, 1971), that in some thawed soils the initial effective stress may not be zero. These soils would therefore have some initial strength upon thaw, and consolidation will not occur unless the ultimate effective stress, after the dissipation of all excess pore pressures, exceeds this initial 'residual stress' -- denoted here as σ'_r. If a residual stress exists in the thawed soil the consequent reduction in the soil's void ratio will be less than that for a soil in which the residual stress is zero, and the pore pressures generated during thaw-consolidation will be lower than those predicted by the thaw-consolidation solution presented here.

Roggenstock (1977), summarizing an extensive testing program on undisturbed specimens, concludes that the residual stress is insignificant in soils where the ice content exceeds

the liquid limit. Since the ice content of the soil at the base of the active layer along the Kivitoo bench slopes is generally greater than the liquid limit (> 30%), and it is the worst possible stability conditions (for given values of α and Cv) that are of interest here, the residual stress in the following analysis is assumed to be minimal. The situation where the residual stress is not zero will be considered later.

Several problems arise when considering the effectiveness of thaw-consolidation in creating critically low soil strength conditions on thawing slopes. Firstly, the process requires soils with low to moderate coefficients of consolidation, or very high values of α, if the thaw-consolidation ratio (R) is to be large enough to predict failure on gentle slopes. As we have noted above, the retention of cryogenic structure during thaw may actually increase the permeability of the thawed soil, raising Cv above critical values (if a confining layer of low permeability does not develop). A second objection raised by Vallejo (1980) in relation to thaw consolidation (and by Chandler (1972) in relation to the ice-blocked drainage mechanism) is the perceived difficulty of generating and maintaining large excess pore-water pressures over extensive areas. Local variability in thaw depth, ice content and physical properties of the soil (such as Cv, $\sigma'r$, kw) could lead to great variations in soil strength, and therefore shear resistance, over relatively small areas.

In the context of the latter, the Kivitoo data indicate that along the bench slopes the active layer thickness later in

the thaw season is areally uniform over short distances (to within 10 cm) and that the icy basal layers may also be areally continuous. It is also possible that since the icy layers just below the depth of average annual thaw accumulate over time, they display less variation in moisture content between closely spaced sites than does the ice profile higher up in the frozen active layer. (The ice profile in the active layer, since it reforms each year, should be more sensitive to local moisture conditions.) The differences in strength between thawing soils of varying high ice contents will be less than that for soils of different lower ice contents, due to such factors as the elimination of all residual stresses. The slowing down of the thaw front in the icy soils would eliminate large spatial variations in active layer development late in the thaw season by allowing the thaw plane to 'catch up' with nearby, deeper thaw penetration. Also, closely spaced differences in ground surface thermal conditions will average out at depth. (This has been demonstrated by Wright (1985, pers. comm.) at a sub-arctic site.)

Thus, deep penetration of the frost table, by exposing a thick zone of high ice-content soil to prolonged thaw and integrating boundary conditions, could 'smooth out' localized spatial variation (in both active layer depth and soil strength). The net result of this deep and prolonged thaw would be the creation of areally uniform thaw-consolidation conditions over relatively large portions of the bench slope. (In more heterogeneous active layers, such as the hummocky slopes discussed by Mackay (1981, 1983), local variations in

active layer depth would present an extremely rough surface over which to develop a continuous failure 'plane' located at the frost table. This rough surface would increase shear resistance and may inhibit failure.)

3. Thaw-consolidation mechanism: Appliction to Kivitoo.

Considering the alternatives, thaw-consolidation is the most reasonable mechanism which can be employed to account for the initiation of landslides on low-gradient slopes in active layer soils. In following analysis, the thaw-consolidation model is applied to the field situation at Kivitoo. First, representative values of the thaw-consolidation parameters (α, Cv) for the Kivitoo landslides are obtained. These values are then used in the thaw-consolidation analysis as outlined above. Following this a number of extensions and qualifications of the basic thaw-consolidation model are considered.

a. Solution of the thermal problem: Derivation of the thermal constant, α, for Kivitoo.

i. Determination of the thermal constant from field measurements

The rate of thaw in a frozen soil is defined by the Neumann solution, Eq. VI.4. If the depth of thaw (x1, x2) is known at times t1 and t2 then the thermal constant (α) can be calculated directly from field data using the following

solution.

$$\sigma = \sqrt{2 \frac{dx}{dt} x'} \qquad \text{(VI.9)}$$

where $dx = x2 - x1$, and $dt = t2 - t1$ and x' is equal to the median depth of thaw between x1 and x2. This analysis makes the assumption that the rate of thaw relative to the square root of time remains constant between t1 and t2.

The values of the thermal constant calculated from the 1983 field data in Table VI.3 fall within a narrow range, 0.02 to 0.036 cm/sec$^{\frac{1}{2}}$ with an average of 0.028 cm/sec$^{\frac{1}{2}}$. The sites where active layer depths were measured represent a variety of soil and ground water conditions along the bench slopes so that the measured values of the thermal constant are representative of a number of possible situations. The values of the thermal constant given in Table VI.3, were determined when the thaw front was in the lower portion of the active layer. As the clean slide scars at Kivitoo are 60-100 cm deep, these values are considered to be the relevant ones for use in a thawing slope stability analysis.

The observed variation in the value of the thermal constant between sites is to be expected and results from local differences in the thermal properties of the thawed soil, the ice content of the frozen soil and other factors, such as site-to-site variation in the relationship between air and ground surface temperature. The value of the thermal constant at any one site will also vary throughout the summer period as air temperature fluctuates and layers of different thermal

properties and ice content are encountered by the thaw plane. (The problems presented by a variable thermal constant will be considered below and in Appendix A.) Thus it is not possible, nor correct, to define a single value of the thermal constant for Kivitoo. Rather, it is more appropriate to use a range of possible values which may then be used to define both average and worst-case situations. The field data do show, however, that the thermal constant in a given year varies over a small range and, as noted above, the effect of small variations in are, ultimately, not as significant in terms of thaw-consolidation and slope stability as are the possible variations in other factors such as the coeficient of consolidation and hydraulic conductivity of the thawed soil. This point will be demonstrated in the stability analysis, below.

ii. Analytical definition of the thermal constant and back-calculation of average seasonal thawing temperatures

In order to assess the representativeness of the values of the thermal constant calculated for the two field seasons and to define expected year-to-year variations in both the thermal constant and maximum seasonal active layer thickness, it is useful to define the thermal constant analytically. Using this analytical solution to the thawing problem, reasonable estimates of seasonal thawing temperatures, thaw rates and active layer depths can be derived for past years from local weather records.

The thermal constant (α) is defined analytically for given soil and thermal boundary conditions by the Stefan solution (e.g. Jumikis, 1977),

$$\alpha = \sqrt{\frac{2Ku \cdot Ts}{L}} \qquad \text{(VI.10)}$$

where Ku is the thermal conductivity of the unfrozen soil, L is the latent heat content of the frozen soil and Ts is the thawing temperature (>0°C) at the ground surface. The thermal boundary conditions in the Stefan solution are defined by Ts and 0°C at the thaw plane, the difference being defined as the step temperature. This solution assumes that all heat transfer into the soil is conductive. The latent heat content of the frozen soil (L) increases with ice content, while the thermal conductivity of the unfrozen soil (Ku) tends to decrease as the water content increases. Thus, for a given step temperature, the value of the thermal constant (as calculated from Eq. VI.10) increases as the ice content of the frozen soil, or as the water content of the overlying thawed soil, decreases. At a given water content, saturated coarse-grained soils tend to have higher thermal conductivity values than fine-grained soils (e.g. Kersten, 1949).

A hypothetical thawing step temperature can be back-calculated from Eq. VI.10 using the α values derived from the Kivitoo field data if the values of Ku and L are known and α is assumed to remain constant throughout the thaw season. Typical values for Ku and L can be found in various sources (e.g. Jumikis, 1977; Kersten, 1949; Johnson, 1980), as well as

in the series of papers by Morgenstern, Nixon, et al., cited above. For a thawing clayey silt of low plasticity with an ice content of 30% and an unfrozen water content of 20% values of L and Ku would be 36 cal/cm³ and 0.0041 cal/cm °C s respectively. Obviously, soil moisture parameters vary from site to site and within a given profile. These values, however, are considered to be representative average values for the soils found along the Kivitoo bench and are used here to derive reasonable estimates of Ts. (See, for comparison, soils data in the landslide case studies, above.) A more detailed analysis might be made for each individual site, but, due to uncetainties about the ice conmtent profile in the upper portion of the active layer, as well as other factors (discussed below), such an analysis would not neccesarily yield more useful results.

Using the set of thermal parameters just defined, hypothetical step temperatures derived for 1983 are 1.8° to 5.7° C with an average value of 3.9°C (Ts+, Table VI.3). For the 1977 data, the average back calculated step temperature is nearly the same, 3.6°, even though the summer of 1977 was warmer than 1983. This discrepancy is probably due to the fact that the soil at the site where the 1977 data were collected (behind the retrogressive active layer failure at K990) was particularly ice-rich. Therefore, the value of L used in the analysis is probably too small and thus, the back-calculated value of Ts too low. If a larger value for L is used, a more reasonable estimate of Ts can be obtained. Further analysis on the sensitivity of the value of Ts to variations in other variables is provided in Appendix A.

A more accurate thermal model for the development of the active layer at Kivitoo can be constructed by acknowledging that the fine-grained soil along much of the bench is overlain by 30-40 cm of colluvial sand with different values of Ku and L. Nixon and Morgenstern (1973) use a modified form of the Stefan solution to solve such a two-layer thawing problem:

$$X = \sqrt{\left[\frac{Ku_2}{Ku_1} H\right]^2 + \frac{2Ku_2 Ts\ (t - t,o)}{L_2}} - \left[\frac{Ku_2}{Ku_1} - 1\right] H \qquad (VI.11)$$

where t,o is the time required to thaw the top layer of thickness H and properties Ku_1, L_1. The term t,o can be calculated by deriving α for the surface layer from Eq. VI.10 and then substituting this result into the Neumann solution (Eq. VI.4), taking the thickness of the upper layer as the depth of thaw (X). Using the following values -- For the upper sandy soil layer: Wu = 15-20%, Wf = 20%; Ku_1 = 0.006 cal/cm °C s, L_1 = 20 cal/cm³. While for the lower fine-grained layer: Wu = 20%, Wf = 32%; Ku_2 = 0.0041 cal/cm °C s, L_2 = 38 cal/cm³ (from Jumikis (1977) -- a graphic solution to Eq. VI.11 can be constructed by plotting thaw depth against thaw season length (in days) for a reasonable range of equivalent step temperatures (e.g. 1°-10° C). This solution is shown in Figure VI.14. The value of the thermal constant (α) in the lower soil layer can be calculated directly from each of the curves in Figure VI.14. This ranges from .017 cm/sec$^{\frac{1}{2}}$ for an equivalent step temperature of 1°C to .049 cm/sec$^{\frac{1}{2}}$ for an equivalent step temperature of 10°C. Yet, when this active layer thermal model is applied uniformly to the Kivitoo field data in Table VI.4,

the back-calculated step temperatures are not significantly reduced, suggesting that the between site variation in thaw rate is, in large part, a result of other factors, such as variations in ground surface temperature.

The meaning of the the hypothetical step temperatures derived above (and in Appendix A) in relation to the actual field conditions is difficult to assess (even if these are corrected for air/ground temperature differences). This is because thawing temperatures in the field do not occur as a step temperature increase, but fluctuate throughout the thaw season. It may therefore be more meaningful to think of the back-calculated step temperature, not in real terms, but rather as representing the total amount of heat available for thawing averaged over the length of the thaw season (or period of measurement).

iii. Year-to-year variation in thaw rate and active layer depth.

Equivalent step temperatures, thaw rates and active layer depths have been derived for the years 1960-1983 using the weather records from Broughton Island; Table VI.4.

The amount of thawing in a given active layer profile depends, ultimately, upon the amount of heat which can be moved into the soil. The best first approximation of the total amount of heat available for thawing during the summer season which can be made from weather data is the number of thawing degree days. (Using the daily mean temperatures, this is the

number of degrees above 0°C per day summed for all days in the thaw season). A single step temperature for the particular thaw season can be defined by dividing the number of thawing degree days by the length of the thaw season (see, for example, Nixon and Morgenstern, 1973). These data are given in Table VI.4 as an 'equivalent' step temperature. (Geometric methods considering idealized temperature time series curves (e.g. Nelson and Outcalt, 1984) have been devised to calculate a single yearly thawing temperature, although for short, low-amplitude thaw seasons these methods probably do not yield more accurate results.) The calculated thaw season length and equivalent step temperature may then be used in association with soil thermal properties to back-calculate expected year-to-year variations in α and thaw depth. If the two-layer model developed above is considered to be a best representation of the soil profile along the bench, then the graphical solution given in Figure VI.14 can be used along with the particular thaw season length and equivalent step temperature from Table VI.4, to define a representative thaw depth and value of the thermal constant for a given year. While this method, when used without correction for air/ground temperature differences, would tend to slightly underpredict active layer depths along much of the Kivitoo bench the magnitude of year-to-year variations are still meaningfully defined.

The exact length of the thaw season is difficult to determine because of day-to-day fluctuations of air temperature above and below 0°C (particularly during change-over periods; Boyd, 1976), as well as differences between ground and air

temperature. For the purposes of this study, the thaw season was considered to begin with the first two consecutive days of mean daily air temperatures above 0°C which are not interrupted by more than the same number of days with negative mean temperatures. The end of the thaw season was similarly determined. An equivalent step temperature was then calculated using a thaw season length derived using two different methods; one in which all of the days in the thaw period were counted, and the other where only those days with a mean temperature above 0°C were used. These two methods give different values for thaw season length and, therefore, different equivalent step temperatres. As the total number of degree-days in either case remains the same, counting all the days obviously gives a lower thaw season equivalent step temperature than when only the days with positive mean temperatures are considered.

Using the first method, the equivalent step temperatures derived from the Broughton Island weather data average 4.5°C ranging from a low of 3.2°C in 1972 to a peak of 7.0°C in 1969. If the longer thaw season is used, the average is 3.8°C, with a low of 2°C in 1970 and a high of 5.6°C in 1966. These values are, at least, in general agreement with the step temperatues back-calculated from the Kivitoo data and the low yearly temperature value of 2.1°C for 1983 is in good agreement with the Ts calculated for the wet site (where the n-factor (Appendix A) is most likely close to unity).

As the back-calculated values of α -- and therefore the thaw consolidation ratio (R) -- will be larger if the higher step temperature is used, the value of the thermal constant

derived from weather data must be interpreted cautiously. As it is the most severe thaw conditions, in terms of slope stability, which are of interest, and the Kivitoo data show that the relevant Ts may exceed air temperature, the higher values of the equivalent step temperature may be used to define a 'worst case'. It must be emphasized that between-site variations of α in any one year may be greater than the predicted year-to-year variations. Still, whichever value of the eqivalent step temperature is used, the calculated yearly values of the thermal constant defined for this idealized soil profile are useful as an indication of the magnitude of year-to-year variations in α which can be expected. These results may then be interpreted in light of the range of α defined locally in any given year.

Even though the thermal constant will vary depending upon the method used to calculate eqivalent step temperature, the maximum depth of thaw obtained using either method is approximately the same. This is because the total number of degree days is constant. (If the longer thaw season is used, the calculated step temperature is correspondingly lower.) Thus, while this analysis can only suggest what the magnitude of year-to-year variation in the thaw rate might be, it gives a better indication of yearly differences in active layer thickness.

Thawing degree days are, obviously, unevenly distributed over time. For a given number of degree days, it is the length of the thaw season and the distribution of thawing heat within this period which affects the rate of thaw. Thus, while short,

warm summers may result in active layer development identical to that of longer, cooler summers, the rate of thaw in the former case will exceed that of the cooler summers, and it is the rate of thaw which is most significant in terms of the analytical thaw-consolidation solution as defined above. Yet, even high thaw rates may not be effective in generating large values of the thaw-consolidation ratio (R) if the soils being thawed have large values of Cv, or, in layered soil profiles, if the overlying soils are highly permeable. Therefore, not only must the thaw rate be sufficiently high, but the soil conditions in relation to the thaw plane, must also be conducive to excess pore pressure generation.

While fluctuations in surface temperature may cause variations in the thaw rate, the maximun depth of thaw at the end of the thaw period remains the same for either a fluctuating temperature regime or a constant step temperature. Yet, it may be significant in relation to thaw-consolidation problems that, in contrast to the rate of thaw under a constant equivalent step temperatue, a variable surface temperature regime could result in marked fluctuations in thaw rate. For example, Nixon and McRoberts (1973) show that while the actual depth of thaw penetration using either a hyperbolic temperature history or an equivalent step temperature is identical, rate of thaw advance under the hyperbolic temperature regime increases markedly later in the thaw season. (McRoberts (1975) has presented field data which show that some thawing active layer soils may, in fact, exhibit this effect.) This accelerated late season thawing (relative to the square root of time) may

be important since (in the case of a hyperbolic thermal regime) it means α values would tend to be greatest later in the thaw season, when the active layer is thickest and the thaw front may be penetrating very icy soil. However, overall, the variations in thaw rate at Kivitoo due to air temperature fluctuations, probably remain within a reletively narrow range. The calculated thaw rates for equivalent step temperatures of 1° to 10°C shown in the plot of the solution to the two layer thawing problem defined above (Figure VI.14) have a range of 0.017 to 0.049 $cm/sec^{\frac{1}{2}}$. If only the range of equivalent step temperatures calculated for the years 1960-1983 (Table VI.4) are used then the variation in α is even less; 0.023 to 0.041 $cm/sec^{\frac{1}{2}}$. Still, in marginal stability situations such small variations may be significant.

The thermal analysis developed above has adopted a two layer active layer model. If a very icy basal soil is present this would represent a third layer. As noted above, when the thaw plane reaches an icy layer at depth its progress may be further damped due to the increase in the amount of heat required to melt the additional ice. Therefore year-to-year differences in active layer depth are probably not, in fact, as great as those just defined. Without engaging in a more detailed numerical treatment, the thermal analysis presented above can be reinterpreted to indicate, not the depth of thaw, but the amount of time during which the icy basal layer is exposed to thaw (at a given thaw rate) and, hence, ultimately, the amount of water released at the thaw plane. [With very icy soils, where ice accounts for most of the soil volume, active

layer thickness cannot be estimated unless the volume of the thawed soil after the expulsion of all excess melt water can be predicted. As the ice content by volume approaches 100%, continued thaw will not result in any thickening of the active layer since, after all the melt water has been expelled, no new soil has been added at the active layer's base (Nixon, 1973).

The maximun, minimum and average depth of thaw calculated using the two-layer model are 110 cm (1975), 63 cm (1983) and 87 cm, respectively. The minimum value from 1983, underpredicts, by 5 to 15 cm, the actual thaw depths measured in the field that year. (This discrepancy may be corrected by assuming different thermal parameters, for example, a lower water content for the upper layer.) The analysis, however, does show large year-to-year differences in thaw depth. If the calculated depth of thaw penetration is effectively mitigated by the presence of icy basal layers, then the back-calculated values may be manifest as variations, not in the depth of thaw, but rather in the amount of time during which these icy soils are exposed to thaw (at a given rate). Since the icy layers would be expected to occur somewhat below the median depth of thaw, then (for reasons given in the previous sections) the thaw plane should just approch this depth in most years and significant melting should not occur. However, in exceptional years, it would penetrate these layers, thawing them at a given rate for a greater or lesser period of time. The suggestion from this analysis that years such as 1962, 1966 and 1975 were ones of significant thaw in the ice-rich basal layers (see Table VI.4) is worth emaphasizing here, and will be considered

later. Also worth pointing out is that thaw seasons such as 1969, which was warm but short, may not result in rapid thaw of icy basal layers since the thaw front does not have sufficient time to reach this depth.

b. Determination of the coefficient of consolidation, Cv, for the fine-grained soils along the Kivitoo bench.

Calculation of the magnitude of excess pore pressures in a thaw-consolidating soil is dependent upon a knowledge of Cv as well as upon σ_z. Determination of the relevant coefficient of consolidation for a given soil must be done by consolidation testing in the laboratory.

The coefficient of consolidation was obtained for several representative soils from Kivitoo using a standard dead load consolidometer with a 6.35 cm (diameter) by 2.54 cm (height) circular sample. Consolidation tests on both fully remolded and frozen/thawed samples were performed in an effort to determine the effect freezing would have on the magnitude of Cv. The tests were carried out at various water contents up to 40% (LI = 4) and a range of consolidation loads: 9.8 - 70 kPa. Reliable tests could not be performed at higher water contents due to excessive sample extrusion around the loading cap. Soil freezing was done by placing a remoulded sample in a perspex odometer ring in a refrigerator freezer. This produced a cryogenic structure of ataxic ice veins (most less than 1 mm thick) which resembled that found in the field. A typical frozen test sample is shown in Figure VI.15.

The value of Cv is determined from the plot of vertical displacement (compression) versus the logarithm of time using the following standard formula (e.g. Lambe, 1951)

$$Cv = \frac{0.197\ (1/2\ H)^2}{t,50} \qquad \text{(VI.12)}$$

where H is the sample thickness and t,50 is the time at which 50% of the total (primary) compression has occurred. Typical consolidation curves for a remolded and frozen/thawed sample are shown in Figure VI.16. In order to determine t,50 it is necessary to define the d,100 point (100% primary consolidation) and a corrected zero point, d,s. Determination of d,s is relatively straightforward for remolded soils in which the initial portion of the compression curve has a gentle slope and the consolidation curve approximates an idealized form. However, the large, rapid vertical strains observed in the frozen/thawed samples make the definition of the early portion of the consolidation curve, and therefore the determination of a corrected zero point, difficult. Thus, d,s for the frozen/thawed samples is, necessarily, approximate, and there is a corresponding loss in accuracy in the calculation of the coefficient of consolidation. In fact, this method most likely gives a value of Cv which is low since, as a result of the extremely rapid initial consolidation, the corrected zero point is well below the initial zero, and the derived t,50 is correspondingly large. Recognizing this, it is still possible to calculate a relevant Cv, for clearly the rapid initial consolidation of frozen/thawed samples gives a 50% compression

time which is much less than that of the corresponding remoulded soil, resulting in the calculation of a coefficient of consolidation which, if not precisely defined, is nonetheless one to three orders of magnitude larger. Also, the conventional division of the consolidation curve into primary and secondary compression portions may not be an adequate practice for frozen/thawed soils. In these structured soils initial rapid consolidation is most likely a result of the closing of cracks between peds, rather than a more uniform consolidation of the sample as a whole.

Typical values of Cv for the frozen-thawed soil are in the range 10^{-2} - 10^{-3} cm^2/s while Cv for the remolded soil is 10^{-4} - 10^{-5} cm^2/s. Coefficients of consolidation for two representative fine-grained soil samples (from Slide 3; Bulk Samples 1 and 2) are given in Table VI.5.

It is interesting to note that for a stage-loaded sample of frozen/thawed soil the consolidation curve returns to the 'normal' form at the larger compression loadings. This is shown by the consolidation curves for both remolded and frozen/thawed, stage-loaded samples in Figure VI.17 and suggests that once the cracks left by the melted ice veins are closed and the compression load exceeds the residual stress present in the overconsolidated soil peds, the relationship between kw and Mv (Eq. VI.3) returns to that of the remolded soil. The 'transition stress' at which the consolidation curve returns to its 'normal' form gives an indication of the overconsolidation stresses to which the soil between the ice partings has been subjected. For the soils tested in the

laboratory, this transition stress is between 35 and 70 kPa, which is greater than the overburden stresses in a thawing active layer less than a metre thick. For a given specimen Cv also tends to decrease as the initial void ratio of the frozen/thawed soil decreases. The reduction in Cv may be by two or three orders of magnitude. For example, Cv decreased from 2.5×10^{-2} cm^2/s under the initial loading to 6.3×10^{-4} cm^2/s under a subsequent, higher load (Bulk Sample 2, test 7; Table VI.5 and Figure VI.17). This is significant since the standard thaw-consolidation model assumes that Cv is a constant for a given soil.

c. Calculation of the thaw-consolidation ratio, R, for the Kivitoo bench slopes.

Now that representative values for α and Cv have been obtained it is possible to use Eq. VI.5 to calculate values of the thaw-consolidation ratio, R, for a soil thawing in the field at Kivitoo. In the following analysis the stability of a 4° slope ($\gamma = 18$ kN/m^3, $\phi' = 32°$) will be considered, as this was the inclination of the lowest-gradient failure at Kivitoo. From Eq.VI.8, the R value necessary to account for failure of this slope is 1.22. (For slopes inclined at 1° to 10°, the values of the thaw-consolidation ratio required for failure ranges from 2.7 to 0.54.)

Using the coefficient of consolidation for the remolded fine-grained soil (initial loading only) -- $6.9 \times 10^{-5} < Cv <$

4.1×10^{-4} cm²/s; Table VI.5 -- and a range of the thermal constant -- from Tables VI.3 and VI.4; $0.02 < \alpha < 0.041$ cm/s$^{\frac{1}{2}}$ -- the calculated extreme values of the thaw-consolidation ratio are 0.49 and 2.5. For these low values of Cv, then, failure on a 4° slope is explicable at the higher rates of thaw. Still, using the lower Cv values for the remolded soils, stability is predicted most of the time, with failure possible only at the highest thaw rates.

However, consolidation tests indicate that the relevant Cv for a frozen/thawed soil may be considerably greater than that for the remolded soil used above. Taking an average value of Cv for the frozen/thawed soil from the laboratory tests -- 1.2×10^{-2} cm²/s -- the computed values are significantly lower; $0.09 < R < 0.19$ (an 88% reduction in the value of R). Minimal excess pore pressures are therefore predicted and even at the higher thaw rates, the slope should be stable. In fact, if R = 0.19, no slope less steep than 15° should fail.

As a further check on these calculations, Eq. VI.5 may be used to calculate some hypothetical α and Cv values necessary for failure, i.e. to attain R = 1.22. If a high range value of α is used -- 0.041 cm/s$^{\frac{1}{2}}$; Ts = 7.0°C -- the coefficient of consolidation must be equal to 2.8×10^{-4} cm²/s, which, according to the laboratory data, is unexpectedly low for a recently thawed soil. However, if a more reasonable value of Cv is used (1×10^{-3} cm²/s, which is still less than the average Cv calculated from the laboratory tests), the thermal constant must equal 0.08 cm/s$^{\frac{1}{2}}$. This α value is unrealistically high for Rivitoo (particularly for ice-rich

soils), corresponding to a step tepmerature increase of 36°C.

These calculations emphasize the extreme sensitivity of the thaw-consolidation model to variations in the magnitude of the consolidation coefficient (as has been noted by McRoberts and Morgenstern, 1974). The degree of variation of this parameter which could be expected in the field is much greater than the potential variation of the thermal constant. The laboratory data do show consistently high Cv values for the frozen/thawed soils and it is these values which should be used in the solution of the single layer thaw-consolidation model. Therefore this analysis, using the larger Cv of the thawing soil coupled with the low values of the thermal constant derived for Kivitoo, can adequately account for the general stability of the Kivitoo bench slopes and the inability to detect any unequivocal excess pore pressures during the 1983 field season. It is, however, incompatible with the fact that failure does, sometimes, occur.

d. The special case of active layers with continuous icy layers at depth.

If, in a thawing soil, thick ice layers are encountered at the thaw plane, a situation is established in which the thickness of the overlying soil, Xo, and the thermal gradient are constant. This is because no recently thawed soil is being added to the thickness of the active layer. For a given step temperature the rate of melting of the ice layer and hence the rate of release of meltwater into the overlying soil can be

calculated. Knowing this and the hydraulic conductivity of the thawed soil overlying the ice layer, a new excess pore pressure gradient can be derived. Nixon (1973) provides a solution for the excess pore pressure gradient at the soil/ice interface

$$D = \frac{\gamma_i \; Ku \; (Ts - Tf)}{kw \; (Po + \gamma' Xo) \; Li} \qquad (VI.13)$$

where D is the dimensionless excess pore pressure gradient, γ_i is the unit weight of ice, Ku is the thermal conductivity of the thawed soil, Ts is the applied temperature at the soil surface, Tf is the temperature at the soil/ice interface (0°C), kw is the hydraulic conductivity of the thawed soil, γ'Xo is the submerged weight of the overlying soil, and Li is the volumetric latent heat content of ice (80 cal/cm^3).

Initially, as the thaw front begins to melt the ice layer, the overlying soil will tend to expand (deconsolidate) in response to the higher pore pressures and lower effective stress conditions involved in the expulsion of the melt water. As the thawed soil increases in volume water, moving from the thaw front to the surface in response to the new excess pore pressure gradient, will be extracted, tending initially to mitigate the induced excess pore pressures. Thus the new steady-state excess pore pressure gradient, D, will not be established immediately. The rate at which the initial excess pore pressure gradient, B (i.e. the excess pore pressure gradient prior to melting of the ice layer which is, for this analysis, assumed to be 0), will approach the new excess pore pressure gradient is a function of time, and is dependent upon

both Cv of the thawed soil and Xo, the thickness of the soil above the ice lens. The time required for the hydraulic gradient to change from B to D is expressed as a time factor, derived from standard consolidation theory but here used for the inverse case of deconsolidation

$$T = \frac{Cv \bullet t}{Xo^2} \qquad \text{(VI.14)}$$

Nixon (1973) redefines the time factor, in terms of the time required to thaw the ice layer

$$Tf = \frac{Cv \bullet tf}{Xo^2} = \frac{Cv \bullet hi \bullet Li}{Ku\ (Ts - Tf)\ Xo} \qquad \text{(VI.15)}$$

where hi is the thickness of the ice layer and tf is the time required to thaw the layer.

In order to calculate D it is necessary to obtain a representative value of kw, the hydraulic conductivity of the thawed soil overlying the icy layer. To this end, infiltration tests were performed at Kivitoo to determine field conductivity. By introducing a volume of water into the piezometer tubes and allowing this water to drain into the soil, what is essentially a falling head permeability test can be done. For this it is necessary to record the height of the water column above the water table at known intervals. Since only a single piezometer tube was used in each location a realistic pressure field about the piezometer tip, which the drainage of the water column into the soil will induce, must be assumed. Only once the hydraulic gradient is thus established can Darcy's Law be invoked to calculate the soil's hydraulic

conductivity.

Kirkham (1945) has considered this situation. The solution assumes that the piezometer is seated in an isotropic soil (i.e. kw horizontal = kw vertical). The analytical description of Kirkham's method and its application to the Kivitroo sites is summarized in Appendix A. Field conductivity for sites along the bench at Kivitoo are given in Table VI.6.

All piezometer tips were located in the fine-grained soils in which the landslides on the bench are seated. Field hydraulic conductivity ranged from 1 X 10^{-4} cm/s to 1 X 10^{-7} cm/s with most conductivity values in the 1 - 5 X 10^{-7} cm/s range. These values are in agreement with the calculated hydraulic conductivities obtained for the same soils, in a remolded state, from consolidation tests; kw = 10^{-4} to 10^{-7} cm/s. The field values are, however, considerably lower than those calculated from consolidation data for the frozen/thawed soils; (kw = 10^{-3} - 10^{-4} cm/s). Laboratory data from tests on undisturbed thawed specimens (Rowley et al., 1973; Watson et al., 1973; Chamberlain and Gow, 1978; Morgenstern and Nixon, 1975; Roggensack, 1977; Harris, 1977) also suggest that the Kivitoo field conductivity values may be too low by one to three orders of magnitude. Yet the Kivitoo data are in agreement with the in situ hydraulic conductivities measured by Chandler (1972) who obtained a kw value of 1 - 5 X 10^{-7} cm/s in a silty active layer soil (< 15% clay; 0.62 < e < 0.75). Such a soil, in a remolded state, would be expected to have a higher conductivity than the clayier Kivitoo soils. Unfortunately, few other in situ active layer conductivity values are

available.

The permafrost literature (e.g. Roggensack, 1977; Chamberlain and Gow, 1978) stresses the increase in hydraulic conductivity which frost action can induce in a soil sample. This increase, due to the retention of the cryogenic structure, may be as great as 10^3. Roggensack, however, has shown that the observed increase in hydraulic conductivity only applies at very low effective stress levels (less than ca 15 - 20 kPa or approximately 75-100 cm depth). At higher effective stresses conductivity tends to return to that of the unfrozen, normally consolidated soil.

The hydraulic conductivity data noted above have been obtained from small samples tested in the laboratory and caution should be used in applying the results to the field situation. It is possible that in a large sample the non-continuity of an ataxic cryogenic structure in combination with the overconsolidation of the inter-lens soil would mitigate the large increases in conductivity noted in short flow distance tests. In addition, much of the laboratory data are from ice-rich soils. The frost-induced structure in much of the Kivitoo active layer was imparted by ice contents below 30%. In their calculations McRoberts and Morgenstern (1974) use a hydraulic conductivity value (derived from laboratory consolidation tests on remolded soil) of 1.05×10^{-6} cm/s for a soil similar to those at Kivitoo. In an effort to explain a discrepancy between the predicted excess pore pressures and the larger excess pore pressures measured in the field, they state that 'a representative field k_v may be significantly less than

1×10^{-5} cm/s.' While it is felt that the pore pressures measured by McRoberts and Morgenstern were not due to thaw-consolidation (but were instead pore slurry pressures generated by post-failure remolding of debris) it is interesting that they feel that the relevant field conductivity may be very low. (Besides mentioning macro-structure, their reasons for this belief are not stated).

Having noted these results of other workers, and recognizing that there should be greater certainty about the representativeness of the conductivity value than there is of Cv since conductivity was measured directly in the field. Nonetheless, some caution must be exersized in using these data. Certainly anisotropic conductivity in the thawed soil may have changed the inferred pressure field about the piezometer tip thereby invalidating the assumptions used in Kirkham's equations and resulting in an inaccurate calculation of kw. Another possible reason for the low conductivity values may be the overconsolidation of the soil between ice partings which, in association with crack closure or a discontinuous crack system, could significantly reduce the bulk permeability of the soil.

Knowing D, T and B it is possible to calculate the magnitude of the excess pore pressure at the soil/ice interface. Nixon (1973) provides a graphical solution, Figure VI.18, for the B=0 case where Tf is the time factor once the ice layer is completely thawed and represents the largest excess pore pressure.

Making reasonable assumptions about the thickness of the

ice-partings (hi), the time factor (Tf) can be derived from Eq. VI.15. Using the following representative values -- Xo = 100cm, Ts = 7.0°C (the most severe case for Kivitoo), Ku = 0.0032 cal/cm °C s (w = 31%), Lw = 80 cal/cm³, hi = 0.2 cm and Cv = 5 X 10^{-3} cm²/s -- a time factor of 0.037 is calculated.

Having obtained a value for the hydraulic conductivity of the overlying thawed soil the excess pore pressure gradient above an ice layer, D, can be calculated from Eq. VI.13. The value of D is extremely sensitive to kw, which can conceivably range from less than 10^{-3} to 10^{-7} cm/s. Using the following field data --[γ_i = 9 KN/m³, γ' = 9 KN/m³, Xo = 100 cm, Ku = 0.0032 cal/cm °C s (w = 30%), Lw = 80 cal/cm³ , kw = 5 X 10^{-7} cm/s and a step temperature increase of 4.5°C (average equivalent step temperature for Kivitoo from Table VI.3)]-- the dimensionless excess pore pressure gradient, D, is 3.4. However, if a higher step temperature of 7.0°C is used (this being the maximum equivalent step temperature for Kivitoo from Table VI.4; 1975) D increases to 5.44.

Figure VI.18, reproduced from Nixon (1973), plots the time factor upon complete thawing of the ice layer, Tf, against the normalized excess pore pressure at the soil/ice contact for a range of D values (assuming B = 0). A normalized excess pore pressure at the ice layer of approximately 0.9 is necessary for failure on a 4° slope. Plotting the D value for a 4.5°C step temperature increase (D = 3.4) against Tf = 0.037 in Figure VI.18, the normalized excess pore pressure obtained is only 0.74 and stability is predicted. Yet, if the D value for the high step temperature of 7.0°C is used (D = 5.4) the normalized

excess pore pressure would now exceed that required for failure. (It should be noted that if the initial excess pore pressure gradient (B) is not equal to zero, the time required to attain the new excess pore pressure gradient would be reduced. Yet, in most cases at Kivitoo, R in the overlying soil would be small (< 0.2, as shown in the previous section).)

This analysis shows that a high equivalent step temperature would increases the probability of failure in two interrelated ways, i.e. by simultaneously increasing both the depth (for a given thaw season length) and rate of thaw. Stability may also be reduced if the period of time during which the icy layer is subject to thaw at any given thaw rate is lenghtened. This would effectively increase the thickness of the icy layer (ice lens), and hence the time factor, with a corresponding decrease in the potential stability of the thawing soil. Thus icy layers exposed to <u>prolonged</u> thaw at a given thaw rate may present more of a stability problem than icy soil subject to a shorter period of thaw at slightly higher thaw rate.

As natural soils will display a range of ice structures, from ice partings of increasing thickness to pure ice layers, there should be a transition from an ice-rich soil -- in which a solution in terms of the thaw-consolidation ratio (R) is applicable -- to an icy soil in which the analysis outlined above is more appropriate. In terms of slope stability the 'icy-layer model' represents an extreme case. Yet, it is still only under unusually severe circumstances, when the thaw front penetrates the ice-rich soil at the base of the active layer,

that pore pressures high enough for failure can be generated in response to a situation which approximates the one assumed in the icy-layer analysis. Nonetheless, considering the year-to-year variations in temperature and thaw season length at Kivitoo such conditions are possible.

e. Application of thaw-consolidation theory to the Kivitoo bench landslides: Discussion

It is obvious from the calculations presented above that the stability analysis using thaw-consolidation theory is extremely sensitive to errors in kw and Cv, parameters which show a wide range in value. Thus the proper selection of kw and Cv is both critical and difficult. Considerable attention must be given to the undisturbed structure of the thawed active layer soil in the field; not only of the in situ physical properties of the specific soil, but also the highly variable nature that is characteristic of layered soil profiles. This task is far from easy in stoney soils of weak bearing capacity which makes undisturbed sampling nearly impossible.

Laboratory tests clearly show that the coefficient of consolidation for a frozen/thawed soil is one to three orders of magnitude greater than that for the same soil in a fully remolded state. Similarly, in situ Cv may change markedly depending upon the magnitude of the residual stress or, for ice-rich soil, the degree of underconsolidation and changes in hydraulic conductivity. The Cv of the previously thawed soil above the descending thaw front may also be very different from

that of the presently thawing soil. Such circumstances would affect the solution for thawing over an icy layer or necessitate a restatement of the analysis in terms of a two-layer system. Yet, in terms of the present analysis, while it is felt that the choice of an exact Cv is difficult, the appropriate Cv to use for a recently thawed soil just above the thaw front is the higher value, since this is obtained from soils which most closely approximate those found in the field. However, Cv for the overlying consolidated soil may be closer to the remolded values. Thus, the active layer profiles at Kivitoo seem to present a thaw-consolidation problem in the form of a two-layer model. This third possible solution would assume that a consolidated soil possessing a relatively low Cv overlies an unconsolidated or consolidating soil with a large value of the coefficient of consolidation. Such a situation would be especially likely at Kivitoo where low ice content fine-grained soils or soils which have reconsolidated to lower void ratios overlie more ice-rich soils at the active layer's base. This model is also consitent with Savel'yev's (1972) qualitative approch, already noted. A detailed analysis will not be considered independently here as the two-layer model constitutes an intermediate situation bracketed by the single-layer and icy-layer cases already presented. Meaningful consideration of the two-layer model would also require a more detailed knowledge of the relevant in situ consolidation and hydraulic conductivity parameters than is presently justifiable on the basis of the available data.

Observations in the field suggest that soil with initially

high ice contents when thawed and reconsolidated (i.e. above the thaw front) retains much less of the cryogenic structure than does soil with frozen moisture contents below ca 35%. These (previously ice-rich) thawed soils therefore most closely resemble the remolded state and, consequently, may possess both its lower hydraulic conductivity and Cv values. This greater breakdown of structure in thawing high ice content soils may be due to three factors: (1) lower residual stresses, (2) greater thaw strains which result in mechanical remolding and deformation of the cryogenic structure and (3) more available water to effect swelling of the overconsolidated soil between ice partings. These observations further support the layered reformulation, suggesting that deep thaw into ice-rich soil presents the most critical stability conditions, not only because of the increased rate of melt water production, but also because of a decrease in the Cv of any already consolidated layers. If, however, substantial consolidation does not occur due to sustained low effective stress conditions, the soil may retain the higher Cv of the recently thawed soil.

In most situations at Kivitoo the thermal constant is small and Cv of the soil sufficiently large that the predicted thaw-consolidation ratio is low, and only very small excess pore pressures are predicted. This is consistent with field piezometer data and the overall appearance of stability along the bench slopes. Still, it is unusual that no excess pore pressures were noted, since, as demonstrated above, circumstances may be such that excess pore pressures are

predicted, even though these may not be large enough to result in slope failure. (The only artesian conditions observed were in soils which had already failed -- and where failure can be accounted for by traditional methods of stability analysis -- or in locations where such excess pore pressures are more reasonably explained by the particular hydrological conditions of the slope.)

Observation suggests that the transition from the 'normal' thawing situation in the field in which no excess pore pressures are generated, to the exceptional case which results in large excess pore pressures and consequently failure, is marked. Such an abrupt shift from stability to potential instability would be expected from a consideration of the ice content profiles, as these show a sudden enrichment near the permafrost table. Thus, the shift from the observed minimal excess pore pressures to pressures of sufficient magnitude to cause failure may occur suddenly due to unusually rapid, deep and/or prolonged thaw. Another reason for the inability to detect any intermediate conditions may be that, throughout most of the thawing active layer, the residual stress is sufficiently large that any excess pore pressures are kept from developing. This is a reasonable suggestion (and one which is consistent with Roggensack's (1977) findings) since the ice content at the frost table in the vicinity of the piezometer tips was usually less than 35%. As only departures from the residual stress -- which may be well in excess of the overburden pressure -- will result in volume reductions, the presence of a residual stress in low ice content soils implies

that most of the active layer does not consolidate very much upon thaw. Also, if only small residual stresses are present, it is the deeper soil, subject to larger overburden stresses (after the dissipation of any excess pore pressures), which will display larger volume changes. This may be another factor favoring failure near the base of the active layer.

The effect of downward suction of melt water into the still frozen ground upon the pore pressure at the thaw plane must also be considered as a possible partial explanation of the low observed pore pressures. In thawing fine-grained soils, particularly those with relatively low ice contents, down-draw of water into the frozen fringe may significantly reduce pore pressures at the thaw plane. In these soils, thaw-consolidation and ice segregation below the thaw plane probably occur simultaneously, the pore pressures being, to some extent, a product of the relationship between the two processes. The effect of downward suctions during thaw upon pore pressures generated by the thaw-consolidation process remains an important topic for further research.

It is also suspected that consolidation occurs in the thawing, as opposed to thawed, soil when some structural support from the ice is still present. Effectively, this would impart a residual stress to the thawing soil, possibly reducing the magnitude of the excess pore pressures, while still allowing consolidation to occur. However, since the rate of thaw, as well as the amount of water which must be expelled remains the same and, ultimately, that transient residual stress imparted by the ice would be eliminated, this may merely

serve to increase the thickness of the consolidating layer. In this case, the effect of a thawing zone would be to change the excess pore pressure gradient, though not necessarily the magnitude of the excess pore pressures. It is still important to note that the frozen/thawed transition, and therefore the onset of thaw-consolidation, is not abrupt (at the 0°C isotherm) as assumed by theory. Where low thermal gradients are present, the thawing zone may be of significant thickness (although it is not possible, in this study to calculate that thickness).

Another situation, not yet discussed, is that in which the consolidation behavior of the thawing soil is non-linear (Nixon and Morgenstern, 1973). There is much evidence (e.g. Davis and Raymond, 1965) to show that in high void ratio soils the void ratio vs. log effective stress curve is not the straight line which standard Terzaghi consolidation theory assumes. This non-linear behavior could result in the production of pore pressures in excess of those predicted by the linear consolidation theory. The deviation from linearity, and therefore the presumed pore pressure increase, would be greatest in the loosest soils, i.e. the ice rich layers at depth. The transition from linear to non-linear consolidation behavior would further enhance the abruptness of the low-ice/high-ice changeover.

f. Application of thaw-consolidation theory to Kivitoo bench slopes: Conclusion

All of these observations, qualitative and quantitative, together with the possible role of non-linear consolidation, seem to be sufficient to explain the general stability of these low-gradient bench slopes at Kivitoo while allowing for the occasional rapid mass-movement to occur when the thaw front penetrates the ice-rich zone at the permafrost fringe in exceptionally warm or prolonged thaw seasons. That instability does in fact occur late in the season is supported by the measured depth of old slide scars, which is generally 60-100 cm. In light of the core data, which show the permafrost beneath the ice-bulge at the base of the active layer to be relatively ice-poor, the initial suggestion that the Kivitoo landslides occur when the active layer descends into a body of high ice content permafrost must also be discounted. Thermal analysis indicates that, at Kivitoo, the length of the thaw season may be a more significant factor in the thawing of icy basal soil than is yearly variation in the average seasonal thawing temperature, as, according to weather records, the former may be expected to vary more widely. Thus, Table VI.4 shows the years 1962, 1966 and 1975 to present the greatest potential for active layer instability during the period of record. Of these years, 1966 may have been the most severe, combining deep thaw penetration with a relatively high thaw rate. Some years of high calculated rates of thaw, such as 1969, may not present as critical a stabilty problem due to the

relatively short length of their thaw season and the consequent limitation in the ultimate depth to which the thaw front penetrates and/or the relatively brief period of time duing which ice-rich layers are subject to melting. Obviously, in limiting situations, the exact stabiltiy conditions will be a trade-off between thaw rate and thaw depth/period of thaw, such that some shorter but warmer thaw seasons may present greater stability problems than slightly longer, but cooler, summers.

4. Post-failure behavior of landslides along the Kivitoo bench

While the preceeding sections have been concerned with the initiation of failure on low-angle slopes, a thorough discussion of the Kivitoo landslides must also address the problem of post-failure behavior: the form and rate of post-failure deformation, possible restabilization of the slide mass and deposition of the debris. Unfortunately, post-failure behavior has received relatively little attention. The emphasis on failure initiation is exemplified by McRoberts and Morgenstern's (1974:461) statement that they (engineers) are "more interested in predicting the onset of unstable conditions ... than ... in predicting the gross movements involved." For the geomorphologist, who is interested in the broader questions of landscape development, this limited view is not sufficient.

The topic of post-failure behavior is extensive, and full development of the issues involved is beyond both the scope of this thesis and the data which could be gathered during the

limited time spent in the field. Still, it is possible -- and, in light of the limited treatment to be found elsewhere, useful -- to develop a generalized mechanical framework for post-failure movements which can be applied, in a less rigorous manner, to the situation at Kivitoo.

Since none of the landslide events was observed, it is impossible to describe the exact nature of their post-failure behavior. Yet some general observations can be made. As noted in the case studies above, the low-angle landslides at Kivitoo display a broad range of post-failure morpholgy; while some break up and continue downslope as a debris-flow (often resulting in the stripping of the entire active layer leaving behind a bare scar), others remain more or less intact and restabilize after only limited displacement. Furthermore there seems to be a tendency for those landslides that restabilize to be relatively small and involve a larger proportion of sandy soil.

In the discussion of failure above we have assumed that the pore-fluid is water ($\gamma_f = \gamma_w$), that full frictional resistance is available to be mobilized at the time of failure ($\phi'_r < \phi' < \phi'_p$) and that the soil is cohesionless. However, once failure has occurred a number of things may happen which can radically change the state of the soil and its rheological behavior. Some indication of the complexity of this problem is indicated by the possible post-failure developments shown by the flow chart presented in Figure VI.19.

Basically, post-failure transformations in the mechanical behavior of a landslide involve changes in the nature of the

pore-fluid (its density and viscosity) and the tendency towards volume change in the shearing soil (i.e. whether the soil will tend to dilate, contract or remain at a constant volume). Volume changes may significantly effect pore-fluid pressures in the landslide mass (as, for example, the pore pressure increases due to undrained consolidating shear) and, possibly, the angle of internal friction in the shearing soil mass. Undrained shear at saturated water contents in excess of those corresponding to the void ratio at the constant volume or dynamic angles of internal friction is probably a major cause of post-failure strain weakening and pore pressure maintainance in the Kivitoo landslides. In terms of the Mohr-Coulomb strength parameters, soil volume and pore-fluid density changes are important in controlling the effective stress and coefficient of internal friction in the soil following failure. Ultimately, these factors will determine whether the landslide will restabilize, or continue, or even accelerate its movement.

Post-failure changes in the geometry of the slide mass may also have a significant impact on post-failure deformation, as this may alter the initial balance of forces (ratio of shear resistance to shear stress, i.e. the factor of safety), which, at the time of failure, is equal to unity. The build up of passive resistance downslope by the bulging at the toe noted above in the case of Slide 8, is an expression of such consequential changes in landslide geometry.

Along the Kivitoo bench slopes, restabilization after only limited displacement appears to occur in small landslides where sandy soils comprise a major portion of the slide mass. Such

soils, containing little fine-grained sediment, are unable to generate the dense muddy pore-fluid necessary for the suspension of the coarser grains and will not degenerate into debris-flows. Disturbance of the structure of high void ratio sandy soils during initial shear may result in short-lived liquefaction failure. Since the saturated water content of the sandy colluvial soils along the bench commonly exceeds the liquid-limit of these soils it is easy to visualize the loss of all strength upon failure of the ground beneath them. These soils may also be loaded by overriding or thrusting from movement of soil upslope. However, the relatively high hydraulic conductivity of sandy soils permits excess pore pressures to be rapidly dissipated, inhibiting the maintainence of low effective stress conditions. Consequently, little subsequent displacement or break up of the slide mass will occur. Evidence of such limited soil flowage is found in Slide 1, where much of the failure zone was within sandy soil. The small size of this landslide (as well as of Slide 2) would also increase the potential significance of any passive resistance to failure which may build up during initial strain and further inhibit large displacements.

If post-failure strain weakening is minor or short-lived, small landslides in muddier, blocky soils may not be able to generate the energy necessary for remolding of these soils and hence will not form debris flows. In contrast, acceleration of movement often occurs in the larger, muddier landslides as post-failure ped breakdown supplements pore pressures by the addition of suspended solids to the pore-fluid. More ped

breakdown can occur in the larger slope failures since these have greater momentum and therefore more of the energy that is required for this remolding. This may explain why the larger landslides tend to leave clean scars.

In several of the Kivitoo cases, there is evidence that collapse of the soil structure (breakdown of soil peds) can be sufficiently rapid and severe that virtually all clast-clast (ped-ped) contacts are destroyed. The active layer is then transformed into a viscous slurry with suspended clasts of 'cohesive' soil. (In saturated bulked sandy soils, collapse of the grain-grain structural skeleton due to shock can lead to a similar, but more instantaneous, transformation from a grain/pore-fluid system to a mixed grain/water suspension, i.e. liquefaction.) Reducing the number of clast-clast contacts reduces the angle of internal friction, possibly to zero. In this case, rather than being a frictional material with an inter-ped muddy fluid, the soil assumes (to some degree) the rheological properties of the pore-fluid itself. (This rheology may be purely viscous, Bingham or frictional/viscous.)

If post-failure mixing is insufficient to maintain the larger clasts in suspension, these will settle in the slurry and start to interlock. Particle settling and the consequent reconstruction of a rigid soil skeleton will serve to both dissipate excess pore pressures and increase the angle of internal friction leading, in turn, to restabilization of the soil. The rate of post-failure excess pore pressure dissipation, and ultimately the rheological properties and longevity of the mobile flow, will depend on particle settling

rates under the given dynamic conditions in the deforming soil mass. In many cases, however, ongoing mechanical disturbance within the moving soil, by continually breaking particle contacts, will inhibit settling and promote a form of sustained consolidating shear.

Pierson (1981) suggested that the structure which builds-up following the settling of clasts is meta-stable (particularly if all of the excess pore pressures have not been dissipated). Mild disturbance of this settling soil may be enough to cause structural collapse and a resultant rise in pore pressure. More extensive testing (Algus, unpublished data) has shown that such disturbance can readily cause steep rises in pore pressure. (The excess pore pressures generated in this way are, however, more rapidly dissipated than the excess pore pressures in the initial fluid soil. This is because the amount of consolidation (fall of grains) which occurs in the previously sedimented soil upon collapse is less than that in the fully mixed soil.) Thus, if the clasts are separated again by disturbance remobilization may occur and the rheology of the slide mass may again become that of a fluid. It is possible that, during its post-failure history, a shearing soil fluctuates between plastic and viscous (or frictional/viscous) rheological response.

Other particle support mechanisms in moving debris are turbulence (in very fluid debris) and dispersive pressures (e.g. Middleton and Hampton, 1976). If the soil mass has sufficient momentum, dynamic forces arising from particle interaction (such as the dispersive stress; Bagnold, 1954)

will tend to keep the mass dilated, lowering ϕ (Bagnold, 1954) and increasing pore pressures as the dilated soil mass attempts to reconsolidate to a lower void ratio.

The net effect of the post-failure strain-weakening processes discussed above is to reduce the factor of safety after failure, offsetting those factors which would tend to restabilize the slide mass. If the failure is plastic (or, during the initial stages of viscous-type deformation, prior to the full mobilization of viscous resistance) the rate of acceleration of the slide mass is a function of the stress imbalance, which is reflected in the factor of safety. If the stress imbalance is increased (the factor of safety reduced) after failure, the rate of acceleration of the soil mass will increase. This, in turn, provides more energy to cause remolding and dynamic particle suspension, further increasing the stress imbalance and leading to greater acceleration.

Once failure has occurred the viscous resistance imparted by the pore-fluid is mobilized. If the pore-fluid is water, with very low viscosity, its effect on the post-failure acceleration of the mass will be slight. If, however, the pore-fluid is transformed into a dense pore-slurry, viscous resistance to shear may be large and effectively dominate the rate of post-failure strain.

For an intact slab which has failed due to low effective stress conditions caused by thaw-consolidation, overriding of the intact soil downslope of the landslide and the concomitant movement of the slab away from the zone of thaw-consolidation

may result in an increase in the effective stress at the base of the landslide and subsequent restabilization. Post-failure changes in the hydraulic conductivity of the intact slab due to cracking of the slide mass may also lead to pore-pressure dissipation as the pore-fluid can drain out of the slide mass more rapidly.

Restabilization can also occur after limited displacement due to the dilation of a densely packed 'blocky' active layer soil. If the shearing soil tends to dilate (excess) pore pressures will be to some degree dissipated by this increase in pore volume. As noted above, Roggensack (1977) has produced data which shows that cryogenically structured soils are dilative at low effective stresses (< 50 kPa).

B. Retrogressive active layer failure

Retrogressive active layer failure, in which a retreating backscarp is maintained by the evacuation of debris within a low-gradient lobe are found along the Kivitoo bluffs. (See Figures VI.20 and 21 for photographs of two of these failures.) This type of instability occurs on undercut gentle slopes in which ice-rich fine-grained soils occupy at least the basal portion of the active layer soil profile. Debris movement is via the repeated backwasting of small scarps (generally less than 1 m tall), with concomitant slow evacuation of debris in a low-angle tongue or debris flow. The net result of this process is the stripping of a layer of soil just slightly less thick than the active layer.

Features similar in form to the Kivitoo retrogressive active layer failures have been described by French and Egginton (1973) (ground ice slumps), Hegginbottom (1978) (retrogressive thaw flowslide) and by Issacs and Code (1972), who noted that "when the icy sediments are lower than the base of the headwall the feature becomes inactive." All of the features described by these authors appear to retreat by an ablation mechanism as ice-rich permafrost and/or massive ground ice is exposed in the backscarp, and waste is evacuated by debris flow in a low-angle tongue. As such, these features resemble the bimodal flows described by McRoberts and Morgenstern (1974), differing mainly in the height of the backscarp. None of thse authors note the development of tension cracks at the backscarp.

The mode of retrogression of the Kivitoo features is fundamentally different from that of the active layer failures described above. As no icy permafrost was exposed in the backscarp, ablation sensu stricto was not an important mechanism of scarp retreat. Retreat appears to be by a 'spalling' mechanism (initiated by slope undercutting). As debris is moved out from the base of the backscarp, lateral earth forces on the soil mass upslope are eased, and a state of active stress is established leading to the development of tension cracks along the backscarp. Undrained failure of the soft soil at the base of the active layer in the tension-cracked block results in the downslope movement of the block and its incorporation into the debris lobe. Continued movement of the lobe away from the backscarp (further reducing

lateral support), is necessary for the removal of these spalled blocks and for the maintainance of a 'high', steep headscarp and therefore continued retrogression. Theoretically, if the undrained strength of the basal soil and debris is low enough, this process could operate even on flat slopes, as the debris lobe creates its own slope gradient along which movement can occur.

The spalling process may be accelerated by overland flow filling tension cracks, and by an increased rate of thaw at the base of the active layer in the backscarp which would rapidly add highly porous soil and result in thaw-consolidation. Scarp retreat should continue as long as the debris tongue remains mobile (moving debris away from and thereby maintaning the backscarp) and the soil at the base of the active layer is of sufficiently low strength. As soon as the tongue is stabilized, the backscarp should degrade. The type of retrogressive failure described here is similar to much larger failures which occur in other strain-weakening sediments, such as quick clays (e.g. Crawford and Eden, 1967; Mitchell and Markell, 1974; Carson, 1977b).

1. Description of retrogressive active layer failures along the Kivitoo bluffs.

A small retrogressive active layer failure (ca 10 m in width) at the base of the bluffs at K896 occurred at the end of the first week in August, 1983. The slope on which the failure was situated was short (< 10m) and inclined at 12°. The toe of

the slope, which extended to the beach, had been undercut by wave action. A profile of the feature (over which an approximate pre-failure profile has been superimposed) is given in Figure VI.20. As seen in Figure VI.20a, the failure was bracketed by two small gullies and backed by a short, steep (36°) nose. The debris-lobe was 9.4m in length, extending beyond the base of the bluffs onto the beach. Overall inclination of the lobe was 7°, while segments of its surface were nearly flat. Backscarp height averaged 40-60 cm but varied considerably depending upon the amount of debris accumulated at its base.

Most of the soil movement occurred during an initial rapid failure (which was not observed) and retrogression of the backscarp contined for a period of about one week. Within one and a half weeks after the initial failure, retrogression of the backscarp had slowed and new tension cracks were no longer developing here. At this time the backscarp had not reached far enough up the 12° slope to undercut the superadjacent slope.

At the failure site the active layer soil profile consisted of 40-50 cm of intact surficial colluvium (mostly a sandy loam) overlying in situ (α) high ice content clayey silt. The depth of the frost table at the backscarp was 55-65 cm (see Figure VI.20). Soils data, given in Figure VI.20, show the stable surficial debris to have a water content of 20-23%. The ice content of the soil at the frost table, both behind the scarp and underneath the debris lobe, was very high (57-86%). Behind the backscarp, immediately downslope of the small nose,

the ice content was slightly lower; 40%. Water content of the thawed mud just above the frost table was much lower than that of the underlying frozen sediments; 19-26%. This was true even beneath the mobile debris lobe. Moisture content of the saturated moving debris in the lobe was 18-19%, (the same or slightly lower than the undisturbed colluvium) indicating that flowage is possible after remolding and structural breakdown, even at these relatively low water contents. (Low flow limits appear to be a function of the poor-sorting of debris; e.g. Rodine and Johnson, 1976.)

A retrogressive active layer failure nearly identical to the one described above, was observed in 1977; Figure VI.21. The feature was located on a small bench and had recently been undercut by rapid incision of the small stream at K900. The inclination of the bench onto which the failure was retrogressing was 7-12°. Tension cracks, developing around the back and sides of the scar can be seen in Figures VI.21a and 21b. These extended through the (unsaturated) colluvial silty sand to the in situ fine-grained soil just above the frost table. Ice contents from the frost table at this site (obtained in 1983) were 58-96%, while the water content of the thawed soil just above the frost table was only 15%.

A third instance of active retrogressive failure is seen in Figure VI.22, which shows the base of the tongue slope in the debris-bowl at K660 (B-2). The soil profile here is comprised of 73 cm of poorly-sorted debris overlying clayey silt with the frost table at 86 cm (July 27, 1983). Ice content at the frost table was 38%, while the water content of

the thawed soil immediately above this was 21-23%. This failure is particularly interesting since it was only a zone of tension cracks about 6 m in width which developed. No further breakdown of the active layer soil or flowage of debris from the zone of failure occurred. Again, this feature is associated with an undercut slope and is seated in muddy sediments. In this case, however, it appears that the initial strain upon failure and any associated strain-weakening in the soil was insufficient to sustain failure. The lower ice content at the frost table may have been the reason for this limited displacement. This feature demonstrates that initial strains involve the rapid propagation of a wide tension zone. If the debris within this initial zone of tension is evacuated, resulting in the development of steep scarp, the sustained retreat of this scarp may occur at a much slower rate.

2. Mechanics of failure initiation

Retrogressive active layer failures are initiated by local slope steepening due to undercutting by wave action at the base of the bluff or by gully incision along the bluff. Failure may also be initiated on a low-gradient slope if it lies upslope of a steeper slope along which failure has occurred. The effect of these processes is to create a vertical scarp which may then retrogress.

Sudden stress concentration at the base of a vertical scarp (due to the removal of the toe) can, under certain circumstances, result in the undrained failure of the soil at

the base of the scarp. The maximum or critical height of a vertical slope which can be supported by a given soil is

$$H = \bar{N} \frac{Su}{\gamma} \qquad \text{(VI.16)}$$

where Su is the undrained cohesive strength of the soil ($\phi'=0$), γ is the soil's bulk unit weight, and where the coefficient $\bar{N}$ (called the stability factor) depends on several circumstances (Terzaghi, 1943; Carson, 1971, p. 103; Carson 1977b). These include the depth of tension crack development prior to failure, the thickness of 'debris spoil' against the backscarp, and the uniformity of strength in the soil profile. Failures involving large retrogression of sensitive clays and tall (> 10m) scarps have been reported with $4 < \bar{N} < 8$ with thick accumulation of spoil at the backscarp (Carson, 1977b, Fig. 16) but are possible with $\bar{N}$ as low as 2 if there is full removal of debris from the backscarp.

No undrained strength data were obtained directly for these Kivitoo soils. The moisture content data, however, show that the soil at the base of the active layer is commonly at or above the liquid limit. Worth and Wood (1978) have reviewed published correlations between the liquid limit and the undrained strength of remolded soil at that water content. They found that this ranges from less than 1 kPa to about 3 kPa. Assuming an undrained strength value for a typical active layer soil at the liquid limit of 2 kPa and a bulk unit weight of 17 kN/m^3, the critical height for failure (with $\bar{N} = 2$) is 23cm. As the height of the backscarps in the Kivitoo failures

is typically 40-60 cm, failure can easily be accounted for, even assuming variations in bulk unit weight and soil strength. The additional assumption implicit in that conclusion is that the soil at the base of the backscarp does become fully remolded due to the local concentration of stress at that site (Bjerrum, 1968; Christian and Whitman,1969). Observations of the actual slow subsidence/flowage taking place at the backscarp seem to confirm that at least partial remolding does occur there, but a quantitative analysis of the remolding process is beyond the scope of this work. Retrogression will progress as long as a backscarp taller than the critical height can be maintained by the removal of debris, and the undrained strength of the soil at the base of the active layer is low.

The retrogressive mode of instability and its dependence on repeated development of stress concentration at a new backscarp is, clearly, fundamentally different from the infinite slope stability approach adopted in the main body of this chapter.

3. Movement of the debris lobe

Monitoring of stakes placed in the debris lobe of the retrogressive failure along the side of the stream at K900 indicated that movement was intermittent, ceasing when the backscarp no longer showed signs of continued retreat. Movement was greatest below the backscarp, decreasing towards the toe of the lobe which was dry. Thus, in this particular slope failure, flow was compressive.

While a movement survey of the failure at the base of the bluff at K896 was not done, the downslope tilting of piezometers placed in the flow indicated that the surficial soil was moving at a faster rate than the soil below demonstrating that movement possessed at least some component of flowage. (The tip of the piezometer was approximately 10 cm above the frost table so that this tilting could not have been the result of a fixed tip position in stationary basal soil.)

As the surface of the debris lobe was 7° and the debris itself was relatively dense ($\gamma_{dry} \geq 19.7$ kN/m^3) and poorly sorted (suggesting that the friction angle was at least 32-35°, if not greater) excess pore pressures are required for movement. Muddy water could be seen in pools on the surface of the debris lobe indicating that a pore-slurry of some density in excess of that of water was, in fact, present. Data from piezometers placed in the lobe, Figure VI.20, confirmed the presence of excess pore pressures. It is probable that the excess pressures here reflect the increased density of the muddy pore fluid (as decribed above) rather than thaw-consolidation at the base of the lobe. (Some pore pressure increase due to thaw-consolidation of the high-ice content soil beneath the debris flow is possible, but as the thawed mud above the frost table had a water content of only 19-22% and was quite stiff, this additional component of excess pore pressure creation was not thought to be significant.)

An infinite slope stability analysis of the debris layer at K896 using the pore pressure data from the piezometers and a friction angle of 35°, indicated that even though excess pore

pressures existed, these were insufficient to account for movement. In the case of the largest pore pressure reading (piezometer 11), the pore pressure ratio required for failure was 0.81 while the in situ pore pressure ratio was only 0.73. (The pore pressure ratio, $Ru = u/\gamma D$, is the ratio of the pore pressure to the total unit weight of the soil overlying the potential failure plane.) However, it is thought that the largest pore pressures which were observed were not the largest that had occurred in the debris lobe during the period of measurement. The data indicate that the piezometric level in the lobe is erratic, suggesting that high pore pressures, and the movements they enable, occur in the form of short-lived surges. Such periods of intermittent movement could be explained by shock-induced structural collapse of a meta-stable particle skeleton within the debris lobe which induces a form of undrained self-loading raising the fluid pressure in the debris. One mechanism for this disturbance may be the spalling taking place at the backscarp. Thus backscarp retrogression and the maintainance of a mobile debris lobe are interdependent. The shock-induced undrained failure just described is different from, and may be supplementary to, the undrained loading situation described by Hutchinson and Bhandari (1971). In this latter mechanism, it is simply the rapid increase in total normal stress, due solely to the sudden loading of the back of the lobe by debris from the backscarp which causes the pore pressure rise, rather than collapse of structure due to dynamic impact. (It may be significant that the movements described by these authors take the form of a

slide rather than that of a flow.)

Following a surge, if the rate of debris movement is insufficient to maintain all the particles in suspension in the slurry, some settling will occur, reestablishing particle contacts, building frictional strength and leading to restabilization of the flow. As the particles may again settle into a meta-stable structure, renewed spalling at the backscarp can reactivate the flow.

It is apparent that there is a critical relationship between the amount of movement which occurs in a surge, the amount of debris which can be removed from the backscarp and the height of the backscarp relative to the surface of the debris at its base. Stabilization of the failure may occur as the height of the backscarp decreases (due to local changes in slope) or if the mobility of the debris is reduced due to drainage, evaporation or the reestablishment of high frictional strength due to settling. All of these factors affect the critical value of $\bar{N}$ for retrogression in Eq. VI.14.

C. Gelifluction.

Solifluction, the slow downslope movement of regolith materials in cold environments, has attracted considerable attention from geomorphologists and civil engineers. Two processes, frost creep and gelifluction are traditionally cited as responsible for these displacements. Frost creep is the net downslope displacement caused by heaving of the ground normal to the slope surface (due to the formation of ice in the soil)

followed by a more nearly vertical settling (upon thaw). This process is easily envisaged and may operate on slopes of any inclination. Gelifluction, which is defined (Washburn, 1967) as seasonal movement in excess of that directly attributabe to frost creep, has proven more difficult to explain. Clearly, gelifluction must involve some form of internal shear strain. However, the reason for the strength loss within the soil, neccessary for movement to occur on gentle slopes, and the rheological behavior of the moving soil (both during and after failure) are still poorly understood. Any gelifluction model must account for failure initiation, post-failure movements and restabilization after only limited displacements.

Geomorphologists have long emphasized the flow characteristics of gelifluction movements, citing such evidence as the form of solifluction lobes, downslope convexity of some (but not all) vertical velocity profiles, lack of distinct shear surfaces, and slope-parallel orientation of elongate particles in solifluction soils. Washburn (1967) has suggested that gelifluction probably only occurs at water contents in excess of the liquid limit, the implication being that failure takes the form of a soil flow rather than a slide.

The soils most commonly encountered on gelifluction slopes are sandy with at least a small percentage of silt and/or clay (making them frost susceptible). The clay-sized fraction seldom exceeds 15°, although some solifluction soils, derived from drift deposits may have a larger clay sized fraction (20% - 50%; Washburn, 1967), probably consisting mainly of rock flour. Solifluction soils typically have low liquid limits

(often < 25%) and plasticity indices (<5%).

Unfortunately, few determinations have been made of the frozen water contents in gelifluction soils. Washburn (1967) reports ice contents of 50-100% (and as high as 247%) in the upper 20 cm of a solifluction slope in Greenland. Frozen water contents of 27% and 35% for a surficial soil were obtained by Williams (1959). At this site frozen water content decreased downward from the surface with a maximum water of 67% content at 20 cm (in a particularly wet location). These ice content data are probably high in relation to most gelifluction soils. The basic trend, however, with ice content relatively high near the surface and a depleted, relatively ice-poor zone at middle-depths in the active layer, appears to be correct. Benedict (1970) and Williams (1959) have made some of the few available observations of the form of ice in gelifluction soils. Both researchers found horizontal ice-lenses of up to 0.5 cm thickness in slightly silty sands, decreasing in both number and thickness with depth.

Reported rates of surface soil movement on gelifluction slopes are 1-6 cm/yr. Rates exceeding this are rare, although in particularly wet locations movements of up to 12 cm/yr or more have been recorded (Washburn, 1967). (Williams (1959) documented one springtime 'surge' of 25 cm within a period of a few days.) Although solifluction movement has generally been monitored on an annual basis, where it has been observed over the course of the thaw season the largest displacements tend to occur in the early spring during initial thaw. (Thorough analysis of movement data is difficult due to problems in

properly separating the frost creep and gelifluction components.)

The vertical velocity profiles from solifluction slopes show that movement rarely extends below 50-60 cm, even where the active layer is considerably thicker. Also, many of the profiles have pronounced downslope concavity, indicating rapidly diminishing displacement with depth. Distinct shear surfaces are absent (except in the profiles from steep slopes, e.g. Jahn,1967). Vegetation seems to have a marked effect, with the profiles displaying the most pronounced downslope concavities tending to be those from bare sites (e.g. Williams, 1966; Price, 1973).

Williams (1959) long ago recognized that shear strain on low-gradient gelifluction slopes must involve drastic reductions in one or more of the Mohr-Coulomb strength parameters. In light of their low clay mineral content of most gelifluction soils they may be considered cohesionless. Williams (1959) and Harris (1977) have attempted to detect excess pore pressures on solifluction slopes. Yet in none of these studies were piezometric levels above the ground surface detected. In most instances the piezometric surface was rapidly drawn down following the loss of water supply from melting snowpacks or descent of the thaw plane into unsaturated, ice-poor soils at depth.

While Williams (1959) discounted unusually low effective stress conditions as a mechanism for the initiation of gelifluction movements, based on the apparent absence of excess

pore pressures, McRoberts and Morgenstern (1974) and Chandler (1972) have revived this idea. Yet it is difficult to envision the generation of large excess pore pressures by the thaw-consolidation mechanism discussed above in sandy solifluction soils due to the high hydraulic conductivity and coefficients of consolidation of such soils.

A special case which may occur in an expanded, unsaturated soil is very rapid thawing brought about by the infiltration of melt water into the frozen soil. Effectively, this raises the value of the thermal constant (α) in Eq. VI.5, radically increasing the value of thaw-consolidation ratio (R). As the frozen sandy soils at Kivitoo are not saturated (Table VI.7), the sudden influx of (warm) melt would result in the rapid loss of ice bonds between grains.

The inability to detect high pore pressures on gelifluction slopes does not neccessarily mean that such conditions do not exist, as they may be very short-lived, areally restricted, and involve small volumes of water, thereby escaping detection. Such spatially and temporally transient excess pore pressures, if they do occur, would be characteristic of localized, shortlived liquefaction rather than continued thaw-consolidation as envisioned above.

Noting that "the soil immediately following thaw is in a very loose state", Williams (1966) suggested that "a further possibility (for failure initiation) is that the friction angle of the soil is to be regarded as very low...". It has been demonstrated (Andresson and Bjerrum, 1967) that the angle of internal friction decreases rapidly above a certain critical

porosity. For well-sorted fine to medium sand the friction angle drops from 28° at a porosity of 46% to 0° (i.e. no particle contacts exist) at a porosity of 48%. Similar values have been given by Rowe (1963) for fine sand.

The mechanism of failure initiation in gelifluction proposed in this thesis is one in which the in situ value of ϕ' for the frozen soil is significantly less than ϕ'_{cv} due to the loss of particle-particle contacts. Lacking significant frictional strength, upon thaw the soil structure collapses upon the loss of cohesion provided by the interstitial ice. This may cause localized shear strain which, if the soil is saturated, and immediate full drainage does not occur, will result in short-lived high pore-pressures. Thus, the initial failure, due in part to the low frictional strength of the sand upon thaw, results in liquefaction of the saturated sand which, in turn, produces and maintains, at least temporarily, low effective stress conditions sustaining downslope shear strain. Spreading of the initial failure may occur as isolated pockets of loose soil may cause loading and consequently, failure and liquefaction of adjacent, slightly stronger soil. Harris (1983) has shown small bubbly voids (vesicles) to be a feature of silty/fine sand solifluction soils. Such voids are often found in soils which have undergone liquefaction. At Kivitoo rounded voids are commonly found in silty /fine sand solifluction soils, but not in coarser-grained ones. These voids provide good circumstantial evidence of liquefaction. Harris does not, however, address the mechanism by which liquefaction is initiated. In his laboratory simulations,

structural collapse is induced by a hand held plunger, thereby inflicting considerably greater stresses upon the soil than could be expected in the field.

Technically, increasing the porosity of the soil such that structural collapse occurs at the in situ effective stress following the loss of cohesion from interstitial ice, amounts to a form of thaw-consolidation. However, in its abruptness it is fundamentally different from the slow thaw-consolidation proposed by McRoberts and Morgenstern (1974) in which, moreover, the entire strength loss is attributed solely to excess pore pressures rather than also including a decrease in the internal friction angle.

Solifluction lobes and solifluction slopes are features of widespread occurrence on both the terrace surface and along the bench at Kivitoo. Several large gelifluction lobes, northwest of the bluffs are actively encroaching on raised beach deposits. Small lobes are commonly found along the bench, typically just below the back slope. A common solifluction feature occurring at the base of the bench back slope is a small pack of soil ripples, Fig. VI.23. Apparently these are the result of compressive gelifluction flow at the bench/back slope junction. Solifluction slopes (or 'sheets' in Washburn's (1967, 1973) terms) comprise portions of the bench. These slopes develop below laterally extensive water sources such as the elongate snowpacks which drift in at the base of the bench back slope. While apparently subject to gelifluction movement, the slopes do not display distinct lobate forms. Subdued

risers do develop along the doemslope edge of the bench in these locations, probably due to the downdraw of the local water table at this point. The 'smooth' uniform surface of these slopes is presumably due to the more or less equal distribution of moisture along the slope (both laterally and downslope) which tends to mitigate the differential movements that ultimately would result in the formation of lobes.

A solifluction slope, along the south side of the valley at K1145, was the subject of limited observations. The study site is shown in Figure VI.24. (The location is also shown in Figure VIII.9.) Piezometers 1 and 9 were located on a bench slope which was about 100 m to the south of the study site. These did not record any high excess pore pressures during the field season. However, the tips were at a depth of 60-65 cm, below the depth of any expected gelifluction movements.

The gelifluction soils at Kivitoo tend to be sandy with less than 20% silt/clay. One solifluction lobe, at the base of a bluff formed in particularly well sorted fine sand, consisted entirely of this sand with no finer particles. These observations suggest that the commonly-cited association of solifluction with slightly silty soils is not correct in all cases, and that sands are also subject to this process.

From examination of frozen sandy gelifluction soils in the field it appeared that the grains of soil were sufficiently separated during freezing for the porosity to be greater than that of the soil in a normally consolidated state. This suggests that the friction angle is lower than that for the constant volume (or residual) state of packing. Sampling of

the gelifluction soils at Kivitoo, however, did not reveal unusually large porosities; the average porosity of specimens of frozen sandy soil was 45% (Frozen moisture content = 24%, γ = 14.24 kN/m³, assuming Gs = 2.65). The largest reliable porosity obtained (based on a high-quality undisturbed frozen sample) was 48%.

In light of Andresen and Bjerrum's data these are marginal values. Yet they are large enough that they just fall within the range for $\phi' = 0$ established by Andresson and Bjerrum (1967). However, the sampling procedure is biased by sample size. If a point method of sampling could be devised it would most likely reveal pockets of high porosity soil. Moreover, while the frozen soils had high porosities they were not saturated. Williams (1959) also found unsaturated frozen soils of high porosity (Table VI.7). While it is generally assumed that sandy soils will not display a substantial frost-related volume increase, Beskow (1953) and Fig. VI.25), has shown that unsaturated sands can expand upon freezing. [It was not possible to obtain reliable bulk unit weight data on thawed soils because of their extreme sensitivity and lack of strong ice bonding. However, disturbed and partially remolded samples had high bulk unit weights relative to the frozen soil (γ_{dry} = 19.4 kN/m³, n = 25%, assuming Gs = 2.65) and low saturated moisture contents (11-14%; Table VI.7.), suggesting that post-thaw collapse had indeed occurred.]

These data, along with the observation that thawed samples had excess water at the surface, show that the soil if disturbed, will tend to consolidate. Thus, while shear failure

in these gelifluction soils seems to be related to low ϕ' values in the highly porous soil, it is probably amplified (and converted to a flow-type movement) by the partial liquefaction which accompanies structural collapse of the soil. However, in such sandy soils excess pore pressures will be rapidly dissipated, and movement will be short-lived resulting in only limited movement. The restraint of nearby stable soils will also limit total displacement. The rapid decrease in gelifluction movements with depth is probably a function of the lower ice-contents and therefore lower porosity of these deeper soils. The larger effective stresses at shallow depth which can also, according to Beskow (1953), repress frost-heaving of unsaturated sands.

D. Endnote

In this chapter the topic of mass movement on low gradient slopes in thawing soils has been adressed in some depth. Aside from the significance of such a discussion to slope stability problems in cold regions in general, these mass wasting processes, particularly single-event translational landslides and retrogressive active layer failure, are considered to be fundamental to the morphological development of the bluffs with debris-bowls and the benched bluffs. In the following chapters, the morphogenesis of these two sections of the Kivitoo coastline is considered.

TABLE VI.1

MORPHOLOGY OF LOW-ANGLE, SINGLE-EVENT LANDSLIDES AT KIVITOO

		ANGLE	WIDTH	LENGTH
Slide 1	K1033	5°	10 m	20 m
Slide 2	1110	5-7°	7 m	20 m
Slide 3	1168	4-7°	30-40 m	15-20 m
Slide 4	1231	4°	11 m	30 m
Slide 5	1227	5°	18 m	30 m
Slide 6	1081	10°	20 m	10 m
Slide 7	1148	4°	10 m	25 m
Slide 8	890	17°	8 m	17 m

TABLE VI.2

SUMMARY OF SOIL PROPERTIES

selected samples from instability features along the Kivitoo Bench

SAMPLE	LOCATION	Sand/Silt/Clay (%)	LL, PL, PI (%)
BS-1	Slide 3	5/61/34	28/17/11
BS-2	"	27/48/25	22/14/8
BS-3	Slide 5	19/56/25	20/14/7
BS-4	"	16/56/28	20/14/6
BS-5	Slope surface K1145	58/35/7	Non-plastic
BS-5	Slide 7	10/61/29	21/15/6
BS-8	Trench 1	11/60/29	23/16/7
T-20	Slide 8, pit B1	42/45/13	
T-22	Slide 8, pit A	12/66/22	
T-55	Core 9, 93-111 cm	48/39/13	
T-56	" 118-126 cm	30/50/20	
T-57	Core 10, 0-75 cm	13/61/26	
T-60	" 120-141 cm	15/56/29	
T-67	Retrogressive failure, K900	16/42/42	22/17/5

TABLE VI.3

THERMAL SOLUTIONS FOR KIVITOO

Location	t1	t2	dt	x1	x2	dx	α	Ts+	Ts*
Piez. Site 1	5/7	19/7	14	45	60	15	0.036	5.7°	5.3°
Slide 2	5/7	13/8	39	55	82	27	0.033	4.8°	4.5°
Piez. Site 2	19/7	13/8	25	63	69	6	0.020	1.8°	1.6°
Piez. Site 3	19/7	13/8	25	73	83	10	0.027	3.2°	3.0°
Piez. Site 5	22/7	13/8	22	72	84	12	0.031	4.2°	3.9°
Above values all 1983									
Retrogressive failure, K900 (1977)	7/8	25/8	18	65	75	10	0.030	4.0°	3.7°
	"	"	18	68	75	7	0.026	3.0°	3.8°
	"	"	18	66	74				
"	"	"	18	66	74	8	0.023	2.3°	3.4°

+ Single layer model: W_u = 20%, W_f = 30%

* Two-layer model (from graphic solution, Figure VI.14)

TABLE VI.4

LENGTH OF THAW SEASON, EQUIVALENT STEP TEMPERATURE, DEPTH OF THAW, AND VALUE OF THE THERMAL CONSTANT FOR THE YEARS 1960 - 1983, AS DETERMINED FROM BROUGHTON ISLAND WEATHER RECORDS

YEAR	Total Degree Days	Thaw Season Length Method 1	Equivalent Step Temperature 1 °C	Thaw Season Length Method 2	Equivalent Step Temperature 2 °C	α Single Layer	Thaw Depth (cm), Single layer	Thaw Depth (cm), Two-Layer Model (from Figure VI.14)	α Two-Layer
1960	357	70	5.1°	70	5.1°	0.034	84 cm	95 cm	0.036
1961	325	65	5.0°	74	4.9°	0.034	81 cm	92 cm	0.035
1962	406	81	5.0°	91	4.5°	0.034	90 cm	103 cm	0.035
1963	233	61	3.8°	64	3.6°	0.029	67 cm	79 cm	0.026
1964	269	60	4.5°	74	3.6°	0.032	73 cm	83 cm	0.033
1965	249	57	4.4°	81	3.0°	0.032	71 cm	83 cm	0.032
1966	408	64	6.4°	73	5.6°	0.038	89 cm	102 cm	0.039
1967	290	64	4.5°	77	3.8°	0.032	75 cm	86 cm	0.033
1968	251	72	3.5°	85	3.0°	0.028	70 cm	82 cm	0.029
1969	330	47	7.0°	66	5.0°	0.040	81 cm	91 cm	0.041
1970	128	39	3.3°	64	2.0°	0.027	50 cm	63 cm	0.029
1971	281	62	4.5°	83	3.4°	0.032	74 cm	88 cm	0.033
1972	141	56	2.5°	56	2.5°	0.024	53 cm	66 cm	0.025
1973	275	58	4.8°	78	3.5°	0.033	74 cm	86 cm	0.034
1974	392	74	5.3°	82	4.8°	0.035	88 cm	98 cm	0.036
1975	501	109	4.6°	109	4.6°	0.032	98 cm	110 cm	0.034
1976	NA								
1977	274	61	4.5°	67	4.1°	0.031	71 cm	85 cm	0.033
1978	183	53	3.5°	59	3.1°	0.028	60 cm	74 cm	0.030
1979	252	76	3.3°	83	3.0°	0.027	69 cm	81 cm	0.029
1980	396	79	5.0°	81	4.9°	0.034	89 cm	99 cm	0.035
1981	311	68	4.6°	79	3.9°	0.032	76 cm	90 cm	0.033
1982	329	74	4.4°	86	3.8°	0.032	81 cm	92 cm	0.032
1983	120	38	3.2°	58	2.1°	0.027	49 cm	63 cm	0.029

SOIL THERMAL PROPERTIES

Single layer case: W_f=30%, W_u=20%; L=36 cal/cm^3, K_u=0.0041 cal/cm °C s

Two layer case: Layer 1 W_f=20%, W_u=20%; L=20 cal/cm^3, K_u=0.006 cal/cm °C s

Layer 2: W_f=32%, W_u=20%; L=38 cal/cm^3, K_u=0.0041 cal/cm °C s

TABLE VI.5

CONSOLIDATION TEST RESULTS

* Frozen/Thawed Sample
Wi Initial water content
Wf Water content at end of test
e,i Initial void ratio
e,f Void ratio at end of test
Δe Change in void ratio
Δe % Change in void ratio as a per centage
Cv Coefficient of consolidation

		Load (kPa)	Wi (%)	Wf (%)	e,i	e,f	Δe	Δe %	Cv (cm^2/s)
Bulk Sample 1	1	35	27.6%	22.6%	0.75	0.61	0.14	18.6%	1.5×10^{-4}
	2	35	31%	26.4%	0.85	0.71	0.14	16.6%	6.9×10^{-5}
	3*	70	30%	20.6%	0.80	0.55	0.25	31%	1.0×10^{-2}
	4*	35	31.3%	23.1%	0.86	0.63	0.23	27%	9.4×10^{-3}
	5*	70	31.7%	21.7%	0.91	0.60	0.31	34.5%	1.0×10^{-2}
	6*	35-70	39.6%	23.8%	1.07	0.74	0.33	31%	7.1×10^{-3}
	7*	35	31.3%		1.0				1.6×10^{-2}
				20.4%		0.54	0.46	46%	1.2×10^{-2}
	8	35	24.9%		0.93				2.3×10^{-4}
		70		22%		0.59	0.34	37%	5.1×10^{-4}
	9	35	33%		0.90				2.0×10^{-4}
		70		21.7%		0.57	0.33	37%	3.4×10^{-4}
	10	9.8	30%		0.88				2.2×10^{-4}
		35							4.3×10^{-4}
		70		21.7%		0.57			2.4×10^{-4}
Bulk Sample 2	1	35	27.3%	20%	0.77	0.53	0.24	31.0%	4.1×10^{-4}
	2	9.8	27%	22.2%	0.75	0.59	0.16	21.3%	2.1×10^{-4}
	3*	9.8	28.6%	22.8%	0.76	0.60	0.15	20.3%	1.1×10^{-2}
	4	9.8	30%	25%	0.84	0.66	0.17	20.5%	------
	5	9.8	26.5%	22%	0.74	0.59	0.15	20.3%	1.2×10^{-4}
	6	9.8	27.1%		0.76	0.61		19.6%	1.2×10^{-4}
		35				0.53		30.0%	5.2×10^{-3}
		70		19%		0.51		33.0%	3.2×10^{-3}
	7*	9.8	28.7%		0.83	0.67		19.8%	2.5×10^{-2}
		35				0.57		31.9%	9.2×10^{-3}
		70		19%		0.53		36.0%	6.3×10^{-4}

Loose loading cap tilted on Ball, T7A. This may have provided excess side friction, slowing the initial consolidation. See data plot, Appendix A. Friction may also have been a problem with T1, T4, T5, T6, in each, Cv of these samples is too low.

TABLE VI.6

FIELD HYDRAULIC CONDUCTIVITY

No.	LOCATION		DATE: 1983	h_1 (cm)	h_2 (cm)	Δh (cm)	t (sec)	K (cm/s)	S/S/C (%)
5	Slide 8	58	14/8	47.0	41.0	-6.0	4 200	4.1×10^{-7}	13/61/26
4	"	69	14/8	44.5	42.0	-2.5	5 700	1.2×10^{-7}	
12	"	40	14/8	38.0	35.5	-2.5	5 400	1.6×10^{-7}	
3	Site 1	50	9/7	15.5	12.0	-3.5	22 500	2.5×10^{-7}	11/60/29
8	Site 3	68	14/8	61.0	39.0	-22.0	900	6.2×10^{-6}	
9	K1145	48	14/8	11.0	0.5	-10.5	2 100	3.3×10^{-5}	58/35/7
9	"	48	14/8	68.0	11.0	-57.0	300	1.3×10^{-4}	"
4	Site 1	51	7/7	24.5	11.0	-13.5	900	4.4×10^{-5}	
5	Site 1	69	7/7	56.5	52.0	-4.5	9 300	1.1×10^{-7}	
6		44	10/7	71.0	1.5	-69.5	98 400	8.7×10^{-7}	

TABLE VI.7

PHYSICAL PROPERTIES OF SOME GELIFLUCTION SOILS FROM KIVITOO

Location: Solifluction site, K1145, see Figure VIII.9.

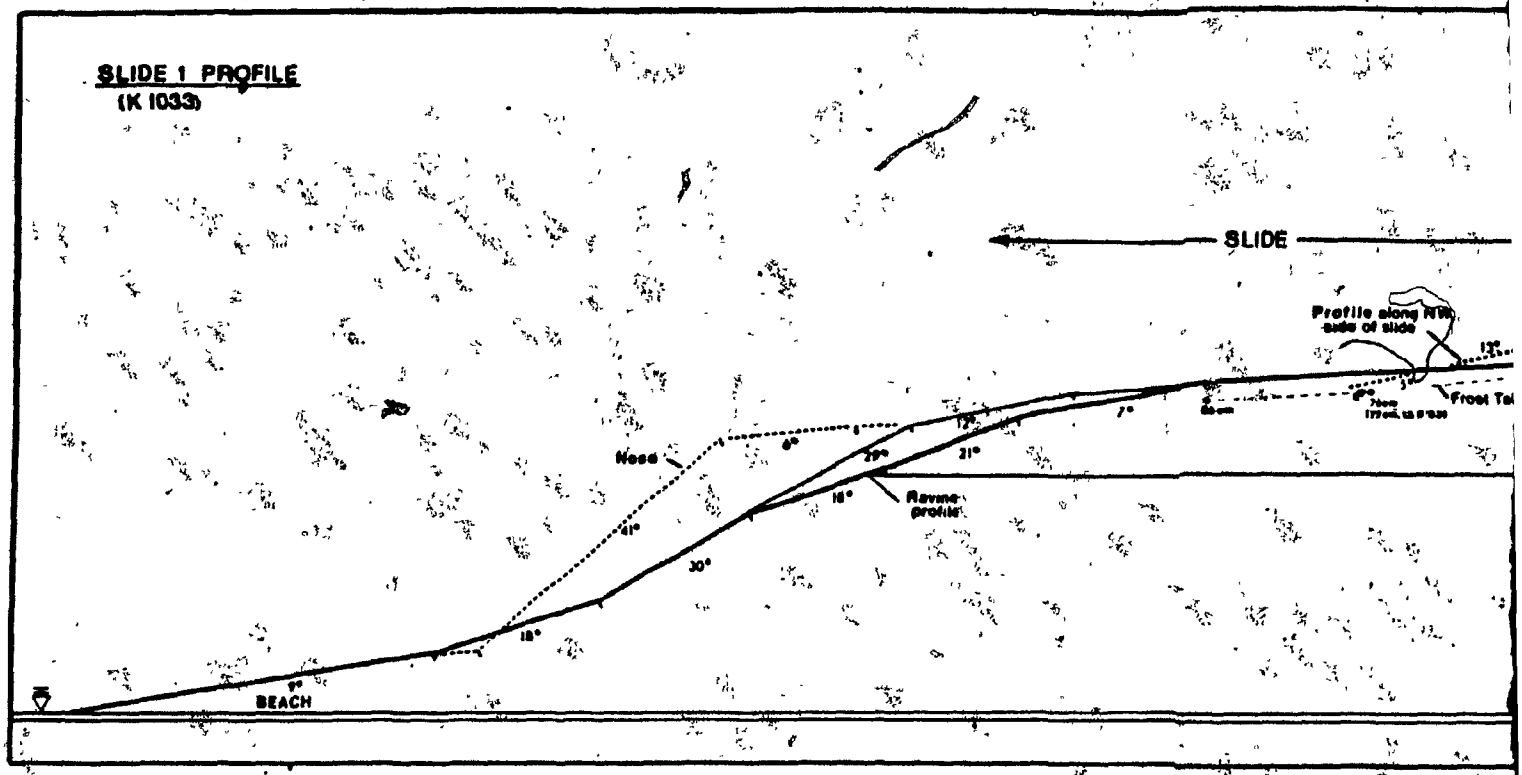
Physical state	Water content (%)	Bulk Unit Wt. (dry, kN/m^3)	Porosity (n = %)	% Sat.
*Frozen, fine to coarse sand	24%	14.24	45%	74%
Thawed, near surface	17%	19.41	25%	100%
Thawed/remolded	12%			100%
Thawed sand with bubbly structure	14%	15.22	41%	50%

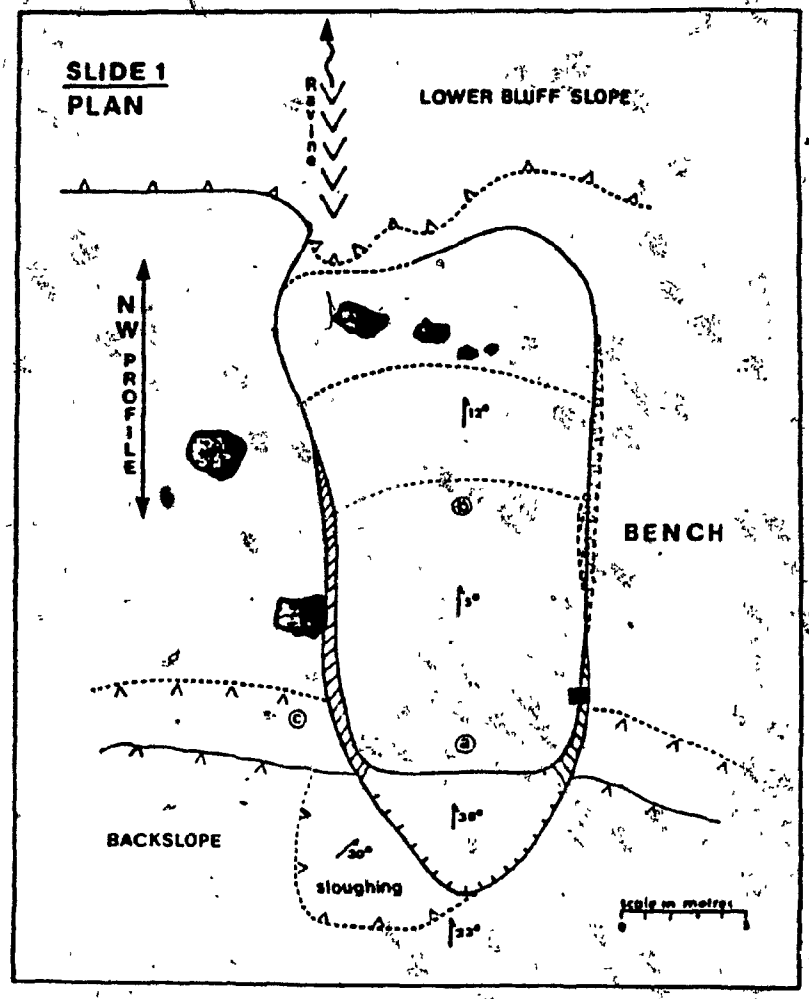
*ice content is highly variable, with a standard deviation of 7% for seven samples. The highest ice content was 39%, the lowest 19%.
Max. unit wt.; 15.1 kN/m^3, n = 43% Min. unit wt.; 14.2 kN/m^3, n = 46%

Porosity and Bulk Unit Weight Data for Some Other Gelifluction Soils

Source	Bulk Unit Wt. (dry, kN/m^3)	Water content (%)	Porosity (n = %)
Harris (1977)	16.3	25%	40%
	15.5	24%	42%
Williams (1959)	14.3		45%
	14.9	19%	43%
Veillette	----	---	44%

Figure VI.1



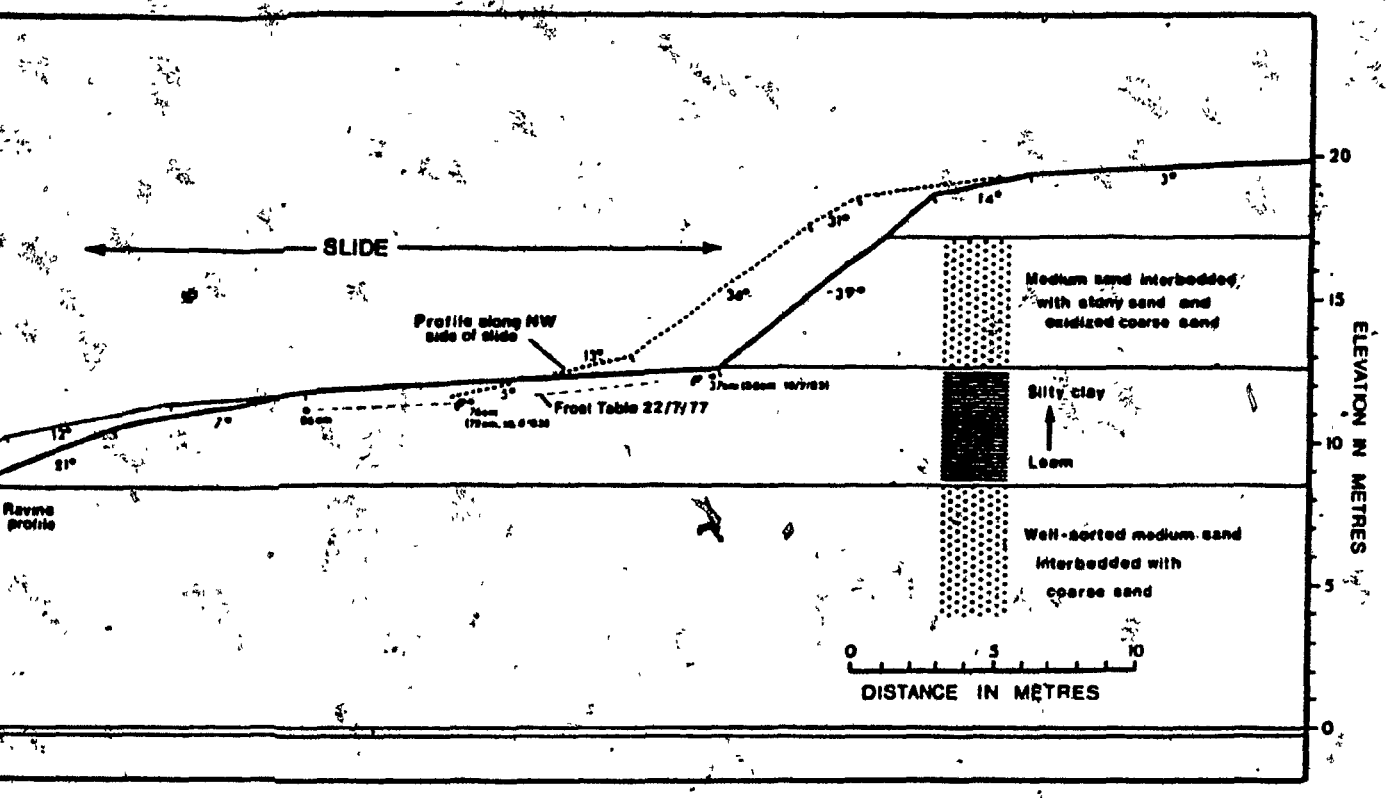


SOIL PIT DATA, SLIDE 1 (W%)

PIT A, Core 6 location (19/7/83)
0-30 cm (18%)
30-35 cm silty loam
soil just above frost table (20%)
Frost table (35 cm; 16%)

PIT B (13/8/83)
0-40 cm oxidized sand
40-72 cm grey silty sand (14%, 60 cm)
Frost table (72 cm; 41-45%)

PIT C (19/7/83)
0-32 cm colluvial sand
32-41 cm silty sand (15%)
41-52 cm sandy loam
soil just above frost table (17%)
Frost table (52 cm; 41%)



SOIL PIT DATA, SLIDE 1 (W%)

PIT A, Core 8 location (19/7/83)
0-30 cm (18%)
30-35 cm silty loam
soil just above frost table (20%)
Frost table (35 cm; 16%)

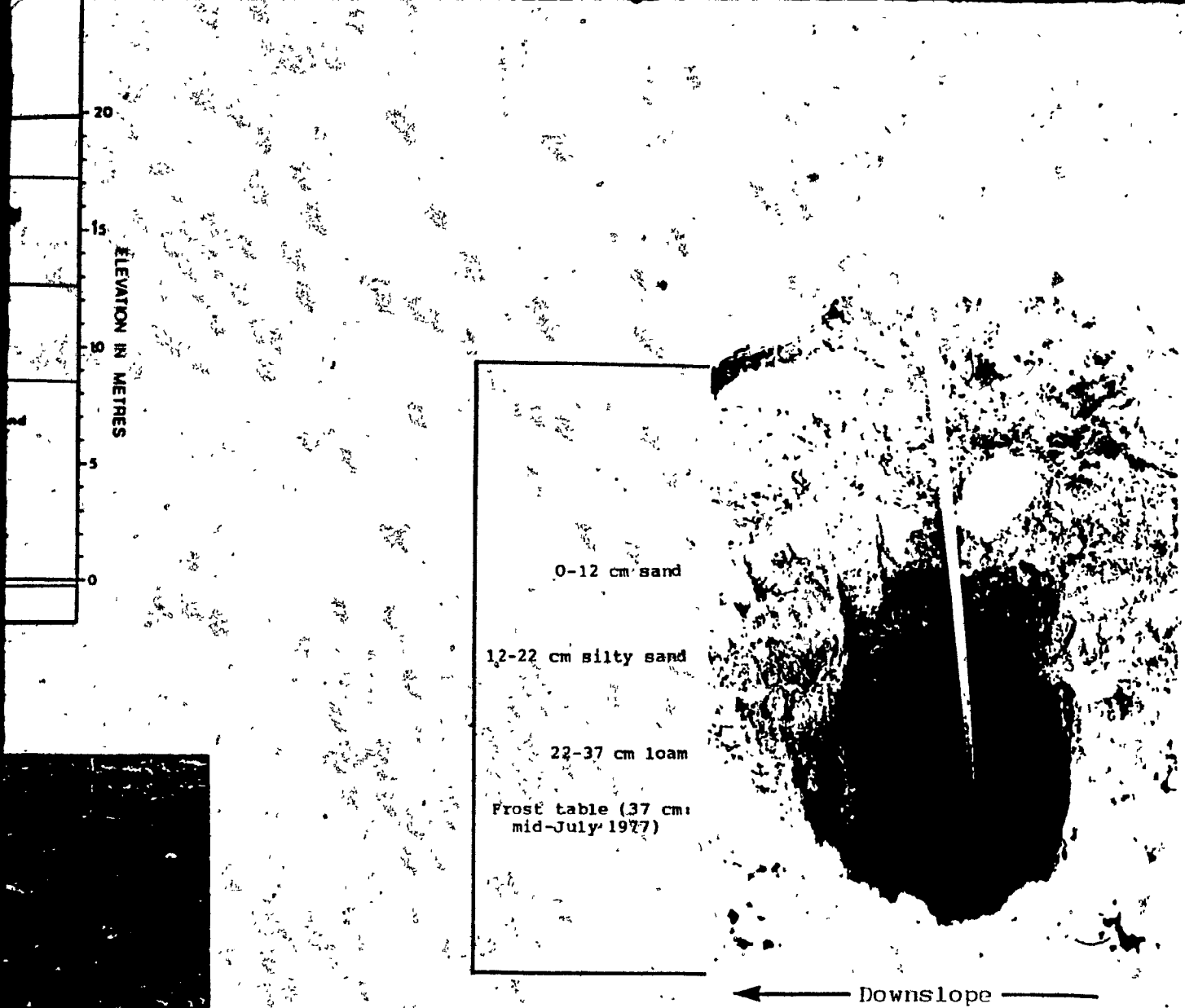
PIT B (13/8/83)
0-40 cm oxidized sand
40-72 cm grey silty sand (14%, 60 cm)
Frost table (72 cm; 41-45%)

PIT C (19/7/83)
0-32 cm colluvial sand
32-41 cm silty sand (15%)
41-52 cm sandy loam
soil just above frost table (17%)
Frost table (52 cm; 41%)



AA

Slide 1 (K1033). View of landslide looking downslope from bench back slope. The distinct rupture with the bench surface along the sides and limited displacement of the failed mass can be seen. (August 1977)



B

Excavation along side of landslide at back of the failure scar. (Location is marked on landslide plan, ■.) ~15 cm of silty loam is overlain by sand and silty sand, frost table is at 37 cm (early July 1977).



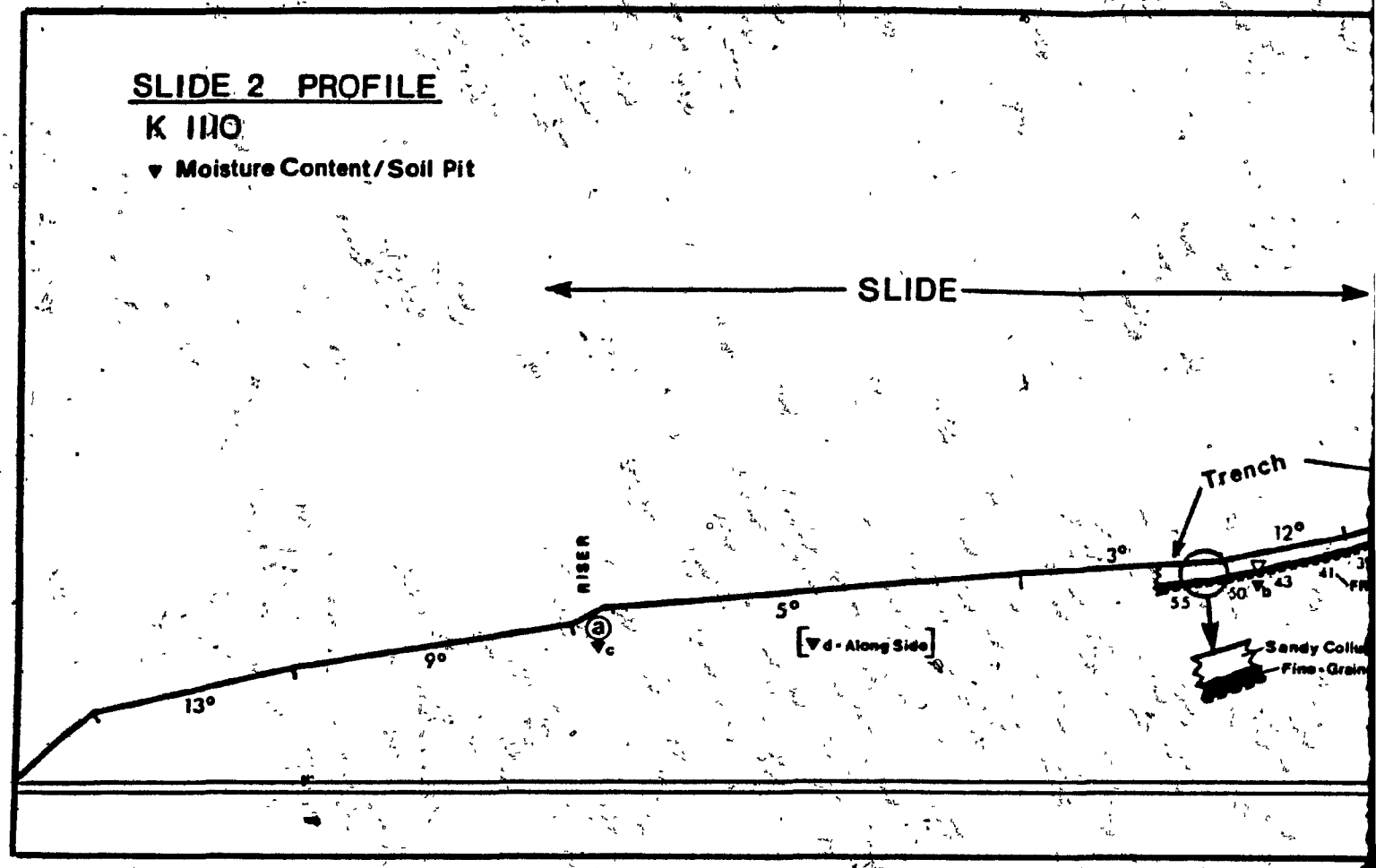
ing downslope from
with the bench
lacement of the

Figure VI.2

SLIDE 2 PROFILE

K 1110

▼ Moisture Content/Soil Pit





AA

Slide 2 (K1110). View of landslide looking downslope from bench back slope. Landslide displays distinct lateral shearing, overriding of the lower bench slope and compression ridge development at toe. Trench shown on profile was located to the left of shovel. Photograph, taken in early July 1977, shows late lying snow pack at back of slide scar.

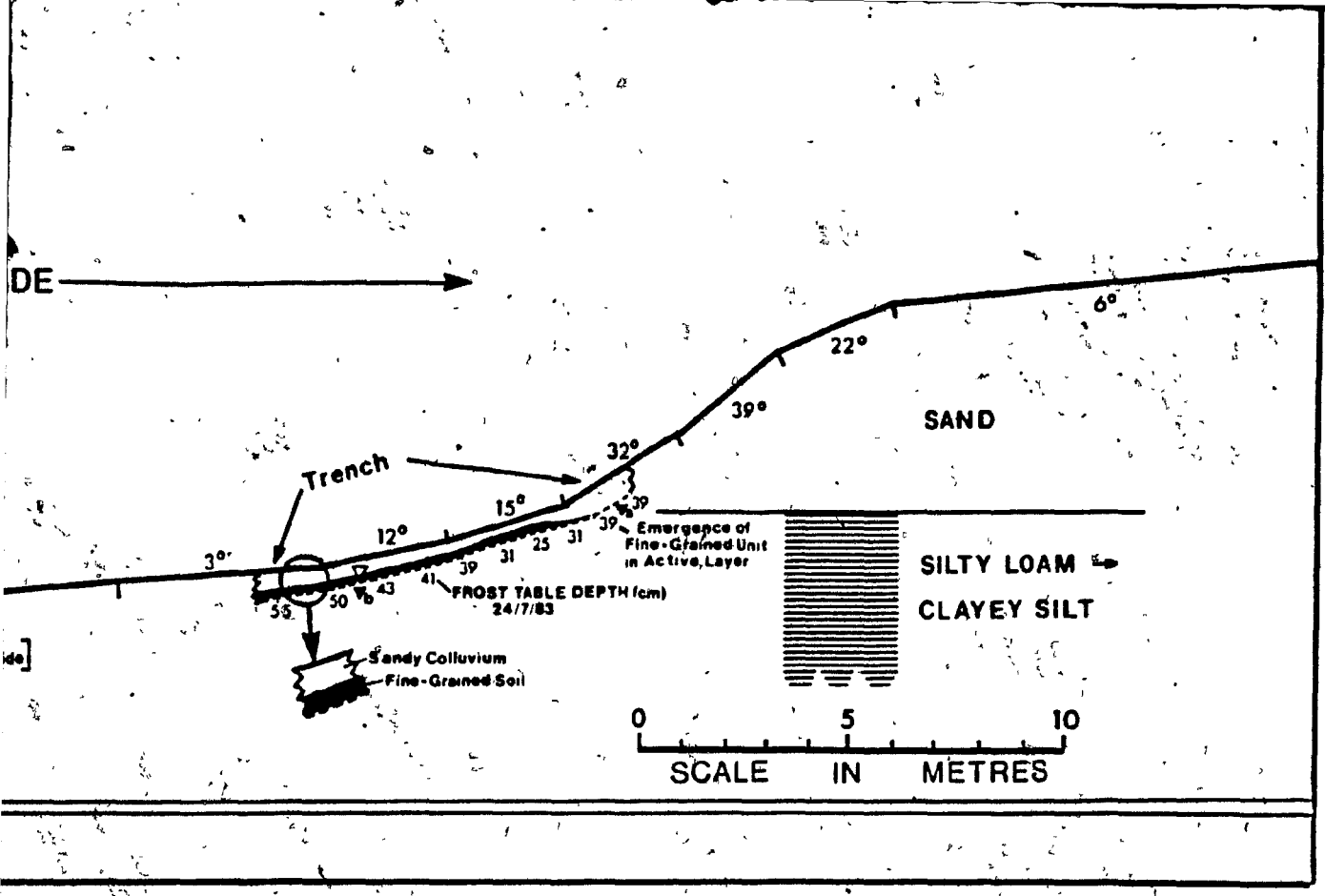
SOIL PIT DATA (W%)

A
0-39 cm sand
Frost table (39 cm; 18%)

B
0-28 cm sandy colluvium
28-45 cm silty loam (24%)
Frost table (45 cm; 24-31%)

C
0-61 cm snady colluvium
61-81 cm sand and silty sand
81-92 cm silty loam
thawed soil just above frost table (90 cm; 22%)
Frost table (92 cm; 30%)

D
Sandy loam just above frost table (20%)
Frost table (63 cm; 24-26%)





C

Excavation at
slide mas has
downslope by o
the buried soi

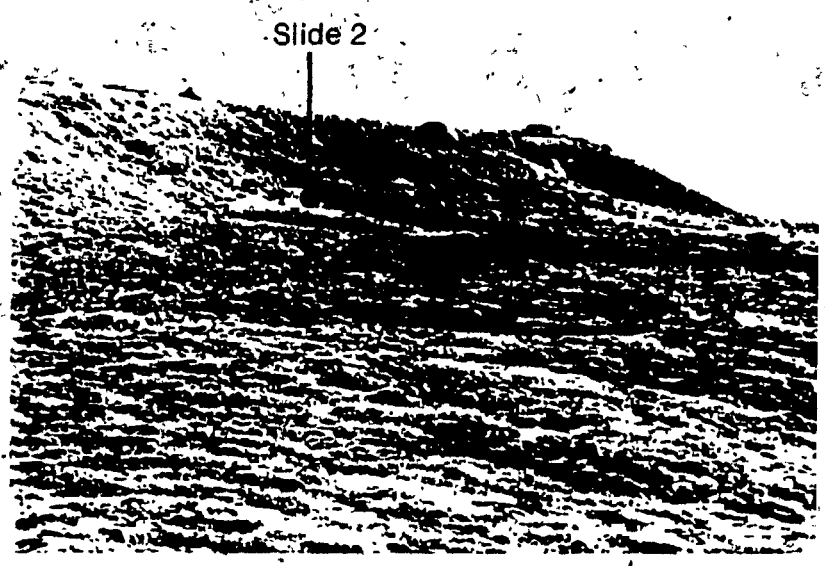
SOIL PIT DATA (W%)

A
0-39 cm sand
Frost table (39 cm: 18%)

B
0-28 cm sandy colluvium
28-45 cm silty loam (24%)
Frost table (45 cm: 24-31%)

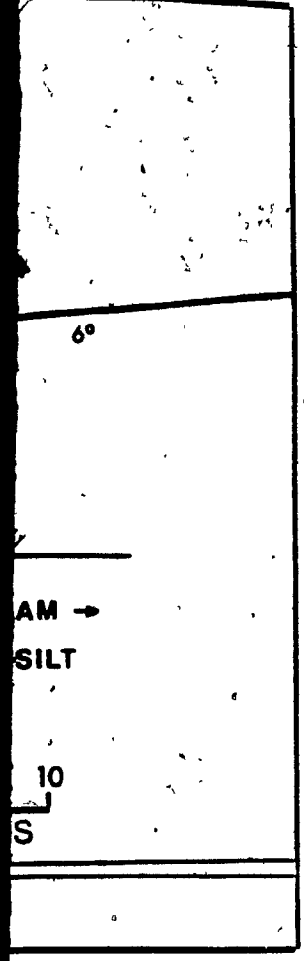
C
0-61 cm snady colluvium
61-81 cm sand and silty sand
81-92 cm silty loam
thawed soil just above frost table (90 cm: 22%)
Frost table (92 cm: 30%)

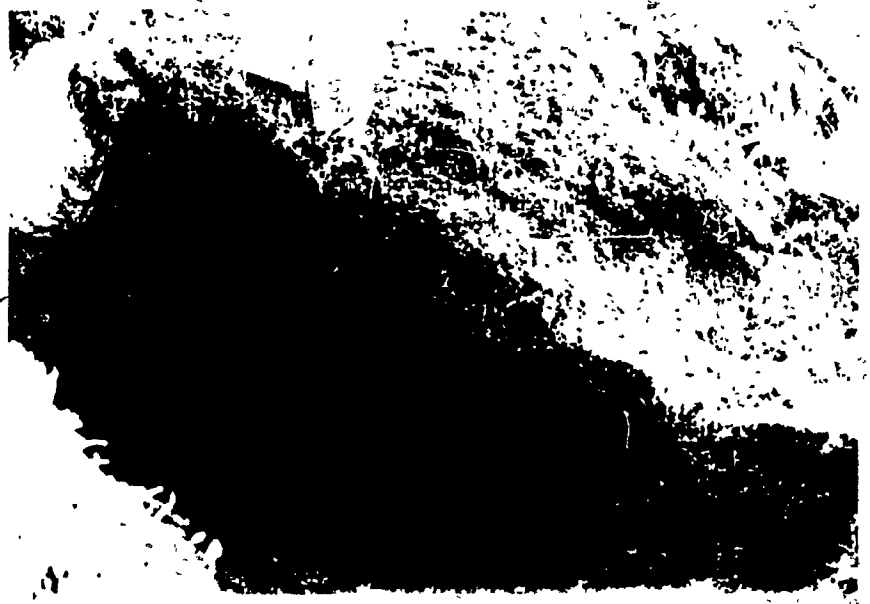
D
Sandy loam just above frost table (
Frost table (63 cm: 24-26%)



B

View of Slide 2 looking west along bench. Note 'older' slide in foreground. (Similar view shown in Figure VIII.3.) Photograph taken August 1977.





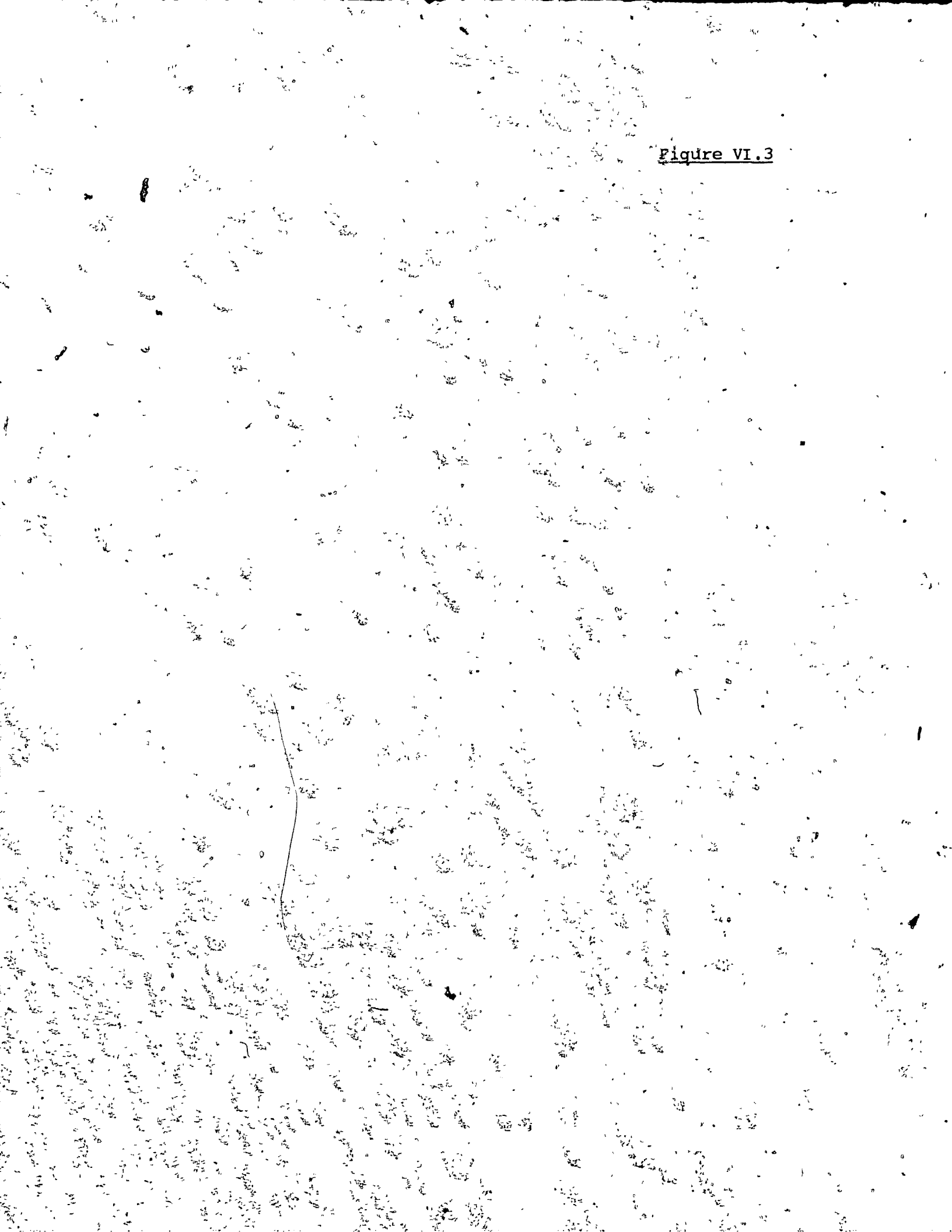
CA

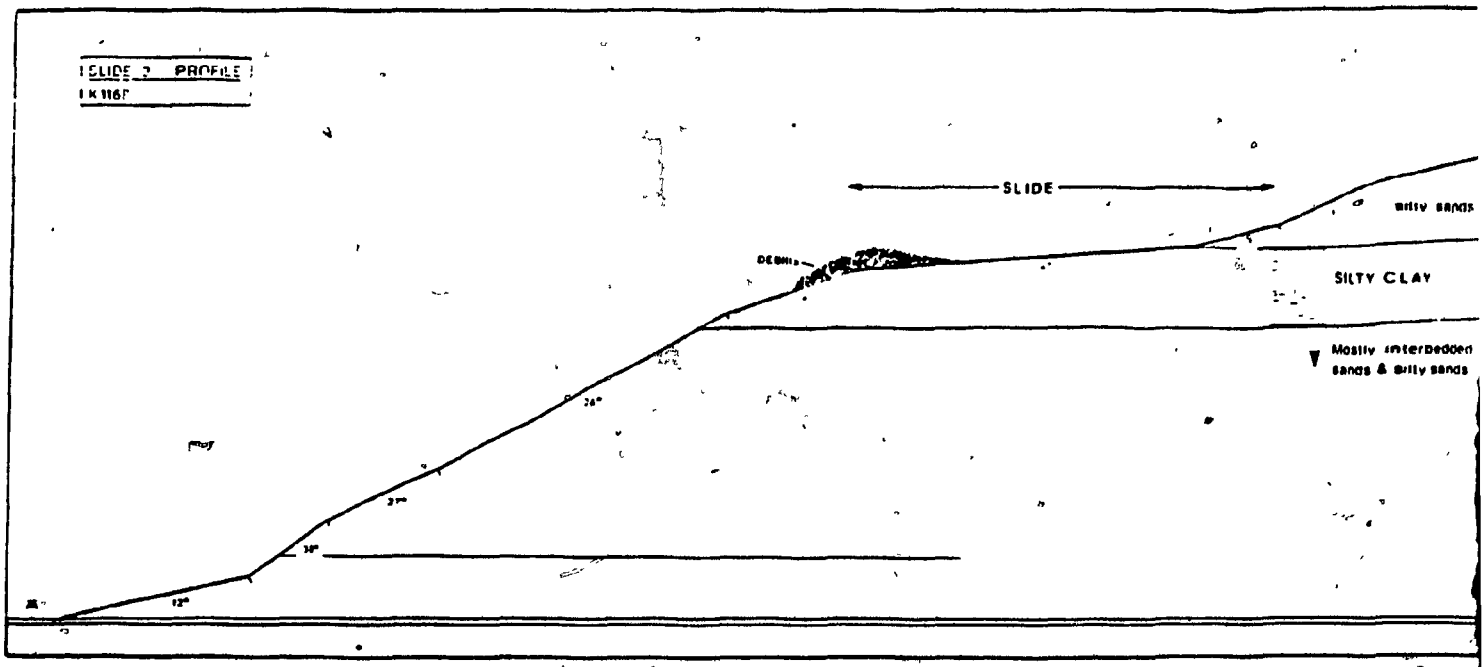
Excavation at toe of Slide 2; location @ on profile. The slide mas has thinned near the toe and overridden the bench downslope by only 30-35 cm (as indicated by the length of the buried soil). (See soil pit data; C.)

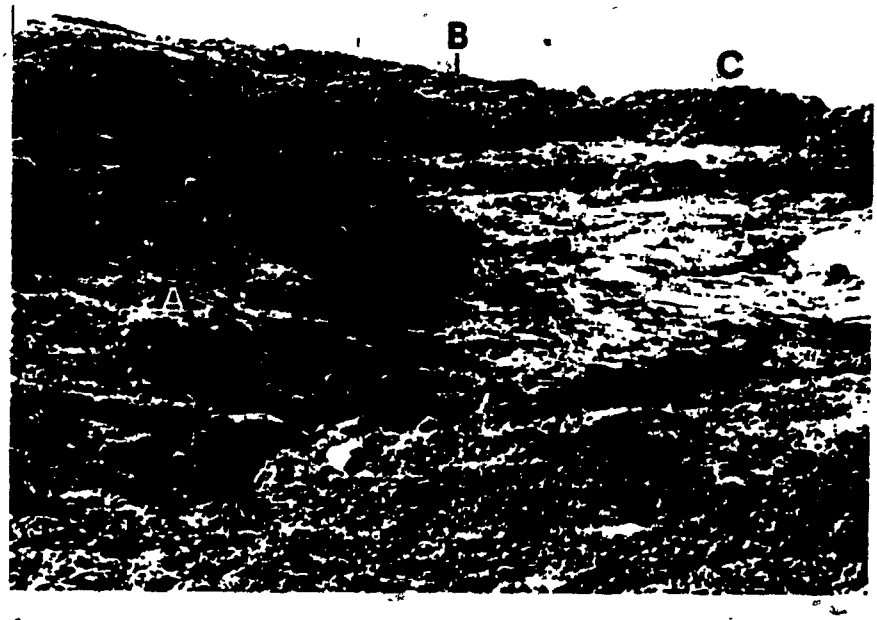


h. Note 'older' slide
Figure VIII.3.) Photo-

Figure VI.3

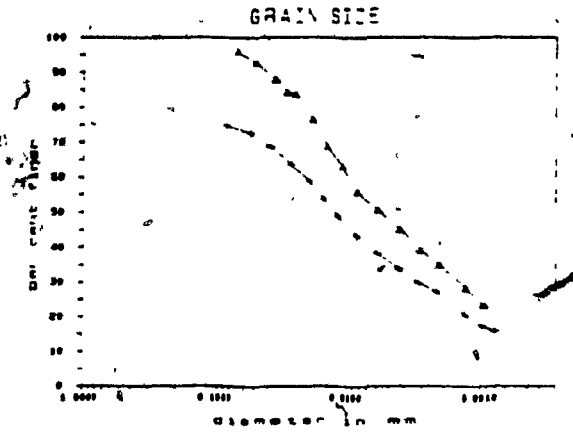




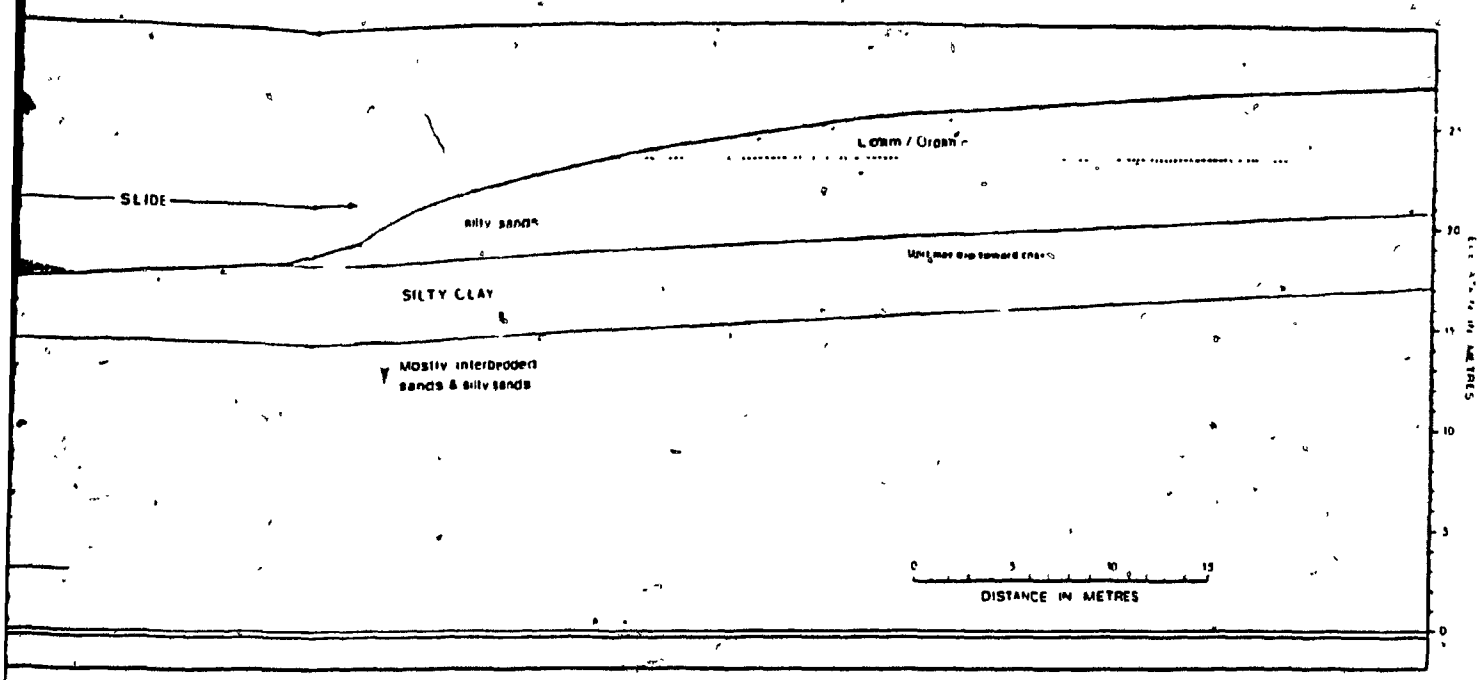


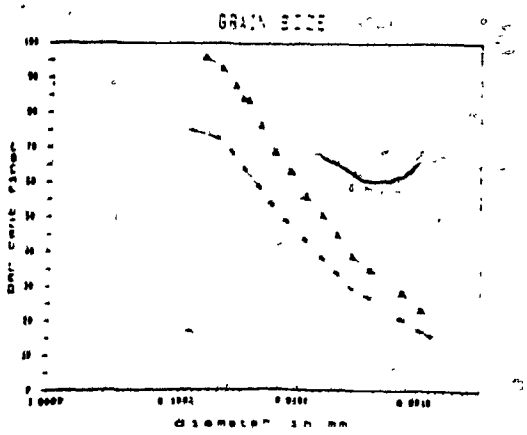
AA

Slide 3 (R1168). View looking west along bench across the bare soil exposed in the slide scar. This landslide was particularly wide (30-40m). The slide mass itself broke-up and continued downslope movement as a debris flow over the base of the bluff. This photograph, taken in August 1977, shows the development of tension cracks along the back slope (A). When first examined (July 1977) no tension cracks were evident. The bench edge is indicated at B. Note also slide debris pushed up at C.



Bulk samples 1 (A) and 2 (-) from Slide 3 scar. Sample - is brown (unweathered) soil from near b of active layer. Sample - is grey (weathered) so from near crack of scar scar.





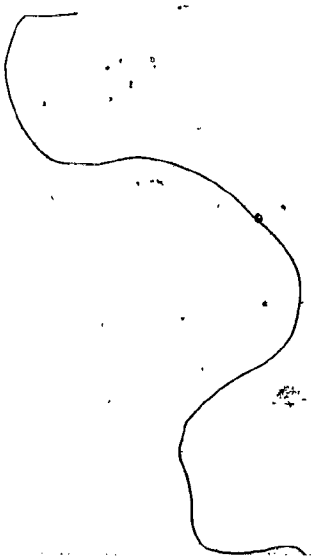
Bulk samples 1 (A) and 2 (B) from Slide 3 scar. Sample 1 is arkosic (unweathered) soil from near base of active layer. Sample 2 is brown (weathered) soil from near surface of scar.



B A

View of the lower portion of Slide 3 looking east along bench. This photograph shows the extensive overthrusting of debris at the landslide toe. The location of piezometers 11, 10 and 13 (in 1983) is indicated by A. See piezometer data for information on moisture content.

Figure VI.4





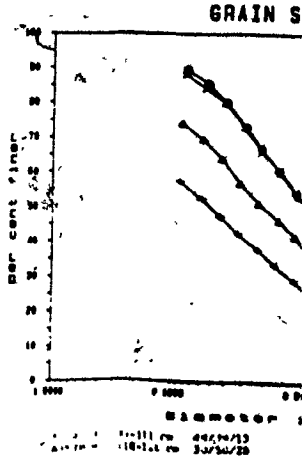
AA

Slide 5 (K1227). View of landslide looking downslope from backscarp. Slide 5 occurred along a particularly wide section of the mid-bluff bench. This feature is similar to Slide 3, both landslides being characterized by debris evacuation and considerable overthrusting at the toe (A). The locations of Cores 10 and 11 (Figure VI.6) are indicated (X). Core 9 is just off the photograph on the intact bench to the right. Surface water, ariseng in a hollow along the bench back slope to the left of the landslide is entering the scar at B. (1977)

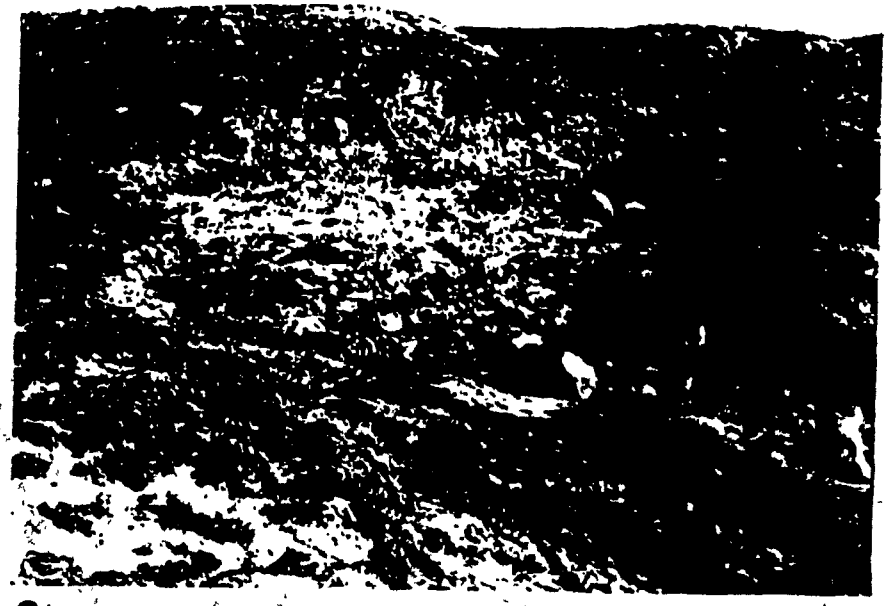


BA

View looking west along wide section of the mid-bluff bench. Slide 5 is indicated (A). Overthrust debris is marked at B. Note also sandy alluvial soil being deposited by slope wash arising in hollow just east of Slide 5. (1977)

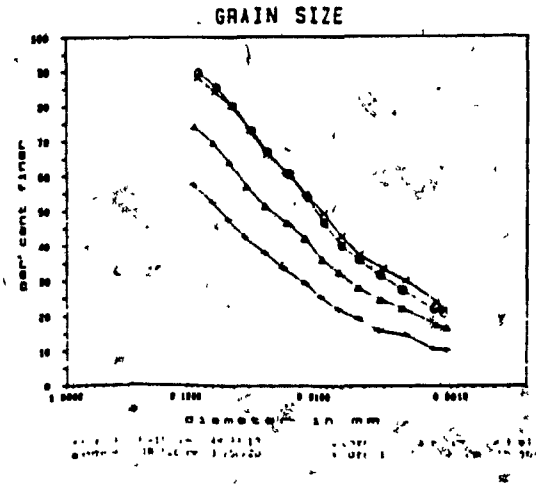


Core 9 ...s from bench slope
Core 10 ...s from Slide 5 sca

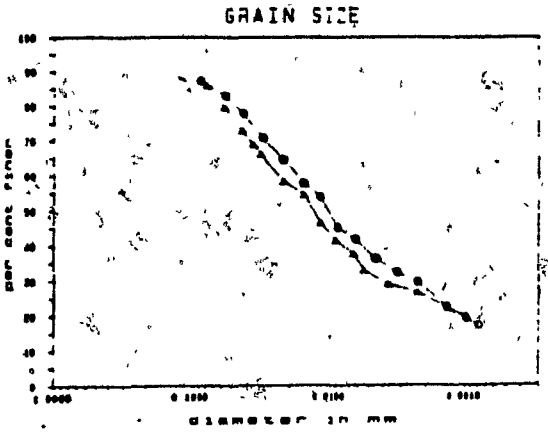


CA

View looking upslope from toe of Slide 5. Note undercutting of the base of the bench back slope. (1977)



Core 9 is from bench slope alongside Slide 5
Core 10 is from Slide 5 scar



Bulk samples 3 (Δ) and 4 (o) from Slide 5 scar

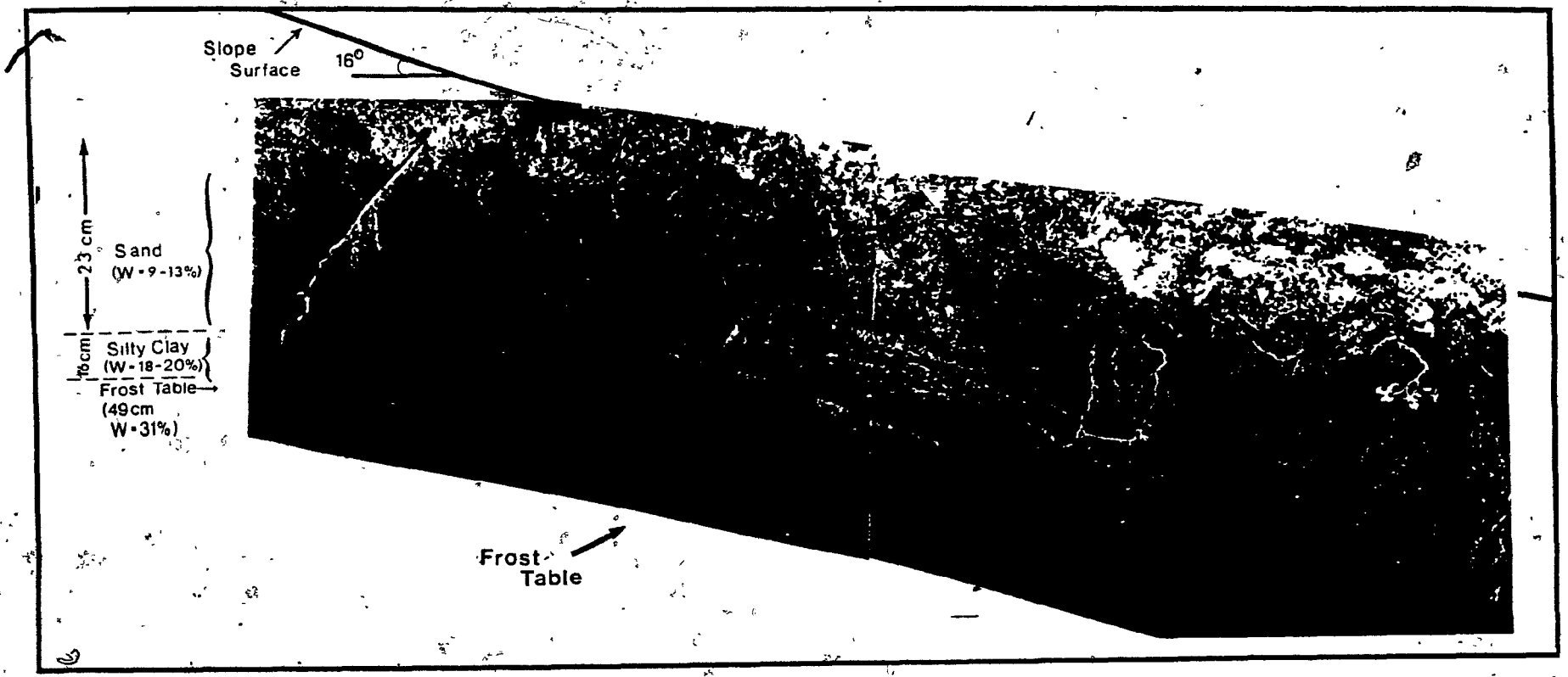


Figure VI.5 Trench across mid-bluff bench at K1063, July 22, 1983. The bottom of the excavation is at the frost table. Soil profile information at left is representative of the trench; the relative thickness of the fine-grained and sandy layers varies slightly along the slope. (The fine-grained layer is 5-20 cm thick, while the frost table depth varies from 45-55 cm.)

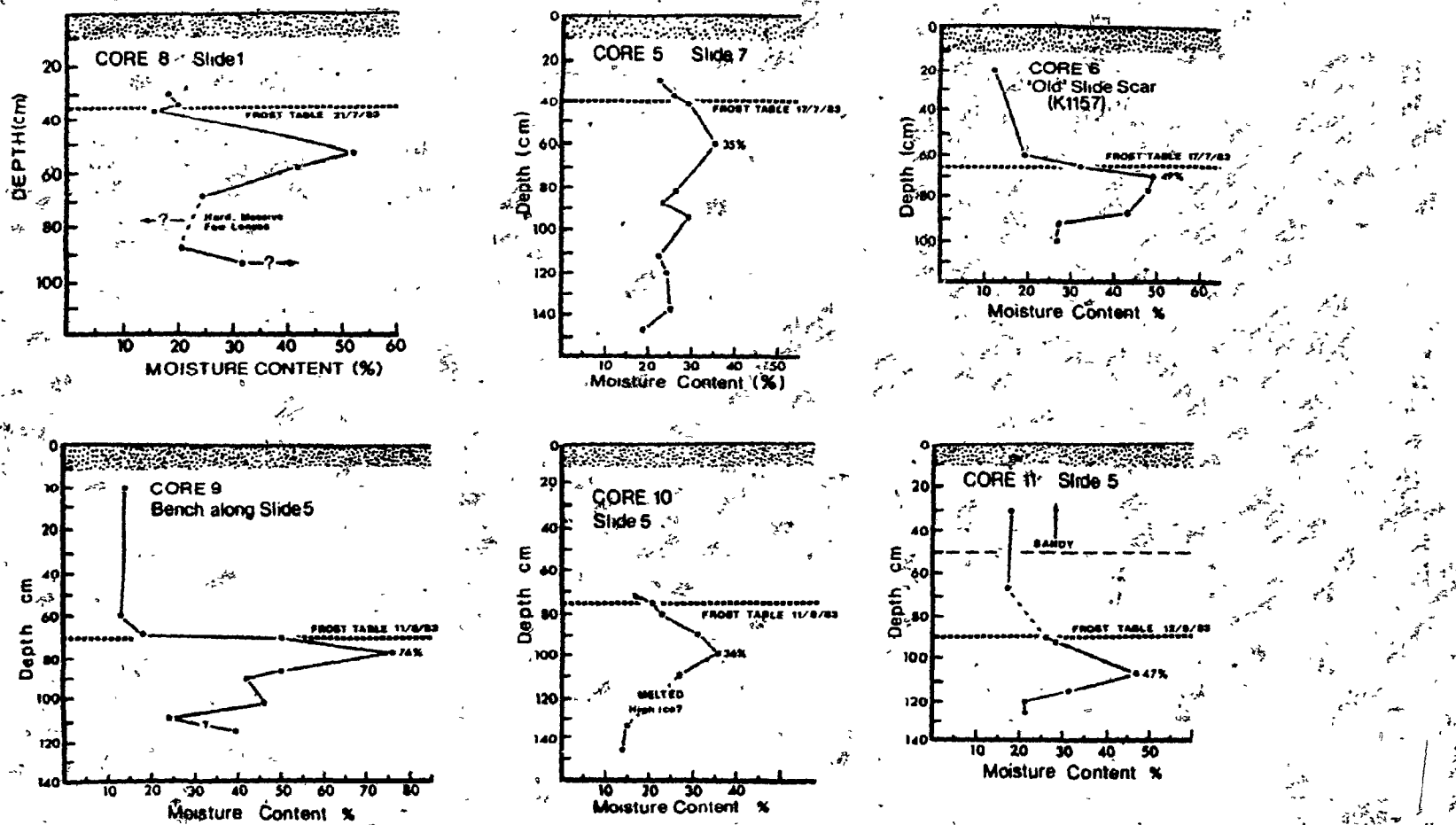


Figure VI.6 CRREL Core data from sites along the mid-bluff bench. Moisture content is per cent dry weight. Data from frost table and below are ice contents.

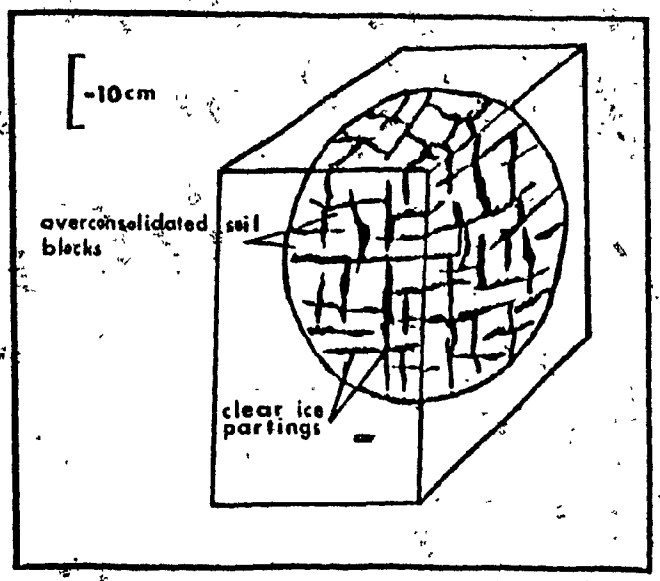


Figure VI.7 Schematic drawing of a frozen fine-grained soil in which a reticulate three-dimensional cryogenic structure has developed.

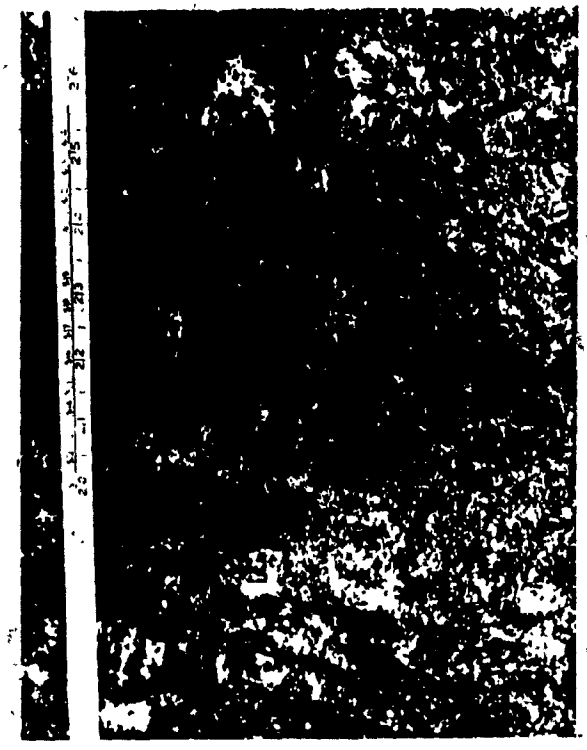


Figure VI.8 Excavation of a frozen silty clay showing the reticulate or blocky cryogenic structure. The white material is granular ice in larger pore spaces. The dark, thin veins form a fine lattice like network through the frozen soil.



Figure VI.9 Exposure of thawed reticulate-structured silty clay, similar to the frozen soil seen in Figure VI.8. In this soil much of the cryogenic structure is retained after thaw.

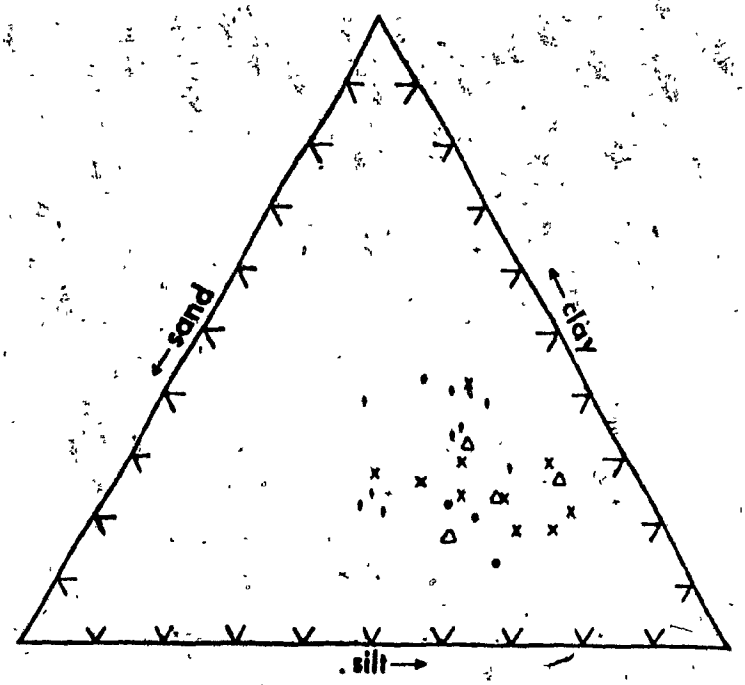
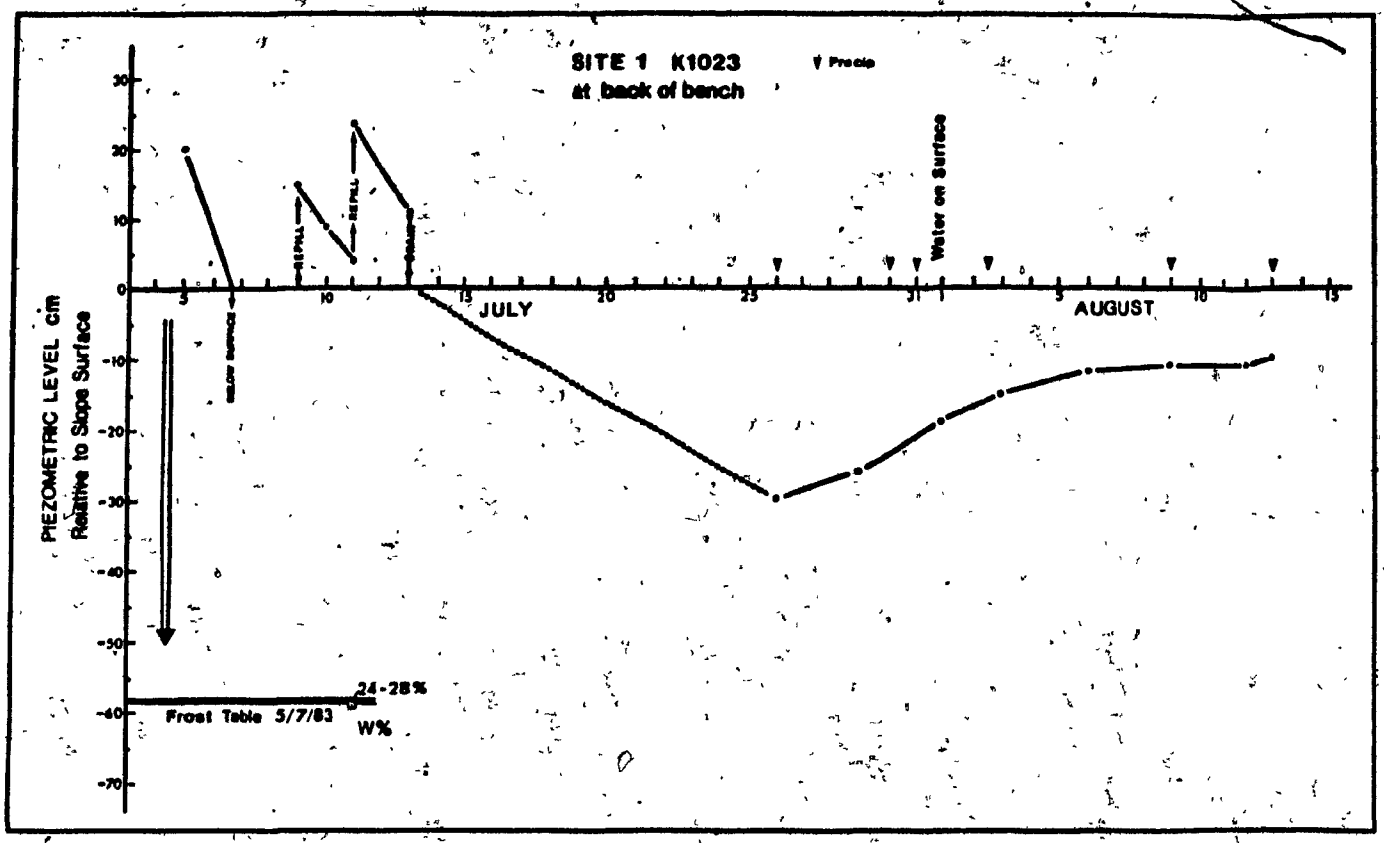
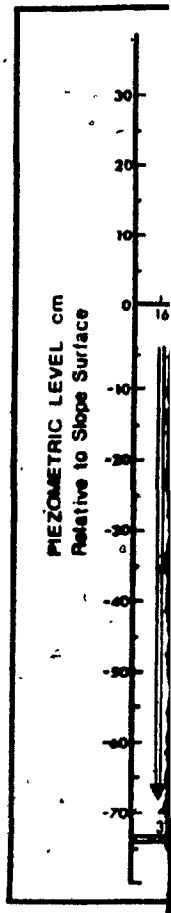
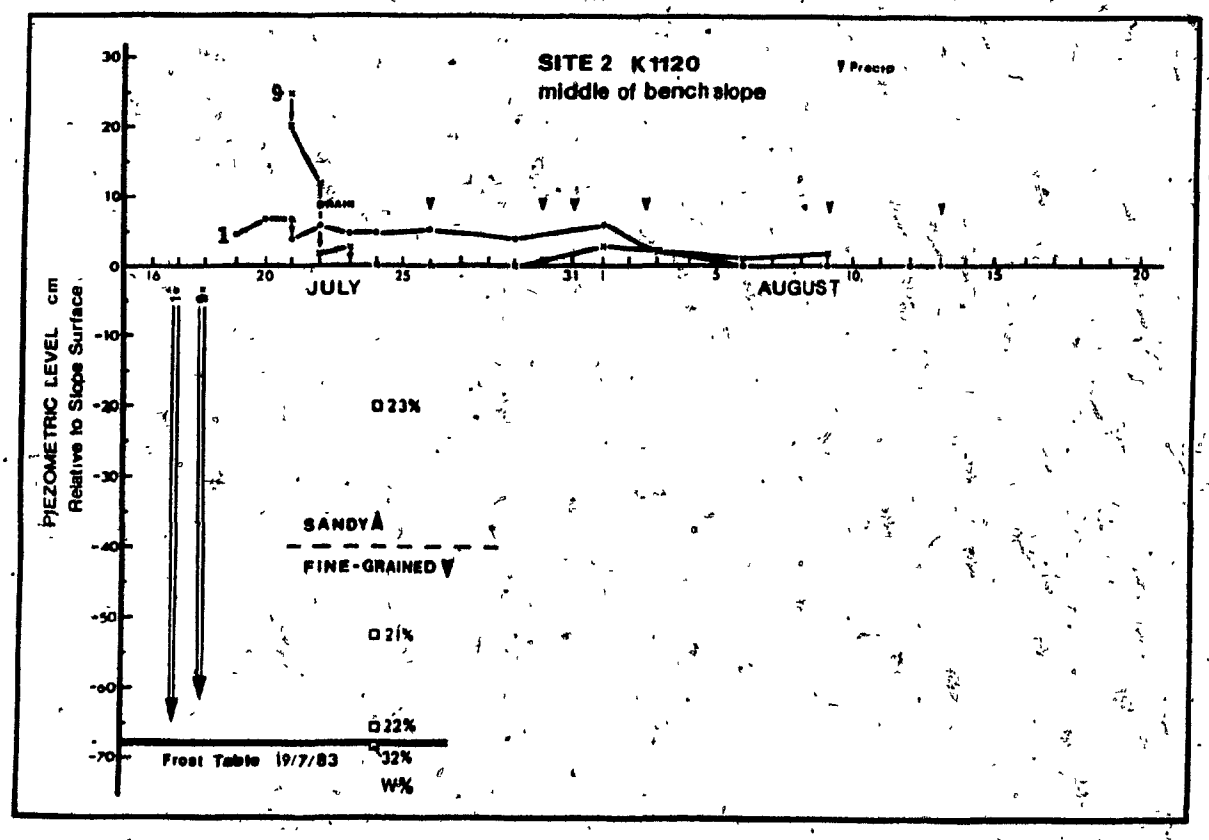


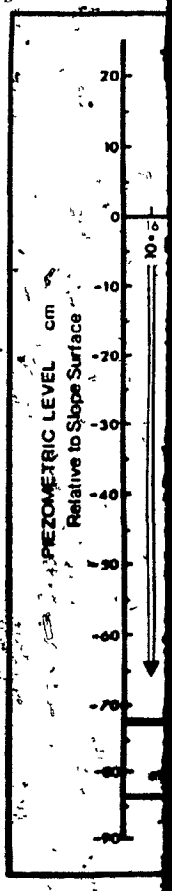
Figure VI.10 Ternary diagram of the grain-size distribution of some soils possessing a reticulate cryogenic structure. x this study; Δ Chandler (1972); • Mackay (1974); + horizontally lensed soil, Mackay (1974)

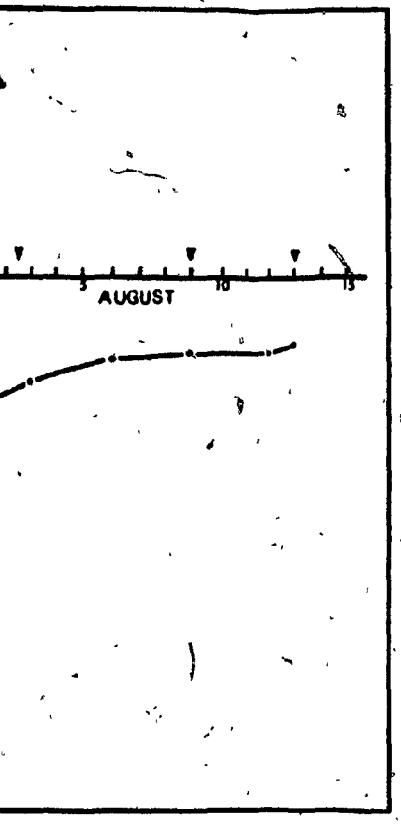
Figure VI.11

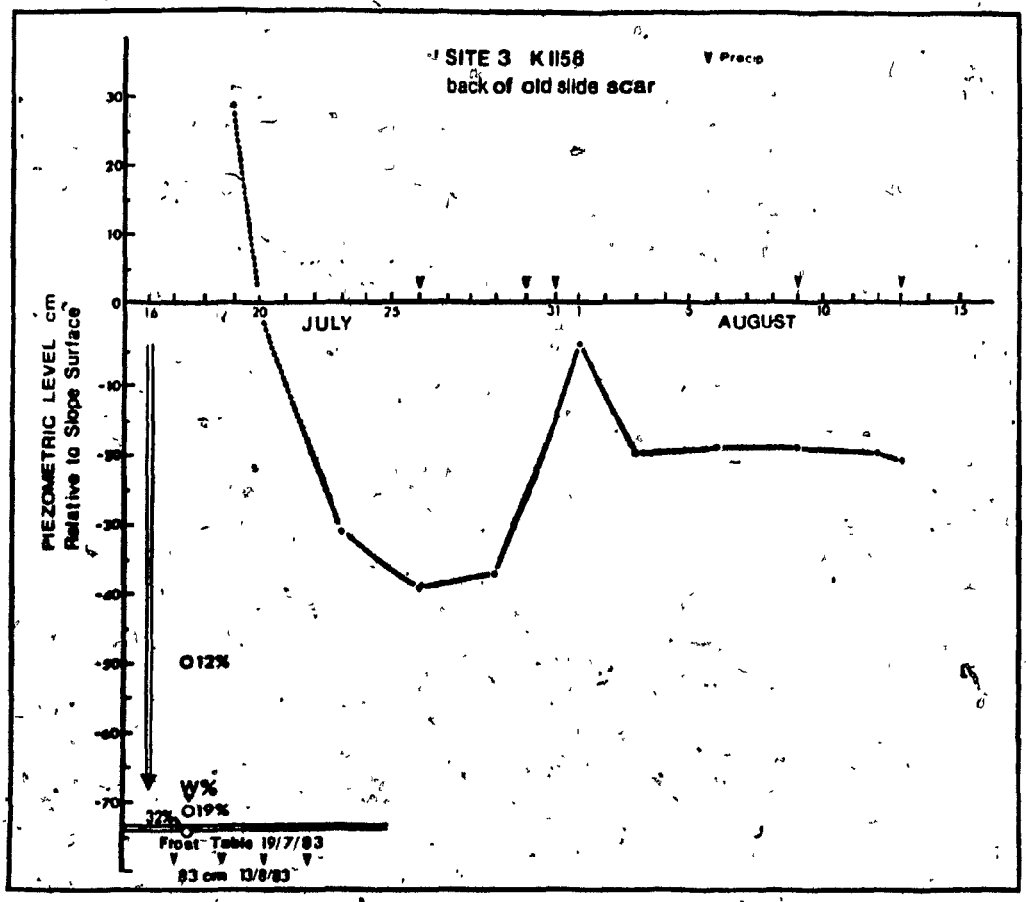

SITE 1 K1023
at back of bench
Precip
Water on Surface
REFILL
REFILL
DRAIN
JULY
AUGUST
PIEZOMETRIC LEVEL cm
Relative to Slope Surface
BELOW SURFACE
24-28%
Frost Table 5/7/83
W%

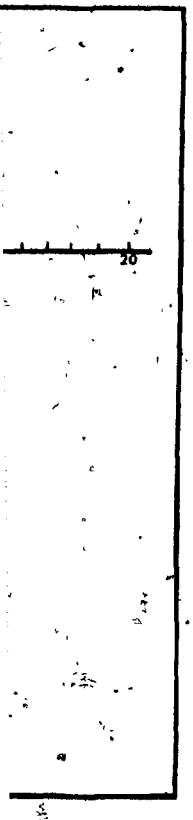

PIEZOMETRIC LEVEL cm
Relative to Slope Surface

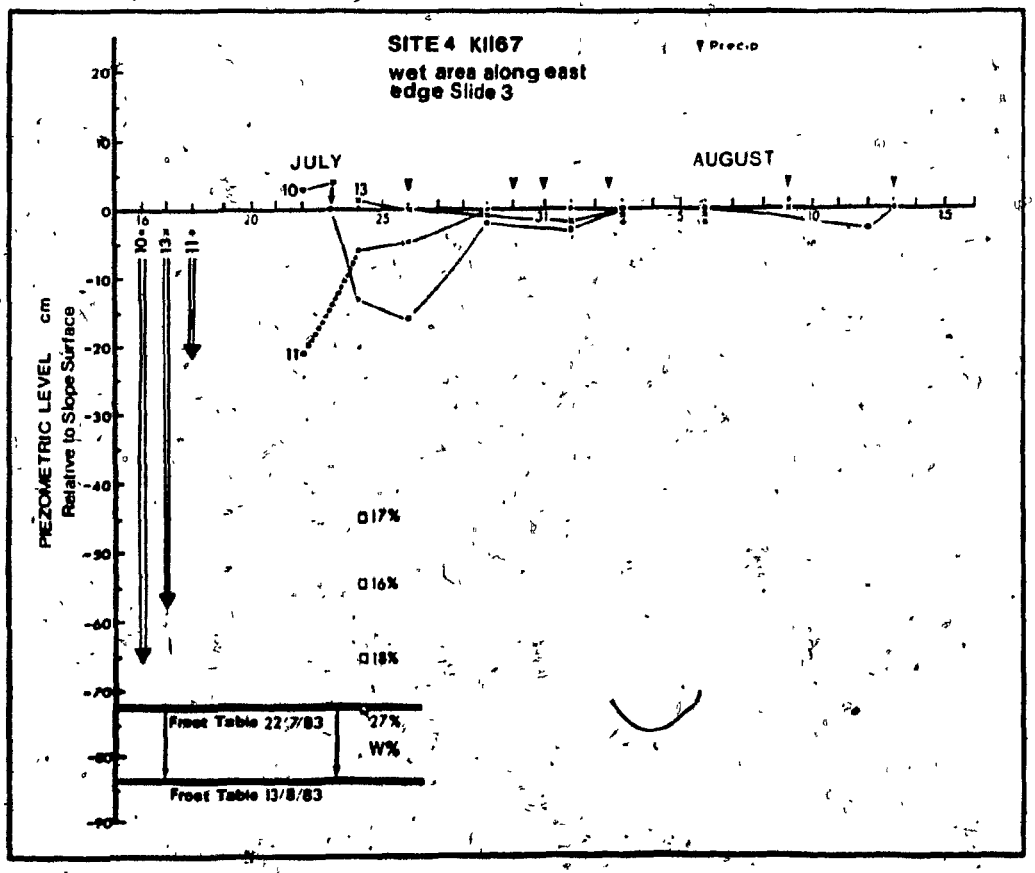

SITE 2 K1120
middle of bench slope
Precip
9
1
DRAIN
JULY
AUGUST
PIEZOMETRIC LEVEL cm
Relative to Slope Surface
23%
SANDY
FINE-GRAINED
21%
22%
32%
Frost Table 19/7/83
W%

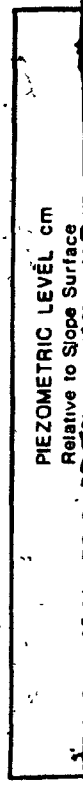

PIEZOMETRIC LEVEL cm
Relative to Slope Surface

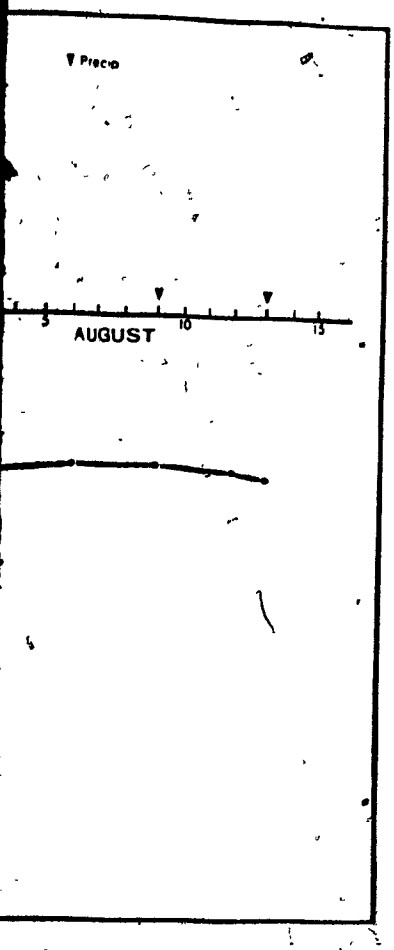

AUGUST
10
15

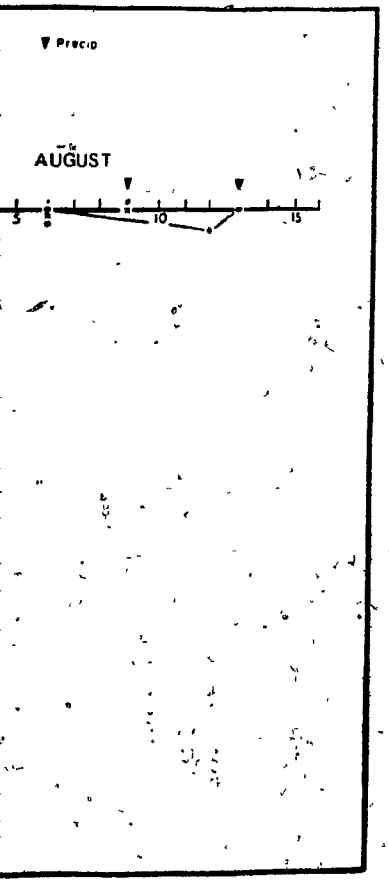

SITE 3 K1158
back of old slide scar
Precip
PIEZOMETRIC LEVEL cm
Relative to Slope Surface
JULY
AUGUST
12%
W%
19%
Frost Table 19/7/83
83 cm 13/8/83


20


SITE 4 K1167
wet area along east
edge Slide 3
Precip
JULY
AUGUST
PIEZOMETRIC LEVEL cm
Relative to Slope Surface
17%
16%
18%
Frost Table 22/7/83
27%
W%
Frost Table 13/8/83


PIEZOMETRIC LEVEL cm
Relative to Slope Surface





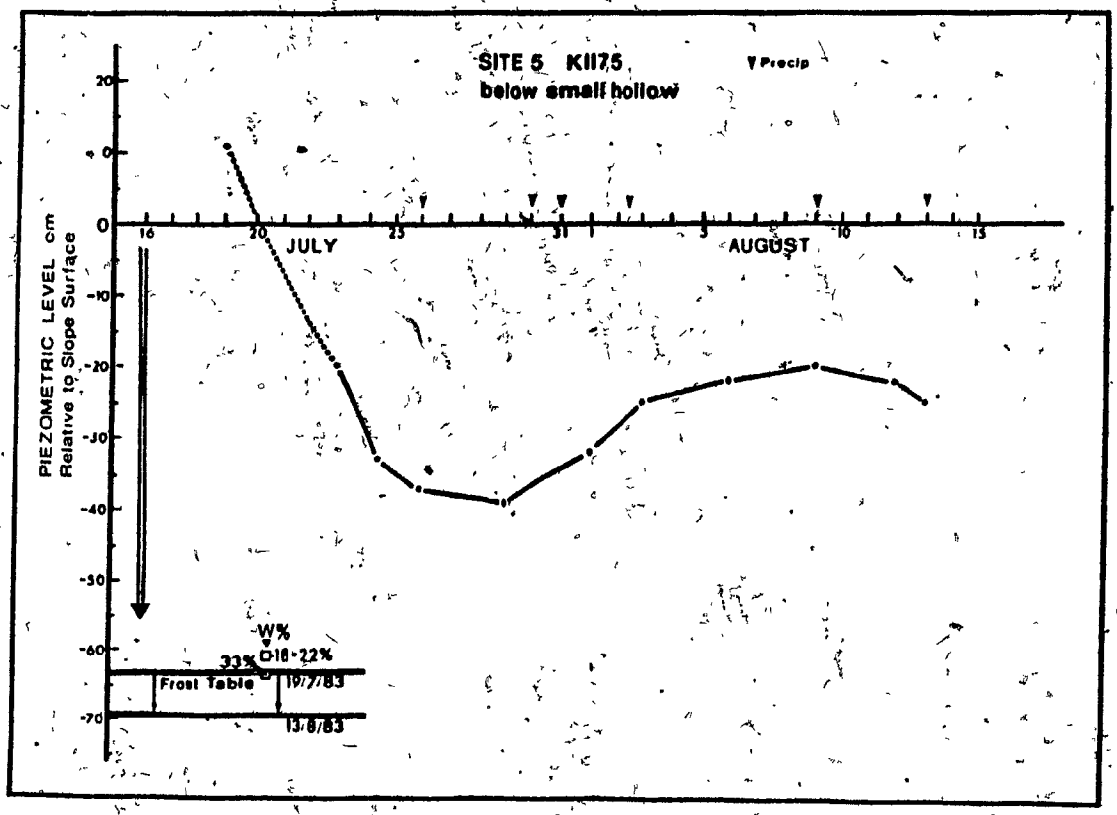
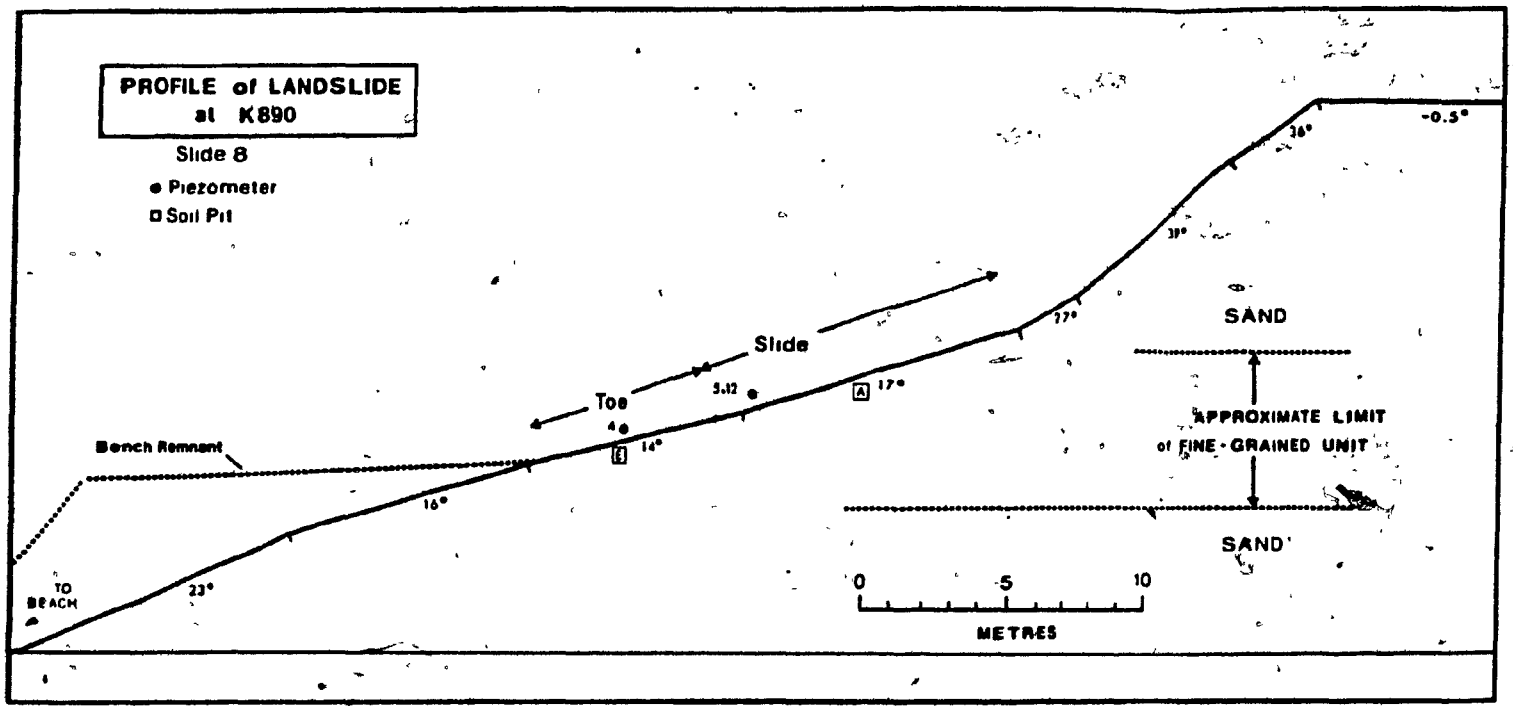
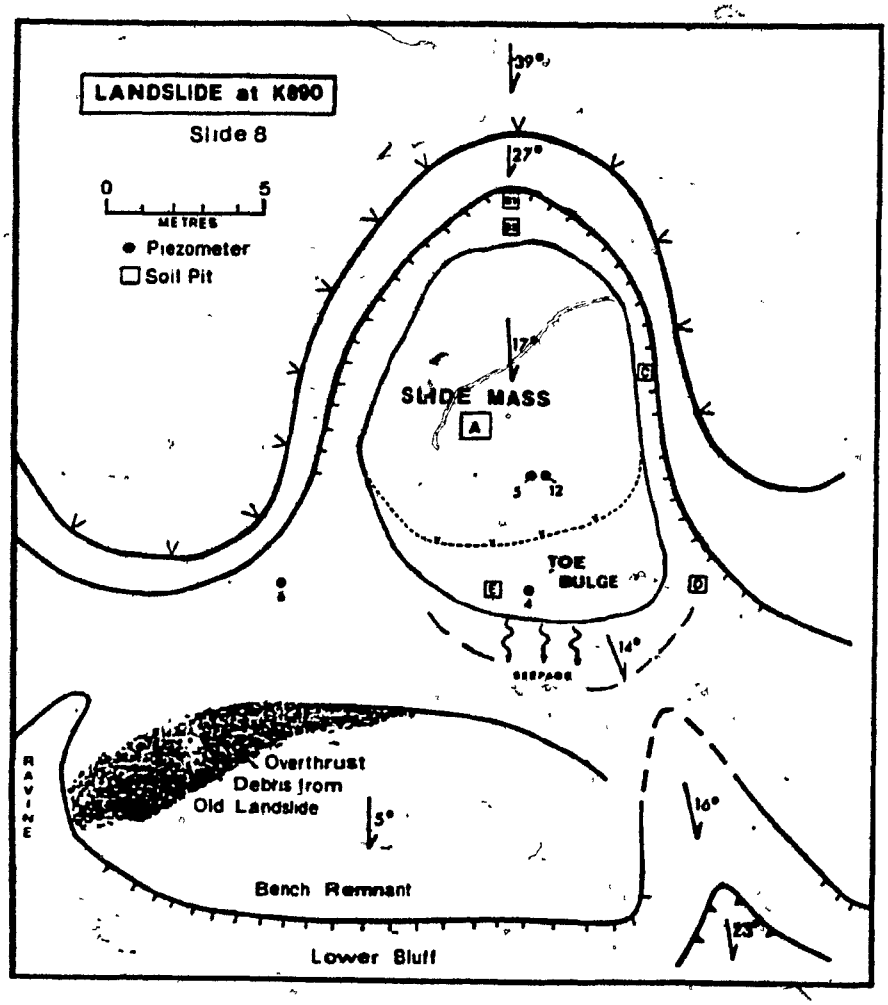


Figure VI. Piezometer data from sites along the mid-bluff bench. Frost table depth and local water content data are also given. Moisture content at or below frost table is from frozen soil.

Figure VI.12





SOIL PIT DATA (M%)

PIT A
0-37 cm sand (12%)
37-52 cm silty sand (20%)
52-57 cm brown loam (22%)
57-60 cm grey clayey silt (26%)
Frost table (60 cm; 49%)

PIT B1
0-37 cm cos-med sand
37-46 cm silty sand (26%)
(top of F-ged unit?)
Frost table (46 cm; 25%)

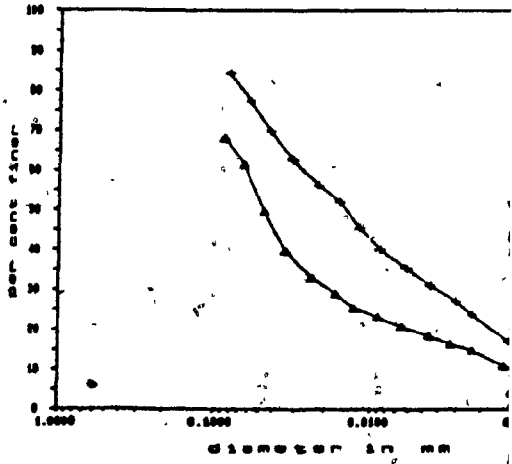
PIT B2
0-35 cm sandy debris at back-scarp, Frost table 35 cm.

PIT C
0-50 cm sand
50-70 cm sil
70-78 cm gre
Frost table

PIT D
Grey clayey
frost table
Frost table

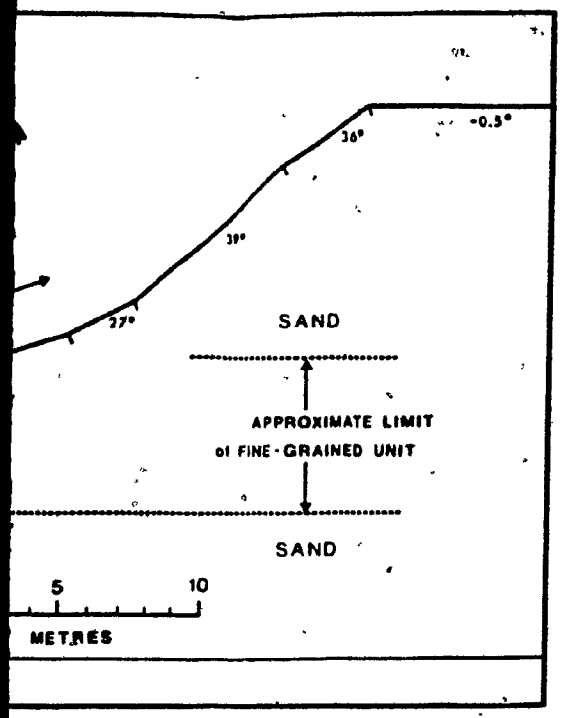
PIT E
0-40 cm sand
40-57 cm loa
Frost table

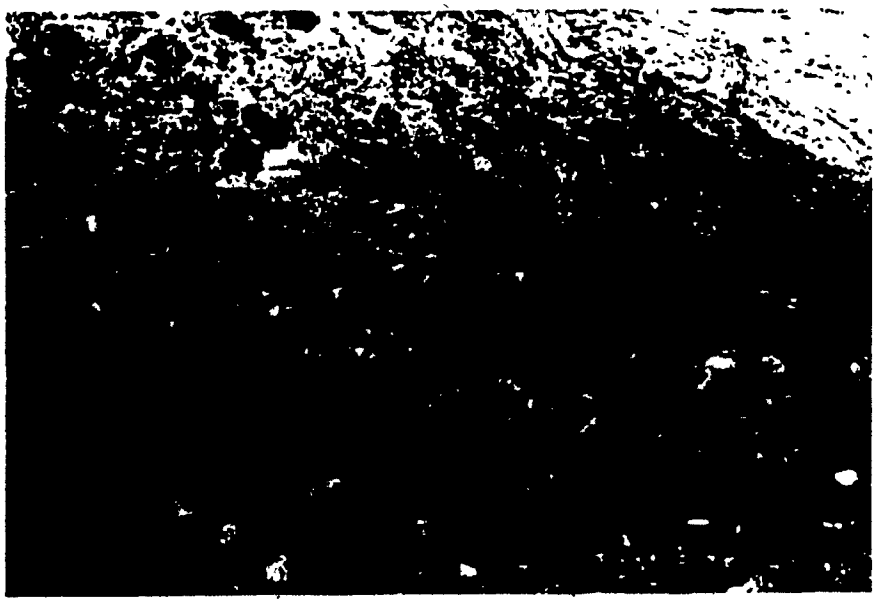
GRAIN SIZE



Soil grain-size from Slide 8, K89

Silty sand (loam) from base of pi
Clayey silt from base of pit A (Δ)





A

Slide 8 observed less than two days after its occurrence. The 2-3 m wide gap at the back of the slide mass shows the limited displacement.

OIL PIT DATA (W%)

IT A
-37 cm sand (12%)
7-52 cm silty sand (20%)
2-57 cm brown loam (22%)
7-60 cm grey clayey silt (26%)
rost table (60 cm; 49%)

IT B1
-37 cm cos-med sand
7-46 cm silty sand (26%)
(top of F-ged unit?)
rost table (46 cm; 25%)

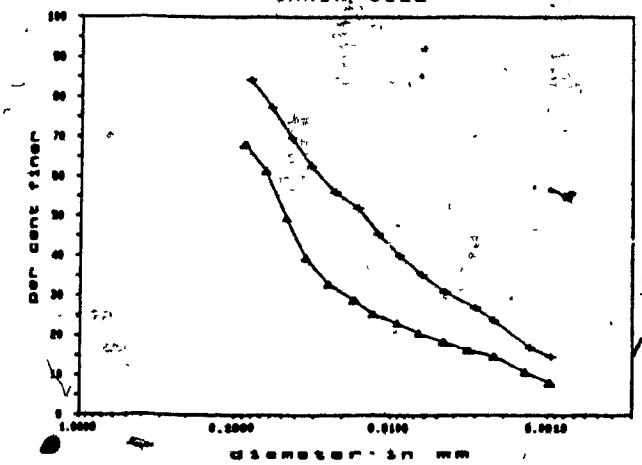
IT B2
-35 cm sandy debris at back-
carp, Frost table 35 cm

PIT C
0-50 cm sand
50-70 cm silty sand
70-78 cm grey clayey silt (25%)
Frost table (78 cm; 66%)

PIT D
Grey clayey silt just above
frost table (34%)
Frost table (ca 75 cm; 71%)

PIT E
0-40 cm sand (11-15%)
40-57 cm loam (20-23%)
Frost table (57 cm; 4[illegible])

GRAIN SIZE



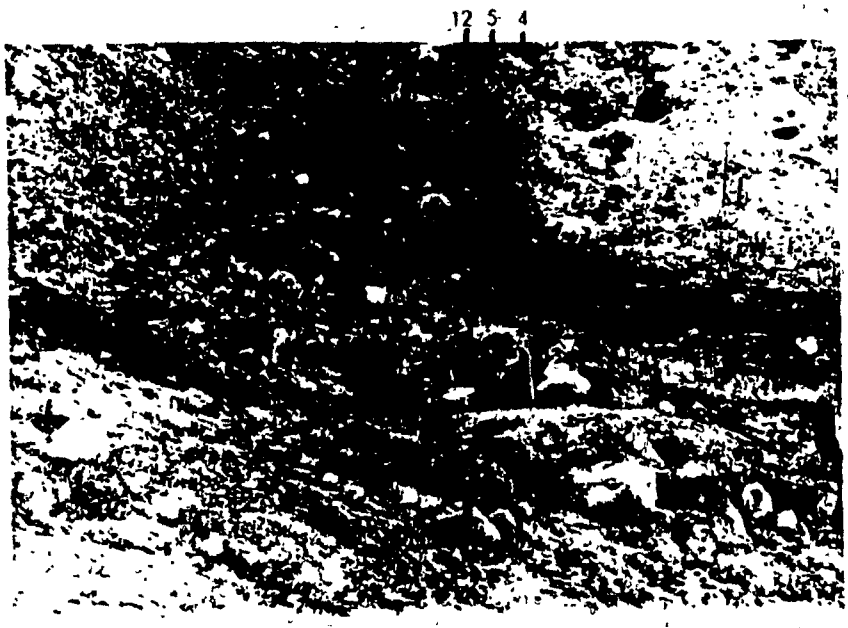
Soil grain-size from Slide 8, K890

Silty sand (loam) from base of pit B1 (+)
Clayey silt from base of pit A (Δ)

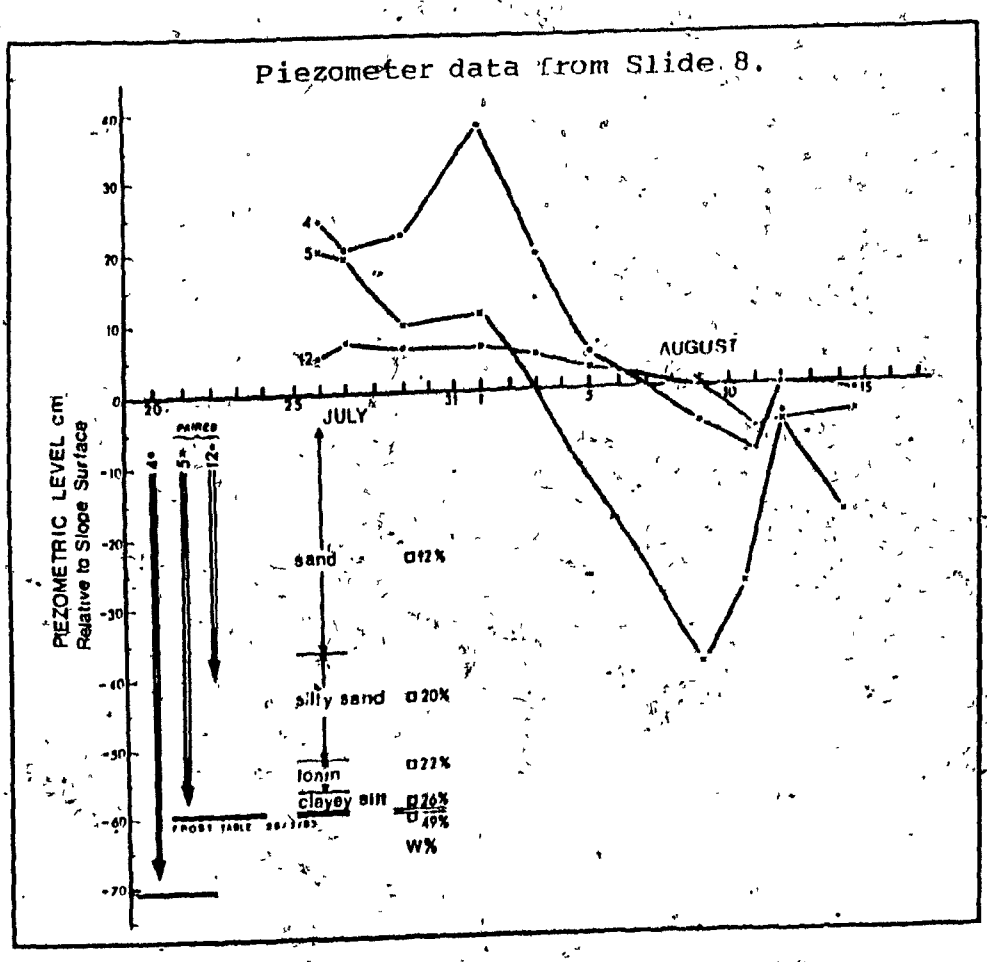


C

Lower portion of soil pit A. The end of the measuring tape lies on the frost table (60 cm). The structure of the clayey silt at the bottom of the soil pit is a loose aggregate of soil peds, often coated with a thin layer of softened mud. The soil water appeared to be clear, not muddy.



B View of Slide 8 looking upslope from bench remnant (see profile). The locations of piezometers 5 and 12, near the center of the landslide, and 4, at the toe, are indicated. Note the distinct bulging of the toe below piezometer 4. (1983)



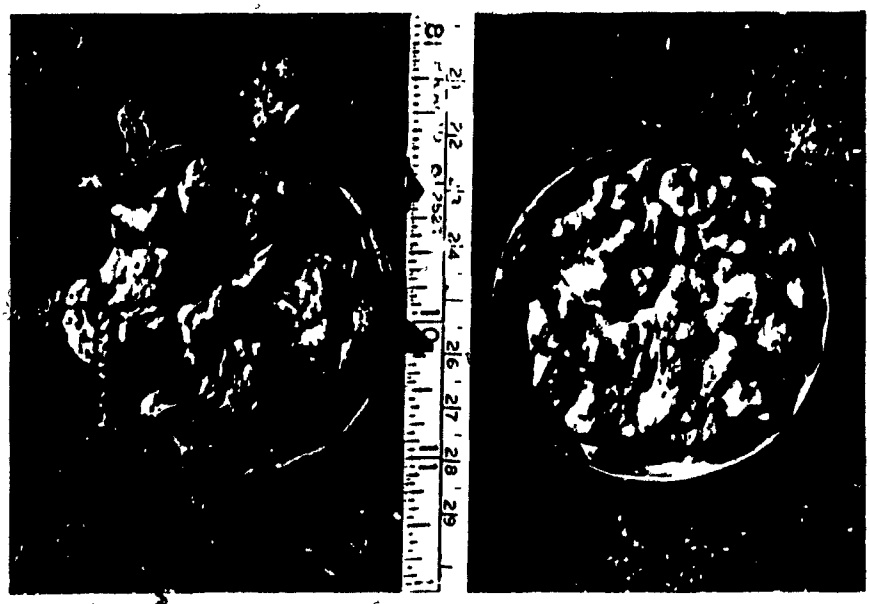


Figure VI.13 Thawed fine-grained soils from the Kivitoo bench. Ice content of these soils was ca 30%. Although these soils have been disturbed by sampling, when thawed they retain much of their cryogenic structure. Some softening of the soil on the outside of the peds has occurred, and the melt water in the sample to the right is slightly muddy. However, this is an artifact of the sampling, and in situ, such accelerated slaking of the peds is not seen.

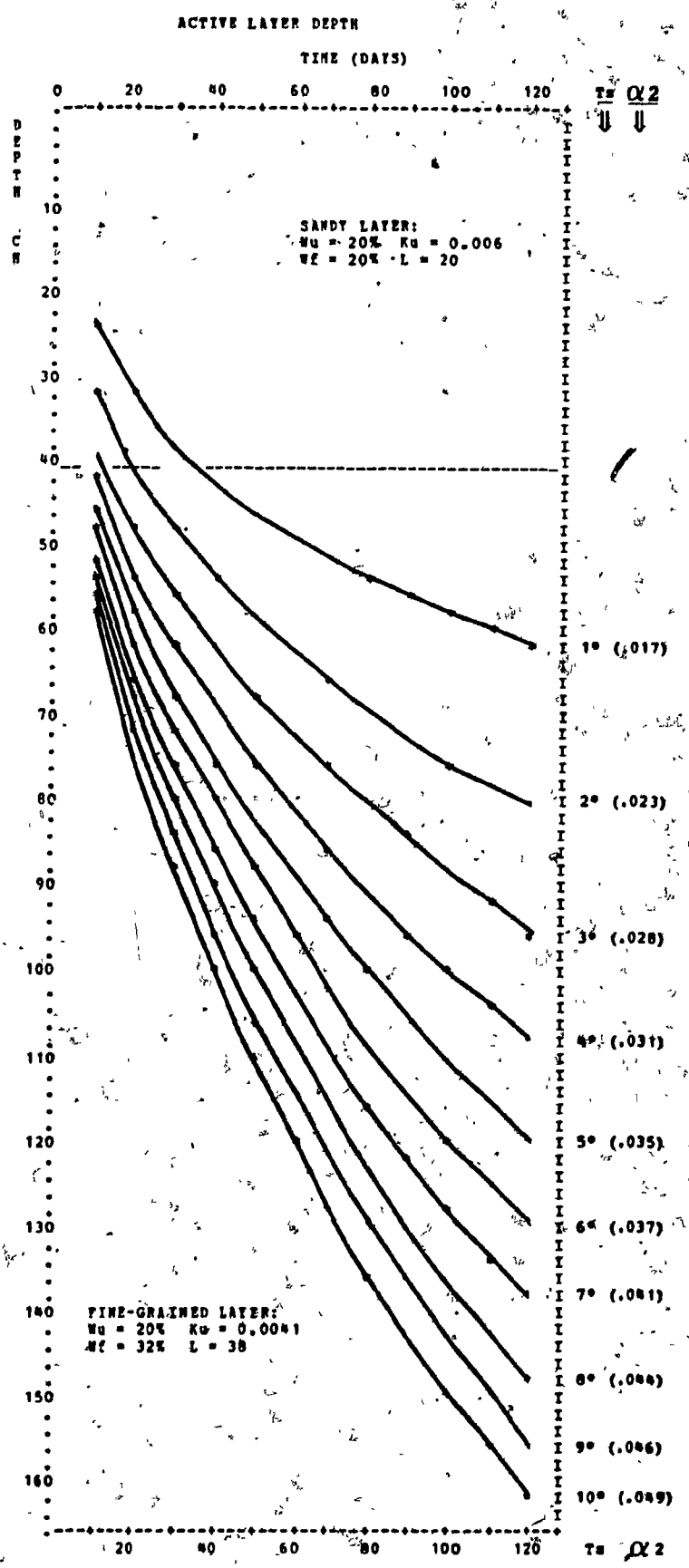


Figure VI.14 Graphic solution to the two-layer thawing problem for a representative active layer profile from the mid-bluff bench. Each curve gives the solution for a specific step temperature increase. The values of the thermal constant ($\alpha 2$) are for the fine-grained layer.

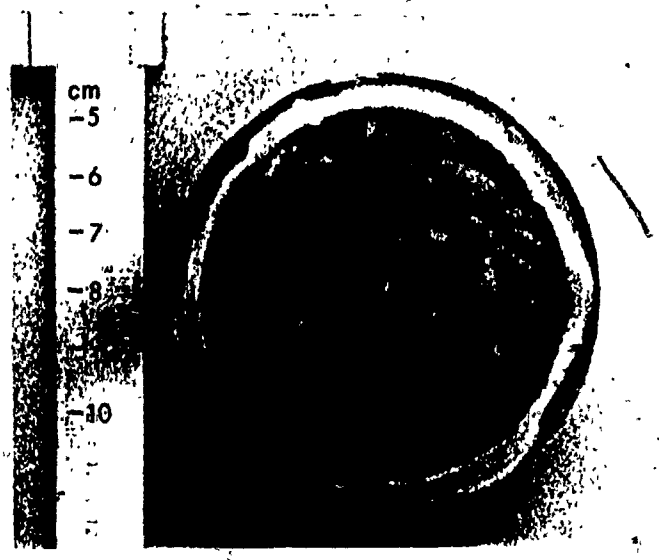


Figure VI.15 Frozen silty clay loam consolidation sample in 6.35 cm diameter ring. The cryogenic structure is ataxic, with ice veins oriented in several different directions. Only those veins oriented in a more or less vertical plane can be seen intersecting the top of the sample. The veins are less than one to two milimetres in thickness.

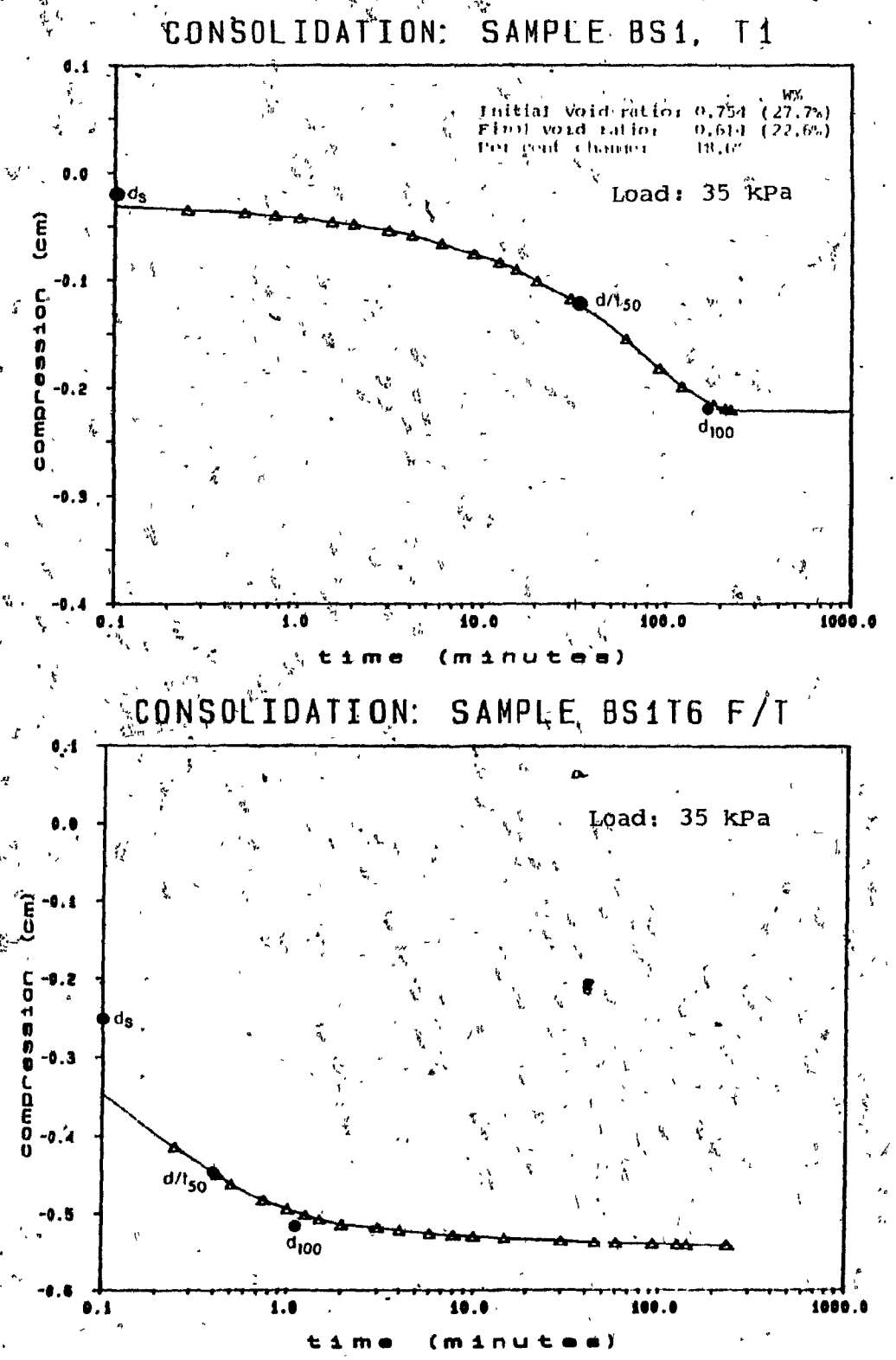
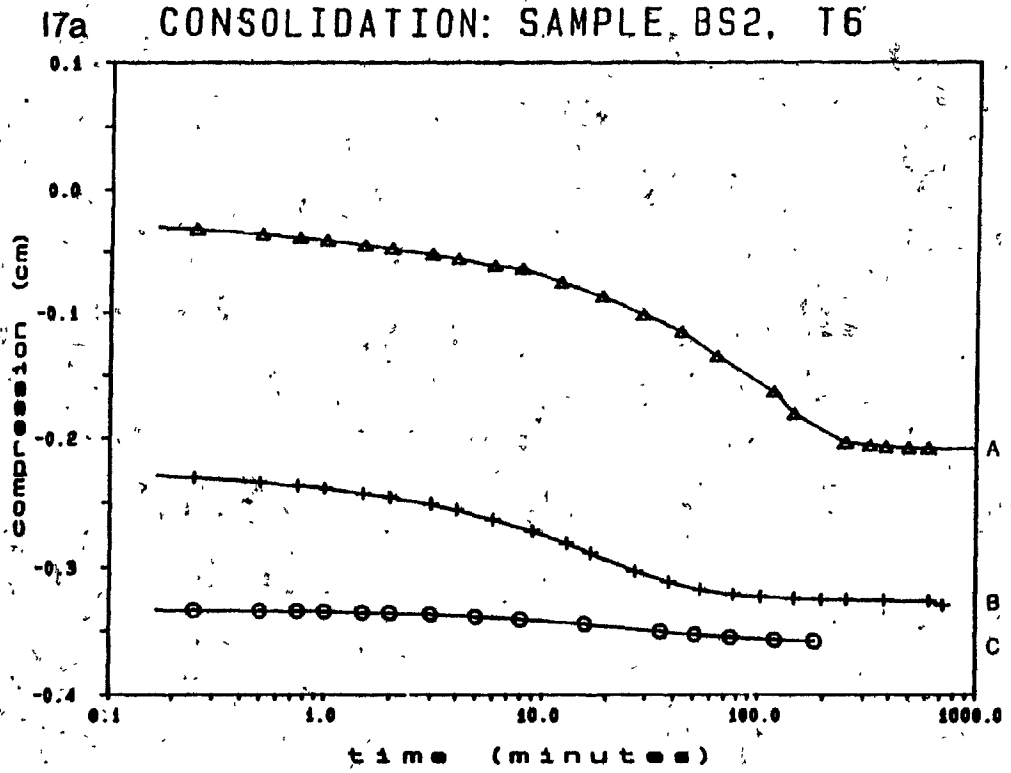


Figure VI.16 Typical consolidation test results for remolded (Curve A) and frozen/thawed (Curve B) silty clay from the Kivitoo bench. (Bulk sample 1, Slide 3; see Table VI.2) In the remolded sample 100% primary consolidation does not occur until after 100 minutes, while in the frozen/thawed sample 100% consolidation is complete by 11 minutes.



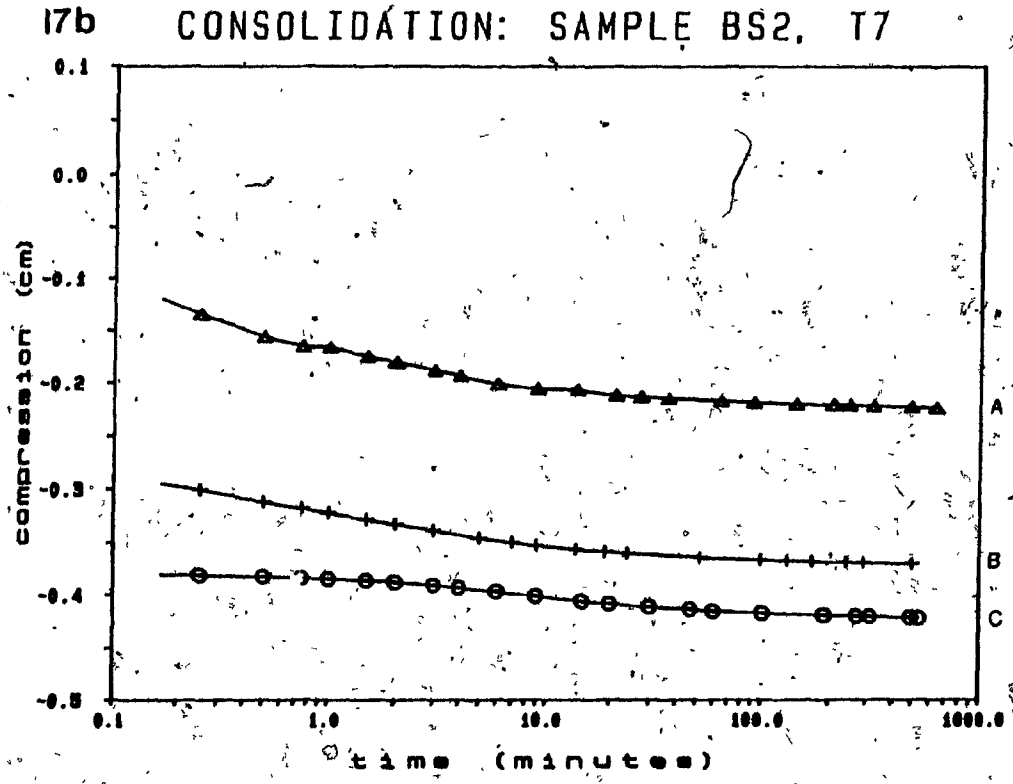


Figure VI.17 Stage-loaded consolidation tests on remolded (17a) and frozen/thawed (17b) silty clay loam. (Bulk sample 2, Slide 3; see Table VI.2). In these tests the sample was subject to three, progressively larger loads (9.8, 35, 70 kPa).

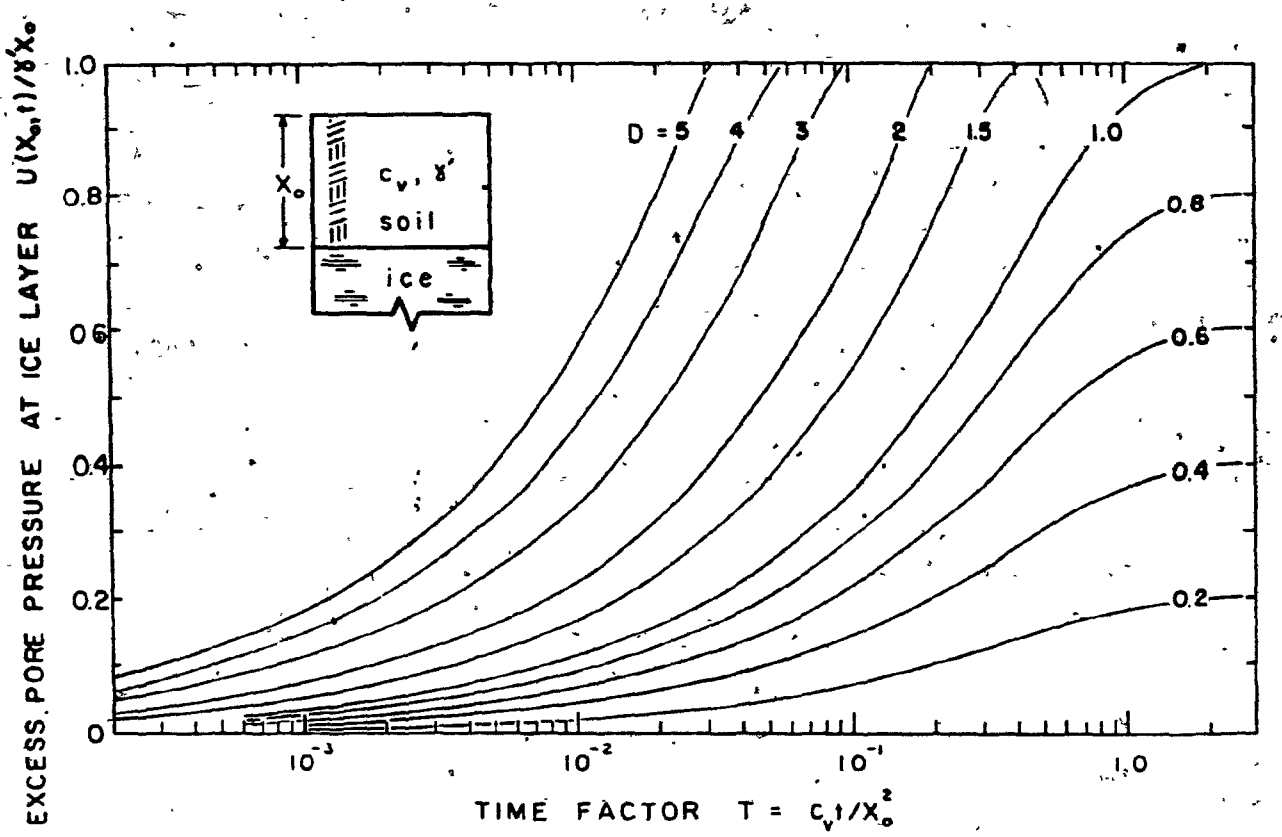


Figure VI.18 Graphic solution for determination of the magnitude of excess pore pressures at a soil/ice interface. The initial excess pore pressure gradient (B) is taken to be zero. See text for discussion. (From Nixon 1973)

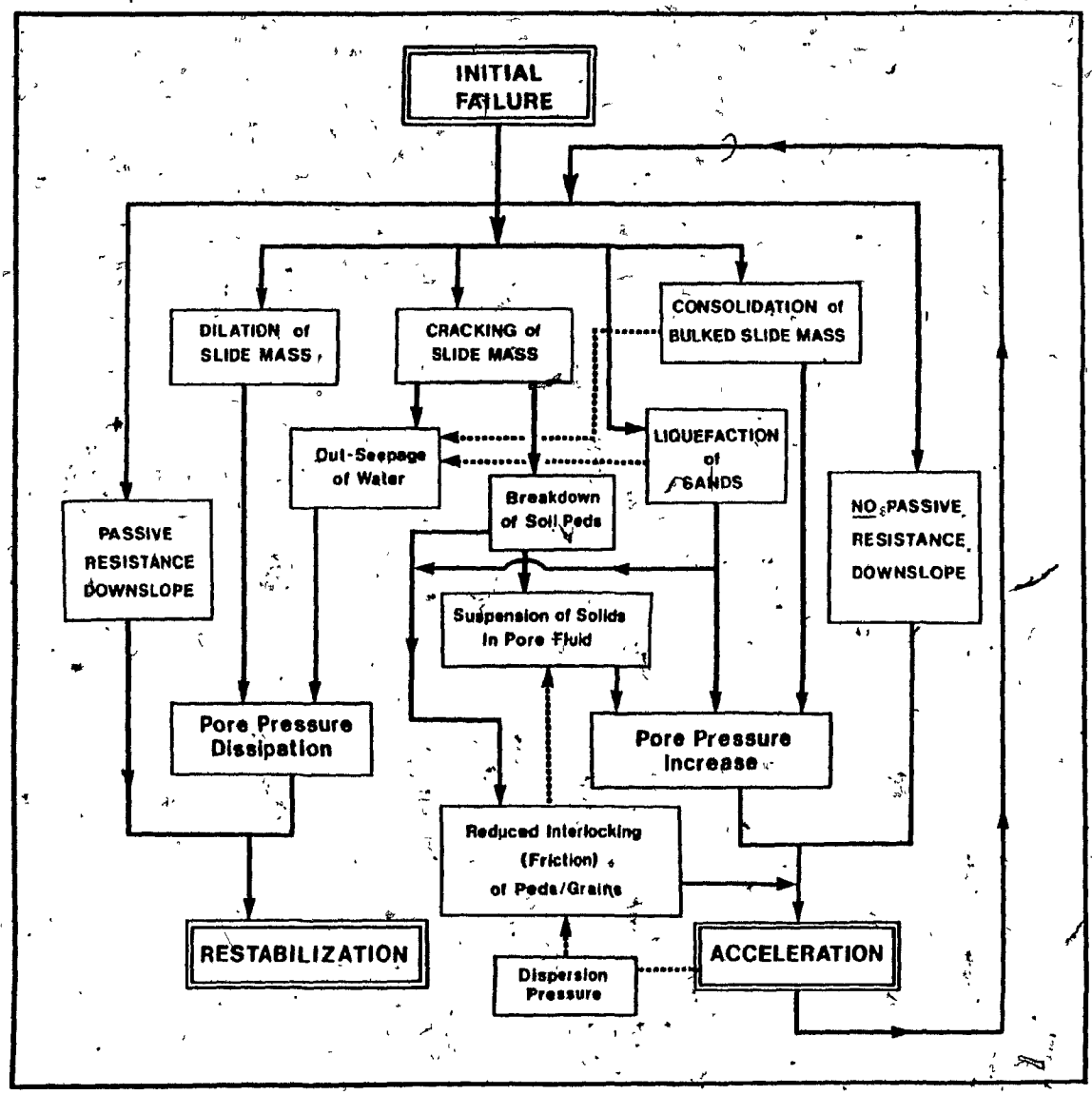
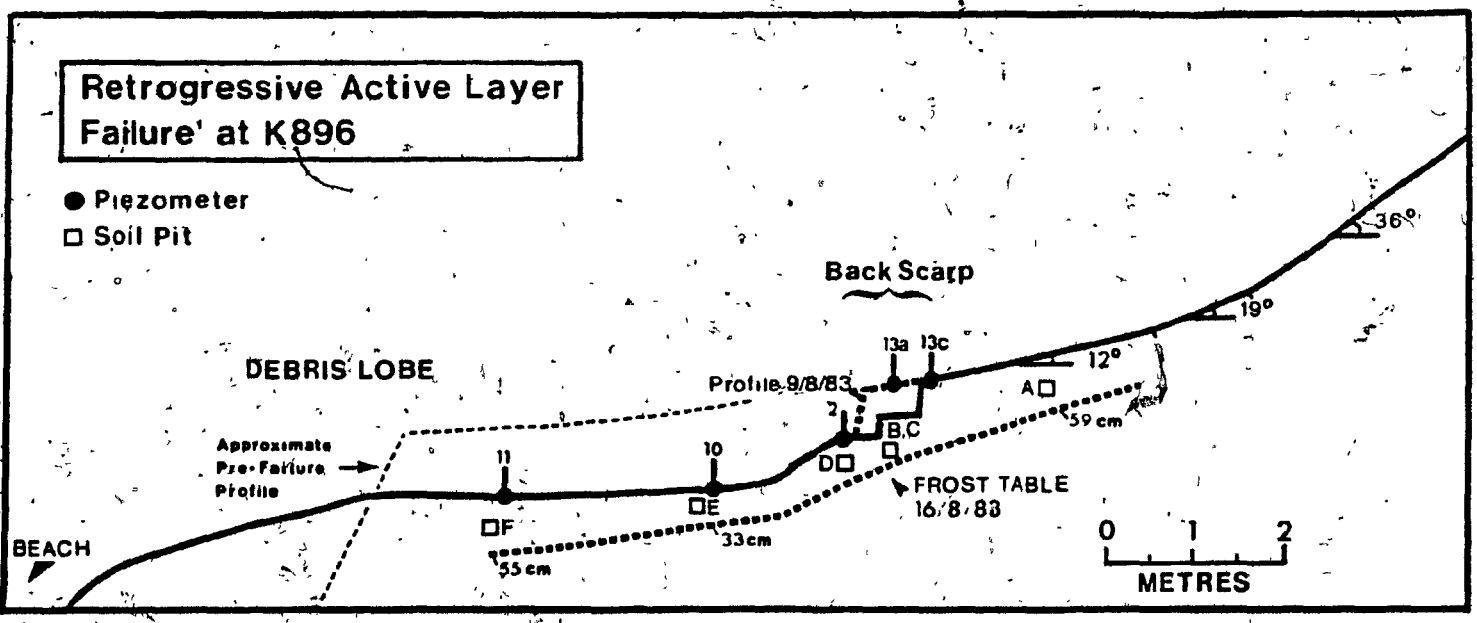


Figure VI.19 Diagramatic presentation of the possible post-failure transformations of a soil mass undergoing shear.

Figure VI.20





SOIL PIT DATA (WK)

PIT A
0-28 cm sand
28-59 cm silty clay
(Thawed soil just above frost table; 23%)
Frost table (59 cm; 40%)

PIT B
0-28 cm sand and silty sand
28-45 cm sandy loam (22%)
45-65 cm silty clay
(Thawed soil just above frost table; 23%)
Frost table (65 cm; 78%)

PIT C
0-24 cm silty sand
24-34 cm stiff brown silty clay (23%)
34-48 cm softer brown silty clay (24%)
48-55 cm grayish silty clay
(Thawed soil just above frost table; 26%)
Frost table (55 cm; 86%)

PIT D
0-43 cm debris (18%)
48-49 cm greyish silty c
(22%)
Frost table (49 cm; 84%)

PIT E
0-31 cm debris
31-33 cm greyish silty c
(19%)
Frost table (33 cm; 57%

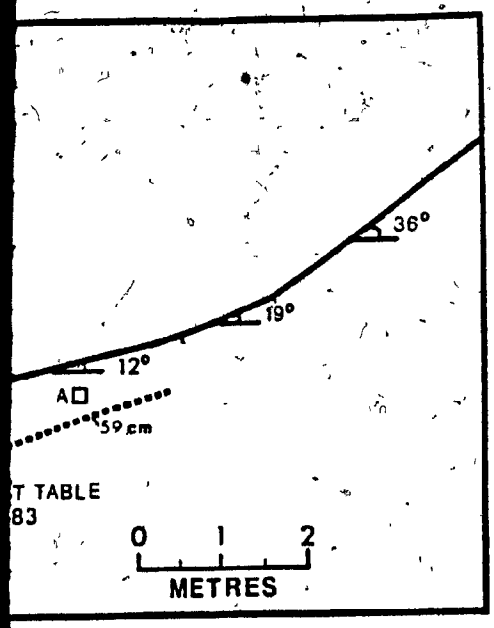
PIT F
0-ca 53 cm debris (14-1
ca 53-55 cm greyish sil
Frost table (55 cm; 53%)

B ▲

Back scarp of the retrogressive failure at K890, August 9, 1983. Piezometers 13a at backscarp and 11 in debris lobe. Note the many small tension cracks in the sandy colluvium in the foreground. This soil is more susceptible to flowage following minor disturbance than the more poorly-sorted colluvium behind the main portion of the failure. Thus retrogression of failure here is more rapid, however, lacking sufficient fine-grained soil to sustain prolonged debris flowage, the total amount of movement after failure is not as great. Piezometer 13b was located in this foreground zone of failure.

C ➤

View of backscarp of retr
failure on August 10, 198
spalling and retrogressio
urred since the previous
(B) was taken. Compare t
of the backscarp in relat
Piezometer 13a. Piezomet
debris lobe, has been til
as spalling has led to re
ment in the debris. Note
subsidence of the spalled
and their incorporation i
debris lobe.





A ▲

Retrogressive active layer failure at base of bluffs at K89O, August 9, 1983. View is upslope from beach. Piezometers 13a, at backscarp, and 11, in centre of debris lobe are indicated. Profile goes across lobe and up small nose behind backscarp. The failure is bracketed by two small ravines. Note also the more limited break-up of the sandier soils along the right side of the failure.

L PIT DATA (W%)

T A
8 cm sand
-59 cm silty clay
Thawed soil just above
frost table; 23%)
ost table (59 cm; 40%)

T B
28 cm sand and silty
and
-45 cm sandy loam (22%)
-65 cm silty clay
Thawed soil just above
frost table; 23%)
ost table (65 cm; 78%)

T C
24 cm silty sand
-34 cm stiff brown silty
lay (23%)
-48 cm softer brown silty
lay (24%)
-55 cm grayish silty clay
Thawed soil just above
frost table; 26%)
ost table (55 cm; 86%)

PIT D
0-43 cm debris (18%)
48-49 cm greyish silty clay (22%)
Frost table (49 cm; 84%)

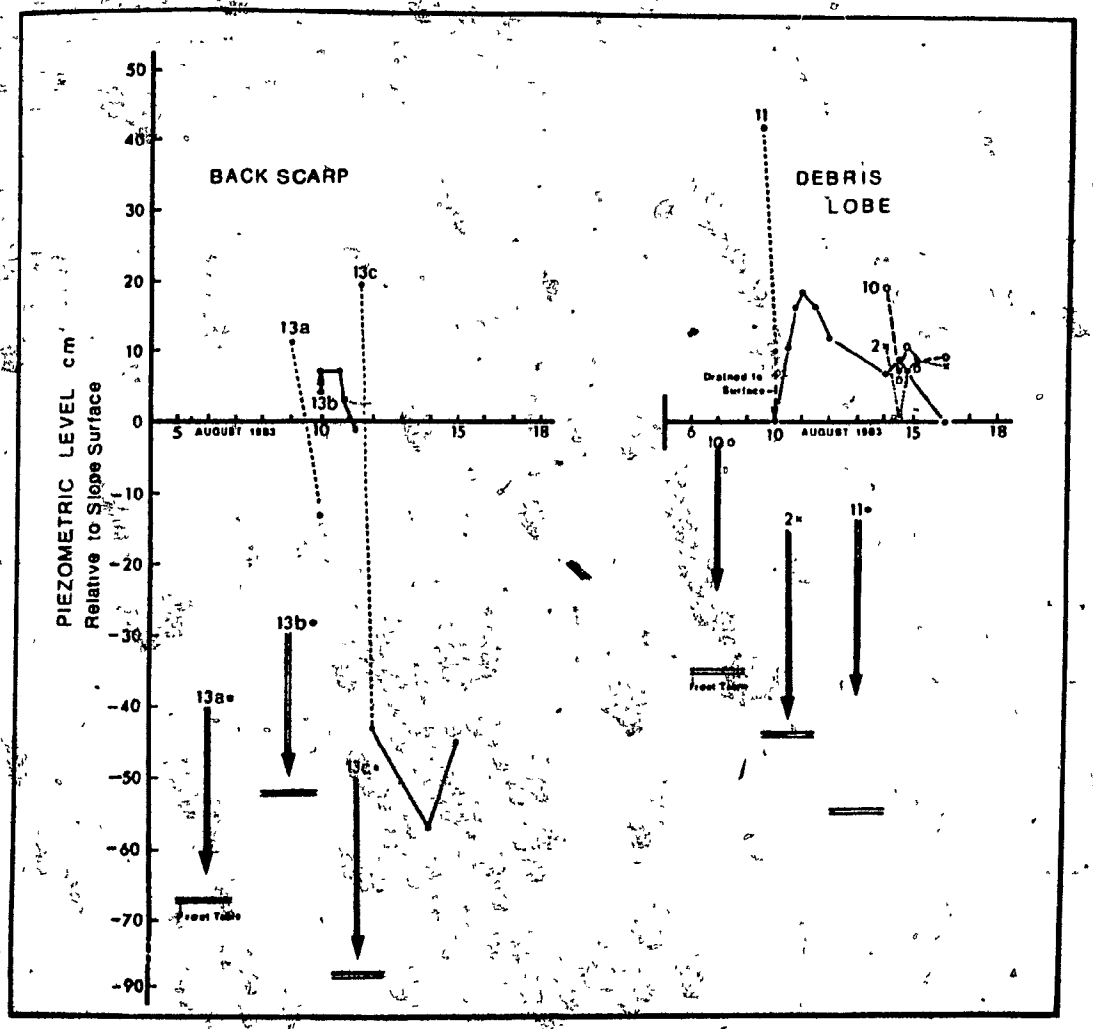
PIT E
0-31 cm debris
31-33 cm greyish silty clay (19%)
Frost table (33 cm; 57%)

PIT F
0-ca 53 cm debris (14-16%)
ca 53-55 cm greyish sity clay
Frost table (55 cm; 53%)



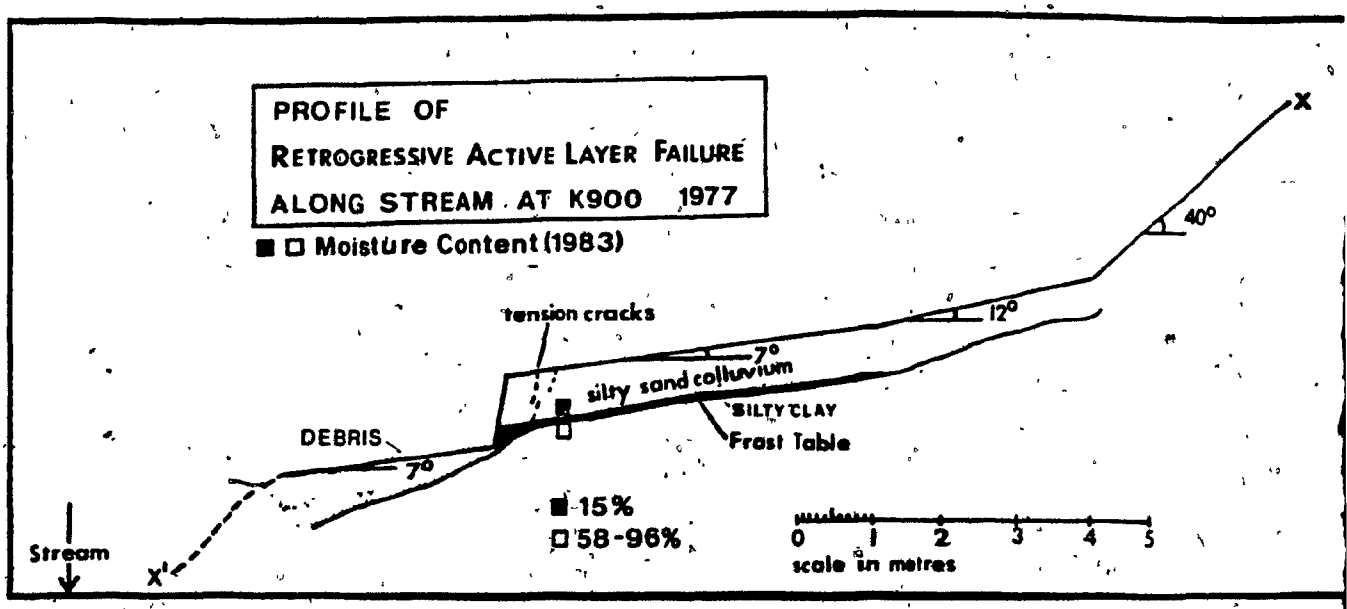
C ►

View of backscarp of retrogressive failure on August 10, 1983. New spalling and retrogression has occurred since the previous photograph (B) was taken. Compare the position of the backscarp in relation to Piezometer 13a. Piezometer 11, in debris lobe, has been tilted forward as spalling has led to renewed movement in the debris. Note also the subsidence of the spalled blocks and their incorporation into the debris lobe.

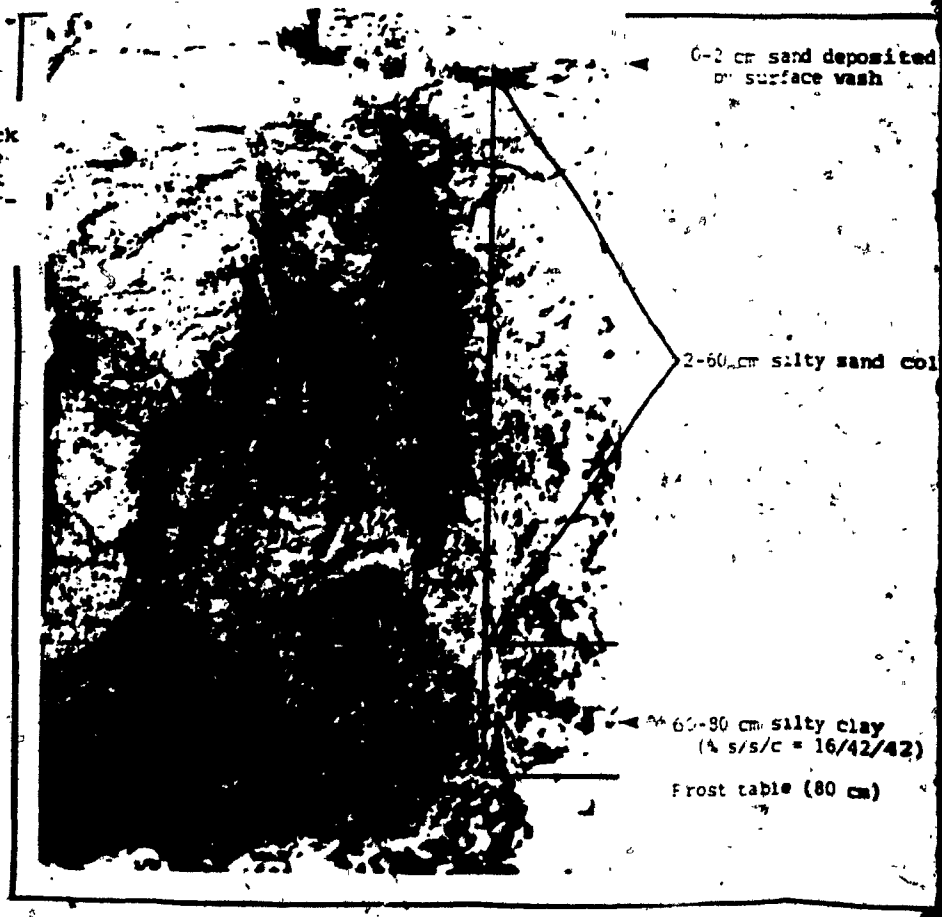


Piezometer data from the retrogressive active layer failure at the base of the bluffs at K890. The locations of the piezometers are indicated on the profile. Piezometer 13b was located at the backscarp of the failure zone to the right in photograph A, and in the foreground in photograph B.

Figure VI.21



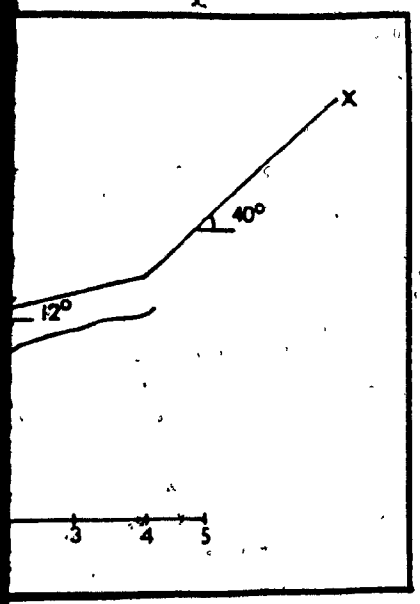
C ►
Excavation through spalling block at the back of the retrogressive active layer failure. The block is separated from the intact surface behind it by deep tension cracks.

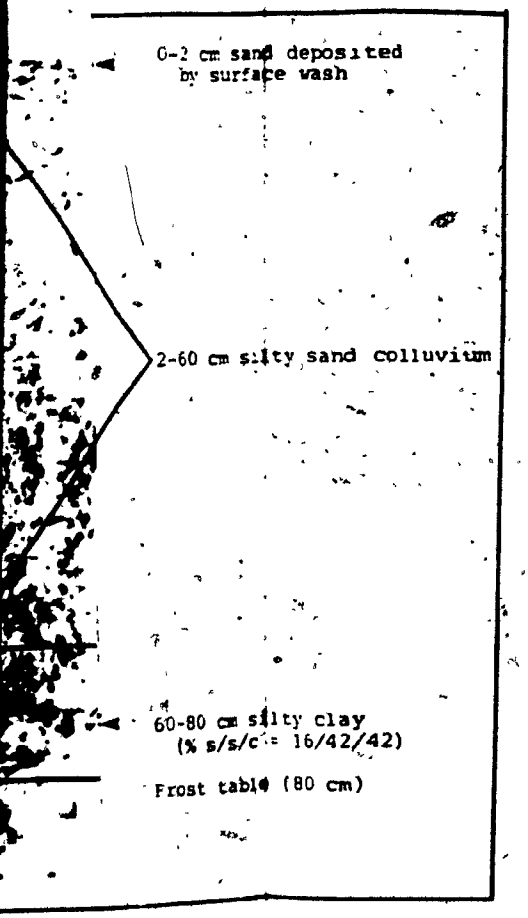




A▲

Retrogressive active layer failure along valley-side bench at small stream at K900, August 1977. The location of this feature is shown in Photograph B, below. Like the slope failure at the base of the bluff, this feature is seated in ice-rich fine-grained soil. At the time this photograph was taken the debris had begun to dry out. X marks site of excavation in Photograph C.







B▲

View inland along the small stream at K900. The active layer failure shown above is seen at A. Above the failure is a small bench (C) mantled by a veneer of sand which has been deposited by slope wash. The bench has developed at the level of a fine-grained unit, from which the soil in which the failure is seated has been derived. The stream has undercone a recent episode of rapid downward incision. This has left the old stream bed, covered by a coarse lag deposit, several metres above the present channel on the side of the valley opposite the active layer failure (B).



Figure VI.22 Arrested retrogressive active layer failure at the edge of the tongue slope of the debris-bowl at K660 (B-2). The soil profile for this failure was similar to those for both of the failures in the vicinity of the stream at K900, and described in the previous figures. However, here significant remolding and flowage of the soil did not occur, resulting in the development of a zone of tensile failure but little displacement.



Figure VI.23 Soil ripples at bottom of bench back slope. These minor features are thought to be caused by compressive gelifluction flow in sandy materials at the base of steep slopes. Such ripples were ubiquitous along the back of the mid-bluff bench.

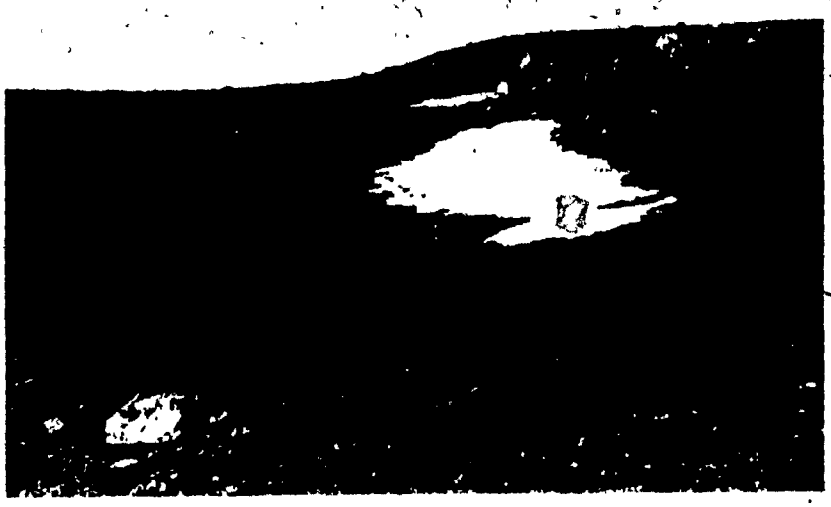


Figure VI.24 Solifluction slope site along stream valley at K1145. (See also Figure VIII.9 for location.) The snow pack lasted until late July in 1983. The slope surface downslope of the snow pack is comprised of a poorly-sorted sand. (July 16, 1983)

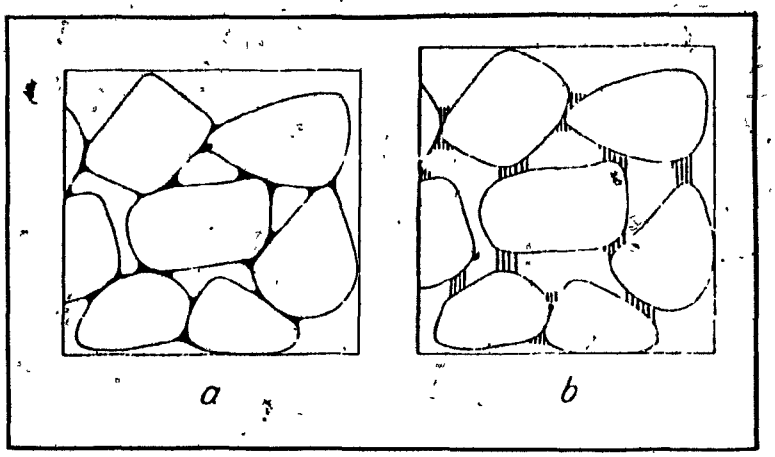


Figure VI.25 Growth of ice at inter-grain contacts in an unsaturated sand (as proposed by Beskow 1935). (a) shows sand prior to freezing, (b) after freezing. This is a possible cause of volume expansion upon freezing of unsaturated sandy soils on solifluction slopes. These soils, when frozen, were loosely ice-bound but did not contain visible ice lenses. (From Williams 1967.)

CHAPTER VII:
MORPHOLOGY AND DEVELOPMENT OF THE BLUFFS WITH DEBRIS-BOWLS

A. Introduction.

The bluffs with debris-bowls constitute the third morphological division of the Kivitoo bluffs. This bluff type extends from K650 to K900 and, like the steep dissected bluffs, includes a range of spatially related features with sufficient genetic and morphological similarities to form an internally coherent grouping. Again the division is identified by its most characteristic and fully expressed features but in reality comprises a continuum of gradational forms. When best developed, as along the section of bluffs shown in Figure VII.1 (as well as between K650 and K735), debris-bowls have steep side and back slopes and gentle tongue slopes, the latter often formed entirely of colluvial debris. Adjacent features are separated one from the other by residual 'ribs'. The well expressed bowl forms grade into features with steeper tongue slopes and less differentiation between the tongue and back slope. In the extreme case the tongue and back slope may merge into a single straighter slope graded to the terrace surface, all but eliminating the characteristic bowl-type profile. These latter slopes are similar in both form and materials to the taluvial lag slopes described in Chapter V.

The development of undercut coast-parallel scarp slopes is limited along the stretch of coast from K650 to K900 due to the lateral expansion of bowl hollows and frequent stream and gully

dissection. Where present, planar slopes are characteristically highly rilled and have (due to the presence of fine-grained sediment from units high in the bluff) a surficial dessication 'crust'. These scarp slopes are notably different from the scarp slopes to the south which have faceted profiles and generally unrilled surfaces.

The development of debris-bowls and their variant forms is again primarily a function of bluff stratigraphy -- which differs significantly from that to the southeast -- and, to a lesser extent, of terrace hydrology. Transitional features tending towards a bowl-like morphology occur along both the steep dissected bluffs and the debris-mantled bluffs. These bowl-like features develop in locations where the stratigraphy has similarities to that found along the section of the coast under consideration here. However, as these bowl-like forms are isolated or poorly-developed along the bluff south of K650, they do not compromize the integrity of the morphological division proposed here, but rather point to the difficulties inherent in ascribing a meaningful morphological framework to a continuum of landscape features. The presence of bowl-like forms along other sections of the coastline also serves to emphasize the fact that gradational rather than ideal forms are typical of morphogenetically complex landscapes.

B. Stratigraphy

The stratigraphy along the bluffs with debris-bowls, which includes Nelson's sections 18-20 (K668) to 12-40 (K875) (Fig.

VII.2), is quite different from that to the southeast due to the presence of thick layers of fine-grained sediments. As shown by Section 18-20, the southeastern extent of the bluffs with debris-bowls coincides with the appearance of a 6 m thick marine clay unit (facies D2: % sand/silt/clay = 45/38/16) near the base of the bluff. Relatively thick fine-grained units (facies D,W and E) are present in all bluff sections northwest of 18-20 (with the notable exception of section 13-10). The facies E2 units found near the top of most sections are the source unit for the fine-grained fraction reponsible for the development of the surface crust on many of the steep bluff slopes.

Sections of debris-mantled bluffs immediately to the southeast of section 18-20 (e.g. section 20-43), may also have thick fine-grained units (although these units tend to contain less clay and more sand than the fine-grained units to the north.) The morphological significance of the fine-grained units in the bluffs to the southeast is mitigated by the thick coarse-grained beach cap (for reasons discussed in Chapter IV). For the most part, the bluffs with debris-bowls lack such thick coarse-grained cap units or where such units do occur, they are thin relative to the height of the bluffs and/or overlain by other, finer-grained units.

C. Terrace conditions along the bluffs with debris bowls

The terrace along the bluffs with debris-bowls has variable surface conditions ranging from dry and sandy to

vegetated with hummocks and substantial overland flow. Much of the run-off, which may last until late in the summer, takes the form of unchannelized surface flow. The bluffs here are also crossed by a number of older stream valleys. Since most of the bluffs along which debris-bowls are developed are lower than the limit of the Late Foxe transgression (i.e. less than 15 m asl), coarse sand and gravel cappings are found along the bluff edge, particularly south of K745. However, extensive development of surface channels and surface wash appears to have removed much of these raised beach deposits and/or increased the percentage of finer material within them, particularly inland of the bluff edge. At the present time, many of the surface channels, such as the one shown in Figure VII.3, carry little run-off and are being actively cut back at the bluff by coastal retreat. Some of the debris-bowls have developed on the bluff slope between these partially abandoned drainage lines, the old channels remaining as rocky buttresses on the face of the bluff.

Between K750 and ca K800 the terrace surface is relatively steep (> 3°) and carries a substantial amount of surface run-off. In 1983, run-off at this location persisted throughout the field season, while in 1977 it lasted until late in July. This particular portion of the terrace is similar in appearence to the steeper wet terrace surface along the dissected bluffs between K150 and K195 and is also associated with the development of bluff slopes graded from the base of the bluff to the knick-line and mantled by coarse lag deposits (taluvium).

Northwest of K830 the bluffs increase in height and the raised beach facies which caps the lower bluffs is not found. The terrace surface along these higher bluffs is comprised of a brown (organic) loam, is well vegetated and remains quite wet throughout the thaw season. Low-angled active layer failure, seated in the loam is commmon along the bluff knick-line as are other active layer forms such as hummocks and silty frost boils. The relatively greater abundance of cryogenic forms is a result of the finer-grained soils and wetter surface conditions.

D. Debris-bowl morphology

1. General characteristics

Individual debris-bowls and bowl-like features range in width from 10 to 20 m and may be as wide as 40 m. Excluding the three exceptionally large 'perched' bowls southeast of the stream at K900, the long profile of the debris-bowls (measured as the horizontal distance from the seaward edge of the tongue to the crest of the back slope: Figure VII.4a) rarely exceeds 30 m.

The low length-to-width ratios and limited expression of coast-parallel scarp slopes between debris-bowls suggests that the Kivitoo features are more efficient at continued lateral expansion than they are at backwasting. Of course, this is due in part to the continual shortening of the longitudial profile by marine erosion while the processes of lateral expansion

proceed unimpeded.

Two morphometric characteristics are responsible for the bowl-like form. One is the nature of the slope profile which consist of slope segments that increase in gradient upslope. A typical debris bowl profile, such as that in Figure VII.4b, is comprised of a steep back slope, a gentler tongue slope, and often a short transitional segment, or foot slope, between them. The second characteristic which helps differentiate the debris-bowl morphology from that of the debris-hoppers, is the path of sediment flow lines within the hollow. Rather than being convergent upon a central point or line (Figure VII.4A), once sediment leaves the back slope of a bowl, the paths are quasi-parallel and, at the edge of the tongue slope, orthogonal to the beach.

Most of the better developed debris-bowls are shallow, being wider than they are long. Sustained landward retrogression does not appear to be characteristic of the Kivitoo bowls. This is in direct contrast to the marked retreat of the backscarps of other 'bowl-shaped' features developed in permafrost described in the literature. Examples of such forms include the bimodal flows described by McRoberts (1973) and the mudflows of Kerfoot (1969). These features, which display retrogression of up to several hundred metres, have length-to-width ratios greater than one, and develop in ice-rich (fine-grained) permafrost which is exposed to thaw in the retrogressing back slope. They also have very active debris tongues comprised of waste shed from the back slope. In comparison, the Kivitoo debris-bowls show comparatively limited

expression, are not backed by slopes in which thawing soils are exposed, nor do they have an active debris tongue which is being fed by continuous sloughing of wet mud from the back slope. Unlike the rapidly developing mass-wasting features such as McRobert's bimodal flows, the Kivitoo debris-bowls are more truly landforms, developing as they do over a period of time by the interaction of a number of different morphogenetic processes.

The morphology of a well developed debris-bowl, the feature at K660 (profile B-2), is described in detail below. Figure VII.5 reproduces profiles of this debris-bowl and shows the relationship between the profile and the local stratigraphy. Also included in Figure VII.5 are a schematic plan, soil pit and water content data and photographic views.

The back slope of this particular debris-bowl stands at 34° and is blanketed by coarse sand and gravel derived from a beach facies (A2) at the top of the bluff. This coarse veneer thins downslope, so that the active layer in the lower portion of the back slope consists mostly of sand derived from the facies B and C units lower down in the section. The surcharge mantle derived from the coarse-grained beach cap, along with the limited run-off intercepted at the bluff edge, provides the primary morphological control on the back slope in a manner similar to that of the debris-mantled bluffs (as discussed in Chapter IV). The coarse-grained unit is not, however, thick enough to stabilize the fine-grained unit at the base of the bluff and inhibit bowl formation. Along the northwest side of

the debris-bowl, lateral expansion is limited by the banks of an adjacent gully -- a situation which occurs elsewhere along this bluff section. The side slopes of this debris-bowl are considerably steeper than the back slope, being in places inclined at more than 45°. A large slope failure, visible in Figure VII.5B, has occurred along the steep northwest side of the bowl. The failed soil was transformed into a debris flow, moving out over the bowl tongue.

Between the tongue and back slope is a short foot slope segment inclined at 23°. Pronounced seepage was encountered along this segment in both 1977 and 1983. Small scarplets, 10-20 cm tall, are actively backwasting onto this slope (see for example Figures VII.5A and VII.6). In most of the debris-bowls, the foot slope is a single, steeper segment inclined at 19-25°.

The tongue slope of the feature at K660 is inclined at 9-11°. While this slope and the tongue slopes of other debris-bowls are quite gentle, there is, in fact, a wide range of slope gradients to be found along the portions of the bluff profile which constitutes the tongue slope. In some cases the 'tongue' may be quite steep (> 20°) but still gentler than the slope either above or below it and therefore maintaining a poorly developed bowl-type profile. Thus, in poorly-developed debris-bowls, the tongue slope may consist only of a short less-steeply inclined segment which interrupts a generally steeper profile. It is significant, for reasons explained below, that these breaks in profile generally coincide with specific stratigraphic units and are therefore

morphogenetically similar to the better developed tongue slopes.

Excavation of the active layer along the tongue of the debris-bowl in Figure VII.5, revealed colluvial debris ranging in texture from silty sand and clayey silty sand to poorly-sorted debris with a high admixture of larger clasts. Only in the lower portion of the tongue was the in situ fine-grained sediment exposed at the base of the active layer. Significantly, this was also the site of the retrogresive failure described in the previous chapter and shown in Figure VI.22. The silty sand found at the base of the back slope (Figure VII.5; Pit 2a) may also be in situ sediment from a stratigraphic unit lying just above the basal fine-grained unit. Seepage, apparently flowing between the frost table and an overlying, less permeable and more poorly-sorted colluvium, was entering into the sample pit on the foot slope, a situation which may result in the development of a confined aquifer.

Along profile B-2, frost table depth increased from 56 cm at the base of the back slope to 73 cm, one metre from the edge of the tongue. The active layer therefore lies almost entirely within colluvium. This was also true along profiles B-1, B-3 and B-4. In none of these locations was the fine-grained unit, in which the debris-bowl is seated, encountered above the frost table. Overlying the colluvial debris along many of the tongue slopes is a variable thickness (up to 20 cm) of well-sorted fine to medium sand which has ben deposited by anastomosing rills and sheet flow arising as seepage along the back slope foot.

Many of the debris-bowls, particularly those where the stratigraphic section contains a larger amount of fine sand and silty sand and thin finer-grained units, have tongue slopes which are formed as a sequence of interbedded colluvial debris and well-sorted alluvial sand deposits. These tongue slopes are found at the base of the bluff and are (at least partly) depositional in origin rather than being formed by mass wasting processes at the level of thick fine-grained units.

Retrogressive failure commonly occurs along the seaward edge of the tongue slope. Such failure takes the form of minor sloughing and flowage of wet debris and is often accompanied by minor rilling along the steepened seaward edge of the tongue slope. Retrogressive instability along the edge of the tongue slope at B-4 (K670) is shown in Figure VII.7. Here, instability is limited in extent (the zone of disturbance is less than 5 m wide) and involves only colluvial sandy silt. The more extensive retrogressive failure, described in the previous chapter was a unique occurrence. Other signs of discrete mass instability seated entirely within the tongue slope, such as tension cracks at the back of instability features, en-echelon tension cracks along shear zones or compression ridges were not found. Neither were distinct failure surfaces or shear zones found in any of the excavations on the tongue. This fact does not preclude such failure since shear or flow zones would probably not be preserved except where obvious textural differences occur on either side of the failure zone. Furthermore, if a substantial thickness of the active layer is subject to flowage or gelifluction, distinct

shear surfaces would not be formed. (A more extensive discussion of debris movement along tongue slopes is undertaken later in this chapter.)

2. Debris-bowl profiles and their relationship to bluff stratigraphy

The longitudinal profiles of 20 debris-bowls and bowl-like features are reproduced in Figure VII.8. The locations of the profiles are marked on the panorama, starting at K656, as B-1 to B-20. While the variation between individual profiles is readily apparent, most of the profiles consist of a relatively steep back slope, (usually greater than 34°), a gentler basal tongue slope of less than 20° and often, a short transitional segment (the foot slope) located between the tongue and back slope and inclined at 19-25°. This sequence of increasing slope segment angle gives the debris-bowl profile an overall concave appearance. Some segment curvature due to wash processes or sloughing may develop at the back of the bowls or where gentler mid-profile slopes merge into steeper basal ones. However, detailed profiling led to the conclusion that the individual slope units along these short profiles are best represented as straight segments.

The detailed stratigraphic section shown alongside the debris-bowl profile in Figure VII.5 indicates that the tongue slope in B-2 is developed within the fine-grained units at the base of the bluff. The back of the tongue slope generally coincides with the top of these units, although this contact

may be obscured by the development of a colluvial foot slope at the back slope base. Examination of the upper contact zone in the well-developed features, B-1 and B-4, also showed that this contact was in the vicinity of the back of the tongue and rarely extended far up the back slope.

Comparison of the bowl profiles (Figure VII.8) with the local stratigraphy (Figure VII.1) again shows the correspondence of fine-grained (Facies D and W) sediments and tongue slopes or gentler breaks in profile. This is particularly evident in the vicinity of Section 16-9 (K729) where the fine-grained sediments and the slope flattening occur in mid-bluff positions.

Some of the features along this section of the bluffs, such as those at K730 (B-13), K844, K849 and K861 have tongue slopes not at the base of the bluff, but higher up in the profile. These 'perched' bowls are associated with thick fine-grained units occupying a mid-bluff position. The relationship between the fine-grained unit and the floor of the debris-bowl is seen in Figure VII.9, which shows the feature at K730. Some of the perched bowls may develop at the top of unusually thick fine-grained units, such as the 10-12 m thick unit which forms the bottom portion of the stratigraphic section between K840 and K865 (Section 13-10). These perched bowls clearly demonstrate that the local profile flattening is not, in most cases, due simply to the development of a basal colluvial tongue, but is intrinsically related to the specific occurrence of thick fine-grained units within a particular bluff section. Tiered profile arrangements are also found.

These may show agreement with two fine-grained units; alternatively, the lower of the tongue slope segments, occurring at the base of the bluff, can simply be a colluvial lobe. In the case of these basal colluvial lobes, the tongue is not clearly associated with development along a particular fine-grained unit and is, as noted below, the product of failure along the upper bluff. Such failure may shed debris which can remain mobile on lower gradient slopes and can therefore build up a gentle colluvial tongue at the slope base.

E. Debris-bowl Development

In order for debris-bowls to form, the upper portion of the slope must retreat, leaving at its base a gentler tongue slope along which the debris can be evacuated to the beach. Debris-bowl development is therefore a function of (1) the rate at which failure along the back and side slopes effects retreat of these slopes, (2) the rapidity with which this debris is removed from the hollow, and (3) the rate of trimming of the tongue and bluff base by marine erosion. The tongue slope is not, in most cases an accumulation area, but rather it is a transportation slope. If debris from failure along the back slope cannot be removed, eventually the backslope itself would be eliminated and replaced by a somewhat lower-angled slope comprised of this debris (the classical slope "replacement" model: Carson and Kirkby, 1972, p.379). Moreover, the tongue slope itself may also assume an active role in maintaining retreat of the bowl's back and side slopes as failure along the

tongue extends to, and thereby undercuts the back slope at its base. Undercutting would then initiate an episode of retrogressive stripping along the back slope. The relative efficacy of these processes of failure and debris removal is dependent upon the rate of basal recession of the bluff, for if the bluff base is retreating more rapidly than these slope processes can operate, debris-bowls will not form. The appearance of the debris-bowl is enhanced if high, steep residual ribs can be maintained between individual features.

1. Initiation of the bowl form

Owing to the limited period of observation and the fact that few clear instances of incipient bowl formation could be found, the mechanisms involved in the initiation of the bowl form are not well understood. The elaboration of a mechanism of bowl formation is complicated by the fact that the active layer soils derived from the fine-grained units along which the debris-bowls develop may possess very different properties on steep dry slopes (where they are characteristically hard and strong, and may be highly cracked imparting a large macro-conductivity) compared to gentler slopes or in hollows.

Development of a debris-bowl is assumed to begin with a steep planar undercut slope (such as that shown in Figure VII.10a). Initial localized failure along the bluff slope profile, presumably associated with high local pore pressures there, would be favored by oversteepening and retreat of the superadjacent slope. Such locally high pore pressures stem

from slope-parallel seepage in the thawed surface layer, the source of water being either drainage from the terrace or the thawing of ground ice in the bluff sediments. The latter source of seepage would be favored in ice-rich fine-grained sediments, the elevation of which then controls the seat of failure within the incipient hollow.

High pore pressures associated with thaw-consolidation of these finer sediments would, at first sight, seem to be an obvious mechanism for preferential failure of fine-grained segments along the bluff profile. However, high pore pressures might also be expected at or just below the level of the fine-grained units because of the lower hydraulic conductivity of these soils compared to the coarser-grained soils upslope.

When slope-parallel seepage in an active layer of constant thickness and gradient encounters soils with reduced conductivity, the rate of seepage movement through the lower slope must be reduced resulting in a thickening of the phreatic zone and effluent flow (seepage out of the ground surface) in the vicinity of the contact. Such an upward component of seepage at that locality would be induced by local artesian pressures at the base of the active layer.

Repeated occurrence of high pore pressures and slope failure would eventually lead to the development of a gentler slope segment emerging along the silt/clay unit reflecting this local pore pressure regime (Figure VII.10B). "Undercutting" of the base of the overlying sand unit by the localized failure in the silt/clay unit would produce retreat of the upper (sand) slope. Provided that sandy colluvium from the upper unit

doesn't accumulate on the new "bench" in sufficient quantity to prevent thaw of the in-situ fine-grained sediment, or function as a surcharge, the process of failure, regrading, and retreat should continue reinforcing the new hollow.

The change in slope geometry from a single straight slope to a lower gradient slope backed by a steeper slope unit will accelerate developmet by changing the hydrology of the slope. If the hydraulic conductivity of the active layer along both slope segments is the same, the gentler slope, in accordance with Darcy's Law, will not be able to discharge the same quantity of water downslope through a saturated active layer of the same thickness as would the steeper (sandy) slope unit. Thus effluent seepage must occur at the break of slope reflecting increased pore pressures at the base of the active layer there. (The argument is analogous to that based on reduced permeability in the silt/clay unit just discussed.) The exact form of the flow net along these slopes is not known, but it is obvious that some upward gradient must exist in the vicinity of the contact between the two slope segments. The situation is shown schematically in Figure VII.11. Thus the new slope geometry, by causing a 'back-up' of subsurface flow at the break in slope, produces localized artesian pressures there. This has the hydrologic effect of inducing effluent seepage, and the geomorphological effect of lowering the critical (threshold) angle for instability at that point.

A change in slope geometry can therefore cause a corresponding change in slope hydrology, the effect of which, if linked with efficient transport processes, may aid in the

perpetuation of the slope form.

While several of the debris-bowls (e.g. B-7, B-10, B-11 and B-12) are clearly associated with fissures or other surface drainage lines, many are not so obviously linked to terrace hydrology. In fact, some of the largest and best developed features (e.g. B-1, B-2 and B-4) are bracketed by gullies or streams into which run-off from the terrace is channeled. A few features are also capped by raised beach deposits, the surface of which may slope away from the bluff edge. Thus soil moisture derived from sources on the bluff face alone, independent of hydrologic conditions on the terrace, appears to be adequate for debris-bowl initiation and development. Initially, this moisture source may be ground-ice or precipitation. Once the hollow has formed, accumulation of snow may provide a significant moisture imput, as it clearly does in several of the debris-bowls.

2. Soil movement along the tongue slope

Since features tending towards a bowl-like form develop along sections of the bluff in which the stratigraphy includes a significant amount of fine-grained sediment, but lacks thick fine-grained units, such units do not seem to be a necessary prerequisite of debris-bowl development. In such cases, colluvium derived from facies C and thin facies D units is capable of continued movement on gentle slopes, and can therefore form low-gradient tongue slopes. In these instances the tongue slope always develops at the base of the bluff where

the debris accumulates.

Debris-bowls are best developed, however, with the gentlest and longest tongue slopes, where thick, clayey fine-grained units are present (e.g. in the vicinity of Sections 18-12, 17-33 and 12-40). The elevation of the tongue slope (or local flattening of profile) is then clearly associated with these fine-grained units. In the case of perched bowls, the tongue slope cannot be explained merely by the accumulation of mobile debris.

The mechanisms which are responsible for the evacuation of debris from the bowl along the tongue slope may be placed into three groups: (a) soil mass movements initiated along tongue slopes, (b) continued movement of debris derived from failure along the back and side slopes, and (c) soil movement related to seepage and slope wash (mass transport) phenomena. These modes of debris movement are discussed below.

a. Stability of the debris-bowl tongue slopes

Examination of the debris-bowl profiles in Figure VII.8 and the bar graph in Figure VII.12 shows that tongue slopes may stand at angles of as low as 9°, with most inclined at 12-16°. Direct shear box tests on a specimen of the clay loam taken from just above the frost table (ca. 90 cm depth) along profile B-2 gave a ϕ' value of 34°. Such ϕ' values are to be expected for clayey glacial sediments (for reasons discussed in Chapter V). Since the specimen was predominantly fine-grained and had a high clay-sized fraction (% sand/silt/clay =

22/40/38) compared to most of the soils found within the tongue, it is reasonable to assume that ϕ' values for the more poorly-sorted colluvium are probably greater than 34°. Substitution of this internal friction value into Eq. III.13, gives a limiting semi-frictional slope angle of 18-19°. This is sufficient account for shallow infinite slope-type failue on the steeper tongue slopes. Yet, larger landslides involving a substantial thickness of the active layer, such as the failure on a 17° slope described in the previous chapter, were not encountered along any of the debris-bowl tongue slopes. There is, on the steeper slopes, ubiqitous shallow sloughing, rarely more than 20 cm in thickness. As noted in Chapter VI, such thin soil movements are more likely to conform to the infinite slope stability assumptions than are the thicker active layer movements.

As infinite slope models with 'normal' pore pressure conditions cannot account for debris movement on the gentler tongue slopes, it is necessary to consider alternative modes of debris mobilization. (Since much of the colluvium is poorly-sorted and has a high admixture of larger clasts, bulk unit weights in many cases are probably not much less than 20 kN/m^3. Thus an explanation of the gentle angles as being a function of low bulk unit weights cannot be applied in all cases, though for some of the steeper tongue slopes comprised of better-sorted silt and sand and with relatively high ice contents, this may be a contributing factor.) Moreover, no low-angle active layer landslides, similar to those found along the bench slopes are described in the previous chapter, were

observed. One reason for this may be the considerable thickness of colluvium along most of the tongue slopes so that the in-situ fine-grained soil was rarely exposed to thawing, except near the edge of the tongue. It is possible that such failure does occur, but only infrequently and in response to stripping of colluvium which reexposes this sediment to ice bulking and subsequent thaw.

Gelifluction-type movements may be a mechanism for the displacement of the better-sorted low-plasticity surficial soils along tongue slopes. A frozen silty sand beneath a snow patch at the back of B-4 had a moisture content of 25%, while that of the thawed, reconsolidated soil was 9-11%. The flow limit of these soils was low (> 15%) indicatng that they may be quite mobile on low gradient slopes immediately following thaw.

Examination of the tongue along profile B-2 during the last week in June, 1983, showed the active layer in the vicinity of Pit 3 (Figure VII.5) to be very weak, so that the soil would readily yield under a person's weight, becoming fluid as he sank in. However, piezometers installed at this location recorded no excess pore pressures indicating that the soil, though loose, was stable. The soil's sensitivity was made evident when disturbance around one of the piezometers caused a temporary rise of the water column to 5 cm above the slope surface indicating the development of transient artesian pore pressures. These observations suggest that the lobes are only marginally stable when saturated early in the thaw season. Retrogressive failure initiated at the undercut base of the tongue slope during this time may therefore result in rapid and

extensive active layer stripping. This process was observed at the steep seaward edge of almost all the tongue slopes. However, in most cases, such failure was very limited in extent, grading into minor shallow sloughing on these short, steep slopes. With the exception of the arrested failure seen in Figure VI.22, extensive stripping such as that described in the previous chapter was not observed in 1977 or 1983, although it probably does occur periodically. In most of the observed cases the effect of retrogressive processes at the tongue edge is limited to regrading of this short slope. Only when the in situ fine-grained unit is exposed to thawing would extensive retrogression and stripping seem to be possible.

An alternative mechanism of failure initiation along the tongue slope may be via debris shed from the back slope which results in an undrained loading of the tongue. This could lead to a rapid rise in pore pressure in the loose active layer soils and, consequently, slope failure.

b. The tongue as a transport slope for failure initiated on the debris-bowl walls

Retrogressive active layer failure seated at the top of the in situ fine-grained unit may be particularly active during the initial stages of bowl development. At a later stage, thick accumulation of debris along the tongue slope by 'burying' the fine-grained sediments in the permafrost will suppress such movements. Mass wasting mechanisms seated entirely within the colluvium will then predominate. As these

processes may be slow, a period of slope steepening due to the accumulation of debris from back slope failure may ensue. Undercutting by wave action could reexpose the (basal) fine-grained unit to thaw initiating a period of rapid tongue slope development by retrogressive active-layer failure.

Much of the debris shed by failure along the back and side slopes of the debris-bowls is capable of continued movement over the tongue slope as it is readily transformed into a debris-flow. Of all the mass-movement processes, this sustained downslope displacement of remolded landslide debris may be the one by which most of the waste produced by back slope retreat reaches the beach.

c. Soil movement by seepage and slope wash

Stripping of sandy colluvial and alluvial deposits by sheet wash and seepage erosion appears to be a significant agent of denudation along tongue slopes. The tiny seepage steps (Hadley and Rolfe, 1955) shown in Figure VII.7 are features, indicitive of these processes, and are found in most of the Kivitoo debris-bowls. These micro-scarps (which are typically 10-20 cm tall) migrate upslope by basal sapping and failure, coupled with downslope transport by liquefation flow and sheet wash. This process may be capable of fully stripping a thickness of soil from the tongue slope. Seepage steps are best developed in sandy alluvial/colluvial deposits underlain by less permeable soils (e.g. the dense poorly-sorted debris

flow deposits). The processes of sheet wash and seepage erosion may also be important in reexposing the in-situ fine-grained unit to seasonal thaw by reducing the thickness of overlying colluvium which in turn, could initiate a new cycle of active mass wasting along the tongue slope.

3. Retreat of the debris-bowl back slope

Once the incipient debris-bowl has formed, continued retreat of the back slope appears to be caused by a combination of spring line sapping and failure at the back slope base due to the localized occurrence of high pore pressures. Seepage at the back slope foot was observed in nearly all debris-bowls and accounts for the surface flow, alluvial sand deposits, and rilling along tongue slopes. The source of seepage may be precipitation, melt from snow which has accumulated in the hollow, overland flow from the terrace, or, where this is intercepted by bracketing channels, meltwater from ice-rich sediment higher in the bluff. It is possible that pipes carry water to the debris-bowls, even where the terrace immediately behind the feature is dry. Yet no evidence for piping was found. Rill wash occurs along some of the back and side slopes, but considering the low precipitation, funneling of terrace run-off into bracketing gullies and streams, and the suspected intensity of mass wasting activity, rill erosion is probably not a primary mechanism of backwasting.

The role of spring sapping in slope development has not received much attention. Schumm (1956) suggested that, while

rill erosion is paramount, basal sapping accounts for some of the retreat of badland slopes and pediment formation. Jones (1978) and Dunne (1980) have discussed spring sapping, but only in relation to drainage net development. More recently, Hutchinson (1982) has pointed to seepage erosion as a mechanism of widespread significance in the back-wasting of steep slopes in bedded deposits where 'water-bearing sands' occur above a layer of lower hydraulic conductivity and erosivity.

A clear distinction must be made here between spring sapping and basal failure. Spring sapping is the undercuting of the slope base by seepage via the removal of discrete soil particles. On the other hand, basal failure is a mass movement resulting from the increased frequency of high pore pressures near the slope base compared to the rest of the profile. Slope failure then occurs in accordance with Eq.III.11 leading to slope regrading along this section of the profile.

Both spring sapping and basal failure are operative at the back of debris-bowls, although their relative importance is difficult to assess given the present observations. It is apparent that they are mutually interactive, and when coupled with debris removal along the tongue lead to retreat of the back slope. Oversteepening of the back slope base by failure along the tongue which extends upslope can also initiate back slope failure. However, in 1977 and 1983 no instability along the tongue slope was observed to have retrogressed as far as the back slope.

Examination of the profiles in Figure VII.8 shows that the back slope is able to remain at inclinations near or above

expected frictional threshold values (> 32°, as determined by Eq.III.11). This indicates that, along most debris-bowl back and side slopes positive pore pressure occurrence is infrequent, relative to the rate of basal undercutting and/or removal.

The mode of back slope retreat described above is very different from that in the bimodal flows studied by McRoberts (1973) and which the Kivitoo features resemble morphologically. Retreat in the bimodal flows is by an ablation mechanism, (as described in Chaptr VI). Both McRoberts (1973) and Kerfoot (1969) describe features, developed in low ice-content sandy sediment, where the active layer remains on the back slope until it 'reaches some critical thickness' at which point failure and stripping of the entire active layer occurs. The mechanics of such a failure were not discussed, but some (minor) cohesive component to regolith strength is implied. No similar late-season failures of the back slopes of the Kivitoo bowls were noted during the 1977 or 1983 field seasons. Exceptional precipitation events may lead to active layer stripping, but such rainfall events are probably infrequent relative to the actual rate of back slope retreat.

4. The foot slope

Limited regrading at the base of the back slope results in the formation of the foot slopes commonly encountered in this position. These slopes are most likely short semi-frictional segments comprised of colluvium derived from the back slope

and/or underlying units. A bar graph derived from the profiles, Figure VII.12, shows a range of 19-27°. Assuming ϕ' for such material is 35-45°, (Carson, 1977a; Statham, 1974) the lower slope segment gradients (19-23°) would seem to correspond to fully saturated 'semi-frictional conditions' for moderately well-sorted sandy colluvium which is the material of which these slopes are usually formed.

5. Inter-bowl ribs, debris-bowl side slopes and planar, coast-parallel slopes

Once a debris-bowl begins to develop, the side slopes will become desiccated since they are now in an unfavorable position to receive seepage from the terrace. The surficial crust which commonly develops on these slopes is derived from facies E2 units which occur in the upper portion of the bluff. These units contribute a fine-grained fraction, with an apparent cohesion (strong capillary suctions) when dry. The surficial crust enhances slope stabilitiy in two ways. Firstly, it lends considerble mechanical (cohesive) strength to the slope; many of the 'crusty' side slopes and coast-parallel slopes stand at angles in excess of 45°. Secondly, since the crust forms a relatively impermeable surface, rill development, rather than mass movement, is favored. Rill erosion itself may lead to some rib and side slope retreat, although for reasons stated above this is considered unimportant.

Failure of over-steepened inter-bowl ribs was observed in several locations. One failure, at K668, and shown in Figure

VII.13, involved forward movement and collapse of a rib end. The newly created slope stood at 64-72° and was slightly concave. A portion of the failure plane apparently passed through frozen soil (determined by thermal criteria since ice partings could not be found). A failure surface may have been able to develop within the frozen sediment because of its very low ice content (<15%), which imparted only a limited amount of cohesion to the slightly clayey, silty sand (45/40/15 %, facies D2, Section 18-20). Apparently, on this steep slope, drainage and desiccation after thaw left an active layer which was, in essence, a poorly ice-cemented aggregation of soil blocks. This particular failure may have been due, in part, to the undrained failure of basal sediments softened by melt-water and wet debris, impounded against the base of the bluff by the ice foot.

Indeed drift snow and the ice foot seem to play an important role in the retreat of the bluff in locations where the basal sediments are fine-grained and susceptible to flowage, Figure VII.14. Figure VII.15, which shows a pocket penetrometer log at the base of the slope in the previous figure gives an indication of this softening. Once 'spalling' of the slope base has occurred, the sediment then softens and becomes mobilized as a basal debris flow apron, which moves out from the bluff over the snow and ice. The underlying ice provides a source of moisture, preventing dessication of the flow material. It is posssible that excess pore pressures (in addition to those due to the presence of a pore-slurry) are generated at the bottom of the debris-flow as melting occurs at

the debris-ice interface, a situation similar to thawing over ice lens (as discussed in Chapter VI). The frictional resistance along the soil-ice interface is also likely to be very low so that the soil may actually be sliding rather than (or as well as) flowing. Only once the snow and ice have melted and disappeared does debris movement cease and the slope base dry out and become restabilized.

F. Taluvial Debris Slopes

Slopes similar to the taluvial debris slopes which occur along the steep dissected bluffs are also found along the bluffs with debris-bowls. Formed of poorly-sorted taluvial lag, these slopes stand at inclinations consistent with the expected semi-frictional thresholds of such debris (24-27°, as discussed in Chapter V). As seen in Figure VII.16, these slopes resemble debris-bowls in being separated by steep residual ribs. However, the typical debris-bowl profile does not develop, either because the rate of slope regrading and debris supply along the back slope is too rapid relative to regrading along a low-gradient tongue, or thaw-related instability is inhibited by the low silt/clay content of the local stratigraphy.

As is the case along the steep, dissected bluffs, the main factors influencing the location and development of taluvial slopes are the local stratigraphy and terrace hydrology. This slope type appears to form in locations where the rate of debris supply along the back slope is more rapid than that at which it can be evacuated in a low-angled tongue slope.

Taluvial slopes will therefore develop in locations where there are stony sediments and a significant amount of non-plastic fine sand and silty sediment (e.g. low clay-content C facies) at the top of the section or where there is a relatively large amount of run-off intercepted at the knick-line (as between K753 and K765, the location of profiles B-18 to B-20). In both these cases regrading of the back slope and debris supply will be relatively rapid. The large amount of run-off will increase the frequency of positive pore pressures and also aid in the eluviation of the finer soil particles and the development of the poorly-sorted taluvial texture. The absence of thick (basal) fine-grained units may further promote the development of a straight taluvial slope by inhibiting tongue formation. (It must be emphasized that, because a slope stands at angles which are in excess of the expected semi-frictional threshold gradient, it does not follow that high or even excess pore pressures do not occur from time to time. If debris is being supplied by rapid back slope failure (relative to basal undercutting), high rates of debris throughput may result in the retention of slopes steeper than would be predicted on the basis of the local pore pressure regime alone.)

Thus, there is a continuum of both form and process between debris-bowls, debris-bowl-like features with steep, lobate profiles along which some flow-type failure is occurring (at angles less than 1/2 $\tan\phi'$) and taluvial slopes. For example, profiles B-16 and B-20 appear to be, essentially, semi-frictional taluvial slopes but display a tendency towards a more 'concave' profile. The taluvial slopes therefore

constitute a limiting case of debris-bowl development.

G. Endnote

Debris-hoppers and debris-bowls are similar features in the both are loci of accelerated debris movement and localized knick-line retreat, i.e. both are hollows in the bluff planform. In one sense, the debris-bowl is an extreme form of debris-hopper in which the axial slope has widened and flattened (as seen in Figure VII.4). Such a broad, gentle axial slope can only arise via mass movement processes where fine-grained sediments susceptible to thaw-related at low angles are significantly present in the bluff stratigraphy. In the case of the taluvial slopes, these appear to be similar features along both the steep dissected bluffs and the bluffs with debris-bowls (see Figure IX.1). In both instances, taluvial slopes arise along sections of the bluffs which are particularly stony and receive large amounts of run-off from the terrace surface. However, along the bluffs with debris-bowls the role of accelerated slope flattening due to failure caused by seepage derived from the thawing of ice-rich sediments in the bluff (or thaw-related instability of these sediments themselves) appears to be of relatively greater importance than it is along the sandier bluffs to the southeast.

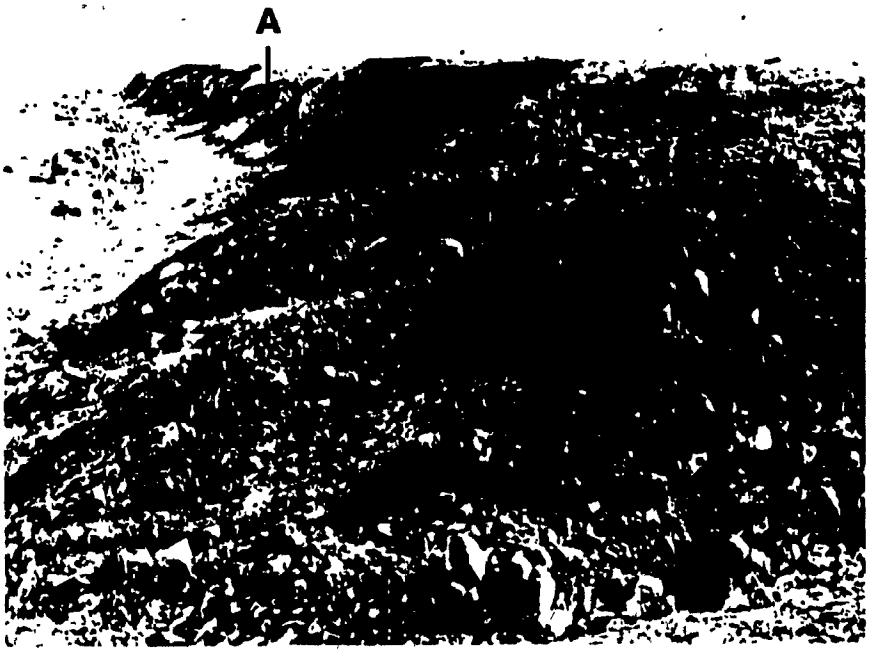


Figure VII.1 View southeast along the bluffs with debris-bowls from K682. The feature described in Figure VII.5 (B-2) is marked at 'A'. In this view the broad arcuate hollow, steep side walls and gentler tongue slope of the debris- bowl form is seen.

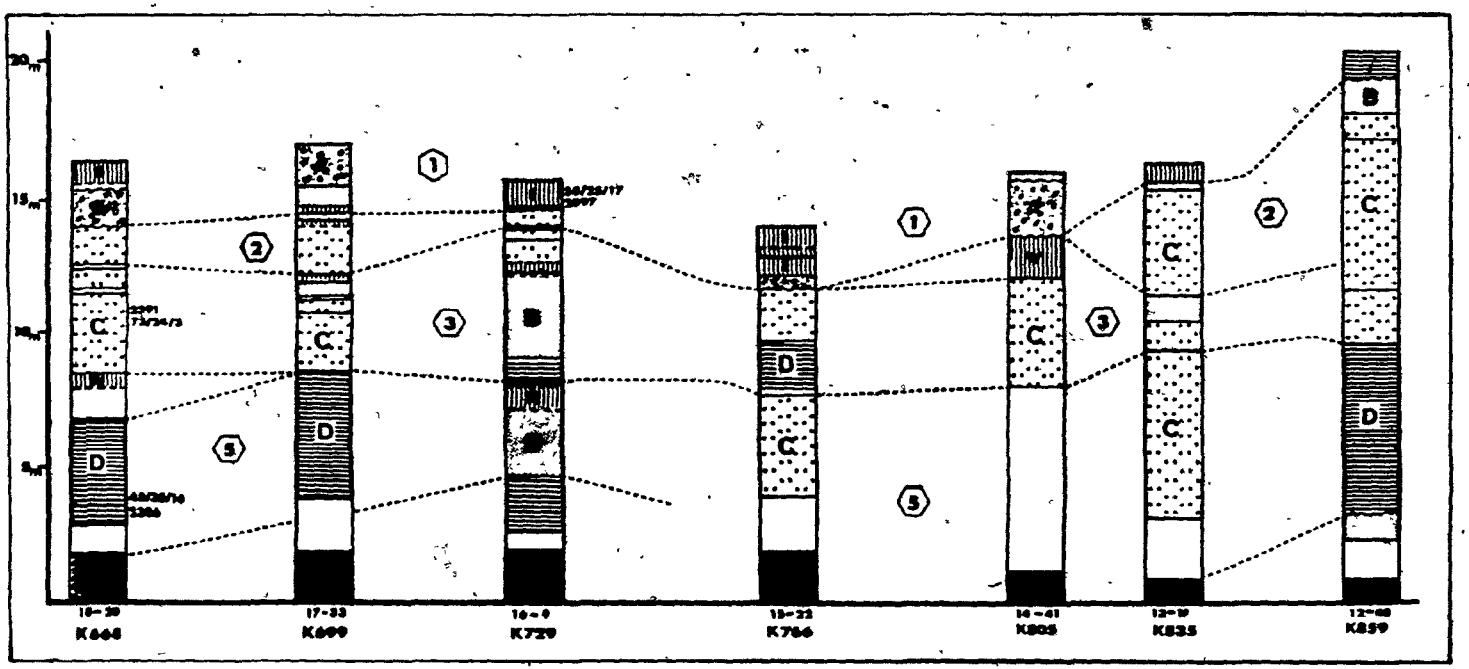
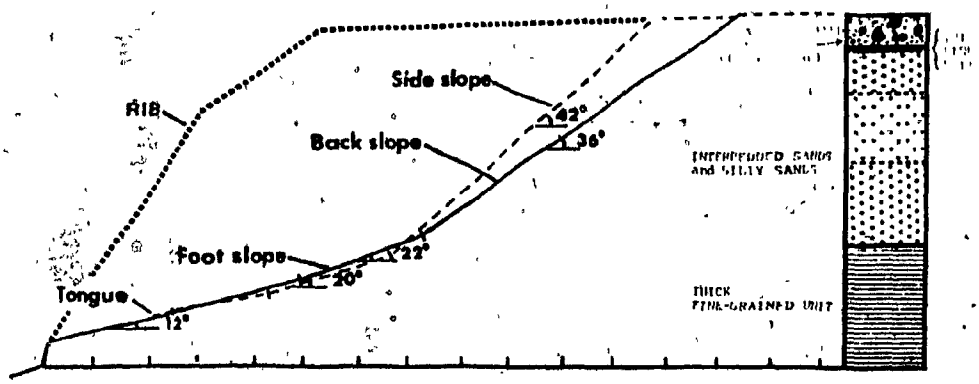


Figure VII.2 Stratigraphy along the bluffs with debris-bowls.

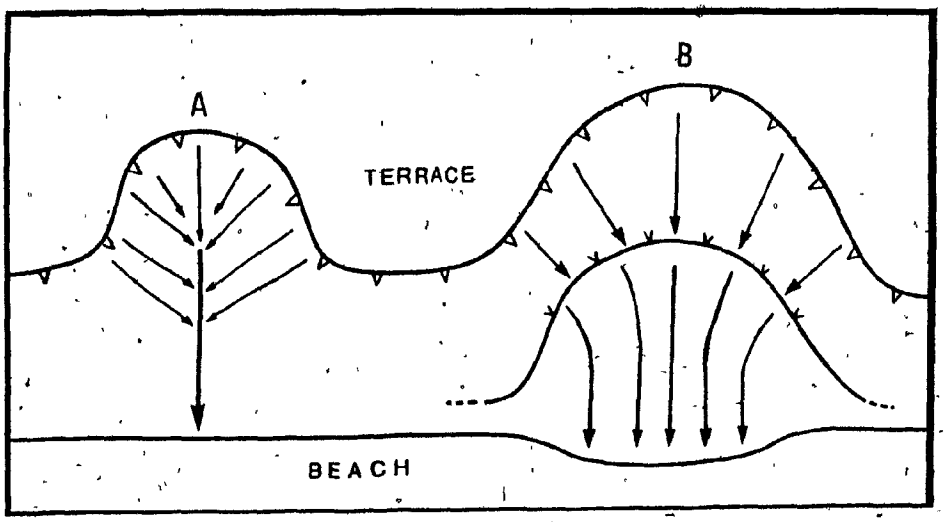
Facies A - Coarse-grained sediments, coarse sand and gravelly sand.
Facies B - Sand. Facies C - Interbedded silt + sand, silty sand.
Facies D, W, and E - Fine-grained sediments.



Figure VII.3 Dry, stabilized channel on terrace surface behind bluff at K667. At present this channel carries very little run-off.



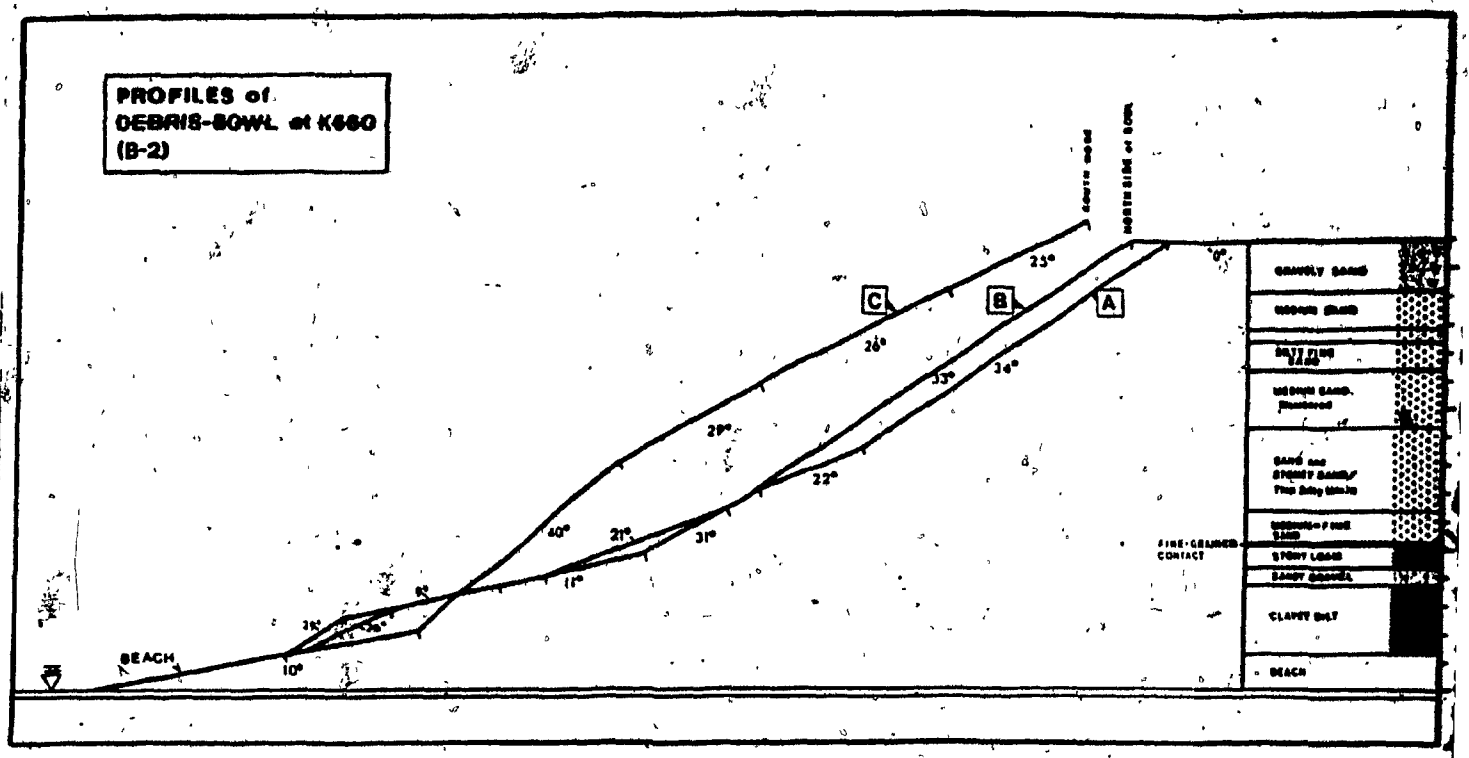
Schematic profile of a debris-bowl showing the typical division of the profile into slope units. The stratigraphy shows that the tongue slope is accordant with the fine-grained unit at the base.

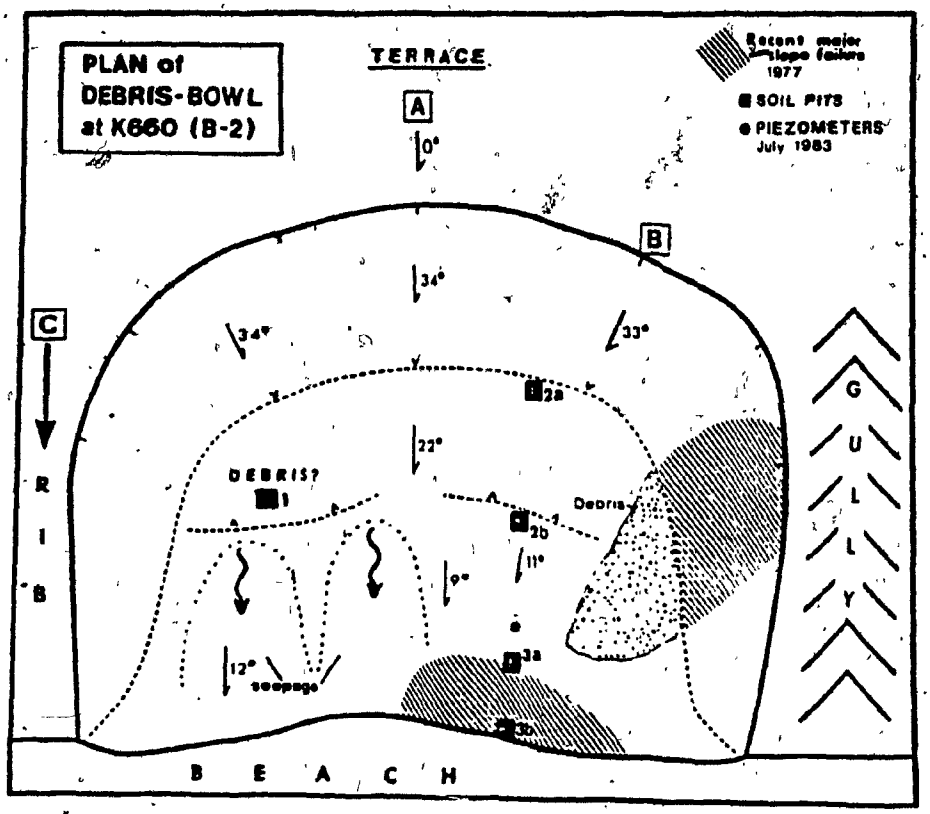


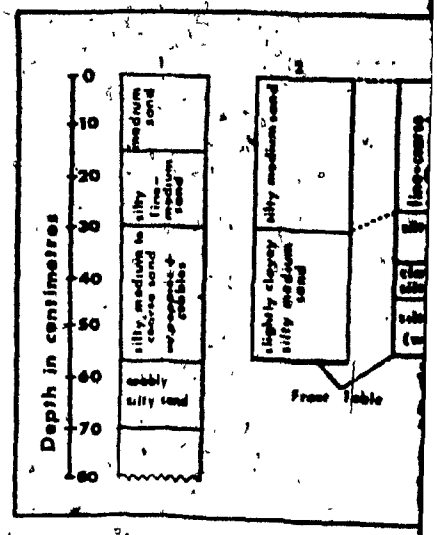
Plan of a debris-hopper (A) and a debris-bowl (B), showing convergent ground water and sediment flow lines in the debris-hopper and parallel flow lines along the debris-bowl tongue slope.

Figure VII.4 Schematic profile and plan of a well-developed debris-bowl.

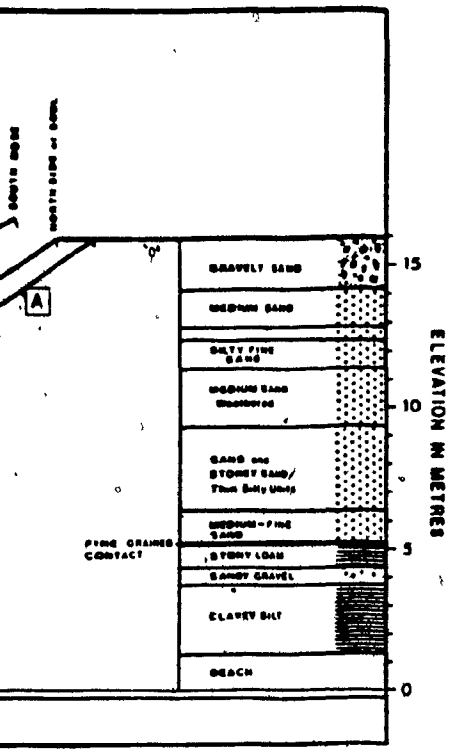
Figure VII.5

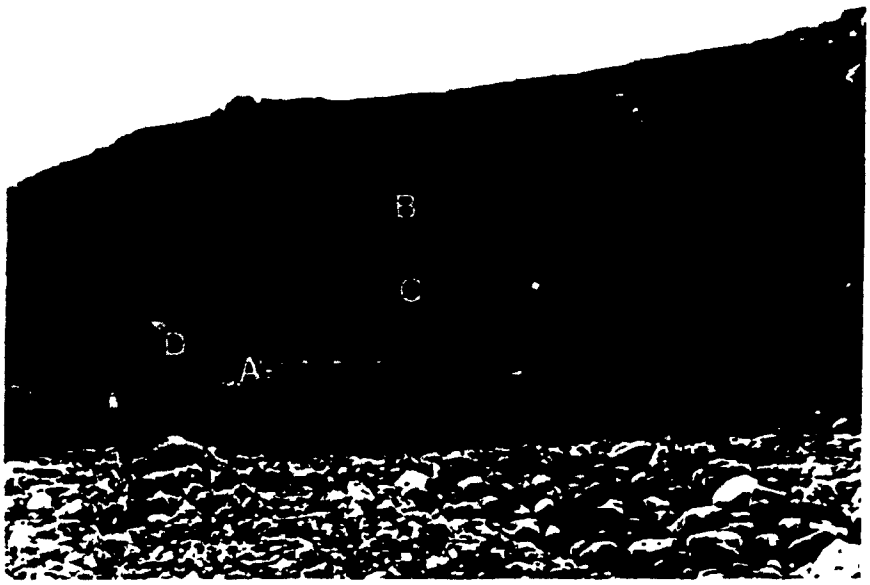






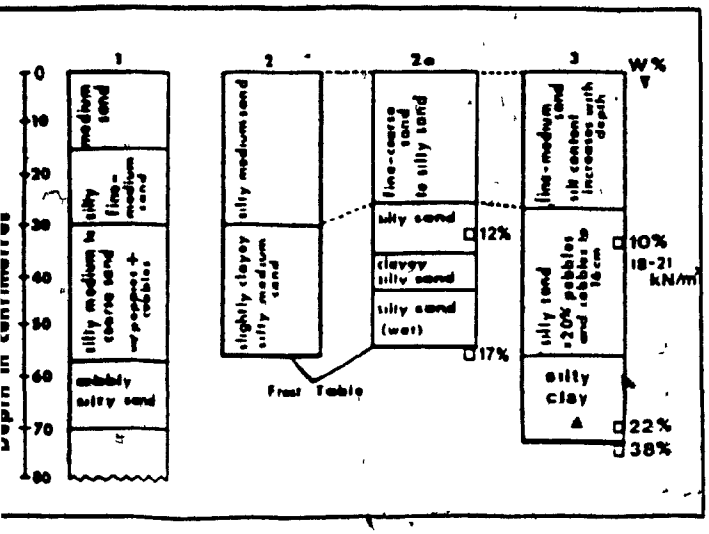
Soil pit data from the debris-bowl at
of the pits are marked on the plan of
The materials above the silty clay in
which, because of its poor-sorting,
location of grain-size sample.



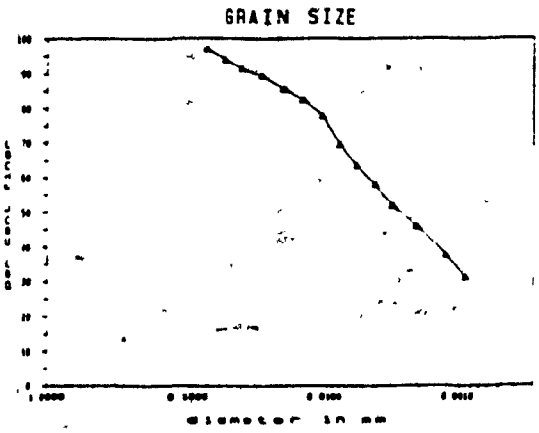


A A

Debris-bowl at K660 (B-2). The photograph shows the feature presented diagramatically at left. The morphology of a well-developed debris-bowl can be seen. This consists of a low-gradient tongue slope (A), a steep back slope (B) and a transitional segment or foot slope (C) inbetween. The back slope is straight in profile and covered by a veneer of coarse-grained sediment derived from the beach deposits which form the cap unit here. (See local stratigraphy on profile to left.) Tension cracks associated with the arrested instability at the edge of the tongue can be seen at D. (This particular failure has been discussed in the previous chapter, and is indicated on the plan to the left.)



it data from the debris-bowl at K660 (B-2). The locations pits are marked on the plan of the feature, Figure VII.5b. terials above the silty clay in pit 3 is colluvial debris because of its poor-sorting, may be quite dense. ▲ denotes on of grain-size sample.

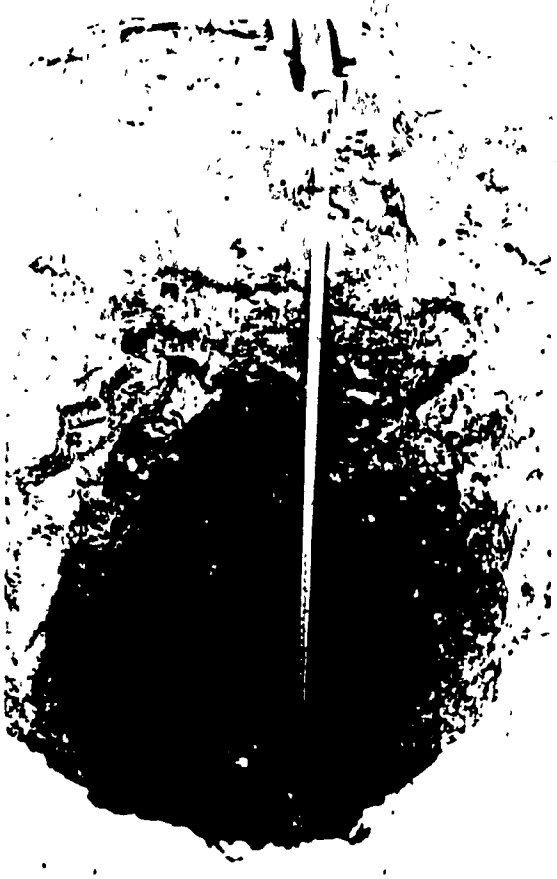


Sample from base of active layer along debris-bowl tongue slope at K660 (B-2), Pit 3a.



B▲

Northwest side of the debris-bowl seen in Photograph A. The soil involved in the failure of the side slope has become transformed into a debris flow, moving out over the surface of the tongue at X. (The location of this slope failure is marked on the plan, to the left.



◄C

Soil pit on tongue slope of the debris-bowl at K660 (B-2). The location of this soil pit is marked on the debris-bowl plan at left. Pit exposes 20 cm of silty clay above the frost table, which is at 72 cm. Overlying this is colluvial debris; see details of soil pits to left.

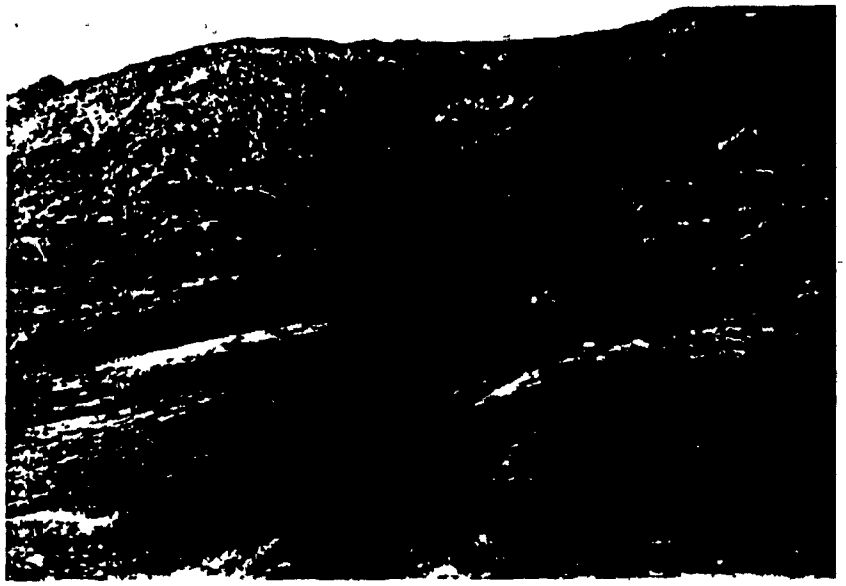


Figure VII.6 Seepage steps retrogressing over debris-bowl tongue slope. The poorly-sorted colluvium which underlies the cover of colluvial/alluvial sand forms a relatively impermeable surface. This contrast in hydraulic conductivity can result in the development of a perched water table, or of a layered phreatic system. The more frequent, and more rapid, groundwater flow in the sands, as well as their ease of entrainment, leads to periodic stripping.



Figure VII.7 Minor retrogressive instability and sloughing at the edge of the tongue slope of the feature at K670 (B-4). The sediments involved in these movements are non-plastic silty loams and silty sands. The finer-grained, in situ sediments are not exposed at the edge of this tongue slope.

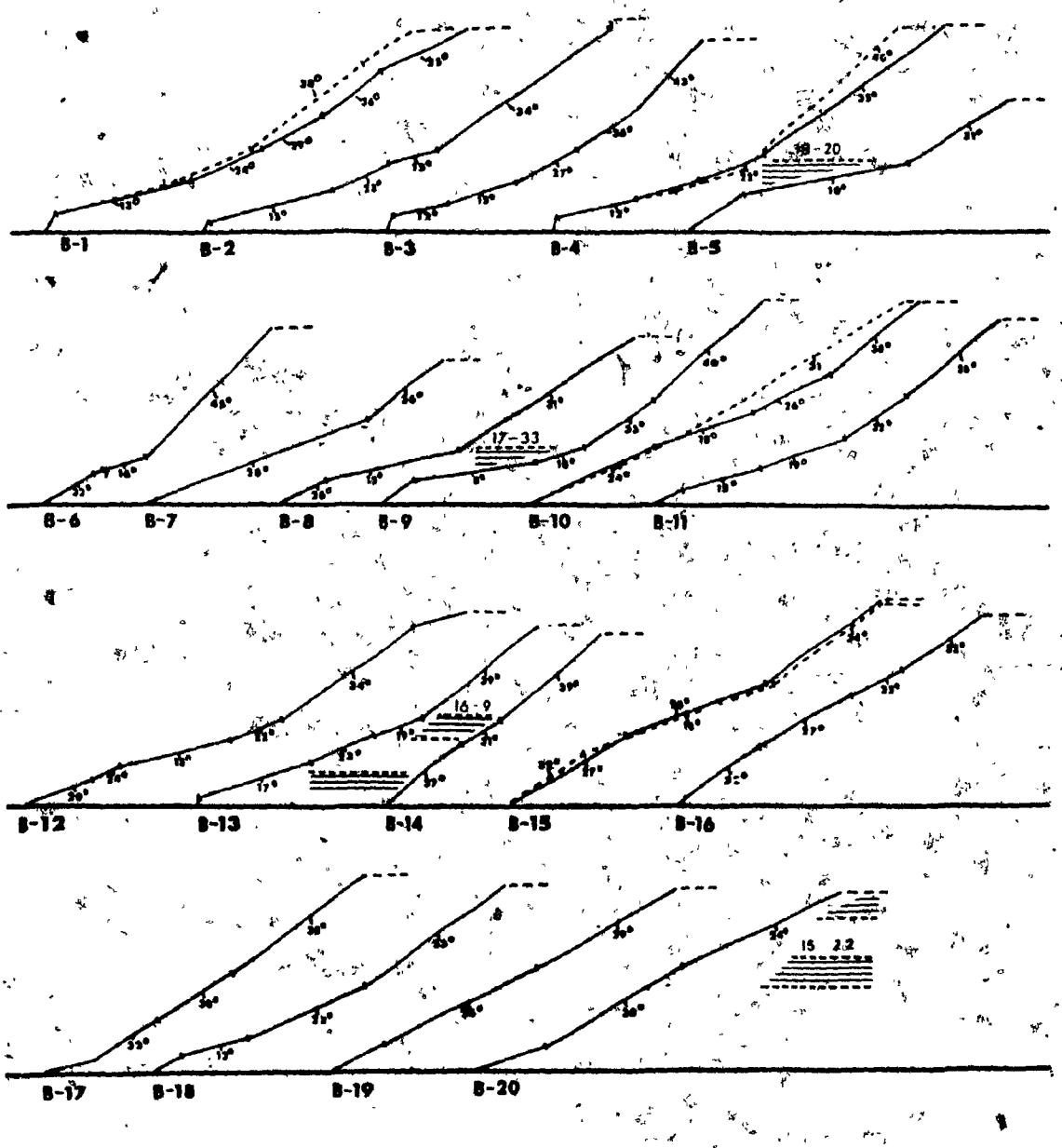


Figure VII.8 Profiles through debris-bowls and related features between K650 and K765. Profile locations are marked on the bluff panorama. Where available the approximate elevations of the major fine-grained units from Nelson's stratigraphy (Figure VII.2) are given. Note the two gentler slope segments in profile B-13 associated with two fine-grained units.



Figure VII.9 Large 'perched' debris-bowl at K860. The floor of this feature is situated near the top of a particularly thick, massive fine-grained unit (see Section 12-40, Figure VII.2). The dark fine-grained sediment can be seen in situ at the base of the bluff.

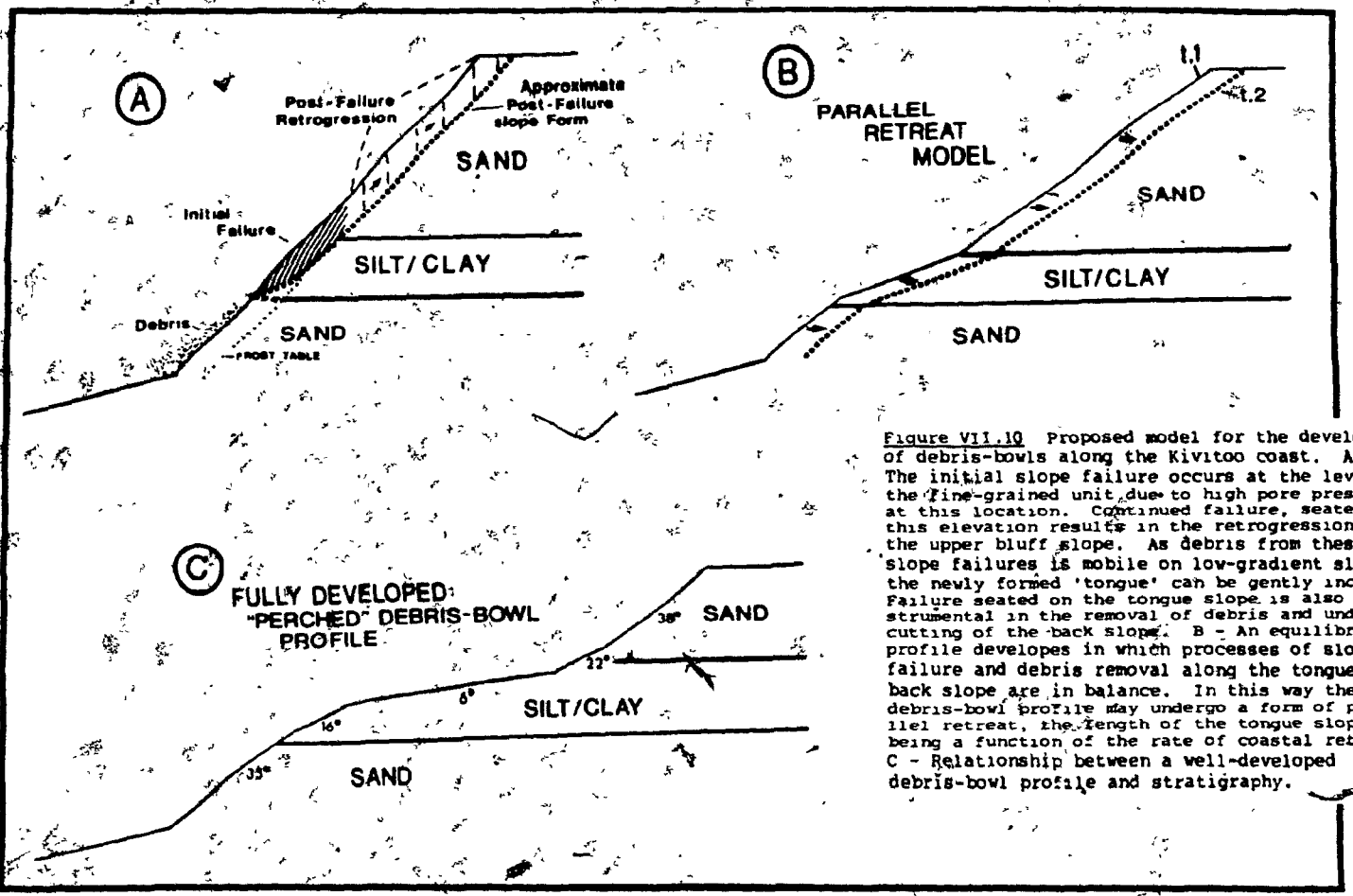


Figure VII.10 Proposed model for the development of debris-bowls along the Kivitoo coast. A - The initial slope failure occurs at the level of the fine-grained unit due to high pore pressures at this location. Continued failure, seated at this elevation results in the retrogression of the upper bluff slope. As debris from these slope failures is mobile on low-gradient slopes, the newly formed 'tongue' can be gently inclined. Failure seated on the tongue slope is also instrumental in the removal of debris and undercutting of the back slope. B - An equilibrium profile developes in which processes of slope failure and debris removal along the tongue and back slope are in balance. In this way the debris-bowl profile may undergo a form of parallel retreat, the length of the tongue slope being a function of the rate of coastal retreat. C - Relationship between a well-developed debris-bowl profile and stratigraphy.

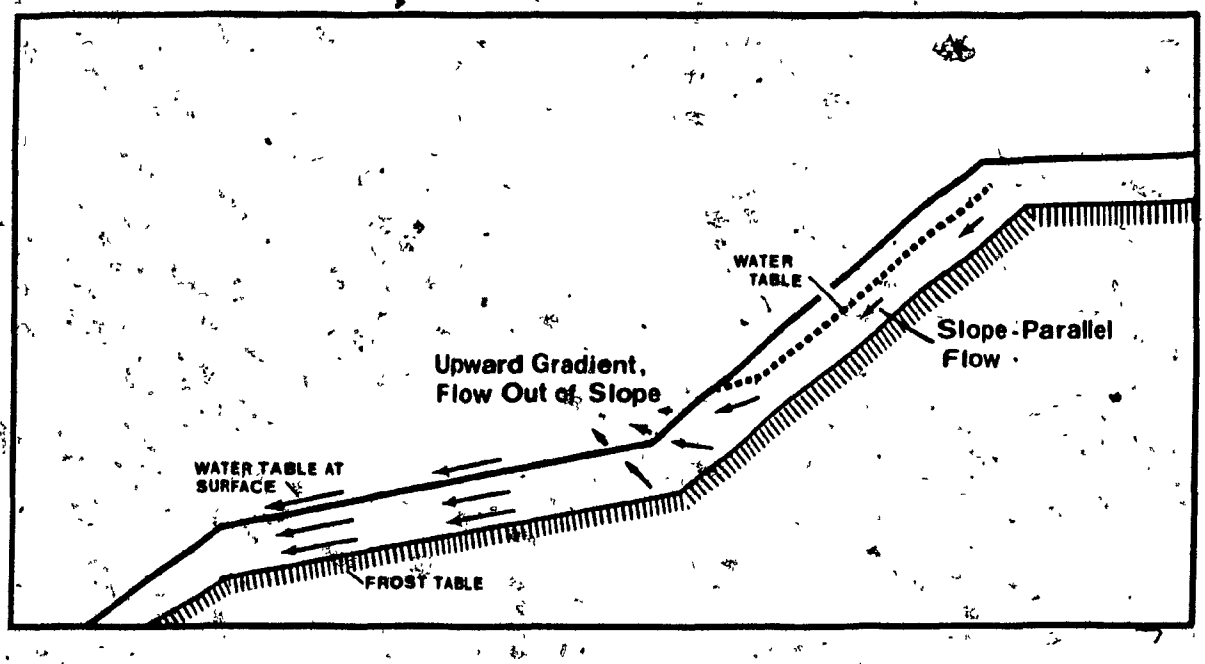


Figure VII.11 Schematic diagram showing hypothetical flow directions along a bluff slope. Upward flow (effluent seepage) occurs at the top of the gentler slope slope due to the reduced along-slope hydraulic gradient, as well as three-dimensional flow convergence and reduced permeability of the lower slope.

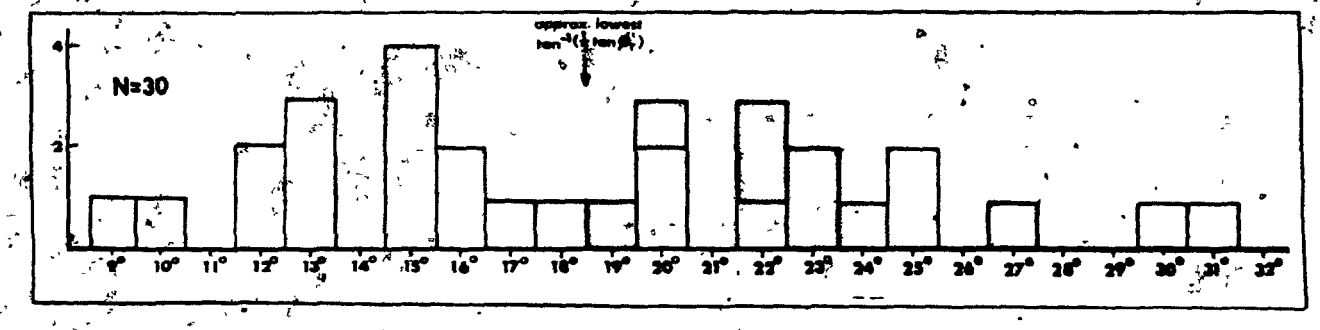


Figure VII.12 Bar graph of slope segment angles along debris-bowl tongue slopes and foot slopes (shaded). Arrow marks approximate semi-frictional threshold gradient for a slope comprised of materials with a residual angle of internal friction of 34^{0}.



Figure VII.13 Failure of rib end at K668. This slope failure is thought to be associated with the softening of sediment at the base of the bluff by wet debris and melt water impounded at the base by the ice foot and drift snow. The soil involved is a blocky loam. A portion of the failure surface apparently passed through frozen soil, which, in this unfavorable location, was particularly dry. Newly created slope stands at 60-70°.



Figure VII.14 Apron of wet and fluid debris over drift snow and the ice foot at the base of the bluff southeast of Profile B-1 (K652). Basal unit is a silty clay - clay loam. Retreat of the slope is via softening of the basal sediments and subsequent spalling. Slope restabilizes only after the snow and ice has melted and the debris drys out. See penetrometer log from base of bluff (Figure VII.19).

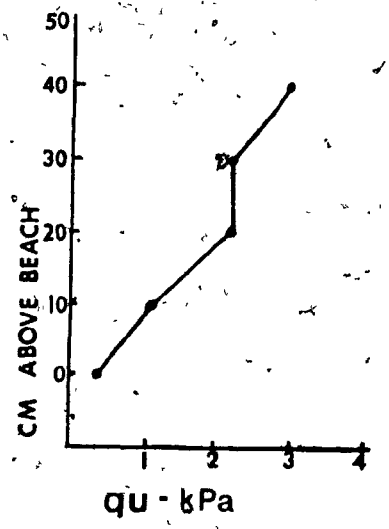


Figure VII.15 Pocket penetrometer log at base of bluff shown in Figure VII.18. Penetrometer gives unconfined compressive strength of the sediment (qu).



Figure VII.16 Taluvial lag slopes, separated by residual ribs, along the bluff between K754 and K765. The terrace surface behind the bluffs at this location carried a relatively large amount of unconcentrated surface run-off to the bluff edge. This has resulted in a rapid supply of coarse debris by slope failure (i.e. relative to the rate of undercutting at the base) at the top of the bluff and the removal of finer materials from the surface of the slope.

CHAPTER VII:

THE BENCHED BLUFFS

A. Introduction.

The mid-bluff bench which characterizes the benched bluffs starts just southeast of Camp II at an elevation of 8-10 m (as measured at the seaward edge of the bench). It is discontinuous, consisting mainly of bench fragments in large hollows, until around K940. The broken bench between K940 and K1020 can be followed visually on the photographic panorama between K940 and K1020 by noting breaks in slope, areas of concentrated instability, and remnants of old bench surfaces. (See profiles H-1 to H-6, Appendix B.) The well developed, continuous bench surface begins at K1052 at an elevation of 10-12 m rising to 15+ m at K1052. Proceeding northwest along the coast, the bench can be traced in the series of 'N' profiles (Appendix B) as it rises from an elevation of 15 m to over 23 m near the end of the bluffs in the vicinity of K1200. Northwest of this, two gentle slope segments are developed at approximately 14 m and 24 m (e.g. profiles N-4 to N-9, Appendix B) forming a 'double' bench.

Figures VIII.1 and VIII.2 show typical sections of the bench surface. The mid-bluff bench ranges from less than 10 m to over 40 m in width. Variations in the width of the bench may be sudden and often appear as 'jogs' in the plan of the bench back slope. Along any one section of the bench the topographic plan is characterized by shallow hollows and

rounded spurs (seen in Figures VIII.1 and VIII.3) at the back slope. At a few locations the bench narrows so that the back slope is nearly continuous with the basal slope. Narrowing is often associated with high sandy 'knolls' (interpreted by Nelson (1978) as small deltas deposited during a period of higher relative sea level) on top of the bluff, as at K1058 and K1082. The thick sand cappings provided by the knolls may inhibit bench development and thus account for the narrowing at these locations.

As shown in the bar graph in Figure VIII.4, the inclination of the bench ranges from almost horizontal to 17° with most slopes inclined at 5-11°. As such, the gradient of the bench is well below expected semi-frictional threshold values. (Direct shear tests on a remolded soil from the base of Slide 5 gave a $\phi'r$ value of 34°. In accordance with Eq. III.13, an angle of limiting stability for a slope comprised of such material is 19°.) Bench slopes are usually gentler than the slopes which constitute the debris-bowl tongues along the bluffs to the southwest. The bench slope itself is fairly straight from the base of the back slope to its downslope edge, where a slightly steeper straight slope segment or a convex slope element typically forms a transitional slope between the bench and the lower bluff slope. A short concave upward segment or foot slope inclined at 18-25° often develops at the back of the bench. Yet, in some locations the contact between the back slope and the bench is abrupt. Both an abrupt change in slope and a transitional foot slope can be seen at the back of the bench in Figure VIII.3.

The surface of the bench is mostly vegetated, indicating, at least general stability. Locally, seepage arising at the base of the back slope may deposit a veneer of sandy sediment on the bench slope. Sheet wash may also be important in moving sand, derived from the back slope, across the bench.

The bench continues inland along the sides of the larger streams which cross this section of the bluffs. Low-angled landslides like those found on the bench surface also occur along these valley sides, particularly near the bluff line where the gradient of the stream steepens.

B. The Origin of the Mid-bluff Bench

The mid-bluff bench at Kivitoo has been interpreted by Pheasant and Andrews (1973) and Andrews et al. (1975) as a marine terrace cut into the bluffs during relative sea level still stands of 15 m and 7 m above present sea level during the late Fox stade. The northwestward rise in elevation of the bench was accounted for by assuming a rather steep (1.5 m/km) crustal tilt in towards the ice source at the head of Narpang Fiord.

The morphological evidence, however, does not support this interpretation: (1) The bench is covered entirely by sandy colluvium. Raised beach deposits were not evident anywhere on the bench surface. (2) The bench back slope is irregular in plan. If marine erosion had cut the bench, the back slope would be more or less linear in plan and the bench more uniform in width. Or it would vary systematically in width in response

to the pattern of coastal erosion following uplift. (3) The bench varies in elevation, often over short distances, rising from less than 10 m in the vicinity of the stream at K900 to over 20 m near the northwest end of the bluffs. This gradient is too steep to have reasonably been the result of isostatic tilting. Pheasant and Andrews (1973) assume bench 'cutting' during two different relative sea levels, but, in fact, there are several bench levels located between these assumed sea level stands (see 'H' and 'N' series profiles, Appendix B). (4) The bench is continuous with similar low-gradient surfaces along the sides of the streams which cross the bluffs. It is doubtful that wave erosion could have reached into these small valleys, particularly without leaving beach deposits.

The bench is interpreted here as having been formed by mass movement processes seated at the level of the thick fine-grained units which occur in the bluff stratigraphy along this stretch of the Kivitoo coastline. Bench development is therefore morphogenetically continuous with the development of the debris-bowls and instability complexes further south. However, under the more moderate rates of marine erosion within the mouth of Narpaing Fiord, the ribs and terrace remnants between individual features have been eliminated and their tongue slopes joined to form a continuous surface at the level of the fine-grained unit. The typical back slope plan of hollows and spurs may be a residuum of this process. (Further evidence for less intense rates of erosion than those which occur along the more exposed coast to the southeast is presented below.)

1. Bench Development

Once terrace remnants separating cells of intensive instability have been eliminated, further modification of the bench surface by low-angled failure seated in the fine-grained unit would 'smooth out' this surface and affect continued retreat of the back slope by undercutting and debris removal. This process would result in continued widening of the bench. As discussed below, present-day instability seems to be preferentially located downslope of spurs in the back slope, thereby aiding in the elimination of rib remnants and straightening the bench plan. (Evidence for, and the mechanics of, present-day instability along bench slopes, has been discussed at length in Chapter VI.) Nevertheless it must be acknowledged that present rates of backwasting seem far too low to have formed the bench in the time available.

The 'terraces' along the sides of streams crossing the bluffs are formed and modified by the same mass wasting processes which are operative on the bluff bench. For example, at present a bench is actively forming along the sides of the stream at K900. This is the location of the retrogressive active layer failure described in Chapter VI and can be seen in Figure VI.21B. Remnants of the old valley-side bench are found along the bluffs just to the southeast of the stream. These bench remnants occur at the level of a fine-grained unit. This particular unit thickens to the southeast where it forms the unit atop which the large perched debris-bowls are developed. (See panorama and profiles H-11 and 13, Appendix B.)

The profiles and stratigraphic sections shown in Figures VIII.5, 8, and 10 (as well as in the illustrations of the individual landslide features presented in Chapter VI) clearly demonstrate the accordance between the bench slope and the fine-grained units. Further comparison of the bench with the fine-grained units may be made with the profiles and stratigraphy given in Appendix B. Excavations, such as those shown in Figures VIII.6 and VIII.7, show that the contact between the in-situ fine-grained unit and the underlying coarser-grained sandy sediment lies just below the downslope edge of the bench. Often, the thickness of the fine-grained unit at this point is just slightly less than the thickness of the active layer. This may be an indication that bench development is, at many locations, in an approximate equilibrium with the rate of undercutting of the bench by failure along the bluff base occasioned by coastal retreat. Once the fine-grained unit is thin enough so that there is no longer any fine-grained soil exposed at the base of the active layer instability along the bench edge will be subdued. Continued undercutting of the bench edge, if it occurred, could lead to a thickening of the fine-grained soil (in relation to the active layer) and renewed instability.

The upper contact of the fine-grained unit is almost always situated at the back of the bench, or else a small distance up the foot slope. This is a result of the continued trimming back of the sands overlying the fine-grained unit by low gradient failure along the bench slope. Also, a steeper back slope, if it is partly developed in the fine-grained

sediment, would tend to fail as a result of the thaw-unstable nature of these sediments so that regrading could occur until the fine-grained layer no longer forms a portion of the steep back slope. In this sense, the bench slope may be thought of as a threshold slope, the gradient of which is determined by the tendency of the fine-grained sediment to develop artesian pore pressures during thaw and its susceptibility to retrogressive active-layer processes.

As detailed stratigraphy and excavations make clear, the bench at Kivitoo is, in all locations, associated with the fine-grained units. This relationship is further substantiated by the bluff profile and stratigraphy shown in Figure VIII.8. Here there are two lower-gradient segments occupying mid-slope positions. Both of these are associated with fine-grained units. Further evidence is found along the sides of valleys crossing the bench where the presence of mudboils (non-sorted circles), which have broken through the cover of colluvial sand bringing fossil shells to the surface, suggest that the soil they contain is being derived from in-situ fine-grained units at the base of the active layer. Excavation confirmed that this was the case.

Other evidence suggesting that bench development results from mass wasting processes is the presence of small sand mounds at the edge of the bench adjacent to stream valleys, Figures VIII.9 and 10 (as well as profile N-30). These mounds are outliers of the original terrace surface which have been left behind while adjacent unstable hollows cut back into the bench back slope and, when enlarged laterally, eventually join

to leave a remnant of the terrace surface at the bluff edge. Such mounds are favored on either side of stream mouths (Figure VIII.9) because soil movements will be directed roughly parallel to the line of greatest slope, which in the case of the bench is seaward, and along the valley side is towards the stream. Thus, a divergence of lines of debris movement will occur, leaving a wedge of ground at the intersection of the bench and stream valley, largely unaffected by such movements. Groundwater flow lines will also diverge, further enhancing the stability of this portion of the bench, and of the bluff slope below it. The profile and stratigraphy in Figure VIII.10 shows the small mound at the bench edge and the relationship between the fine-grained unit and the bench. Here, suppression of instability by the mound and groundwater flow divergence seems to have been resposible for the maintainance of a relatively thick layer of fine-grained sediment below the seaward edge of the bench.

2. Other instances of bench formation

Bench formation is common in temperate regions along bluffs developed on mixed lithologies. Many of these benches may be attributed to ground subsidence associated with deep-seated rotational slumping. Others, however, are due to the differing stability characteristics of the sediments which comprise the bluff stratigraphy, as is the case at Kivitoo. In such cases bench formation is usually associated with clay units, as these provide materials of relatively low frictional strength (and therefore are favored shear surfaces), and are

susceptible to debris flowage. The upper contact of fine grained units may form the base of a zone of seepage (perched phreatic layer) and is therefore a preferred location of basal sapping and slope failure. Downslope transport of debris by flowage is favored in these wet, fine-grained soils, maintaining retreat of the superadjacent bluff and the continued development of the bench.

Yet, few of these reports give clear evidence that the debris along the bench is moving, or that failure is being initiated, on slopes less steep than the semi-frictional threshold angle of the constituent materials. Barton (1973), for example, calculated factors of safety of 1.06 and 1.56 for two bench slopes in clay rubble. Accordingly, Barton suggested that transient excess pore pressures due to undrained loading (Hutchinson and Bhandari, 1971) may be operative.

Bench development has also been reported along permafrost slopes. Miles (1977) identified 'composite' features, where low ice content units underlie high ice content fine-grained material. Instability at the level of the fine-grained unit results in a typical bench morphology. Miles did not, however, discuss the mechanics of bench development, nor did he elaborate upon the nature of the relationship between the bench and the fine-grained unit. B. Mode (pers. comm.) and P. Drake (pers. comm.) have noted the association of bench morphology and fine-grained units along the Clyde bluffs, 400 km north of Kivitoo. These bluffs are stratigraphically and morphologically similar to the Kivitoo bluffs. Loken (1965), working at the head of Inugsuin Fiord, identified a wave cut

terrace at 9 m asl. Comparison with the stratigraphy shows that the break in slope occurs at the level of a silt/clay unit. It is possible that this 'terrace', also, was the result of mass wasting processes and not marine action.

Similarly-situated 'paleo-shorelines' are reported by Washburn (1947). These observations demonstrate that both the morphology and stratigraphy of the bluff must be looked at together when making genetic interpretations.

3. Location of low-angled landslides

Of the six low-angle slope failures examined along the bench, four occurred below steep, convex-in-plan slopes (spurs) at the back of the bench. Figure VIII.11 shows the location of slides 4 and 5 on the particularly wide bench between K1216 and K1240. The bench back slope consists of a series of hollows and spurs. The spurs are the remnants of 'ribs' which once separated individual debris-bowls or instability complexes. Figure VIII.11 shows that unchannelized surface wash has deposited a cover of well sorted fine to medium sand below the hollow. Soil auger probes at the back of the bench below the hollow show these deposits to be thicker than the active layer. (The frost table is at 75 cm.) The sands are well sorted, very wet and liquefy easily when disturbed.

The cover sands thin downslope so that at auger hole B (Figure VIII.11), they grade into silty sand and clayey silty fine sand at a depth of 80 cm, just above the frost table (which was at 92 cm). Auger hole C is in a short, high (ca 105

cm) gelifluction lobe located just below a spur. No indications of recent mass movement activity could be found on the bench below this gelifluction lobe. The auger hole showed a regolith composition similar to that of hole A.

In contrast to these regolith profiles, blocky clay or loam is encountered at shallow depth (<30 cm) beneath the other spurs, e.g. the soil pits in Slides 4 and 5. Thus the 'unstable' loam lies closer to the slope surface below spurs, and is therefore within the active layer and exposed to thawing. Below hollows both erosion of the loam unit (by prior instability) and recovering by sand is greater. The frost table is therefore unlikely to penetrate the 'unstable' loam or only exposes a thin layer of it to thaw. The result of these spatial variations in the active layer soil profile is that instability is, currently, preferentially located below spurs.

A similar case of layered soils of differing stability characteristics and varying thicknesses is described by Egginton (1981) focusing on the instability of the 'gravel pads' (coarse, raised beach deposits), which were overlying a fine-grained till. Some of these 'pads' are moving down a (10°?) slope at a rate of up to 18 mm/yr. Egginton found that the stable pads were particularly thick and that it was only when the pad was sufficiently thin that the seasonal frost table could dip into the underlying fine-grained till, that instability was observed.

C. Rates of Toe Erosion and the Development of Vegetated Colluvial Slopes

It has been assumed that the mid-bluff bench forms northwest of Camp II, because the rate of toe erosion is lower along this stretch of coast than it is to the southeast. The less severe erosional environment would allow the morphogenetic processes on the bluff slope a longer period in which to work. Evidence of less intense wave attack is abundant. This portion of the coastline is within the mouth of Narpaing Fiord, and is therefore less directly exposed to incoming swell from Davis Strait. Islands further inhibit wave attack. Removal of debris supplied to the beach by failure along the bluff slope appears to be relatively slow. For example, Figure VIII.12 shows the bluff downslope of the particularly wide section of the bench between K1215 and K1230. This portion of the coast is actually a large colluvial apron formed of landslide debris derived from instability along the bench. Wave attack appears to be insufficient to remove this debris or cut the lobe back to conform with the coast.

The most convincing argument for lower rates of basal erosion is the developement of vegetated slopes along the lower portion of the benched bluffs. Many of these slopes show little or no signs of instability. As seen in Figure VIII.13 these slopes are typically mantled by a sandy or silty sand colluvium. Measurements of twenty 20 m long stable and quasi-stable lower bluff slope segments showed that these stand at 19-23°, Figure VIII.14. This coincides with a (weak) modal

grouping on the bar graph of all lower bluff slope segments derived from the N profiles, Figure VIII.15. (Profile descriptions and comparison with the panorama indicate that most of those slopes less than ca 24° are vegetated, while those greater than ca 30°, are unvegetated and occur mostly beneath spurs or adjacent to stream valleys, both of which are hydrologically 'unfavorable' locations.)

Direct shear tests (drained), preformed at low normal stresses on a sample taken from a quasi-stable 22° slope, gave a ϕ' value of 34-35°. Substitution of this value in Eq.III.13 gives a semi-frictional threshold angle of 19-20°, which is in agreement with the modal grouping of observed straight slope segments (Figure VIII.15), supporting the contention that these are semi-frictional threshold slopes.

The bar graph in Figure VIII.15 also shows that some of the basal slopes along the benched bluffs stand at inclinations less steep than 19° (i.e. below the expected semi-frictional angles). These gentle segments occur mainly along the colluvial apron below the wide bench (location of Slides 4 and 5) and in other locations where the regolith appears to have a particularly large fine-grained fraction relative to other basal slopes along the benched bluffs (although this has not been confirmed by systematic sampling). As such, these slopes may also be, along with the bench and tongue slopes previously described, 'artesian slopes' (Carson, 1976) the ultimate angle of limiting stability being controlled by the frequent occcurrence of excess pore pressures. The processes which are operative on the gentle slopes below the bench are

not as evident as they are along the bench and tongue slopes; signs of slope failure are not obvious. Minor gelifluction features occur locally but are not ubiquitous. Further investigation of these lower bluff slopes and the source of the excess pore pressures (if they do indeed occur) is necessary.

The fact that many of the slopes below the bench have regraded to semi-frictional angles and have been colonized by vegetation is the most convincing evidence for lower rates of basal erosion along the benched bluffs. Since the stratigraphy of the lower bluff slope along the benched bluffs is similar to that of the planar debris-mantled and steep, dissected bluffs further south along the coast (Chapters IV and V), if the rate of undercutting along the bluffs in those two areas were to decrease substantially, at least parts of them would flatten to semi-fricitonal angles. Moreover, the presence of small gelifluction lobes on these 'stable' basal slopes in the northern area, and basal slopes less steep than predicted semi-frictional angles, implies that, given low rates of basal undercutting and over long enough periods of time, the slopes will continue to flatten under the influence of particular mass wasting processes controlled by excess pore pressure conditions.

D. The Bench Back Slope

Comparison of the lower bluff slope bar graph with one from the bluff slopes above the bench, Figure VIII.16, indicates that these upper slopes are significantly steeper

with most standing at 26-35°. This implies that the upper slopes are drier and/or subject to more intense basal trimming. As such they tend to stand at angles closer to frictional than semi- frictional threshold values. (The very gentle slope "segments" included in the bar graph are all either near the base or the crest of the bench back slope; as such, they may be part of concave or convex slope elements which have formed in response to slope wash or creep processes.)

E. Endnote

It has been noted above that present rates of backwasting along the bench slopes appear to be too low to account for the formation of the bench since post-Foxe emergence. This suggests that the initial stages of bench development were quite rapid, as they appear to be along the actively undercut bluffs in the vicinity of Camp II where highly unstable, incipient bench/bowl - type features are currently found. Once a gentle bench slope has formed, with its end-points graded to the upper and lower limits of the fine-grained unit, its surface mantled by a thickness of sandy colluvium and a new active layer ice profile established, low-gradient failure may be substantially suppressed, occurring only sporadically in response to exceptional thaw seasons. It is therefore probable that the Kivitoo bench formed soon after late-Foxe emergence, a period which also coincided with the Holocene hypsithermal (ca 7,000 - 5,000 BP: Deevy and Flint, 1956; Miller, 1973). Given the inferred low rates of basal trimming along this portion of

of the Kivitoo coastline, the bench has probably only been modified and somewhat widened -- most likely during warm episodes when rapid mass movement processes may have been significantly reactivated -- since its primary post-glacial morphogenesis.



Figure VIII.1 View west along the mid-bluff bench from K1020. Slide 1 is marked at A. Photograph shows the typical arrangement of small spurs and hollows at the back of the bench. A small slope failure, exposing the in situ fine grained unit has occurred below the spur in the foreground. Piezometer 3 was located near 'x' at the base of the back slope. Note also the sharp break between the downslope edge of the bench and the steeper, unvegetated slope at the base of the bluff.

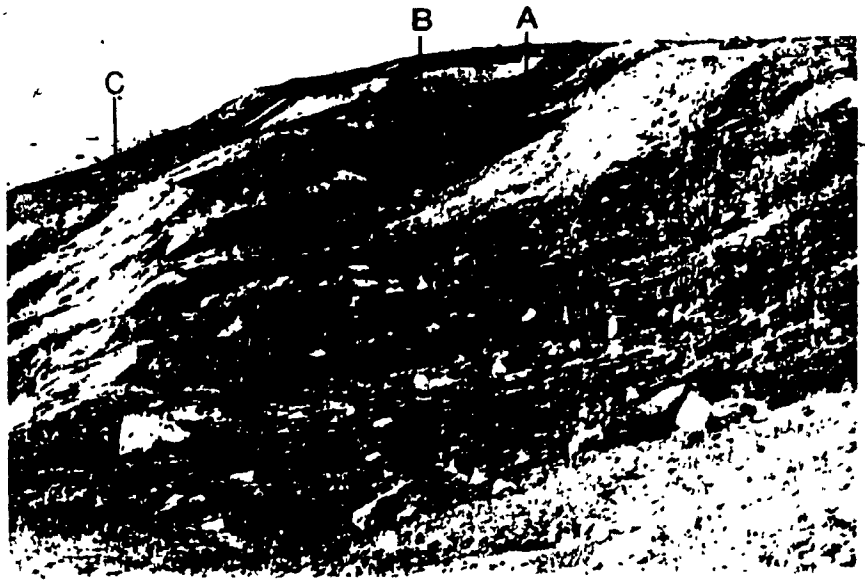


Figure VIII.2 View from ca K1245 east along a particularly wide section of the mid-bluff bench. Slide 5 (A), Slide 4 (B) and gentle basal colluvial slope (C) are marked. A planform of three spurs and intervening hollows along the bench back slope can be discerned.



Figure VIII.3 Bench and back slope west of K1105. Slide 2 is seen (A), as is another, older feature in front of it in the photograph (B). As seen here the junction between the bench and back slope may be either abrupt (as in the foreground) or occupied by a transitional foot slope (as in the vicinity of Slide 2). A profile of this section of the bench and further description of Slide 2 are given in Figure VI.2.

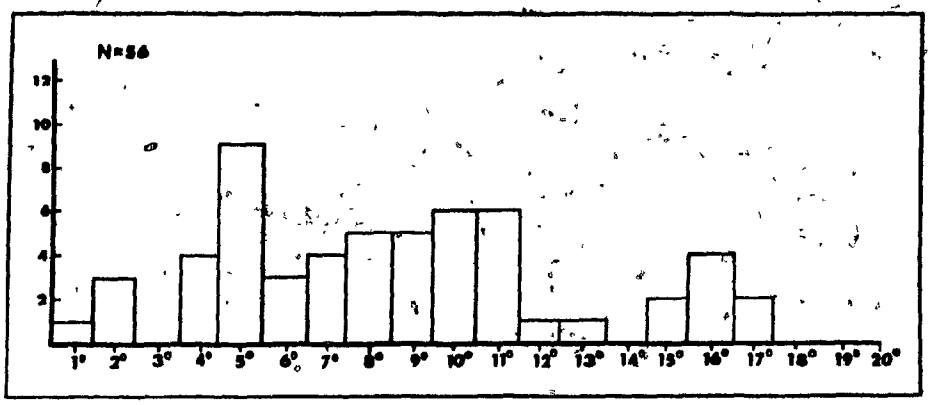


Figure VIII.4 Bar graph of slope segment angles along the mid-bluff bench. (Taken from N-series profiles, Appendix B.)

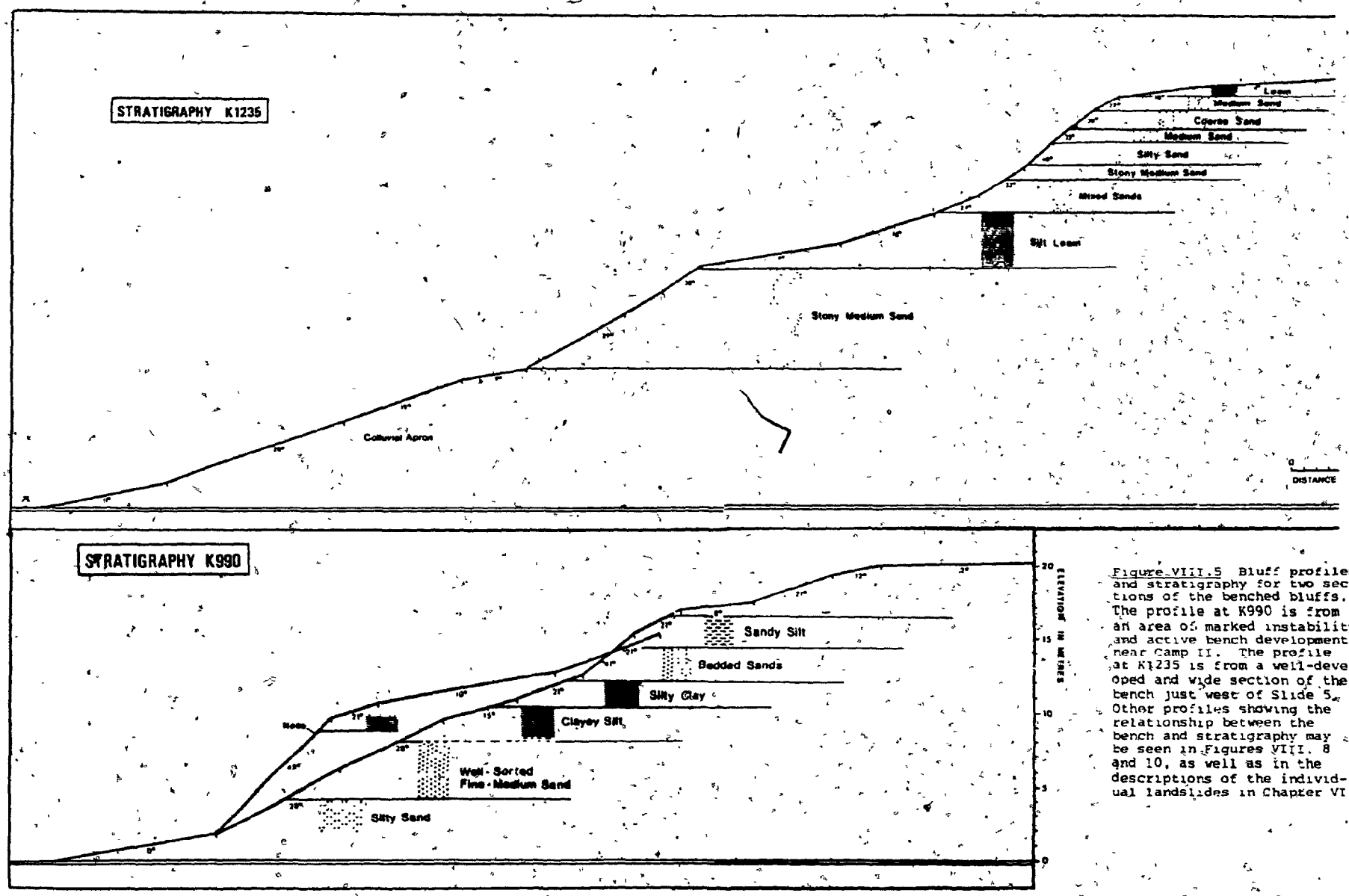


Figure VIII.5 Bluff profiles and stratigraphy for two sections of the benched bluffs. The profile at K990 is from an area of marked instability and active bench development near Camp II. The profile at K1235 is from a well-developed and wide section of the bench just west of Slide 5. Other profiles showing the relationship between the bench and stratigraphy may be seen in Figures VIII. 8 and 10, as well as in the descriptions of the individual landslides in Chapter VI.



Figure VIII.6 Excavation at the downslope edge of the bench slope at K955. The contact between the basal sandy unit and the overlying fine-grained unit is seen in situ. The thickness of the fine-grained unit at this location is only slightly less than that of the active layer. On either side of this bench remnant gullies are actively incising.



Figure VIII.7 Excavation at the downslope egde of a bench segment near K1250. The photograph shows the lower of two bench segments developed along this section of the bluffs. The bluff profile and stratigraphy at this site are reproduced in Figure VIII.8. Again, the fine-grained unit at this location is slightly less thick than the active layer.

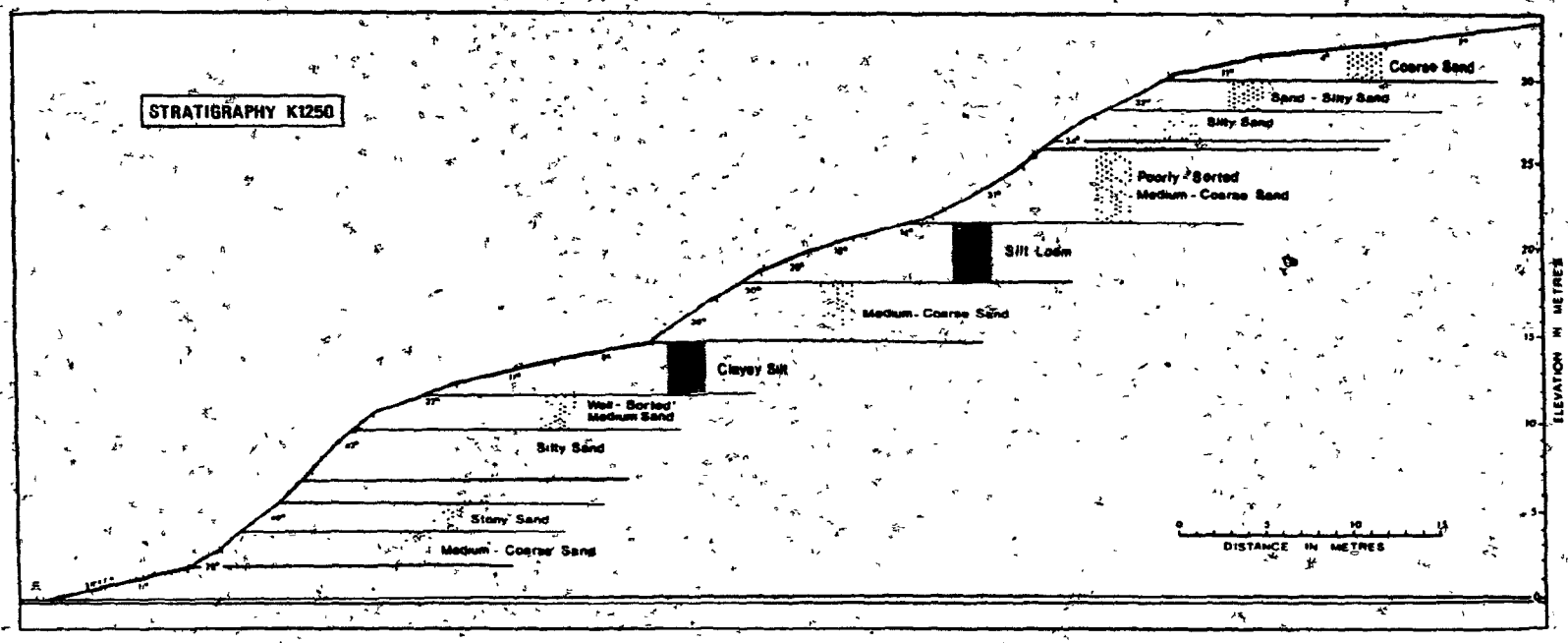


Figure VIII.8 Profile and stratigraphy at K1250, near the western end of the Kivitoo bluffs. Here two bench segments are developed at the level of two fine-grained units. An excavation at the downslope edge of the lower bench segment is shown in Figure VIII.7.

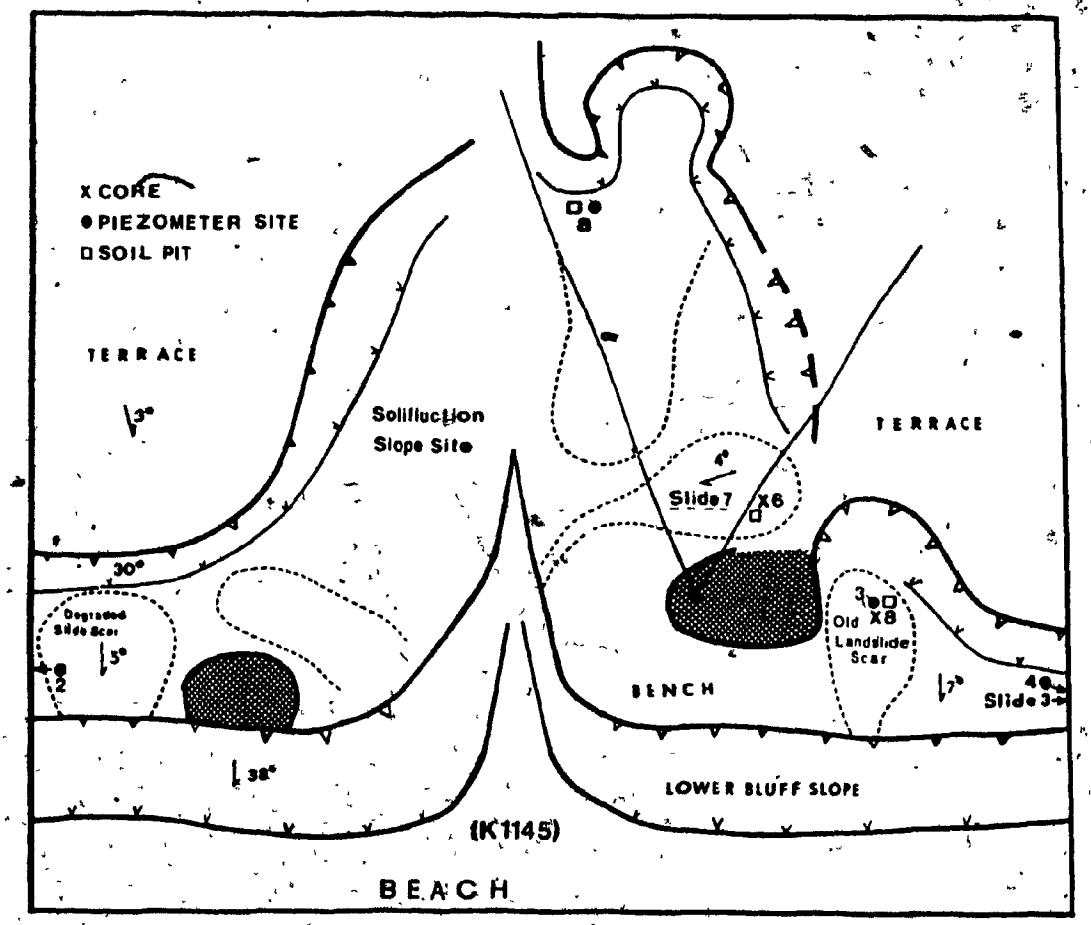


Figure VIII.9a Schematic plan of the mid-bluff bench and its extension along the sides of the stream at K1145. The profile in Figure VIII.10 runs across the small mound to the left of the stream (cross-hatched). The origin of this mound, and that to the right of the stream, is discussed in the text. The photograph, Figure VIII.9b (below), is the view inland from the mound to the right of the stream. Slide 7 is in the foreground.

Figure VIII.9b



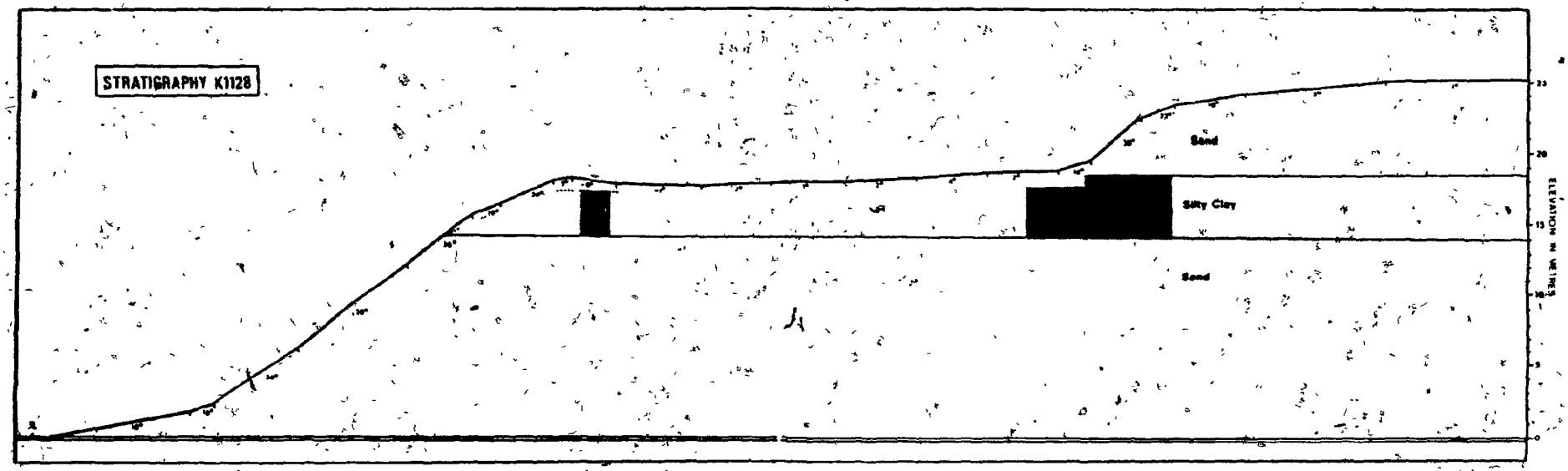


Figure VIII.10 Profile and stratigraphy across mid-bluff bench at K1128. The profile shows the small mound at the seaward edge of the bench, as well as the unusual thickness of the fine-grained unit at this location (i.e., below the mound). The location of the profile is also maked on Figure VIII.9a.

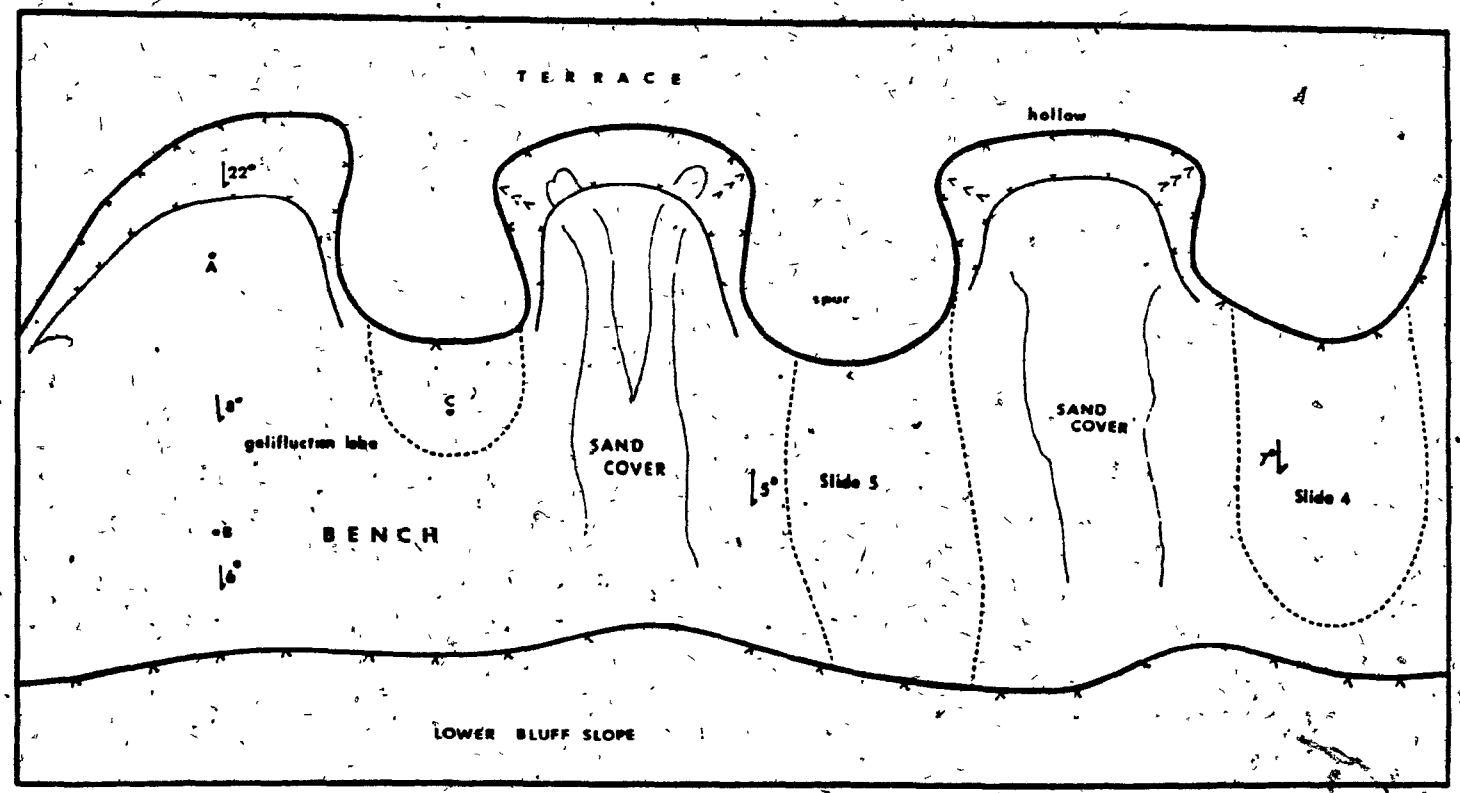


Figure VIII.11 Schematic representation of the wide section of the mid-bluff bench between K1215 and 1235. Landslides are preferentially situated below spurs (noses) in the back slope plan. Downslope of hollows the bench is covered by a thick layer of sands deposited by slope wash. Thus, in the latter locations, the active layer must be unusually thick if the in situ fine-grained soil is to be exposed to prolonged thaw.



Figure VIII.12 View east from K1250. The large colluvial slope (A) below a particularly wide section of the mid-bluff bench is shown extending out beyond the general trend of the coastline. Wave action, along this relatively protected section of the coast, is unable to cut the apron back to conformity with the coast and a beach has developed on this debris.



Figure VIII.13 Quasi-stable vegetated colluvial slope below the mid-bluff bench. Slope angle is 22°. Shallow instability is marked at A. These slopes, which are commonly encountered along the benched bluffs, are considered to be semi-frictional threshold slopes.

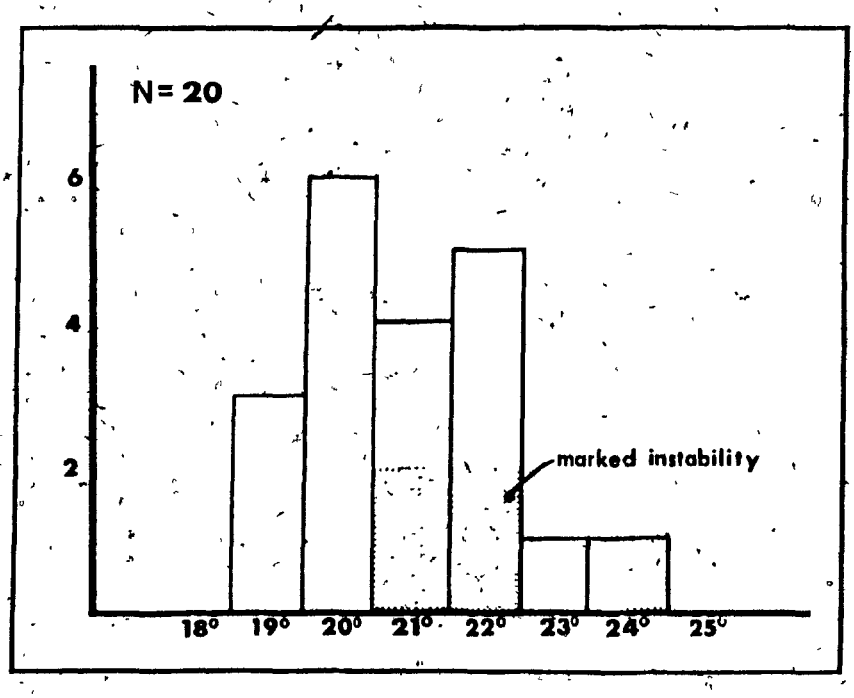


Figure VIII.14 Bar graph of stable and quasi-stable vegetated colluvial slope segments from the lower bluff slope along the benched bluffs. Shaded areas indicate segments with marked instability.

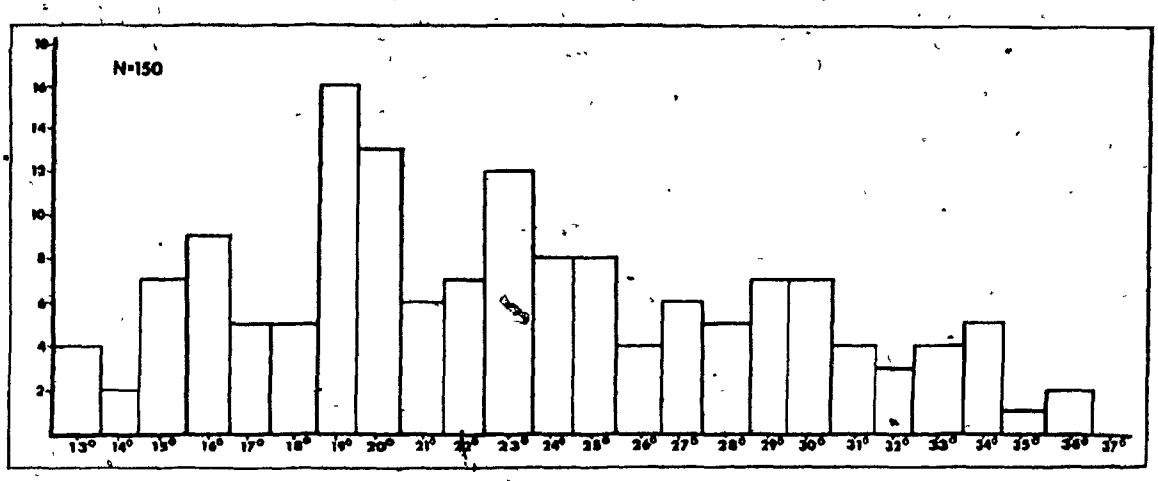


Figure VIII.15 Bar graph of lower bluff slope segment angles along the benched bluffs. The segments are taken from the N-series profiles.

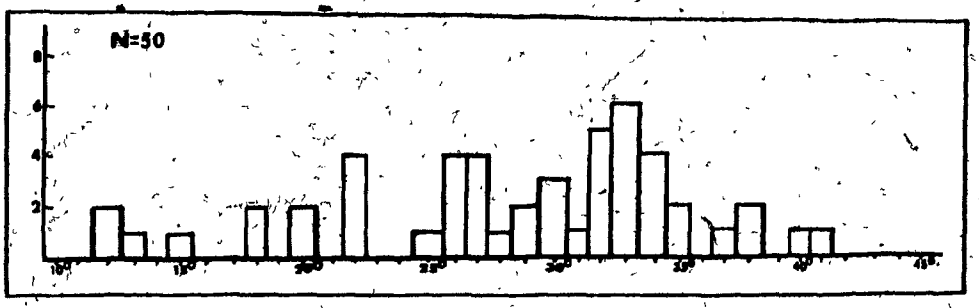


Figure VIII.16 Bar graph of slope segment angles along the bench back slope. The slope segments are culled from the N- series profiles.

CHAPTER IX:

DISCUSSION and SUGGESTIONS FOR FURTHER RESEARCH

A diagramatic summary of the morphological development of the Kivitoo Bluffs is presented in Figure IX.1. Although the stratigraphy along the Kivitoo coast is complex and spatially variable, four distinctive bluff types characterized by the occurrence of specific form-elements, have been identified. The principal factor in the determination of the specific bluff morphology is the local stratigraphy. Particularly important is the occurrence of thick fine-grained units along which gentle slope segments may develop, or thick coarse-grained cap units which may provide a freely draining mantle inhibiting slope flattening and dissection. (Undercut bluffs possessing intermediate lithologies, lacking these two sedimentary units, tend to develop types of steep shallow hollows.) The intensity of basal marine erosion is also important in that it, ultimately, determines the amount of time during which the relevant processes can act upon a given slope. If the rate of undercutting and basal retreat is rapid relative to the rate at which slope failure, regrading and, consequently, the development of individual slope features can occur, bluff dissection may be inhibited and steep slopes maintained. If, however, the rate of basal trimming is reduced, well expressed features and gentler, regraded slopes, such as the mid-bluff bench, can develop. To this extent the bluff morphology is an expression of the local balance between undercutting of the

bluff slope and the rate of operation of bluff-face processes. Along certain sections of the coast the hydrology of the terrace surface behind the bluff may play a significant role in bluff development, primarily as it effects the amount and distribution of run-off and seepage along the bluff face. In many cases, particularly where ice-rich sediments are not abundant, the terrace hydrology is the critical factor in determining the rate of slope flattening (frequency of slope failure) and the location of individual bluff features.

When well developed, as they are along the Kivitoo coastline, the bluff types identified here are distinct entities. In reality however, a continuum of form exists such that the conditions which give rise to a particular bluff morphology may be present to some extent along portions of the coast where other morphogenetic processes predominate. Thus, in some locations complex transitional features -- for example debris-hoppers with axial regrading and widening and therefore tending towards bowl-like form -- would be expected. The geographic integrity and good elaboration of the individual morphological units at Kivitoo is due, in large part, to the lateral continuity of specific stratigraphic and erosive conditions there. Other coastlines may not possess morphological divisions which are as clearly defined spatially.

Associations of morphological features similar to those found at Kivitoo have been recognized along the the Clyde bluffs (B. Mode and P. Drake, pers. comm.) and along river banks on Banks Island, N.W.T. (Miles, 1977). They have also been noted south of Kivitoo and along wave-cut raised deltas on

the coast of Frobisher Bay. These observations suggest that the model of bluff development presented here is widely applicable to coastal bluffs and other undercut slopes developed in unconsolidated or lightly cemented sedimentary deposits in permafrost regions. The morphological model proposed here may therefore serve a useful interpretive function for those interested in the stratigraphy of such bluffs, since a general knowledge of their morphology, as can be obtained from aerial or ground photography, can provide useful information about the nature and sequencing of the bluff sediments. (At Kivitoo it was often easier to locate fine-grained units by noting breaks in slope than it was to find these in good exposures.)

Slope forms resembling those found at Kivitoo also occur along coastal bluffs in unconsolidated sediments or weak rocks in non-permafrost regions. Although the significance of the slope dissection represented by the formation of steep hollows (debris-hoppers) is little appreciated, it appears to be a fundamental form of the degradation of undercut slopes in all environments. In this respect, the main difference between debris-hopper development in temperate and permafrost environments may be that, in the latter, melting snow and ground ice are more significant sources of seepage. Conversely, the presence of permafrost may restrict hollow development somewhat by limiting the amount of time during which the morphogenetic processes can operate, restricting hollow growth and development relative to bluff retreat.

As the processes responsible for hollow development are

predominantly shallow forms of mass wasting and seepage erosion, this type of slope dissection is distinct from the embayment of coastal slopes caused by more deep-seated (often rotational) failures (such as those described by Hutchinson (1969) and Brunsden and Jones (1972) along the coast of England). It is not likely that such deep-seated failure could occur along the Kivitoo coast because of the presence of permafrost. McRoberts and Morgenstern (1974b) have identified large scale, deep-seated landslides in frozen ground. However, these landslides were seated in unfrozen soil beneath the permafrost base. The permafrost at Kivitoo is too thick for such failure to occur.

Bluffs with low gradient slope segments and which exhibit benched morphologies or bowl-like landforms are also found in non-permafrost regions. The (usually deep-seated) mass wasting processes reponsible for their formation (noted in Chapters VII and VIII) are, in these cases, fundamentally different than those operative at Kivitoo. Most often gentle slopes along temperate bluffs are situated beneath steep slopes formed in muddy sediments either by basal erosion or exposure in the backscarps of large deep-seated landslides. Typically, these low gradient slopes are transport slopes along which debris, shed by failure of the steeper superadjacent bluff, is moving downslope as a mudflow. However, shallow, infinite slope-type soil movement is seldom initiated along these gentle non-permafrost slopes, although such mechanisms as undrained loading (Hutchinson and Bhandari, 1971) may produce sufficiently large excess pore pressures to remobilize

quasi-stable muddy soils.

While, threshold slopes have been recognized as significant components in the development of non-permafrost landscapes (Carson, 1975), their existence in permafrost environments was questionable due to the expectation of ubiquitous artesian pore pressure conditions in thawing active layer soils. The documentation of quasi-stable semi-frictional slopes presented in Chapter VIII provides evidence that such threshold slopes may indeed be important in the development of permafrost slopes, at least in non-muddy soils. In muddy soils episodic failure in response to excess pore pressures generated by thaw-related processes can lead to the development of slopes gentler than the expected semi-frictional threshold and in such soils the concept of a threshold slope may not strictly apply (as suggested by Carson, 1976). Furthermore, it is evident that the slow, continuous and shallow soil movements of solifluction which depend upon artesian conditions do not, in most cases, affect the overall stability of the slope on which they occur. In this respect solifluction bears resemblance to soil creep phenomena, imposing a second order of process over the primary shaper of slope form (along the Kivitoo bluffs); rapid mass movement. In concert with the observations and stability analysis presented in Chapters VI and VIII demonstrating infrequent landsliding along bench slopes (under present conditions), these observations provide further evidence running counter to the general perception of widespread (rapid) instability along most periglacial slopes. (Gelifluction, in contrast, may indeed be found on most soil

slopes.)

Lacking suitably extensive observations, the significance of long-term climatic variation in bluff development is difficult to assess. In Chapter VI it was concluded that year-to-year differences in air temperature and insolation effects the depth and rate of seasonal thaw penetration and can lead, in exceptional years, to failure along even gentle slopes in fine-grained soils. Long-term warming trends, by increasing the average seasonal active layer thickness and exposing icy basal layers to accelerated thaw, may therefore result in episodes of intensive instability. However, once a new average seasonal active layer thickness has been established (at the new, higher thaw season temperatures) further instability may be substantially suppressed. This is because a new equilibrium ice profile should develop with the icy basal zone reforming at a deeper level near the base of the newly thickened active layer. This supports the contention, raised in Chapter VIII, that some geomorphic features at Kivitoo, in particular the mid-bluff bench, are, to an extent, 'fossil' forms, presently inactive, which have developed primarily during periods of climatic warming. A corollary of these observations is that the morphogenesis of the bluff slopes in general would be more rapid during periods of warming due to increases in the supply of phreatic water from melt of ground ice, as well as accelerated rates of thaw at those sites where thaw-related instability is a significant factor in slope development.

Perhaps the most dramatic consequences of climatic warming would be variations in the erosional environment related to

changes in sea ice cover. If the period of open water is extended, rates of marine undercutting could be substantially increased. The relationship between ice cover and erosion rates, however, is not straightforward since changes in climate may cause corresponding changes in other factors, such as storminess and the direction of prevailing winds and the thickness of sea ice.

It has been suggested that the significance of extreme rainfall events at Kivitoo is not great considering the rate of basal undercutting and the predominant contribution of melt-derived seepage. In many locations in permafrost environments saturated conditions could be expected for a considerable portion of the thaw season regardless of rainfall amounts. Certainly, active layer saturation as a result of moderate to severe rainfalls is a factor in failure on some of the more persistant, steeper slopes. (For example, the failure at the back of a bench remnant at K890 described in Chapter VI.) However, the overall importance of the extreme rainfall event as an initiator of slope failure in the semi-arid eastern Canadian arctic is not clear. It is possible that, in addition to providing active layer saturation along dryer slopes, warm late season rains, by providing an influx of heat when the active layer is thickest, could result in accelerated thaw, and consequently excesss pore pressure conditions. Although noted many times in the preceeding analysis, it is, however, important to emphasize again that saturation of the active layer alone is insufficient to cause failure <u>on low-gradient slopes</u> and that excess pore pressures and the consequent low

effective stress conditions must be present. Underscoring this point is necessary, since many geomorphologists persist in linking all slope instability to saturated flow conditions, and such simplifications only serve to divert attention from meaningful pursuit of correct process definition.

While recent studies have been of fundamental importance in increasing understanding of the behavior of thawing soils, most of this work has been concerned with the development of an analytical foundation for the modeling of thaw-consolidation processes. Testing of this framework, using both artificially prepared and 'undisturbed' samples of thawed soil, has been carried out by a number of researchers (e.g. Watson et al., 1973; Morgenstern and Smith, 1973; Nixon and Morgenstern, 1974; Roggensack, 1977). These data, when analyzed in conjunction with modifications to the basic thaw-consolidation model which take into account the residual stress, have provided good experimental verification of the analytical solution. However, in laboratory tests soil and thermal boundary conditions are rigorously defined and material homogeneity is maintained. The soil and boundary conditions in the field are certainly more variable and complex than those which apply in the laboratory. Thus, while thaw-consolidation theory appears to provide a valid physical model, its application to geomorphological problems is severely limited by a lack of both appropriate field data and good definition of actual field conditions.

The simplifications involved in the analytical solution (such as a single 'step' thawing temperature) have been shown to present significant problems if thaw-consolidation theory is to be meaningfully applied to the field situation. This has been recognized, and to a degree addressed, by Nixon and his colleagues (e.g. the extensions to the thawing problem discussed in Nixon and McRoberts (1973)). However, these reconsiderations have been largely theoretical, and rigorous verification in the field is again lacking. McRoberts' (1973) and McRoberts and Morgensterns' (1974) investigation applying theory to slope stability problems and backed by field investigations are pioneering in this respect. Yet, these investigations were not concerned with true active layer failures, concentrating as they did on debris lobes in large scale retrogressive failures. The present work has applied thawing soils mechanics theory to the more general problem of active layer processes.

Because the mechanics and thermal dynamics of the thaw-consolidation problem, as manifest in the field, are extemely complex, simplification is unavoidable. Yet, complex numerical models (considering actual active layer profiles, and incorporating a detailed solution to the thawing problem) could be usefully constructed. Then, not only must the soil thermal conditions be correctly modeled, but these solutions must be linked to the soil mechanics model (incorporating information on the in situ mechanical properties of the specific thawing soils). Such detailed modeling remains a promising path for future research.

In Chapter VI a first attempt has been made to redress some of the problems noted above. As such, this portion of the present research has been concerned first with putting existing analytical models to rigorous field testing and, secondly, with attempting to define (in a semi-quantitative manner) the true nature of the thaw-consolidation problem as it exists in nature. Certainly, one of the main points to emerge from the field is the non-representativeness of much of the laboratory data which has been used previously in hypothetical solutions to perceived field thawing conditions. The identification of the icy basal layer, its widespread occurrence in active layer soils, and its potential significance for the instability of thawing slopes is notable as a preliminary linkage of actual field conditions and active layer slope processes. The materially heterogeneous (layered) nature of active layer soils, both in terms of mechanical and thermal properties, must also be fully recognized, as should the widespread significance of such seemingly special cases as large residual stresses and low hydraulic conductivity.

Aside from the determination of in situ soil properties (hydraulic conductivity, compressibility, soil strength) more field data concerned with active layer thermal problems are needed. These should include detailed measurement of thaw rates, their spatial variability and the reasons for these observed variations. Central to the analytical definition of the field thawing problem is a detailed knowledge of the active layer ice profile and how this changes through time. While relatively large amounts of information from deep permafrost

cores are available, detailed data from the active layer and the near-surface permafrost are still scarce. Although the presence of basal icy layers has been documented, virtually nothing is known about ice profiles in the upper active layer. The work of Mackay and Outcalt is notable for its consideration of these topics, but this work is still preliminary and of limited application to geotechnical investigations since the data have not been collected within the context of slope stability problems.

Pehaps the most useful direction for future investigations of thawing slopes will be the development of instrumented study sites. Here, a variety of parameters relevant to the stability of thawing slopes could be measured simultaneously. Such a site would include an array of recording transducer piezometers, thermisters and weather instruments to record air and ground surface temperature. In situ shear tests (shear vane or penetration tests) preformed at regular intervals over the thaw season, along with tests on large undisturbed specimens, would provide necessary soil strength data. Periodic core sampling to keep track of soil water migration throughout the yearly cycle of freezing and thawing should also be a part of such a program.

Further verification of the gelifluction model presented in Chapter VI requires additional data on the in situ porosity of frozen solifluction soils. Also needed are data from strength tests, performed on undisturbed soil specimens at low effective stress levels in order to determine the value of the coefficient of internal friction immediately following thaw.

Instrumentation of thawing solifluction slopes with sensitive transducer piezometers capable of providing a continuous record of pore pressures would be particularly useful, allowing for the detection of the short-lived and areally confined liquefation failures that are suspected to be responsible for gelifluction movements. Similar scale experiments could be attempted in the laboratory.

Stress controlled strength testing of thawing soils is also an avenue for further research. (Most test methods are strain controlled.) Since natural slopes are subject to stress controlled conditions, this type of testing, by more accurately reproducing field conditions, has the potential of yielding more accurate and relevant information. Stress controlled tests may be particularly useful in thawing soils, where the mechanical behavior of the soil is dependent upon a number of factors which may be continually changing over time; for example the swelling of soil peds and the time-dependent creep deformation of the cryogenic structure (which may, for a number of reasons, lead to substantial strain weakening in soils with large in situ water contents).

This research has attempted to integrate detailed geomorphological investigation of a complex landform (the Kivitoo Bluffs) with explanations of the observed slope processes and differences in slope morphology in terms of physical principles. Such an integrative geotechnical approach to the study of natural slopes has not been frequently pursued and the present research is one of the few studies to examine

permafrost slopes in such depth. In the recent past, geomorphologists studying slope processes and desiring a more 'quantitative' approach to the disipline have tended to concentrate on measurement of rates of process operation rather than on the more fundamental problems involved in the mechanics of these processes. As the body of engineering literature concerning permafrost soils develops, the new insights must be taken up and extended by geomorphologists. Such an understanding of earth physics, when coupled with process rate data, provides a powerful lens through which to view the larger problems of landscape development.

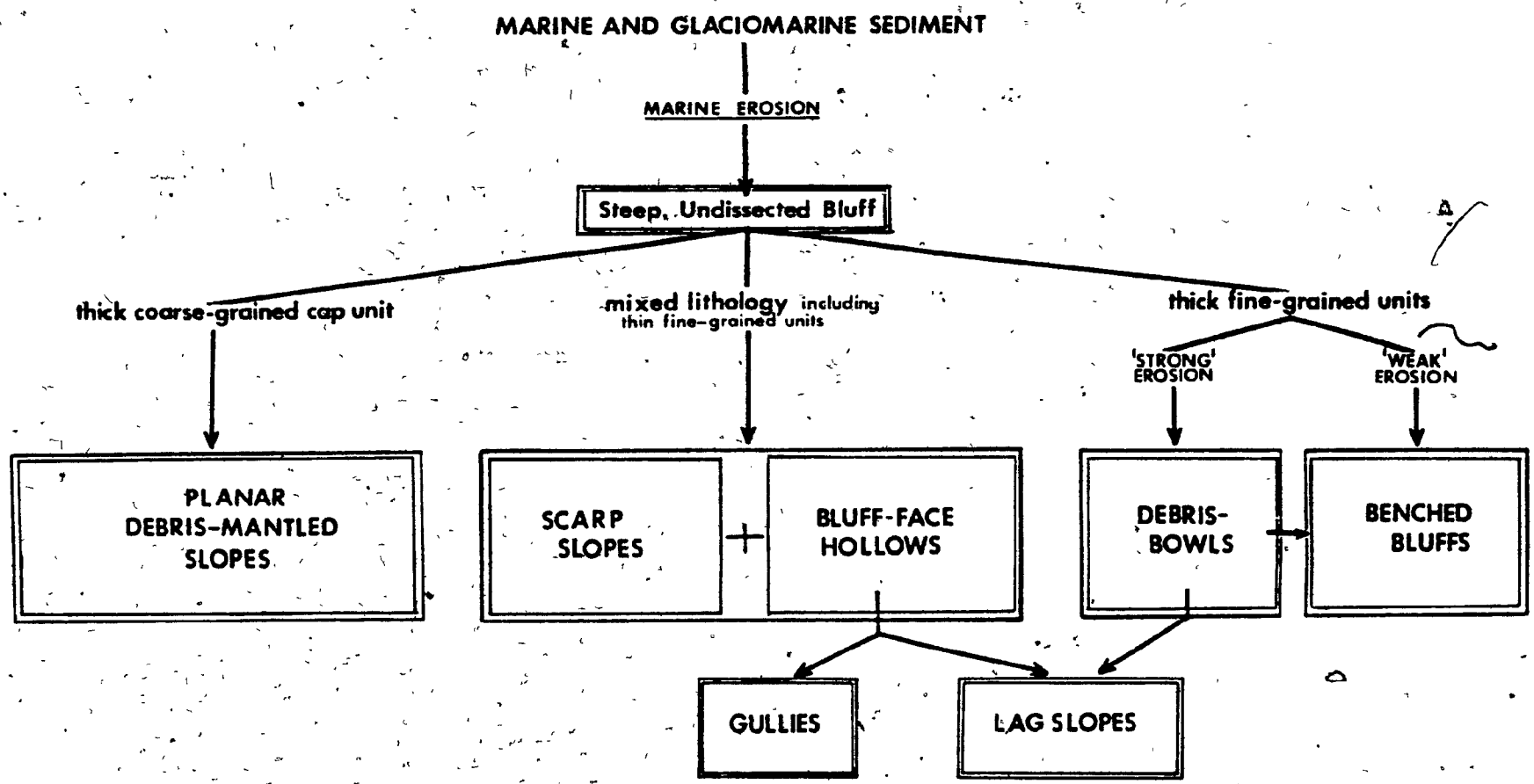


Figure IX.1 Morphological development of the Kivitoo bluffs.

REFERENCES

Allen, J.R.L., 1969, 'Maximum slope attainable by surfaces underlain by bulked equal spheroids with variable dimensional ordering', Bull. Geol. Soc. Am., 80: 1924-1930.

Anderson, J.G., 1906, 'Solifluction, a component of sub-aerial denudation', Jour. Geol., 14: 91-112.

Andresen, A. and Bjerrum, L., 1967, 'Slides in subaqueaous slopes in loose sand and silt', Marine Geotechnique, (A.F. Richards, ed.), University of Illinois, Urbana: 221-239.

Andrews, J.T., 1968, 'Late Pleistocene history of the Istoq Valley, north-central Baffin Island', Meanges de Geog, University Liege, Belgium: 118-133.

_____, Isherwood, W. and Szabo, B.J., 1975, 'Multiple tills, radiometric ages and assessment of the Wisconsin glaciation in Eastern Baffin Island, N.W.T.; Canada: A progress report', Arctic and Alpine Research, 7: 39-59.

_____, and Barry, R., 1972, 'Present and paleo-climate on the glaciation of Cumberland Peninsula, Baffin Island, N.W.T., Canada', Annual Reviews Earth and Planetary Science, 6: 205-228.

_____, and Barry, R.G., 1978, 'Glacial inception and disintegration during the last glaciation' Earth and Planetary Science Letters Annual Review, 6: 205-228.

_____, Barry, R.G., Bradly, R.S., Miller, R.H., and Williams, L.D., 1972, 'Past and present glaciological responses to climate in eastern Baffin Island', Quaternary Research, 2: 303-314.

_____, and Miller, G.H., 1972, 'Quaternary history of northern Cumberland Peninsula, Baffin Island, N.W.T., Canada: Part IV, Maps of the present glaciation limits and lowest equilibrium line altitude for north and south Baffin Island', Arctic and Alpine Research, 4(1): 45-59.

Bagnold, R.A., 1954, Experiments on a gravity-free dispersion of large solid spheres in a Newtonian fluid under shear', Proc. Roy. Soc. Series A, 225: 49-63.

Bjerrum, L., 1968, 'Progressive failure in slopes of Overconsolidated plastic clay and clay shales', Norwegian Geotech. Inst. Pub. No. 77, Oslo, 29pp.

Barry, R.G., Andrews, J.T. and Mahaffy, M.A., 1975, 'Continental ice sheets: conditions for growth', Science, 190: 979-981.

_____, Arindale, W.H., Andrews, J.T., Barry, R.S. and Nichols, H., 1977, 'Environmental change and cultural change in

the eastern Canadian Arctic during the last 5000 years', Arctic and Alpine Research, 9: 193-210.

Barton, M.E., 1973, 'The degradation of Barton Clay Cliffs at Hampshire', Quart. Jour. Eng. Geol., 6: 423-440.

Benedict, J.B., 1970, 'Downslope soil movement in a Colorado Alpine Region: Rates, processes and climatic significance, Arctic and Alpine Research, 2: 165-226.

Beskow, G., 1953, 'Tjalbildningen och tjallyftningen' in Soil Freezing and Frost Heaving with Special Application to Roads and Railroads, Northwestern University, Evanston, Ill., (also, Penner, 1967; op. cit.).

Bird, J.B., 1977, 'Coastal morphology and terrain studies, Kivitoo Peninsula, Baffin Island', Geol. Surv. Can. Paper 77-1C: 53-55.

Boyd, D.W., 1976, 'Normal freezing and thawing degree-days from monthly temperatures', Can. Geotech. Jour., 13: 176-180.

Bradley, R.S., 1972, 'The problem of inversons in estimating the height of glaciation limits in arctic regions', Arctic and Alpine Research, 4: 359-360.

_____ and Miller, G.H., 1972, 'Recent climatic change and increased glaciation in eastern Canadian Arctic', Nature, 237: 385-387.

Brown, J., 1969, 'Ionic concentration gradients in permafrost; CRREL Research Report 272, 25 pp.

Brown, R.J.E., 1972, 'Permafrost in the Canadian Arctic Archipelago Zeit. fur Geom., Suppl. BD 13: 102-130.

Brunsden, D. and Jones, D.K.C., 1972, 'The morphology of degraded landslide slopes in south west Dorset', Quart. Jour. eng. Geol., 5: 205-222.

Bryan, R.B. and Price, A.G., 1980, 'Recession of the Scarborough Bluffs, Ontario, Canada', Zeit. fur Geomorph., Suppl. 34: 48-62.

Carrigy, M.A., 1970, 'Experiments on the angle of repose of granular materials', Sedimentology, 14: 147-158.

Carson, M.A., 1969, 'Models of hillslope development under mass failure', Geol. Analysis, 1: 76-100.

_____, 1971, 'An application of the concept of threshold slopes to the Laramie Mountains, Wyoming', Inst. Br. Geog. Spec. Publ. 3: 31-47.

_____, 1975, 'Threshold and characteristic angles of straight slopes', 4th Guelph Symposium on Geomorphology, (E.

Yatsu, ed.): 19-34.

_____, 1976, 'Mass-wasting, slope development and climate', Geomorphology and Climate, (E. Derbyshire ed.): 101-136.

_____, 1977a, 'Angles of repose, angles of shearing resistance and angle of talus slopes', Earth Surface Processes, 2: 363-380.

_____, 1977b, 'On the retrogression of landslides in sensitive muddy sediments', Can. Geotech. Jour., 14: 582-602

_____ and Kirkby, M.J., 1972, Hillslope Form and Process, Cambridge University Press, Cambridge, England, 475 pp.

_____ and Petley, D.J., 1970, 'The existence of threshold slopes in the denudation of the landscape', Trans. Inst. Brit. Geog. 49: 71-95.

Chamberlain, E.J. and Gow, A.J., 1978, 'Effect of freezing and thawing on the permeability and structure of soils' Proc. First Int. Symp. on Ground Freezing, Ruhr Univ., W. Germany, 31-44.

Chandler, R.J., 1970, 'Solifluction on low-angled slopes in Northamtonshire', Quart. Jour. Eng. Geol., 2: 65-69.

_____, 1972, 'Periglacial mudslides in West Spitzbergen and their bearing on the origin of fossil 'solifluction' shears in low-angled clay slopes, Quart. Jour. Eng. Geol., 5: 223-241.

_____, 1973, 'The inclination of talus, Arctic talus terraces, and other slopes composed of granular material', Jour. Geol., 81: 1-14.

Cassagrande, A., 1976, 'Liquefaction and cyclic deformation of sands: A critical review', Harvard Soil Mechanics Series, No. 88, 27 pp.

Castro, G., 1975, 'Liquefaction and cyclic mobility of saturated sands', Jour. Geotech. Energy Division, A.S.C.E., 6, 551-569.

Christian, J.T. and Whitman, R.V., 1969, 'A one-dimensional model for progressive failure', Proc. 7th Int. Conf. Soil Mech. Fndn. Eng.: 541-545.

Church, M., Stock, R.F. and Ryder, J.M., 1979, 'Contemporary sediment environments on Baffin Island, N.W.T., Canada: Debris slope accumulations', Arctic and Alpine Research, 11: 371-402.

Crawford, C.B. and Eden, W.J., 1967, 'Stability of natural slopes in sensitive clay', Jour. Soil Mech. Fndn. Div., ASCE, 93: 419-436.

Czudek, T. and Demek, J., 1970, 'Thermokarst in Siberia and its influence on the development of lowland relief', Quaternary

Research, 1: 103-120.

Davies, J.L., 1964, 'A morphogenic approach to world shorelines', Zeit. fur Geomorph., 8: 127-142.

_____, 1972, Geographical Variation in Coastal Development, Oliver and Boyd, Edingurgh, 204pp.

Davis, E.H. and Raymond, G.P., 1965, 'A non-linear theory of consolidation', Geotechnique, 15: 161-174.

Deevy, E.S. and Flint, R.F., 1957, 'Postglacial hypsithermal interval', Science, 125: 182-184.

Dekin, A.A. Jr., 1972, 'Climatic change and cultural change; A correlative study from eastern arctic prehistory', Polar Notes, 12: 11-31.

Derbyshire, E., Gregory, K.J., and Hails, J.R., 1979, Geomorphological Processes, Dawson Westview Press, Boulder Colorado, 312 pp.

Dolan, R., Hayden, B., Hornberger, G., Zieman, J. and Vincent, M., 1972, Classification of the Coastal Environments of the World, Part 1, The Americas, Univ. of Virginia, Charlottesville.

Dredge, L.A. and Thom, B.G., 1976, 'Development of a gully-flow near Sept-Isles, Quebec', Can Jour. Earth Sci., 13: 1145-1151.

Dunne, T., 1980, 'Formation and controls of channel networks', Prog. in Phys. Geog., 4: 211-239.

Dusseault, M.B. and Morgenstern, N.R., 1978a, 'Characteristics of natural slopes in the Athabaska Oil Sands', Can. Geotech, Jour., 15: 202-238.

_____, 1978b, 'Shear strength of Athabaska Oil Sands', Can. Geotech. Jour., 15: 216-238.

_____, 1979, 'Locked sands', Quart Jour. Eng. Geol., 12: 117-131.

Dyke, A, 1977, 'Quaternary geomorphology, glacial chronology and sea-level history of Southwestern Cumberland Peninsula, Baffin Island, Northwest Territories, Canada' (unpublished Ph.D. thesis), University of Colorado, Boulder, 185 pp.

_____, 1979, 'Glacial and sea-level history of southwestern Cumberland Peninsula, Baffin Island, N.W.T., Canada', Arctic and Alpine Research, 11: 179-202.

EBA Engineering Consultants Ltd., 1979, 'Geotechnical Evaluation; Arctic Pilot Project, Melville Island Pipeline, EBA Eng. Consul., Edmntn. Alta., 144pp. and Appendicies.

Egginton, P.A., 1981, 'Stability problems associated with sand and gravel pads, central district of Keewatin', Scientific and Technical Notes in Current Research, Part A, Geol. Surv. Can., Paper 81-1A: 385-388.

Embleton, C. and King, C.A.M., 1975, Periglacial Geomorphology, John Wiley and Sons, New York, 203 pp.

Feyling-Hanssen, R.W., 1976, 'The stratigraphy of the Quaternary, Clyde Foreland Formation, Baffin Island, illustrated by the distribution of benthic foramifera', Boreas, 5: 77-94.

French, H.M., 1975, 'Man-induced thermokarst, Sachs Harbour airstrip, Banks Island, Northwest Territories', Can. Jour. Earth Sci., 12: 132-144.

_____ and Egginton, P.A., 1973, 'Thermokarst development, Banks Island, Western Canadian Arctic', Proc. 2nd Int. Permafrost Conf., National Academy of Sciences, Washington, D.C.: 203-212.

Gilbert, G.K., 1880, 'Report on the geology of the Henry Mountains', U.S. Geographical and Geological Survey of the Rocky Mountain Region: 109-118.

Guymon, G.L., 1976, 'Summer moisture-temperature for arctic tundra', Jour. of the Irrigation and Drainage Division, ASCE, 102: 403-411.

Hack, J.T. and Goodlett, J.C., 1960, 'Geomorphology and forest ecology of a mountain range in the central Appalachians', U.S. Geol. Surv. Prof. Paper 347.

Hadley, R.F. and Rolfe, B.N., 1955, 'Development and significance of seepage steps in slope erosion', EOS Am. Geophys. Union Trans., 36: 792-804.

Hamilton, A.B, 1966, 'Freezing shrinkage in compacted clays', Can. Geotech. Jour., 3: 1-17.

Harper, J.R., 1978, 'Coastal erosion rates along the Chukchi Sea coast near Barrow, Alaska', Arctic, 31: 428-433.

Harris, C., 1977, 'Engineering properties, groundwater conditions, and the nature of soil movement on a solifluction slope in north Norway', Quart. Jour. Engng. Geol., 10: 27-43.

_____, 1984, 'Vescicles in thin sections of periglacial soils from north and south, Norway', Permafrost Conference.

Hartwell, A.D., 1972, 'Coastal conditions of arctic northern Alaska', in Terrain and Coastal Conditions on the Arctic Alaskan Coastal Plain, (Sellman et al. eds.), CRREL Special Report 165: 32-72.

Hegginbottom, J.A., 1978, 'An active retrogressive thaw flowslide

on eastern Melville Island, District of Franklin', Scientific and Technical Notes, Current Research, Part A, Geol. Surv. Can. Paper 78-1A: 535-526.

Holtendahl, H., 1959, 'Den norske strandflate, med saerlig henblikk pa dens utvikling i kystomradene pa More', Norske Geogr. Tidsskr., 16: 285-303.

Horner, P.B., Milne, W.G., and McMechan, G.A., 1975, 'Canadian Earthquakes -- 1970', Seismic Series No. 69, Energy, Mines and Resources, Ottawa.

Hutchinson, J.N., 1967, 'The free degradation of London Clay cliffs', Proc. Geotech. Conf. (Oslo), 1: 113-118.

_____, 1969, 'A reconsideration of coastal landslides at Folkestone Warren, Kent',

_____, 1970, ' A coastal mudflow on the London Clay cliffs at Beltinge, North Kent', Geotechnique, 20: 412-438.

_____, 1973, 'The response of London Clay cliffs to differing rates of toe erosion', Geol. Appl. Idrogeol. Univ. Bari., 8: 221-239.

_____, 1974, 'Periglacial solifluction: an approximate mechanism for clayey soils', Geotechnique, 23: 438-443.

_____, 1982, 'Damage to slopes produced by seepage erosion', in Landslides and Mudflows, Reports of the ALMA-ATA International Seminar, Moscow, 250-268.

_____ and Bhandari, R.K., 1971, 'Undrained loading, a fundamental mechanism of mudflows and other mass movements', Geotechnique, 21: 353-358.

Issacs, R.M. and Code, J.A., 1972, Proc. Can. North. Pipeline Conf., Ottawa, Canada, N.R.C.C. Tech. Memo 104: 147-178.

Ives, J.D. and Andrews, J.T., 1963, 'Studies in the physical geography of north-central Baffin Island, N.W.T., Geogr. Bull., 19: 5-48.

_____, Andrews, J.T. and Barry, R.G., 1975, 'Growth and decay of the Laurentide Ice Sheet and comparisons with Fennoscandinavia', Naturwissenschaften, 62: 118-125.

Jackson, G.D. and Taylor, F.C., 1972, 'Correlation of Aphebian rock units in the northeastern Canadian Shield', Can. Jour. Earth Sci., 9: 1650-1669.

John, B.S. and Sugden, D.E., 1971, 'Raised marine features and phases of glaciation in the South Shetland Islands', British Antarctic Survey Bull., 24: 45-111.

_____, 1975, 'Coastal geomorphology of high latitudes',

Prog. in Geog., 7: 53-132.

Johnson, G.H., 1981, Permafrost: Engineering Design and Construction, John Wiley and Sons, Toronto, 540pp.

Johnson, R.G. and McClure, B.T., 1976, 'A model for Northern Hemisphere continental ice sheet variation', Quaternary Research, 6: 325-353.

Jones, J.A.A., 1978, 'Extending the Hewlett model of stream run-off generation', Area, 11: 110-114.

Jumikis, A.R., 1977, Thermal Geotechnics, Rutgers Univ. Press, New Brunswick, N.J., 375pp.

Kerfoot, D.E., 1969, 'The geomorphology and permafrost condition of Garry Islands, N.W.T.', Unpubl, Ph.D. thesis, Univ. Brit. Columbia, Vancouver, B.C.

Kersten, M.S., 1949, 'Laboratory research for the determination of thermal properties of soils' Final Report, Eng. Exp. Station, Univ. Minnisota, Minneapolis.

King, C.A.M., 1969, 'Some Arctic coastal features around Foxe Basin and in east Baffin Island, N.W.T., Canada', Geografiska Annaler, 51A: 207-218.

King, L.H., 1972, 'Relation of plate techtonics to the geomorphic evolution of the Canadian Atlantic Provinces', Geol. Soc. Am. Bull., 83: 3083-3090.

Kirkby, M.J., 1978, Hillslope Hydrology, John Wiley and Sons, New York: 389.

Kirkham, D., 1945, 'Proposed method for field measurement of permeability of soil below the water table', Soil Sci Soc. Am. Proc., 10: 58-68.

Kirkpatrick, W.M., 1965, 'Effects of grain size and grading on the shearing behavior of granular materials', Proc. 6th Int. Conf. Soil Mech. Found. Eng., Univ. of Toronto Press: 273-277.

Lambe, W.T., 1951, Soil Testing for Engineers, John Wiley and Sons, New York, 165pp.

_____, and Whitman, R.V., 1969, Soil Mechanics, John Wiley and Sons, Inc., New York, 553 pp.

Lane, K.S., 1948, 'Treatment of frost sloughing slopes', Proc. 2nd Int. Conf. Soil Mech. Eng. (Rotterdam), 3: 281-283.

Leffingwell, E. de K., 1919, 'The Canning River region, northern Alaska', U.S. Geol. Surv. Prof. Paper 109: 251 pp.

Lewellen, R.I., 1970, 'Permafrost erosion along the Beaufort Sea coast', Arctic Inst. North America, Tech. Report ONR-382 1: 25

pp.

Linell, K.A., 1966, 'Description and classification of frozen soils', Proc. Permafrost Int. Conf., National Academy of Sciences, Washington, D.C., 481-487.

Lohnes, R.A. and Handy, R.L., 1968, 'Slope angles in friable loess', Jour. of Geol., 76: 247-258.

Loken, O.H., 1965, 'Postglacial emergence at the south end of Inugsuin Fiord, Baffin Island, N.W.T.', Geog. Bull., 7: 243-258.

_____, and Hodgson, D.A., 1971, 'On the submarine geomorphology along the east coast of Baffin, Canada', Can. Jour. Earth Sci., 8: 185-195.

Luckman, B.H., 1971, 'The role of snow avalanches in the evolution of alpine talus slopes', Inst. Brit. Geog. Spec. Pub. No. 3: 93-110.

Lunardini, V.J., 1981, Heat Transfer in Cold Climates, Van Nostrand Reinhold Company, New York, 731 pp.

Mackay, J.R., 1963, 'Notes on the shoreline recession along the coast of the Yukon Territory', Arctic, 16: 195-197.

_____, 1966, 'Segregated epigenetic ice and slumps in permafrost, Mackenzie Delta Region, N.W.T., Geogr. Bull. Can., 8: 59-80.

_____, 1972a, 'The world of underground ice', Ann. Assoc. Am. Geog., 62: 1-22.

_____, 1972b, 'Offshore permafrost and ground ice, Southern Beaufort Sea, Canada', Can. Jour. Earth Sci., 11: 1550-1561.

_____, 1974, 'Reticulate ice veins in permafrost northern Canada', Can. Geotech. Jour., 11: 230-237.

_____, 1977a, 'Pulsating pingos, Tktoyaktuk Peninsula, N.W.T.', Can. Jour. Earth Sci., 14: 209-222.

_____, 1977b, 'Probing for the bottom of the active layer', G.S.C. Report of Activities, Part A: 327-328.

_____, 1980, 'The origin of hummocks, western Arctic Coast, Canada', Can. Jour. Earth Sci., 17: 996-1006.

_____, 1981, 'Active layer slope movement in a continuous permafrost environment, Garry Island, Northwest Territories, Canada', Can. Jour. Earth Sci., 18: 1666-1680.

_____, 1983, 'Downward water movement into frozen ground, western arctic coast, Canada', Can Jour. Earth Sci., 20:

120-134.

Manley, G., 1959, 'The late-glacial climate of northwest England', Proc. Liverpool and Manchester Geol. Soc., 1: 188-215.

McGhee, R., 1972, 'Climatic change and the development of Canadian Arctic cultural conditions', in Climate Changes in Arctic Areas During the Last Ten Thousand Years, (Y. Vasari, H. Hyvarinen, S. Hicks, eds.), Acta Univ. Ouluensis, Ser. A, No. 3, Geol;. No. 1: 39-60.

_____, and J.A. Tuck, 1976, 'Un-dating the Canadian Arctic, in Eastern Arctic Prehistory and Paleoeskimo Problems (M.A. Maxwell ed.), Mem. Soc. Amer. Archaeol., 31: 6-14.

McGill University, 1963, 'A Report of the Physical Environment of Central Baffin Island', RAND Research Mem. 2837, 375pp.

McMillan, N.J., 1973, 'Shelves of Labrador Sea and Baffin Bay Canada', in Future Petrolium Provinces of Canada, (R.G. McGossan ed.), Am. Soc. Petrol. Geol. Mem. 1: 473-517.

McRoberts, E.C., 1973, 'Stability of slopes in permafrost', (Unpubl. Ph.D. thesis), Univ. Alberta, Edmonton, Alberta.

_____, 1975, 'Field observations of thawing in soils', Can. Geotech. Jour. 12: 126-130.

_____, and Morgenstern, N.R., 1974a, 'The stability of thawing slopes', Can. Geotech. Jour., 11: 447-469.

_____, 1974b, 'Stability of slopes in thawing soil', Can. Geotech. Jour., 11: 554-573

_____, and Nixon, J.F., 1975, 'Reticulate ice veins in permafrost, Northern Canada: Discussion', Can. Geotech. Jour., 12: 159-162.

Middleton, G.V. and Hampton, M.A., 1976, 'Subaqueous sediment transport and deposition by sediment gravity flows', in Marine Sediment Transport and Environmental Management, (Stanley, D.J. and Swift, D.J.P., eds.), John Wiley and Sons, New York: 197-218.

Miles, M.J., 1977, 'Coast and riverbank stability on Banks Island, N.W.T., Canada', Proc. Third Natl. Hydrotech. Conf., 2: 972-1001.

Miller, G.A., 1973, 'Late Quaternary glacial and climatic history of Northern Cumberland Peninsula, Baffin Island, N.W.T., Canada', Quaternary Research, 3: 571-583.

_____, and Bradley, R.S., 1976, 'The shaping of a land: Geology, climate and ice age history', in The Land That Never

Melts Auyuittyg National Park, R. Wilson ed., 1-61.

_____, Andrews, J.T. and Short, S.K., 1977, 'The last interglacial/glacial cycle, Clyde Foreland, Baffin Island, N.W.T.:Stratigraphy, biostratigraphy and chronology', Can. Jour. Earth Sci., 14: 2824-2857.

Mitchell, R.J. and Markell, A.R., 1974, 'Flowsliding in sensitive soils', Can. Geotech. Jour., 11:11-31.

Morgenstern N.R. and Nixon, J.P., 1971, 'One-dimensional consolidation of thawing soils', Can. Geotech. Jour., 8: 558-565.

_____, 1975, 'An analysis of the performance of a warm-oil pipeline in permafrost, Inuvik, N.W.T.', Can. Geotech. Jour., 12: 196-208.

_____, and Smith, L.B., 1973, 'Thaw-consolidation tests on remoulded clays', Can Geotech Jour., 10: 25-40.

Mosley, M.P., 1972, 'Evolution of a discontinuous gully system', Ann. Accoc. Am. Geog., 62: 655-663.

Nansen, F., 1922, 'The strandflat and isostacy', Oslo: 313 pp.

Nelson, A.R., 1978, 'Quaternary glacial and marine stratigraphy of the Qivitu Peninsula, North Cumberland Peninsula, Baffin Island, Canada', Unpubl. Ph.D. thesis, Univ. of Colorado: 299 pp.

_____, 1980, 'Chronology of Quaternary landforms, Qivitu Peninsula, Northern Cumberland Peninsula, Baffin Island, N.W.T., Canada', Arctic and Alpine Research, 12: 256-286.

_____, 1981, 'Quaternary glacial and marine stratigraphy of the Qivitu Peninsula, north Cumberland Peninsula, Baffin Island, Canada', Geol. Soc. America Bull. , Pt. II, 92: 1143-1261.

Nelson, F., and Outcalt, S.I., 1984, 'A frost index number for spacial prediction of ground-frost zones', Proc. 4th Int. Conf. Permafrost, National Academy of Sciences, Washington, D.C., 907-911.

Newbury, R.W., Beaty, K.G. and McGullough, G.K., 1978, 'Initial shoreline erosion in a permafrost affected resevoir', Proc. 3rd Int. Conf. Permafrost, National Research Council, Ottawa: 833-839.

Nichols, H., 1967, 'The post-glacial history of vegetation and climate at Ennadai Lake, Keewatin, and Lynn Lake, Manitoba, (Canada)', Eiszeitelter und Gregenwart, 18: 176-197.

Nicholson, F.H. and Lewis, J.S., 1976, 'Active layer and suprapermafrost groundwater studies; Schefferville, Quebec',

Proc. 2nd Conf. Soil Water Problems in Cold Regions, Edmntn. Alta.: 15-30.

Nielson, N., 1979, 'Icefoot processes. Observations of erosion on a rocky coast, Disko, Greenland', Z. Geomorph., N.F., 23: 321-331.

Nixon, J.F., 1973, 'Thaw-consolidation in some layered systems', Can. Geotech Jour. 8: 558-565.

_____, and McRoberts, E.C., 1973, 'A study of some factors affecting the thawing of frozen soils', Can. Geotech. Jour., 10: 439-452.

_____, and Morgenstern, N.R., 1973a, 'The residual stress in thawing soils', Can. Geotech. Jour., 10: 617-631.

_____, 1973b, 'Practical extensions to a theory of consolidation for thawing soils', Proc. 2nd Int. Conf. Permafrost, NAS, 369-377.

_____, 1974, 'Thaw-consolidation on undisturbed fine-grained permafrost', Can Geotech. Jour., 11: 202-214.

Oceanographic Atlas of the Polar Seas, 1958, Part II, Arctic. U.S. Naval Oceanographic Office, Washington, D.C., H.O. Pub. No 705.

Outcalt, S.I., 1982, 'Massive near-surface ground ice in arctic Alaska: Description and modeling analysis, Physical Geography, 3: 123-147.

Parmuzina, O.Yu., 1978, 'Cryogenic texture and some characteristics of ice formation in the active layer', (In Russian: cited in Mackay, 1983; op. cit.).

Pelletier, B.R., Ross, O.I., Keen, C.E. and Keen, M.J., 1974, 'Geology and geophysics of Baffin Bay', in Offshore Geology in Eastern Canada, Geol. Surv. Can. Paper 74-30, 2: 247-258.

Penner, E., Johnson G.H. and Goodrich, L.E., 1974, 'Thermal conductivity laboratory studies of some Mackenzie Highway soils', Can. Geotech. Jour., 12: 271-289.

Pettibone, H.C. and Kealy, C.D., 1971, 'Engineering properties of mine tailings', Jour. Soil Mech. and Fndn. Division, ASCE: 1207-1225.

Pheasant, D.R., 1971, 'The glacial chronology and glacio-isostacy of the Narpaing-Quajon Fiord area Cumberland Peninsula, Baffin Island', (unpubl. Ph.D. thesis), Univ. of Colorado, Boulder: 232 pp.

_____, and J.T. Andrews, 1973, 'Wisconsin glacial chronology and relative sea level movements, Narpaing Fiord -

Broughton Island area, eastern Baffin Island, N.W.T.', Can. Jour. Earth Sci., 10: 1621-1641.

Pierson, T.C., 1981, 'Dominant support mechanisms in debris flows at Mt. Thomas, New Zealand, and implications for flow mobility', Sedimentology, 28: 49-60.

_____, 1983, 'Soil Pipes and slope stability,' Quart. Jour. Engng. Geology, 16: 1-11.

de Ploey, J., 1977, 'Some experimental data on slopewash and wind action with reference to Quaternary morphogenesis in Belgium', Earth Surface Processes, 2: 101-115.

Pollard, W.H. and French, H.M., 1980, 'A first approximation of the volume of ground ice, Richards Island, Pleistocene Mackenzie Delta, Northwest Territories, Canada, Can. Geotech. Jour., 5: 1381-1386.

Potrashkov, G.D. and Khrustalev, L.N., 1961, ' Concerning the effect of thawed clayey soils', (in Russian: cited in Savely'ev, 1972; op. cit.)

Price, L.W., 1973, 'Rates of mass wasting in the Ruby Range, Yukon Territory', Proc. 2nd Int. Permafrost Conf., National Academy of Sciences, Washington, D.C.: 235-245.

Pufahl, D.E. and Morgenstern, N.R., 1979, 'Stabilization of planar landslides in permafrost', Can. Geotech. Jour., 16: 734-747.

Quigley, R.M., Gelinas, P.J., Bou, W.T., and Packer, R.W., 1977, 'Cyclic erosion-instability relationships: Lake Erie north shore bluffs', Can. Geotech. Jour., 14: 310-323.

Rapp, A., 1960, 'Recent developments of mountain slopes in Karkevagge and surroundings, northern Scaninavia', Geogr. Annlr., 42: 71-200.

Reusch, H., 1894, 'The Norwegian coast-plain', Jour. Geol., 2: 347-349.

Rodine, J.D. and Johnson, A.M., 1976, 'The ability of debris, heavily freighted with coarse clastic materials, to flow on gentle slopes', Sedimentology, 23: 213-234.

Roggensack, W.D., 1977, 'Geotechnical Properties of Fine-Grained Permafrost', (unpubl. Ph.D. thesis), University of Alberta, Edmonton.

Rowe, P.W., 1963, 'Stress-dilatancy, earth pressures and slopes', Jour. Soil Mech. Found. Division, 3: 37-61.

Rowley, R.K., Watson, G.H., Auld, R.G. and Wilson, T.M., 1973, 'Performance of a 48-inch warm-oil pipeline supported in permafrost', Can. Geotech. Jour., 10: 282-303.

Rycroft, D., 1971, 'Drainage investigations in the Southwest', Ann. Rep., Exp. Unit, Ministry of Agriculture, Fisheries and Food, Cambridge, (cited in Carson, 1976; op. cit.), 7-15.

Savel'yev, V.S., 1972, 'Effects of groundwater on stability of slopes and structures erected on them on thawing of frozen soils', U.S. CRREL Draft Translation TL 369, Hanover, N.H.: 10 pp.

Savigear, R.A.G., 1965, 'A technique of morphological mapping', Ann. Ass. Am. Geogr., 55: 514-538.

Schumm, S.A., 1956, 'The role of creep and rainwash in the retreat of badland slopes', Am. Jour. Sci., 254: 693-706.

Seed, H.B., 1968, 'Landslides during earthquakes due to soil liquefaction', Jour. Soil Mech. Fndn. Eng., ASCE, 94: 1055-1122.

Sharp, R.P., 1966, 'Kelso dunes, Mohave Desert, California', Geol. Soc. Am. Bull., 77: 1045-1074.

Siple, P.A., 1952, 'Ice blocked drainage as a principal factor in frost heave, slump and solifluction', in Frost Action in Soils, Highw. Res. Bd. Spec. Rept. No. 2: 172-175.

Skempton, A.W., and Bishop, A.W., 1950, 'The measurement of shear stress in soils', Geotechnique, 2: 90-108.

_____, and DeLory, F.A., 1957, 'Stability of natural slopes in London Clay', Proc. 4th Intl. Conf on Soil Mech. and Found. Eng., 2: 90-108.

Smalley, I., 1971, 'Nature of quick clays', Nature, 231: 310.

Stangl, K.O., Roggensack, W.D., and Hayley, D.W., 1982, 'Engineering geology of surficial soils, eastern Melville Esland', 4th Canadian Permafrost Conf., 136-147.

Statham, I., 1974, 'The relationship of porosity and angle of repose to mixture proportions in assemblages of different sized materials, Sedimentology, 21: 149-162.

Strahler, A.N., 1950a, 'Equilibrium theory of erosional slopes approached by frequency distribution analysis: Part I', Am. Jour. Sci., 248: 673-696.

_____, 1950b, 'Equilibrium theory of erosional slopes approached by frequency distribution analysis: Part II', Am. Jour. Sci., 248: 800-814.

Sugden, D.E. and Watts, S.H., 1977, 'Tors, felsenmeer, and glaciation in northern Cumberland Peninsula, Baffin Island', Can. Jour. Earth Sci., 14: 2817-2823.

Swithinbank, C., 1960, Ice Atlas of Arctic Canada, Defense

Research Board, Ottawa.

Taber, S., 1943, 'Perenially frozen ground in Alaska: its origin, and history', Geol. Soc. Am. Bull., 54: 1433-1548,

Tam, S.W., 1975, 'Mechanisms and spatial patterns of erosion in the Toes River Basin, Barbados', Unpubl. Ph.D. thesis, McGill University,

Taylor, R.B., 1980, 'Coastal environments along the northern shore of Somerset Island, District of Franklin', in The Coastline of Canada, (S.B. McCann, ed.), G.S.C. Paper 80-10: 239-250.

Terzaghi, K., 1943, Theoretical Soil Mechanics, John Wiley and Sons, New York.

_____, 1962, Stability of steep slopes on hard unweathered rock', Geotechnique, 12: 251-270.

_____, and Peck, R.B., 1948, Soil Mechanics in Engineering Practice, John Wiley and Sons, New York, 566pp.

Tsytovich, N.A., 1955, 'Investigation of effects of freezing and thawing conditions on porosity of water-saturated sands', U.S.S.R. Academy of Science Press, Moscow. (in Russian: cited in Savael'vey, 1972: op. cit.).

_____, 1975, The Mechanics of Frozen Ground, (Trans. from Russian), McGraw Hill, Washington, D.C., 426pp.

Tuckfield, C.G., 1964, 'Gully erosion in the New Forest, Hampshire', Am. Jour. Sci., 262: 795-807.

Vallejo, L.E., 1980, 'A new approach to the stability analysis of thawing slopes', Can. Geotech. Jour., 17: 607-612.

Washburn, A.L., 1947, 'Reconnaissance geology of portions of Victoria Island and adjacent regions', Geol. Soc. Am., Memoir 22, 142pp.

_____, 1967, 'Instrumental observations of mass-wasting in the Mesters Uig District, Northeast Greenland', Medd. am Gronland, 166: 318 pp.

_____, 1973, Periglacial Processes and Environment, Edward Arnold, London: 320 pp.

_____, 1980, Geocryology: a survey of periglacial processes and environments, John Wiley and Sons, New York, 406pp.

Watson, G.H., Slusarchuk, W.A. and Rowley, R.K., 1973, 'Determination Some frozen and thawed properties of permafrost soils', Can. Geotech. Jour., 10: 592-606.

Weeks, A.G., 1969, 'The stability of natural slopes in S.E. England as affected by periglacial activity', Quart. Jour. Eng. Geol., 2: 49-61.

Wentworth, C.K., 1943, 'Soil avalanches on Oahu, Hawaii', Bull. Geol. Soc. Am., 54: 53-64.

Williams, P.J., 1959, 'An investigation into the processes occurring in solifluction', Am. Jour. Sci., 251: 481-490.

_____, 1966, 'Downslope soil movement at a subarctic location with regard to variations with depth', Can. Geotech. Jour., 3: 191-203.

_____, 1967, 'Properties and behavior of freezing soils', Norwegian Geotech. Inst. Publ. 72: 119 pp.

Worth, C.P. and Wood, D.M., 1978, 'The correlation of index properties with some basic engineering properties of soils', Can. Geotech. Jour., 15: 137-145.

Wright, R.K., 1981, 'The water balance od a lichen tundra underlain by permafrost', McGill Subartic Research Paper No. 33, Centre for Northern Studiea and Research, McGill University, Montreal, 110pp.

Wu, T.H., 1966, Soil Mechanics, Allyn and Bacon, Inc., Boston: 431 pp.

_____, and Sangrey, D.A., 1978, 'Strength properties and their measurement', in Landslides: Analysis and Control, Special Report 176, Trans. Res. Bd., National Academy of Sciences, 139-154.

Youd, T.L., 1973, 'Liquefaction, Flow and Associated ground failure, U.S. Geological Survey Circular 688, 12 pp.

Young, A., 1971, 'Slope profile analysis: the system of best units', in Slopes Form and Process, (D. Burnsden, ed.), Inst. of Brt. Geog. Spec. Pub. 3: 1-13.

_____, 1972, Slopes, Oliver and Boyd, Edinburgh, 288 pp.

Zenkovitch, V.P., 1967, Processes of Coastal Development, Edinburgh, Oliver and Boyd: 738 pp.

APPENDIX A

1. Addenda to text
   a. Solution for hydraulic conductivity measurement from a single piezometer tube
   b. Further comments on the thawing of active layer soils
2. Tilting box data set
3. Consolidation test data from thawed and frozen/thawed soil specimens from Kivitoo bench slopes

Solution for hydraulic conductivity measurement from a single piezometer tube

The in situ hydraulic conductivity (ku) of a soil may be determined by introducing a volume of water into the piezometer tube and allowing it to drain into the soil. If the depth of the piezometer tip and the height of the water column at times t1 and t2 are known then the following equation (from Kirkby 1945) may be used

$$ku = \frac{\pi b^2 \ln[(l1 - d)/(l2 - d)]}{(t2 - t1) A}$$

where b is the radius of the tube at the soil surface, l1 and l2 are the height of the water column above the piezometer tip at t1 and t2 respectively, d is the height of the water table above the piezometer tip, and A is a function of the piezometer outlet area and the depth of the tip below the water table (d). For a sperical cavity

$$A = \frac{4 \pi [1 + (r/d)^2]}{(1/rw) - [(1/2)d]}$$

where rw is the radius of the cavity, the term $(r/d)^2$ is small and can be neglected. Since the tips of the piezometers used at Rivitoo were not spherical, but cylindrical, A was calculated for a sphere of the same surface area as the cylinder and found to be equal to 14.5 cm.

Further comments on the thawing of active layer soils

As air temperature would be expected to be the same at all the sites, the observed range in the back-calculated step temperature values must be due to other factors. The two most probable reasons for the observed variations are (1) between-site differences in soil thermal properties so that the values of Ku and L used in Eq.VI.10 are not appropriate for all the sites, and (2) real differences in Ts due to spatially variable air/ground surface temperature relationships. While the values of Ku and L which have been used are considered to be representative average values for the active layer along the bench as a whole, the specific values (especially the value of L) may vary widely between sites leading, in part, to the observed variations in thaw rate. The Kivitoo data indicate that the effect of expected variations in the moisture content of the frozen soil (i.e. L) on thaw rates would be greater than that of the thawed soil (on Ku), as the latter typically has a relatively narrow moisture content range 15-30%.

Site specific differences between air and ground surface temperature are another probable cause of between-site variation in thaw rate and, therefore, back-calculated step temperature. Lunardini (1981) provides a correction, or 'n-factor', to comply with this relationship. (See also Johnson, 1981.) The n-factor is defined as $n = Ts/Ta$ where Ts is the temperature at the ground surface and Ta is the air temperature. Typical values of the n-factor are 0.73 for bare soil, 1.0 for a wet surface, 1.3 - 2.0 for gravel and 0.37 for peat. Values close to unity are

reasonable for much of the bench slope at Kivitoo, where the water table is close to the surface. However, at some of the drier sites, the n-factor may be estimated to be as high as 1.5-2 (although no actual measurements were made). (The value of the n-factor may be effected not only by air temperature, but also by the amount of direct solar insolation (particularly on dry surfaces), and therefore upon the reletive cloudiness, of the particular thaw season.) Significantly, the lowest back-calulated value of the step temperature (1.6@C) was obtained for a site where the water table was at the surface during the entire thaw season. This site would be most likely to have an n-factor close to unity. Consequently, the back-calculated step-temperature from this site may be the one most truely representative of the average air thawing step temperature for the summer season. N-factors in excess of unity would also partly account for the relatively deep thaw depths which were noted early in the thaw season (if the time of thaw initiation is predicated using air temperature data alone). If the value of the n-factor is large, for example in dryer snow-free sites, the active layer may be tens of cms thick before daily mean air temperature has risen above 0@C.

Between-site variation in thaw rate may also arise from local differences in mass heat transfer by such vectors as groundwater through-flow and rainfall infiltration. Although the magnitude of such transfers at Kivitoo is unknown, it is likely to be small, due to the relatively low thaw season temperatures (compared to other arctic and sub-arctic locations), thick phreatic zones (promoting run-off of rainfall), and gentle slope gradient and low hydraulic conductivity soils (which would reduce through-flow and

infiltration rates). Since thermal conductivity of unsaturated soil tends to be lower than that of saturated soil, fluctuations in the local water table could also give rise to variations in the thermal conductivity of the active layer, and thereby affect thaw rates. However, since a dryer surface may have a larger n-factor, these effects may be, to some degree, mitigated.)

Tilting Box Test Results

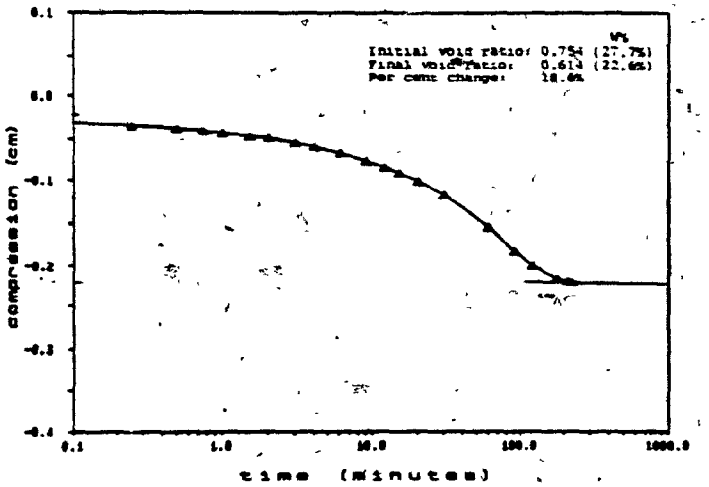
Test No.	Angle of initial yield	Angle of repose slope
1	41.5°	34°
2	43.5°	33.5°
3	40°	35° (small avalanche)
4	38°	34°
5	38.5°	34.5°
6	45° (tamped)	34°
7	44° (tamped)	32.5°
8	41°	34°
9	42.5° (tamped)	35°
10	40°	35°
11	41°	34°
12	39.5°	33.5°
13	41.5°	34.5°
14	38.5°	33.5°
15	41°	34.5°
16	37.5°	34°
17	39°	34.5°
18	38°	33°
19	45°	34.5°
20	41°	34.5°
	$\bar{x}$ = 40.3°	$\bar{x}$ = 34.1°
		sd = 0.77°
		$S_{\bar{x}}$ = 0.17°

95% chi² limits = 34.4-33.8°

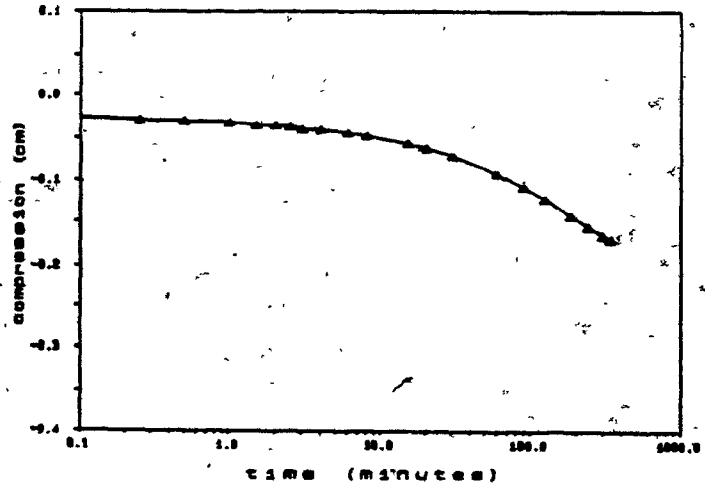
ϕ_i = 38-45° (depending upon packing)

ϕ_{rep} = 34°

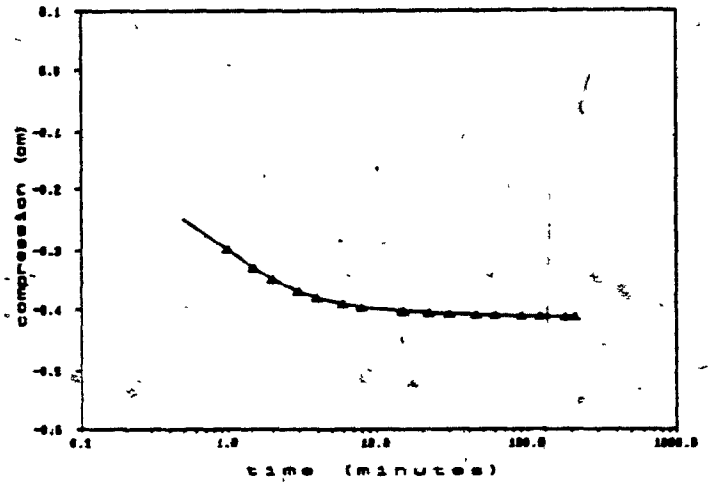
CONSOLIDATION: SAMPLE BS1, T1



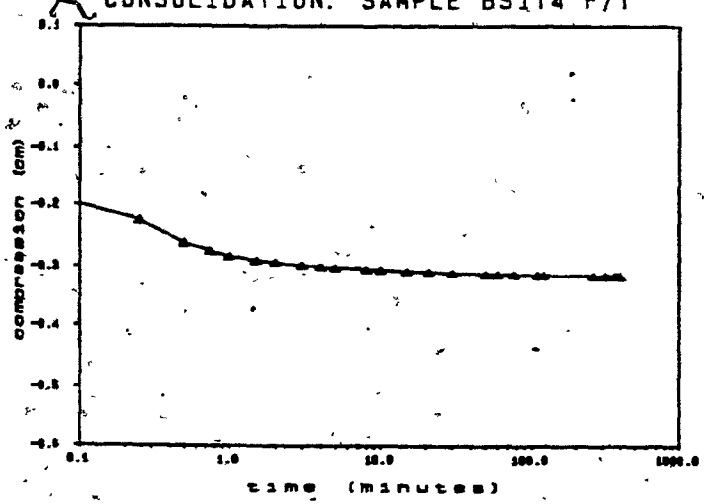
CONSOLIDATION: SAMPLE BS1, T2



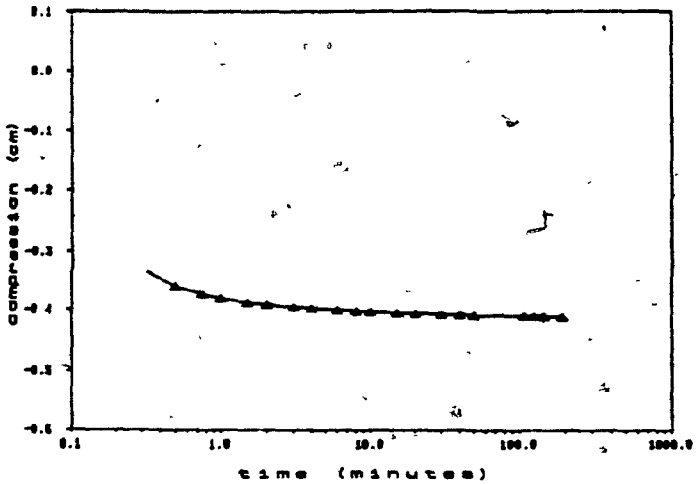
CONSOLIDATION: SAMPLE BS1T3



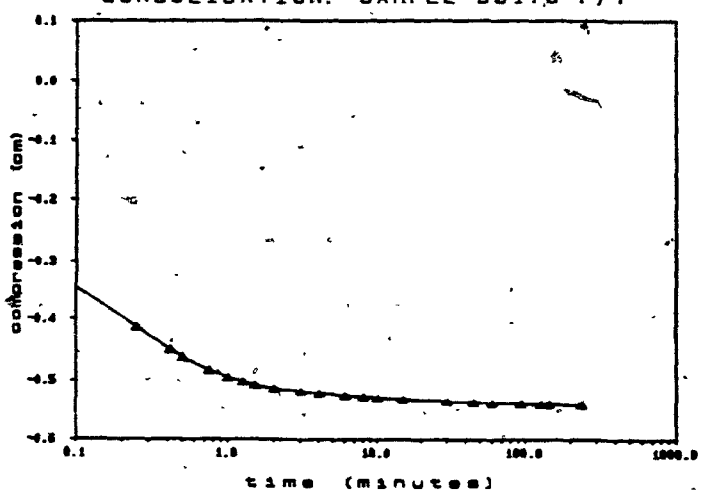
CONSOLIDATION: SAMPLE BS1T4 F/T



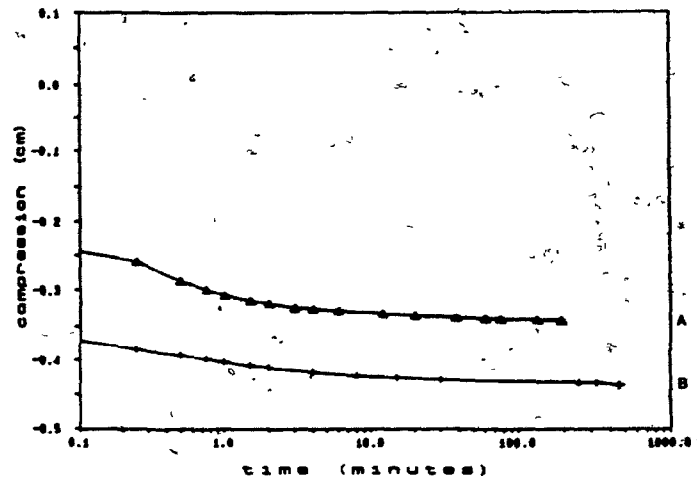
CONSOLIDATION: SAMPLE BS1T5 F/T



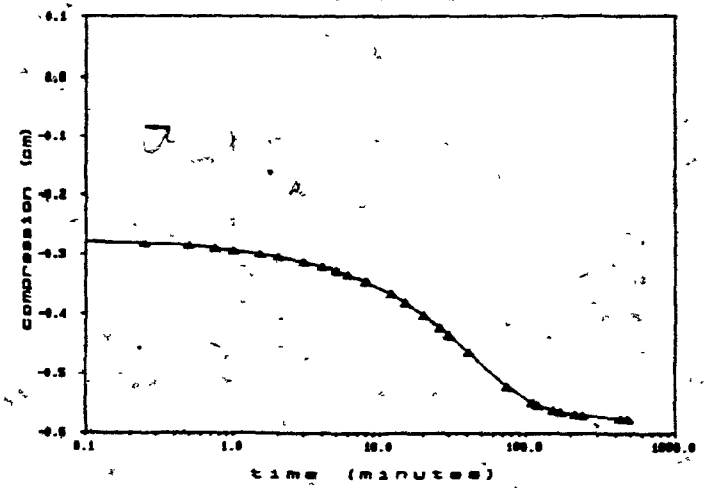
CONSOLIDATION: SAMPLE BS1T6 F/T



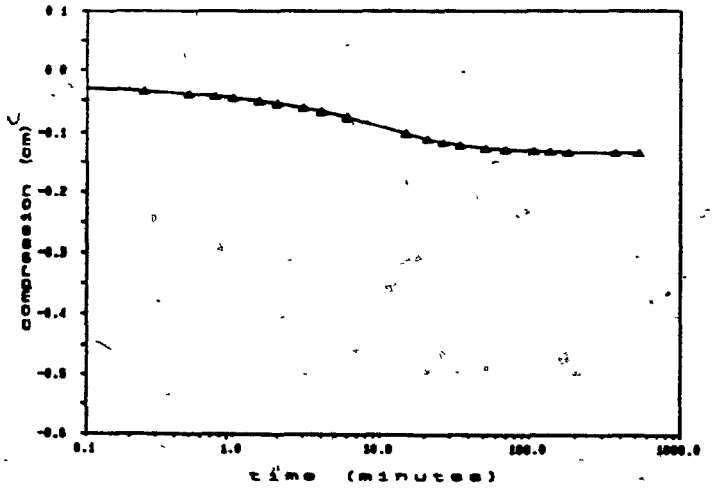
CONSOLIDATION: SAMPLE BS1_ T7 F/T



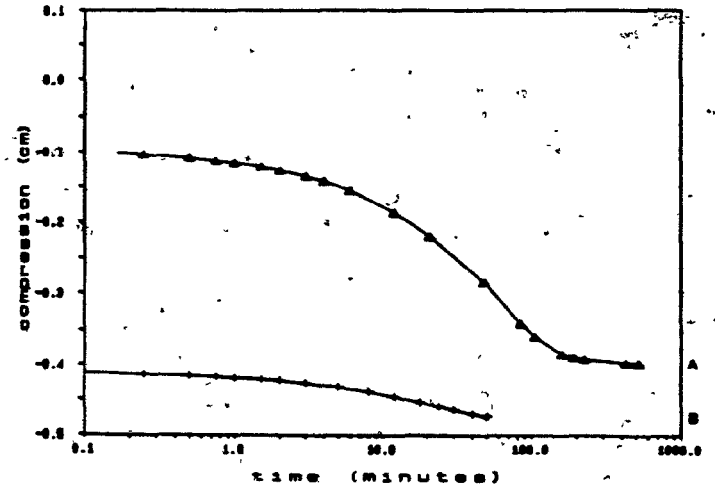
CONSOLIDATION: BS1T8A



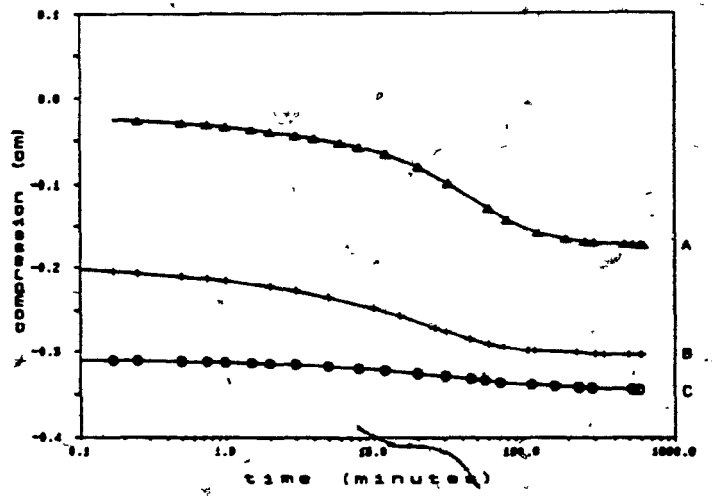
CONSOLIDATION: SAMPLE BS1, T8B



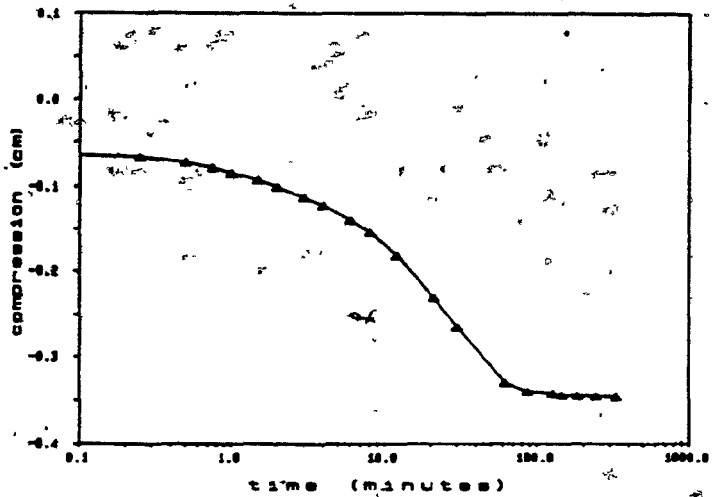
CONSOLIDATION: SAMPLE BS1, T9



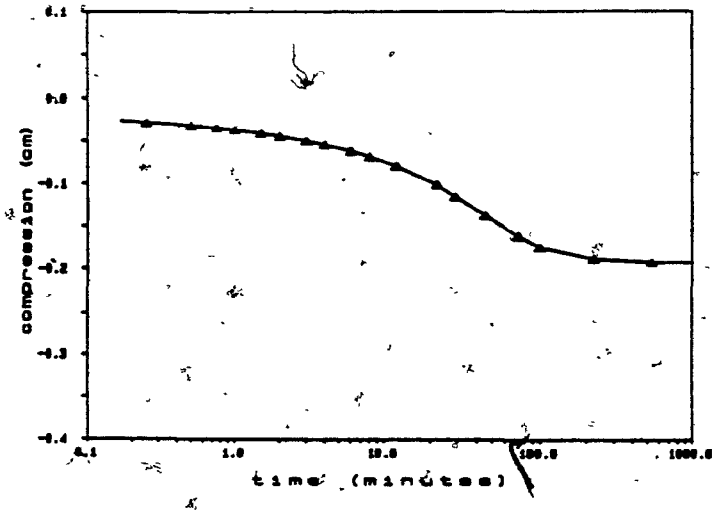
CONSOLIDATION: SAMPLE BS1, T10



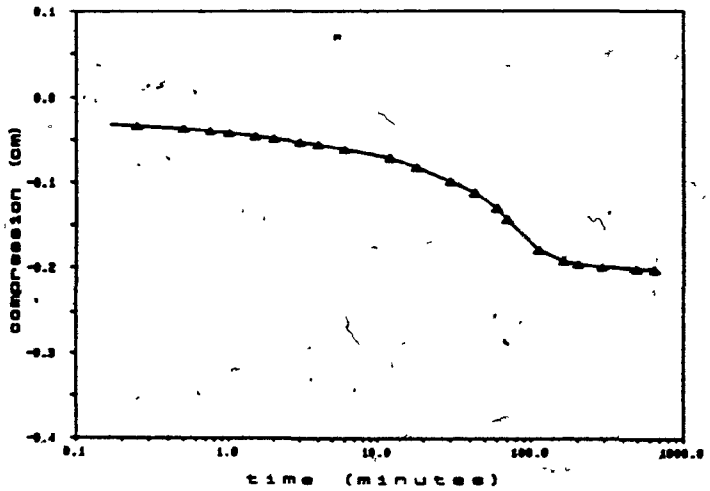
CONSOLIDATION: SAMPLE BS2, T1



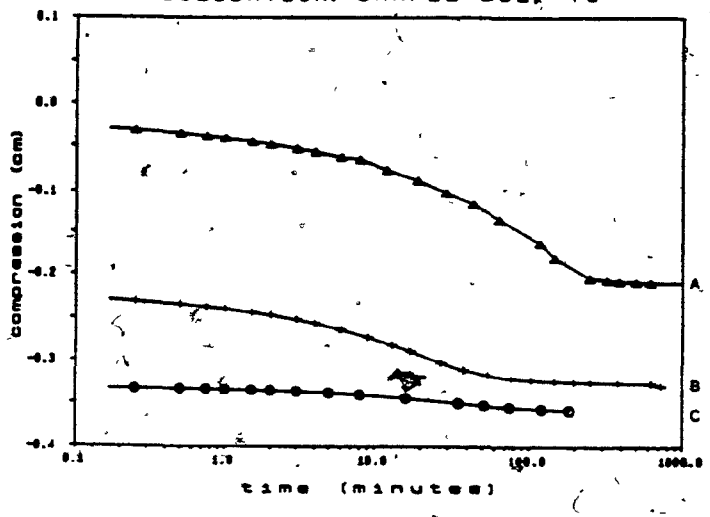
CONSOLIDATION: BS2, T2



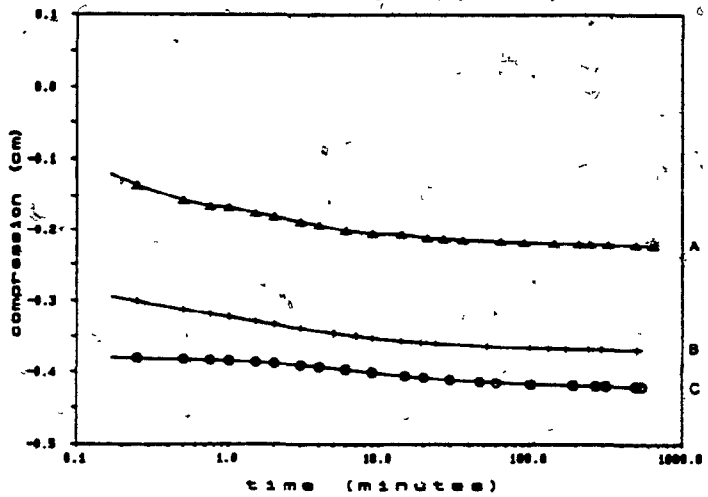
CONSOLIDATION: SAMPLE BS2, T5



CONSOLIDATION: SAMPLE BS2, T6



CONSOLIDATION: SAMPLE BS2, T7



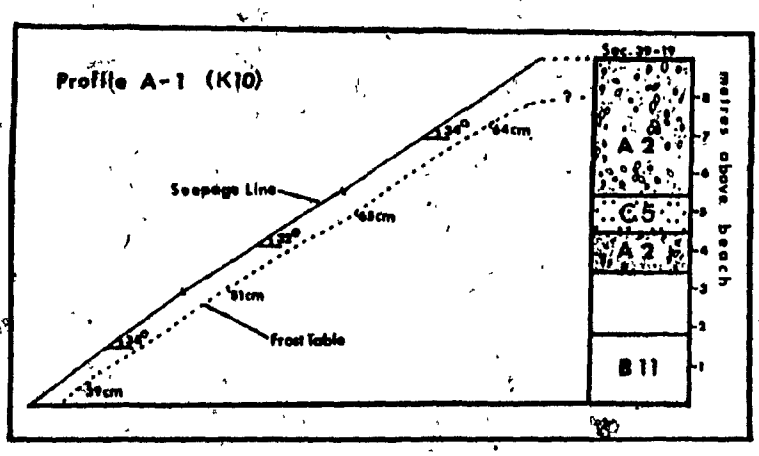
APPENDIX B

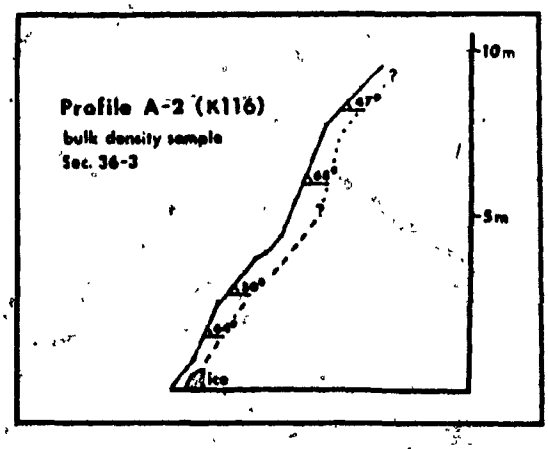
1. A-series bluff profiles (1977)
   Profiles along the debris-mantled bluffs and the steep dissected bluffs including frost table depths (mid-August, 1977) and stratigraphy

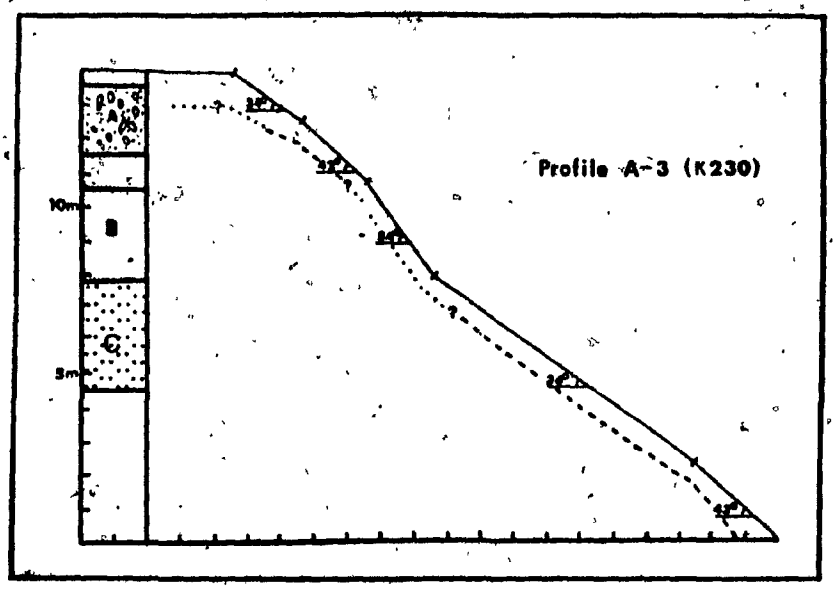
2. H-series profiles (1977)
   K886; H-13 to K1012; H-1

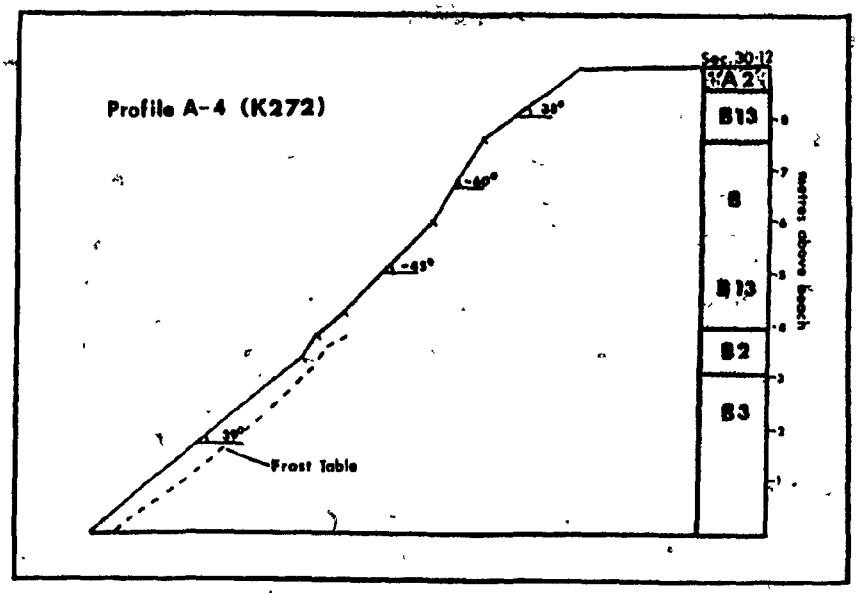
3. N-series profiles (1977)
   K1020; N-50 to K1272; N-3
   Profiles N-1 and N-2 are immediately to the northwest of K1300

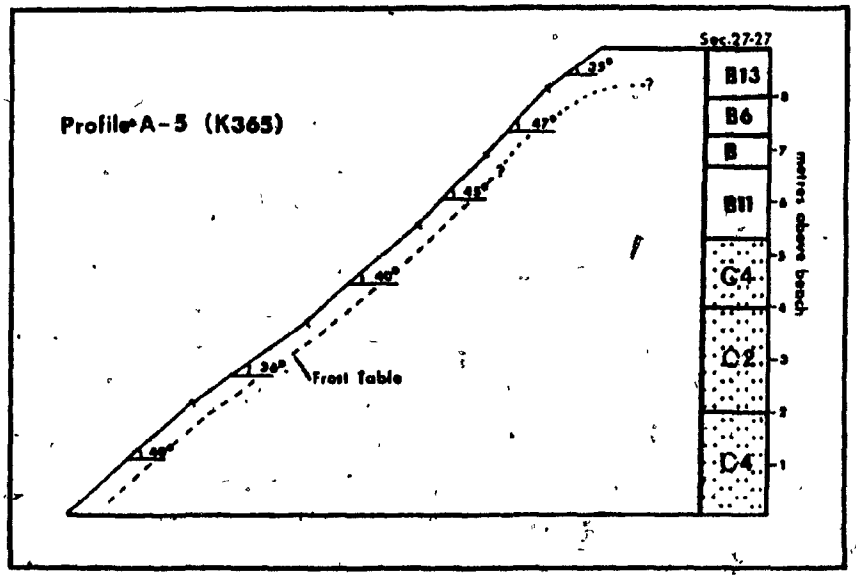
4. Bluff top/terrace survey lines

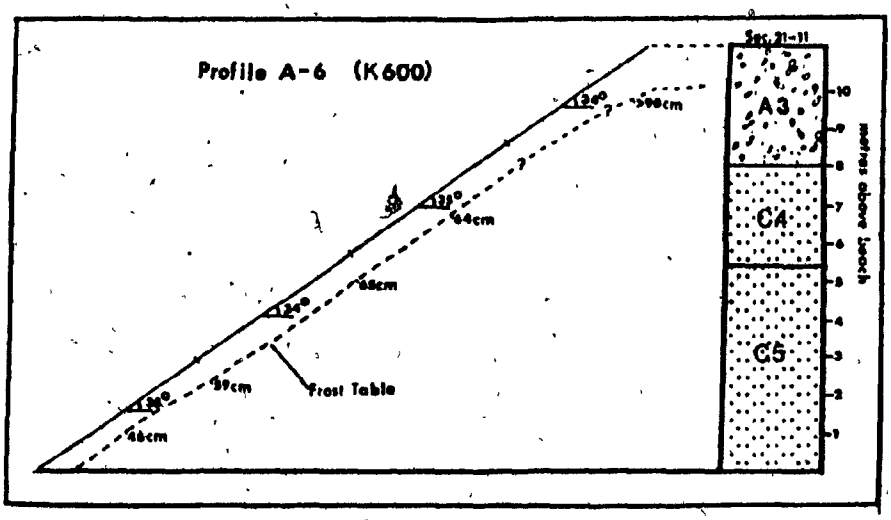

Profile A-1 (K10)
Sec. 29-19
metres above beach
A 2
C5
A 2 h
B 11
Seepage Line
Frost Table
34°
64cm
68cm
91cm
34°
39cm

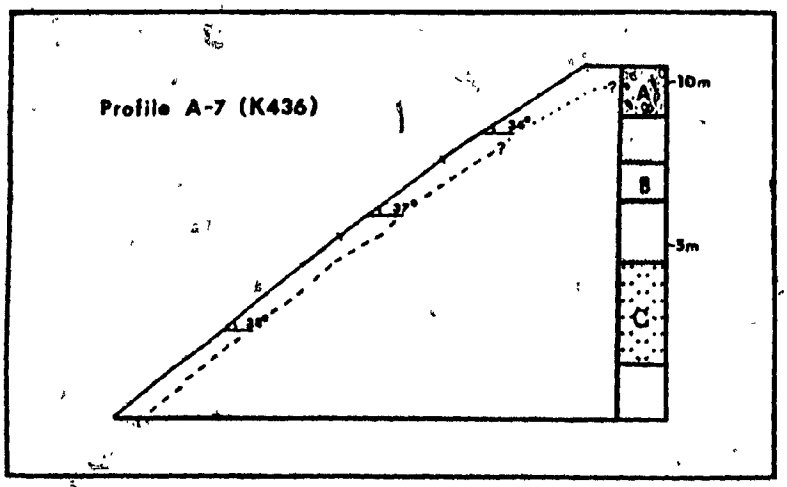

Profile A-2 (K116)
bulk density sample
Sec. 36-3
10m
5m
47°
40°
36°
Ice

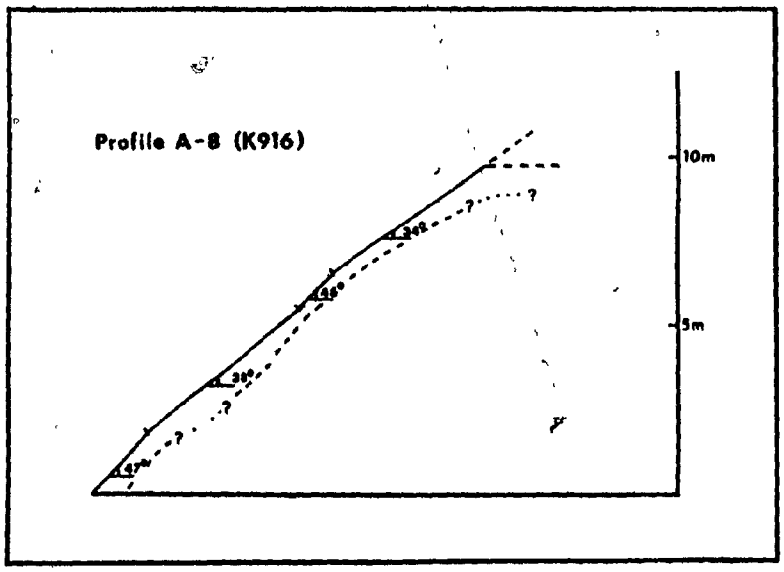

Profile A-3 (K230)
A
B
C
10m
5m
32°
32°
25°
25°

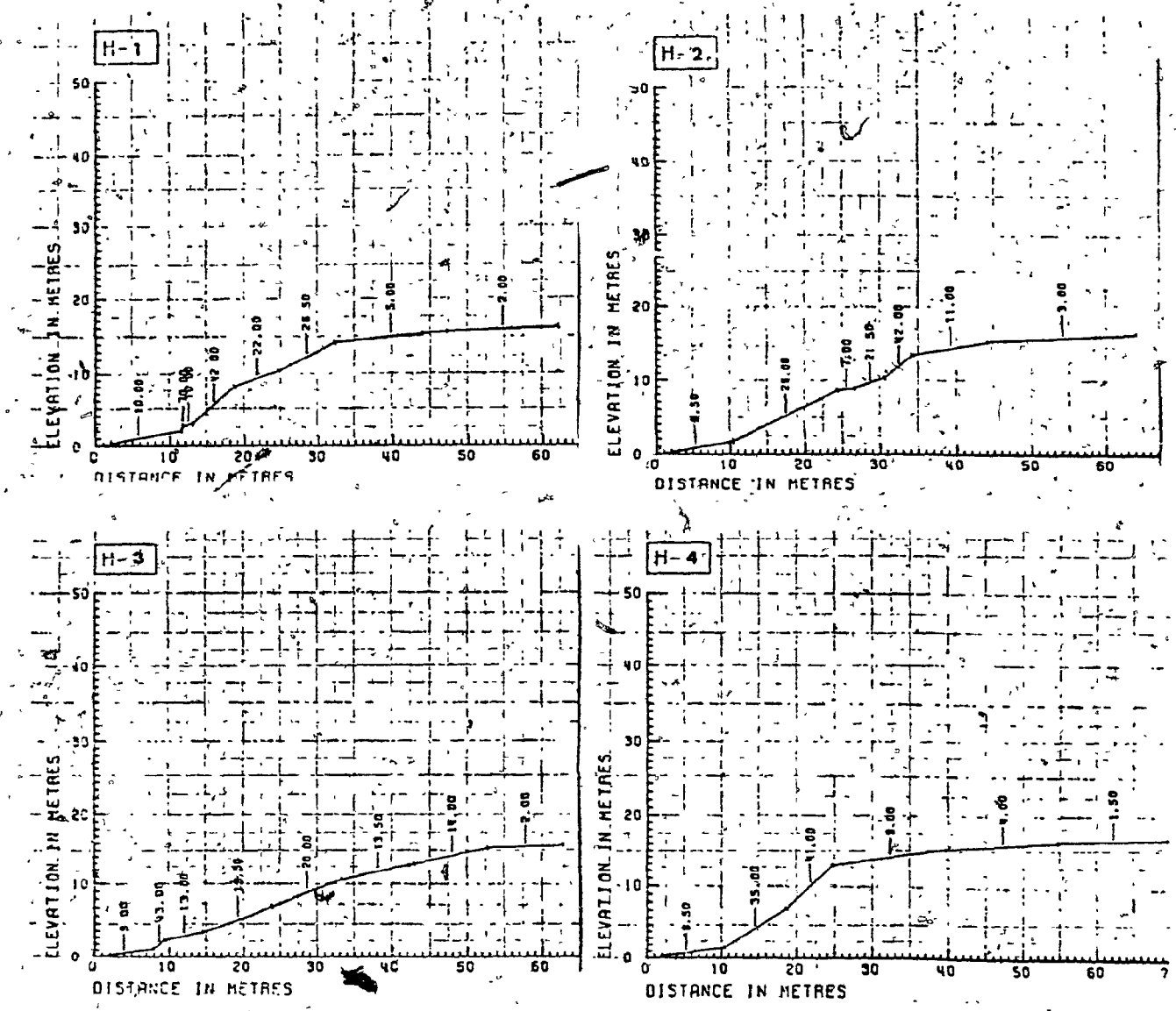

Profile A-4 (K272)
Sec. 30-12
A2
B13
B
B13
B2
B3
35°
40°
45°
39°
Frost Table
metres above beach

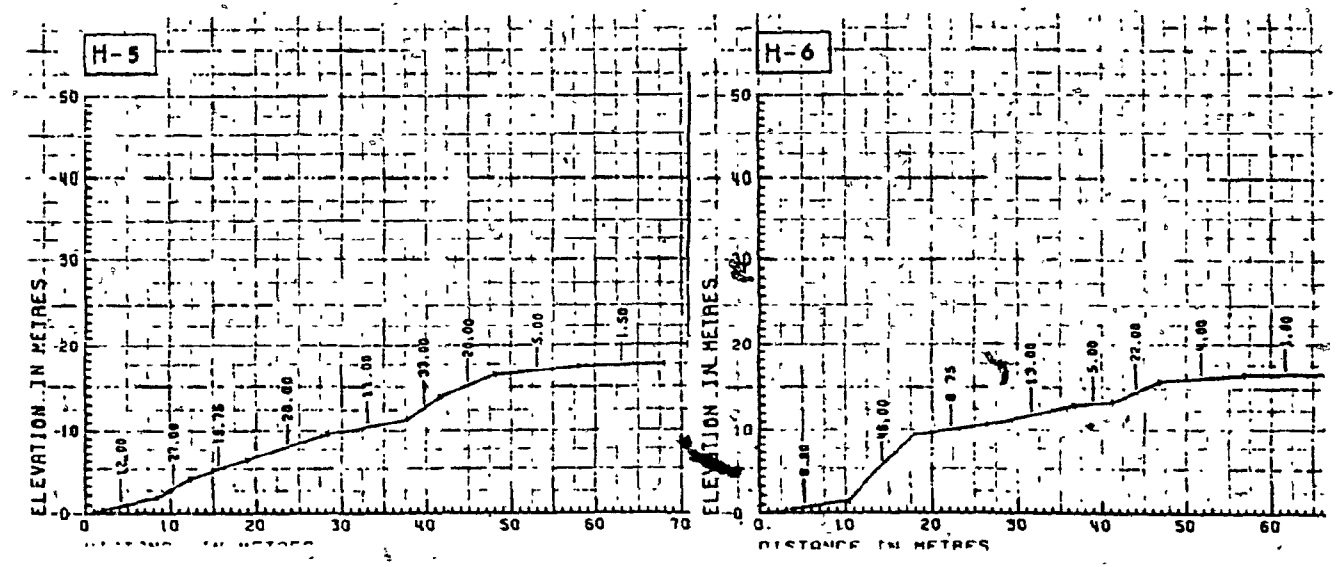

Profile A-5 (K365)
Sec. 27-27
B13
B6
B
B11
C4
C2
C4
35°
42°
45°
40°
36°
Frost Table
metres above beach


Profile A-6 (K600)
Sec. 21-11
A3
C4
C5
24°
>90cm
33°
64cm
68cm
24°
59cm
Frost Table
36°
46cm
metres above beach

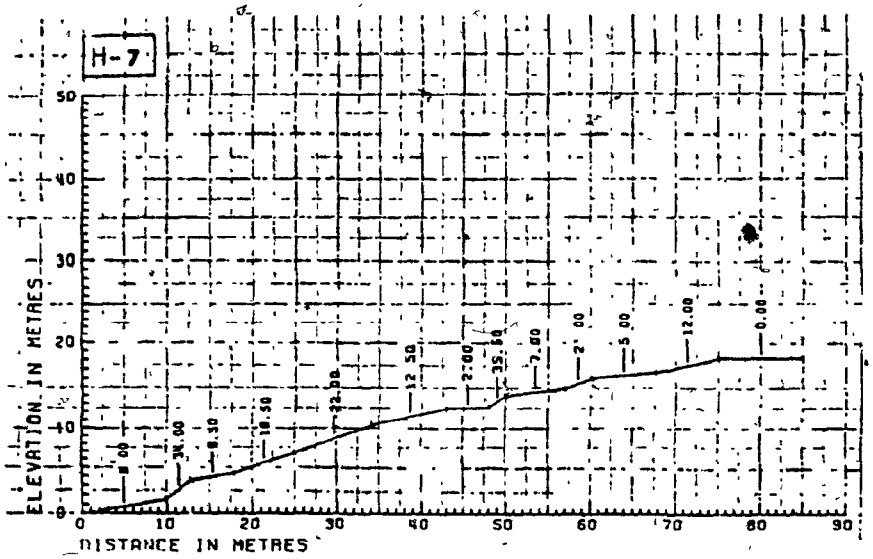

Profile A-7 (K436)
A
B
C
10m
5m
?
34°
37°
36°

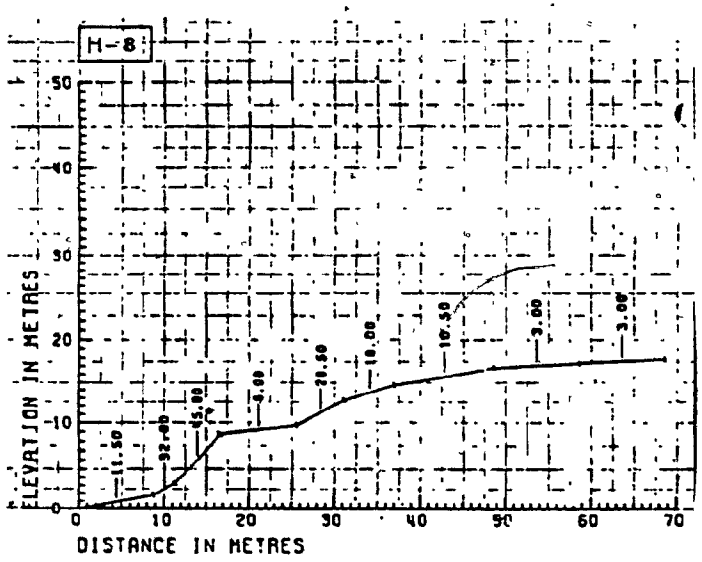

Profile A-8 (K916)
10m
5m
?
34°
38°
36°
47°

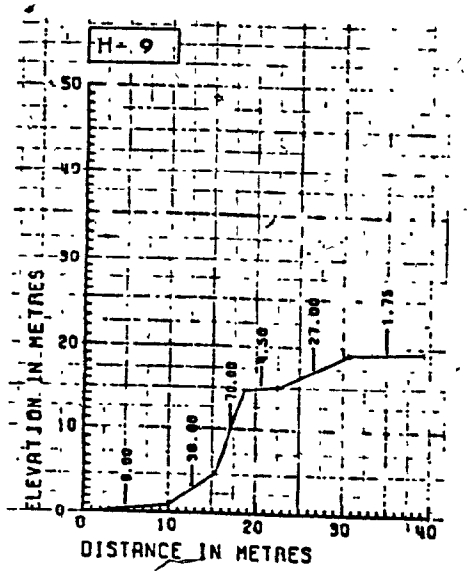

H-1
ELEVATION IN METRES
DISTANCE IN METRES
10.00
7.00
12.00
22.00
28.50
5.00
2.00
H-2
ELEVATION IN METRES
DISTANCE IN METRES
8.50
28.00
7.00
21.50
12.00
11.00
9.00
H-3
ELEVATION IN METRES
DISTANCE IN METRES
5.00
13.00
20.00
13.50
19.00
2.00
H-4
ELEVATION IN METRES
DISTANCE IN METRES
8.50
35.00
11.00
9.00
9.00
1.50

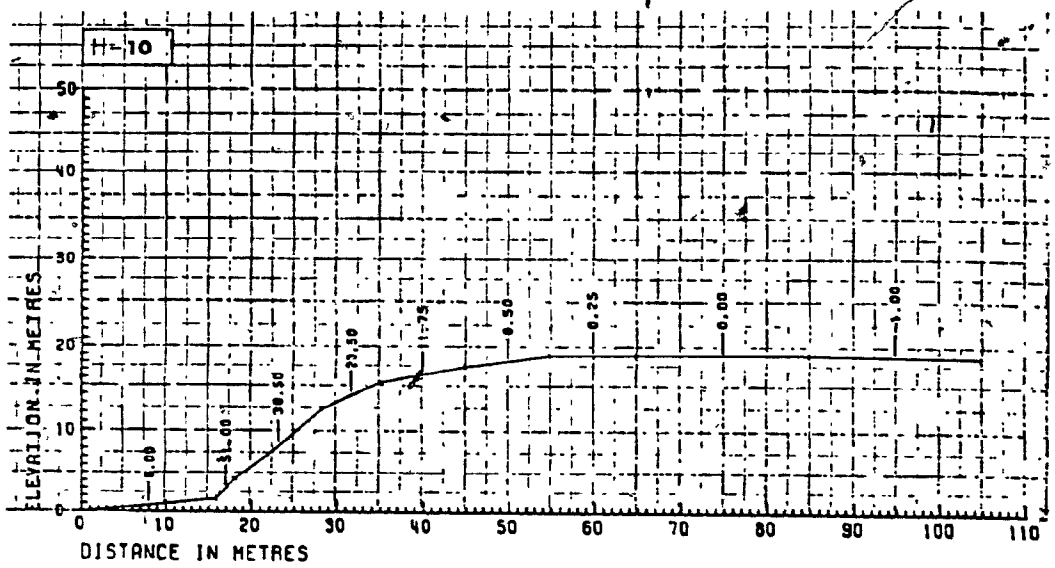

H-5
ELEVATION IN METRES
0
10
20
30
40
50
60
70
12.00
27.00
18.75
20.00
11.00
33.00
20.00
5.00
1.50

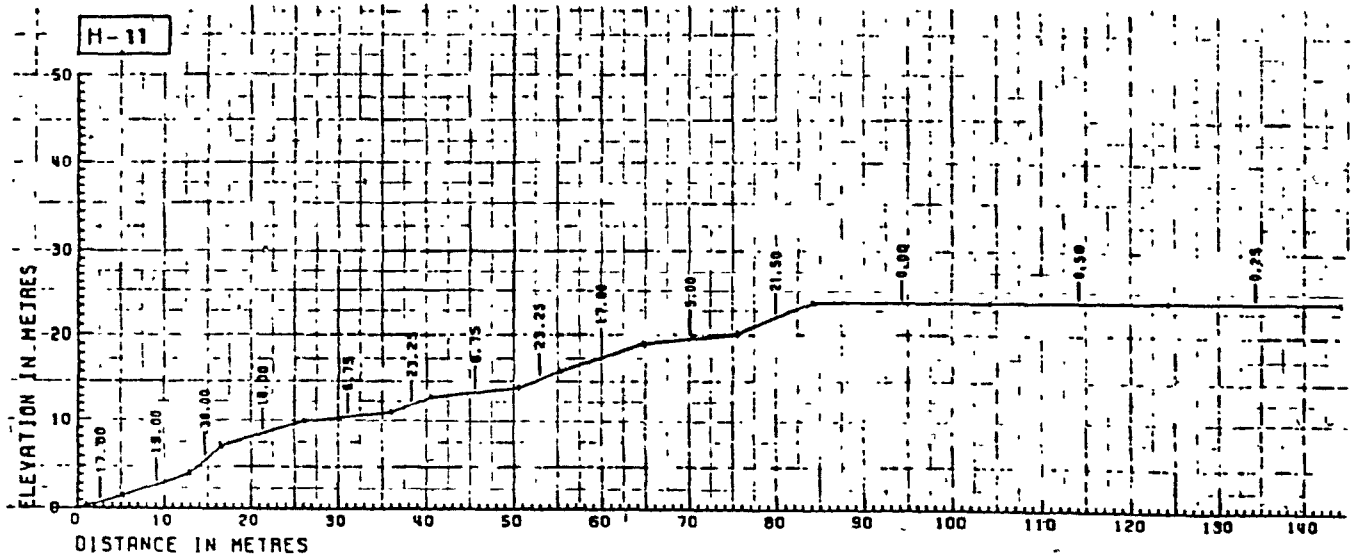
H-6
ELEVATION IN METRES
0
10
20
30
40
50
60
16.00
13.00
5.00
22.00
4.00
3.00

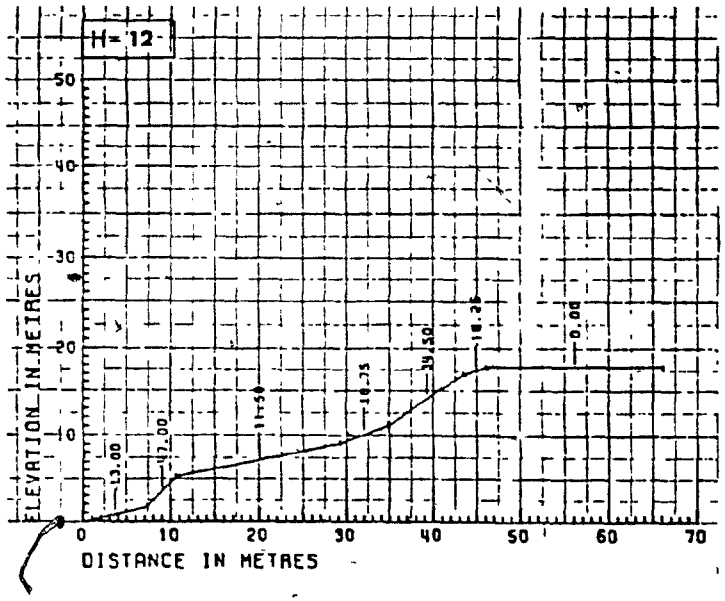

H-7
ELEVATION IN METRES
0
10
20
30
40
50
60
70
80
90
DISTANCE IN METRES
34.00
18.50
32.00
12.50
35.00
7.00
5.00
12.00
0.00

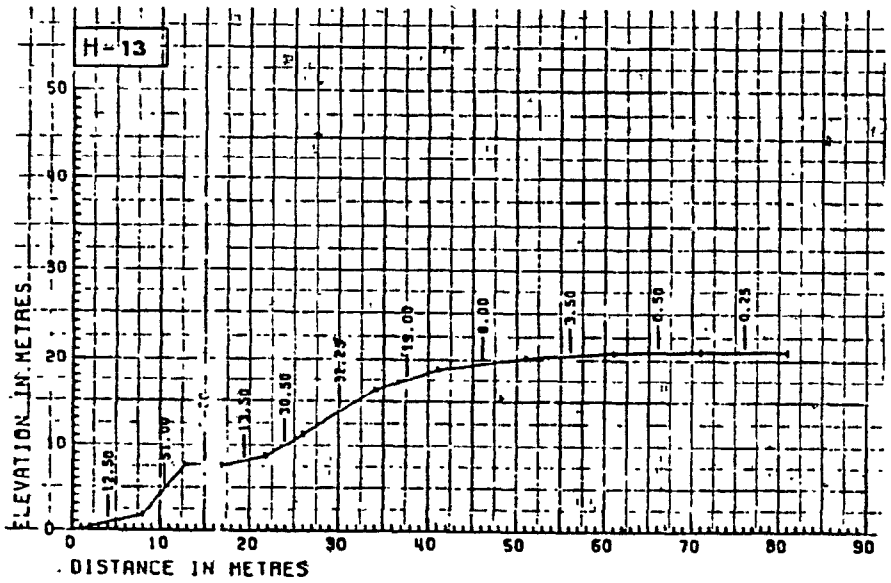

H-8
ELEVATION IN METRES
DISTANCE IN METRES
0
10
20
30
40
50
60
70
11.50
32.00
45.00
4.00
21.50
10.00
10.50
3.00
3.00

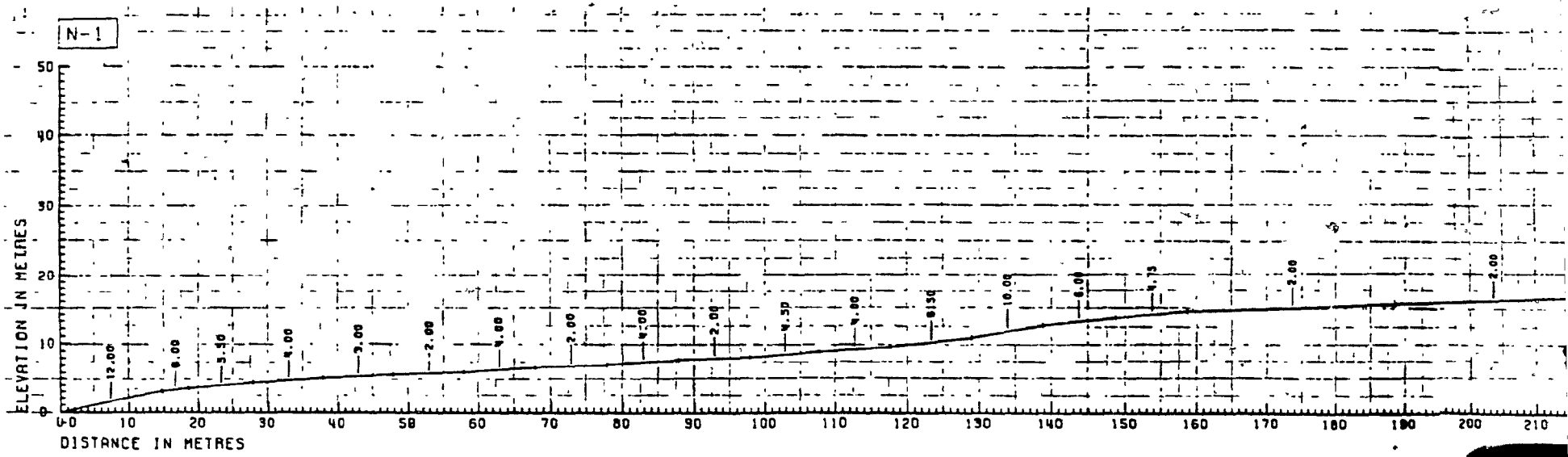

H-9
ELEVATION IN METRES
DISTANCE IN METRES
0
10
20
30
40
50
0.00
30.00
10.00
4.50
27.00
1.75

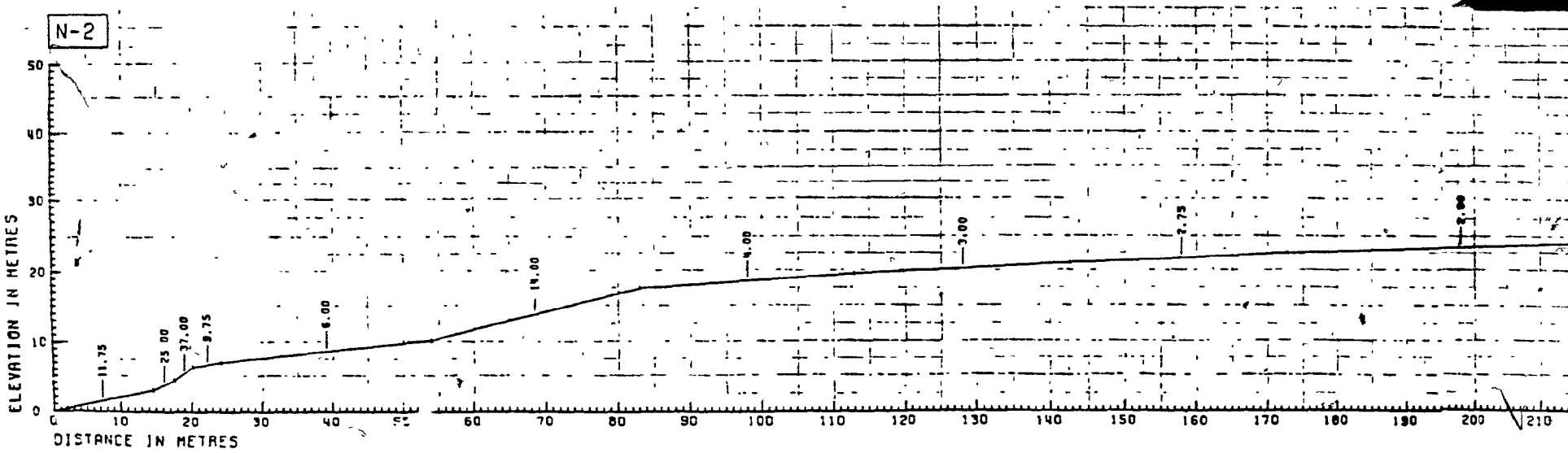

H-10
ELEVATION IN METRES
DISTANCE IN METRES
0
10
20
30
40
50
60
70
80
90
100
110
5.00
31.00
30.50
23.50
11.75
0.50
0.25
0.00
5.00

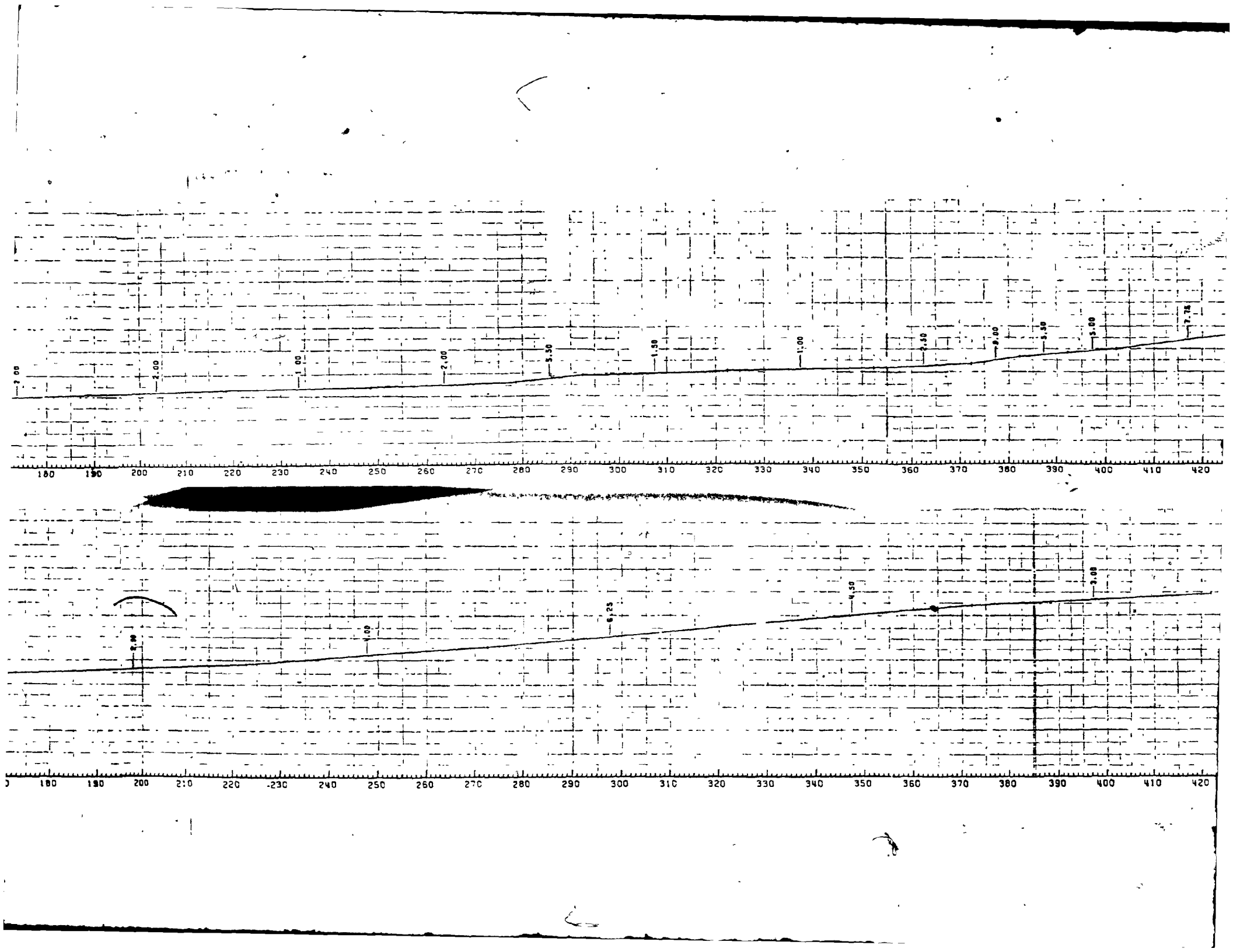

H-11
ELEVATION IN METRES
DISTANCE IN METRES
0
10
20
30
40
50
60
70
80
90
100
110
120
130
140
17.00
19.00
30.00
18.00
6.75
23.25
6.75
23.25
17.00
9.00
21.50
0.00
0.50
0.25

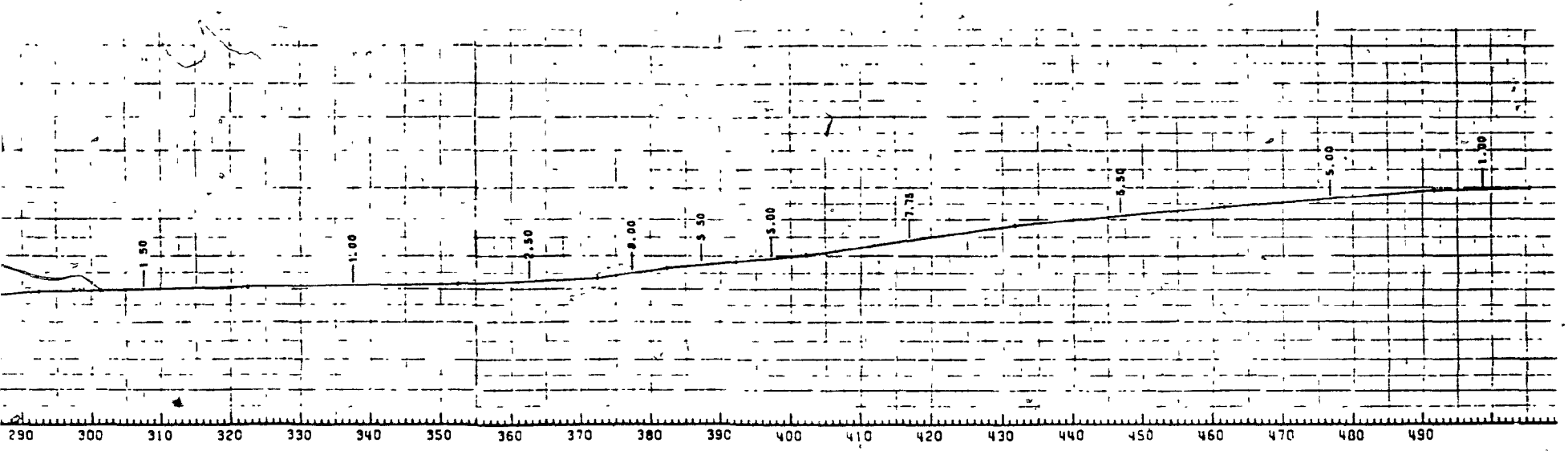

H-12
ELEVATION IN METRES
DISTANCE IN METRES
0
10
20
30
40
50
60
70
13.00
12.00
11.50
18.75
34.50
18.25
0.00

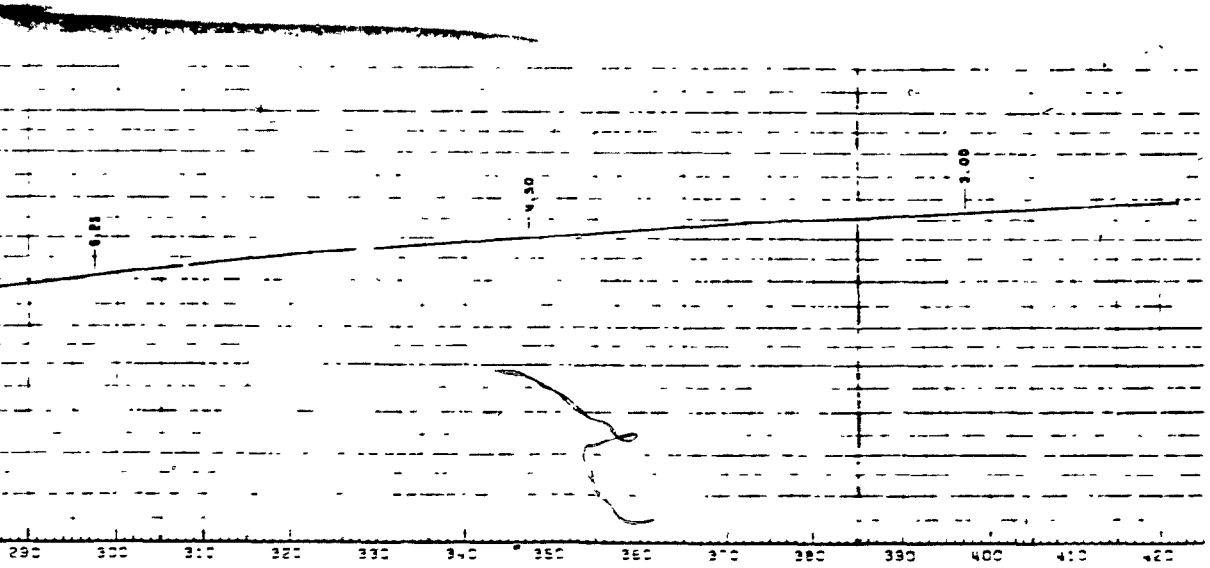

H-13
ELEVATION IN METRES
DISTANCE IN METRES
0
10
20
30
40
50
60
70
80
90
12.50
31.00
13.50
30.50
31.25
19.00
0.00
3.50
0.50
0.25

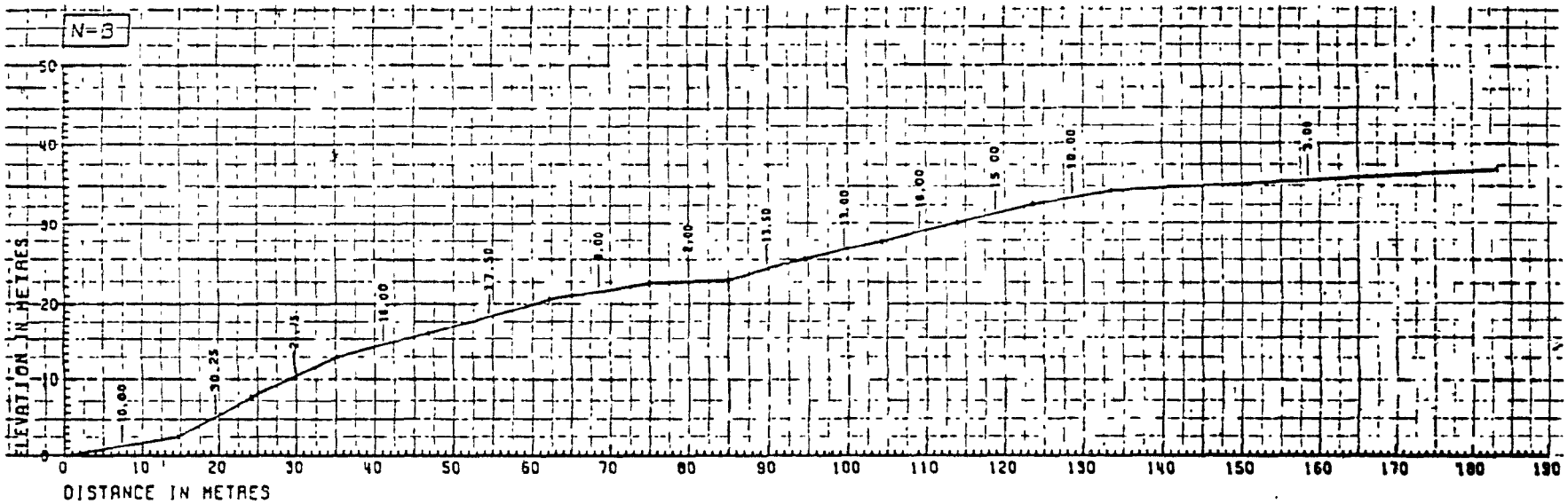

N-1
ELEVATION IN METRES
DISTANCE IN METRES
0
10
20
30
40
50
60
70
80
90
100
110
120
130
140
150
160
170
180
190
200
210
12.00
6.00
3.50
4.00
3.00
2.00
4.00
2.00
4.00
2.00
4.50
4.00
8.50
10.00
6.00
4.75
2.00
2.00

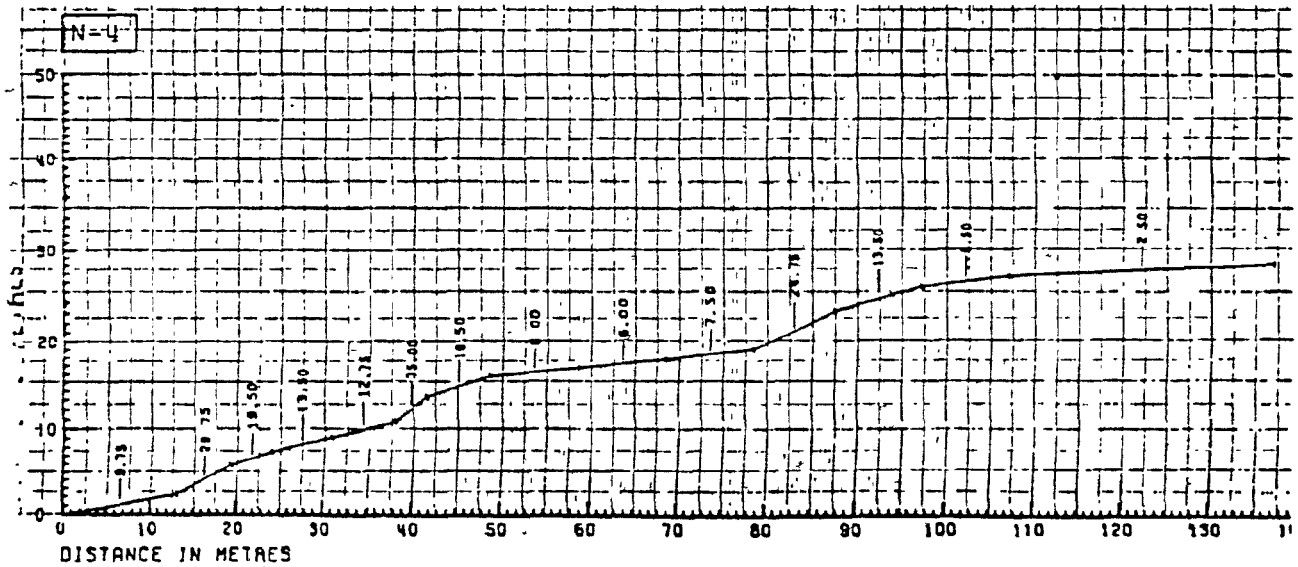

N-2
ELEVATION IN METRES
DISTANCE IN METRES
0
10
20
30
40
50
60
70
80
90
100
110
120
130
140
150
160
170
180
190
200
210
11.75
25.00
37.00
8.75
6.00
18.00
4.00
3.00
2.75
2.00

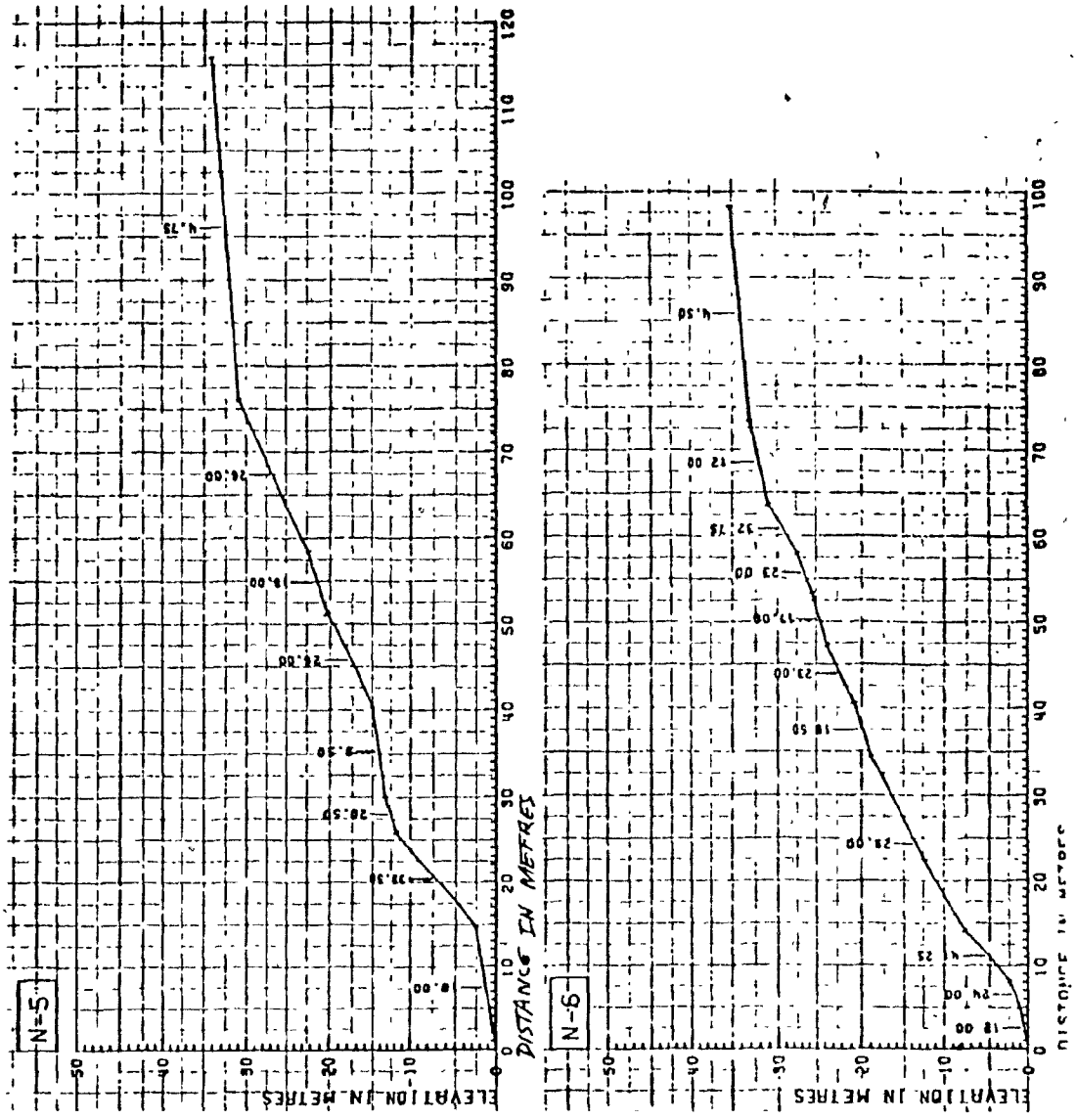

2.00
2.00
1.00
2.00
3.50
1.50
1.00
2.50
9.00
5.50
5.00
7.75
180
190
200
210
220
230
240
250
260
270
280
290
300
310
320
330
340
350
360
370
380
390
400
410
420
2.00
1.00
6.25
4.50
3.00
180
190
200
210
220
230
240
250
260
270
280
290
300
310
320
330
340
350
360
370
380
390
400
410
420

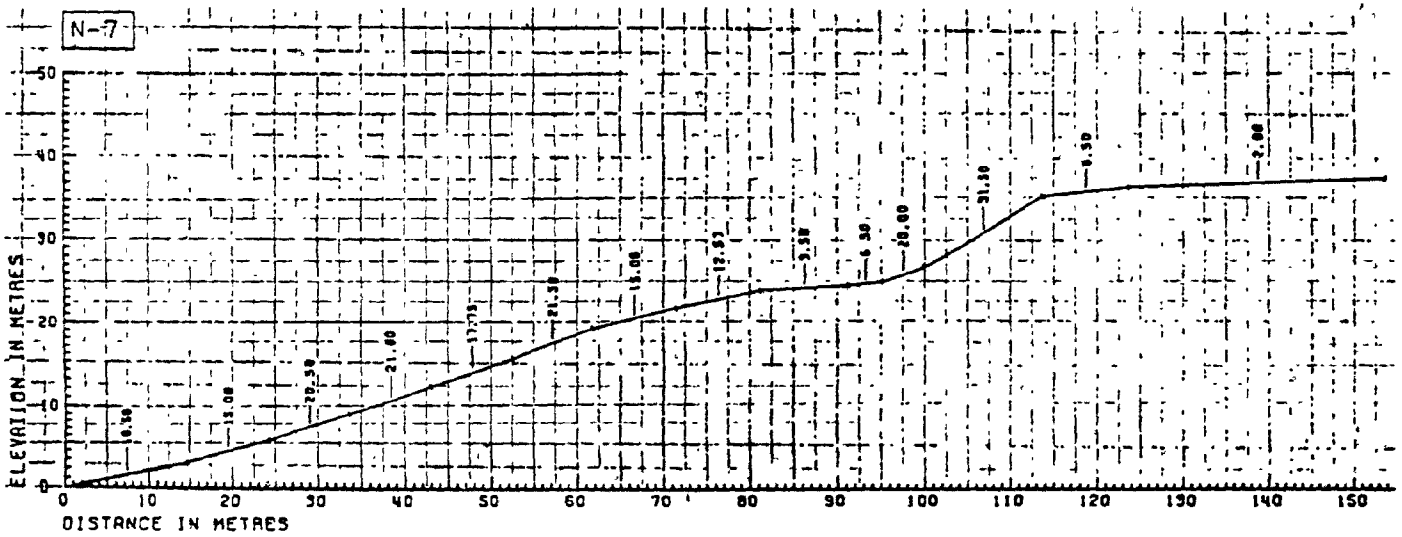

1.50
1.00
2.50
8.00
5.50
5.00
7.75
6.50
5.00
1.00
290
300
310
320
330
340
350
360
370
380
390
400
410
420
430
440
450
460
470
480
490

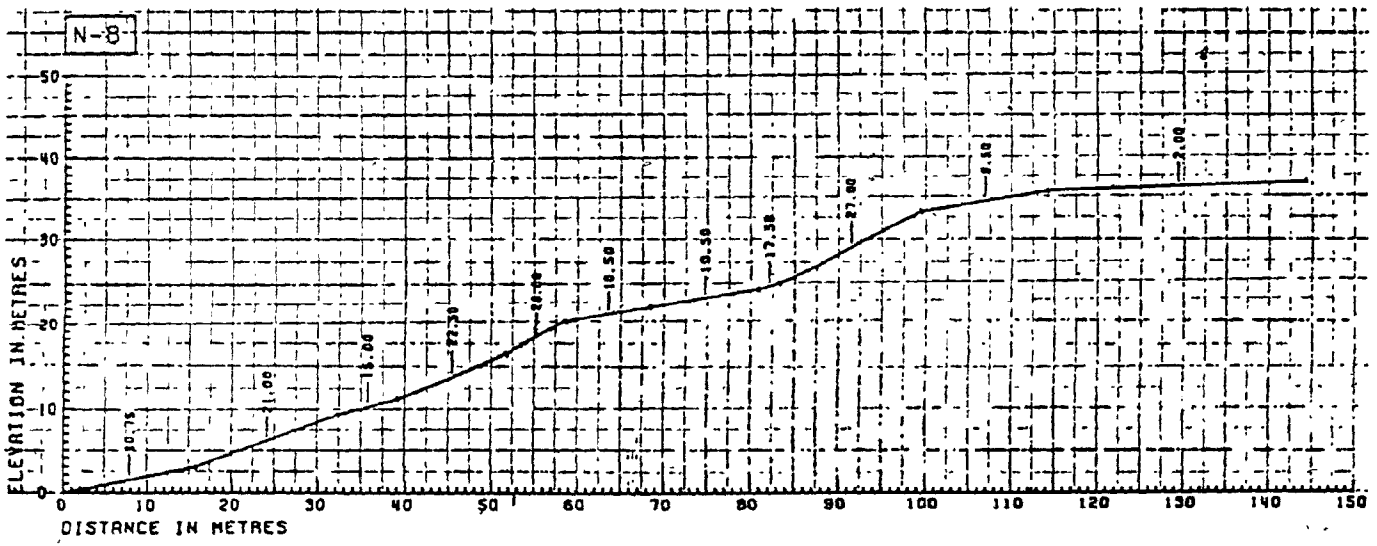

6.25
4.50
3.00
290
300
310
320
330
340
350
360
370
380
390
400
410
420

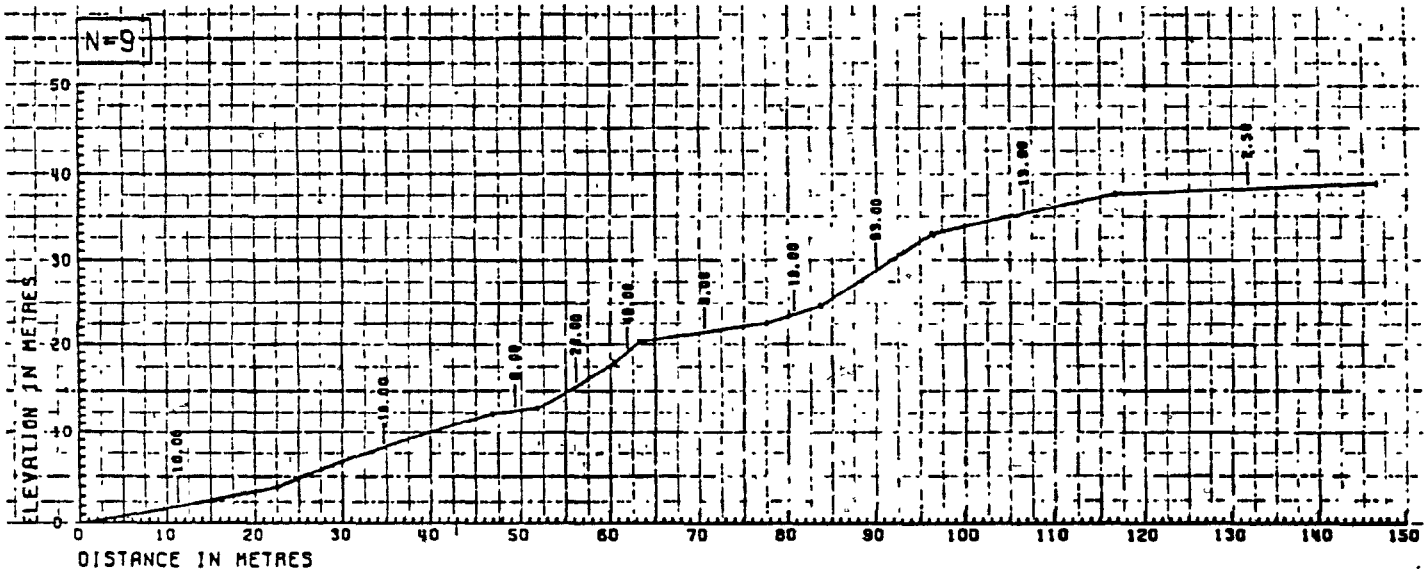

N=3
ELEVATION IN METRES
DISTANCE IN METRES
0
10
20
30
40
50
60
70
80
90
100
110
120
130
140
150
160
170
180
190
10.00
30.25
21.75
18.00
17.50
8.00
8.00
13.50
13.00
16.00
15.00
18.00
3.00

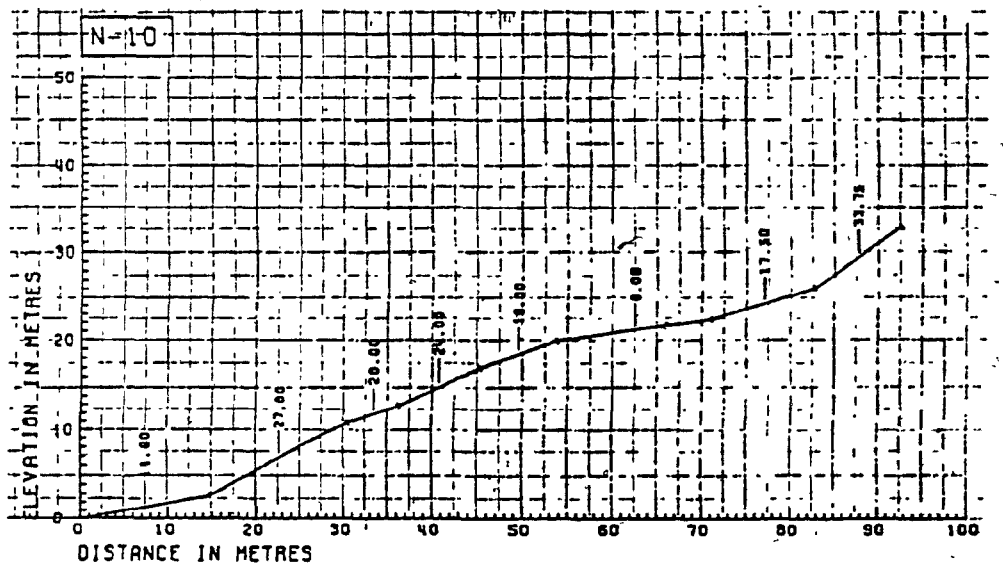

N=4
DISTANCE IN METRES
0
10
20
30
40
50
60
70
80
90
100
110
120
130
8.75
28.75
19.50
13.50
12.75
15.00
10.50
8.00
8.00
7.50
24.75
13.50
4.50
2.50

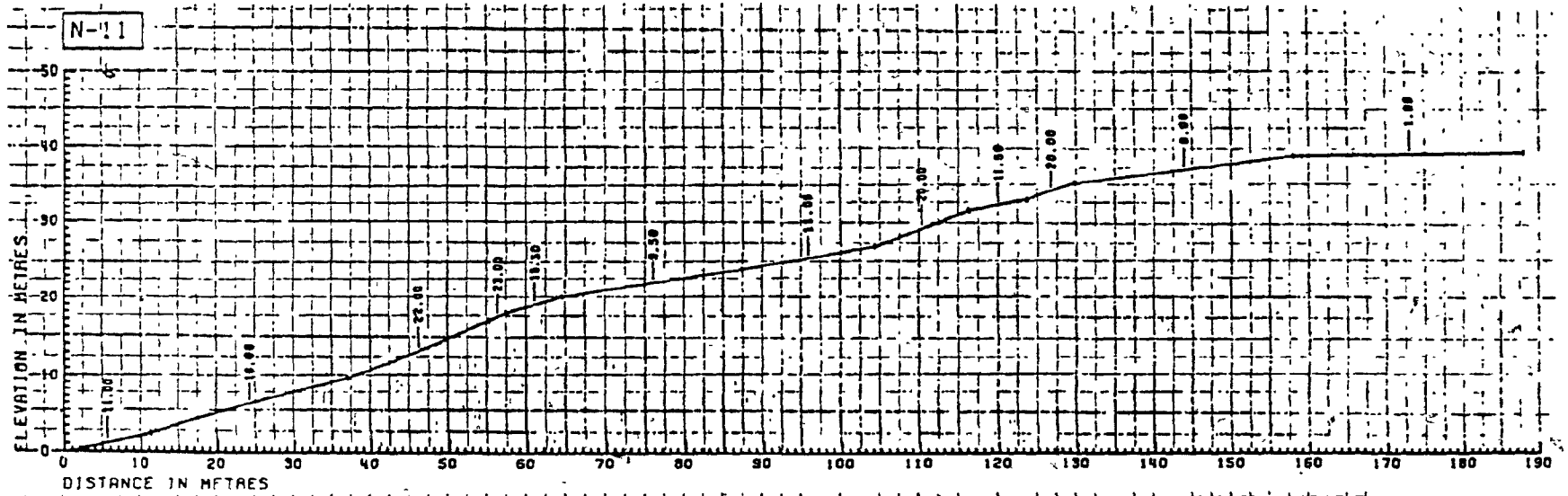

N-5
N-6
ELEVATION IN METRES
DISTANCE IN METRES

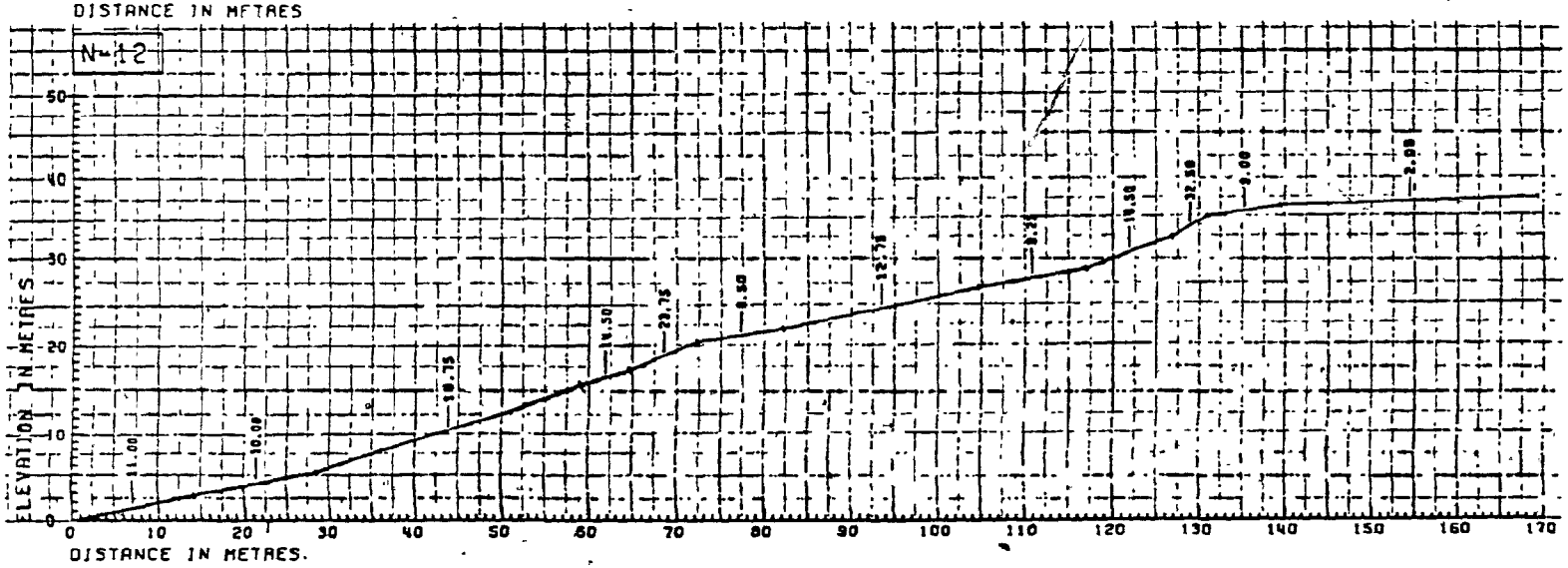

N-7
ELEVATION IN METRES
DISTANCE IN METRES
0
10
20
30
40
50
60
70
80
90
100
110
120
130
140
150
10.50
15.00
20.50
21.00
17.75
21.50
15.00
12.53
5.58
6.50
28.00
31.50
6.50
2.00

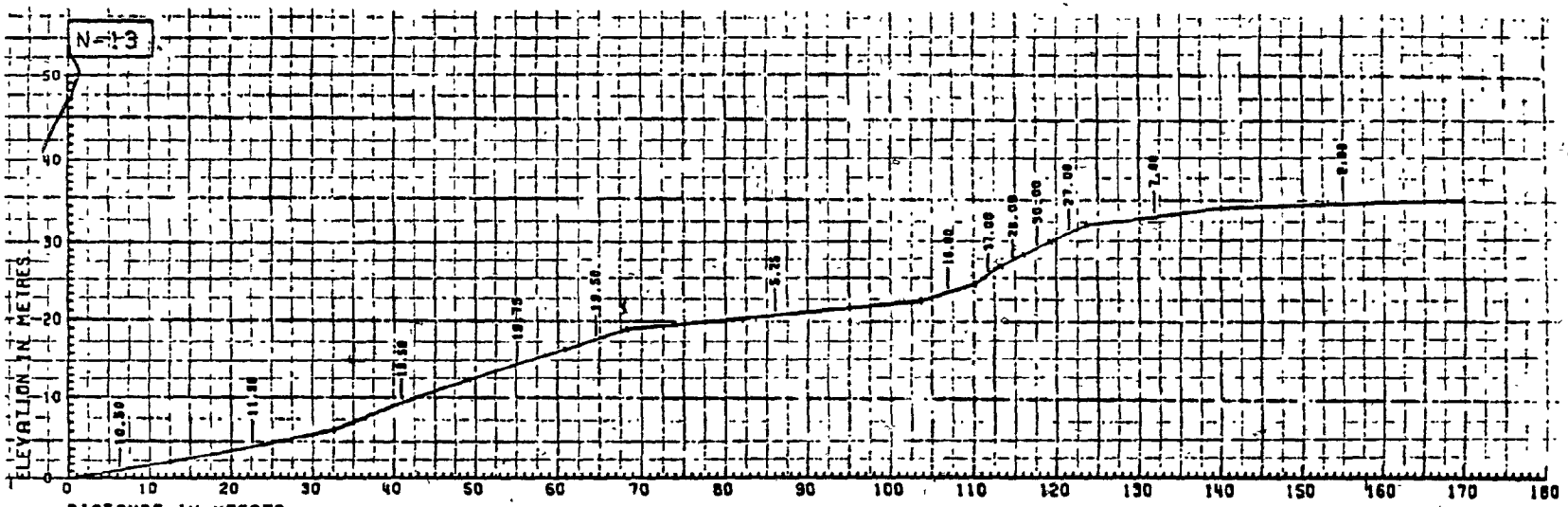

N-8
ELEVATION IN METRES
DISTANCE IN METRES
0
10
20
30
40
50
60
70
80
90
100
110
120
130
140
150
10.75
11.00
15.00
22.50
28.00
18.50
18.50
17.38
27.80
6.10
2.00

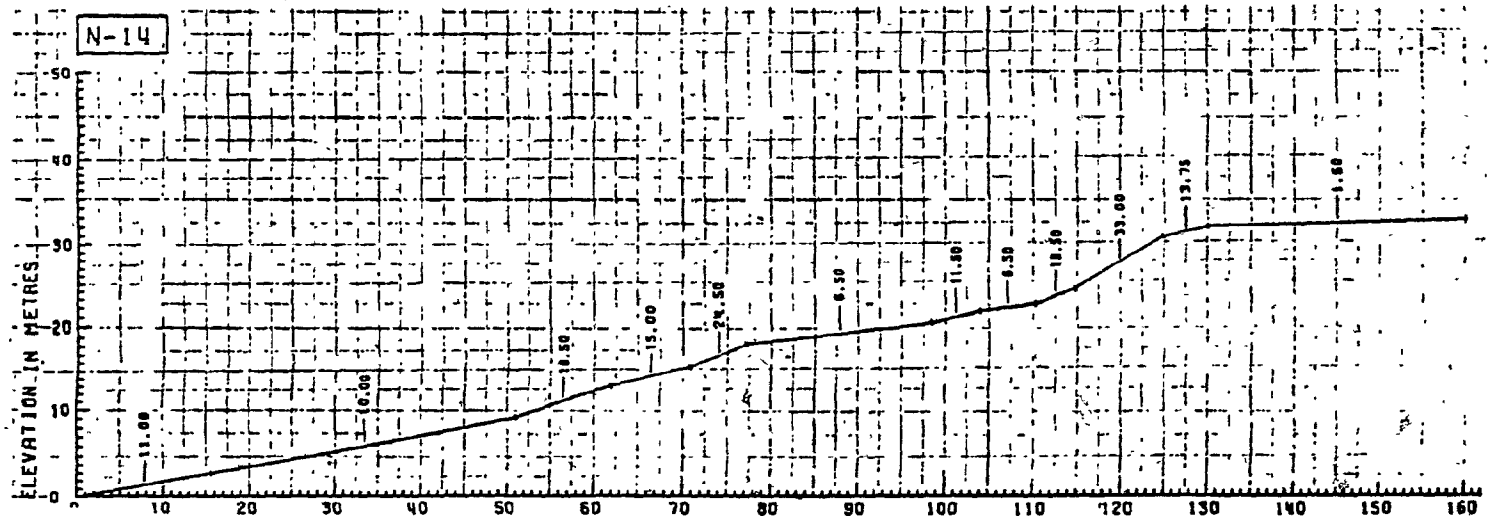

N=9
ELEVATION IN METRES
DISTANCE IN METRES
0
10
20
30
40
50
60
70
80
90
100
110
120
130
140
150
10.00
18.00
8.00
27.00
40.00
8.00
18.00
33.00
19.00
2.50

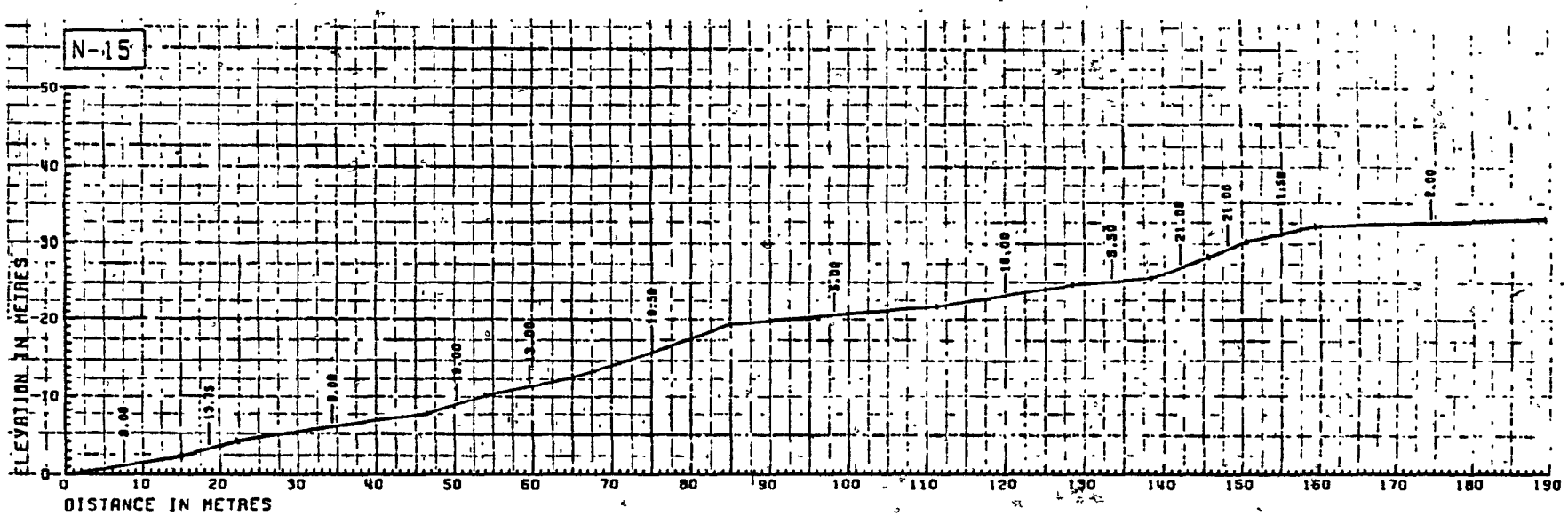

N=10
ELEVATION IN METRES
DISTANCE IN METRES
0
10
20
30
40
50
60
70
80
90
100
1.00
27.00
20.00
24.00
18.00
8.00
17.50
33.75

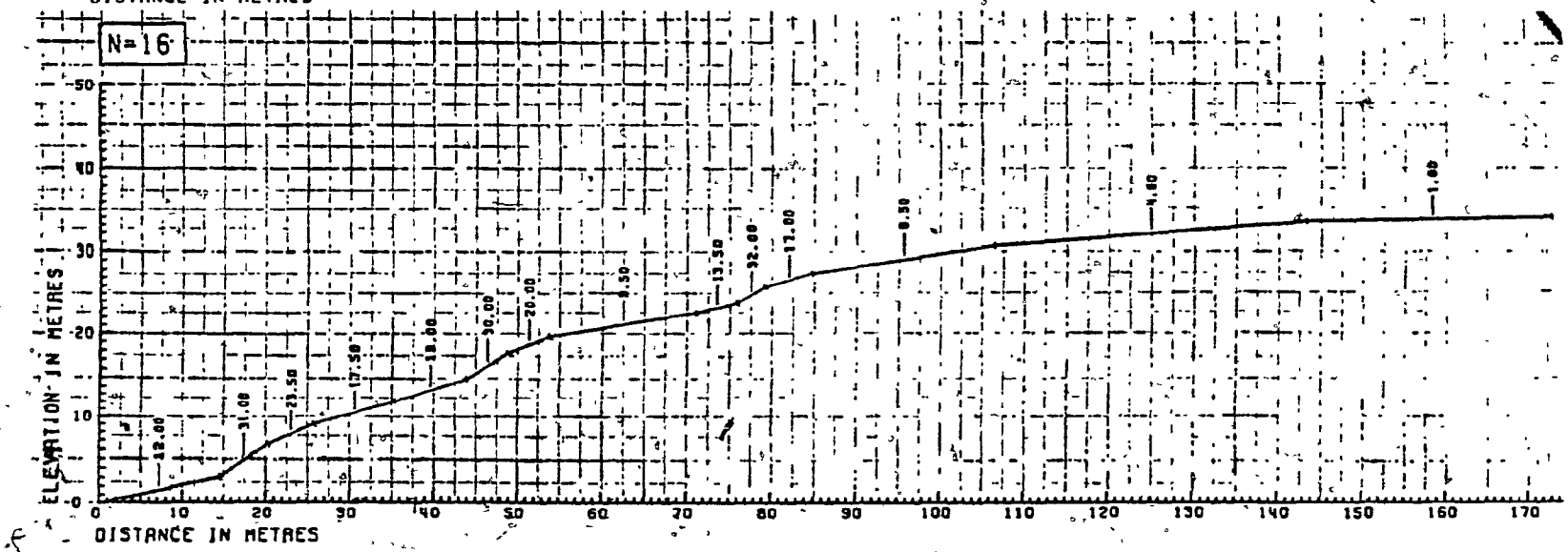

N-11
ELEVATION IN METRES
DISTANCE IN METRES
0
10
20
30
40
50
60
70
80
90
100
110
120
130
140
150
160
170
180
190

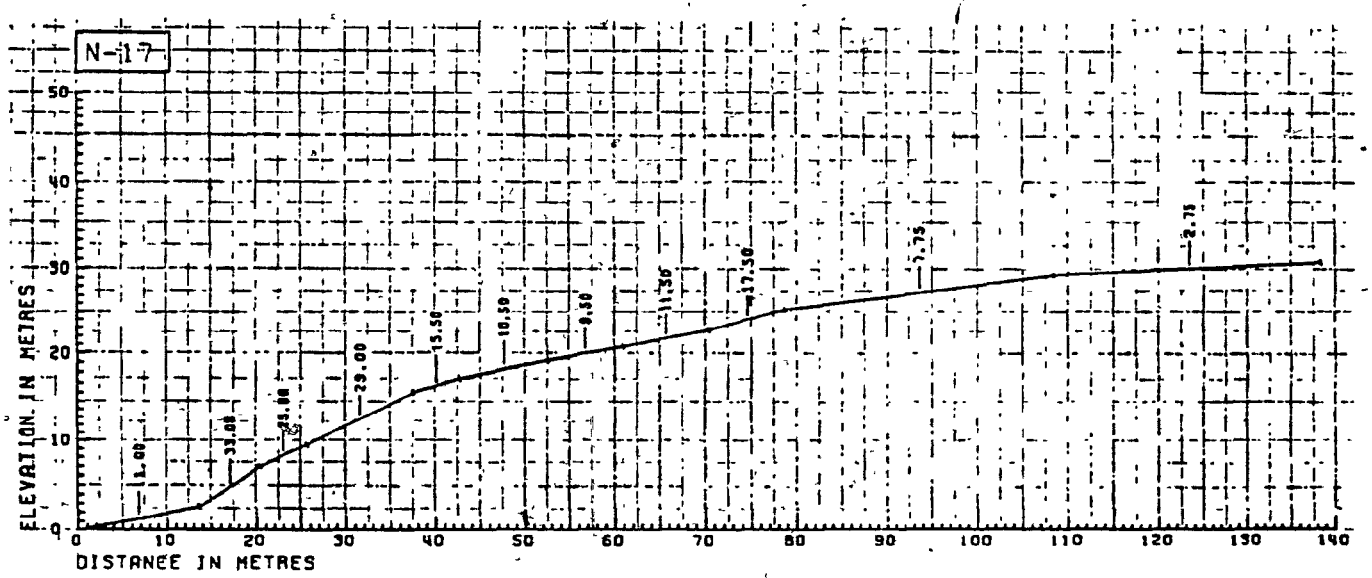

N-12
ELEVATION IN METRES
DISTANCE IN METRES.
0
10
20
30
40
50
60
70
80
90
100
110
120
130
140
150
160
170

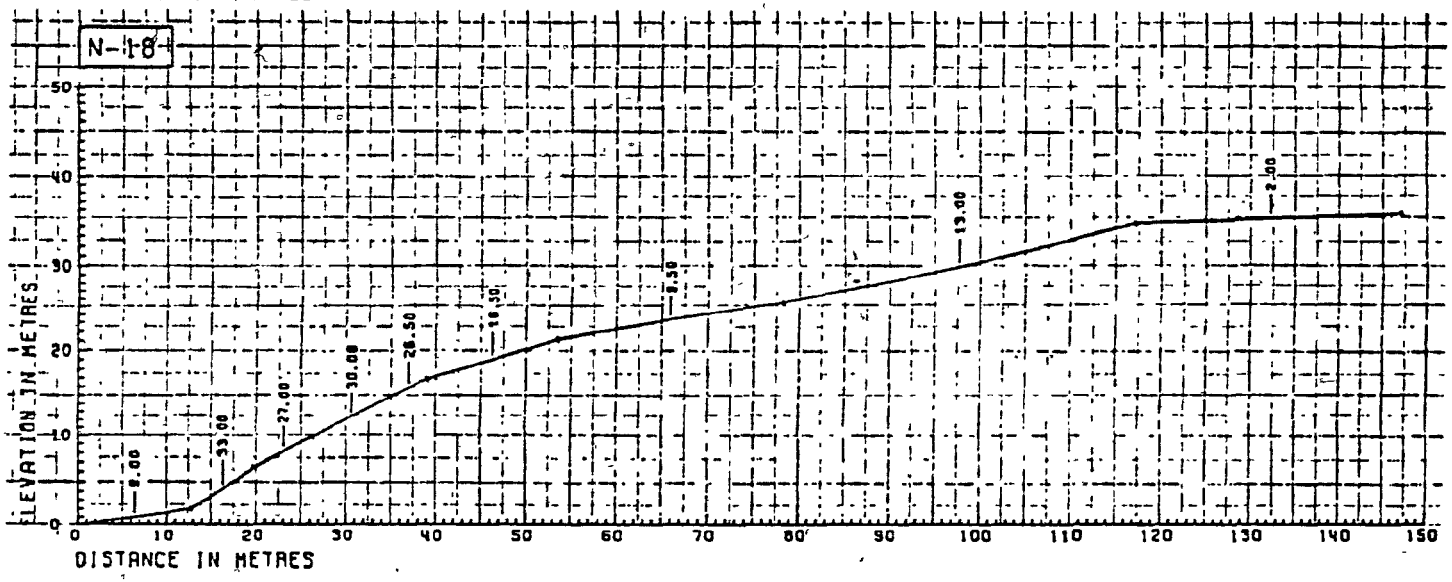

N-13
ELEVATION IN METRES
DISTANCE IN METRES
0
10
20
30
40
50
60
70
80
90
100
110
120
130
140
150
160
170
180

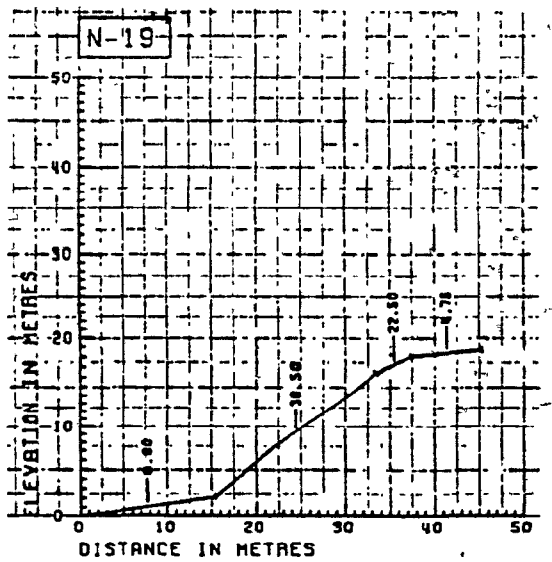

N-14
ELEVATION IN METRES
0
10
20
30
40
50
60
70
80
90
100
110
120
130
140
150
160

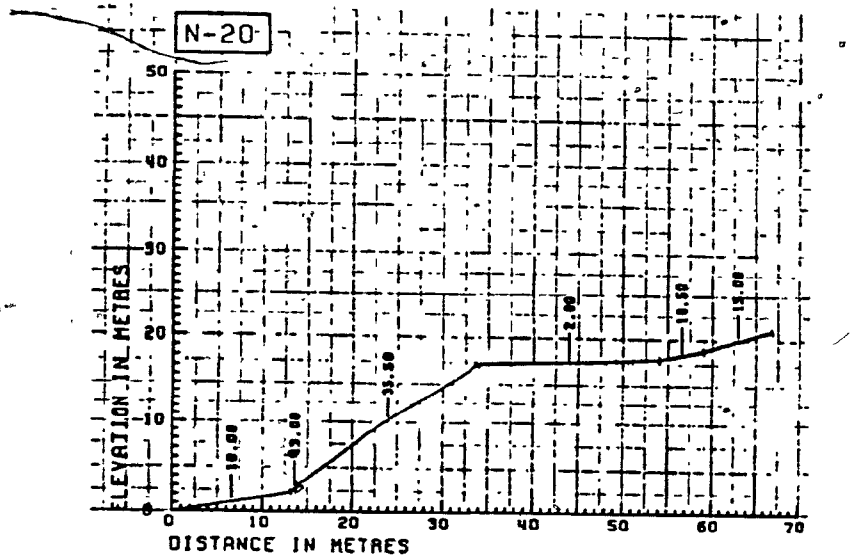

N-15
ELEVATION IN METRES
DISTANCE IN METRES
0
10
20
30
40
50
60
70
80
90
100
110
120
130
140
150
160
170
180
190
8.00
13.15
8.00
19.00
13.00
19.50
5.00
18.00
5.50
21.00
21.00
11.50
8.00

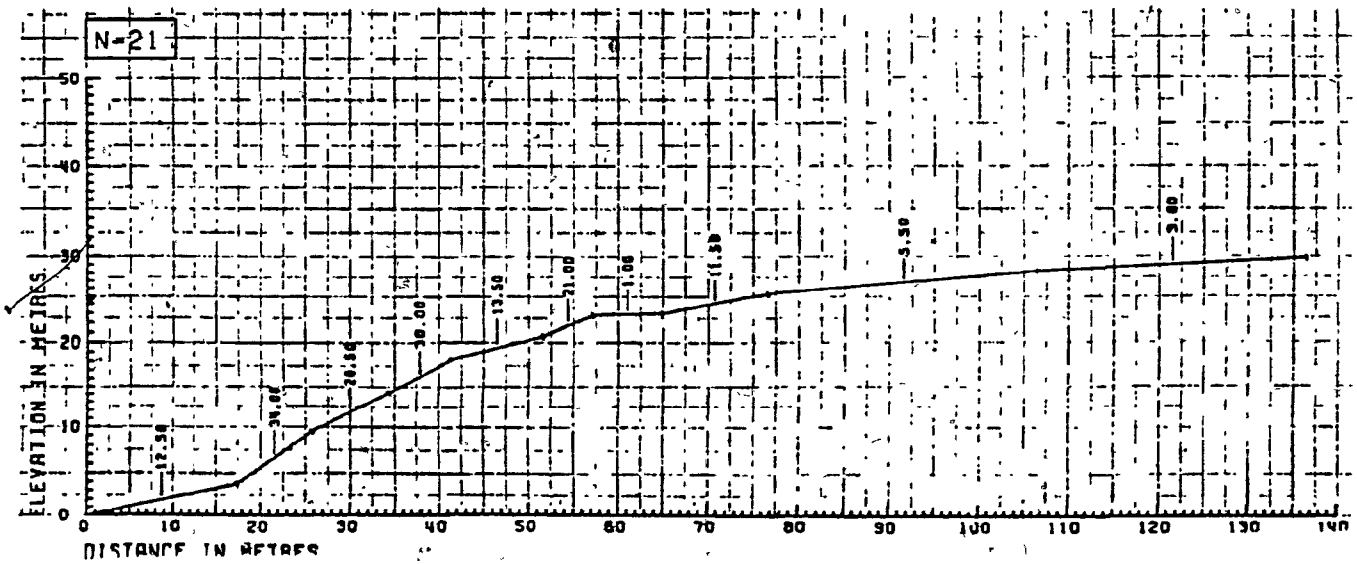

N=16
ELEVATION IN METRES
DISTANCE IN METRES
0
10
20
30
40
50
60
70
80
90
100
110
120
130
140
150
160
170
12.00
21.00
23.50
17.50
18.00
30.00
20.00
8.50
13.50
12.00
17.00
8.50
4.00
1.00

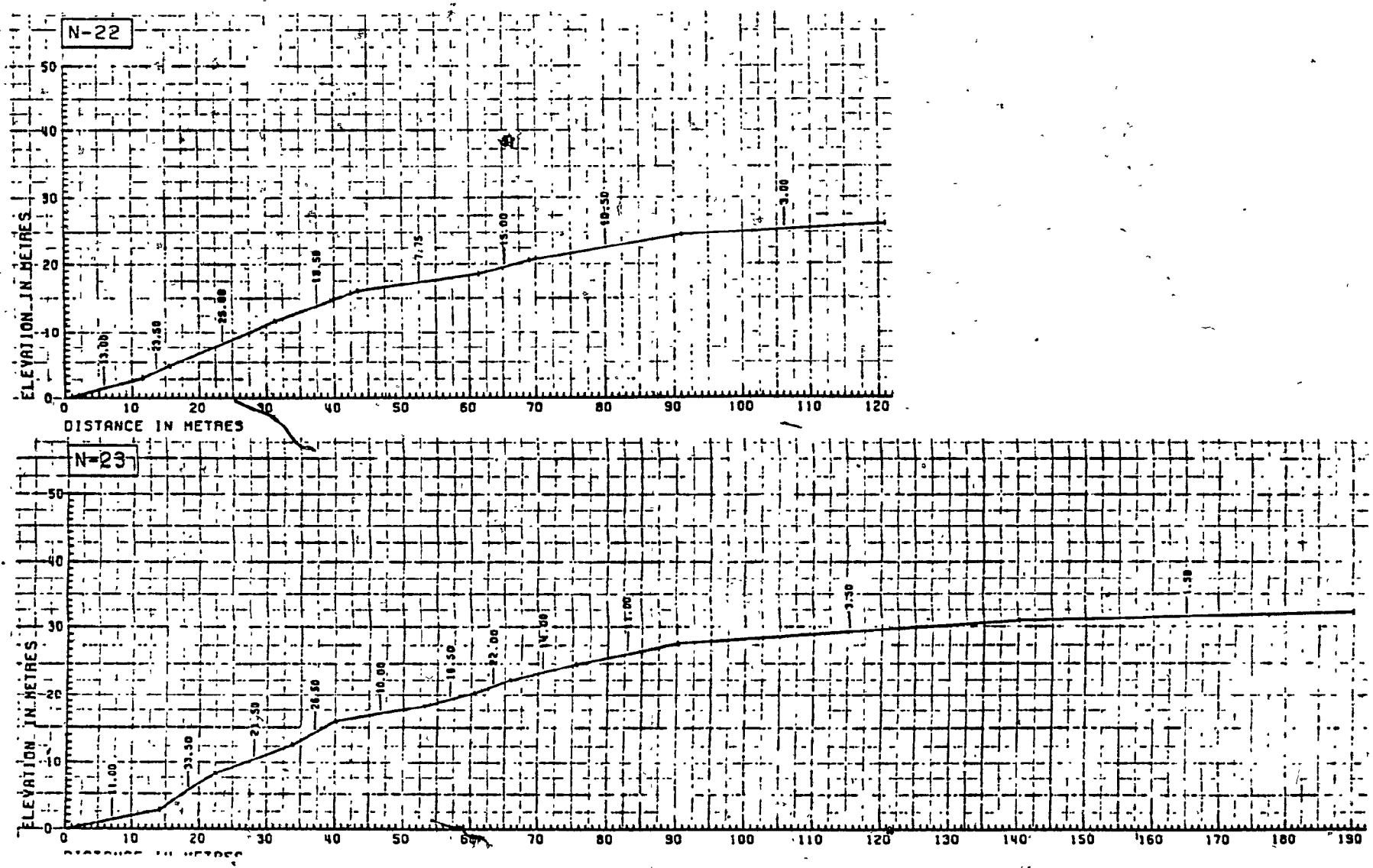

N-17
ELEVATION IN METRES
DISTANCE IN METRES
0
10
20
30
40
50
60
70
80
90
100
110
120
130
140
1.00
33.00
25.00
29.00
15.50
10.50
8.50
11.50
12.50
5.75
2.75

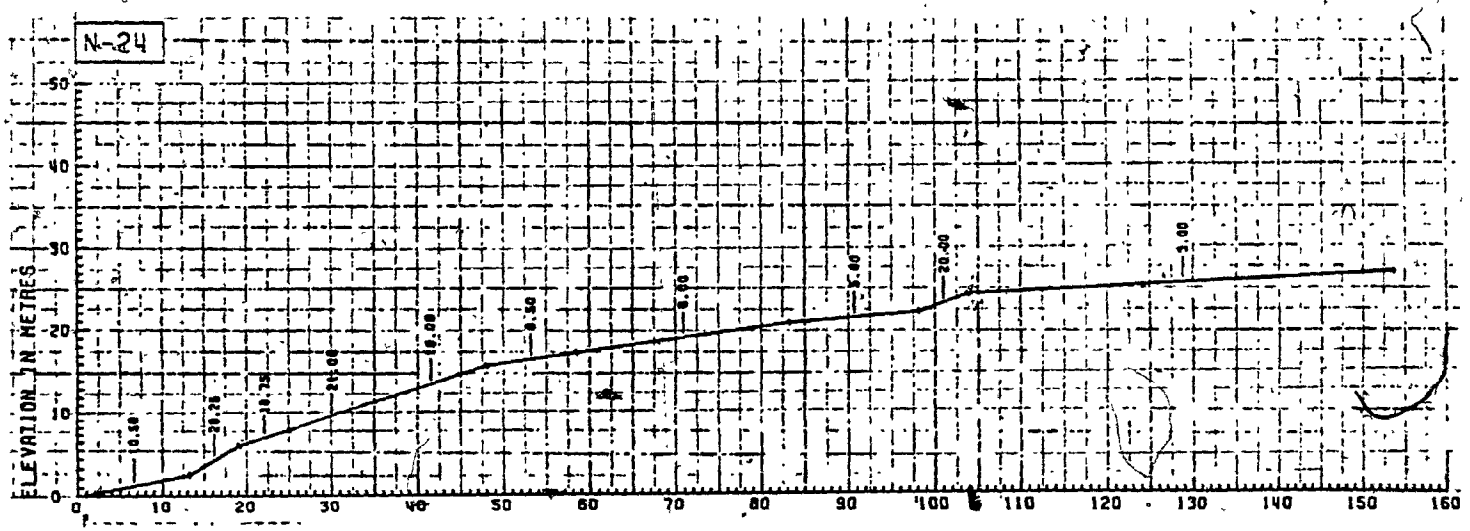

N-18
ELEVATION IN METRES
DISTANCE IN METRES
0
10
20
30
40
50
60
70
80
90
100
110
120
130
140
150
8.00
33.00
27.00
30.00
28.50
16.50
8.50
13.00
2.00

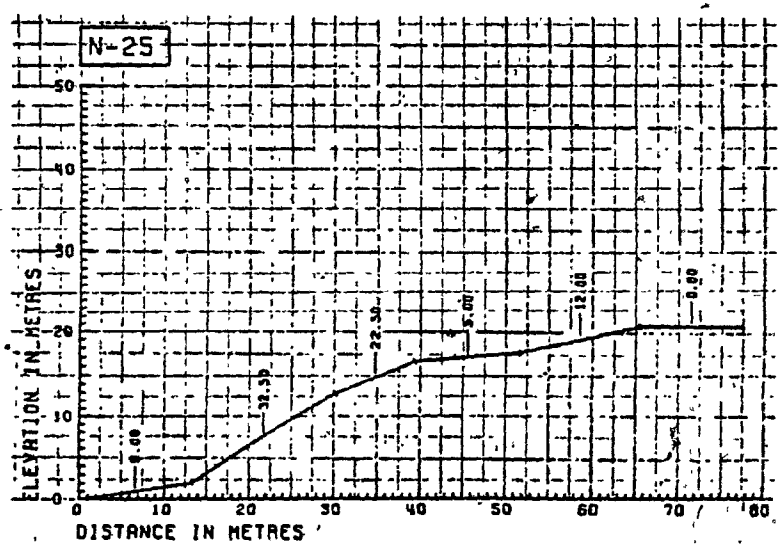

N-19
ELEVATION IN METRES
DISTANCE IN METRES
0
10
20
30
40
50
6.00
38.50
22.50
4.75

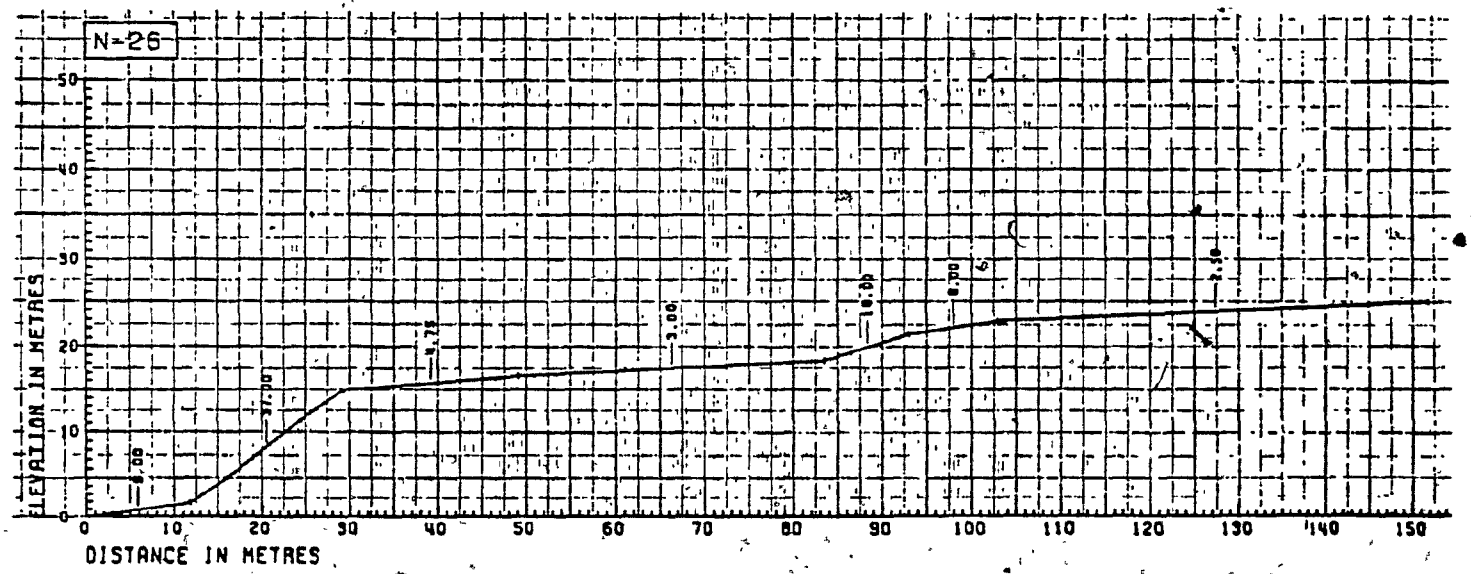

N-20
ELEVATION IN METRES
DISTANCE IN METRES
0
10
20
30
40
50
60
70
19.00
43.00
35.00
2.00
10.50
13.00

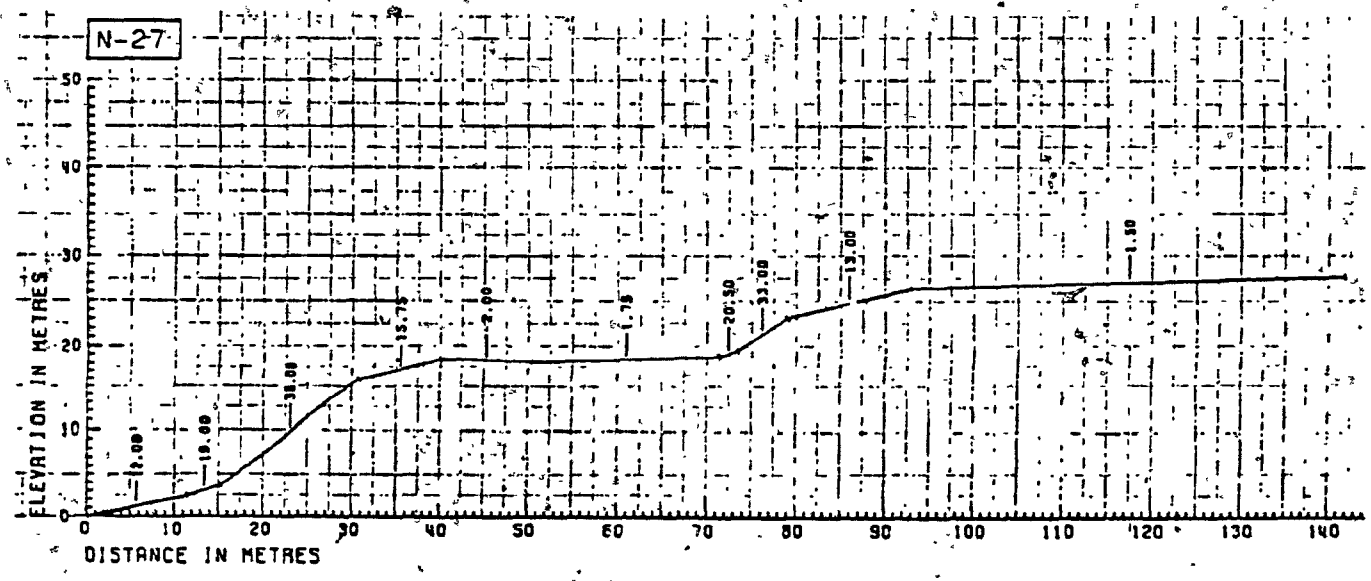

N-21
ELEVATION IN METRES
DISTANCE IN METRES
0
10
20
30
40
50
60
70
80
90
100
110
120
130
140
12.50
28.00
28.50
38.00
13.50
21.00
1.00
11.50
5.50
3.00

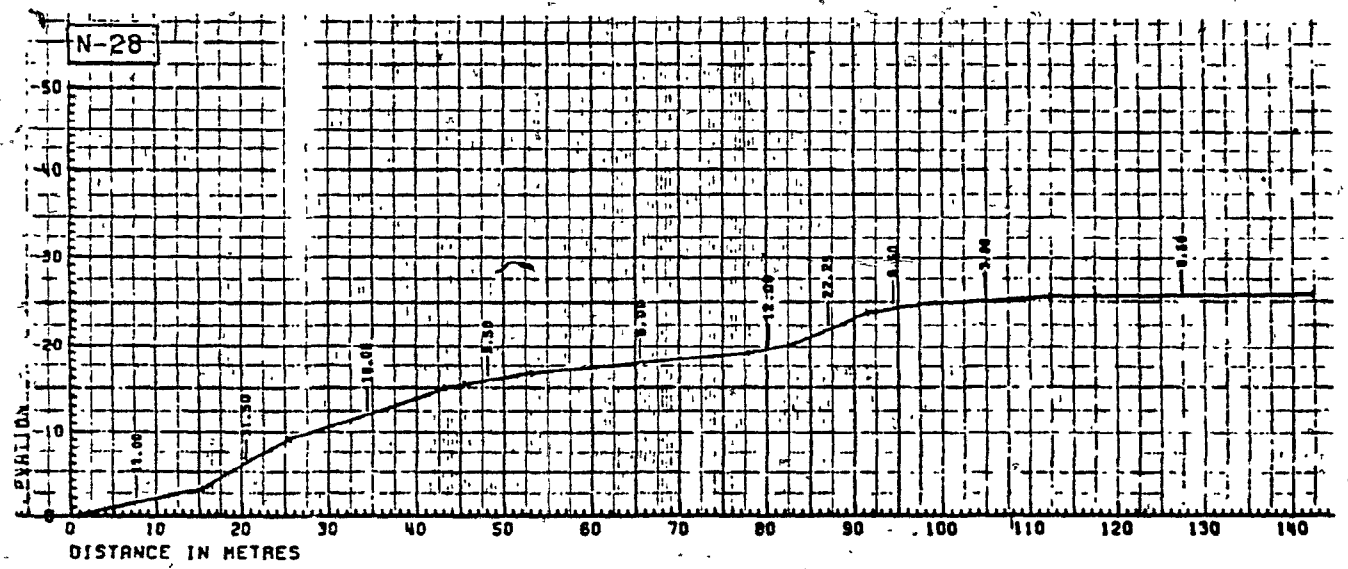

N-22
ELEVATION IN METRES
DISTANCE IN METRES
N-23
ELEVATION IN METRES

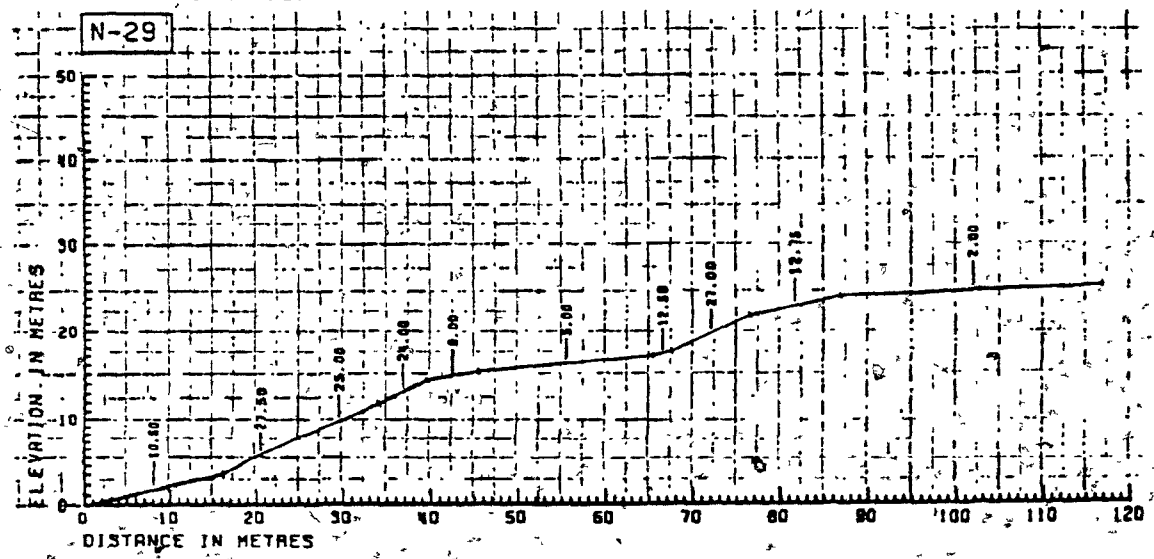

N-24
ELEVATION IN METRES
0
10
20
30
40
50
60
70
80
90
100
110
120
130
140
150
160
10.50
20.25
10.75
21.00
18.00
8.50
8.00
5.00
20.00
3.00

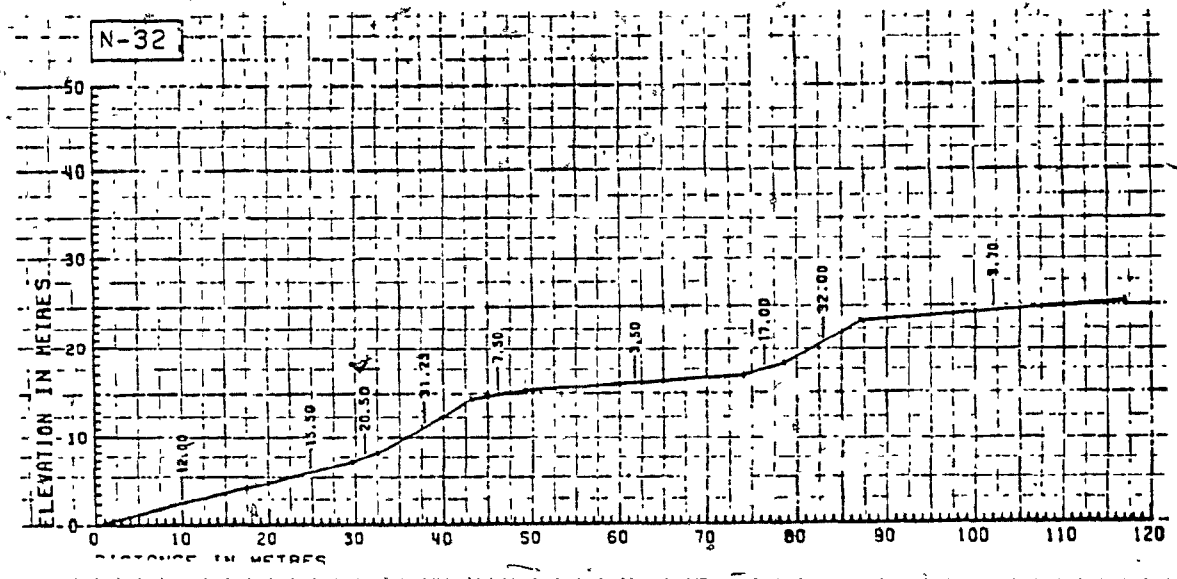

N-25
ELEVATION IN METRES
0
10
20
30
40
50
60
70
80
DISTANCE IN METRES
8.00
32.50
22.50
5.00
12.00
8.00

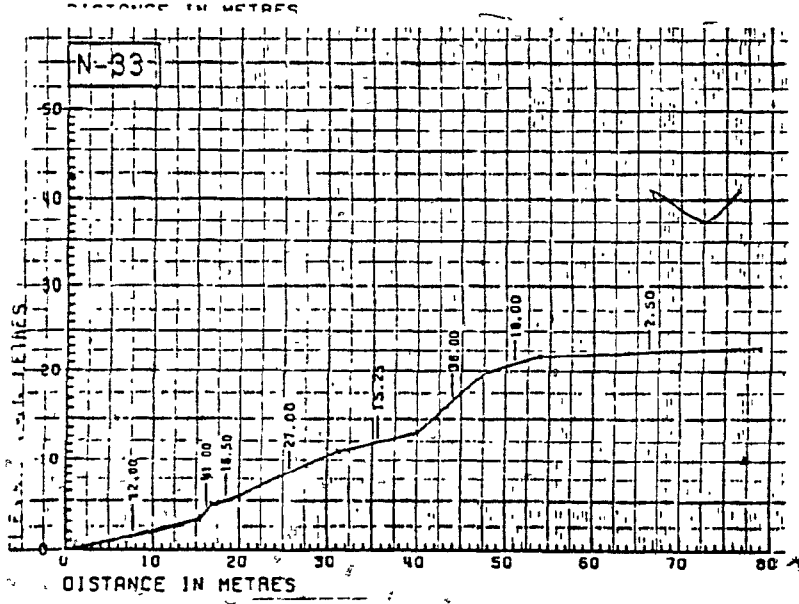

N-26
ELEVATION IN METRES
DISTANCE IN METRES
0
10
20
30
40
50
60
70
80
90
100
110
120
130
140
150
6.00
37.00
4.75
3.00
18.00
8.00
2.50

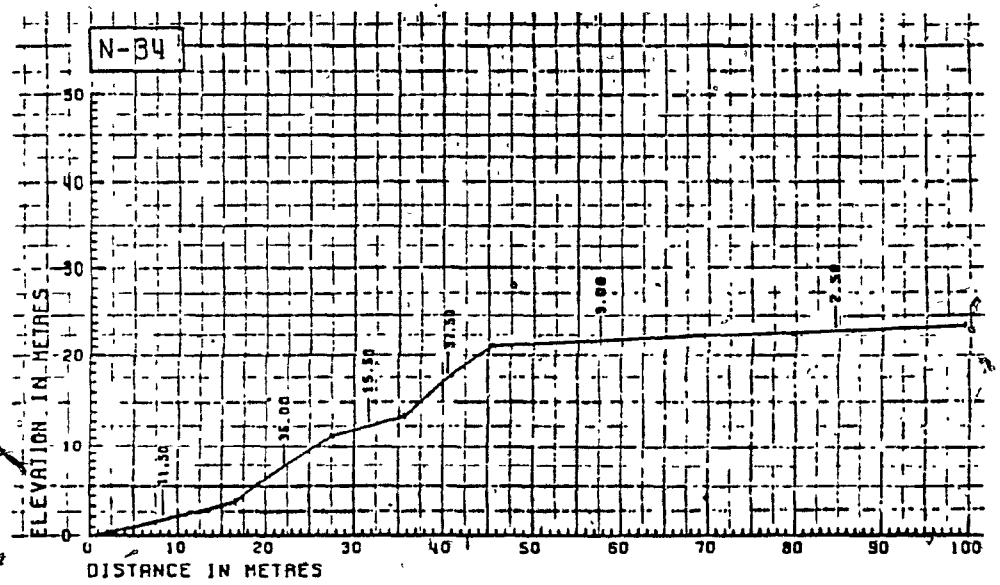

N-27
ELEVATION IN METRES
DISTANCE IN METRES
0
10
20
30
40
50
60
70
80
90
100
110
120
130
140
12.00
10.00
38.00
15.75
2.00
1.75
20.50
33.00
13.00
1.50

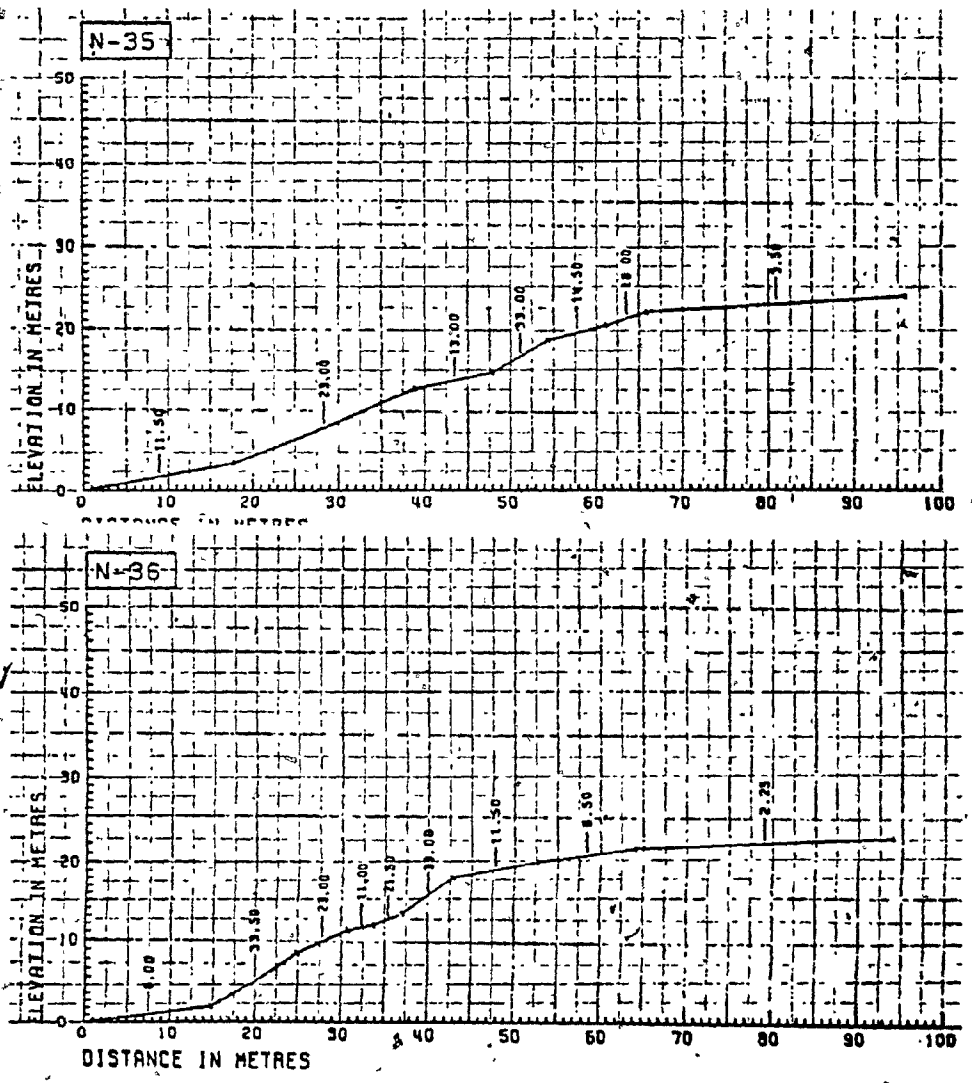

N-28
ELEVATION
DISTANCE IN METRES

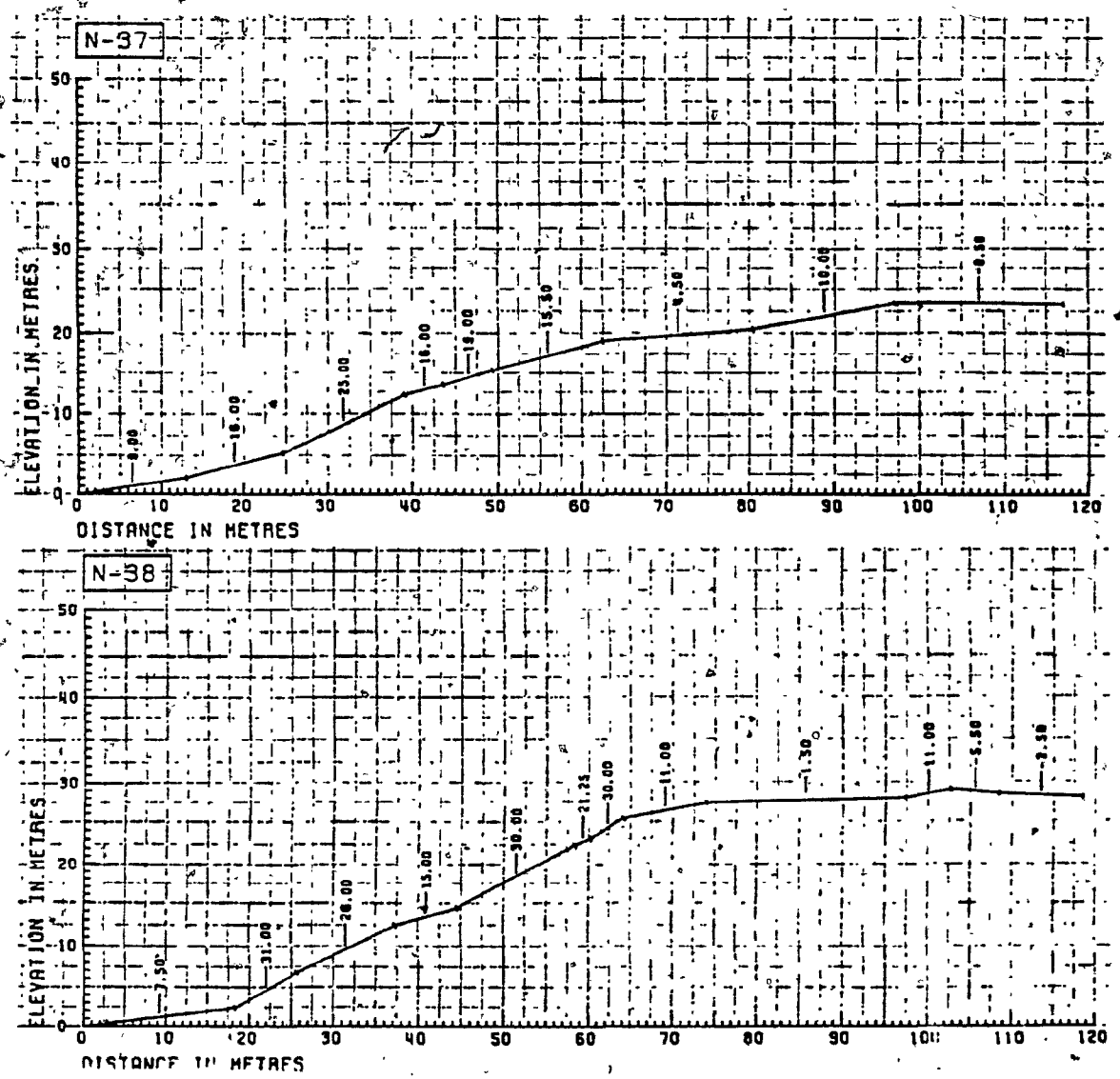

N-29
ELEVATION IN METRES
DISTANCE IN METRES

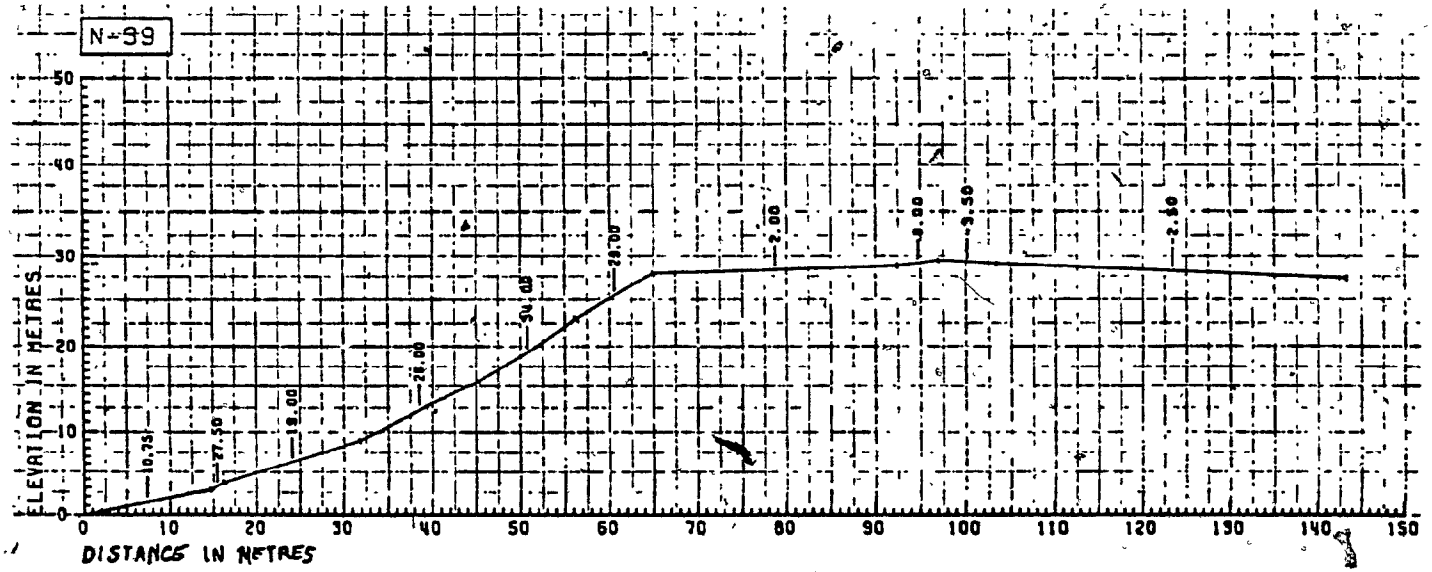

N-32
ELEVATION IN METRES
0
10
20
30
40
50
60
70
80
90
100
110
120
12.00
13.50
20.50
31.25
7.50
3.50
17.00
32.00
3.70

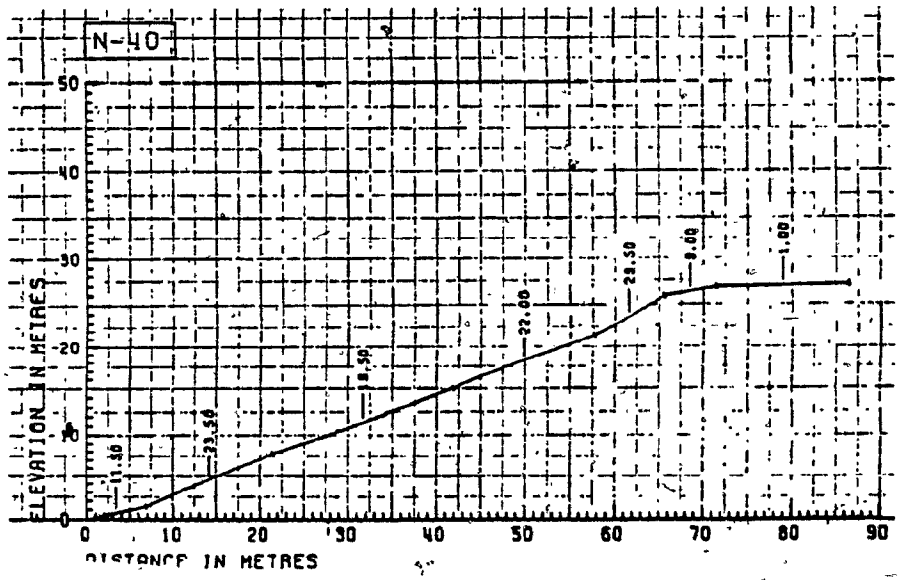

N-33
ELEVATION IN METRES
DISTANCE IN METRES
0
10
20
30
40
50
60
70
80
12.00
11.00
18.50
27.00
15.25
36.00
18.00
2.50

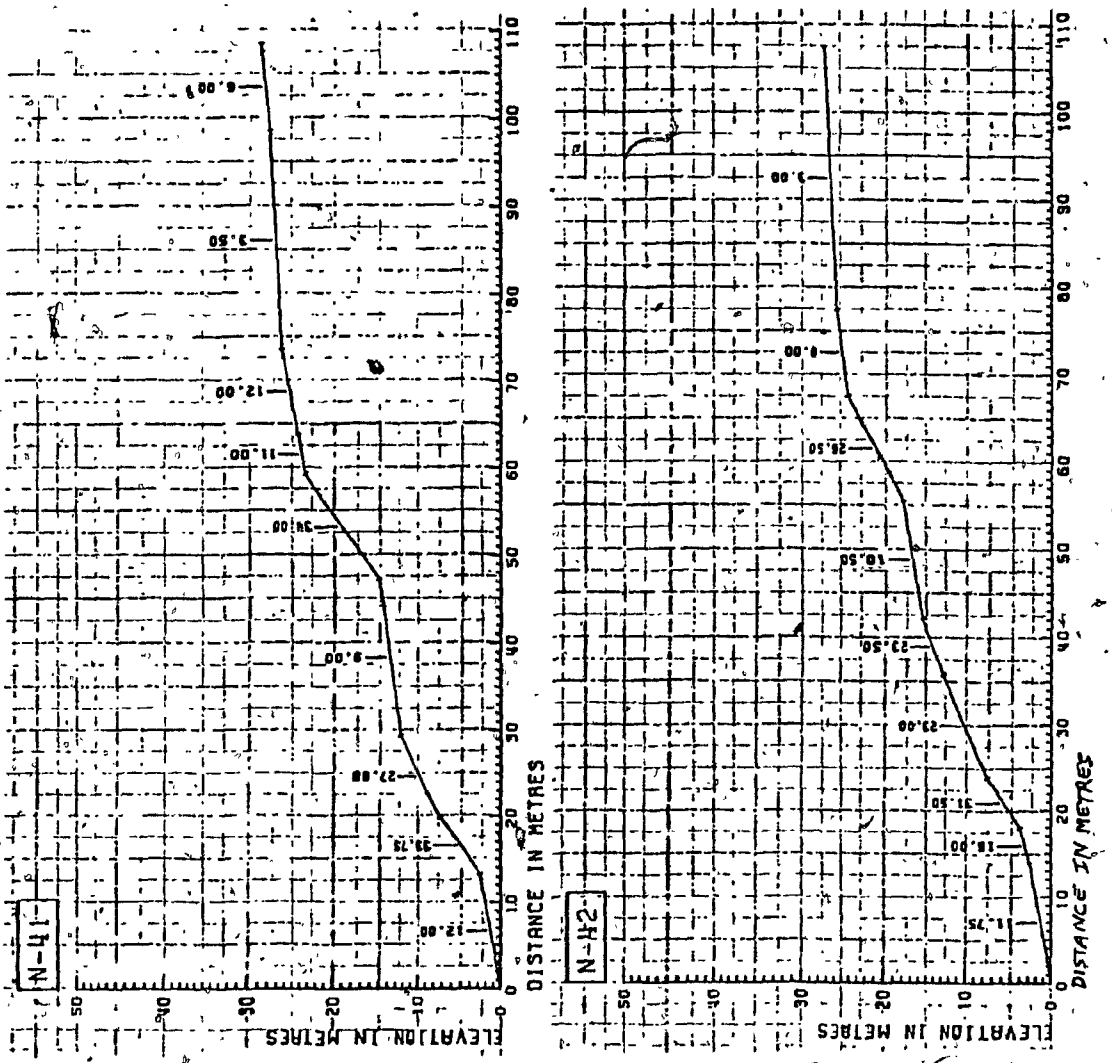

N-34
ELEVATION IN METRES
DISTANCE IN METRES
0
10
20
30
40
50
60
70
80
90
100
11.50
36.00
15.50
37.50
9.00
2.50

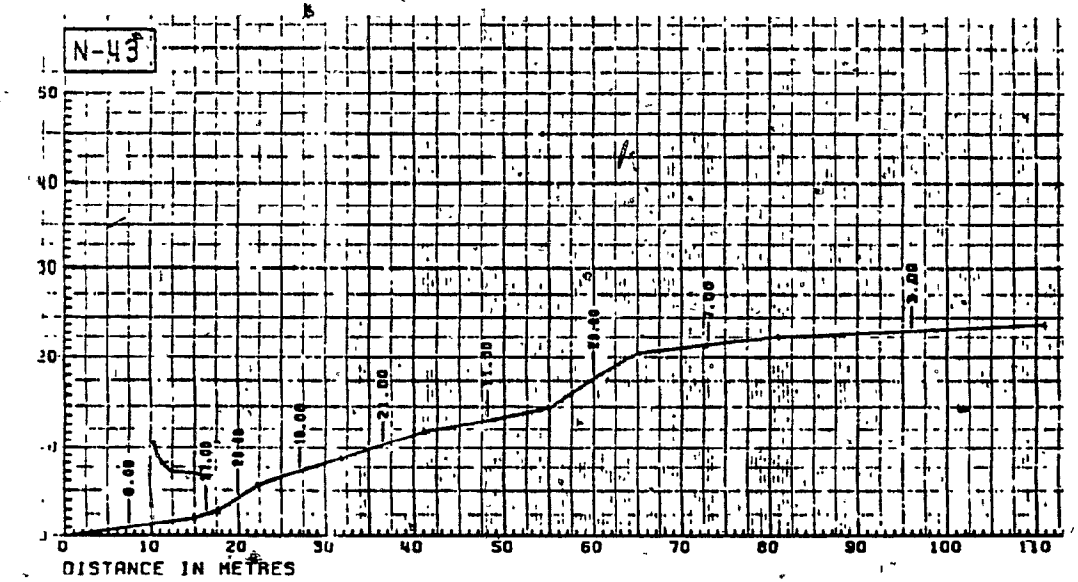

N-35
ELEVATION IN METRES
0
10
20
30
40
50
60
70
80
90
100
11.50
23.00
13.00
33.00
14.50
18.00
3.50
N-36
ELEVATION IN METRES
DISTANCE IN METRES
4.00
33.50
23.00
11.00
21.50
13.00
11.50
8.50
2.23

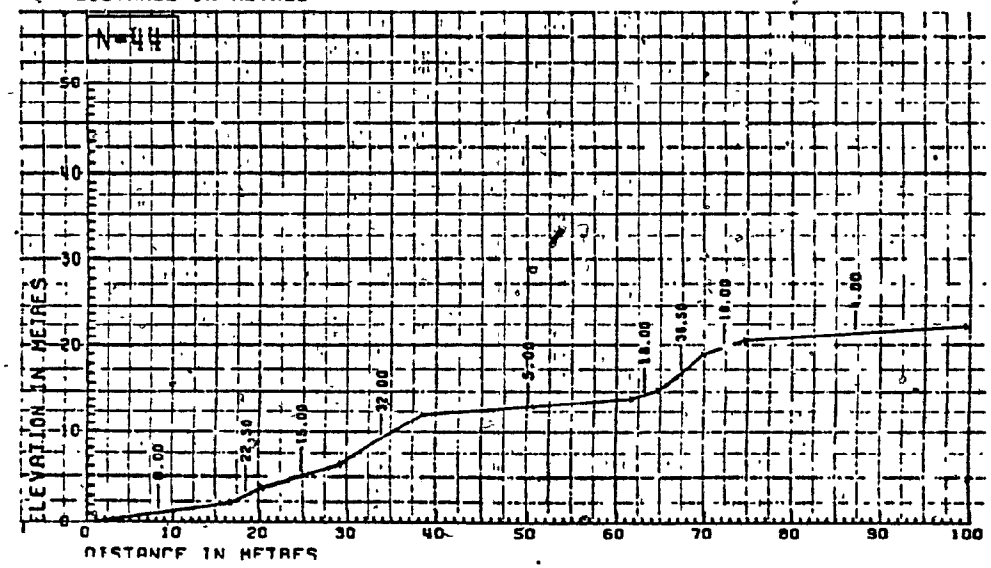

N-37
ELEVATION IN METRES
DISTANCE IN METRES
0
10
20
30
40
50
60
70
80
90
100
110
120
8.00
16.00
23.00
30.00
38.00
45.30
49.50
50.00
49.50
N-38
ELEVATION IN METRES
DISTANCE IN METRES
3.50
31.00
38.00
45.00
50.00
51.25
50.00
51.00
51.30
51.00
49.50
49.38

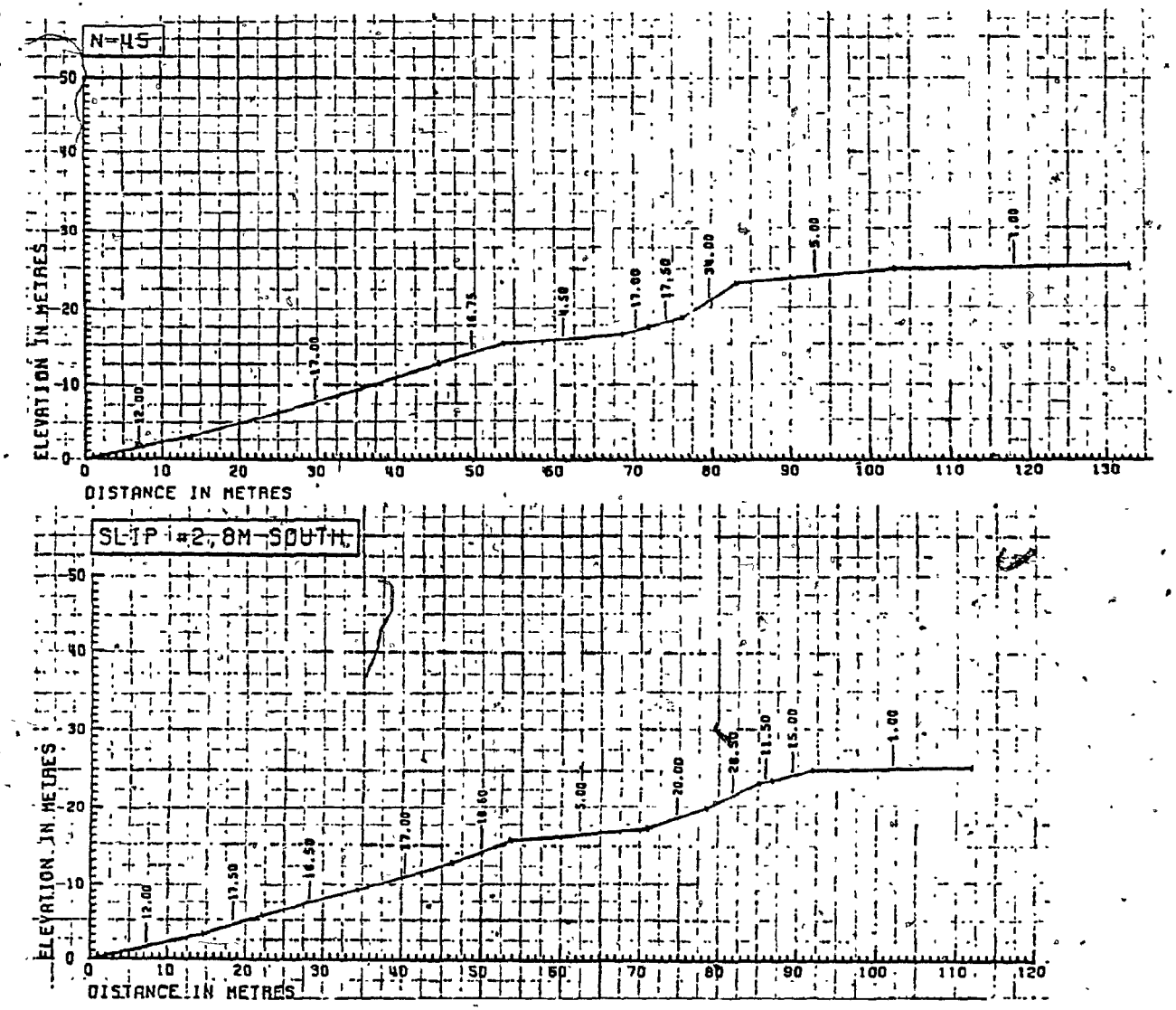

N-39
ELEVATION IN METRES
DISTANCE IN METRES
0
10
20
30
40
50
60
70
80
90
100
110
120
130
140
150
10.75
27.50
18.00
28.00
34.00
29.00
2.00
8.00
3.50
2.50

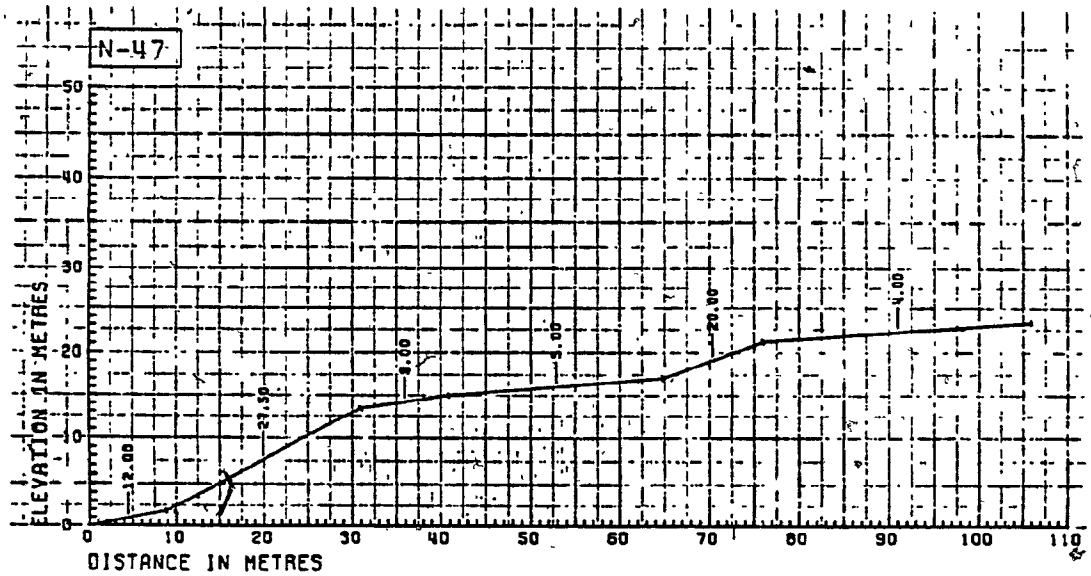

N-40
ELEVATION IN METRES
DISTANCE IN METRES
0
10
20
30
40
50
60
70
80
90
11.50
23.50
8.50
22.00
28.50
8.00
1.00

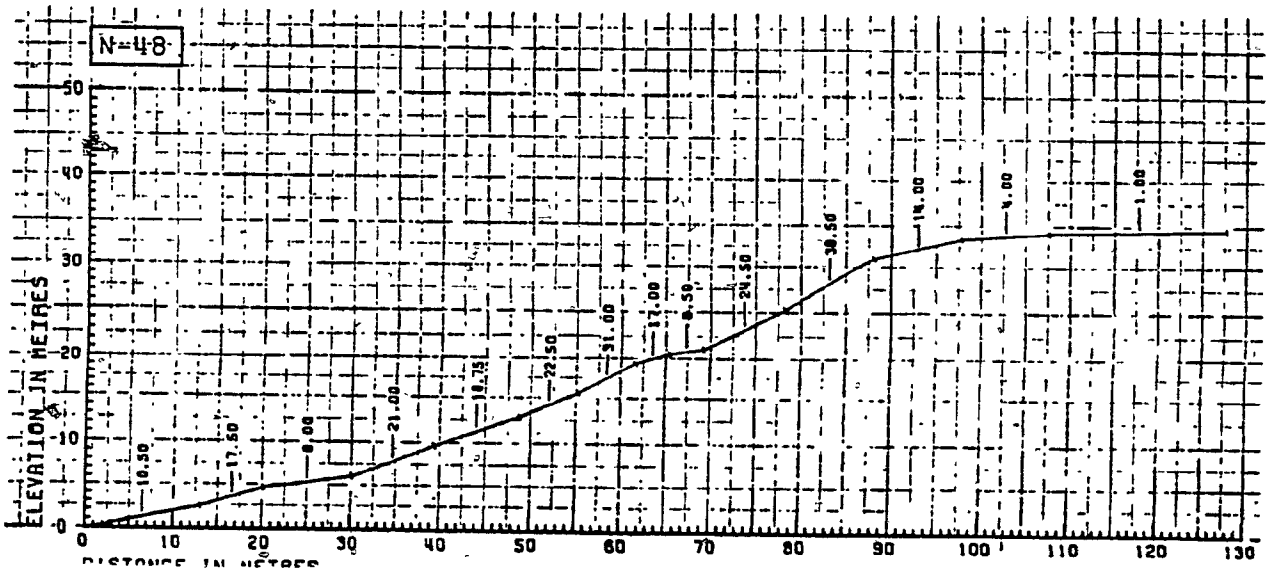

N-41
N-42
DISTANCE IN METRES
ELEVATION IN METRES

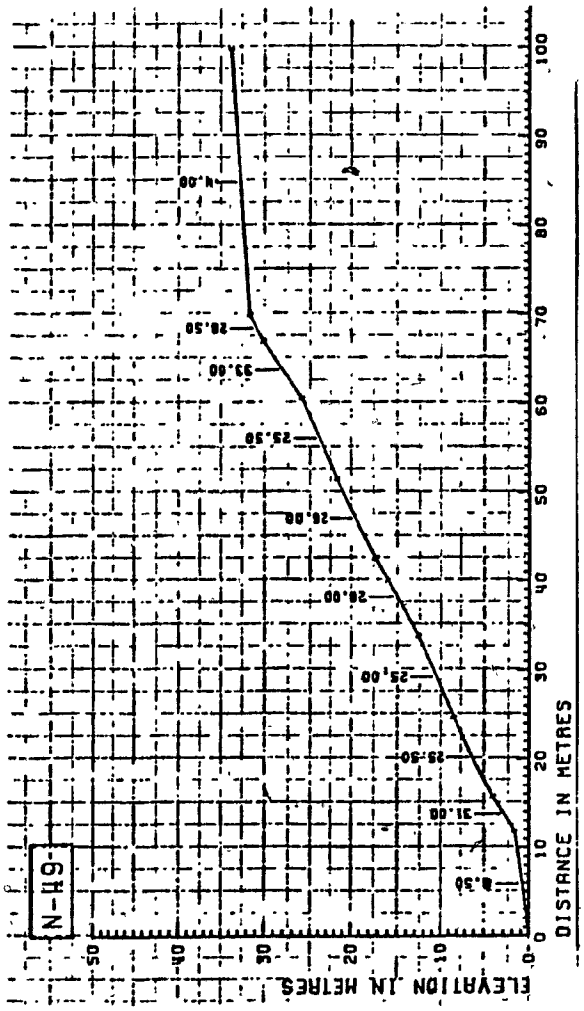

N-43
0.00
17.00
20.10
18.00
21.00
11.00
20.00
7.00
3.00
0
10
20
30
40
50
60
70
80
90
100
110
DISTANCE IN METRES

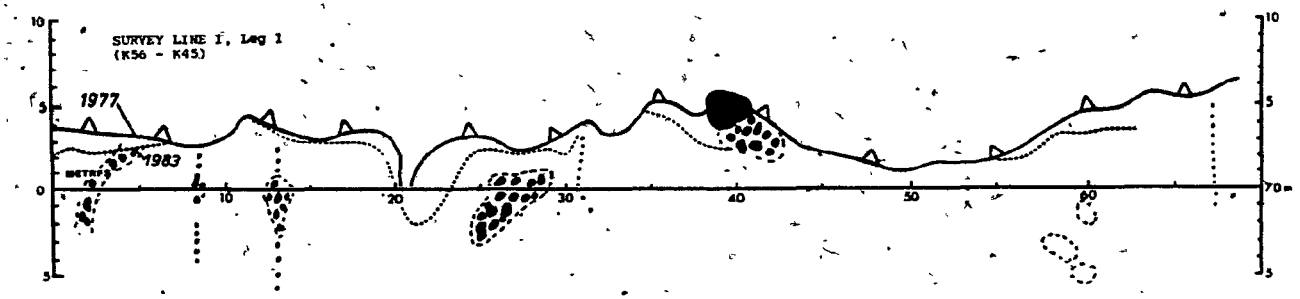

N-44
ELEVATION IN METRES
0.00
22.30
15.00
32.00
9.00
18.00
38.50
19.00
1.00
0
10
20
30
40
50
60
70
80
90
100
DISTANCE IN METRES


N-45
ELEVATION IN METRES
DISTANCE IN METRES
SLIP #2, 8M SOUTH
ELEVATION IN METRES
DISTANCE IN METRES

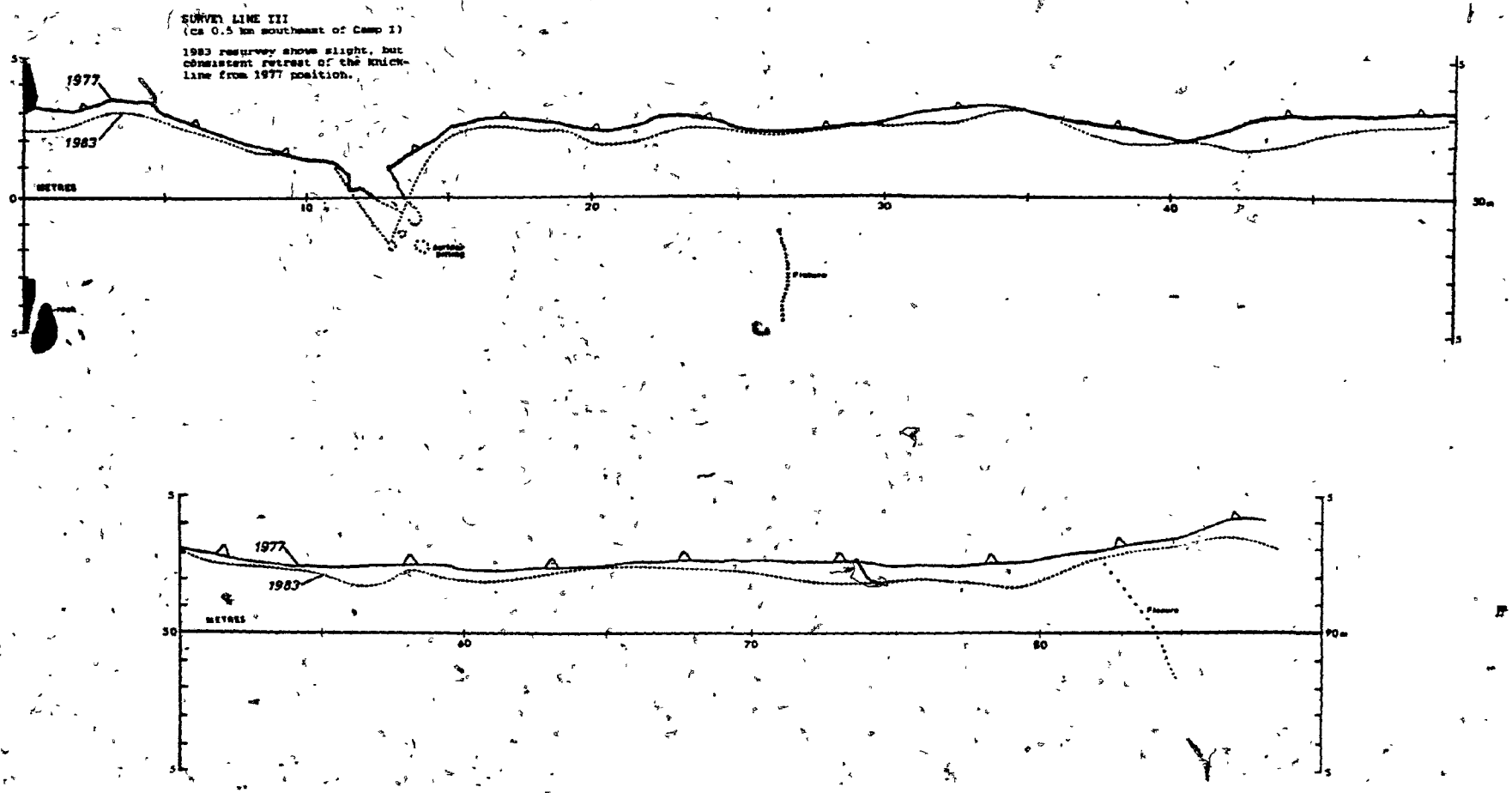

N-47
ELEVATION IN METRES
DISTANCE IN METRES
0
10
20
30
40
50
60
70
80
90
100
110
12.00
23.50
8.00
4.00
20.00
4.00

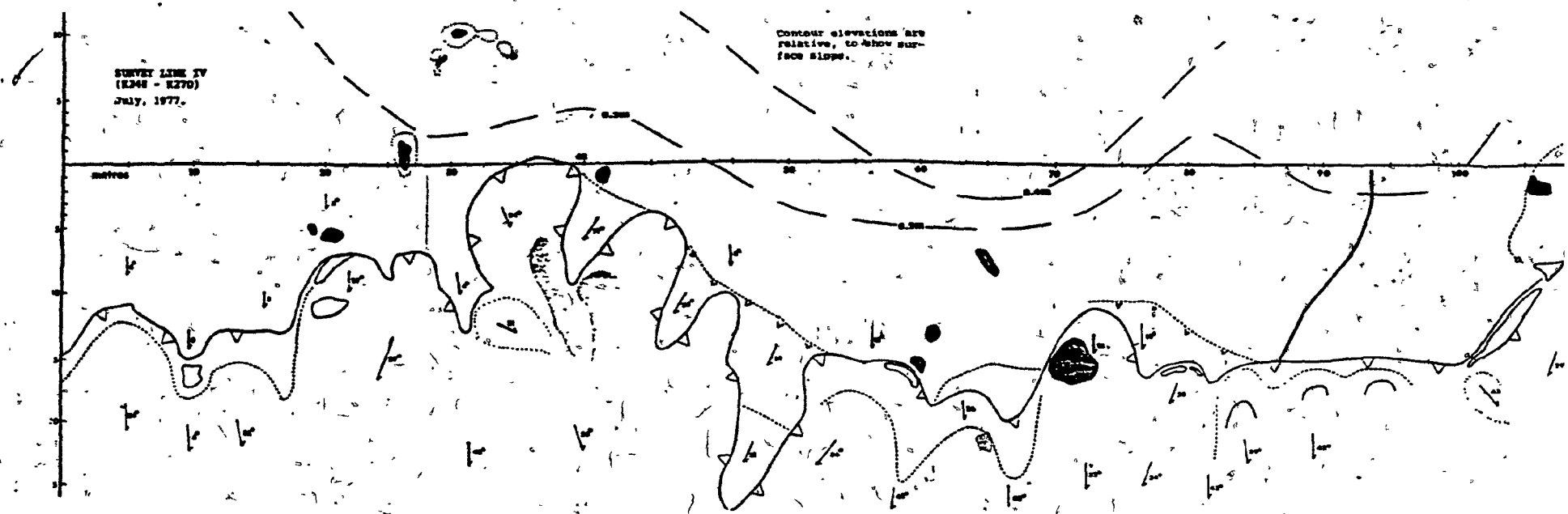

N-48
ELEVATION IN METRES
0
10
20
30
40
50
60
70
80
90
100
110
120
130
10.50
17.50
8.00
21.00
18.25
22.50
31.00
11.00
8.50
24.50
30.50
18.00
4.00
1.00

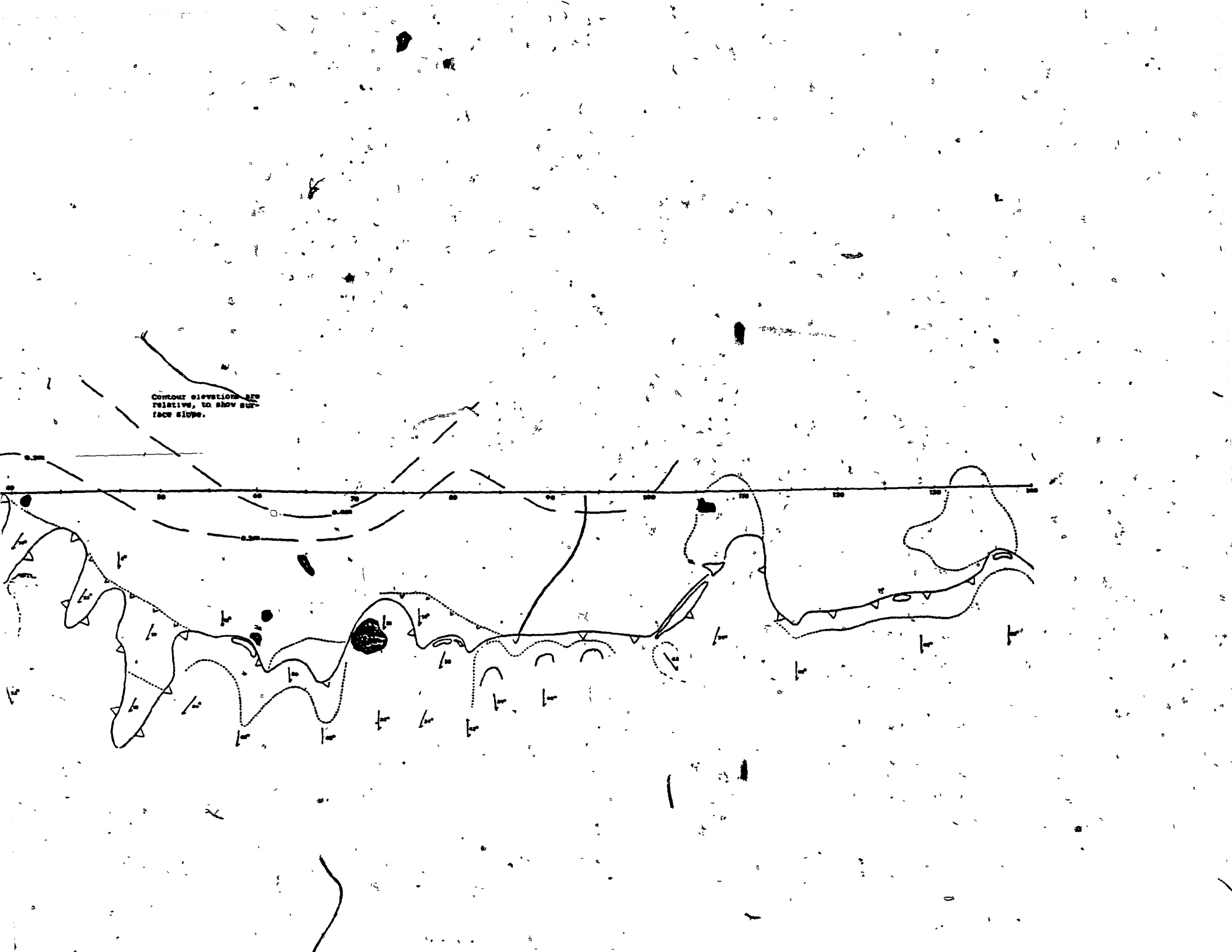

N-H9
ELEVATION IN METRES
DISTANCE IN METRES
14.00
28.50
33.00
25.50
26.00
26.00
25.00
23.50
21.00
8.50

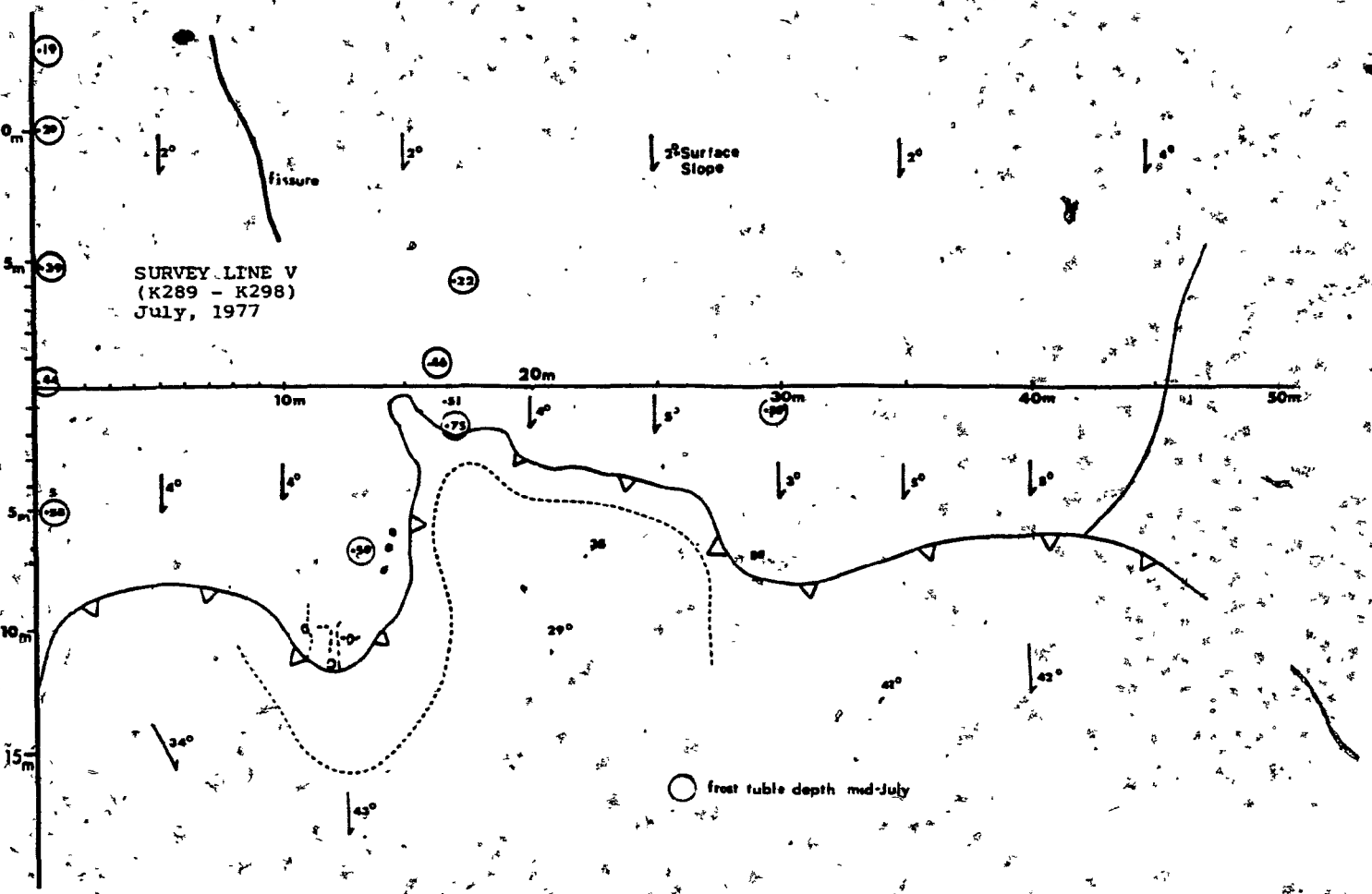

SURVEY LINE I, Leg 1
(K56 - K45)
1977
1983
METRES
10
5
0
5
10
20
30
40
50
60
70m

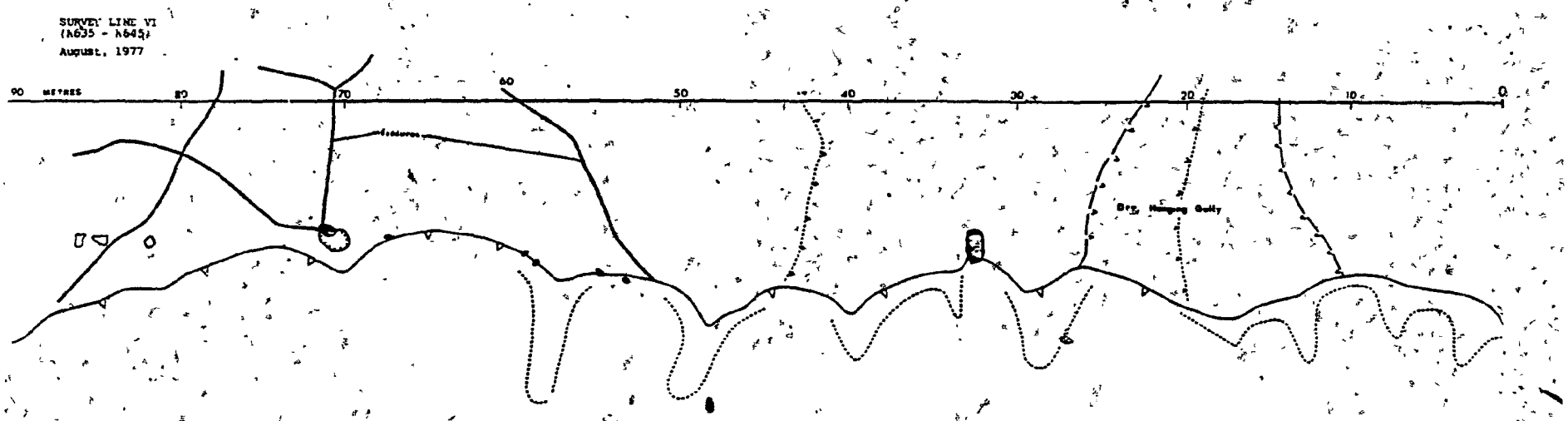

SURVEY LINE I, Leg 2
(K45 - K25)
1977
1983
METRES
Gully
10
5
0
5
10
20
30
40
50
60
70
80
90
100m

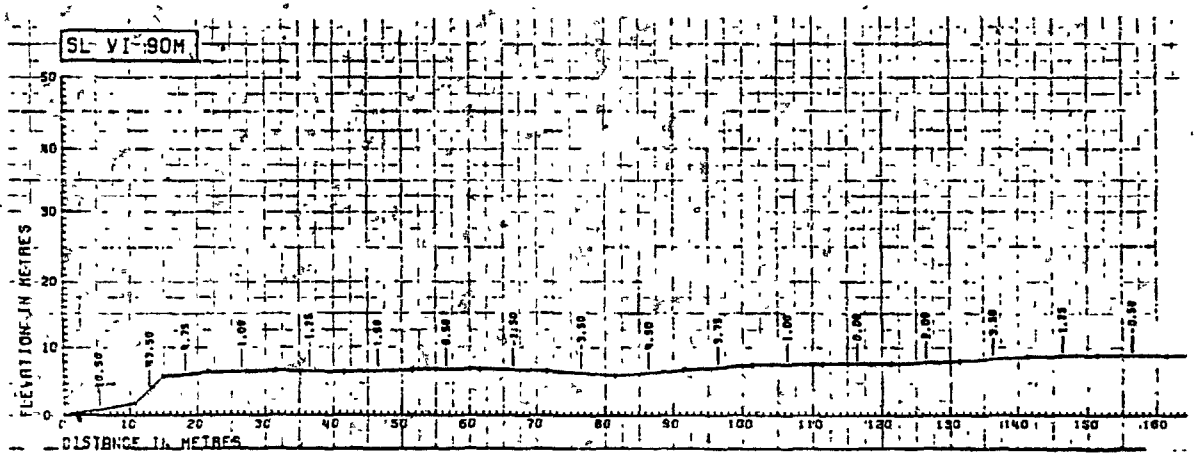

SURVEY LINE III
(ca 0.5 km southeast of Camp I)
1983 resurvey shows slight, but consistent retreat of the knick-line from 1977 position.
1977
1983
METRES
0
10
20
30
40
50
60
70
80
90m


SURVEY LINE IV
(E248 - E270)
July, 1977.
Contour elevations are relative, to show surface slope.
metres

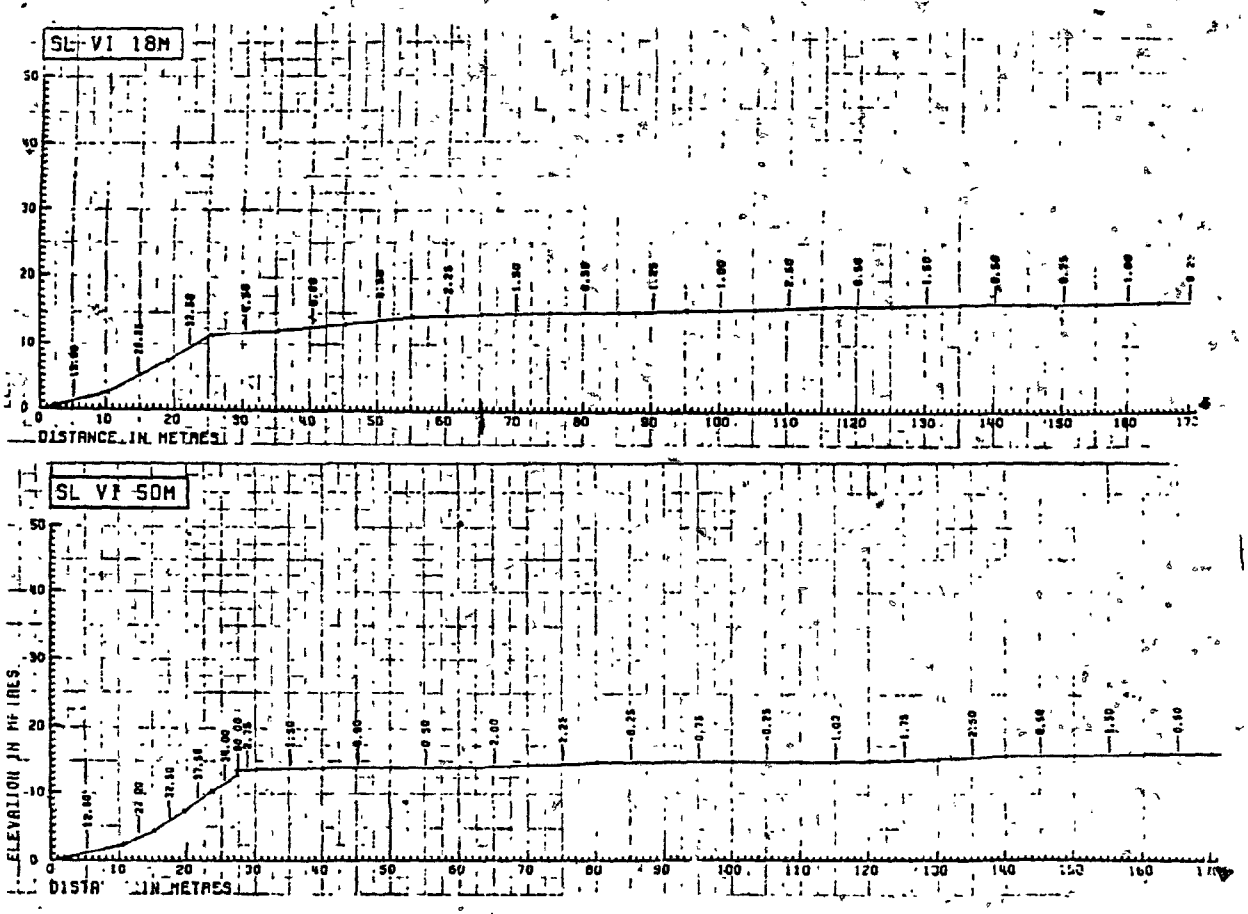

Contour elevations are relative, to show surface slope.

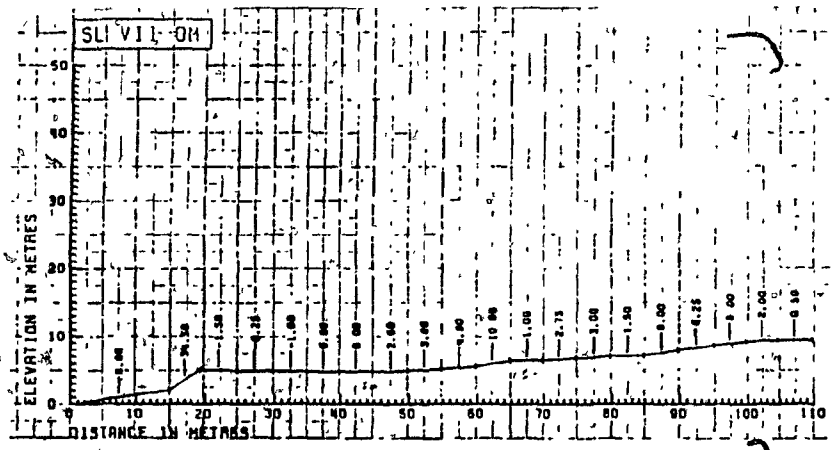

SURVEY LINE V
(K289 - K298)
July, 1977
fissure
Surface Slope
10m
20m
30m
40m
50m
frost table depth mid-July

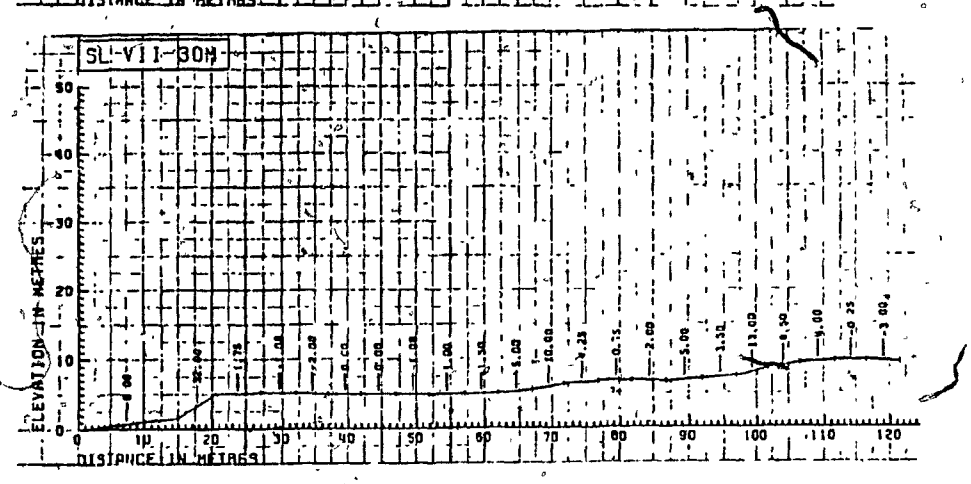


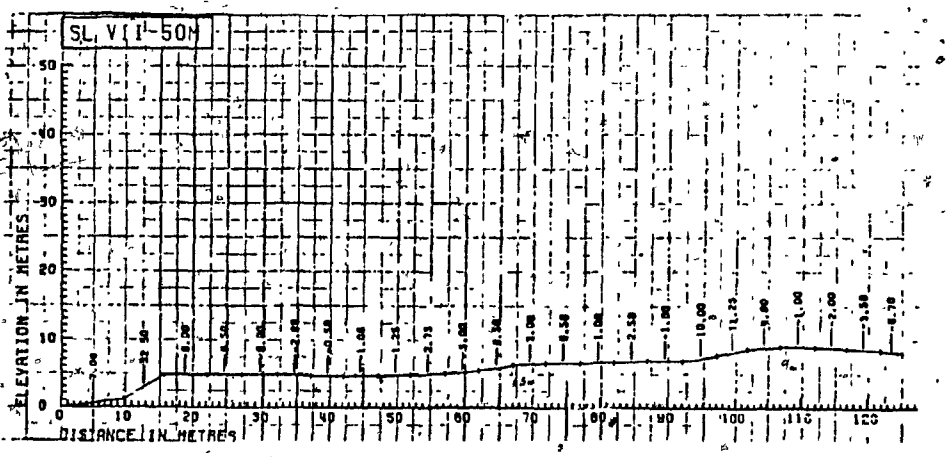


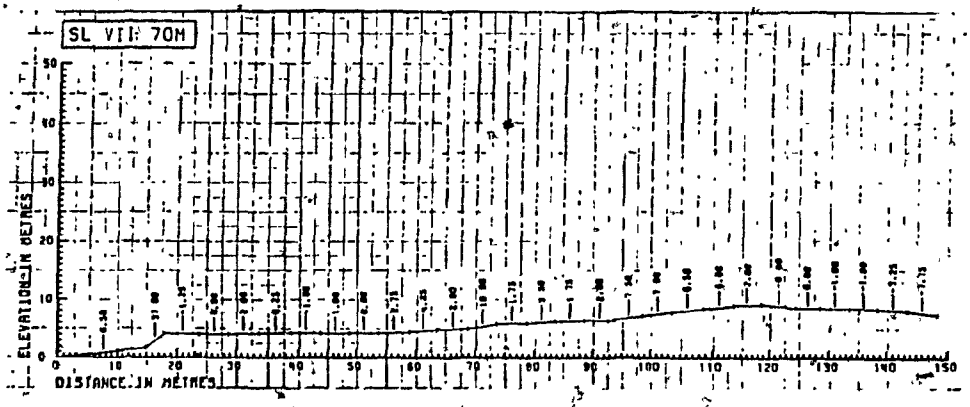
18m and 50m transects on following page


SL VI 18M
DISTANCE IN METRES
SL VI 50M
ELEVATION IN METRES
DISTANCE IN METRES


SL VII-0M
ELEVATION IN METRES
DISTANCE IN METRES


SL-VII-30M
ELEVATION IN METRES
DISTANCE IN METRES


SL VII-50M
ELEVATION IN METRES
DISTANCE IN METRES


SL VII-70M
ELEVATION IN METRES
DISTANCE IN METRES

APPENDIX C

1. Photographic Panorama of the Kivitoo Bluffs

Part 1: K0 - K450
Part 2: K451 - K880
Part 3: K881 - K1302

2. Stratigraphy of the Kivitoo Bluffs (Nelson, 1978)

Part 1: Sections 54-16 to 16-9; K729
Panorama begins between sections 39-19 and 38-14

Part 2: Sections 15-22; K766 to 1-30; K1247

Appendix C

Kivitoo Bluff Panorama

Part 1: K0 - K450



← Survey Lines III + VIII



35-4

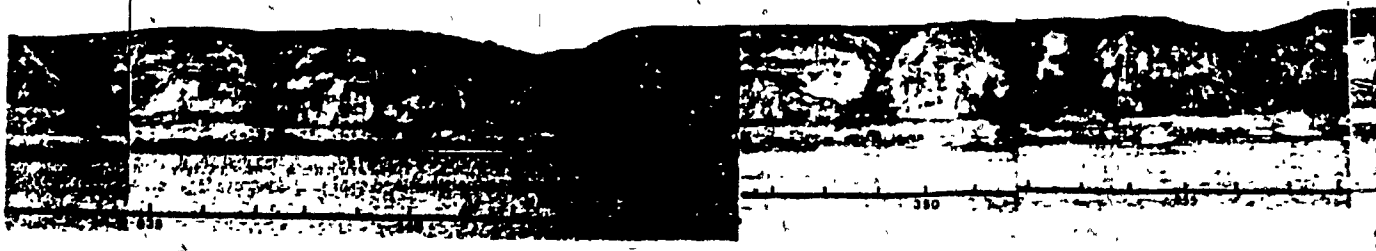
SURVEY LINE II



29-34

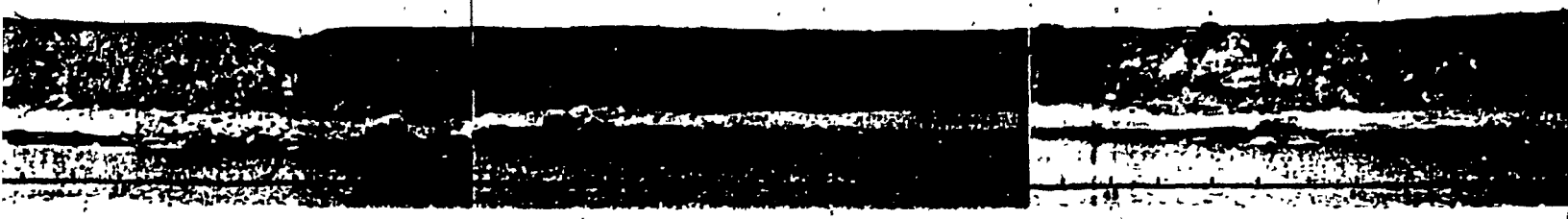


28-13



38-14

SURVEY LINE I



34-2



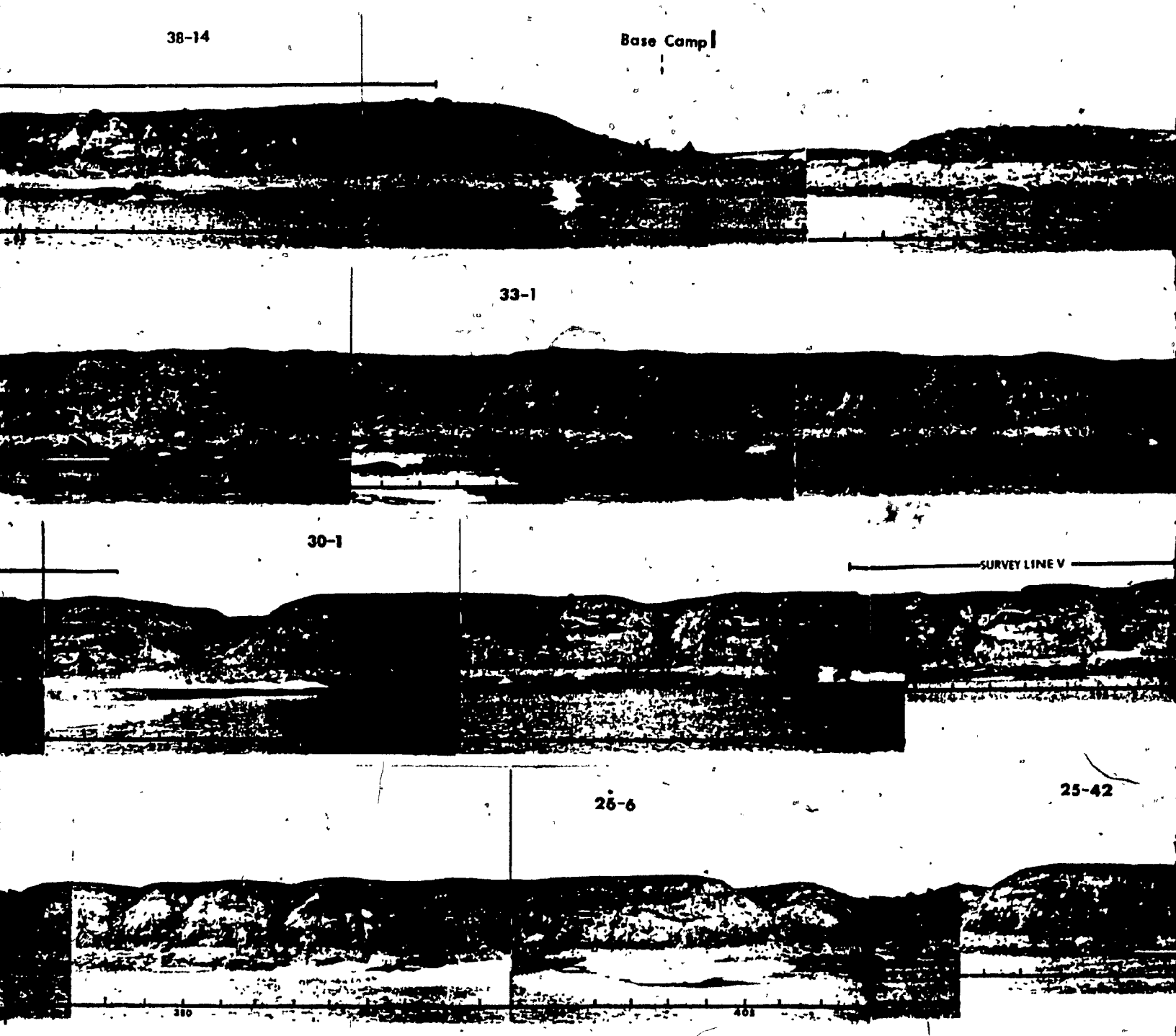
30-1

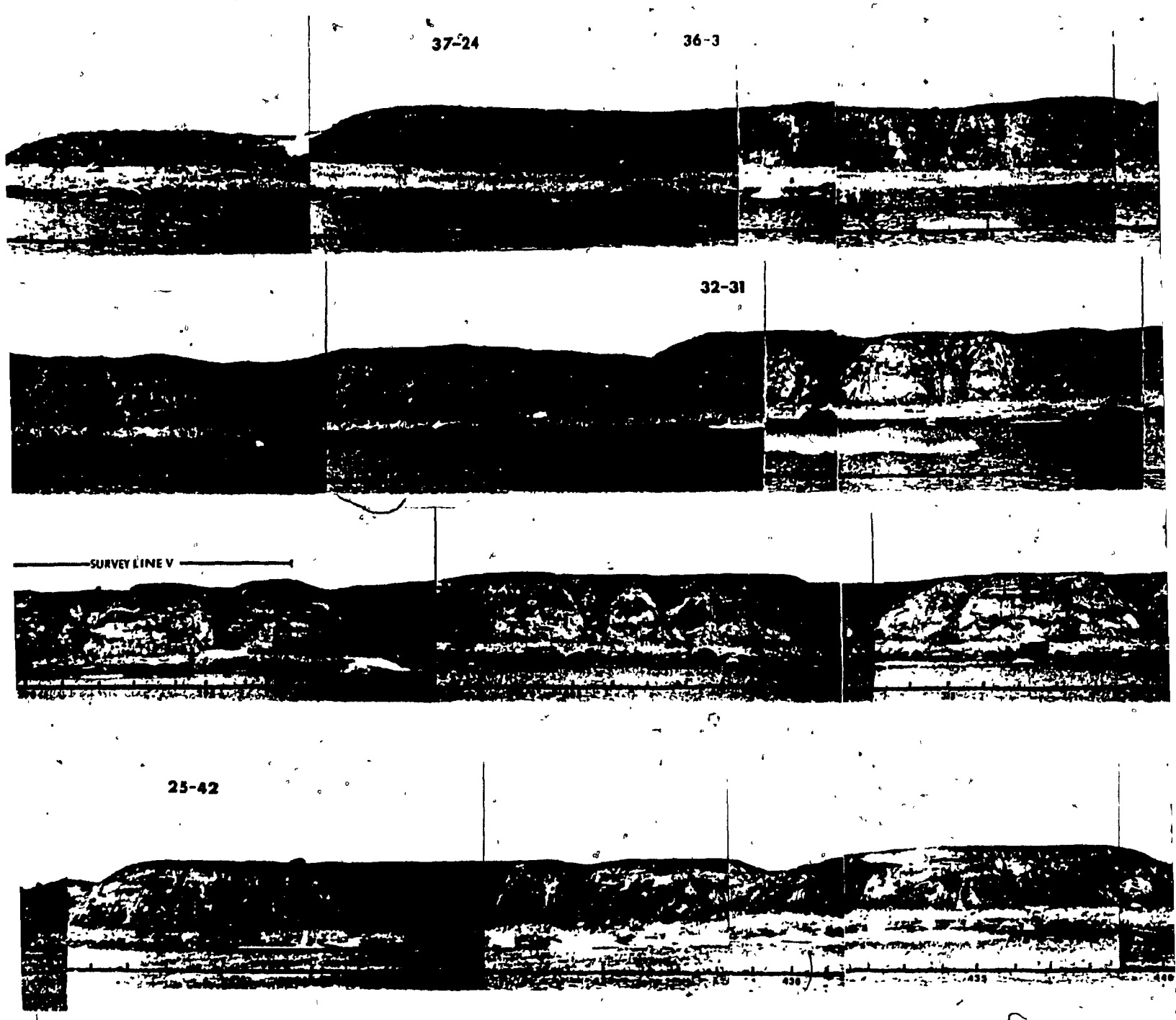
SURVEY LINE IV



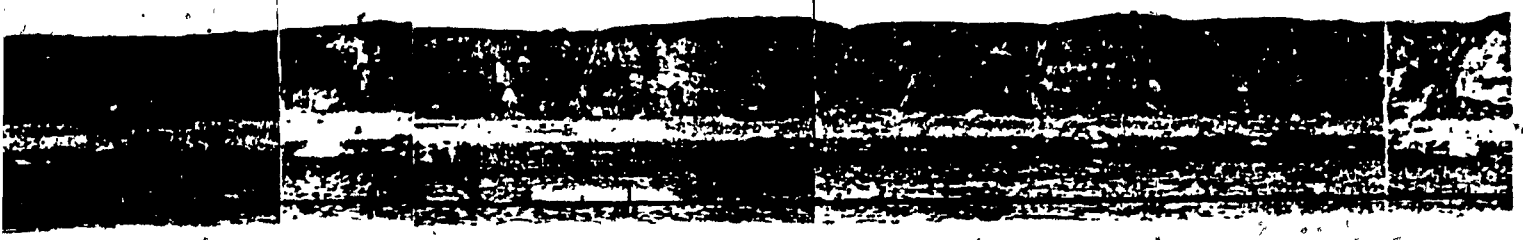
27-27




38-14
Base Camp
33-1
30-1
SURVEY LINE V
25-6
25-42
350
400

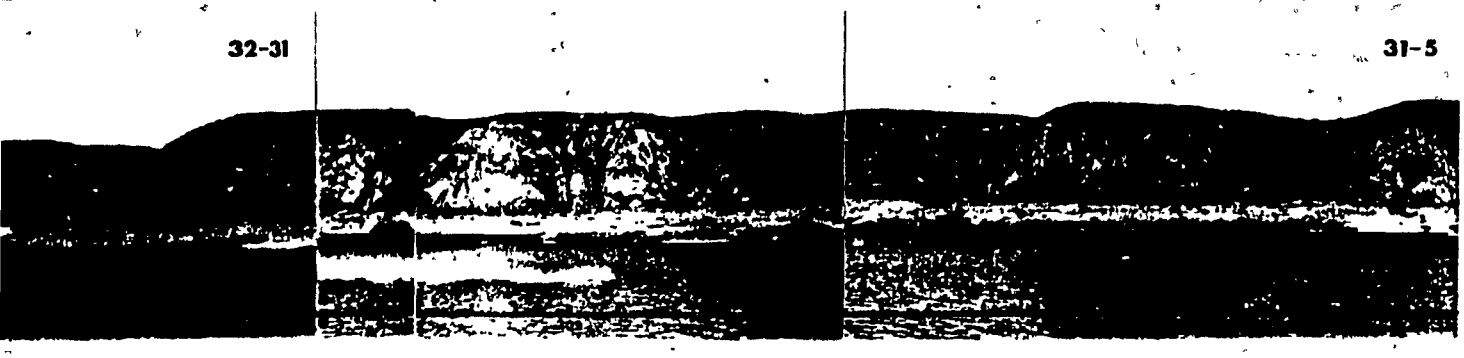

37-24
36-3
32-31
SURVEY LINE V
25-42

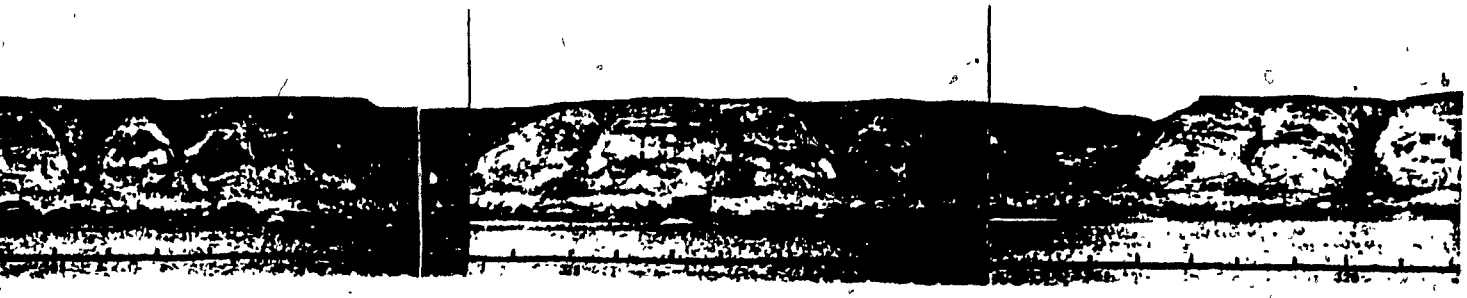
36-3



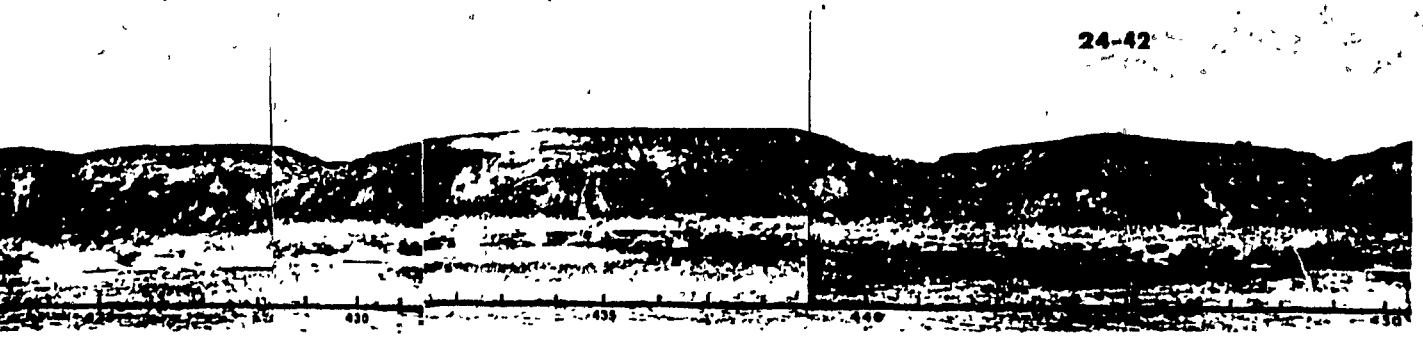
32-31

31-5





24-42



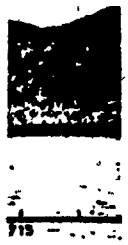
Appendix C

Kivitoo Bluff Panorama

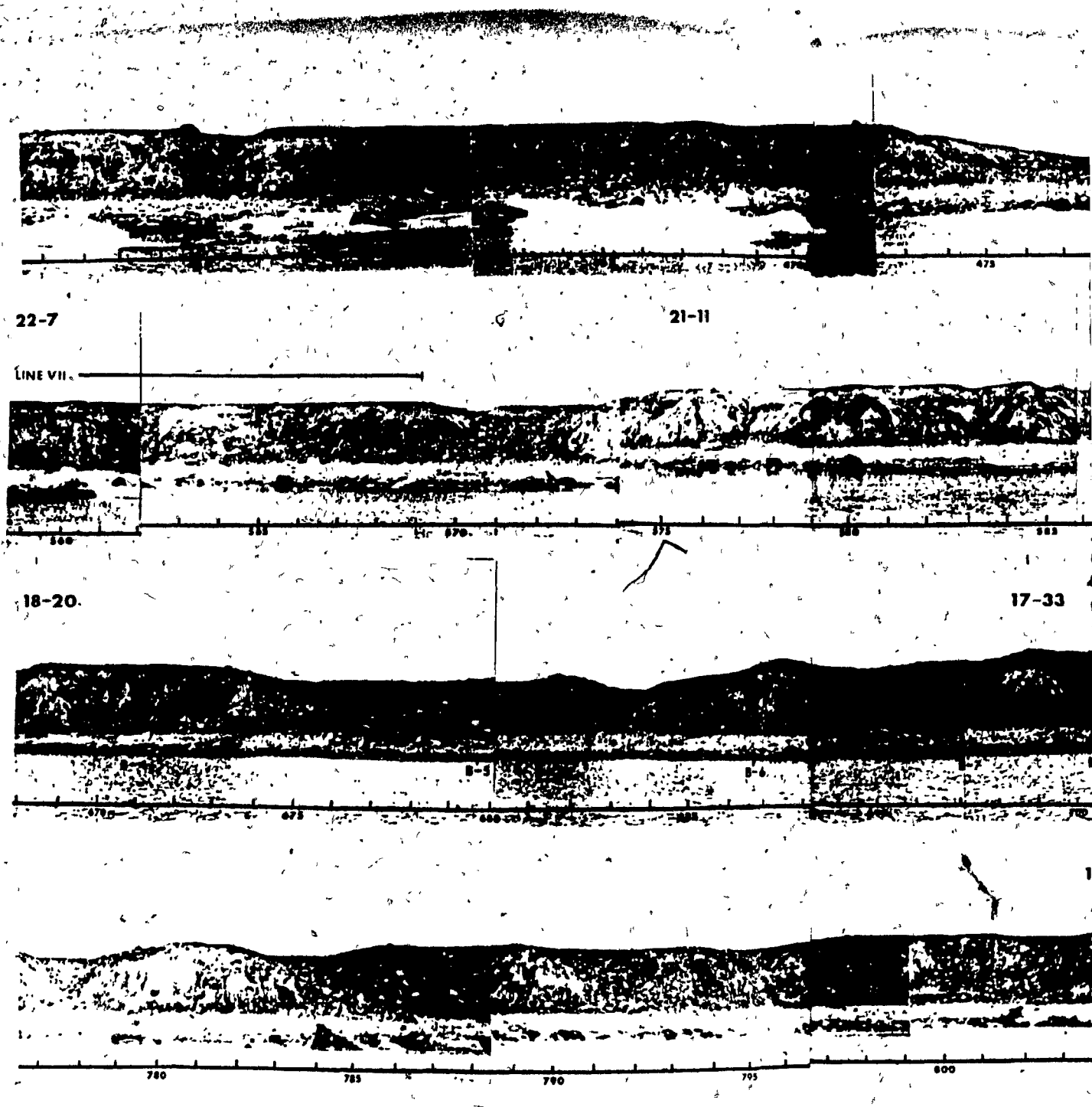
Part 2: K451 - K880

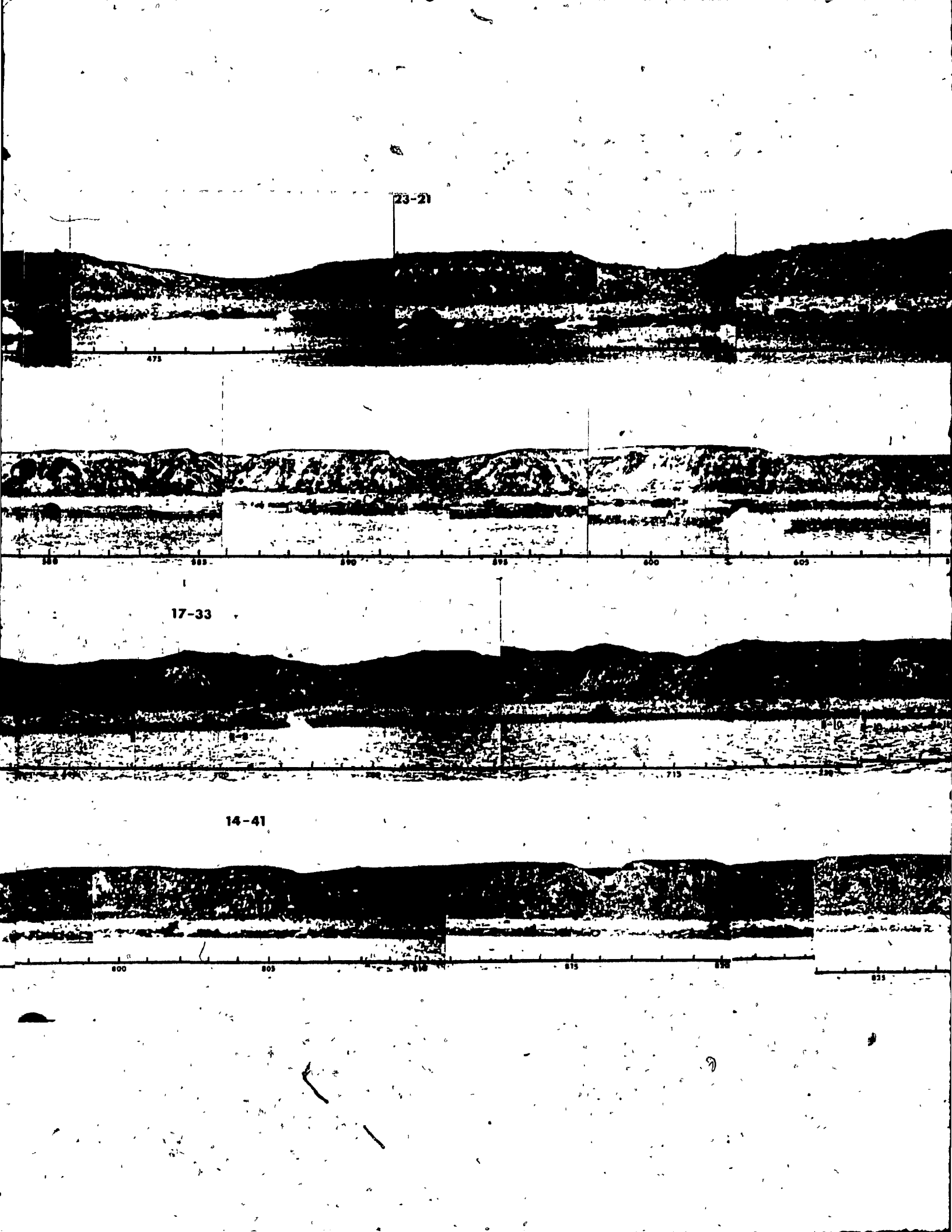


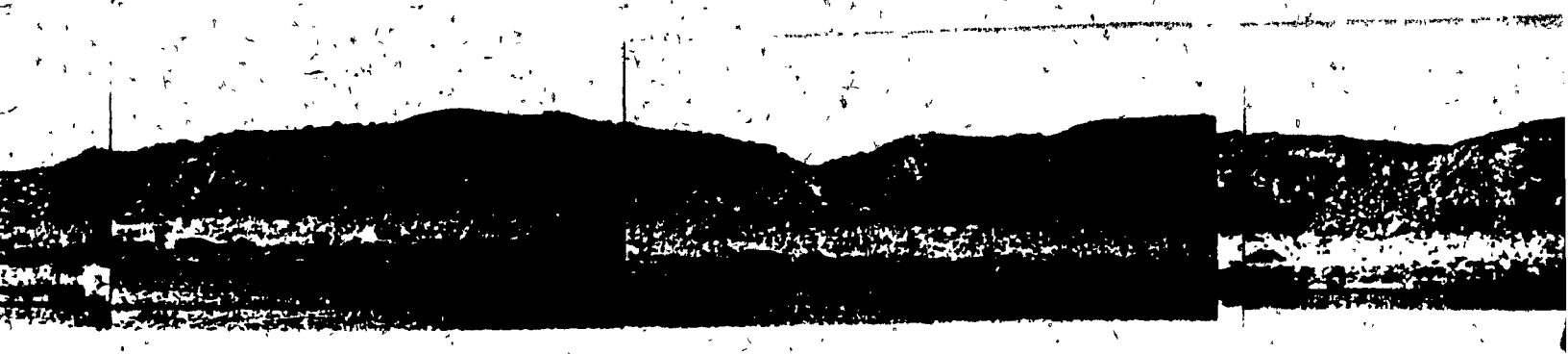







22-7
21-11
LINE VII
18-20
17-33
B-5
B-6
700
705
710
715
720
725

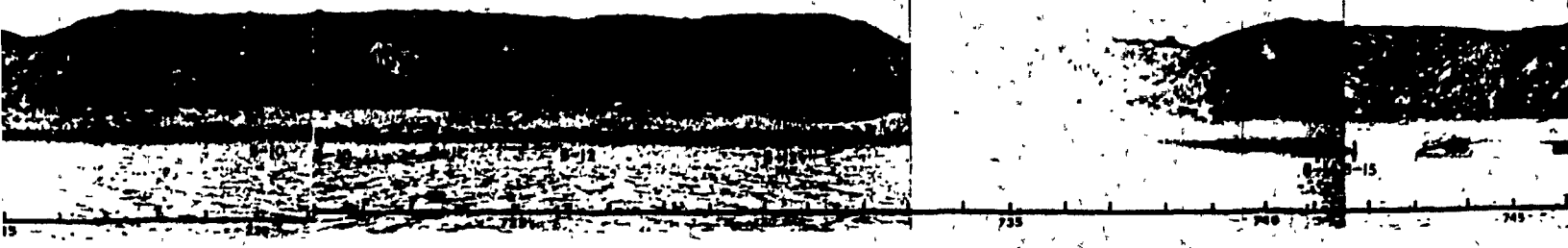

23-21
17-33
14-41



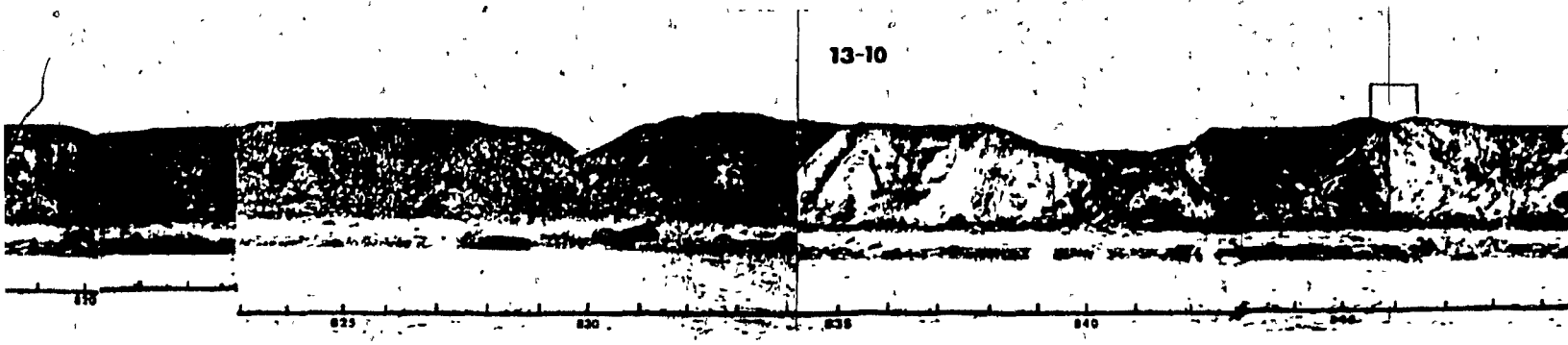
20-43

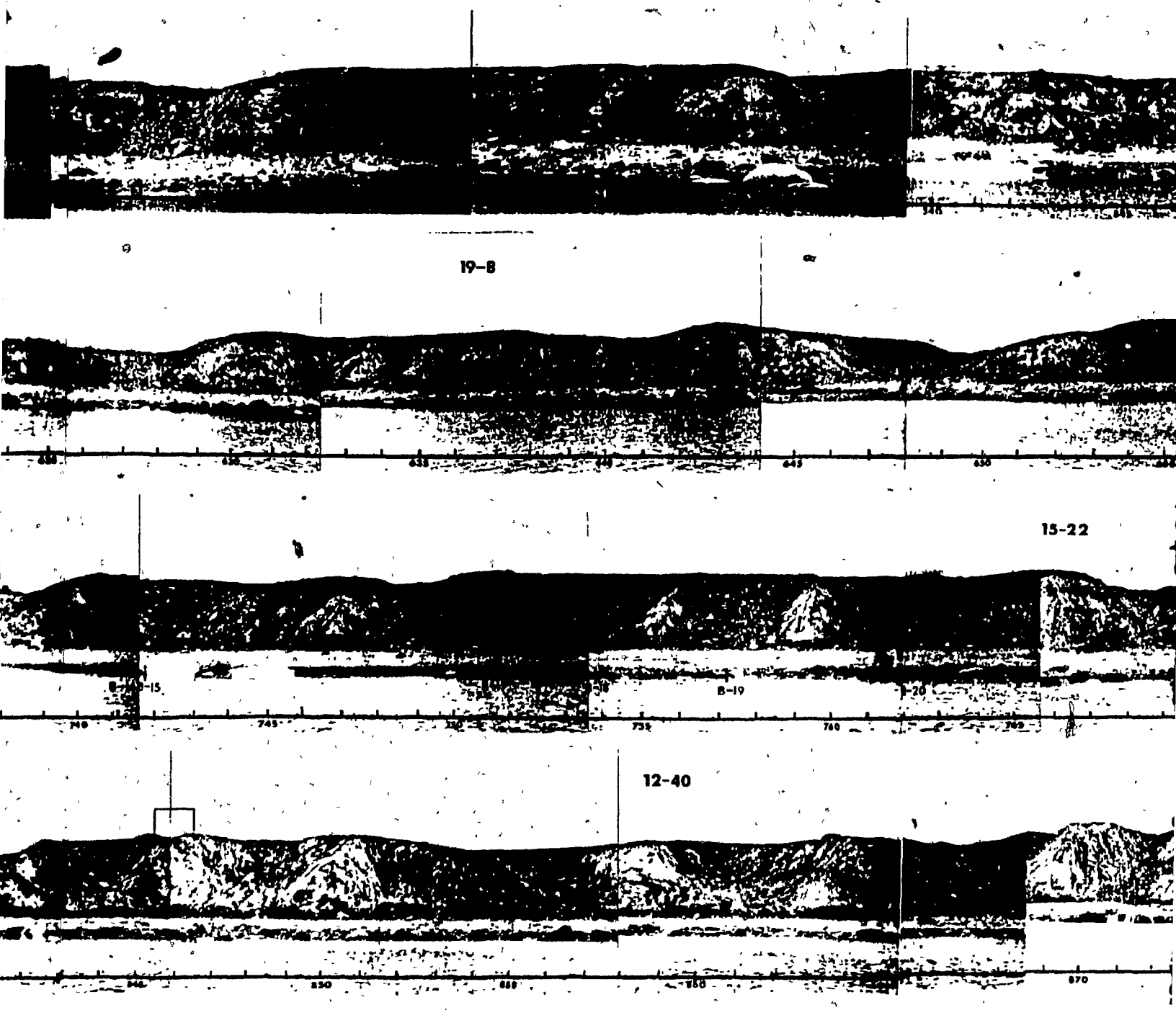


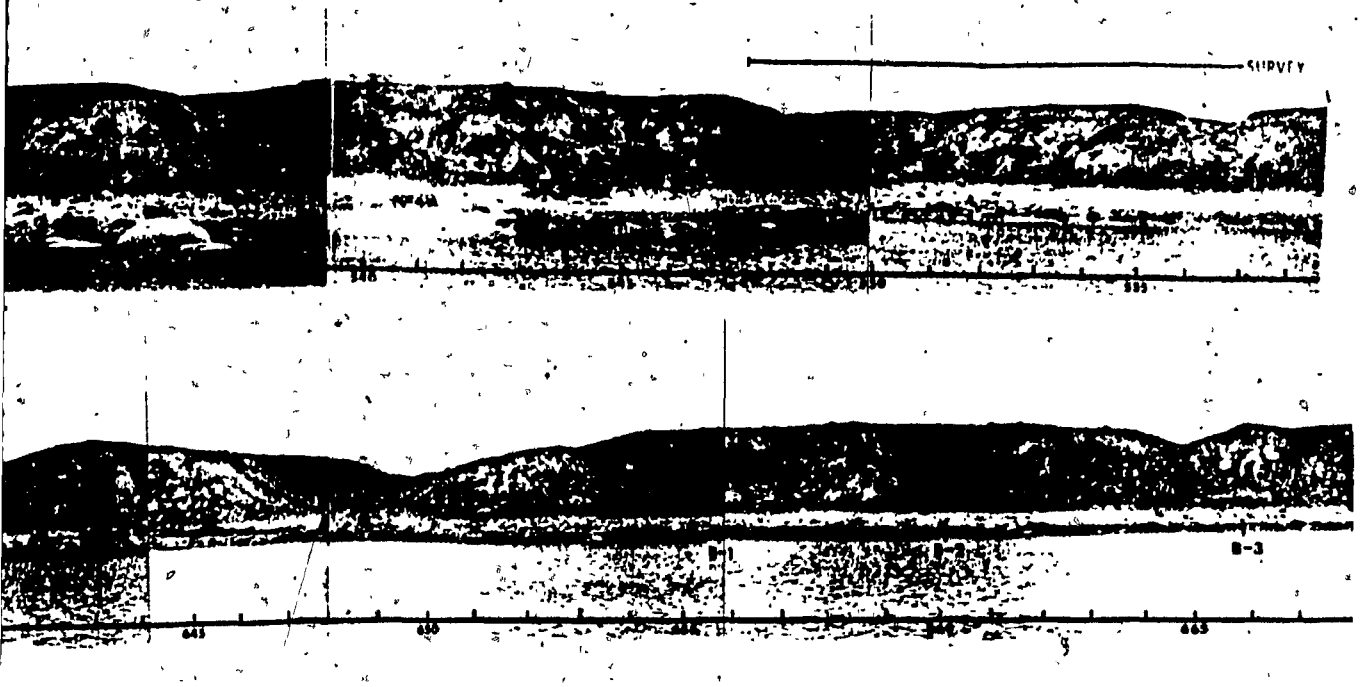
16-9



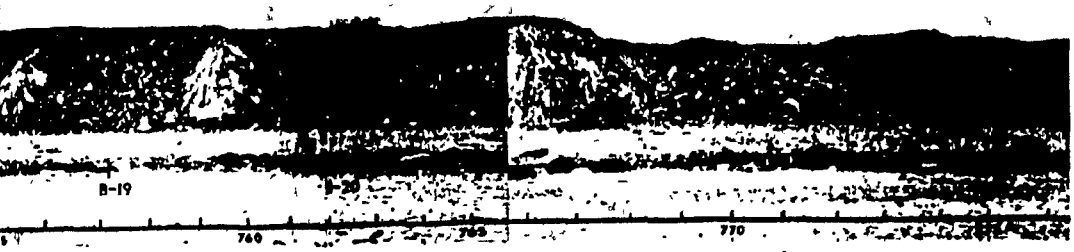
13-10



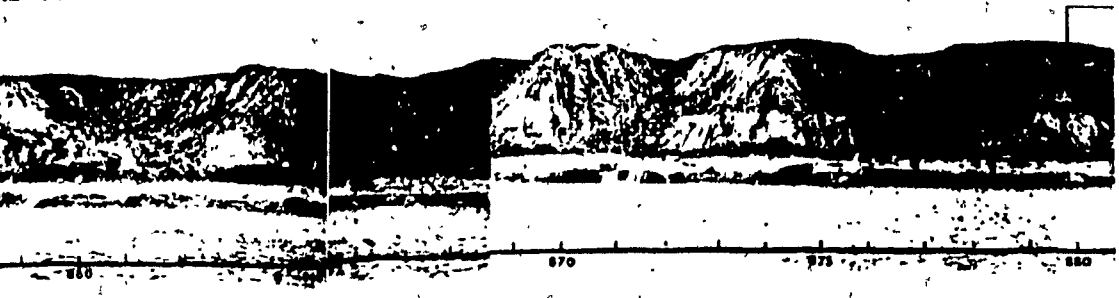

19-8
15-22
B-19
12-40



15-22



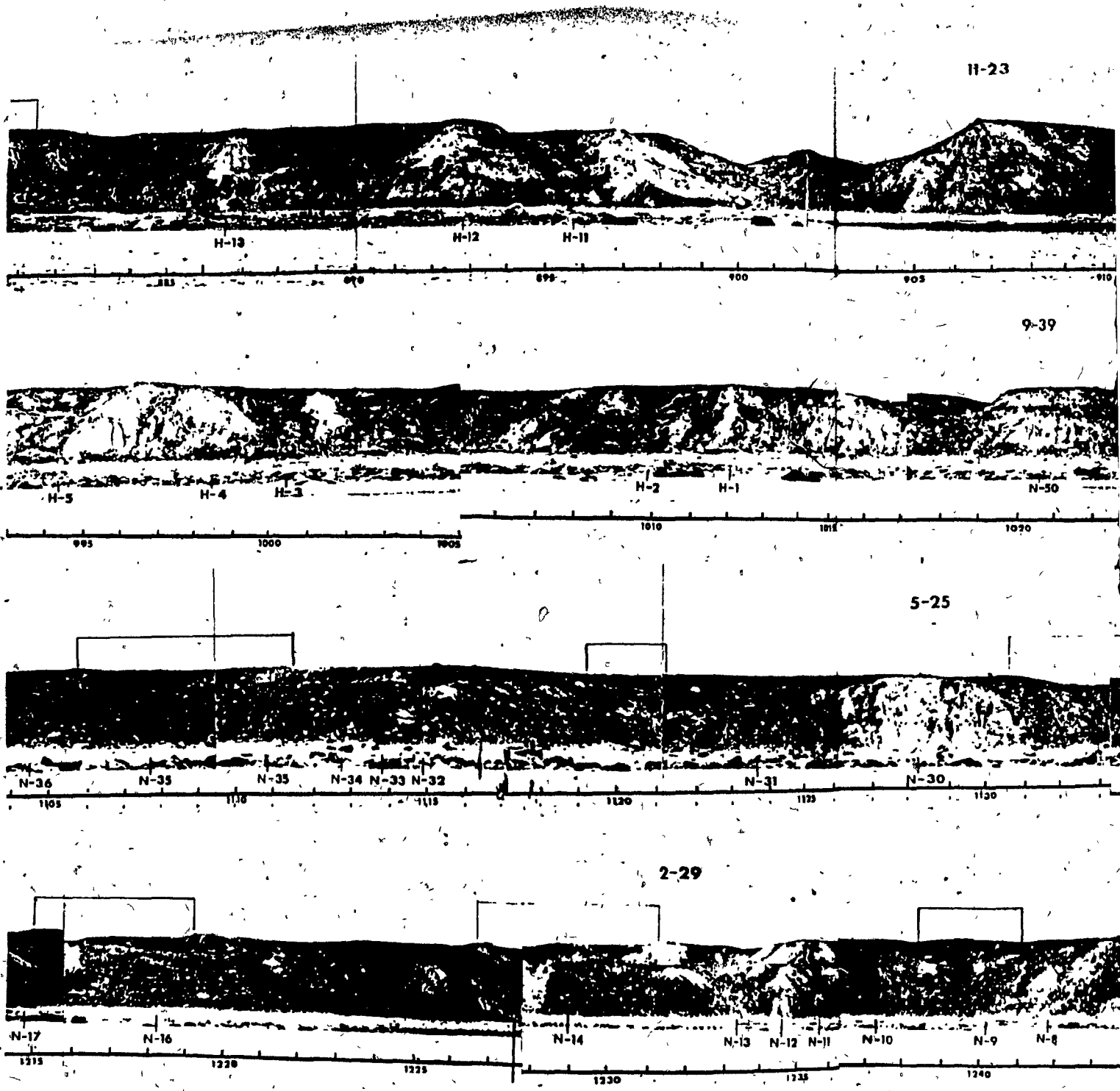
12-40

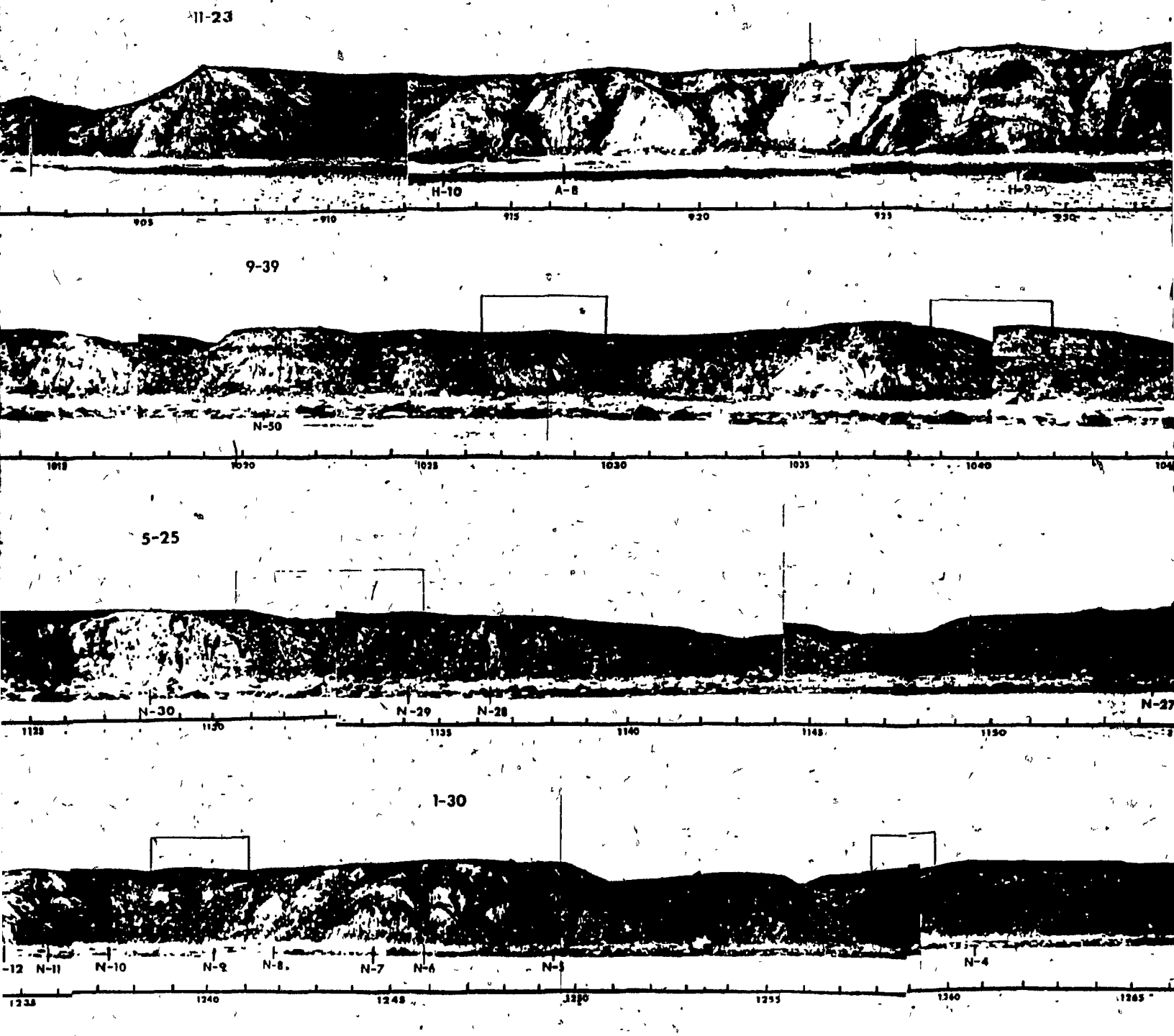


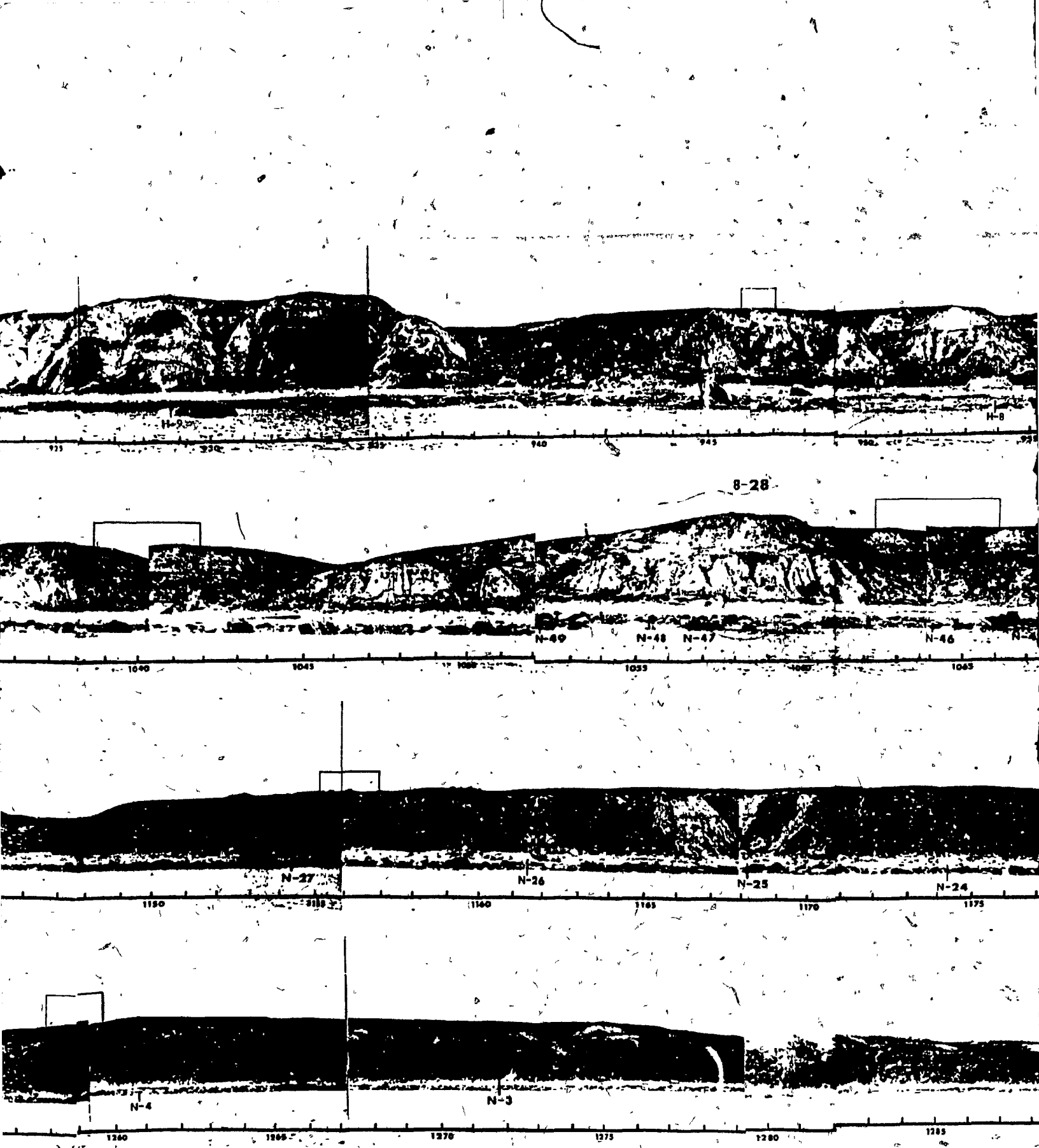
Appendix C

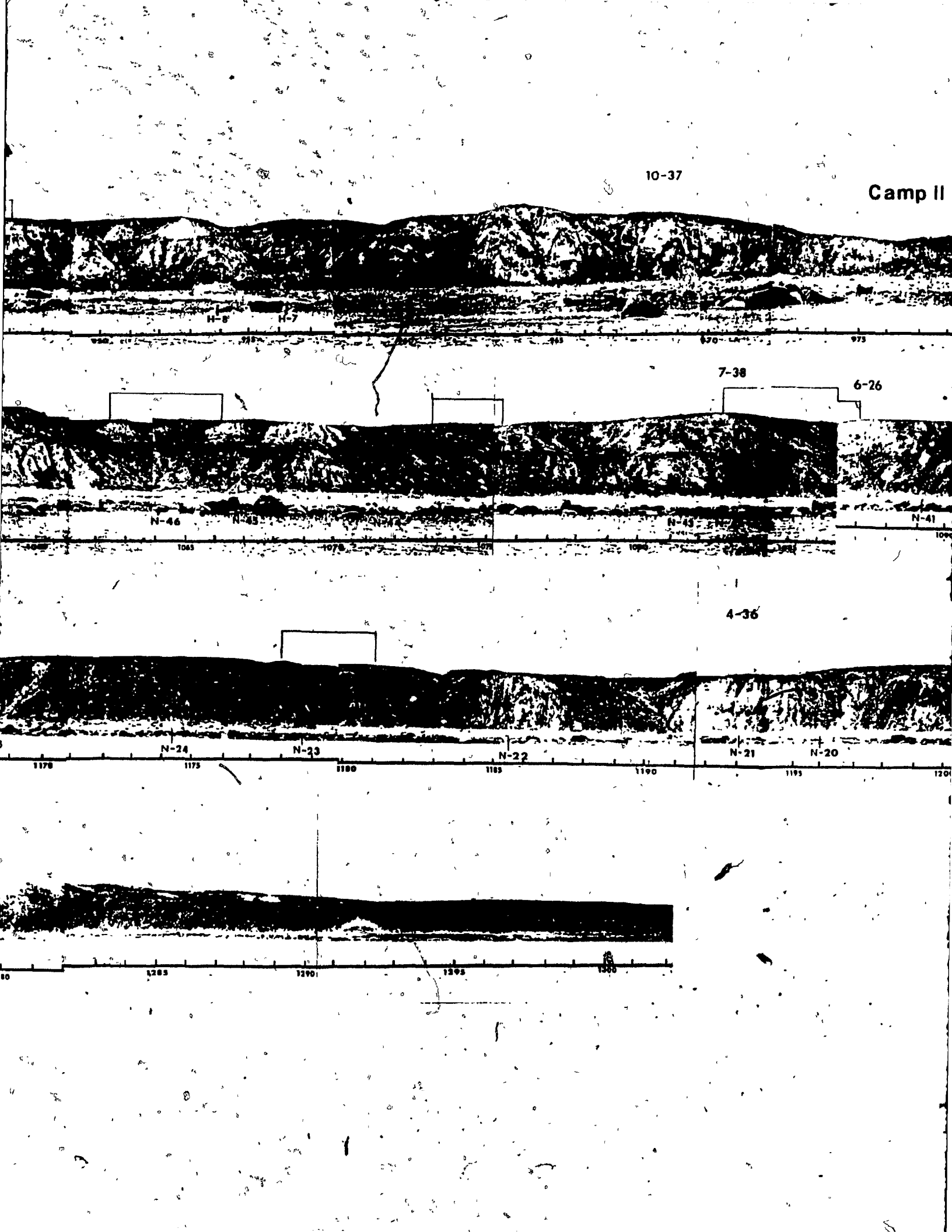
Kivitoo Bluff Panorama

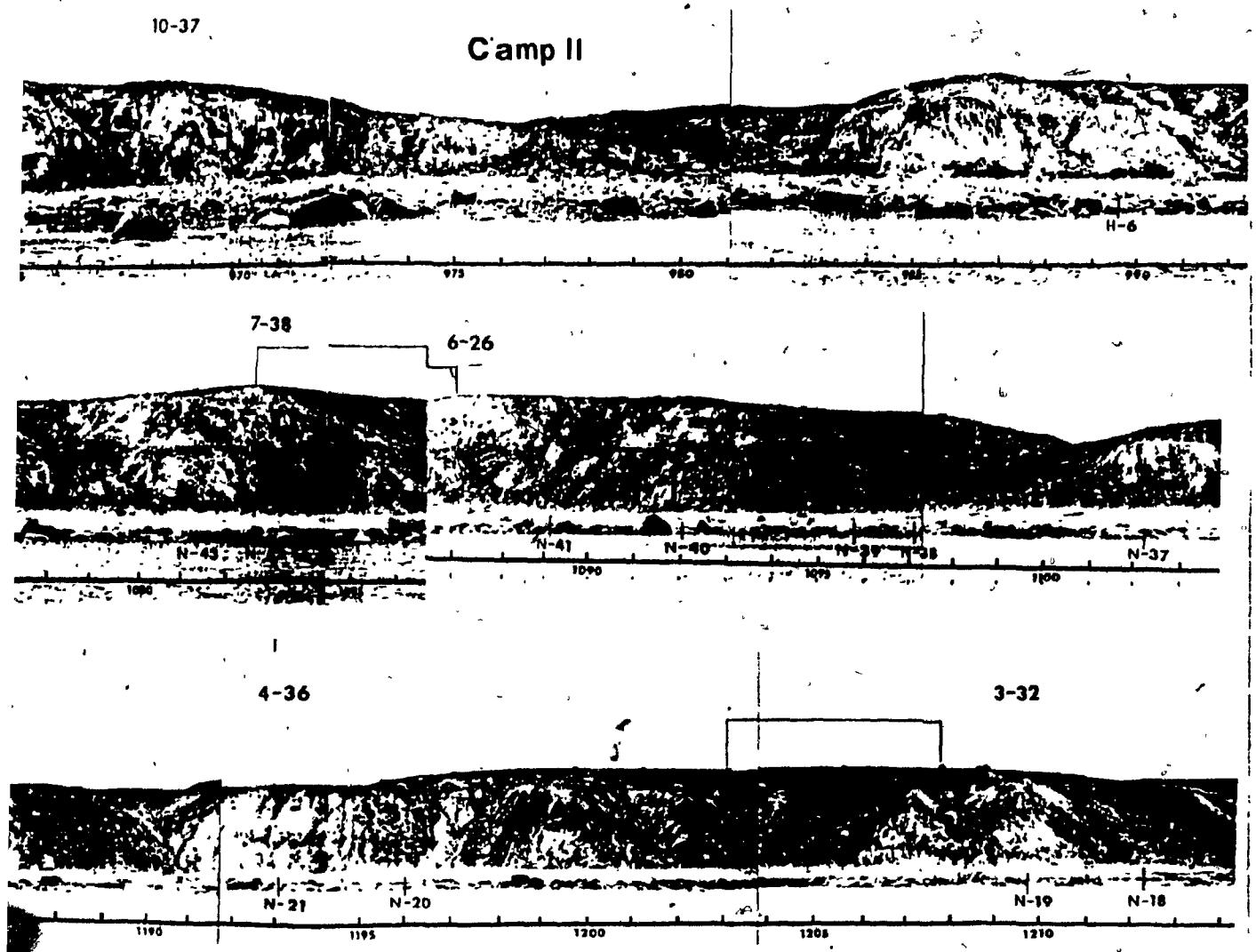
Part 3: K881 - K1302


11-23
H-13
H-12
H-11
885
890
895
900
905
910
9-39
H-5
H-4
H-3
H-2
H-1
N-50
995
1000
1005
1010
1015
1020
5-25
N-36
N-35
N-35
N-34
N-33
N-32
N-31
N-30
1105
1110
1115
1120
1125
1130
2-29
N-17
N-16
N-14
N-13
N-12
N-11
N-10
N-9
N-8
1215
1220
1225
1230
1235
1240


11-23
H-10
A-8
905
910
915
920
925
9-39
N-50
1015
1020
1025
1030
1035
1040
5-25
N-30
N-29
N-28
N-27
1130
1135
1140
1145
1150
1-30
-12
N-11
N-10
N-9
N-8
N-7
N-6
N-5
N-4
1235
1240
1245
1250
1255
1260
1265


H-9
H-8
940
945
8-28
N-49
N-48
N-47
N-46
1040
1045
1055
1065
N-27
N-26
N-25
N-24
1150
1160
1165
1170
1175
N-4
N-3
1260
1270
1275
1280
1285


10-37
Camp II
H-8
H-7
7-38
6-26
N-46
N-45
N-41
4-36
N-24
N-23
N-22
N-21
N-20

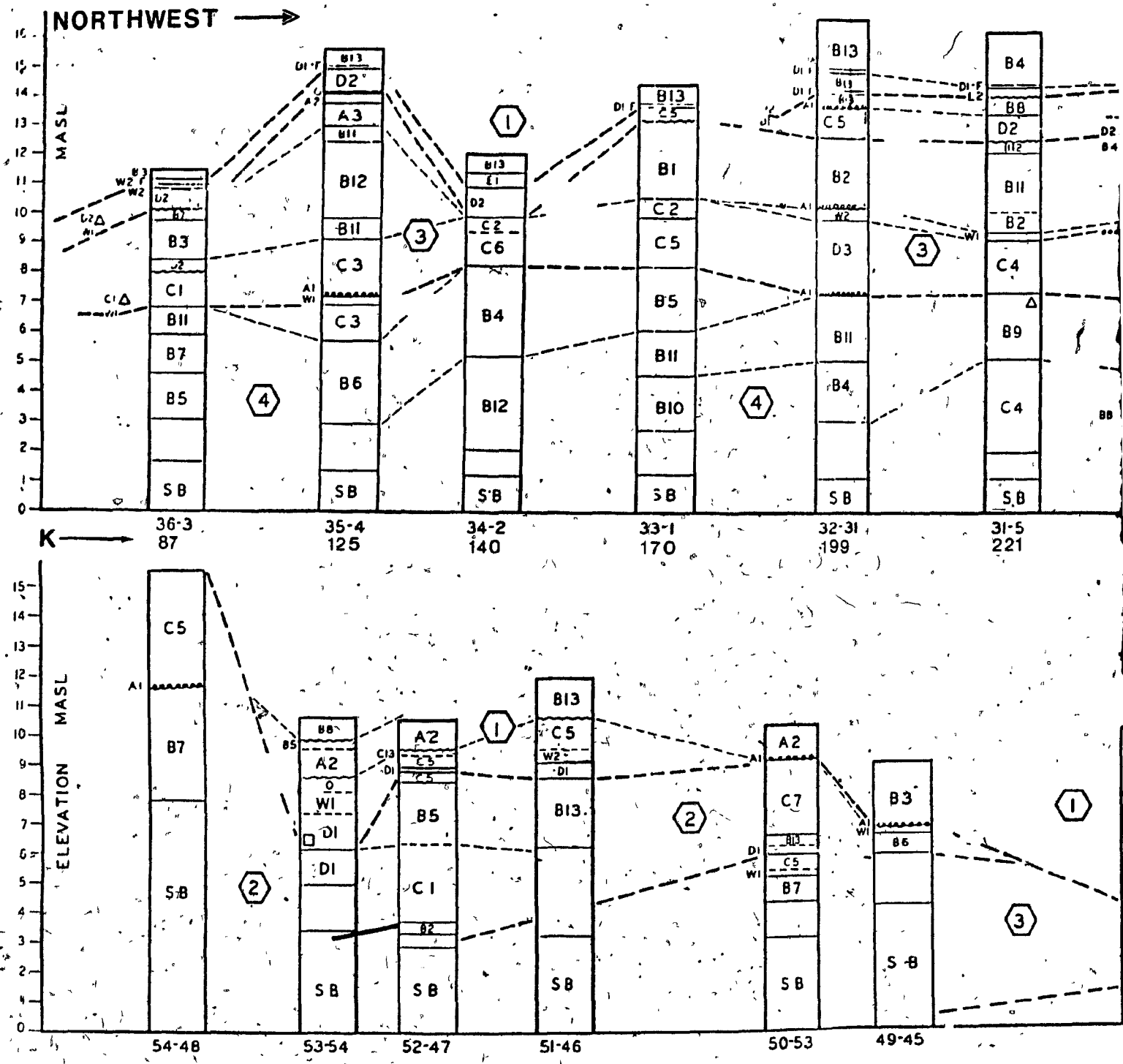

10-37
Camp II
H-6
970
975
980
985
990
7-38
6-26
N-43
N-41
N-40
N-39
N-38
N-37
1080
1090
1095
1100
4-36
3-32
N-21
N-20
N-19
N-18
1190
1195
1200
1205
1210

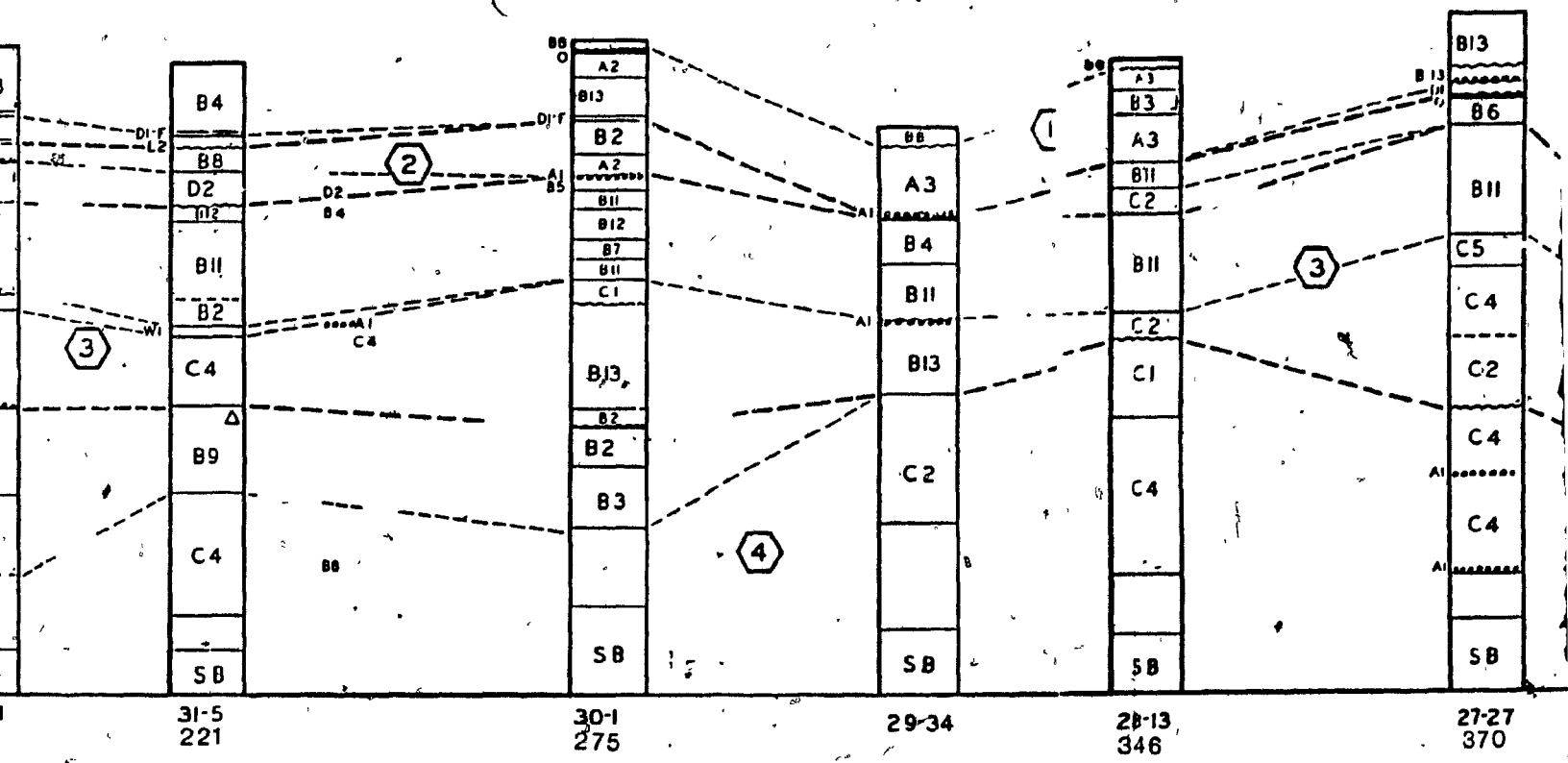
Appendix C

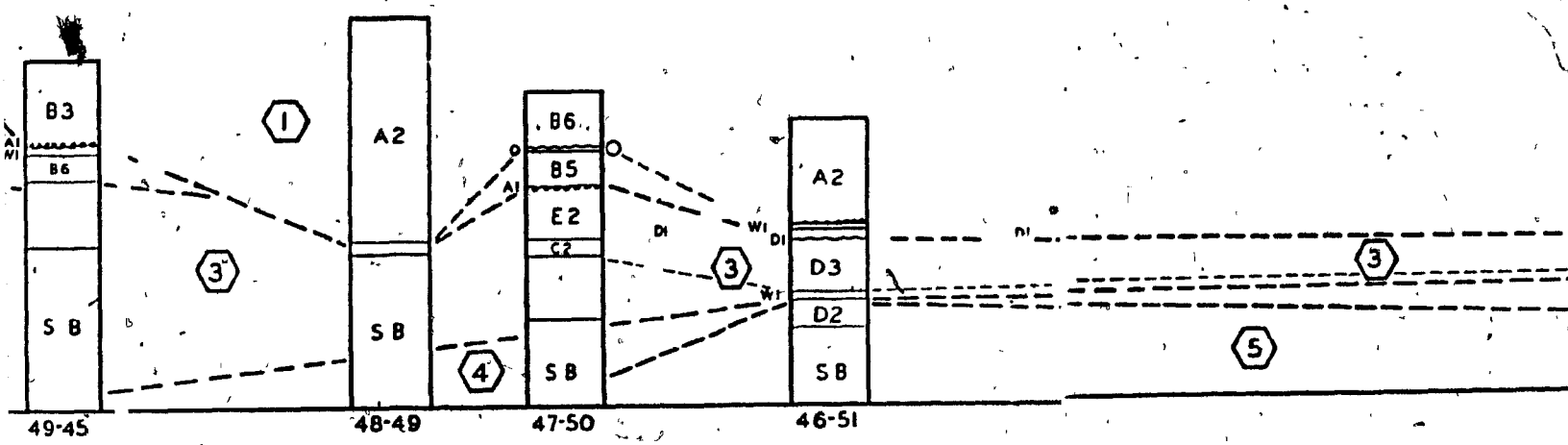
Stratigraphy: Part 1

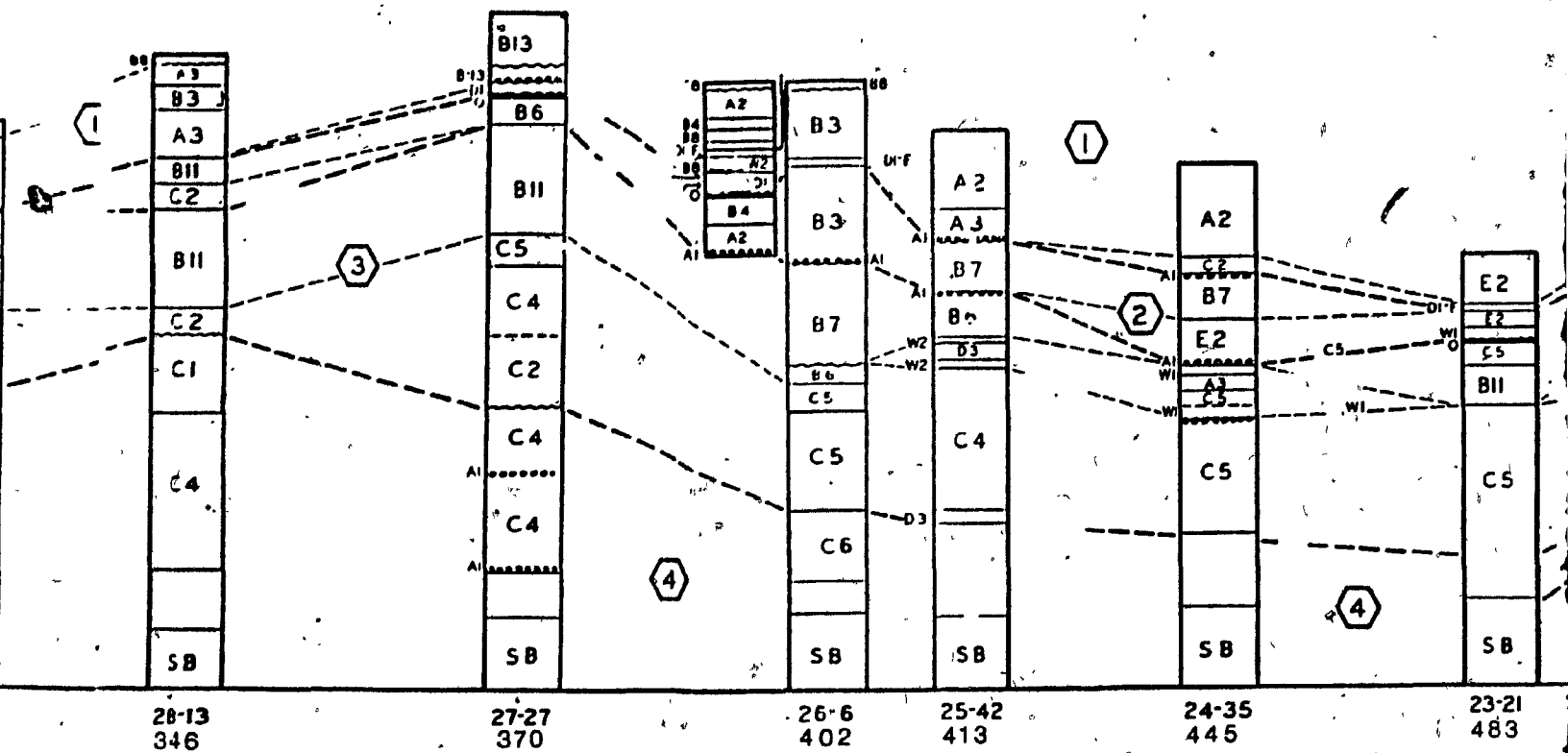
Sections 54-48 to 16-9 (K729)

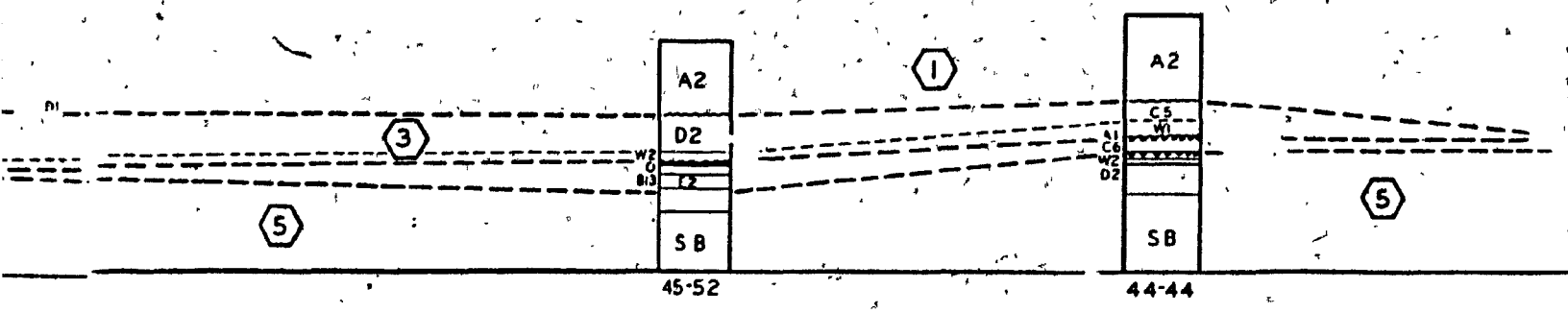
For key to facies notation see Table II.3

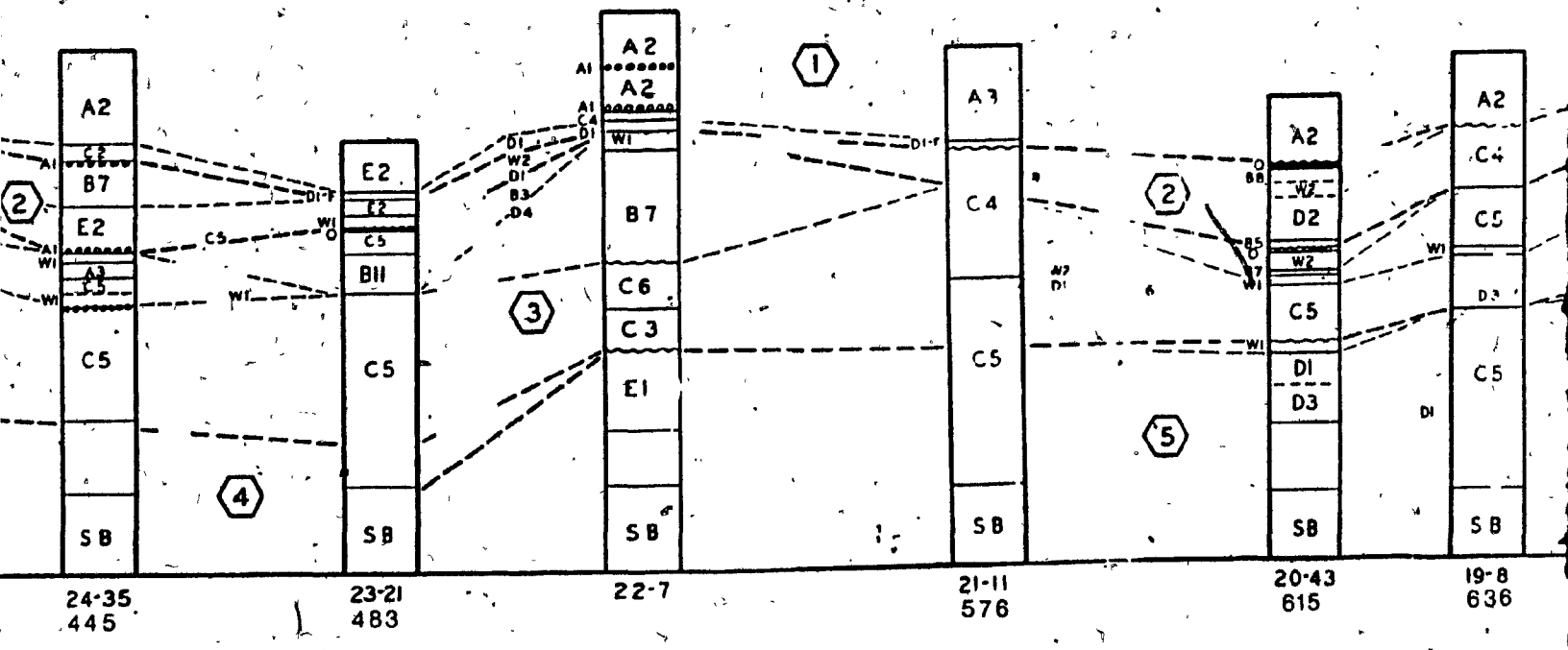

NORTHWEST
MASL
K
36-3
87
35-4
125
34-2
140
33-1
170
32-31
199
31-5
221
ELEVATION MASL
54-48
53-54
52-47
51-46
50-53
49-45

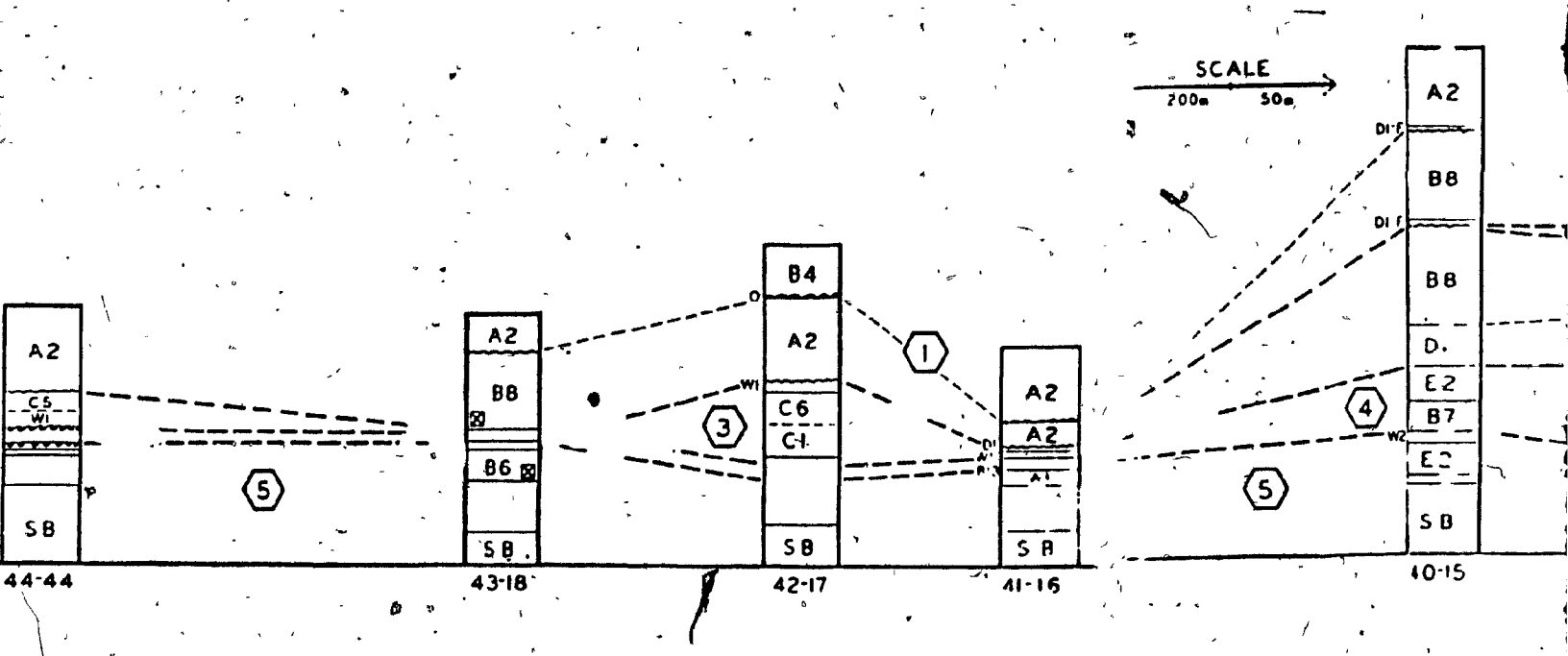

B4
B8
D2
B11
B2
C4
B9
C4
SB
B8
A2
B13
B2
A2
B11
B12
B7
B11
C1
B13
B2
B2
B3
SB
A3
B4
B11
C2
SB
A3
B3
A3
B11
C2
B11
C1
C4
SB
B13
B6
B11
C5
C4
C2
C4
C4
SB
31-5
221
30-1
275
29-34
28-13
346
27-27
370

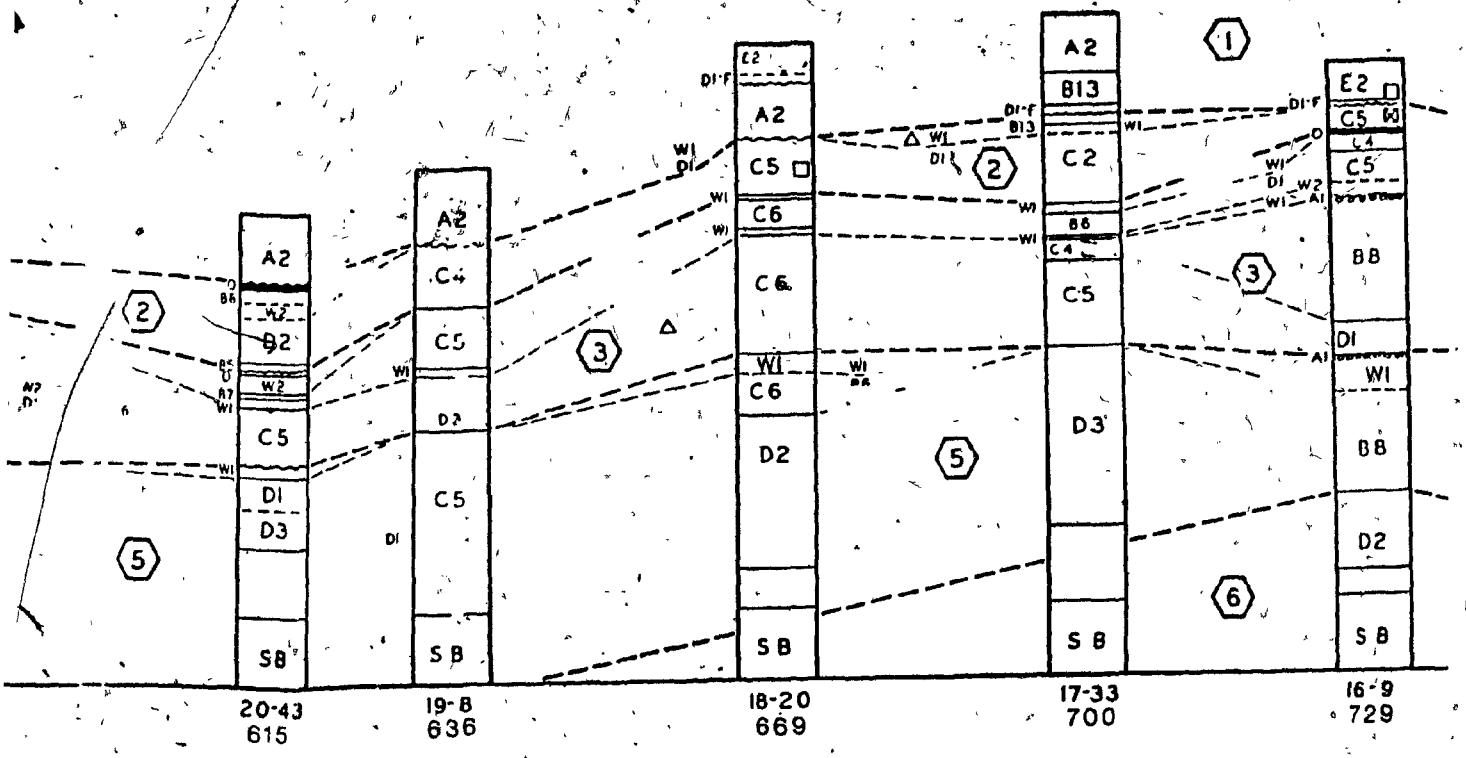

B3
B6
S B
A2
S B
B6
B5
E2
C2
SB
A2
D3
D2
SB
49-45
48-49
47-50
46-51

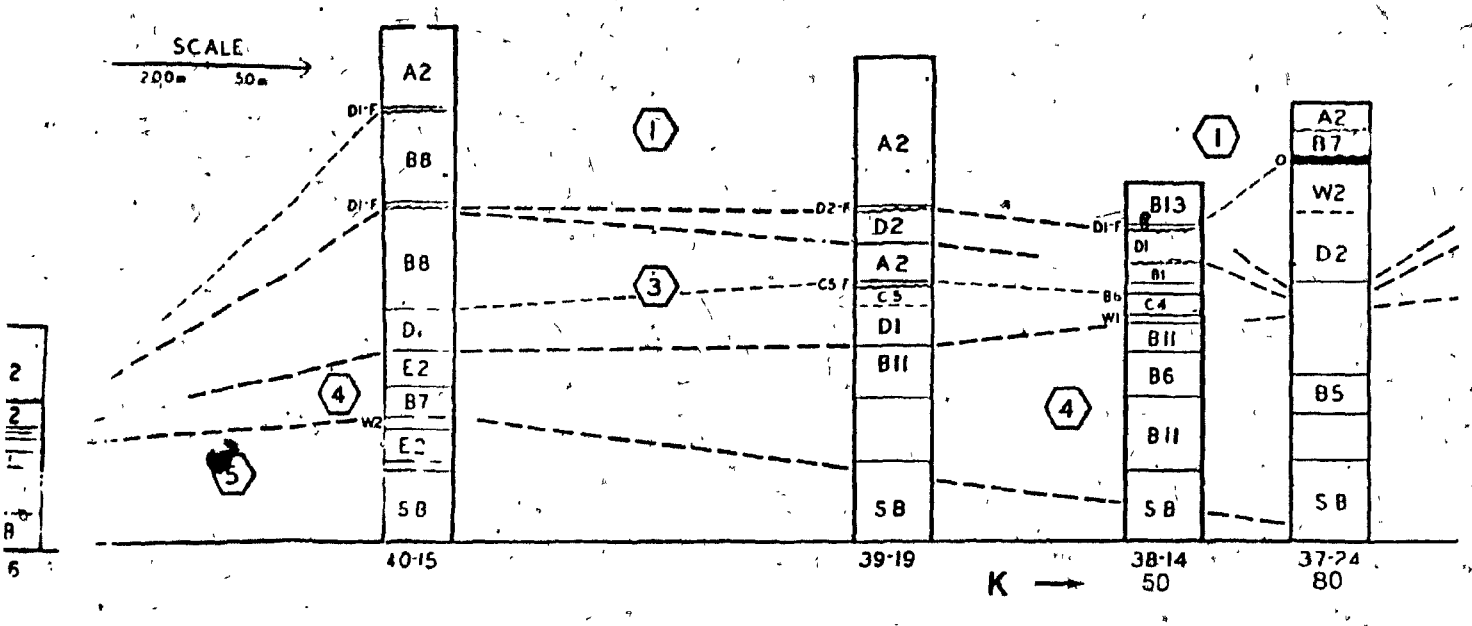

28-13
346
27-27
370
26-6
402
25-42
413
24-35
445
23-21
483
SB
C4
C1
C2
B11
A3
B3
B13
B6
C5
C6
B7
B4
A2
E2
D1
D2
D3
W2
A1


45-52
44-44
SB
A2
D2
C2
B13
C5
W1
C6
W2
D2
D1


A2
B7
E2
C5
SB
E2
B11
C5
SB
A2
A2
B7
C6
C3
E1
SB
A3
C4
C5
SB
A2
D2
C5
D1
D3
SB
A2
C4
C5
D3
C5
SB
24-35
445
23-21
483
22-7
21-11
576
20-43
615
19-8
636


SCALE
200m 50m
A2
C5
SB
A2
B8
B6
SB
B4
A2
C6
C1
SB
A2
A2
SB
A2
B8
B8
D.
E2
B7
E2
SB
44-44
43-18
42-17
41-16
40-15

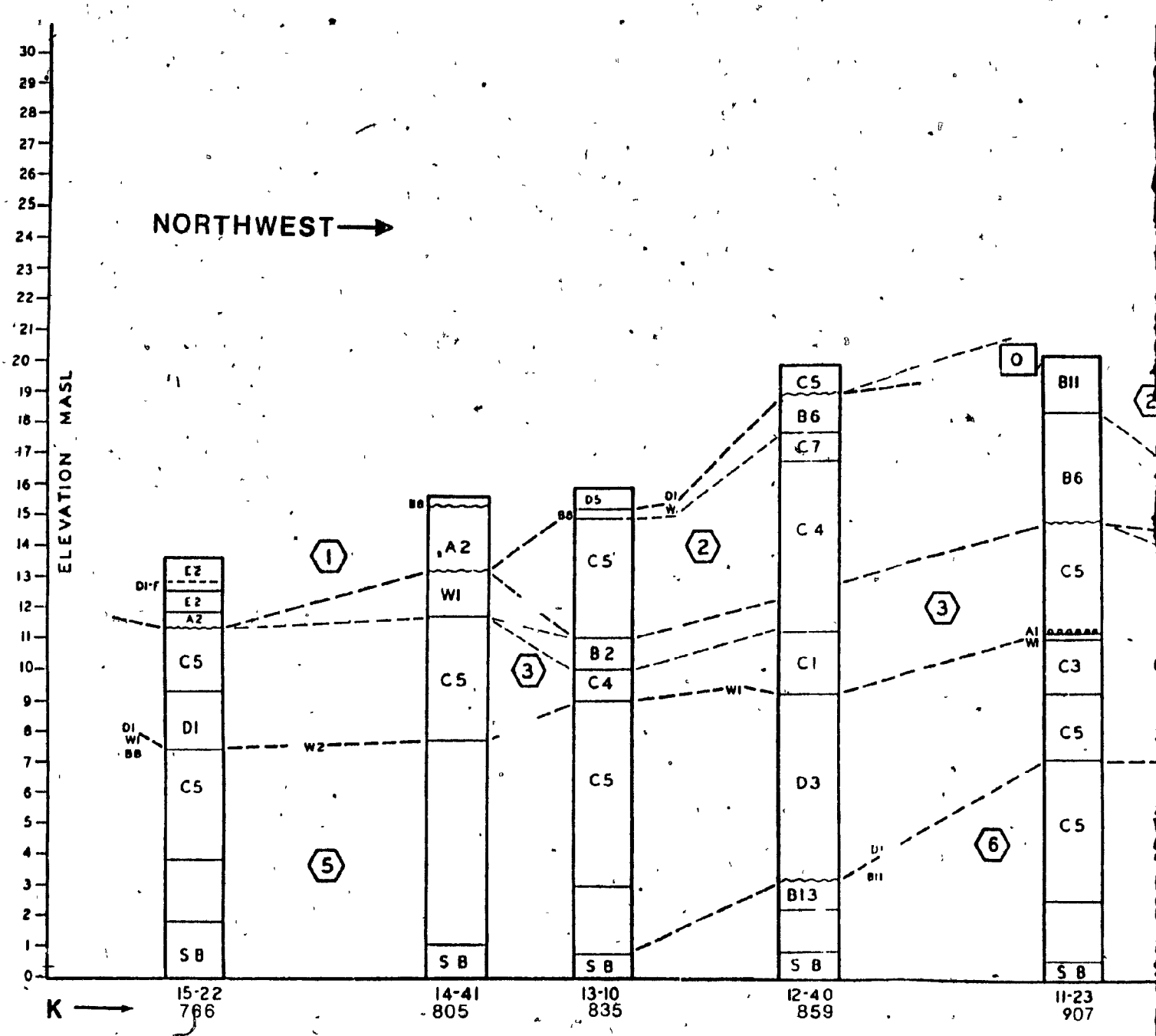

A2
B2
C5
D3
D1
SB
C4
C6
D2
B13
C2
B6
E2
B8
W2
W1
D1-F
20-43
615
19-8
636
18-20
669
17-33
700
16-9
729

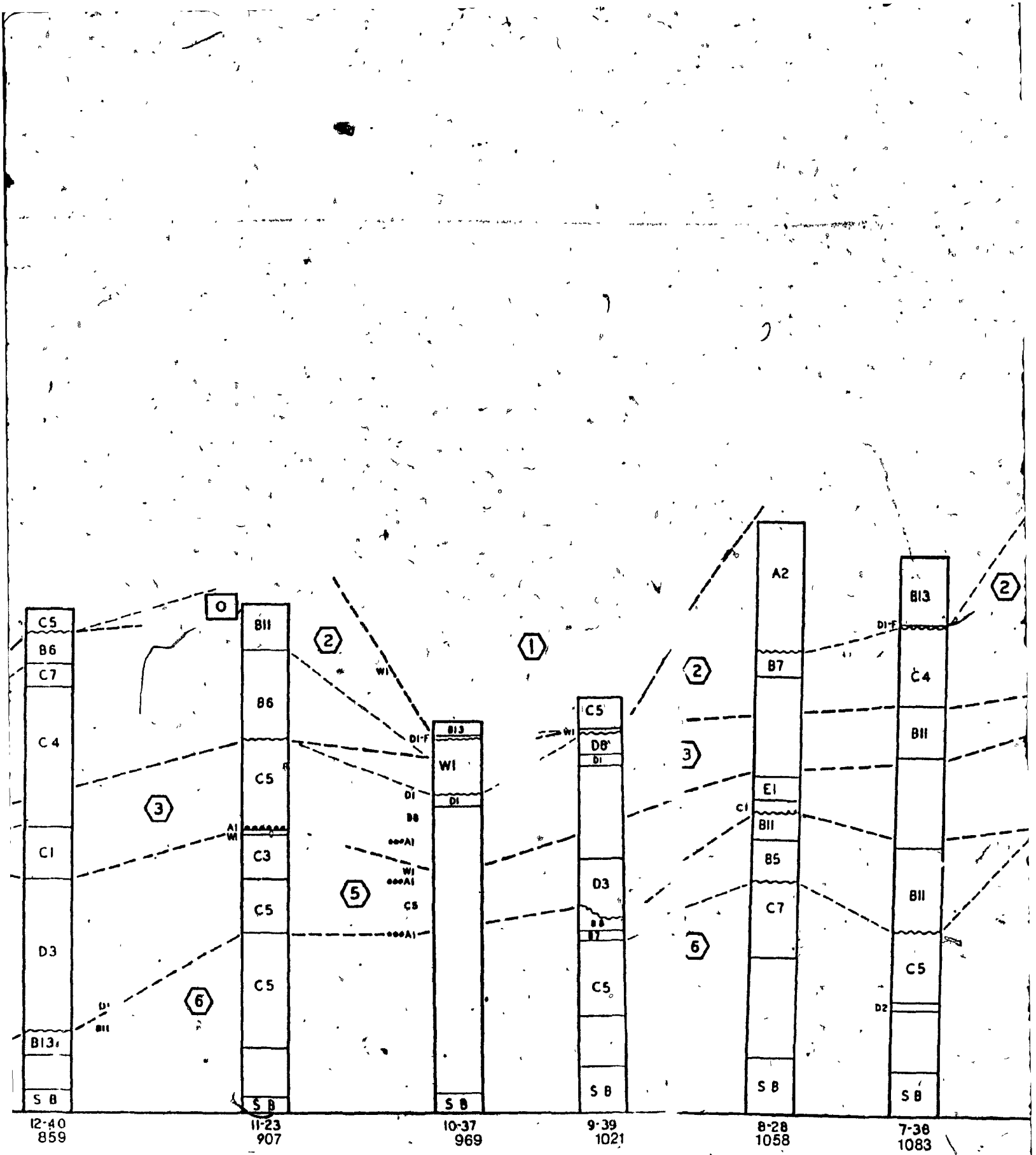

SCALE
200m
50m
A2
B8
D1
E2
B7
W2
SB
B11
B6
B5
B13
D2
C4
C5
40-15
39-19
38-14
50
37-24
80
K

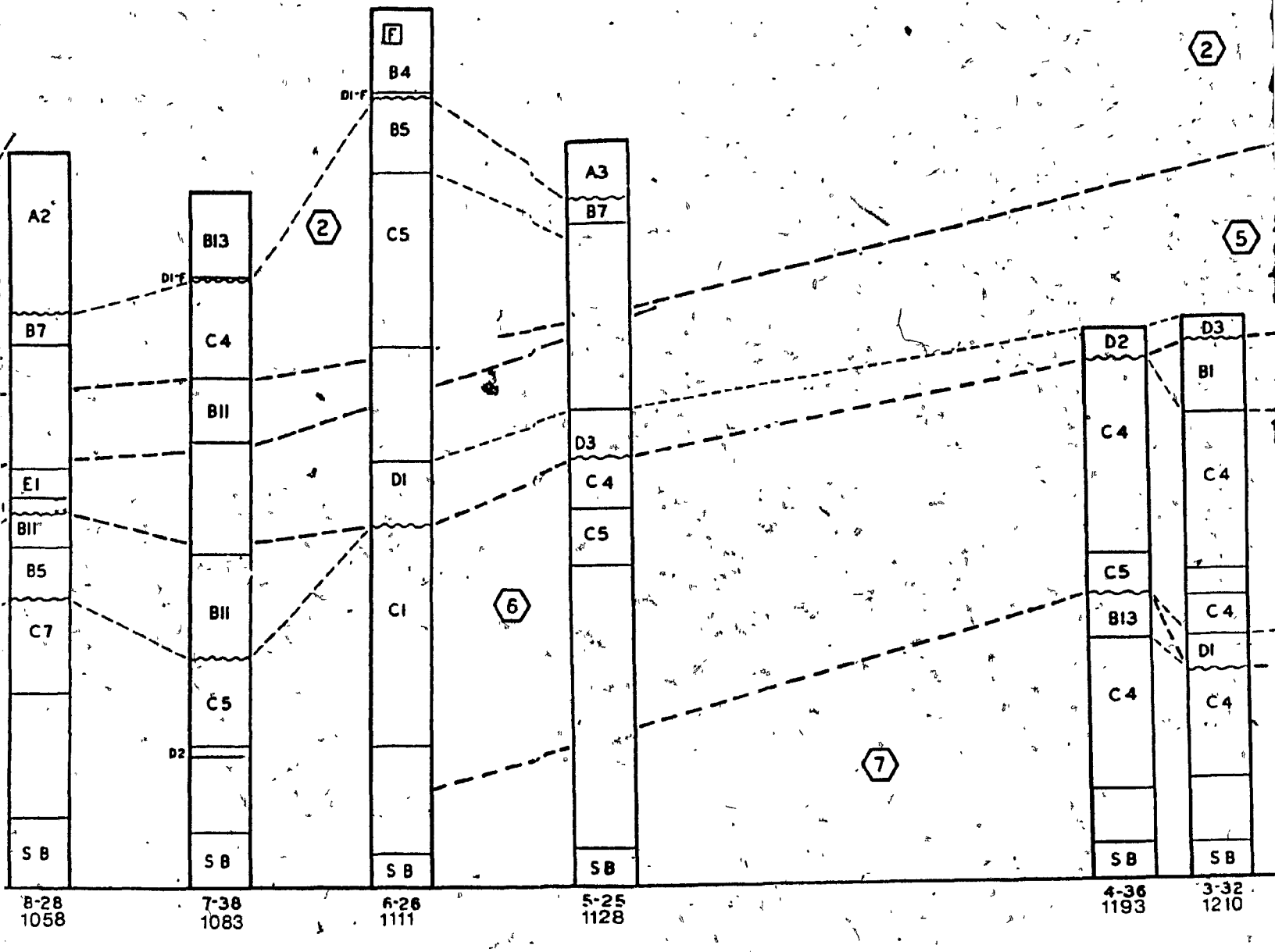
Appendix C

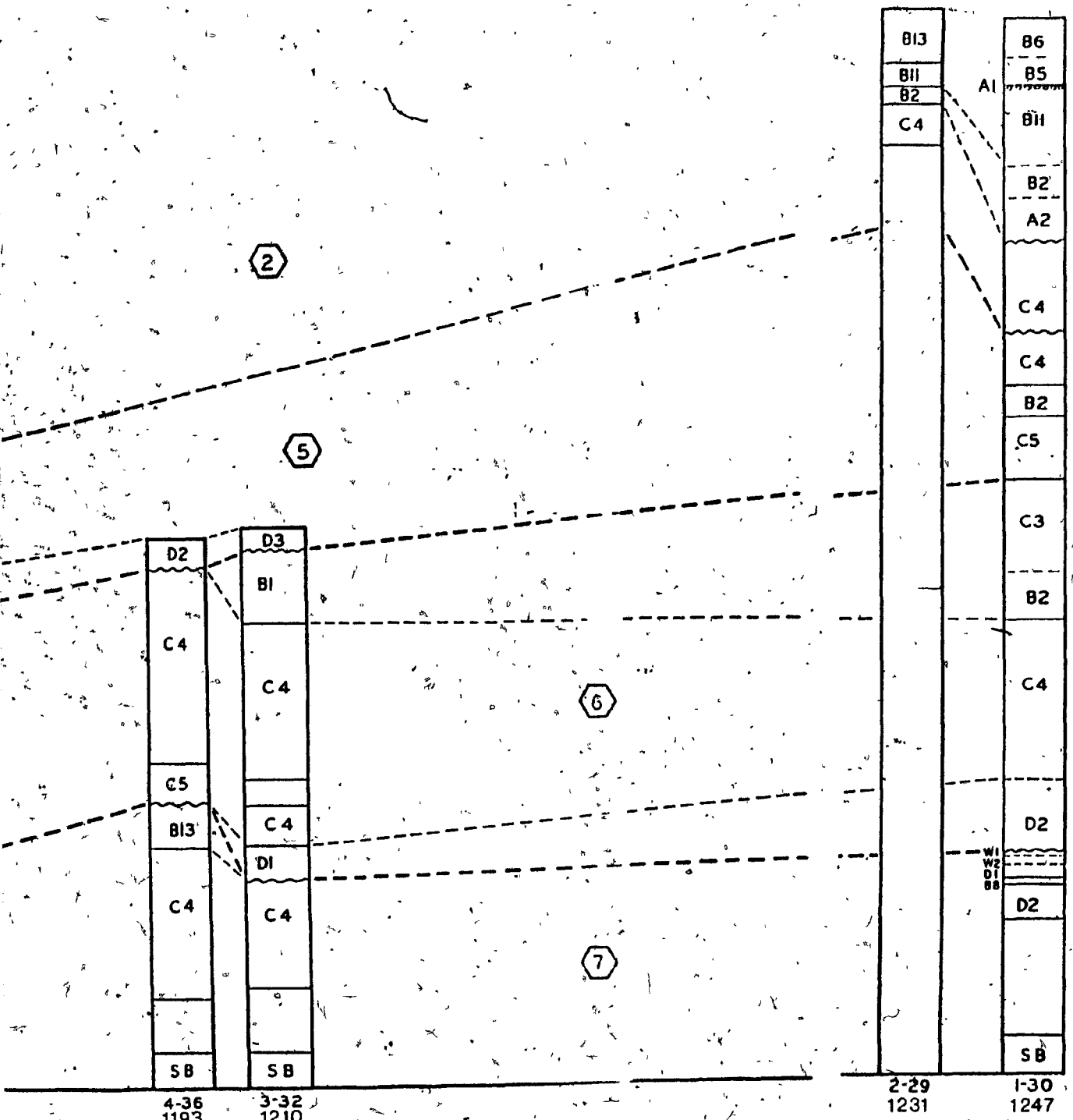
Stratigraphy: Part 2
Sections 15-22 (K766)
to 1-30 (K1247)

For key to facies
notation see Table II.3


NORTHWEST
ELEVATION MASL
30
29
28
27
26
25
24
23
22
21
20
19
18
17
16
15
14
13
12
11
10
9
8
7
6
5
4
3
2
1
0
K
15-22
766
14-41
805
13-10
835
12-40
859
11-23
907
E2
E2
A2
C5
D1
C5
S B
D1-f
D1
W1
B8
W2
A2
W1
C5
S B
B8
D5
C5
B2
C4
C5
S B
D1
W1
C5
B6
C7
C4
C1
D3
B13
S B
D1
B11
B11
B6
C5
A1
W1
C3
C5
C5
C5
S B
0
1
2
3
5
6


C5
B6
C7
C4
C1
D3
B13
S B
B11
B6
C5
A1
W1
C3
C5
C5
S B
W1
B13
D1-F
D1
D1
B6
A1
W1
A1
C5
A1
S B
C5
D8
D1
D3
C5
S B
A2
B7
E1
C1
B11
B5
C7
S B
B13
D1-F
C4
B11
B11
C5
D2
S B
0
1
2
3
5
6
12-40
859
11-23
907
10-37
969
9-39
1021
8-28
1058
7-38
1083


A2
B7
E1
B11"
B5
C7
S B
8-28
1058
B13
DI-F
C4
B11
B11
C5
D2
S B
7-38
1083
F
B4
DI-F
B5
C5
DI
C1
S B
6-26
1111
A3
B7
D3
C4
C5
S B
5-25
1128
D2
C4
C5
B13
C4
S B
4-36
1193
D3
BI
C4
C4
DI
C4
S B
3-32
1210
2
2
5
6
7


B13
B11
B2
C4
A1
B6
B5
B11
B2
A2
C4
C4
B2
C5
C3
B2
C4
D2
W1
W2
D1
B8
D2
SB
2
5
6
7
D2
C4
C5
B13
C4
D3
B1
C4
D1
C4
SB
4-36
1193
3-32
1210
2-29
1231
1-30
1247

KIVITOO

STRATIGRAPHY OF THE COASTAL BLUFFS

from NELSON 1978

